Dielectrophoretic Investigations Of Bacterial Cells

Andrew Paul Brown

A thesis submitted for the degree of Doctor of Philosophy

THE UNIVERSITY *of York*

Department of Biology

York

U.K.

December 1996

DEDICATION

This thesis is dedicated to the memory of Mr Philip Brown, dearly loved and sadly missed by us all. He was here to see me begin this undertaking but unfortunately could not be around to see it come to an end.

"The more I see, the more I know. The more I know, the less I understand."

Paul Weller

ABSTRACT

Dielectrophoresis (DEP), movement of particles or cells in non-uniform electric fields, has been increasingly investigated over recent years. The majority of this work has primarily consisted of theoretical considerations, though many practical applications have begun to emerge. These often involve the DEP of bacterial cells, many of which are of great importance in areas of microbiology, particularly medical and environmental science.

The phenomenon of DEP relies upon the relative polarisability of the cells (caused by an electric field) compared to the medium in which they are suspended. This is a frequency dependent process which is highly specific to the nature of the cells, particularly their surface and cell wall properties. The selective nature of DEP has enabled its application for identification purposes, bacterial species having characteristic DEP collection patterns over a frequency range. Explanations relating to bacterial cell wall peptidoglycan structure have been offered to account for some of the differences in resulting spectra.

Work undertaken in this thesis has involved the use and development of a previously described rapid dielectrophoresis system, which utilises a continuous flow rather than the earlier methods using non-flowing media (static dielectrophoresis). Many physical parameters have been found to influence the extent of dielectrophoretic movement and subsequent collection of cells at electrodes. A range of these conditions (e.g. conductivity, duration of applied field, pump speed, voltage, etc.) have been examined in more detail in this thesis and a set of standardised experimental conditions for examination of bacterial cells and polystyrene latex particles proposed. Some parameters such as electrode quality are difficult to standardise. Therefore a calibration method using latex particles has also been examined.

Particle or cell concentration present in the sample has been found to greatly affect the extent of DEP collection, though linear correlations were discounted on the basis of normalisation experiments. Sigmoidal relationships were proposed, relating to a co-operative effect brought about by an increase in electric field non-uniformity by the initial collection of cells. The existence of such relationships between particle or cell concentration and DEP collection has enabled the use of this system as a novel particle counting device. This has certain advantages over other counting systems and the dielectrophoretic effect allows a selective collection and enumeration of a desired cell type from a mixture on the basis of applied frequency.

Interspecies variation between bacterial spectra was observed, though variations within a particular species were also in evidence. Even isogenic strains or species which are closely related were also found to have great differences in spectra. Bacterial cells are subject to

variation in structure from growth effects and the nature of the suspending medium. Investigations have been undertaken on these effects, and explanations proposed relating DEP effects at a particular frequency to alterations in bacterial cell structure.

The production of exopolysaccharide (EPS) material in some bacterial species is known to vary according to growth medium, particularly nitrogen and carbon source. Changes in DEP spectrum were shown following changes in growth medium, and possible links with EPS variations have been proposed. However, other explanations relate to variations in properties of the outer membrane and bacterial cell structure. Further to these experiments, *Klebsiella* spp. mutagenesis was performed using N-methyl-N'-nitro-N-nitrosoguanidine (NTG) resulting in loss of slime producing function. This was confirmed by colony morphology and EPS dry weight measurements. Resulting spectra, comparing mutants and parent strains were found to have major differences. While this may be due to the lack of EPS present on the cell surface (altering the polarisability of the cell), a much greater level of collection was produced implicating additional cell structure changes.

The effect of cell physiology and morphology was examined by the use of the antibiotics; nalidixic acid, chloramphenicol and ampicillin. These three antibiotics have different mechanisms of action, causing major effects on cell structure even at sub-inhibitory levels. Nalidixic acid, a quinolone, caused significant cell elongation at sub-MIC levels, resulting in a shift in the peak of dielectrophoretic collection from around 2 MHz to 800 kHz. This was attributed to enhanced surface conductivity effects, or inhibition of nucleic acid replication and septation responses reducing intracellular polarisation effects in the higher frequency range. Antibiotic binding to cell surfaces was thought unlikely to contribute to spectral changes of *E. coli* since the spectrum of a resistant strain was found to be unaffected by growth in antibiotic containing medium. Chloramphenicol mediated inhibition of protein synthesis resulted in significant cell wall thickening by the continuation of peptidoglycan synthesis in *B. subtilis* cells. This thickening caused a significant reduction in cell polarisability between 20 kHz and 1 MHz compared to the control sample grown in absence of antibiotic. Proposed explanations are the loss of structural proteins from the cytoplasmic membrane which have potential roles in enhancing cell polarisation, or by the increased wall thickness reducing charge transport and subsequent polarisation. Ampicillin treatment caused cell elongation and bulge formation but produced little change in dielectrophoretic spectrum at sub-MIC concentrations.

Many of the treatments experienced by cells produced changes in spectral frequency response. It is however, an inherently difficult procedure to isolate the spectral effects of normal growth from the effect of a treatment, due to the highly interlinked processes ongoing in cell synthesis. Indeed, minor changes in cell structure may actually have more notable effects on polarisation responses than more major visible changes. Adequate controls are therefore also difficult to

enforce. In its current form the dielectrophoretic system used, although offering major advantages in terms of reproducibility and analyses, is still inadequate for attribution of specific changes in cell structure due to the examination of whole cell polarisation.

TABLE OF CONTENTS

LIST OF FIGURES

Figure A5.1 : Scanning electron micrographs of several bacterial species.

LIST OF TABLES

ACKNOWLEDGEMENTS

First of all I would like to thank Dr Bernard Betts, my friend and supervisor for his help and encouragement over the years. Without his confidence in my ability I wouldn't have been able to get this far.

Jo Bryenton has been with me for the past five years, four of which I have been involved with this DPhil. Throughout that time she has been unfaltering in her support and love. When you undertake something as big as this, it doesn't just involve you, but all of the people around you and Jo will be as happy to see this thesis finished as I will. Now I think it is time for me to return some of that devotion. I will never forget all that she has done.

Someone that has been with me even longer than Jo is Adrian Harrison. He is a constant source of companionship and loyalty. Adrian is always good to discuss ideas with, invariably knows the quick way to get things done, and is always there when things go wrong.

Thanks also go to other lab. members, both past and present for their help. I would like to thank several of them in particular : Carmel Quinn (who was a great source of inspiration and a good friend), Barry Daly, Richard Beal and Mark Ripley. Thanks for all of your encouragement.

On a more personal note I would like to mention Drs. Dave Cattrall and Iain Checkland. They helped to shape me in the formative years and inspired me to become what I am today.

I would also like to acknowledge the help of Meg Stark, Pete Crosby and Mike Hopgood for their electron microscopy and photography, everyone in electronics notably Duncan Allsopp, Jonathan Cremer and Malcolm Law for providing electrodes and other friends and family, especially Andy Vickers and Jayne Graham.

Last but not least I would like to acknowledge all those other people who made allowances to enable me to finish writing when life could have been very difficult.

DECLARATION

I declare that all of the results presented in this thesis are my own and original work except where acknowledged. This work has neither been accepted for, nor is being submitted for any other degrees.

Journal Papers

Brown A.P., Harrison A.B., Betts W.B. & O'Neill J.G (1996) A dielectrophoretic particle counting device. In preparation.

Brown A.P., Harrison A.B., Betts W.B. & O'Neill J.G. (1996) A novel method for quantifying grid based dielectrophoresis. In preparation.

Betts W.B. & Brown A.P. (1996) Dielectrophoresis in real-time analysis and separation of cells. Review article, accepted for publication.

Conference Proceedings

Brown A.P., Harrison A.B., Betts W.B. & O'Neill J.G. (1996) A dielectrophoretic device for real-time counting of bacteria in water. *In* Health Related Water Microbiology. 6-10th October, Mallorca, Spain.

Posters

Brown A.P., Betts W.B., Harrison A.B., Milner K. & Allsopp D.W.E. (1996) Microelectronic systems for the dielectrophoretic analysis of biological particles. *In* Microfabrication Technology for Biomedical Applications. 24-25th October, San Jose, California.

Harrison A.B., Brown A.P., Betts W.B. & O'Neill J.G. (1994) Dielectrophoretic analysis of biofilms. Society For Applied Bacteriology, 20th September (Autumn Meeting), University of Leicester, Leicester, U.K.

Published Abstracts and Conference Presentations

Betts W.B., Brown A.P., Goodall D.M. & Allsopp D.W.E. (1996) Dielectrophoresis : instrumentation and biological applications. *In* Scientific Instrument Association Conference. 16-18th April, Wembley, London, U.K.

Publication were also produced in additional research areas :

Journal Papers

Harrison A.B., Brown A.P., Betts W.B. & O'Neill J.G. (1995) A laboratory biofilm generator adaptable for recirculatory or flow-through operation. *Microbios* **84**, 53-62.

Conference Proceedings

Brown A.P. & Betts W.B. (1995) Survival of micro-organisms in frozen food. *In* 2nd European Congress on Food Freezing. 6-7th April, University of York, York, U.K.

Candidate.....

Supervisor.....

Date.....

Chapter 1 : The Dielectrophoretic Phenomenon

1.1 Dielectrophoresis

1.1.1 General Definition of Dielectrophoresis

Dielectrophoresis (DEP) has been defined as the translational motion of particles brought about by the application of non-uniform electric fields (Pohl, 1951, 1958, 1978; Crane & Pohl, 1968, 1972; Pohl & Crane, 1972; Pethig, 1991).

The term was used first in the early 1950's by Herbert Pohl (Pohl, 1951). Since then it has been documented considerably fewer times than the more widely established technique of electrophoresis which is currently a common practice in many biological laboratories all over the world. To date, this potentially very resourceful phenomenon has produced relatively few applications, though encouragingly, greater interest has begun to emerge steadily over recent years.

In contrast to electrophoresis, dielectrophoresis can occur with overall neutral particles and only in non-uniform electric fields (either a.c. or d.c.). The dielectrophoretic force may be thought of as a two phase force, the first being a polarising force which causes dipole formation in the particle and the second being the translational movement to specific areas produced by a non-uniform electric field (Pohl, 1973).

There are other electrical effects produced in non-uniform electrical fields though these will not be considered in any great detail here. These processes, such as electrorotation, electroporation and electrostriction have been extensively studied and discussion of these can be found in Arnold & Zimmermann (1988), Neumann *et al.* (1989) and Pohl (1973) respectively.

1.1.2 Dipole Formation

A dipole is caused when there is a finite separation of equal and opposite positive and negative charges with respect to each other (Pohl & Hawk, 1966). Generally, dipoles can be of two types, *permanent* or *induced.*

1.1.2.1 Permanent Dipoles

If the atoms of an element have more affinity for electrons than the atoms of another element, it is termed more *electronegative*. When a very electronegative atom e.g. chlorine, or oxygen is bonded to a less electronegative atom e.g. hydrogen, the more electronegative atom will draw the electron cloud involved in the chemical bond towards itself producing slight positive and negative charges within the molecule i.e. a dipole is formed. This difference in electronegativity exists in the absence of an applied electric field, so is known as a *permanent dipole*. All polar molecules have these permanent dipoles. A well known example is that of water, in which electrons are pulled towards the oxygen atom, so giving it a δ- charge, leaving a slight positive charge on each of the hydrogen atoms (figure 1.1). Randomisation of the molecular dipoles in water, however, means there is no overall polarisation of the bulk water unless an electric field is applied (Grant & Phillips, 1990).

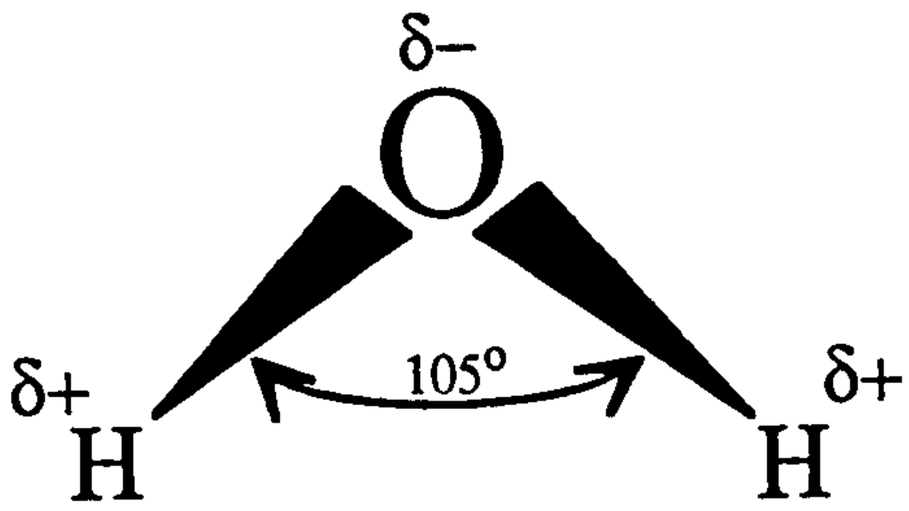

Figure 1.1 : Representation of the permanent dipole structure of a water molecule.

A measure of the size of this polarisation is given as a *dipole moment*. The magnitude of a dipole moment (μ) is equal to the product of the size of the charges (q) and the distance separating them (a) and is often given in Debye units (1 Debye = 3.33×10^{-30} C m)

An electric field applied to a permanent dipole at an angle θ to the field causes a torque to be exerted, turning the dipole into alignment with the field, with a force $qaE \sin\theta$. The Brownian motion effects shown by other molecules present in the field will minimise the extent of this organisation (Grant *et al.*, 1978). Nevertheless, permanent dipole rotation of many such molecular dipoles will often have an overall summation effect leading to better polarisability and dielectrophoretic mobility.

These permanent dipoles are present in many molecules, including biological macromolecules, and their polar nature leads to attractive, repulsive and orientational forces in response to applied electric fields.

1.1.2.2 Induced Dipole Formation

When a dielectric (an insulating material) is placed within a uniform electric field, the atoms constituting the material become polarised, and the centres of positive and negative charge (figure 1.2) become slightly shifted with respect to each other (Grant & Phillips, 1990). Everywhere except at the surfaces of the dielectric, this movement of electrons is balanced by the movement of the positive nucleus in the opposite direction. One face of the dielectric gains an overall negative charge since at this surface no positive nuclei can move to counteract the electron displacement. Equally, the positive nuclei at the opposite surface will not be balanced so that surface will acquire a net positive charge.

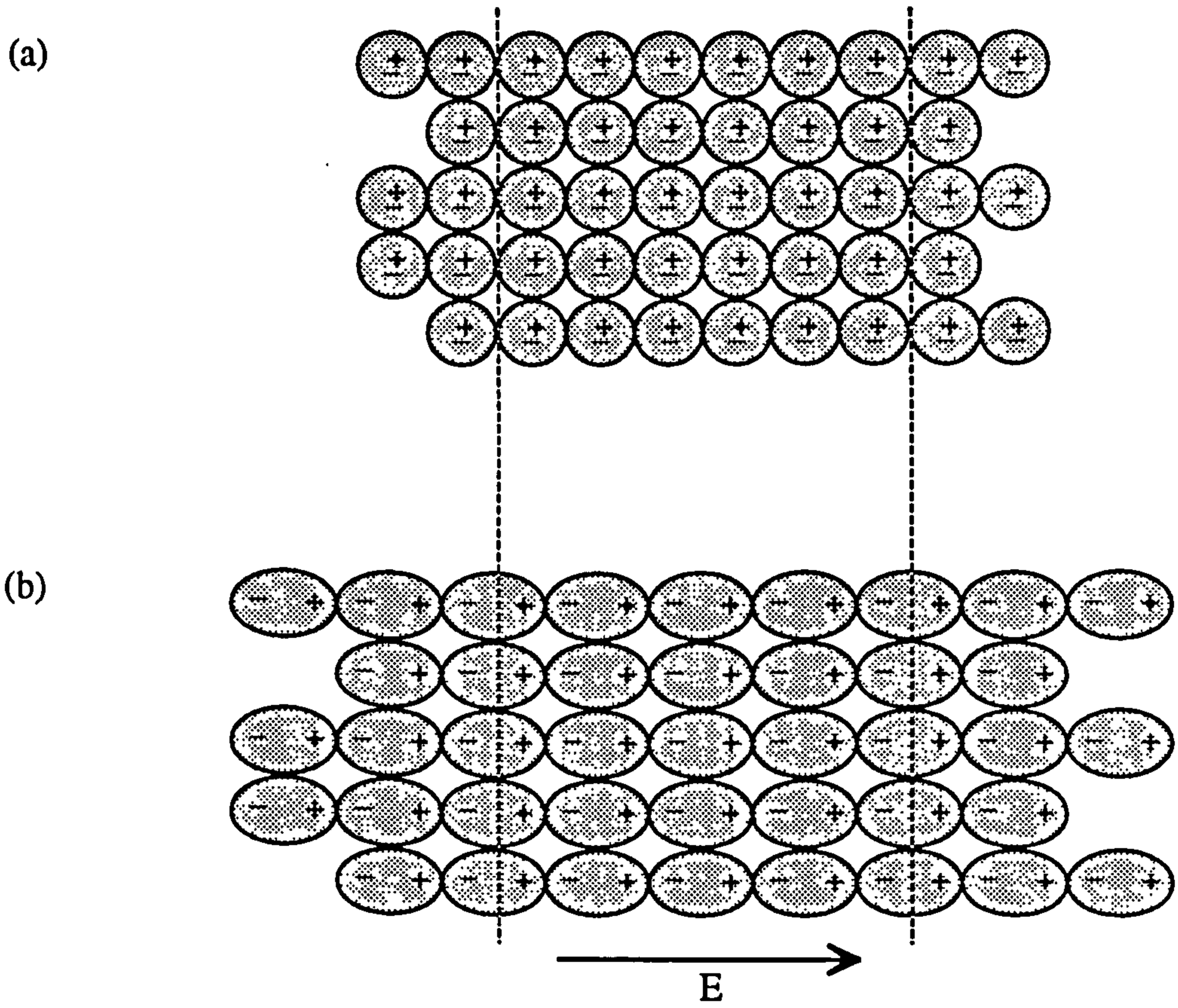

Figure 1.2 : Induced polarisation of a dielectric material. (a) In absence of an electric field, (b) In presence of an electric field, E (after Grant & Phillips, 1990).

These permanent dipoles are present in many molecules, including biological macromolecules, and their polar nature leads to attractive, repulsive and orientational forces in response to applied electric fields.

1.1.2.2 Induced Dipole Formation

When a dielectric (an insulating material) is placed within a uniform electric field, the atoms constituting the material become polarised, and the centres of positive and negative charge (figure 1.2) become slightly shifted with respect to each other (Grant & Phillips, 1990). Everywhere except at the surfaces of the dielectric, this movement of electrons is balanced by the movement of the positive nucleus in the opposite direction. One face of the dielectric gains an overall negative charge since at this surface no positive nuclei can move to counteract the electron displacement. Equally, the positive nuclei at the opposite surface will not be balanced so that surface will acquire a net positive charge.

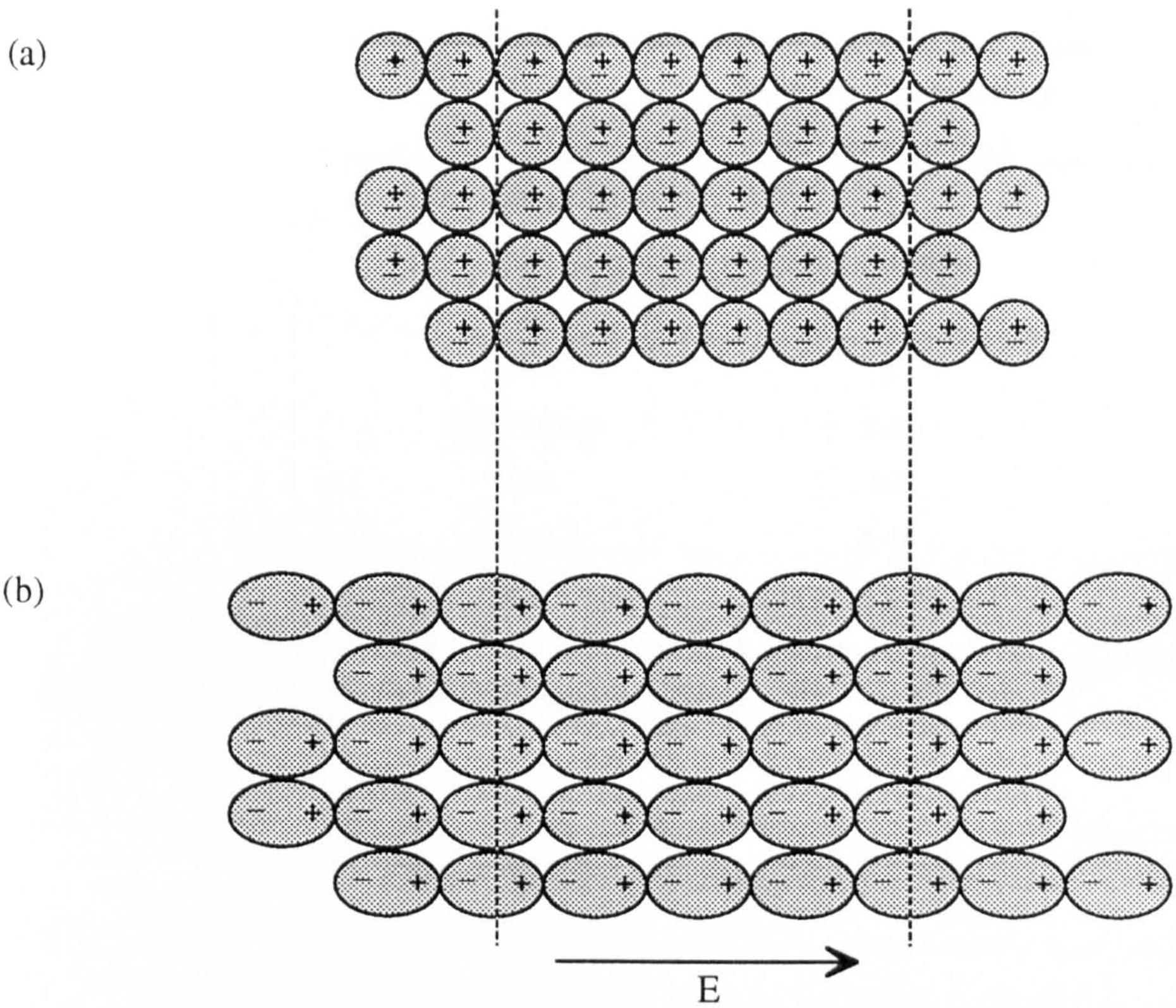

Figure 1.2 : Induced polarisation of a dielectric material. (a) In absence of an electric field, (b) In presence of an electric field, **E** (after Grant & Phillips, 1990).

Thus the overall effect of these individual atomic dipole moments is a polarisation of the dielectric, known as *electronic polarisation*, in the direction of the applied field. This is expressed as a polarisation vector, **P** (total dipole moment per unit volume) where

$$\mathbf{P} = (\varepsilon_s - 1)\varepsilon_o\mathbf{E} \qquad (1.1)$$

ε_o being the permittivity of free space and ε_s being the relative permittivity of the dielectric filling the electrode space (ε_s - 1 is also known as the constant of proportionality, or electric susceptibility, and may be replaced by χ_E).

The presence of this polarisation in the dielectric material opposes the applied electric field passing through the material and is known as a *depolarising field* (Grant & Phillips, 1990). A measure of the electric field reduction caused by the presence of the dielectric (relative to that of a vacuum) is known as the *relative permittivity* of the dielectric. Values of relative permittivity for some dielectric materials are shown in table 1.1 below.

Material	Relative Permittivity (at room temp.)
Vacuum	1
Air	≈ 1 (1.00054)
Water	78
Mica	5
Polyethylene	2.25
Paper	3.3
Glass	5-10
Most solids and liquids	between 2 and 100

(compiled from Eisberg & Lerner (1981); Cutnell & Johnson (1989); Whelan & Hodgson (1989)).

Table 1.1 : Relative permittivities of a number of materials.

Thus the electric field between parallel electrode plates in a vacuum, E_o, where :

$$E_o = \frac{q}{\varepsilon_o A} \tag{1.2}$$

becomes reduced to E_m by the presence of a dielectric material

$$E_m = \frac{q}{\varepsilon_s \varepsilon_o A} \tag{1.3}$$

where A is the area of the electrode plates and q represents the charges on the plates. In other words, the electric field is inversely proportional to the relative permittivity of a dielectric.

The dielectrophoretic force exerted on a dielectric when placed in an external electric field is caused by polarisations contributed by both any permanent dipoles in existence and the induced dipoles caused by the field (Pohl, 1978; Pethig, 1979). When considering a suspension of particles, it should be noted that these polarisations occur in both the particle and the suspending medium dielectrics. Hence, dielectrophoretic motion is dependent upon the relative polarisabilities and thus the permittivity (ε_m, ε_p) and conductivity (σ_m, σ_p) properties of the medium and particles.

1.1.3 The Nature of Dielectrophoresis

1.1.3.1 Uniform Electric Fields

When particles, either charged or electrically neutral are placed within a uniform d.c. field, established by a pair of parallel plates, they experience a force. This is the familiar action of electrophoresis, resulting in an attraction of a charged body towards the oppositely charged electrode and a stasis of a neutral particle (figure 1.3).

The equal and opposite charges within the neutral particle are induced to separate by the field and establish a dipole (Grant *et al.*, 1978). In addition to that described in section 1.1.2.2, there are other proposed ways by which this particle polarisation can occur and these will be discussed in detail later. Physical orientation of a particle in this uniform field may occur due to the alignment of these dipoles, but because the particle is within a uniform field the attractive forces will be equal on both sides, resulting in no net translational movement.

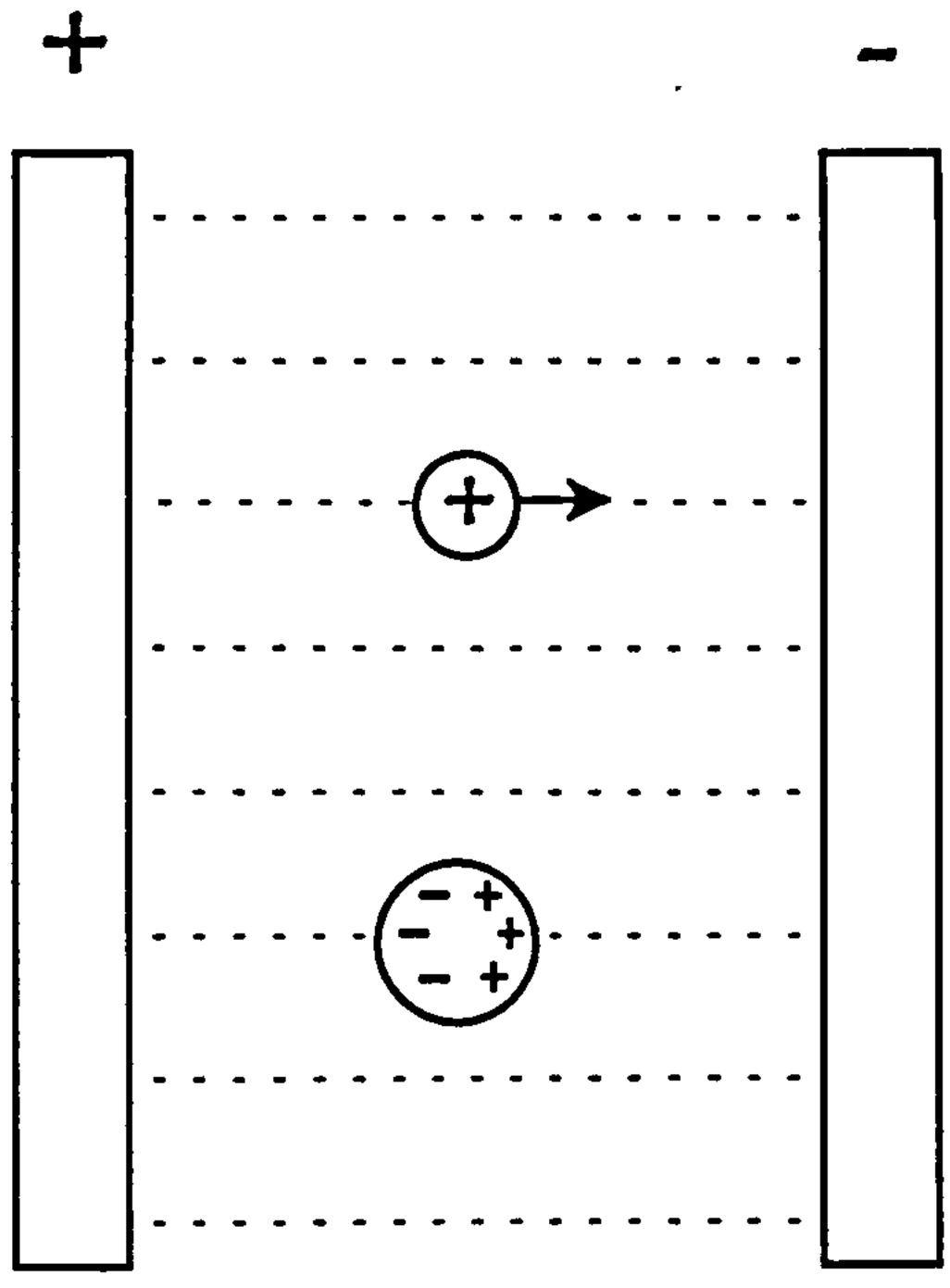

Figure 1.3 : Effect of a uniform electric field upon both charged and neutral particles.

If placed in a uniform field which is alternating (a.c.), the charged particle will maintain its movement towards the oppositely charged electrode, resulting in an oscillating motion around a central position as the field switches. In the alternating field, the dipole of the neutral particle also changes direction. However, the forces in the region of the particle are equal, meaning there is still no net movement even though there is a flipping of the dipole.

1.1.3.2 Non-uniform Electric Fields

There is negligible movement of charged particles in a.c. fields, causing little effect of electrophoretic movement on dielectrophoresis except at low frequencies where the field is switching at such a low rate that electrophoresis may be able to occur. In reality, the ideal case of a uniform field is very difficult to achieve (Pohl, 1973). The uniformity caused by a pair of parallel plates lasts for as little as a fraction of a second, after which the field becomes quite non-uniform due to microscopic deformities in the electrode surfaces.

It has been hypothesised, however, that in contrast to neutral particles, oscillating charged spherical particles also undergo slight repulsion from the high field intensity region of alternating non-uniform fields over time (Pohl, 1978).

In neutral particles the dipole formation will become asymmetric by the field non-uniformity. Individual molecular dipole moments will align differently across the particle and charge movement over the particle is altered by this field. Forces on these charges will be greater on one side of the particle due to the non-uniform alignment causing an imbalance in force upon the particle, being greater in the high field intensity region due to maximum non-uniformity. This force imbalance leads to a translational movement of the particle through the suspending medium (Pohl & Crane, 1971). This movement is known as *dielectrophoresis* (figure 1.4).

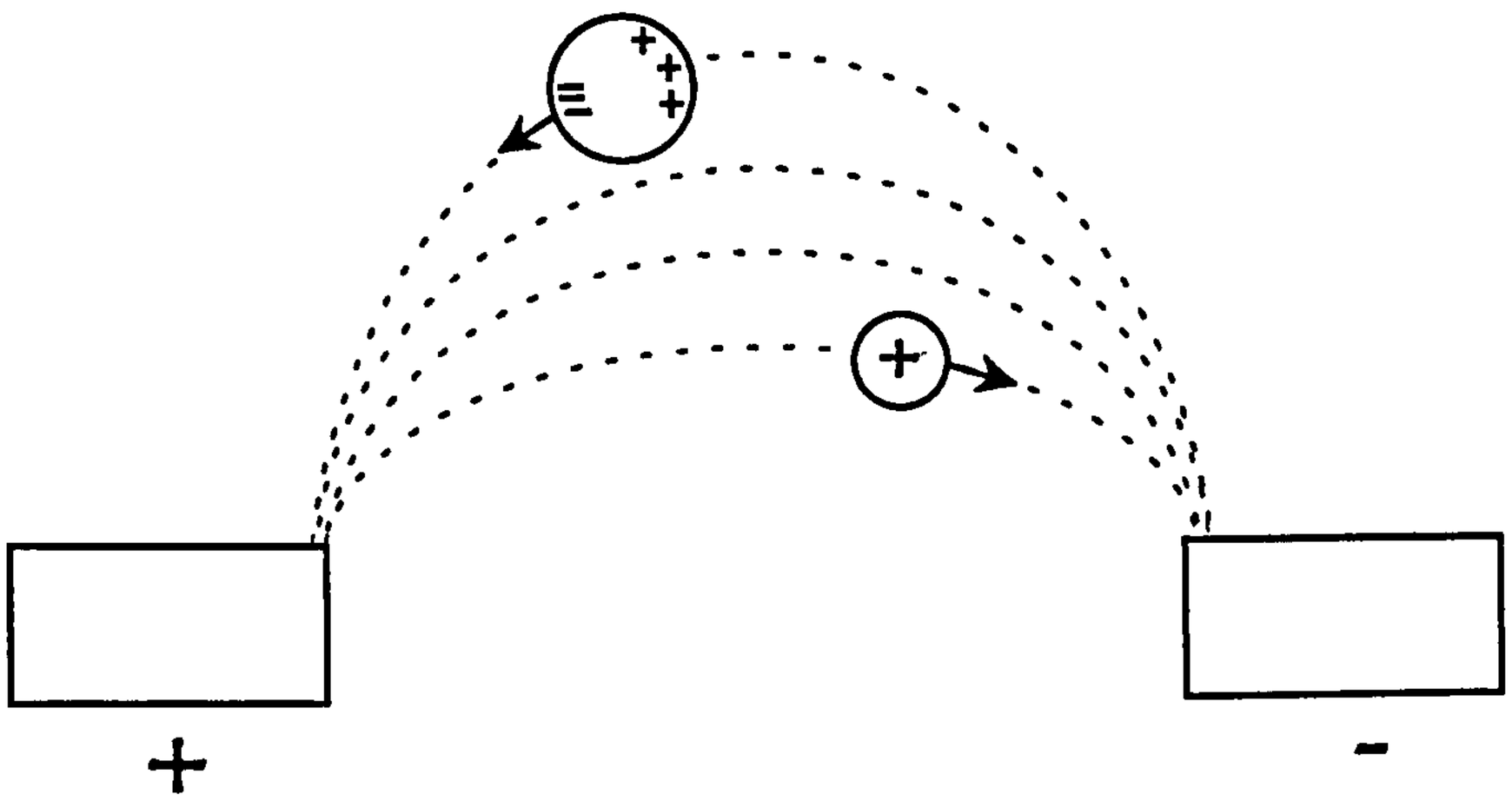

Figure 1.4 : Effect of a non-uniform electric field upon both charged and neutral particles.

The equation often used to demonstrate the dielectrophoretic force is related to the relative polarisability of the particle over that of the medium, the electric field strength and its divergence (the gradient of the electric field) :

$$\mathbf{F} = \mathbf{P}\, v\, (\mathbf{E} \cdot \nabla)\, \mathbf{E} \qquad (1.4)$$

$$= \tfrac{1}{2}\, \mathbf{P}\, v\, \nabla\, |\mathbf{E}|^2 \qquad (1.5)$$

where **P** is the relative polarisability of the particle (dipole moment per unit volume), v is the particle volume, **E** is the applied electric field vector and ∇ is the mathematical del vector operator (i.e. $\mathbf{E} \cdot \nabla$ represents the divergence, or non-uniformity of the electric field).

When the non-uniform field is made to alternate, the dipole of the neutral particle will also switch. However, even when the dipole realigns in the opposite direction, the areas of

non-uniformity will still exist in the same positions relative to the particle due to the electrode arrangement. This means that the polarised particle will still move in the same direction towards the highest field non-uniformity regions i.e. movement will be in the same direction irrespective of the polarity of the electrodes and so will occur in both a.c. and d.c. fields.

The examples described above are for the cases where the dielectric constant of the particles are greater than that of the suspending medium, leading to paraelectric behaviour called *positive dielectrophoresis*. When the opposite is true, apoelectric behaviour is exhibited, resulting in a translational movement of the particles away from the highest field strengths. This is known as *negative dielectrophoresis.*

1.1.4 Basic Theory of Dielectrophoresis

To gain a fuller understanding of the general description of dielectrophoretic motion it is helpful to discuss the underlying theory of its occurrence. It is useful to begin with the case of ideal dielectrics, those which have a "finite dielectric constant and infinite resistivity" (Pohl, 1978).

1.1.4.1 Ideal Dielectrics

When a perfectly insulating particle is suspended in a perfectly insulating liquid medium and subjected to an external electric field, the observed motion is dependent upon the relative forces exerted on each, and thus related to the individual permittivities of both particle and medium.

As shown previously, the dielectrophoretic force,

$$\mathbf{F} = \tfrac{1}{2}\mathbf{P}v\nabla|\mathbf{E}|^2 = \mathbf{P}v(\mathbf{E}.\nabla)\mathbf{E} \qquad (1.6)$$

Therefore the net force on the particle, **F** is given by (see Appendix 1) :

$$\mathbf{F} = (\tfrac{1}{2})(4\pi a^3)(\varepsilon_o K_m)\left(\frac{K_p - K_m}{K_p + 2K_m}\right)\nabla|E_e|^2 \qquad (1.7)$$

or

$$\mathbf{F} = 2\pi a^3 \varepsilon_o K_m \frac{K_p - K_m}{K_p + 2K_m} \nabla|E_e|^2 \qquad (1.8)$$

where a is the particle radius, ∇ is the del vector operator and $\mathbf{E_e}$ is the external electric field. K_m and K_p represent the relative permittivities and ε_m and ε_p are absolute permittivities of the medium and particle respectively.

The force is a vector which has a magnitude proportional to the square of the electric field magnitude. This demonstrates from theory that the dielectrophoretic force is indeed independent of the sign of the applied field and can occur in both a.c. and d.c. fields. For perfect dielectrics (i.e. perfectly insulating), when the permittivity of the particle is greater than the medium permittivity, positive dielectrophoretic collection occurs, moving the particle to the highest field strength regions, as may be observed by examination of the above equation. Should the medium permittivity exceed that of the particle, movement of the particle to low field strength regions i.e. negative dielectrophoresis, will result.

Terms in the equation relate to the difference in permittivity of the particle over that of the medium. It should be noted, however, that the dielectrophoretic force does not increase limitlessly with greater particle permittivity but will only increase up to a magnitude determined by the medium. For very large particle permittivity (K_p near infinity), the terms in the equation for the dielectrophoretic force will become proportional to K_m, the permittivity of the medium i.e. the force will be limited by the suspending medium permittivity. However, if the medium permittivity increases (with fixed particle permittivity), the term $K_m\left[\frac{K_p - K_m}{K_p + 2K_m}\right]$ will tend towards -∞, meaning that as the permittivity of the medium increases past that of the particle, the direction of the dielectrophoretic force will change and a limitless negative DEP force will be produced.

Using the DEP system of Pohl (1978), differences in permittivity of ≥ 1 between the particle and medium were normally necessary for efficient positive dielectrophoresis. In that system, the motion was caused by a very weak force and easily prevented by turbulence, heating effects or electrophoresis.

The DEP force as already described is also related to the particle volume meaning that more efficient movement is seen with larger particles. Under previously used experimental conditions, dielectrophoretic motion has been shown to occur down to particle sizes of around 0.1 μm where disturbances by Brownian motion are known to be significant (Chen, 1972); in contrast, electrophoresis is often used with atomic and molecular ions (Pohl, 1978). However, since the equation of dielectrophoretic motion is also dependent upon the field strength, even smaller particles may potentially be manipulated using higher voltages or micron sized electrode separations. Care must be taken, though, to avoid electrical breakdown or heating of the particle and medium when using high field magnitudes.

1.1.4.2 Real Dielectrics

Non-ideal dielectrics are systems made of a conduction mechanism and a polarisation mechanism and are described as "*lossy dielectrics*" (Mognaschi & Savini, 1985). Since both particle and medium are real dielectrics, they are not 'ideal' perfect insulators so also have finite conductivities, σ_p and σ_m. The effective polarisability of real dielectrics is a complex function relating both permittivity and conductivity. Both, mechanisms which affect polarisation and mechanisms which affect conduction are accounted for in the theory of dielectrophoresis of real particles (Pohl & Crane, 1972). There are many different theories presented to describe these mechanisms, some or all of which may be important in dielectrophoresis, and each with different relaxation times and frequencies.

To account for these conductivity and frequency effects, it was proposed that the permittivity terms in the above equations should be replaced by the real parts of their complex quantities (Pohl, 1978; Sher, 1968) :

i.e.
$$F = 2\pi a^3 \varepsilon_m \, \mathrm{Re}\left[\frac{\varepsilon_p^* - \varepsilon_m^*}{\varepsilon_p^* + 2\varepsilon_m^*}\right] \nabla|E|^2 \qquad (1.9)$$

where $\varepsilon_m^* = (\varepsilon_m^{'} - i\varepsilon_m^{"})$ and $\varepsilon_p^* = (\varepsilon_p^{'} - i\varepsilon_p^{"})$ for medium and particle respectively, ε' and $\varepsilon"$ representing the real and imaginary parts of the complex functions and where $\varepsilon"$ (the dielectric loss term) is related to conductivity and frequency by the relationships, $\varepsilon_m^{"} = \sigma_m/\omega$ and $\varepsilon_p^{"} = \sigma_p/\omega$ where ω is the angular frequency.

Since polarisation is a relationship between permittivity and conductivity, for more conducting particles and medium, the permittivity terms of equation (1.9) may be equally replaced by complex conductivity terms :

i.e.
$$F = 2\pi a^3 \sigma_m \, \mathrm{Re}\left[\frac{\sigma_p^* - \sigma_m^*}{\sigma_p^* + 2\sigma_m^*}\right] \nabla|E|^2 \qquad (1.10)$$

where the complex conductivities $\sigma^* = \sigma + j\omega\varepsilon$ for particle and medium.

At higher frequencies, the equation is dominated by the permittivity terms, with the conductivity equation being applicable to low frequency events. Therefore at these low

frequencies, the dielectrophoretic force can also be determined by the excess in conductivity of the particle over that of the medium. Medium conductivities can be made to dictate the direction of the dielectrophoretic force by being greater or lesser than that of the particle. Indeed, the particle conductivity can be found by altering the medium conductivity until there is no dielectrophoretic motion at these low frequencies as demonstrated by Markx *et al.* (1994).

1.1.5 Mutual Dielectrophoresis

When dielectrophoretic collection occurs at the electrodes, often the particles do not simply cover the whole of the electrode surface. Collection typically occurs in chains, where particles are preferentially attracted to the vicinity of another cell, *mutual dielectrophoresis*. This chain formation, which was originally seen with yeast cells led to the term *"pearl chains"*.

Pearl chain formation is caused because the polarisation of one particle results in a local distortion of the electric field around that particle, creating a region of high field non-uniformity. The theory of dielectrophoresis means that particles collect at areas of high non-uniformity. Therefore a second particle can become attracted to these secondary non-uniform field effects around the first particle and so form a chain of particles. These chains will ultimately be collected on the electrode surface due to the higher non-uniformity.

Collection of cells is increased by the formation of pearl chains due to field induced cell-cell interactions which make the effective volume of the cell aggregation bigger, increasing the dielectrophoretic force as seen from equation 1.6. This could become very significant when using high cellular concentrations due to large amounts of pearl chain formation.

1.1.6 Dielectric Relaxation

Polarisation is a competition between the aligning force caused by the field and the randomising force of Brownian motion. When the external field is removed, only the randomising force remains, causing the polarisation to decay.

The dipole formation for a spherical particle in an insulating medium is established with the characteristic relaxation time constant, τ, described above. It follows therefore that there is also a frequency dependence for this polarisation. The frequency at which relaxation can no longer occur efficiently is known as the *relaxation frequency*.

At low frequencies, the polarisation proceeds quite easily. Since the induced polarisation of the particle is brought about by charge separation and alignment, there is a finite time taken following alternation of the field where the charges need to become random and realign in the

opposite direction. This randomisation is known as *dielectric relaxation* (Grant *et al.*, 1978). As the frequency of the applied field increases, the switching of the polarisation and reorientation of molecular dipoles becomes progressively unable to follow the increasingly rapid reversal of the field. Energy begins to be absorbed by the system, since the field begins to oppose the movement of charge as the relaxation frequency is approached and a dielectric loss (ε") is observed.

1.1.7 Dielectric Dispersions in Cells

Cells have a very complex nature and consist of many different parts, each having a different chemical composition and size. The length of time for repolarisation to occur following switching of the field is dependent upon the characteristic components of the cell or molecular structure. Grant *et al.* (1978) quoted values of greater than 10^{-8} s for large protein molecules to relax after the field is removed. Even very small molecules demonstrated relaxation times of up to 10^{-11} s. In addition, the time for relaxation to occur is also intrinsically related to the mechanism by which polarisation has occurred.

Pohl & Crane (1972) proposed that since a cell is made up of many polarisation mechanisms each with their own characteristic relaxation frequency, over a frequency range the particle is seen to have a *dielectric dispersion* curve. This is manifest as successive decreases in relative permittivity caused by dielectric loss, as each respective mechanism reaches its relaxation point and the polarisation systems are successively removed.

Typical dielectric dispersions are shown in figure 1.5 for a dielectric material (e.g. a particle or cell) and a salt water medium. Permittivity is thus influenced by frequency and experiences a decrease with increasing applied field frequencies.

It was noted that when the dielectric dispersions of particle and medium are overlayed, it can be seen that there are frequency regions where the magnitude of the particle dielectric constant exceeds that of the medium (figure 1.6)(Pohl & Crane, 1972). Where the difference between the two permittivities are calculated and plotted against frequency, a typical dielectrophoretic frequency spectrum results. It was stated that a typical spectrum of dielectrophoretic collection, or yield, may simply be a composite of the two dispersions which relax and decrease as frequency is increased as implied by the above equations.

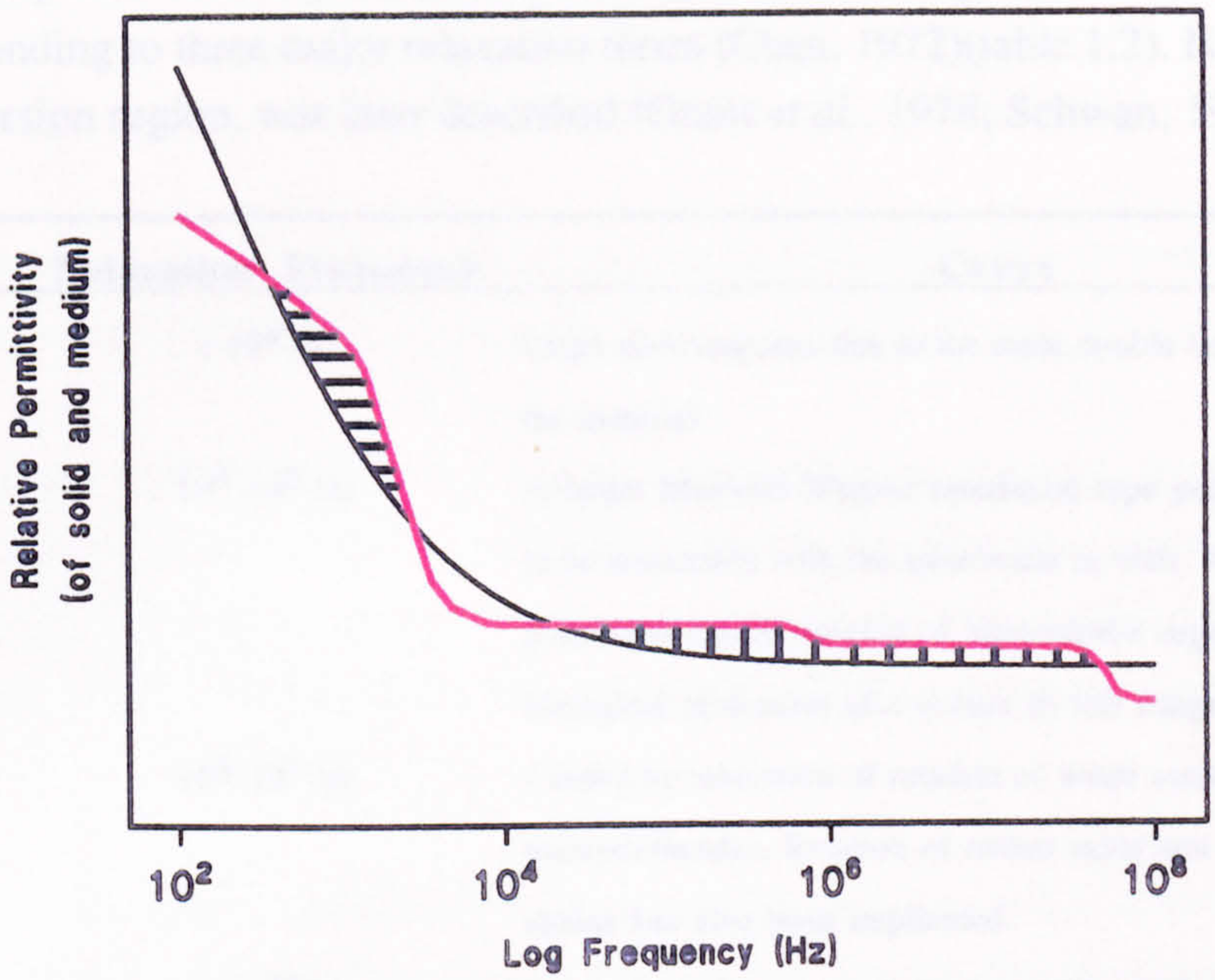

Figure 1.5 : Dielectric dispersion of both a solid material and salt water medium. (—) dispersion of medium, (—) dispersion of particle (after Pohl & Crane, 1972).

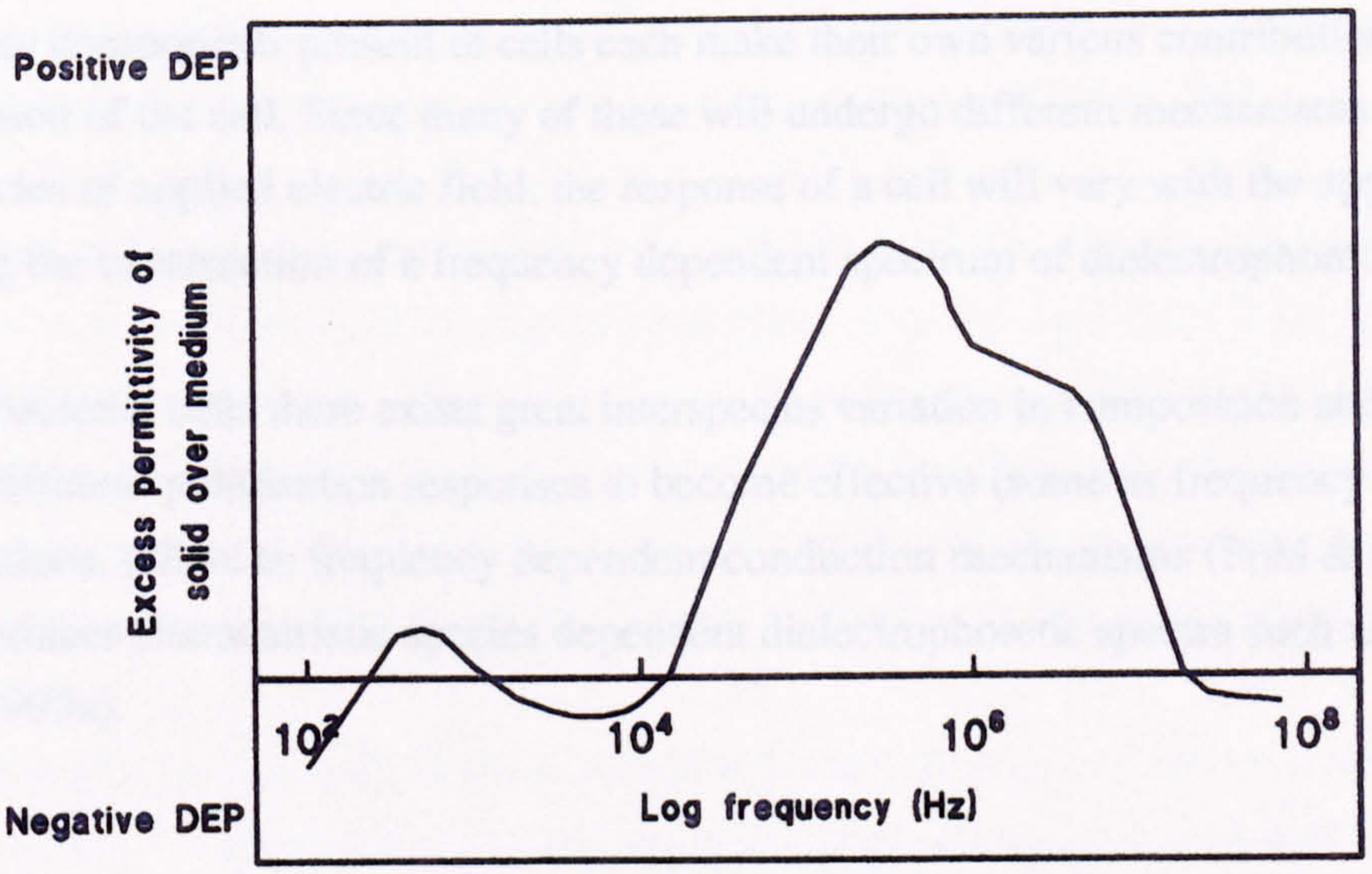

Figure 1.6 : Excess permittivity of a solid particle over that of the medium at a range of frequencies (after Pohl & Crane, 1972).

The frequency spectra of biological cells was thought to contain up to three dielectrophoretic areas corresponding to three major relaxation times (Chen, 1972)(table 1.2). However a fourth minor δ-dispersion region, was later described (Grant *et al.*, 1978; Schwan, 1981).

Dispersion	Relaxation Frequency	Cause
α-dispersion	1-10^4 Hz	Large slow response due to the ionic double layer surrounding the material
β-dispersion	10^4-10^8 Hz	A larger Maxwell-Wagner interfacial type polarisation thought to be associated with the membrane in cells. Relaxation of permanent dipole rotation of intracellular organelles and other biological molecules also occurs in this range.
δ-dispersion	10^8-10^9 Hz	Caused by relaxation of rotation of water associated with macromolecules. Rotation of amino acids and protein side chains has also been implicated.
γ-dispersion	2 x 10^9 Hz	Relaxation of permanent dipole rotation of bulk water molecules.

Table 1.2 : Characteristics of dispersion regions typically found in biological cells.

It is likely that each of these bulk relaxations present in a spectrum is made up of a much larger number of relaxation times, brought about by individual components present within the cells.

The many components present in cells each make their own various contributions to the overall polarisation of the cell. Since many of these will undergo different mechanisms at different frequencies of applied electric field, the response of a cell will vary with the applied frequency, allowing the construction of a frequency dependent spectrum of dielectrophoretic collection.

Within bacterial cells there exists great interspecies variation in composition and logically this causes different polarisation responses to become effective (some as frequency dependent polarisations, others as frequency dependent conduction mechanisms (Pohl & Crane, 1972)). This produces characteristic species dependent dielectrophoretic spectra such as those shown in Betts (1995a).

1.2 Ionic Double Layers

1.2.1 Ion Atmosphere

Aqueous suspensions of particles or cells acquire an *ionic double layer* formed from ionic species present within their local environment.

When two different materials are present together, their differing electrical properties (conductivity and permittivity) lead to variations in the charge upon the materials. The material of higher permittivity generally gains a positive charge with the other material becoming negative (Coehn, 1898). This results in formation of a potential difference between the interfaces.

Ionisation of surface groups (especially on bacterial cell surfaces) and adsorption of various charged molecules also occurs. Therefore, it may be seen that the charge of the particles vary according to the pH and temperature of the surrounding medium. The conducting cytoplasm of cells is normally surrounded by insulating layers such as membranes and are seen to have a net negative surface charge when in aqueous suspension. Bacterial cells such as *Micrococcus lysodeikticus* have been measured to have a surface charge of -1.5 $\mu C.cm^{-2}$ (Price & Pethig, 1986). Positive counterions such as metal cations and protons become rigidly bound to these oppositely charged ions. This rigid layer is possible due to the overcoming of thermal randomisation by strong attractive forces causing positively charged counterions to line up opposite the negative charges on the cell surface. A build up of charges at the surface of the particle results in the formation of an electrostatic potential (Pethig, 1979).

Several models have been proposed in past years to describe ionic double layers. The now accepted theory of Stern (1924) entails a combination of the rigid layer theory of Von Helmholtz (1879) and the diffuse layer ideas of Gouy (1910) and Chapman (1913), consisting of a distinct rigid layer of adsorbed counterions at the interface and a diffuse counterion layer further away (figure 1.7). The initial theory of Von Helmholtz is shown by the line (a) in figure 1.8, where there is a linear change in potential as distance is increased from the surface.

At the particle surface, anions are adsorbed and water dipoles become oriented (Pohl, 1978). Counterions to this negatively charged surface of potential ψ_o, align opposite and are held in a fixed rigid 'Stern layer'. This layer acts as a basic parallel plate capacitor and extends for around 0.5 nm over which there is a linear fall in potential as predicted by the Von Helmholtz theory. Close to the fixed counterion layer, thermal randomisation is very small leading to little movement and cations being held close to the surface, attracted by the negative charge density.

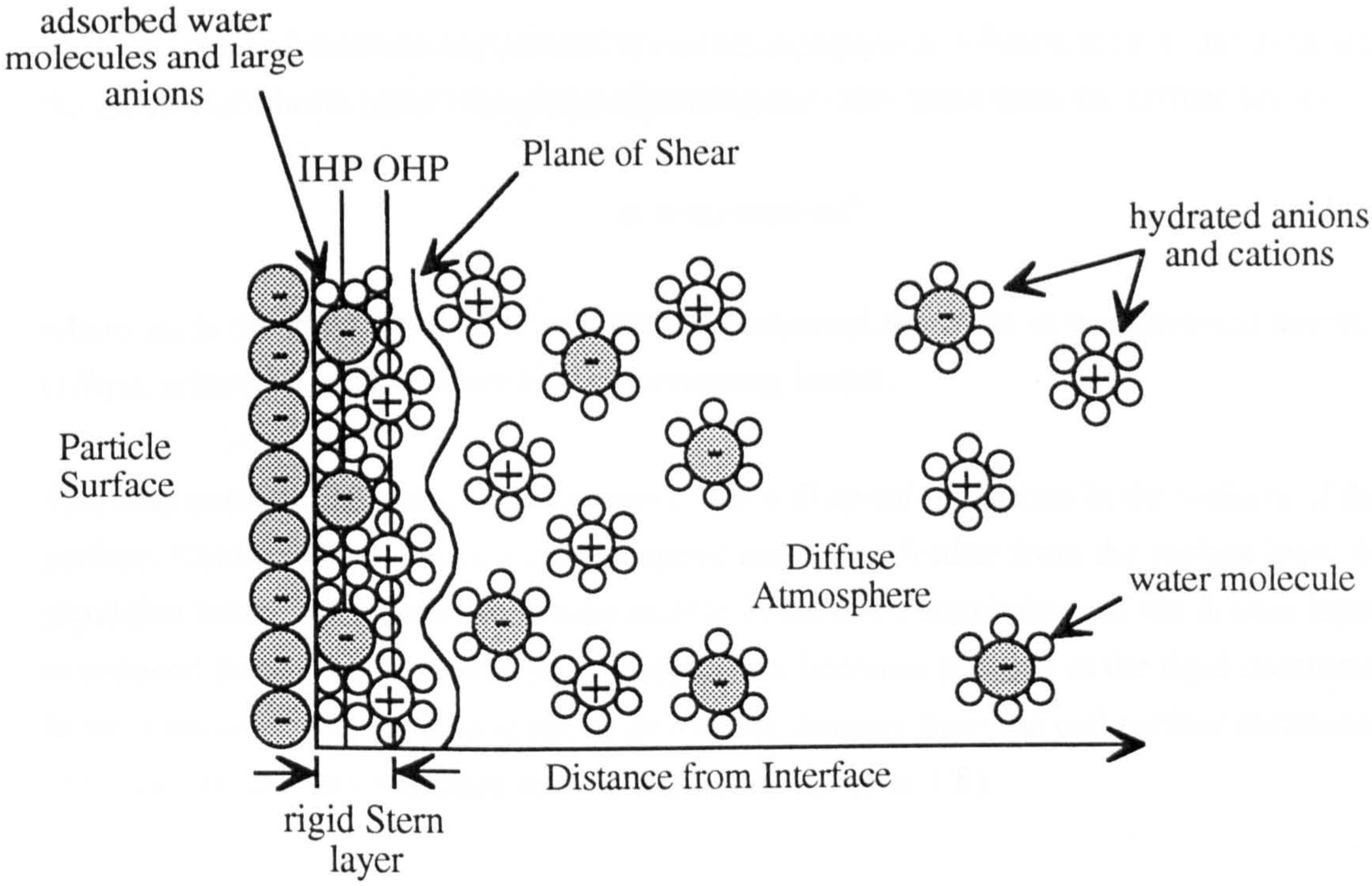

Figure 1.7 : The Stern model of electrical double layers (after Bone & Zabar, 1992).

The Stern model was improved and both an *inner Helmholtz plane* (IHP) and an *outer Helmholtz plane* (OHP) were identified (Grahame, 1947). The IHP represents the centre of negative ions which become dehydrated on adsorption to the surface, the OHP being the closest distance of approach of the positively charged solvated counterions which are attracted to the negative surface charge. The charge in Stern layer may be of opposite sign and greater than at the surface and this leads to reversal of sign as seen in line (c) of figure 1.8.

Further from the particle surface, a second layer was proposed. Gouy (1910) considered that the thermal forces overcome the electrostatic forces further away leading to a 'diffuse atmosphere' of charge to form, the density of counterions being a maximum at the interface and falling off exponentially into the liquid. From this structure of co- and counter-ions arises a potential difference which decreases with distance, such that it tends towards zero at distances far from the surface (line b, figure 1.8).

This exponential decrease in potential ψ can be expressed as a function of d, the distance from the Outer Helmholtz plane (the plane separating the Stern layer from the diffuse layer) :

$$\psi = \psi_d \exp(-\kappa d) \qquad (1.11)$$

where ψ_d is the potential at OHP and κ is the reciprocal thickness of the electrical double layer ($1/\lambda_D$), where λ_D is the Debye-Hückel screening length.

The time averaged scenario is that positive ions will spend more time in the vicinity of the surface. Conversely, negative ions will spend more time further from the surface layer due to repulsive forces. These ions are freely mobile in the outer atmosphere of the double layers due to reduced forces. The potential at the cell surface becomes positive as the rigid counterion layer is encountered and then tends to zero as the distance from the cell surface increases and the ionic atmosphere becomes more diffuse (line c, figure 1.8).

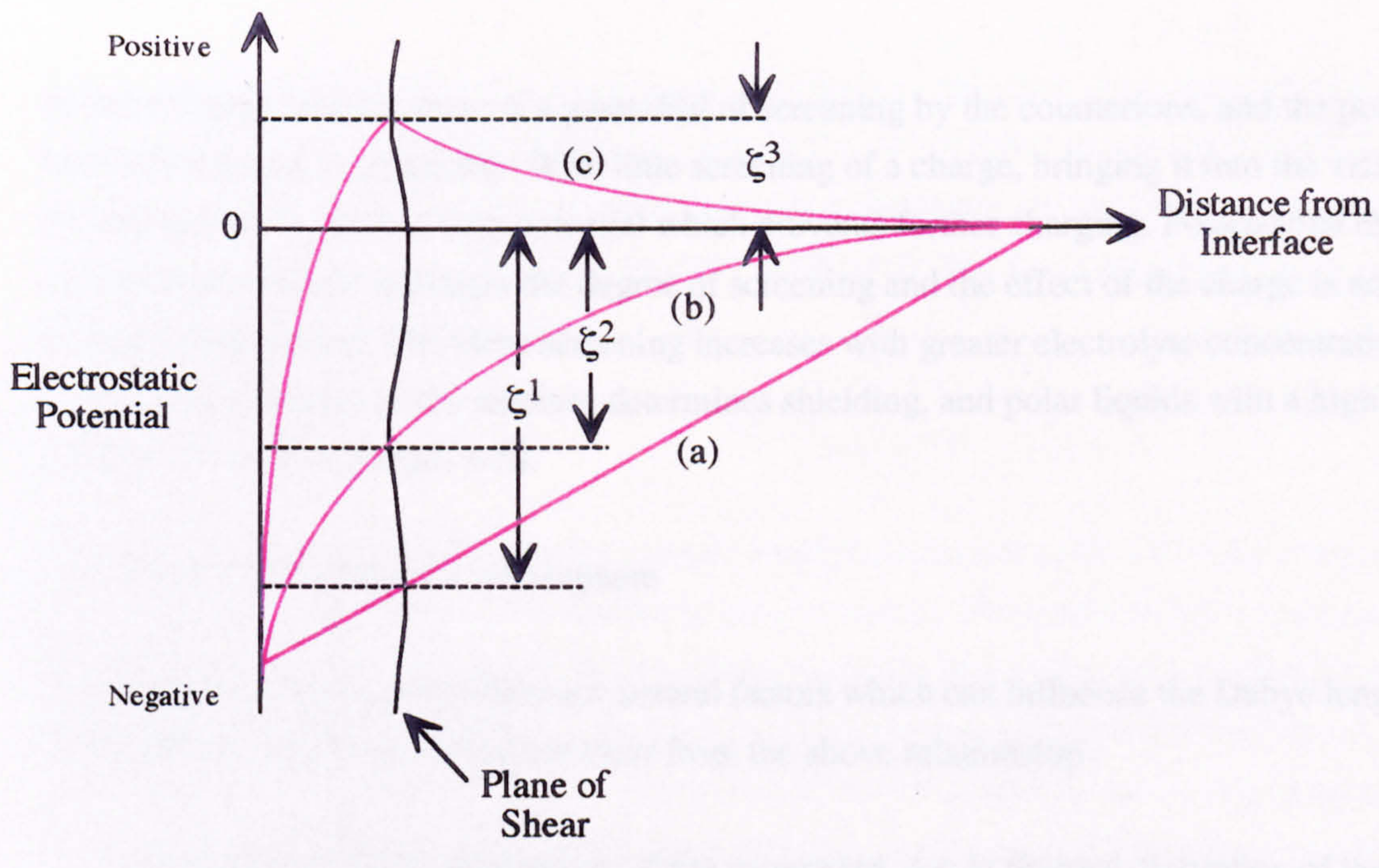

Figure 1.8 : Changes in electrostatic potential at distances from a particle surface (after Chen, 1972).

The congregation of counterions at the interface results in a shielding of the field produced by the surface ions leading to a further dampening of the potential difference.

The extent of screening and speed of potential decrease is determined by the Debye-Hückel screening length (λ_D). This value can be thought of as the distance at which the potential becomes reduced by 63.2 % of its value at the particle surface (Pethig, 1979) and is given by :

$$\lambda_D = \left(\frac{\varepsilon_o \varepsilon_s kT}{2z^2 q^2 n_o} \right)^{1/2} \qquad (1.12)$$

where ε_s is the medium permittivity, z is the ion valency and n_o is the volume density of ions in the medium (Pethig, 1979).

In aqueous solution at 298K, κ is related to the ionic strength of the medium (I, mol.dm^{-3}) as :

$$\kappa = 3.291 \times 10^9 \, I^{1/2} \qquad (1.13)$$

For *M. lysodeikticus*, λ_D has a value of 3.1 nm for 10 mM NaCl and 0.76 nm for 160 mM NaCl.

At short Debye lengths, there is a great deal of screening by the counterions, and the potential becomes reduced very quickly. With little screening of a charge, bringing it into the vicinity of the cell surface leads to a high potential which prevents further charging. Polarisation of the surrounding medium increases the degree of screening and the effect of the charge is not so strongly experienced. Therefore screening increases with greater electrolyte concentration. The relative polarisability of the medium determines shielding, and polar liquids with a high permittivity screen charges well.

1.2.2 Factors Affecting Ion Atmosphere

According to Atkins (1978) there are several factors which can influence the Debye lengths surrounding particles and these are clear from the above relationship :

- λ_D increases with the temperature of the suspension due to thermal disruption of the ionic shielding atmosphere

- Greater suspending medium permittivities decrease the field strength caused by the particle surface charge. This reduces the attraction for counterions and results in larger Debye lengths.

- Decrease in Debye length is observed with increasing concentrations of ions in the atmosphere surrounding the particles due to greater shielding effects, and vice versa. Müller (1933) stated that low electrolyte concentrations (below 0.1 M) resulted in double layer thicknesses of significantly greater than an atomic diameter. In addition, the zeta potential will also become decreased.

- The valency of the counterions is also known to influence the counterion layer, more rapid decreases in double layer thicknesses being observed with ions of higher valency.

At large distances from the particle the attraction of the negatively charged surface for its counterions is very weak and the amount of positive and negative ions after this point in the atmosphere is essentially equal (Müller, 1933). Here, there is no preference for a particular charge polarity, effectively attaining a neutral environment around the particle. Therefore the negative charges of bacterial cells become neutralised overall by the diffuse ionic cloud allowing dielectrophoresis to occur. Thus, even charged particles are often amenable to dielectrophoretic effects.

The potential difference due to these ion layers is likely to influence the movement of charges across the interface of the particles and so govern the rate of many cellular processes. In addition, certain mechanisms involved in dielectric polarisation are regulated by the movement of charges around the particle surface through these layers and are especially active at low frequencies of applied electric field.

1.2.3 Zeta Potential

Of notable importance to the electrical properties of particles and cells is the *zeta potential*, ζ. There is often some degree of movement of the atmosphere surrounding the charged particle surface, though part of the double layer remains rigidly bound to the surface. This is caused by orientation of water molecules near the surface which prevent tangential flow of liquid. Further away, the diffuse counterion cloud is able to move from the particle and its bound layer. This occurs at the *plane of shear* and the potential measured at this point is known as the zeta potential (as demonstrated in figure 1.8), a characteristic which has been implicated in dielectrophoretic responses to applied electric fields.

1.3 Polarisation Mechanisms

The polarisations found in biological material have been studied in detail and several basic mechanisms have been described (Pohl & Crane, 1972; Pohl, 1973; Pohl, 1978)(table 1.3). Any or all of these may be effective in the polarisation of cellular material, depending on local parameters such as frequency and conductivity.

Polarisation Mechanism	Comment
Electronic Polarisation	Most common type of polarisation. External field induces dipole moment by disturbing electron cloud surrounding the nucleus, shifting centres of positive and negative charge by around 10^{-18} m and polarising the material.
Atomic Polarisation	Especially noticeable in ionic solids where oppositely charged ions are displaced relative to each other by applied field.
Orientational Polarisation	Molecules having permanent dipoles respond by orientating themselves in the field to minimise their potential energy. Flexible macromolecules with permanent dipoles may become physically rotated by the field. This response can be very significant. High dielectric constant of water mainly contributed by orientational polarisation.
Nomadic Polarisation	Long polymers often have fixed charges with associated counterions. Applied electric field causes shift in counterions, moving them along the molecules - often termed 'charge hopping'. For efficient polarisation, should be many counterions present and sufficient sites to move to. Predominant in homogeneous materials, but does become limited at higher frequencies due to time necessary for such large ion movements.
Interfacial Polarisation (Maxwell-Wagner Polarisation)	Many real materials are inhomogeneous with layers having different dielectric characteristics, conductivity and permittivity. Differences cause charge distributions across interfaces since charges move easier through one layer compared to the next. This obstruction of movement is manifest as a polarisation. Build up of charge at interfaces can take a long time, yet often occurs with cellular material and is largely responsible for very high observed dielectric constants (often up to 10^4), due to compartmentalisation and layered structure.

Table 1.3 : Basic mechanisms of dielectric polarisation.

These last three mechanisms have been studied in detail with respect to cellular material and particularly bacterial cell structure. To explain the movement and responses of bacterial cells to applied alternating fields, it is necessary to look in more detail at these mechanisms and their frequency characteristics. Pictorial representations of the mechanisms of polarisation are shown in figure 1.9.

1.3.1 Electronic/Atomic Polarisation

As previously discussed, the dielectric dispersion of a material is due to the successive inability of certain polarisation mechanisms to keep up with increasing field frequencies. Generally, atomic and electronic polarisations correspond to optical frequencies meaning that relaxation does not occur below 10 GHz. These mechanisms are therefore outside the frequency range normally used to examine cell or particle suspensions by dielectric or dielectrophoretic techniques.

1.3.2 Permanent Dipole Rotation

One of the earliest modelled polarisation mechanisms was that of *permanent dipole rotation*, first proposed by Debye for protein suspensions.

The relaxation time of dipolar orientation is intrinsically related to the size of the molecule and the viscosity of the suspending medium. As an electric field is applied to the suspension, particularly of proteins, the dipoles present on the molecules, namely ionised forms of amino acid residues become orientated in the field opposed by the medium viscosity.

The relaxation time, τ, proposed for this mechanism is :

$$\tau = \frac{4\pi\eta a^3}{kT} \qquad (1.14)$$

where a is the effective radius of the rotating particles, assumed to be spherical, η is viscosity, and k is the Boltzmann constant.

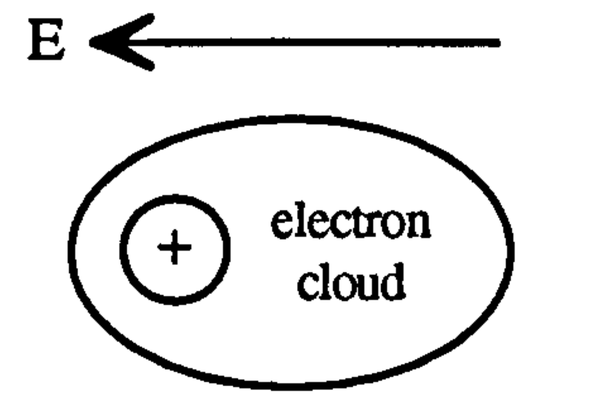

Electronic Polarisation

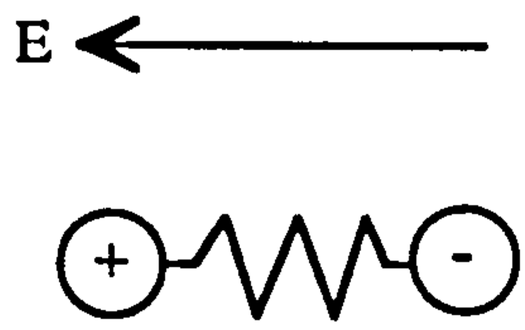

Ionic Polarisation

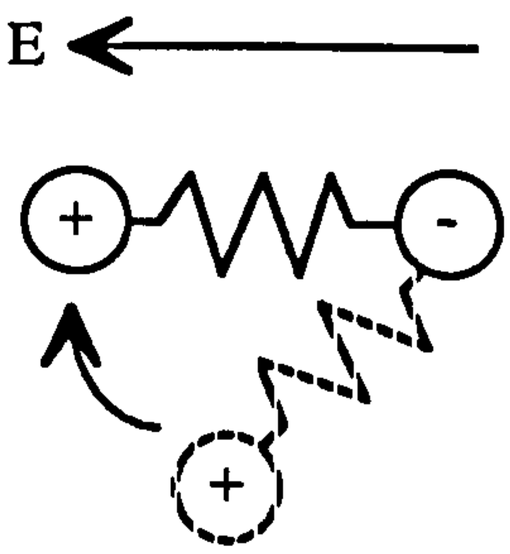

Dipole Rotation

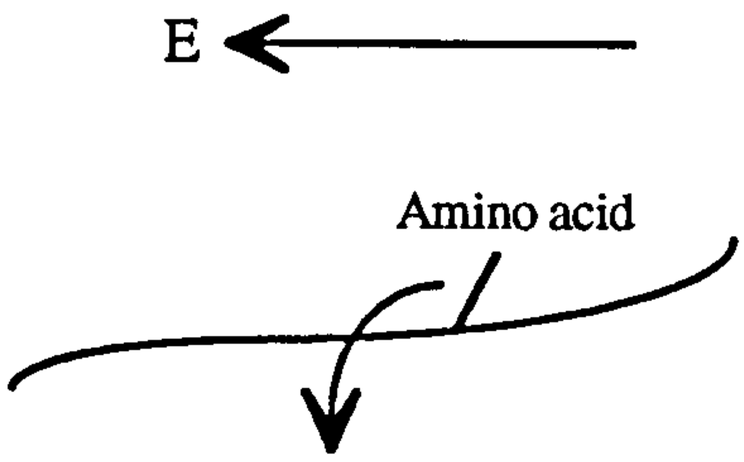

Structural Dipole Rotation

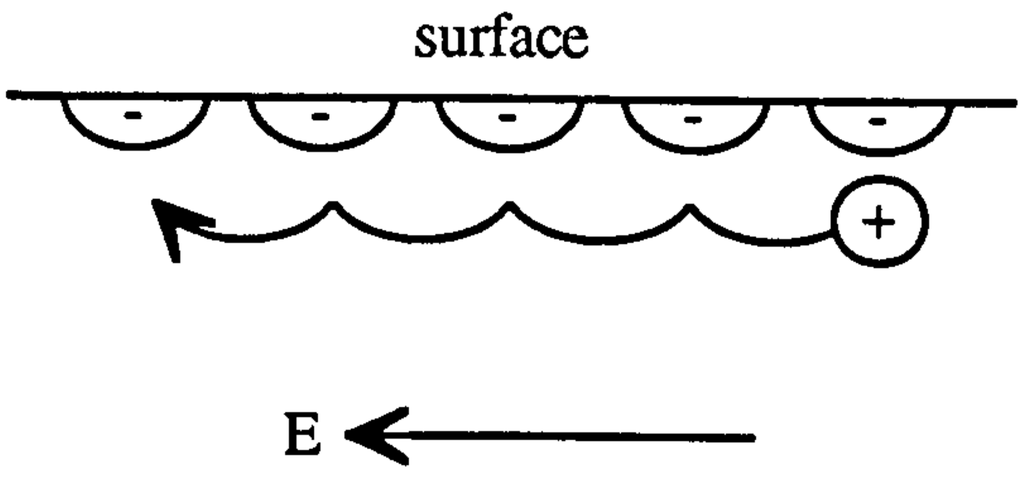

Nomadic Polarisation
(charge hopping)

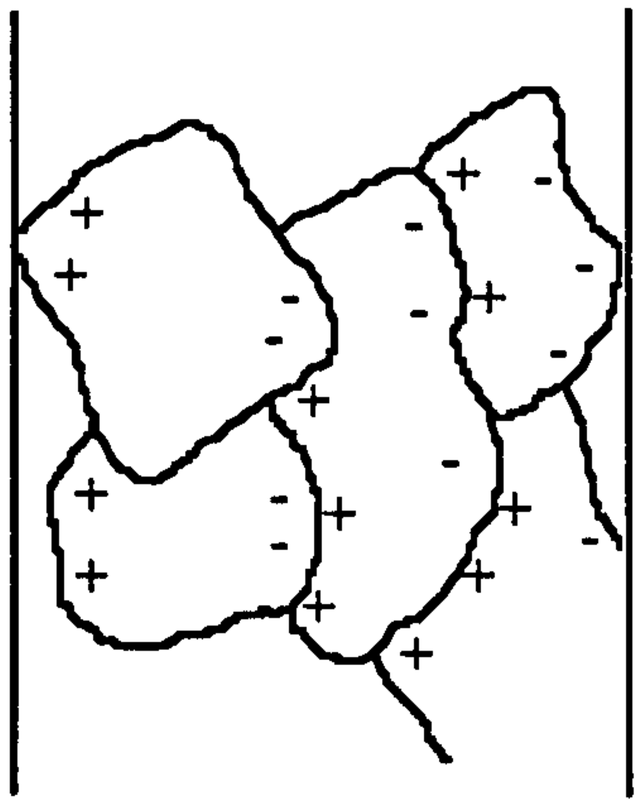

Interfacial Polarisation

Figure 1.9 : Pictorial representation of the basic mechanisms of dielectric polarisation (after Harrop, 1972).

As the size of the molecule, or its constituents parts becomes greater, the relaxation time increases, decreasing the frequency of dispersion. This mechanism has a wide frequency range and can have its relaxation between 0.1 Hz and 10^{12} Hz, compared with up to 10^{14} Hz for electronic and atomic polarisations. For protein molecules the critical frequency is ≈ 1 MHz. Since the function is proportional to the third power of the radius, a small change in size will be expected to have a profound influence on relaxation time. As described above, water molecules are also polarised by this mechanism and have relaxation frequencies as high as 20 GHz.

From the equation, viscosity of the medium is also an important determinant for this mechanism relaxation, being slower in media of high viscosity. Polarisations by this method do not simply relate to conductivity and permittivity characteristics but also the physical characteristics of the medium including viscosity and temperature.

For macromolecular structures there may be a range of dispersions associated with rotation of individual molecular parts, side chains and also that of whole macromolecular orientations. This results in a flattened dielectric loss curve, rather than that corresponding to a single relaxation.

One might expect that a protein which contains a high degree of polar amino acids will exhibit significant polarisations upon application of an external field. However, this is not always the case. When more than one permanent dipole is present within a molecule, the overall dipole is created by vectorial addition of the individual component dipoles, where opposing dipoles cancel each other out. Therefore polarisation of protein components will depend on primary, secondary and tertiary structures.

Amino acids all have their own dipole moment properties which determine the overall nature of the protein molecule due to their zwitterionic form. Since dipole moments are related to the separation of charge, greater dipoles are found with amino acids having larger distances between the ionised carboxyl and amine groups (Pethig, 1979). In addition, many amino acids have polar side chain molecules which may add to the amino acid dipole and may become physically rotated at appropriate field frequencies. However rotation may be restricted by stearic hindrances. Bulky side chain groups may result in a lower relaxation frequency caused by a slower orientation due to these interactions. Presence of these side chains on amino acids and the overall amino acid composition dictates the polarisability of proteins. It may be implied that membranes and cellular components containing substantial amounts of more polar amino acids such as Tyr, Trp, Arg, His and Phe, may (though conformational effects must be remembered) confer a greater degree of polarisability to the cells, at least over specific frequency ranges.

It might be expected that even slight changes in amino acid composition may have significant effects on protein folding. Protein size and polarisability differences will result, influencing relaxation time and modifying the dielectric dispersion. Changes in bacterial membrane protein composition, for instance, caused by changes in growth conditions, are likely to have considerable repercussions on the dielectrophoretic frequency polarisations of the whole cell.

1.3.3 Proton Fluctuation

The nature of protein molecules gives rise to another polarisation mechanism, that of *proton fluctuation*. The pH of the surrounding environment regulates the ionic nature of proteins, acidic pH causing a shift to the protonated state of the amino acids giving the proteins a more positively charged form (Kirkwood & Shumaker, 1952). Near the isoelectric point (pI) of the amino acid, protons can easily dissociate and associate with the molecule by only slight changes in pH and so can transmit charge quite easily. Amino acids near their pI have both positively and negatively charged groups, both of which can contribute to the dipole moment. Therefore it may be expected that there is a high polarisation response at medium pH near the pI of the protein. Bacterial cells containing a high proportion of amino acids with their pI near that of the suspending medium, would be likely to have a substantial proportion of them in an ionised form with high dipole moments, enabling greater polarisation than cells with amino acids with pI far removed from the medium pH.

Protons are highly mobile ions and in media where they can become easily dissociated they may have a very active role in charge movement polarisation mechanisms. Their mobility allows them to bring about polarisation at even higher frequencies than other ionic species. Many amino acid side chains are acidic or basic and can lose or gain protons, occurring alongside proton movement from ionisation of amino and carboxyl groups. In all but very acid solutions, the number of basic binding sites greatly outweighs the number of acidic sites allowing a wide range of proton movements.

In contrast to the counterions, protons chemically bind to specific sites and must first dissociate before moving to another binding site. Pethig (1979) described the probability of having a bound proton as $(1 + 10^{pH - pKa})^{-1}$, implying that at lower pH values the likelihood of having a bound proton is much greater. Therefore, the relaxation and dielectric dispersion of proton fluctuation is governed by the pH of the suspending medium.

The relaxation of this polarisation is related to the time at which protons are bound at each successive site, longer bound time on a molecule leading to greater relaxation times and

slower repolarisation i.e.

$$\tau = \frac{1}{k_D} \qquad (1.15)$$

k_D being the dissociation constant.

Pethig (1979) quoted values of around 10^{-3} s for relaxation times at pH 7 by this mechanism, relaxation in the MHz range only being able to occur at very low pH values.

Where several amino acids of the same types are present near to each other, their isoelectric points may assist in proton conduction. Where the medium pH is near to this pI, protons will be able to dissociate and associate easily thus minimising the time of binding and facilitating their passage along similar amino acid groups, so causing more rapid relaxation.

Therefore, proteins containing greater amounts of amino acids such as alanine (ala), glycine (gly) or histidine (his) (which have pI around 7) at physiological pH may exhibit higher dipole moments. However, it must be remembered that side chains of amino acids are often not in an ionised form at physiological pH. For example, arginine (arg) has a side chain pI of 12.48, aspartic acid (asp) has a side chain pI of 3.86, so do not contribute much to proton fluctuation.

This proton fluctuation mechanism lends towards polarisation by another mechanism, that of surface conductance. In this process, ions are able to move over the surface from one charged group to another. Despite this, amino acids and side chains can be polar without being ionised, due to the presence of C=O or C-NO_2 groups contributing to polarisation by dipole rotation mechanisms. The movement of protons over membrane surfaces along the head groups of phospholipid molecules was demonstrated by Teissié *et al.* (1985) using pH dependent fluorescent probes. Conduction was found to be around 20 times more rapid over the surface than through bulk water, independent of the nature of the head groups. Therefore in bacterial membranes, the presence of proteins and lipids together may allow this very rapid proton conduction mechanism to occur. This enables polarisation to occur up to higher frequencies than that observed by proton movement through the bulk ionic layers surrounding the cells.

Counterion surface conductivity processes were first discussed by Schwarz (1962) and Debye & Falkenhagen (1928).

1.3.4 Surface Ion Conductivity

At pH values far from the isoelectric point, molecules such as proteins will gain a net charge overall. Counterions are electrostatically attracted to these fixed charges as previously described, producing an ionic double layer which surrounds molecules or even cells. These counterions lie at the bottom of potential energy wells, meaning that it is difficult for them to move away from the fixed charges. A large amount of energy is required to move them. As the distance of the counterion from its bound ion increases, the energy necessary to move the ion becomes reduced and eventually the counterion will be able to move freely and exchange with the bulk liquid. This occurs after around 0.86 nm for potassium ions (Pethig, 1979), and it is much easier for the ion atmosphere to move tangentially along the surface, rather than radially away, allowing polarisation.

When many bound ions are present on the macromolecular surface, the potential energy wells tend to overlap, reducing the energy barrier. This allows the counterions to move by only small inputs of energy. The ability for the counterions to move allows charge conduction over the surface and causes a polarisation event. A higher surface charge density allows easier polarisation since there is a greater reduction in the potential energy barrier.

For low energy barriers (0.5 kcal.mol^{-1}) and a 1 μm diameter particle, the relaxation has a dispersion at around 0.3 kHz. This demonstrates that there is quite a large and slow relaxation process and is in fact diffusion controlled. This process is likely to be significantly influenced by the local environmental conditions such as pH and temperature due to ionisation of proteins and other macromolecules present on the surface of cells which aid ion passage. The fluidity of lipid bilayers will also effect charge carrying, by allowing mobilisation of macromolecules such as globular proteins throughout the cell surface layers, while remaining embedded within external membranes. Their defined migration, induced by the electric field would tend to amass charges, enabling polarisation on a macroscopic scale.

According to Schwarz (1962), this low frequency dielectric dispersion (α dispersion) relaxes with a time which is determined by the rate of diffusion of counterions along the particle :

$$\tau = \frac{a^2}{2ukT} \qquad (1.16)$$

This relaxation time is also related to particle size, larger particles taking longer to relax. Ranges of particle size in a suspension gives a variety of relaxation times and so the dispersion may be much flatter than that having a single relaxation time. This is of great relevance to

growing cells such as bacteria and causes a range of relaxation times and thus flatter dielectrophoretic spectra.

This original Schwarz model only accounted for processes occurring due to ions in the fixed Stern layer. Later models such as those of O'Konski (1960) and Dukhin *et al.* (1969) have incorporated the effects of the diffuse ion layer as conductivity processes. These surface conductance mechanisms need to take into account the action of charge carriers and ions as well as the particle size and shape (Dukhin & Shilov, 1974).

O'Konski also used the model of Polder & Van Santen (1946) which also had a term involving the volume fraction of the particles in suspension. Therefore this process was presumably related to the concentration of particles in suspension, the permittivity increasing linearly with particle concentration (Fricke, 1955). At these high concentrations, interactions between particles become more important. Dukhin & Shilov (1974) also showed that relaxation time increases slightly with increasing concentration.

One might also expect the conductance to vary according to the direction of counterion movement in non-spherical particles. Equations proposed by Fricke (1955) for ellipsoid particles have three relaxation times related to the different axes of rotation of the particles and three dispersion regions.

At low frequencies, the large size of this conductance response dominates the polarisation and dielectric dispersions. At higher frequencies, the ionic atmosphere polarisation is too slow to account for polarisations and dispersions in the MHz region. This is generally explained by Maxwell-Wagner interfacial polarisations.

1.3.5 Interfacial Polarisation

Compartmentalisation is necessary in many cells for their metabolic processes, and this is often achieved by the action of insulating membrane structures. When conducting phases are present with these insulating layers, as in cells, charges will move through the conducting regions when subjected to electric fields. However, as would be expected, when the insulating layer is encountered the charge builds up at the interfaces between the two layers. Each of these conducting regions act as dipoles which can be added to existing dipole moments of the material. This accumulation of charges takes a finite time and is possible to occur at lower frequencies. At these frequencies, dipole flipping is efficient and high values of the dielectric constant result. At very high frequencies, there is little time for the build up of charge and the dipoles are therefore small, corresponding to low dielectric constants. At intermediate frequencies, the acquired moments lag behind the field, the lag depending upon the particle

shape but not the size. This phenomenon is known as *interfacial polarisation* or the *Maxwell-Wagner effect*, and its relaxation is exhibited in the β-dispersion region (Maxwell, 1891; Wagner, 1924).

The membrane of cells is primarily made up of lipids and proteins. Oncley (1943) commented that the relaxation frequency for these materials is in the range of 10^5-10^7 Hz, though as discussed above, other mechanisms may give minor contributions with wider relaxation times. In a complicated particle or cell, there is a whole set of polarisation mechanisms, each with a different set of relaxation times. It is this which produces the overall dielectrophoretic spectrum.

Membranes are, to a large extent, responsible for the dielectrophoretic responses of the cell and are greatly affected by polarisation.

Cellular material can be considered to be made up of a lipid bilayer, bounded by polar material on either side. These polar surfaces have both bound and diffuse counterion layers as explained in section 1.2.1. The ionic double layers are subject to very high polarisability especially in low and moderate frequency a.c. fields (Pohl, 1978).

Many studies have been performed on bacterial cells and several models produced to explain observed results.

1.4 Electrical Properties of Bacterial Cells

The majority of dielectric experiments conducted to date used two bacterial species, one Gram positive (*Micrococcus lysodeikticus*), the other Gram negative (*Escherichia coli*). A model was proposed by Carstensen *et al.* (1965) and Carstensen (1967) to relate the dielectric properties of these bacteria to their structure. As a basic model, the bacterial cell is described as a conducting cytoplasm core, within a thin insulating plasma membrane and then surrounded by a porous conducting cell wall.

Generally *Micrococcus* has relatively high conductivity and dielectric constant at low frequencies below 500 kHz. This has been attributed to the effects of the cell wall and the concentration of ions in the wall is predicted to be almost as great as that in the cytoplasmic core. In fact, the ion concentration in the wall can be a factor of ten times more than that in the suspending medium, even though the wall is porous (Chen, 1972). At these frequencies, the plasma membrane underlying the cell wall acts as an insulator, preventing penetration of the applied field into the highly conducting interior (Carstensen, 1967). Values of 1.1 $mho.m^{-1}$

were originally reported for the cell wall conductivity (Carstensen, 1967), with the cell cytoplasm around 2 $S.m^{-1}$ (Tempest, 1969). Further experiments however, found *M. lysodeikticus* to have a lower wall conductivity and values of 0.4 $mho.m^{-1}$ have been quoted (Carstensen & Marquis, 1968). The mobile ions responsible for this high conductivity are thought to act as counterions to the fixed ions present on the wall polymers (Carstensen, 1967; Carstensen & Marquis, 1968; Einolf & Carstensen, 1969). At low medium conductivities, the cell conductivity is determined by these wall charges. However, at higher medium conductivities the wall conductivity will be more proportional to the medium, since ions will penetrate into the wall and increase wall conductivity.

Carstensen (1967) calculated conductivities from the equation :

$$\frac{\sigma-\sigma_1}{\sigma+2\sigma_1} = p\frac{\sigma_2-\sigma_1}{\sigma_2+2\sigma_1} \qquad (1.17)$$

where σ is conductivity of suspension, σ_1 and σ_2 are medium and particle conductivities respectively and p is the volume fraction of the particles.

Overall cell conductivity of *Micrococcus lysodeikticus* has been found to be between 0.15 to 0.3 $mho.m^{-1}$ compared with the much lower cell conductivity of *E. coli* of around 0.03 $mho.m^{-1}$ (Carstensen *et al.*, 1965). The conductivity of the latter is always less than that of its environment, probably due to the presence of its outer membrane preventing an influx of ions from the medium and ionisation of wall material. The cell properties were found to be dependent upon the growth conditions of the bacteria, those in the stationary phase of growth having greater conductivities, while those in early growth phase being more dense (Carstensen & Marquis, 1968). In addition, isolated cell walls change size depending upon medium conductivity, shrinking by a factor of 0.5 in volume when NaCl is added to the suspension (increase in conductivity from 0.005 to 5 $mho.m^{-1}$).

Einolf & Carstensen (1969) showed using *Micrococcus lysodeikticus* protoplasts that both the cell conductivity and dielectric constant are significantly reduced at low frequencies by removal of the cell wall. The dielectric constant is reduced by two orders of magnitude and conductivity reduced to 0.001 $mho.m^{-1}$ in protoplasts at frequencies below 100 kHz. It was, however, found that removal of the cell wall did not alter the β–dispersion, relaxation occurring above 0.5 MHz in both intact cells and protoplasts. This dispersion was shown to be solely due to the membrane rather than the cell wall (Pauly, 1962).

The membrane acts as a resistance and a capacitance in parallel. At low frequencies, the resistance is predominant but as the frequency of the field is increased, there is a short

circuiting of the membrane resistance by the capacitance allowing the field to penetrate further into the cell. Therefore at high frequencies the internal cellular components start to have an effect on the polarisation mechanisms of the cell.

For *Micrococcus lysodeikticus*, the relaxation time, τ, of the polarisation associated with the membrane can be calculated from the equation :

$$\tau = \frac{\varepsilon_p + 2\varepsilon_s}{\sigma_p + 2\sigma_s} \qquad (1.18)$$

where typical values are $\varepsilon_p = 330$ and $\sigma_p = 0.04$ S.m^{-1}.

This relaxation time was found to be around 1.1×10^{-7} s, corresponding to a characteristic frequency of 1.5 MHz. At this frequency the dielectrophoretic force begins to drop in magnitude. It is at this point that the electric field begins to penetrate further into the cell.

Asami *et al.* (1980) found a similar dispersion using *E. coli* in the MHz region and assigned it to be a Maxwell-Wagner dispersion. This relaxation frequency was seen to decrease from 1.4 MHz to 1.2 MHz with decreasing cell concentration and increase with increasing NaCl concentration in the medium.

1.5 Modelling Electrical Characteristics of the Bacterial Cell

One of the earliest models to explain the electrical responses of cells was put forward by Maxwell (1891). This demonstrated that the cell, made up of a sphere of highly conducting cytoplasm circled by an insulating membrane, could be replaced by a homogeneous shell of the same external radius (which had been effectively "smeared out") without altering the external field. Wagner (1914) extended this theory and derived the effective complex permittivity of the system. This process can be repeated many times, expressing two concentric spheres as a single homogeneous sphere and so, by having a smeared out sphere inside another can be used to model different cell structures (Pethig, 1991b).

Crane & Pohl (1972) modelled live and dead yeast cell dielectrophoretic responses by a two-shelled system where the cytoplasm was bounded by a membrane of finite thickness overlaid by a second cell wall layer. In these models, the relative thicknesses of each layer has been found to be a contributing factor to the predicted response of the cells.

Their model predicted the observed response of a disappearance of the normal low frequency minimum (at 10 kHz) and a lowering of the cut off frequency in the MHz range for the dead cells. This was attributed to an increased porosity of the membrane in dead cells, equilibrating the cytoplasmic conductivity with that of the medium and also to an overall decrease in cell size (to 2 μm) of the dead yeast.

This type of model was furthered when Irimajiri *et al.* (1979) used a multishell model of heterogeneous spherical particles, where the general dispersion produced was made up of several individual dispersions, ε_k, each corresponding to relaxation of an interface separating the different dielectric layers.

The effective value for the particle permittivity, ε_p^*, was given as :

$$\varepsilon_p^* = \varepsilon_\infty + \sum_{k=1}^{n+1}\left[\frac{\varepsilon_k}{1+j\omega\tau_k} + \frac{\sigma_0}{j\omega}\right] \qquad (1.19)$$

where ε_∞ is the limiting high frequency absolute permittivity, σ_0 is the limiting low frequency conductivity and ε_k is the dielectric dispersion associated with the relaxation time τ_k.

Multishelled particles gave several dispersions corresponding to their interfaces. Therefore, cells with a greater number of interfaces may be expected to have a wider range of relaxation frequencies causing the dielectrophoretic spectrum to be broader across the frequency range.

Einolf & Carstensen (1973) extended their model for ionic conductivity effects associated with surface ion movements to include the case of a porous surface. The Gram negative outer membrane may be thought of as being porous to certain ions. Pethig (1979) demonstrated the effect of having a porous dielectric with water filled pores running completely through the dielectric. The water filled pores, which may be compared to porin proteins present in the lipid outer membrane, were found to give dielectric losses proportional to the volume concentration of the pores. Comparisons may be drawn which suggest that greater proportion of porins in the membrane increases the size of dielectric losses occurring at relaxation frequencies.

1.6 Orientation of Particles

It has often been reported (Chen, 1972; Bernhardt & Pauly, 1973; Dukhin & Shilov, 1974; Pohl, 1978) that especially ellipsoidal or elongated particles can become orientated by the electric field, depending upon the frequency applied.

In low frequency electric fields elongated cells tend to align along the field lines, whereas high frequency fields cause them to align perpendicular to the field. This change in orientation is due to a change in the type of polarisation mechanisms at different frequencies.

At low frequencies, the field induced ion movement is predominant. This large polarisation current is at its maximum when the displacement of the surface bound charge is greatest. The charge displacement is such that ions tend to move as far from their oppositely charged ions as possible i.e. to the ends of an elongated particle. This polarisation is only effective at low frequencies and is at a maximum when the particle is aligned along the field. At high frequencies, the double layer response begins to fail and membrane capacitance charging is favoured. The polarisation of the membrane will be highest if it presents its maximum cross section to the field. Therefore, the cells will collect at right angles to the field at these frequencies. At very high frequencies, the membrane capacitance may fail to respond quickly enough and other mechanisms may take over, e.g. dipolar orientation.

Therefore there is a frequency at which the orientation of the particle switches at right angles from alignment with the field, to being parallel to it. Experiments with Euglena show the cells to orientate with the field lines at frequencies less than 10 MHz, perpendicular to the field at up to 100 MHz and parallel to the field again, at frequencies greater than 100 MHz, as different mechanisms come into action and others cease to have an effect (Pohl, 1978).

Bernhardt & Pauly (1973) found that the shape of the particle is important and described changes in relaxation frequency for ellipsoids having differing dimensions. These workers predicted alignment perpendicular to the field for frequencies up to 1.06 MHz, flipping to a parallel orientation at higher frequencies.

For prolate and oblate spheroids, increasing the long axes lengths resulted in decreases in relaxation frequency as they become unable to repolarise in time with the switching field. In addition, they also showed that this change in orientation could be brought about by changes in the medium conductivity, by moving the relaxation frequency.

This change in orientation is quite significant to dielectrophoretic measurements since the 'yield' of collection in static systems is related to the length of pearl chains observed at electrodes. Elongated particles aligning end to end will increase the overall chain length and may lead to errors in calculated yields. Presumably pearl chain formation is thus much more efficient and common at the lower frequencies, or very high frequencies, where cell collection occurs parallel to the field. Pearl chain formation also increases the observed level of collection since the effective volume is greatly increased by aggregation of cells, resulting in an even greater dielectrophoretic force.

Chapter 2 : The Bacterial Cell - Consideration of Structure

2.1 Overview

The basic bacterial cell structure is a layered material, beginning at the interior with the cytoplasm containing the nuclear material, extending out through the cytoplasmic membrane, the cell wall with its many polymers and to the outer membrane of Gram negative bacteria. Further layered cell structures such as rigid layers, flagella and exopolysaccharide material may also be considered. This capacity for variation in composition, coupled with the wide range of shapes and sizes of bacterial cells, is responsible for the diversity of form of the dielectrophoretic spectra of bacterial species.

Exceptions to the basic structure of bacterial cells exist, such as *Mycoplasma* spp., and its relations of the 'soft bodied' species which have no cell wall structure but are surrounded by a cytoplasmic membrane; and *Mycobacteria* spp. which possess a waxlike material in their cell wall causing them to be highly hydrophobic.

Although it is recognised that the highly conducting cytoplasmic contents interior to the procaryotic cell membrane are of notable importance to the growth and survival of the cell, it is surface and wall properties which are under examination here. Nevertheless it is anticipated that the internal structures, including insulating membrane mesosomes, will exhibit their major dielectrophoretic polarisations at higher frequencies as described in section 1.4. Since the frequency range used for experiments described in this thesis was limited by the capability of the function generator, the range 1 kHz to 50 MHz may be unlikely to cover a significant proportion of the ranges for observable effects due to internal properties of the cell.

2.2 Capsules

Several of the layers outlined above are common to both Gram positive and Gram negative bacteria. Capsules, may be considered to be the outermost physical structure and therefore is the first point of contact with the local environment and the most external structure to be influenced by the applied electric field. The most common form of capsules found surrounding the bacterial surface are polysaccharide in nature, though some have been found to have polypeptide composition. Relatively few species, such as *Bacillus megaterium, Bacillus anthracis* and *Bacillus subtilis*, exhibit this latter type, generally being a γ-linked polypeptide of

D-glutamic acid in one form or another, sometimes being interspersed with polysaccharide material (Salton, 1960).

The capsulated species studied in this thesis produce polymers of polysaccharide composition, thus attention will be focused on the dielectrophoretic contribution of this type.

2.2.1 Exopolysaccharides

Many bacterial species of most genera secrete exopolysaccharides, in the form of either a discrete capsule attached to the bacterial cell surface or as amorphous slime secreted into the surrounding area (Troy, 1979)(figure 2.1).

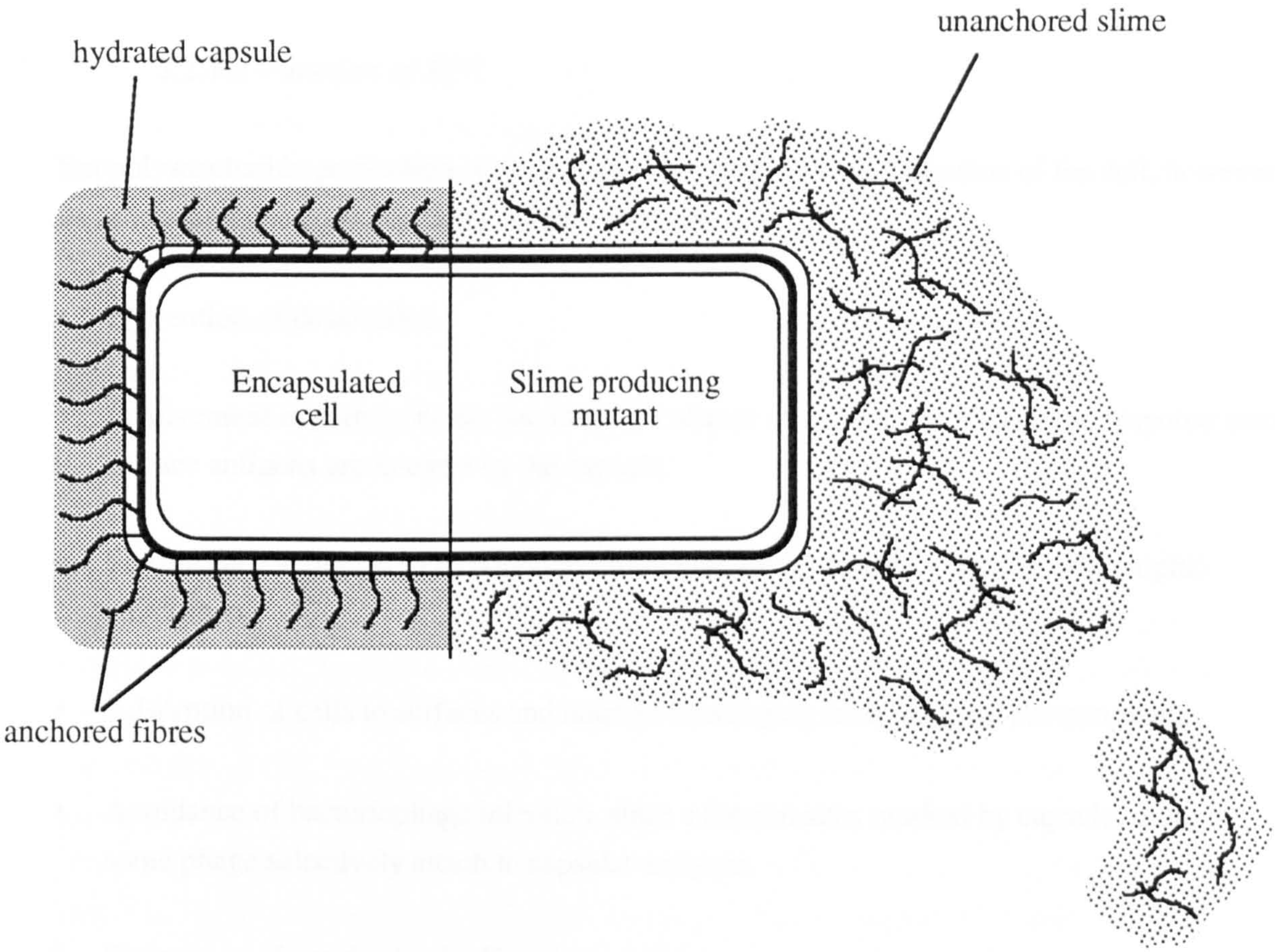

Figure 2.1 : Forms of exopolysaccharide secreted by some bacterial cells.

2.2.1.1 What Is Exopolysaccharide ?

Exopolysaccharides (EPS) can be basically described as highly hydrated linear or branched polysaccharide polymers of many varieties of monomeric, often repeating, subunits. Bacterial exopolysaccharide slime and capsules are particularly hydrophilic, being up to 99 % water (Handley, 1991).

Both capsule and slime have the same basic chemical composition and therefore the distinction between the two is fairly arbitrary; indeed capsule material is often lost into the medium. It is known that the many different chemical compositions of species specific EPS are independent of the type of carbon source as demonstrated using *Klebsiella aerogenes* (Wilkinson *et al.*, 1955), i.e. the chemistry of the polymer is the same even when the cell is cultured in a variety of growth media.

2.2.1.2 Function of EPS

Exopolysaccharide production is not essential for the growth and division of the cell, however its production does provide many useful functions :

- Prevention of dessication.
- Involvement in pathogenesis, due to the avoidance of an immune phagocytic response since surface antigens are masked by the capsule.
- Storing carbon or energy in polymeric form which may be catabolised in oligotrophic conditions.
- Adsorption of cells to surfaces and nutrient scavenging from the local environment.
- Avoidance of bacteriophage infection, since adhesion sites masked by capsule, though some phage selectively attach to capsular antigens.
- Serotyping of species by the K antigen epitope type.
- Importance as a resistance mechanism. Of great consequence in the protection of biofilm related organisms from chlorine, assisting in antibiotic resistance and defence against other antibacterial agents.

2.2.1.3 Structure

Capsules are normally made up of acidic polysaccharides having anionic charges from uronic acid residues, sialic acid, pyruvic acid, phosphate and 3-deoxy-D-manno-octulosonic acid (KDO) (Hancock, 1991). These polymers, when dehydrated, are fibrous structures. Certain capsules have been known to extend up to a cell diameter into the medium under optimum conditions (Hancock, 1991), compared to the much smaller length of the O-antigenic chain of LPS 0.02 μm.

The structure of bacterial EPS polymers is determined by the monomeric component types and numbers, their linkages, the sequence, and non-carbohydrate parts, as well as the overall molecular weight. Since exopolysaccharides may be considered as the outermost physical layer, their structures are likely to be highly influential on the dielectrophoretic response of these bacterial cells.

Polysaccharide polymers such as bacterial EPS can be broadly classified into two groups, those which consist of the same monomeric sugar units, the homopolysaccharides, and those which have more than one type of monomer, the heteropolysaccharides. According to Sutherland (1972), even though EPS appear to be very complex polymers, they are much more simple than the polysaccharides of LPS.

Sutherland (1982) further classified these into five distinct groups, three of them being independent of carbon source for EPS production (table 2.1).

2.2.1.4 Chemical Composition

The capsules of many species have been examined and their structures often characterised, including common species such as *Escherichia coli* , *Klebsiella pneumoniae* (Fischer *et al.*, 1982; Amako *et al.*, 1988) and *Proteus mirabilis* (Beynon *et al.*, 1992). The sequences and composition of EPS have been frequently found by degradation of the polymers by specific hydrolases and subsequent analysis of products by chromatographic or colourimetric methods (Troy, 1979). Many bacteriophage types produce hydrolases specific for the EPS of certain bacteria. These have been used to degrade the EPS of species such as *Klebsiella aerogenes* Type 54 (Sutherland, 1967). The most commonly found constituent monomers of EPS are D-glucose, D-mannose, D-galactose and D-glucuronic acid. Often sugar acids are also found which confer a negative charge on the polymers. This is of special note to the hydrophobicity and adhesion properties of the cell described later in section 2.10. Charge on the surface of bacterial cells brought about by these monomeric groups is fundamental in determining the electrical response of these cells to non-uniform electric fields.

Type	Comments
Homopolysaccharides	Repeating monosaccharide units of single type e.g. dextrans, levans, mutan. Generally produced by bacteria needing specific carbon source for EPS production, normally sucrose. Often produced by *Streptococcus* and *Leuconostoc*.
Homopolysaccharides produced from non-specific carbon sources	Some formed solely from carbohydrate monomers e.g. cellulose, while others possess acyl groups e.g. N-acetylneuraminic acid (sialic acid).
Heteropolysaccharides produced from specific carbon source	Formed from more than one monosaccharide subunit types.
Heteropolysaccharides containing repeating subunits	Most common and diverse in structure and composition. Range from disaccharide to octasaccharide subunits. Examples are colanic acid (produced by *E. coli*, *Salmonella*, *Enterobacter cloacae*) or that produced by the widely studied *Enterobacter (Klebsiella) aerogenes* strains. Specific carbon source unnecessary.
Two subunit heteropolysaccharide exopolysaccharides	The two subunits of this group not found as repeating units and may be found as irregularly sequenced monomers e.g. alginate (contains D-mannuronic acid and L-guluronic acid). The formation of L-guluronic acid is an exception in that unlike other sugars it is not formed via a nucleotide precursor (Sutherland, 1982).

Table 2.1 : Broad classification of EPS structures.

2.2.2 Homopolysaccharides

Several types of homopolysaccharides are commonly produced by certain bacterial species, some of which are described in table 2.2.

Name	Comments
Cellulose	Linear polymer with repeating units of cellobiose (two glucose monomers linked by a β1,4 glycosidic bond). Rotation of alternate glucose units by 180° gives two configurations. Arrangement of terminal residue determines which chemical groups exposed at the surface. Important in movement of charged groups through the capsule. Rotation of neighbouring cellulose polymers may assist or hinder charge hopping polarisation processes.
Levans	Fructose based polymers having β 2,6 glycosidic linkages. High molecular weights of ≥ 10^6 Da.
Dextrans	Polyglucose polymers linked by α 1,6 glycosidic bonds. Less than 40 monomers long, though have been found as long as 550. Branched chain positions 2, 3 or 4 on successive glucose residues allow range of dextrans with different dipole moments and polarisation characteristics.
Mutan	Specific to *Streptococcus mutans*. Glucose monomers linked by α 1,3 glycosidic bonds. Of prime importance in the formation of dental caries.

Table 2.2 : Homopolysaccharide structures of EPS.

The chemical structures of some of these homopolysaccharides are also shown in Appendix 2.

These are less common than the more widely studied heteropolysaccharides and are much simpler in structure. Since heteropolysaccharides can consist of many monomeric groups, there is a range of chemical groups available for polarisation which are likely to transfer charge in different ways. The different branch arrangements imply different stearic hindrances for heteropolysaccharide polymers and different bond angles. This obstruction to physical rotation of the residues will likely dictate the frequency range over which permanent dipole rotations can occur.

2.2.3 Heteropolysaccharides

The very complex nature of the heteropolysaccharides makes it difficult to make generalisations about the structure and composition of this EPS type. The structure of polymers would be

likely to alter as often as mutations can occur in cells, since these capsule and slime arrangements are determined by genetic and enzymic capabilities. Nevertheless, a few common examples of heteropolysaccharide EPS compositions are outlined below (table 2.3). The most widely studied bacterial capsules and slimes are those of Gram negative *Klebsiella (Enterobacter) aerogenes* and *E. coli.* Gram positive cells also synthesise extracellular polymers, however, the majority of these species are normally considered of lesser medical importance and so have not been examined in such great detail.

Name	Monomers	Comments
Colanic Acid	fucose (30-32 %) galactose (33-34 %) glucose (16-17 %) glucuronic acid (17-20 %)	Trisaccharide branch on trisaccharide linear chain. Degree of branching of significance to polarisation. Often produced as slime by Gram negative Enterobacteriaceae, e.g. *E. coli.* Similarities in structure between certain bacterial species.
Klebsiella EPS Type 1	fucose glucose glucuronic acid	Contains pyruvate in the normal structure. Negatively charged molecule, so contributes to dipole moment of the capsule fibres. Glycosidic bonds with 1,3 linkage found.
Klebsiella EPS Type 8	galactose (50 %) glucose (25 %) glucuronic acid (25 %)	Based upon a tetrasaccharide repeating unit as shown in Appendix 2.
Klebsiella EPS Type 54	fucose (10 %) glucose (46 %), glucuronic acid (27 %)	Similar to Type 1. Highly branched. Each tetrasaccharide unit contains formate with alternate tetrasaccharides being acetylated.

Table 2.3 : Heteropolysaccharide structures of EPS.

The chemical structures of some of these heteropolysaccharides are also shown in Appendix 2.

2.2.4 Biosynthesis

2.2.4.1 Nucleotide Precursors

Production of capsule begins with the activation of the sugar components by conversion to nucleotide derivatives within the cytoplasm (Boulnois & Roberts, 1990). These active forms of the sugar monosaccharides have high free energy of hydrolysis and are precursors to the repeating units of the polymer, except in the production of dextrans, mutan or levans where

they are not involved. In addition to EPS, sugar nucleotides form the basis for the production of wall polymers such as LPS and teichoic acids (Sutherland & Norval, 1970).

2.2.4.2 Lipid Intermediates

Activated sugar nucleotides are subsequently passed onto lipid intermediates (identified as C_{55} isoprenoid alcohol, undecaprenyl phosphate), where the polysaccharide chains elongate in a sequential reaction (figure 2.2). The repeating units, such as tetrasaccharide chain portions, are then polymerised to form the polysaccharide. These intermediates have been most studied in strains of *Klebsiella aerogenes* and have been implicated in the production of many other cell wall polymers e.g. lipopolysaccharide (Weiner *et al.*, 1965; Wright *et al.*, 1965) and peptidoglycan (Anderson *et al.*, 1965).

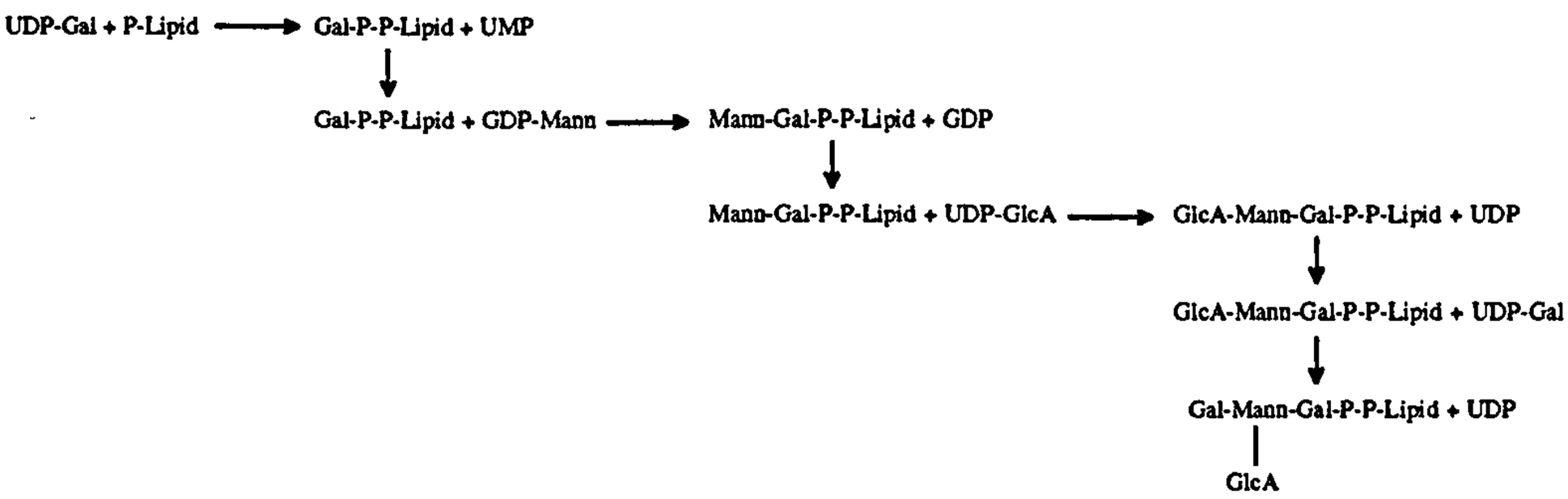

Figure 2.2 : Elongation of EPS polymers utilising lipid intermediates.

Since isoprenoid lipids are also involved in the production of LPS and peptidoglycan alongside the EPS production, it is the availability of the isoprenoid lipids which determines the extent of EPS formation, as lipid must be relinquished before it can then participate in peptidoglycan and lipopolysaccharide formation. When lipid is not required for synthesis by the other systems, EPS formation becomes maximised and occurs particularly in non-growing cells.

2.2.4.3 Transport and Attachment of EPS

Following the polymerisation sequence and polymer elongation by the isoprenoid sequence, the finished product is translocated through the periplasmic space and the outer membrane to an acceptor molecule present on the cell surface where it is attached and organised (Jann & Jann, 1990). Current knowledge suggests that this mechanism is poorly defined, though export is

probably through Bayer patches (areas of attachment between the cytoplasmic and outer membranes).

There have been several suggestions as to the nature of the acceptor molecules on the cell surface though the identification is made difficult due to the large EPS size compared to that of the linkage (Troy, 1979).

There are thought to be three possible ways of capsule attachment :

- Anchored within the membrane
- To the outer leaflet of the outer membrane, either by protein or lipoprotein linkage
- To the inner side of outer membrane or to the peptidoglycan layer. This method is thought the most unlikely of the three.

Extracellular polysaccharide comprises hydrated fibres. Thus there may be a finite number of sites to which these fibres are attached. It can be expected that when all of these sites are filled, no further EPS can attach to the cell and subsequent polymer is lost into the medium. These sites may also anchor only correctly sized EPS. Often EPS which is either very large or small is lost as slime into the surrounding environment. Ørskov & Ørskov (1990) thought it likely that not all K molecules were bound to the surface, possibly due to this feature. Therefore even mild extraction procedures such as a resuspension of cells in saline can cause loss of some capsule from the surface and suspension of K antigens and LPS.

Capsulate cells are able to mutate to become slime producing cells, lacking the ability to attach a discrete capsule. Slime forming mutants are often found in strains that are capsulate. These mutants are potentially caused by an absence of these acceptor molecules or binding sites to which the polymer can attach. These sites may be lost due to mutations or by a loss of enzyme involved in binding process. Further mutations of these cells are possible. Mutations of K^+ capsulate cells to K^- cells lacking EPS have often been described (Ørskov & Ørskov, 1990), due to ease of seeing the differences in colony morphology.

Sutherland (1972) described the possible inter-relationship between possible mutations from a capsulate wild type as in figure 2.3.

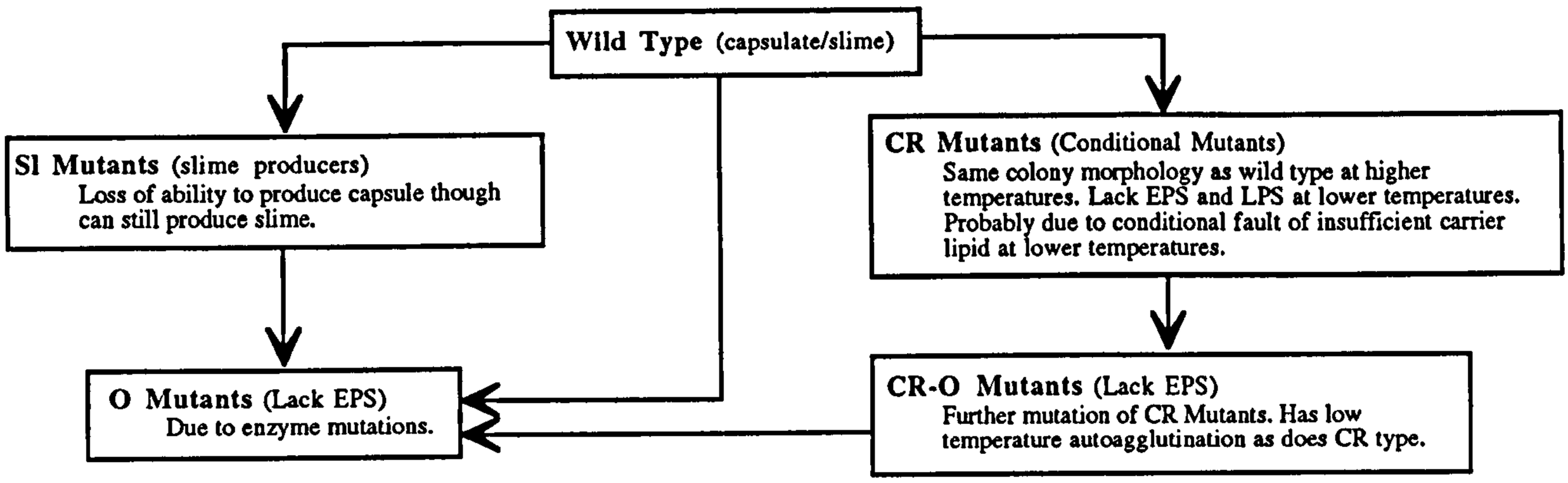

Figure 2.3 : Process of mutation from wild type capsulate bacterial strains (after Sutherland, 1972).

2.2.5 Factors Affecting Synthesis

2.2.5.1 Growth Medium

The extent of EPS production has been shown to vary considerably with the nutrient availability in the growth medium (Duguid & Wilkinson, 1953; Duguid & Wilkinson, 1954; Wilkinson *et al.*, 1954). However the composition of these polymers has been demonstrated to be quite invariant. Wilkinson *et al.* (1955) used a strain of *Klebsiella* (A3(Sl)) to grow on a wide variety of growth substrates. Subsequent chemical analyses found the composition of the slime produced to consist of glucose, fucose and uronic acid, in proportions common in the polymer produced on all carbon sources, namely 50%, 10% and 29% respectively.

The formation of bacterial extracellular polymers has been shown to be greatest when limiting conditions are imposed and a common feature is that polymer production is normally enhanced by high carbon to nitrogen ratios in the growth medium (Wilkinson, 1958). The composition of EPS is not altered by these limitations to the nutrient status, it is the extent of production which is attenuated. Intracellular glycogen has also been found to accumulate in conditions of excess energy over that necessary for growth (De Souza & Sutherland, 1994). The levels of both extracellular polysaccharide and intracellular glycogen storage are likely to have profound effects on the frequency dependent dielectrophoretic response.

Duguid & Wilkinson (1953) estimated the ratio of extracellular polysaccharide to cell growth (expressed as non-dialysable nitrogen) under a variety of nutrient conditions using *Klebsiella*

aerogenes strain A3 (Serotype 54). The cells, using ammonium sulphate as a nitrogen source, expressed 5 times more polysaccharide production under limiting nitrogen conditions (0.015 % w/v ammonium sulphate) compared to the rich growth medium. This is due to the ability of *Klebsiella* in the latter medium to completely utilise the carbon source for growth thus allowing only minimal EPS production.

Maximal polysaccharide production may also be produced by exerting other nutrient limitations, while maintaining aerobic conditions and excess carbohydrate within the medium (Duguid & Wilkinson, 1953; Wilkinson *et al.*, 1954).

2.2.5.2 Growth Phase

Duguid & Wilkinson (1953) also demonstrated greater rates of capsule production throughout the exponential phase of growth. Although EPS production is favoured when normal cell synthesis mechanisms are slowed due to increased availability of isoprenoid lipids (as described in section 2.2.4.2), the rate of EPS production is greatest when the cell is growing and multiplying very rapidly and all mechanisms of cell growth are favoured. Due to the accumulation of the material, most EPS was found after around 4 days of growth.

There are important cytological differences between cells in different growth phases and between those grown under different media conditions. Cells grown in carbon deficient media have small capsules compared to the much larger capsules of cells limited by nitrogen, phosphate or sulphate. The accumulation of EPS over time means that cells taken from different stages of the culture growth would be likely to have significant differences in capsule size possibly leading to very different responses of the bacteria to non-uniform electric fields. The differences in growth medium could be expected to have similar consequences. However, both medium composition and growth phase have also been shown to alter the general cell structure, for instance protein expression and size, making it virtually impossible to attribute dielectrophoretic spectral differences solely to EPS modifications.

2.2.5.3 Aeration

Broth cultures have been found to lead to a lesser EPS production compared with bacteria grown on solid media due to the quantity of aeration.

The majority of bacterial species which produce EPS polymers are known to be aerobes or facultative anaerobes and thus maximisation of polymer production is noted under non limiting oxygen conditions (Sutherland, 1982).

2.2.5.4 Temperature Effects Upon Polymer Synthesis

Experiments with Gram negative bacterial cells have shown that EPS production can be favoured at temperatures between 15-18 °C under certain conditions (Troy, 1979). Lower temperatures of growth depresses the turnover of cell wall polymers and liberates the necessary undecaprenyl phosphate. The expression of polymer is related to the fluidity of the membrane at different temperatures. A mobile lipid phase is required for the membrane associated enzymes to work properly and elongate the EPS polymers on the carrier lipids. Below the transition temperature of the membrane the lipids are very immobile, above the transition temperature the membrane is fluid and allows passage of proteins and incorporation of extra carrier lipid. The various compositions of bacterial membranes attribute different transition temperatures. Proper membrane function needs mobile states and below the membrane lipid transition temperature exogenous lipid is not inserted.

Temperature dependence is also likely to be of importance to dielectrophoresis. Higher membrane fluidity gives rise to greater movement of protein molecules and other charged moieties through the lipid bilayer allowing faster polarisation.

2.3 S-Layers

On the surface of both Gram negative and especially Gram positive species of bacterial cells, highly organised patterned layers can often be visualised (Rogers, 1983). These have a proteinaceous composition which form crystalline structures surrounding the whole cell. Their occurrence in Gram positive species is known to overlay the peptidoglycan wall structure, being found external to the outer membrane (though under any capsular material) in Gram negative cells. The layers are but a few nanometres in thickness and consist of a regular hexagonal array of protein molecules, normally separated by 8-15 nm. The function of S-layers is generally considered to be one of exclusion, the pores between the protein structures barring passage of molecules greater than about 30,000 Da. The presence of S-layers has a masking effect over the hydrophilic LPS side chains, making the cell surface more hydrophobic.

In the absence of capsular material, S-layers will be in direct contact with the environment. Their protein composition and ionisation of amino acid components depending on pH conditions would influence the binding of various ions and charged molecules to this structure. Hancock (1991) commented that these layers have an asymmetrical structure. The inner face has more exposed negatively charged amino acid carboxyl groups due to the folding of the protein molecules. In comparison, the outer face has a more equal distribution of positively

charged amino groups and negatively charged carboxyls, effectively neutralising the overall charge on the outer face.

2.4 Gram Negative Outer Membrane

2.4.1 Structure

Gram negative cell walls are multilayered in appearance, consisting basically of a thin layer of peptidoglycan bounded on either side by two membranes, an inner cytoplasmic membrane and a thin outer membrane. The structure of these organisms will cause compartmentalisation, with each layer having its own unique conductivity and permittivity. The outer membrane is 60-100 Å in thickness (Glauert & Thornley, 1969) and both membranes correlate with the typical model of lipid bilayers, even though there are many other structural differences between the two.

The basic structure of the Gram negative outer membrane consists of a typical phospholipid bilayer. However, in this membrane, the outer leaflet has a substantial proportion of the phospholipids replaced by amphipathic molecules known as lipopolysaccharides, LPS. Also embedded within the membrane are four or five specialised protein types.

2.4.2 Outer Membrane Phospholipids

Phospholipids are amphipathic molecules consisting of both a hydrophobic fatty acid part, and a hydrophilic polar head group (figure 2.4). The phospholipid composition of both cytoplasmic and outer membranes are similar. Common phospholipids, especially within species of the Enterobacteriaceae family, are mainly of the phosphatidylethanolamine (PE) group, though phosphatidylglycerol (PG) and diphosphatidylglycerol (diPG) are also found.

In general the composition does not vary greatly with growth conditions, and overall the ratio of phosphatidylethanolamine to phosphatidylglycerol (or diphosphatidylglycerol) is normally constant. However, in the stationary growth phase of a cell culture the content of diPG increases relative to that of PG.

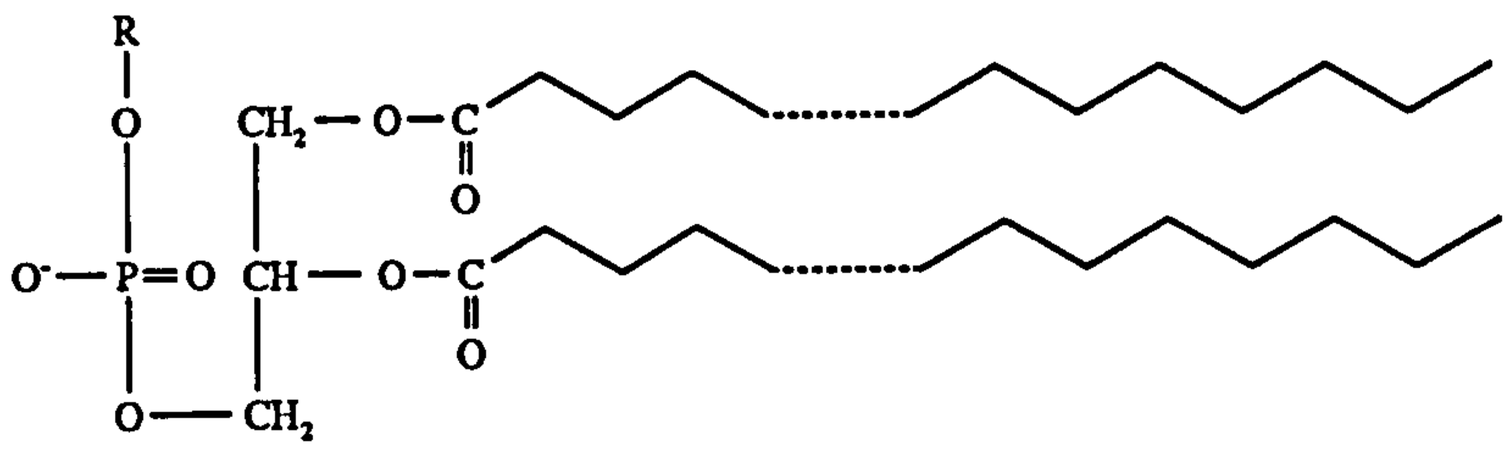

Figure 2.4 : Representation of a typical phospholipid molecule (Hammond *et al.*, 1984).

The structures of PE, PG and diPG are shown in figure 2.5 (a-c). PG and diPG contain a single or double negative charge respectively, carried by the ionised phosphate groups and PE has both positive and negative charges. These charged groups are likely to participate closely in the movement of charge along the membrane bilayer. Therefore, the relative extents of each phospholipid types can cause significant changes in surface charge and counterion levels, and in the conduction of ions and charged groups along the membrane surface. The outer membrane has an asymmetrical arrangement of its lipid bilayer, with the outer leaflet being much reduced in phospholipid, and replaced by LPS and protein molecules. Therefore conduction mechanisms utilising phospholipid head groups may not be such a significant mechanism as in eucaryotic cells, and this may be supplanted by other mechanisms involving the LPS portion.

Phospholipids contain long chain fatty acid molecules which are essentially the same in all phospholipid types. Though phospholipid type is not significantly influenced by growth conditions, the fatty acid component can be modified by several factors. For the survival and activity of membrane associated mechanisms, a consistently fluid membrane is necessary over all conditions and temperatures. Therefore, the outer membrane needs both fluid and non-fluid fatty acids at all temperatures and thus saturated and unsaturated fatty acid types are present in the membrane. Unsaturated and branched fatty acids have a lower melting point, making them more fluid than saturated fatty acids at lower growth temperatures. Mindich (1973) noted that there were areas of different lipid types within the membranes, having different temperature characteristics. Therefore at a specific temperature, there may be areas which are more fluid than others. Movement of charged molecules may occur in the fluid areas yet have restricted movement in the non-fluid domains. Charge interfaces could build up at these limiting

boundaries and act as a type of Maxwell-Wagner interfacial polarisation as described by Harrop (1972), which contribute to overall polarisation of the cell.

(a)

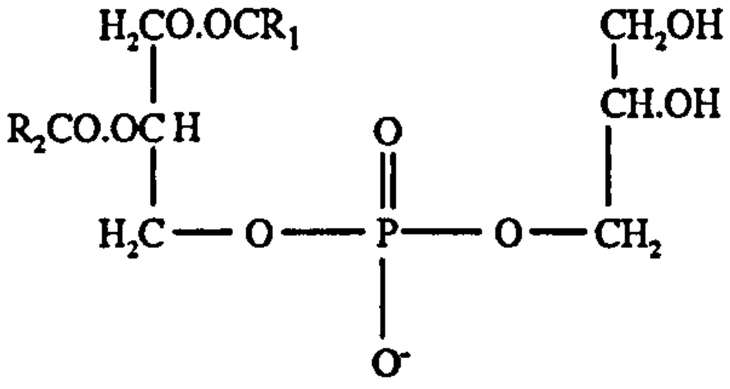

(b)

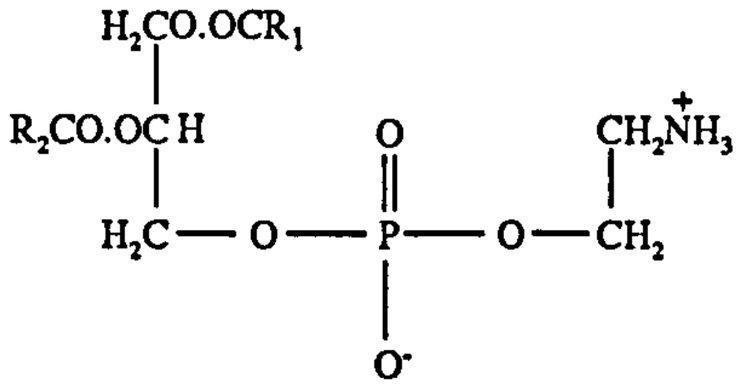

(c)

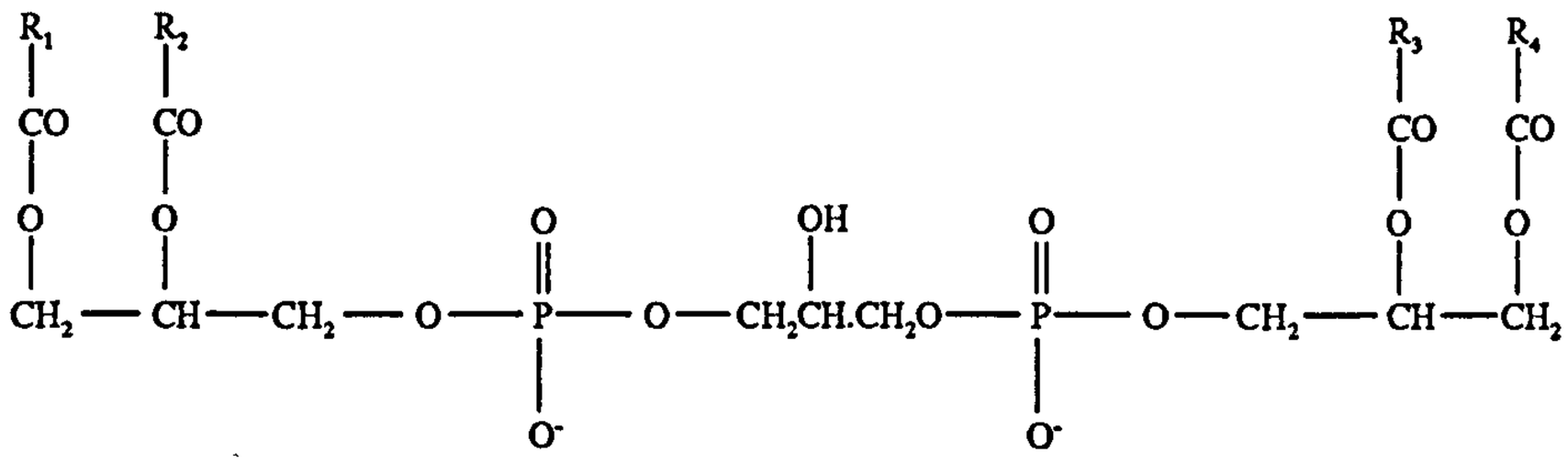

Figure 2.5 : Common membrane phospholipids in dissociated form. (a) Phosphatidylglycerol, (b) Phosphatidylethanolamine, (c) Diphosphatidylglycerol (cardiolipin) (after Rogers, 1983).

Fatty acid composition varies both between species and within species grown in different conditions and has been known to be limited by essential amino acid deprivation. Bacteria able to grow at a range of temperatures are able to substitute these forms of fatty acids within their membranes, producing more of the unsaturated fatty acids at lower temperatures, the converse holding for higher temperatures. Increased membrane thickness will alter capacitance mechanisms of membranes, and the frequency at which the field short circuits the membrane making the length of the fatty acid chains an important additional factor in polarisation of bacterial cells over a frequency range.

Often bacterial membrane phospholipids are found in amino acylated forms, commonly by lysine or alanine. The negatively charged head groups of these phospholipids can allow binding and cleavage of protons and other positively charged ions, allowing a charge conduction over the surface of the membrane phospholipids. Amino acylation further modifies the charge on these phospholipids and the extent of the acylation can be dependent upon the growth conditions and pH of the medium. Lysine has an additional NH_3^+ group donating charges on amino acylated phospholipids to contribute to polarisation responses. These amino substituted groups have a range of pK values for the ionisation of functional groups, meaning that their respective contributions to dielectrophoretic polarisation will occur at different pH values. The polarisation of these cells may be closely related to the nature of the phospholipid groups and substituents.

The migration of lipids throughout the membrane is a rapid process, diffusion being at a rate of 10^{-8} $cm^2.s^{-1}$ in *E. coli*, being able to move the length of a cell in about two seconds (Rogers *et al.*, 1980). In the cytoplasmic membrane, the protein components are free to move easily, though in the outer membrane, this movement does not occur as readily, potentially caused by the rigidity of the LPS layer or other strong interactions inhibiting movement. A higher degree of fluidity increases the rate of diffusion by facilitating movement of these molecules. Charged ions would also be assisted to move along the head groups of mobile lipids more rapidly by the presence of these unsaturated fatty acids. As well as increasing the fluidity of the membrane portion, increased temperatures also increase the conductivity of ions, thus increasing the speed of polarisation by several mechanisms and allowing more efficient polarisation and relaxation up to higher frequencies. Greater degree of fluidity in the membrane would also be likely to decrease the resistance of the membrane to penetration by the electric field, allowing it to occur at a lower portion of the frequency spectrum, bringing into action additional mechanisms of polarisation.

2.4.2.1 Biosynthesis

The basic membrane phospholipid structures are produced from a combination of fatty acids, *sn*-glycerol 3-phosphate, and serine.

Fatty acid production occurs by normal membrane phospholipid biosynthetic pathways using acyl carrier proteins (ACP). The mechanism begins by the combination of acetyl CoA and malonyl CoA. Additional malonyl CoA units are sequentially added, elongating the fatty acid chain. The reaction is then terminated, detaching the fatty acid and allowing the ACP to participate in further synthetic reactions. Fatty acids with odd numbers of carbon atoms can be produced by initial condensation between propionyl CoA and malonyl CoA rather than acetyl CoA.

The assembly of the 3 component parts begins by the acylation of *sn*-glycerol-3-phosphate (initially formed from dihydroxyacetone phosphate) at the C-1 position by the fatty acid, to form phosphatidic acid. Reaction of the phosphatidic acid with CTP, produces a transient intermediate, CDP-diglyceride, which is then able to form completed phospholipids. Should the CDP-diglyceride react with L-serine, phosphatidylethanolamine (PE) results, whereas a reaction with further *sn*-glycerol-3-phosphate produces phosphatidylglycerol (PG). Rapid conversion of PG to diphosphatidylglycerol (diPG) may follow (Mindich, 1973; Hammond *et al.*, 1984).

Following synthesis, the phospholipid fraction is inserted into existing membranes, though membrane elongation and insertion of new lipids is thought not to occur at specific sites but generally over the whole membrane structure (Mindich, 1973).

2.4.3 Lipopolysaccharide

Lipopolysaccharides are amphipathic molecules which are typically made up of three parts, a specific hydrophobic lipid section (lipid A) which is embedded in the lipid bilayer (consisting of fatty acid chains linked to a glucosamine backbone), a short carbohydrate core region and a long polysaccharide chain (the O-side chain) which extends outwards up to 300 Å from the cell surface into the surrounding medium.

It is likely that surface characteristics and membrane structure are of great significance to the dielectrophoretic response. Therefore, it can be seen that LPS molecules are very important to conserve in the membrane and so agents which act on LPS could quite easily change this response.

There is a large degree of chemical diversity in the structure and composition of the O-side chain part of the molecules, and it is these polysaccharides which have been found to have an importance in the functions of the outer membrane. The side chain has been found to be quite unaffected by cultural conditions (Rogers, 1983) and therefore LPS has been used with very great effectiveness in the serotyping and identification of bacteria on the basis of these O-somatic antigens, especially in the study of *Salmonella* species. Many bacterial genera have been examined for their LPS structures including *Escherichia, Shigella, Klebsiella, Proteus* and *Pseudomonas*, and there has been found to be a large amount of conservative regions between species (Rogers, 1983)

The most commonly studied LPS structure is that of *Salmonella typhimurium* and its structure, as a typical example of LPS, is shown in figure 2.6.

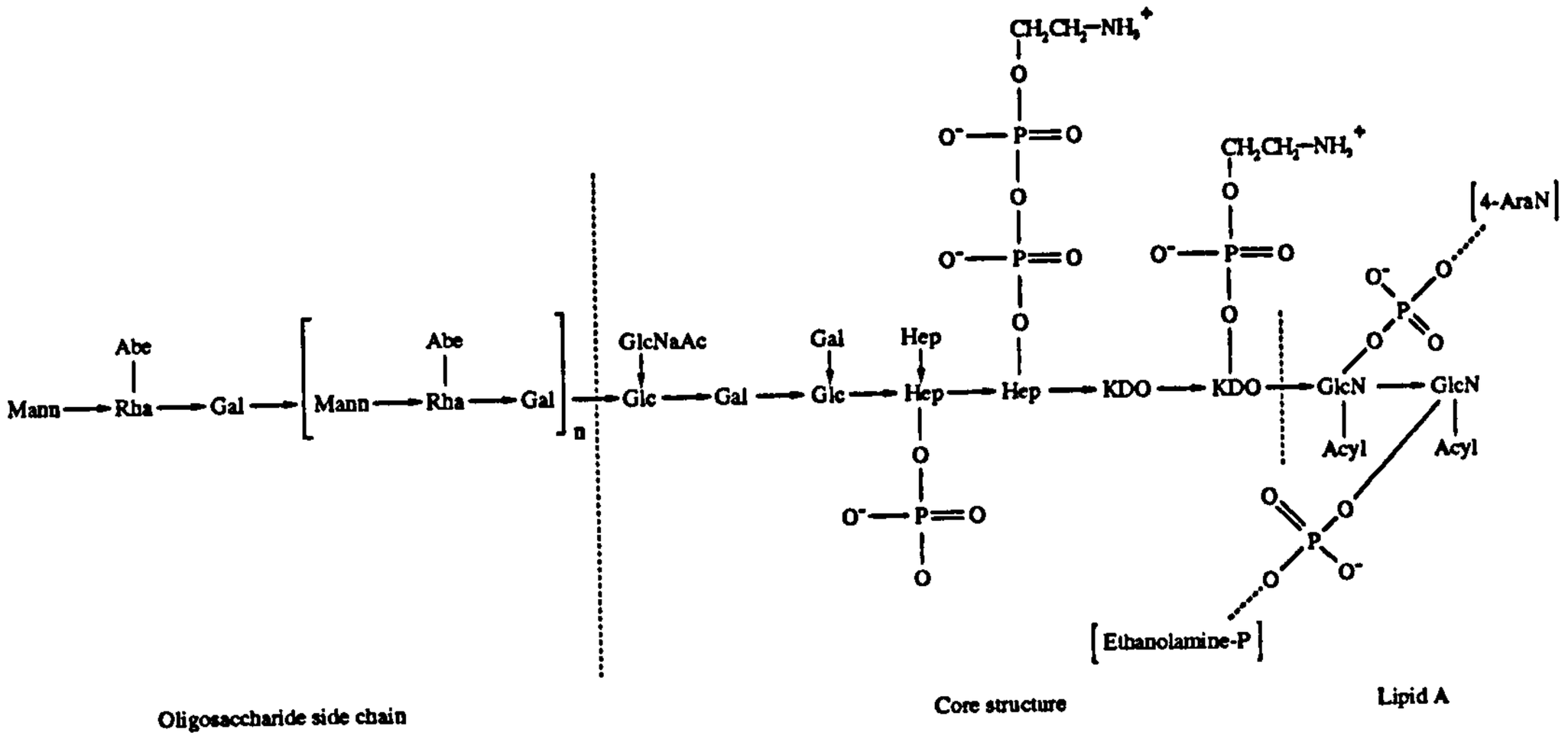

Figure 2.6 : Typical LPS structure (after Nikaido, 1973).

2.4.3.1 Lipid A

This specific lipid found in LPS is composed of a backbone of two disaccharide units of D-glucosamine. These have often been found in *Salmonella, Serratia, Shigella,* and *Pseudomonas* spp. to be linked by a β 1,6 linkage, though β 1,4 bonds have been found. These sugars are substituted with fatty acids, normally via an amide and ester link to C-2 and C-3 respectively.

The lipid A disaccharides often have phosphate groups which may or may not be attached to phosphorylethanolamine and amino-arabinose. These phosphate groups can confer negative charges on the lipid A portion in the absence of neutralisation by substituents. Lipid A molecules are held together in the outer membrane by the presence of divalent cations, possibly binding to the negative charges of the molecules (or of the inner core region) or by interactions between the LPS and protein molecules (Hammond *et al.*, 1984). The presence of these stabilising ions will be likely to facilitate the passage of charges along the surface of the outer membrane of Gram negative species. During the surface conductivity polarisation mechanisms, these stabilising ions may exchange with other co-ions so continuing the surface conductivity effects, or may also allow the conduction of electrons or counterions. The application of the

electric fields and resulting polarisation may thus cause some destabilisation of the membrane, due to the movement of these divalent ions and lead to ion leaching from the cytoplasmic interior, resulting in rises in suspension conductivity.

2.4.3.2 LPS Core

The lipid A sugars are linked to a complex carbohydrate core region which is generally composed of arrangements of D-glucose, D-galactose, N-acetyl-D-glucosamine and L-glycero-D-mannoheptose. The core is bound via a linkage through a sugar acid dimer of KDO (2-keto-3-deoxyoctonic acid). This KDO is essential for LPS formation, though the outer part of the core can often be mutated. Mutants produced by such mutations are commonly referred to as deep rough mutants (Hammond *et al.*, 1984).

The core may also contain substituent groups such as zwitterionic O-phosphorylethanolamine and O-pyrophosphorylethanolamine, bound to KDO and the L-glycero-D-mannoheptose respectively. Thus the phosphorylethanolamine may be thought of as having a similar structure to membrane phospholipids, and this appearance may allow more efficient incorporation and binding within the membrane bilayer.

2.4.3.3 O-Side Chain

The O-side chain which forms the most antigenic part of the LPS molecule consists of repeating oligosaccharide units normally having repeating sequences of 2-4 monosaccharides attached to the core molecule (Hammond *et al.*, 1984).

The length of side chains creates the possibility for several mutant strains to be produced. Generally, complete LPS molecules are found in 'smooth' strains, leading to a colony morphology which is circular in appearance. Mutations to LPS molecules, in contrast to deep rough mutants, normally result from premature terminations at various points in the oligosaccharide chain or an inability to attach or synthesise the chains. These are known as 'rough' mutants, due to their formation of an irregularly shaped undulate colony on solid media. Some semi rough mutants do exist which are unable to polymerise the sugar subunits (Hammond *et al.*, 1984).

As a result, bacteria with such mutations would be expected to generate abnormal dielectrophoretic spectra compared with their parent strains. The long chains of the polysaccharide O-antigen may be influenced by the field to interact with charge passage and rotate under the influence of the field. However, unlike other polysaccharides, these do not appear to be highly charged molecules, responding less to the field presence. Nevertheless, the

charges on lipid A and core regions may have sufficient action in the passage of charge to cause polarisation, and the whole molecules may have enough mobility in the membrane to move in response to the field. The presence of divalent cations, especially magnesium, as stabilisers of LPS may be able to become removed from their interactions by the strong field. Should these divalent ions be released, this may also cause a loss of rigidity in the membrane, leading to loss of charged LPS molecules into the medium, influencing its polarisability and conductivity, or allowing further mobility of LPS to occur.

2.4.3.4 Biosynthesis

The pathway begins by an amination of glucose-1-phosphate to N-acetylglucosamine followed by addition of two (or more) 3-OH fatty acids at C-2 and C-3 of the sugar forming diacyl-1-glucosamine phosphate. This is then activated by the addition of nucleotides and subsequently condensed with another diacyl glucosamine, making the backbone of lipid A. The lipid A is then phosphorylated, producing an acidic precursor which may bond phosphorylethanolamine from serine and 4-amino-arabinose to modify it to a neutral precursor. This reaction is once again dependent upon the nature of the bacterial strain and growth conditions.

The lipid A precursor is then reacted with CMP-KDO (formed by enzymic action on ribulose-5-phosphate) by membrane bound enzymes causing sequential addition of two KDO molecules at the C-6 position of one of the glucosamine sugars. Consequently the inner R-core region is formed by sequential passage of the nucleotide sugar monomers, phosphate groups and ethanolamine to the lipid-KDO-KDO structure, by the action of enzymes. According to Hammond *et al.* (1984), before the initial sugar unit can be added in the outer core region, a phosphorylation step of the heptose sugars must occur to allow continuance of enzyme reactions of sugar transfer.

Once the core region has been synthesised, the O-side chain is formed by use of the same C_{55} polyisoprenoid units met previously in other polymer synthetic mechanisms. In essence, the activated sugar nucleotides are transferred to the carrier lipid in the cytoplasmic membrane and sequentially added in an elongating chain present on the carrier molecule. The lipid carrier and tetrasaccharide carbohydrate chain is then translocated from the inner to outer leaflet of the cytoplasmic membrane, where tetrasaccharide units are cleaved from the carrier and added onto existing carrier-sugar chain molecules. Thus, a long polymer of identical subunits is formed on a single lipid carrier. This releases the other lipid-P-P molecules to participate in further synthetic mechanisms, possibly of other polymer types, once it has been dephosphorylated and recycled.

The cytoplasmic membrane allows free movement of molecules within the bilayer, and so as the completed O-chain and carrier lipid come into the vicinity of the lipid A-core, the elongated oligosaccharide chain is transferred to the lipid forming the completed LPS molecule.

The completed unit on the isoprene carrier is then transferred to the outer membrane for expression at the surface. It is thought that for ease of transport, the translocation occurs at the sites of adherance between the cytoplasmic and outer membranes, Bayer patches (Bayer & Thurow, 1977). Once in place, they are held firmly by protein interactions in the outer leaflet and by the stabilisation effect of divalent ions.

The O-side chains comprise the hydrophilic portion of the amphipathic LPS molecule. Thus mutants, lacking parts of this oligosaccharide, are likely to become more hydrophobic binding less water molecules to the bacterial surface. This loss of water will cause changes to the polarisability of the cell and modifications to the dielectrophoretic spectrum. Nikaido (1973) also noted that there is a high proportion of ionisable groups in the LPS molecule, especially negative charges in the inner core region associated with KDO-heptose portion. LPS is thus likely to exhibit some significant repulsion effects. These effects are neutralised by the presence of cations and moderates this repulsion, binding positive ions, sequestering them and preventing their free movement in response to an applied field.

2.4.4 Protein Structure of the Outer Membrane

Outer membrane proteins (Omp) are significantly different to those of the inner cytoplasmic membrane. Electrophoretic examination of cytoplasmic membranes show the presence of greater than 200 protein types, ranging from 1,500-100,000 Da in molecular weight (Rogers, 1983). The cytoplasmic membrane has a very active and extensive enzymic system, compared with that of the outer membrane, which has practically no enzyme activity at all. There are only a few types of proteins in the outer membrane, all donating particular functions to the membrane. These are divided into two categories, Major and Minor Outer Membrane Proteins.

2.4.4.1 Major Outer Membrane Proteins

These consist of four or five main types, shown in table 2.4 for *E. coli*. However, the nature, size and amount of these proteins can vary significantly with different species and growth conditions. Since many of them are expressed on the surface of the membrane their nature will have variation in the polarisations of bacterial cells, and as a result will be greatly affected by species and growth conditions.

Protein name	Molecular weight, Da	Function
Lipoprotein	7,200	Anchors outer membrane to peptidoglycan
OmpA	35,160	Has a function in bacterial conjugation
OmpC	36,000	Porin for passage of hydrophilic solutes
OmpF	37,200	Porin for passage of hydrophilic solutes
Protein A	40,000	Protease activity

Table 2.4 : Major outer membrane proteins.

Several of the proteins act as non-specific transmembrane pore channels, or 'porins' spanning the outer membrane and tightly bound to the peptidoglycan. OmpC and OmpF are of this nature and are responsible for the conductance of small molecules and excluding hydrophilic molecules of weight greater than 600-700 (Rogers, 1983; Hammond *et al.*, 1984). These outer membrane porins have a trimeric structure (composed of non-hydrophobic amino acids), and form a channel of around 8 nm in diameter. Both OmpC and OmpF span the membrane and are found exposed at the cell surface. This open presence causes these proteins to act a phage receptors, and have an influence on the cell surface characteristics, such as charge movement and hydrophobicity.

Lipoprotein constitutes the majority of the outer membrane protein and up to 6% of the outer membrane protein can be found in this form. Some of this lipoprotein was shown by Braun (1975) to be linked covalently with the peptidoglycan layer, though it may also be found as free molecules in the membrane fraction. Lipoprotein has a significant function in the outer membrane, binding it to the peptidoglycan wall structure and stabilising the membrane. It has been found in several species including *E. coli, Salmonella* strains and *Serratia marcescens* and extends for around 12-14 nm containing a large amount of alpha helix structure (Costerton *et al.*, 1974). The molecule has both lipid and protein portions and in *E. coli*, consists of 58 amino acids with cysteine at the N-terminus (linked to diacylglycerol in the membrane fraction) and lysine at the C-terminus (linked through diaminopimelic acid to muramic acid).

2.4.4.2 Minor Outer Membrane Proteins

The minor proteins of the outer membrane are often inducible by suitable conditions, the majority of them specifically involved in uptake of essential substances such as iron, phosphate and certain sugars or vitamins which cannot utilise the normal porins due to their large size. A more detailed account of function can be found elsewhere (Hammond *et al.*, 1984). Specific conditions which may be limiting, can cause an increase in their expression so they can actually

reach levels comparable to those of the major Omp types. Therefore different growth conditions can yield outer membrane protein compositions of very different profiles.

The usual low numbers of minor proteins would probably not normally have an effect on the standard dielectrophoretic polarisations of the cell. When they undergo an upshift in expression however, more significant contributions to polarisation may begin to occur. The diverse nature of minor outer membrane protein structure will have a wide range of amino acids each ionised to different extents, giving altered response of the cell to electric fields under different conditions and protein profiles.

Under the outer membrane of Gram negative bacteria exists a cell wall layer conferring the stress bearing function to the cell. In Gram positive organisms this layer is also present and makes up the greatest proportion of the cell wall.

2.5 Cell Wall Material

2.5.1 Overview

Electron microscopy studies of bacterial cells have revealed a great deal of information about the nature of cell walls. In Gram positive cells, fixing in OsO_4 reveals an electron dense layer of >30 nm in thickness (Rogers, 1983). The majority of this layer is known to be made up of peptidoglycan and is found to overlay a cytoplasmic membrane which is of around 7.5 nm in thickness (Davis *et al.*, 1980). In Gram positive cells peptidoglycan and associated polymers are often the outermost structures covering the cytoplasmic membrane. These anionic chains have been shown by lectin binding to extend into the medium from *B. subtilis* cell surfaces (Doyle *et al.*, 1975). Since they may be the most external structures these charged polymers will be able to influence and interact with ionic double layers of charge surrounding the surface and affect movement and polarisation responses to alternating non-uniform electric fields.

2.5.2 Peptidoglycan

2.5.2.1 Function of Peptidoglycan

A bacterial cell needs both strength and molecular sieving properties to maintain its viability. In most bacterial cells the strength is afforded by a tough polymer called peptidoglycan. This polymer is present in nearly all bacterial cells except for the *Mycoplasmas* and *Archaebacteria* species, stable L-forms and other more complex organisms such as cyanobacteria. In these groups the peptidoglycan is substituted by other polymeric material giving stress bearing

qualities and osmotic protection. Research undertaken on *Mycoplasma* by Carstensen *et al.* (1971) showed that the lack of peptidoglycan in the cell wall has important effects upon the dielectrophoretic response of these cells and, at low frequencies, it is the cell wall which is responsible for the high nature of the dielectric constant.

Selectivity and exclusion processes are also achieved by peptidoglycan in Gram positive cells, in comparison to the outer membrane function in Gram negative cells. Assessments of the exclusion limits of the peptidoglycan layer in Gram positive cells showed molecules of greater than around 60 kDa were prevented from entering the cell (Hancock, 1991).

2.5.2.2 Structure

Peptidoglycan consists of glycan chains of alternating N-acetylglucosamine and N-acetylmuramic acid linked by β 1-4 bonds, first discovered by Strange & Dark (1956). To the carboxyl groups of the muramic acid residues are attached short polypeptides consisting of a limited number of amino acids. These can be then used to cross link the glycan chains, giving the very high tensile strength to the cell walls. The cross bridge is typified by a link between the terminal D-alanine residue of one peptide chain, often to the amino groups of the L-centre of a diamino group such as lysine or diaminopimelic acid of the next chain. These cross linking structures can be very species specific in nature.

Peptidoglycan is fairly uniform in chemical composition in a species and can constitute up to 10 % of the cell volume and between 50-60 % by weight in Gram positive cells compared with only 10-20 % in Gram negatives (Rogers, 1983; Hammond *et al.*, 1984). The structure of peptidoglycan in many Gram negative and some Gram positive rods is commonly found to be similar to that shown in figure 2.7 for *E. coli.* Additional components of the Gram positive cell wall can be anionic polymers such as teichoic acids, teichuronic acids and other polysaccharides covalently linked to muramic acid residues. There may be as many as one anionic polymer for every 10 disaccharide repeating units of peptidoglycan.

The amount of peptidoglycan is highly variable between bacterial species, though considerably more peptidoglycan is found in Gram positive species. The polymer is a layered material, and there may be between 20-40 layers of peptidoglycan chains separated by distances of 4.2 nm. In Gram negatives however, peptidoglycan can be as thin as one layer with a much lower extent of cross linking (Braun *et al.*, 1973). This larger mesh structure could be inducive to better ion movement and increased polarisability. Wall thickness can be particularly variable, especially following changes in growth conditions. Incubation of cultures, in conditions which allow growth of wall material but not protein synthesis e.g. by addition of antibiotics, or by omission of a necessary amino acid can cause thickening over the whole cell wall. Older

cultures (i.e. non-exponential phase of growth) may also result in this type of wall thickness variation due to a relaxation of control over peptidoglycan biosynthesis, allowing synthesis of other cell polymers as described in section 2.2.4.2. Other irregularities in polymer structure have been found in actively growing Gram positive cells, attributed to incomplete cross linking and forshortened chain lengths. It can be envisaged that spectral differences will occur between exponential and stationary phase cells, not least for these reasons.

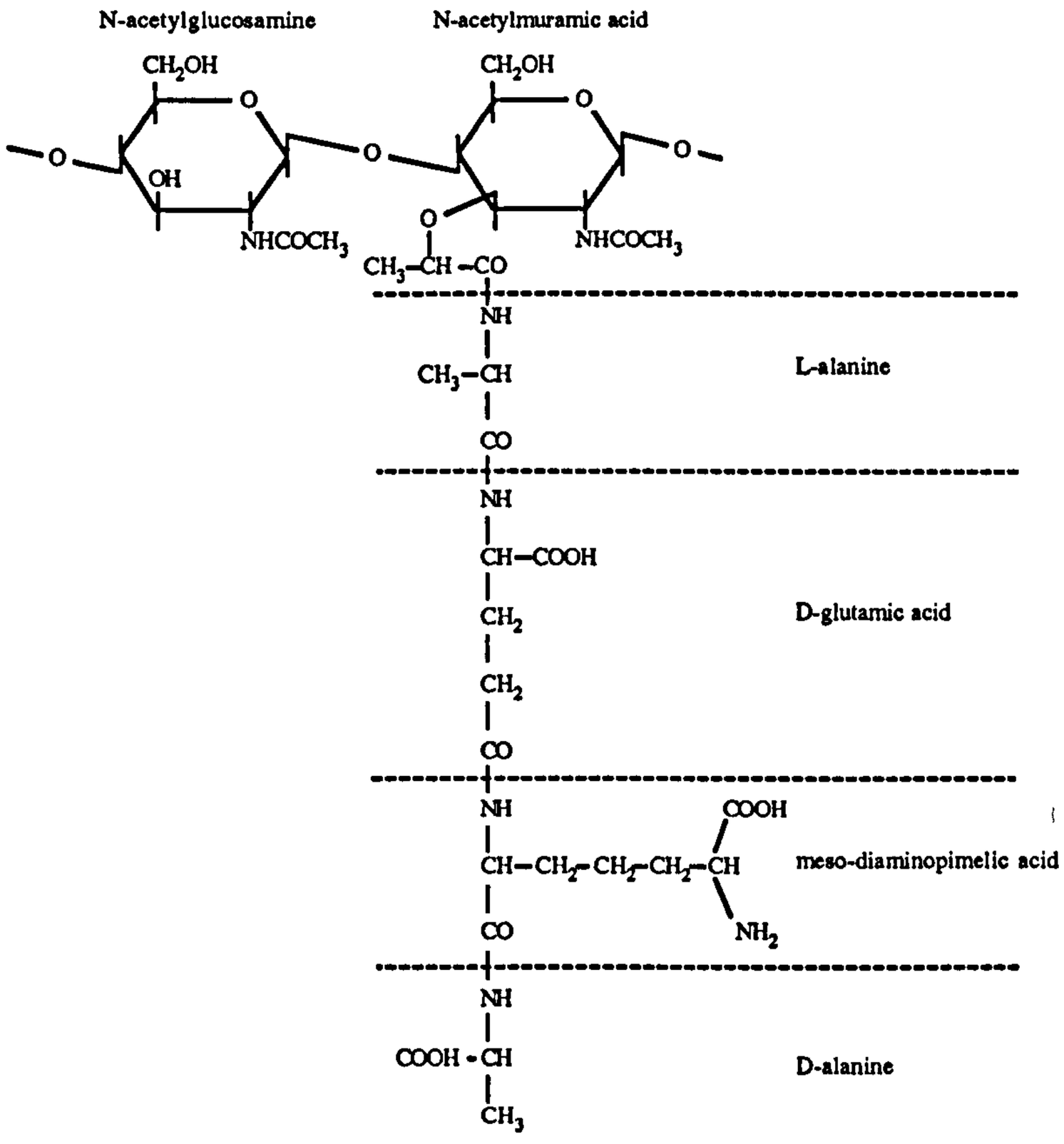

Figure 2.7 : General peptidoglycan structure (after Hammond *et al.*, 1984).

The conformation of peptidoglycan polymers in cell walls is still not precisely determined but it is thought that the strands are similar in nature to chitin (Formanek *et al.*, 1974; Keleman & Rogers, 1971; Rogers *et al.*, 1980) and run parallel to the bacterial surface, accompanied by a considerable amount of hydrogen bonding (Tipper, 1970). Calculations have revealed that a rod shaped cell of 1.5-3 μm x 0.6 μm would need either 10-20 long chains stretching along the length of cell, or around 13 chains surrounding the cell short axis to form the cell wall (Rogers

et al., 1980). Indeed, Hammond *et al.* (1984) suggested that this latter method is present in bacteria such as *B. subtilis* and *E. coli*.

2.5.2.3 Peptide Chains

Inter-species variation arises predominantly from the different amino acids in the peptide portion of peptidoglycan, and the degree and nature of the cross linking between these chains.

A regularly found tetrapeptide sequence consists of the first amino acid which is often L-alanine bound directly to the carboxyl groups of the muramic acid residues by amide links. A D-amino acid, commonly D-glutamate or D-glutamine, is bonded to an L-alanine residue and often to meso-2,6-diaminopimelic acid. The major variation in these peptides is the amino acid at position 3 in the chain. Meso diaminopimelic acid is most common, though L-lysine, L-ornithine, L-diaminobutyric acid or L-homoserine can be found. Diaminopimelic acid also contains a free carboxyl group not involved in any linkage. The terminal amino acid of the tetrapeptide is almost always D-alanine.

Cross links are often formed between the free amino group of the meso-2,6-diaminopimelic acid of one peptide and the carboxyl group of the terminal D-alanine of another peptide. The cross link may be either a direct link (as in many Gram negatives), or may consist of a bridge of 3 or 4 further amino acids, commonly glycine, serine or threonine (found in several Gram positive species). These different types of amino acid groups all have different charges and structures associated with them, each of which could contribute to polarisation of the whole cell, due to their extensive presence in the cell walls.

The variations of linkage bring chains into different orientations and may vary in the proximity of interaction. This leads to a range of mesh sizes, some having particularly large or small pore sizes. This is of fundamental importance when considering the passage of charged molecules along glycan chains and through the peptidoglycan structure. It is, perhaps, implicit that less cross linking should lead to better passage of charges through the more loosely structured polymers. Less cross linking may also allow movement of the glycan chains with respect to each other in response to the application of non-uniform electric fields, assisting cell polarisation. Short cross bridges would mean a more rigid structure and an inability for chain shifting.

The degree of cross linking is very species specific and can be expressed as an index of cross linking. This is given as given as the percentage ratio of amino acids at the third (R_3) position having bound amino groups to the total number of R_3 amino acid residues in the

peptidoglycan. This can vary from in 93.5 % (highly cross-linked) in *Staph. aureus* to 20-30% (low cross-linking) in *E. coli* (Rogers, 1983; Hammond *et al.*, 1984) as in table 2.5.

Bacterial Species	**Cross Linking Index** (Bound R_3 Amino Groups : Total R_3 Amino Groups, %)
Escherichia coli	20.4-33
Proteus mirabilis	33
Proteus vulgaris	33.7
Micrococcus lysodeikticus	20.2
Bacillus subtilis	41
Clostridium perfringens	50
Bacillus megaterium (Exponential)	50
(Stationary)	56
Bacillus cereus	61
Staphylococcus aureus	93.5

Table 2.5 : Peptidoglycan cross linking indices in different bacterial species.

2.5.2.4 Peptidoglycan Biosynthesis

The mechanism of formation is analogous to the formation of EPS previously described. Biosynthesis begins with the production of active precursors within the cytoplasm of the cell. The precursors consist, in this case, of UDP-N-acetylmuramic acid residues linked to the peptide chain, and of UDP-N-acetylglucosamine, formed from sugar-1-phosphate molecules. The energy of hydrolysis of these activated monomers allow polymer formation to occur. The muramic acid residues are formed by the reaction of the active form of UDP-N-acetylglucosamine with phosphoenolpyruvate (CH_2CPO_4COOH). This reaction releases the phosphate group and allows the free carboxyl group to then attach a pentapeptide chain (Hammond *et al.*, 1984). The process of amino acid addition to form this pentapeptide chain proceeds with the first three amino acids being added sequentially to the active muramic acid, followed by the addition of the final two added as a dipeptide of D-alanine.

These subunits are then passed onto the pyrophosphate lipid carrier, undecaprenyl phosphate, where they are linked to form the disaccharide. The active UDP-muramic acid and its conjugated pentapeptide is linked to the carrier lipid phosphate, becoming pyrophosphate. Consequently the UDP-glucosamine is then added, forming the lipid linked disaccharide repeating unit and releasing the UDP.

The subunit is moved through the cytoplasmic membrane and added to an existing elongating glycan chain at a growing point, often without any further modifications. The acceptor exists probably as a lipid linked pyrophosphated glycan strand and the muramic acid part of the disaccharide is joined to the reducing end of the chain, in turn attached to the lipid carrier. Since both existing chain and disaccharide are attached by a pyrophosphated lipid, one of the lipids becomes relinquished upon bonding and is free to recycle back through the membrane to accept another precursor upon cleavage of one of the phosphates. For insertion of the nascent glycan chains into the existing peptidoglycan network, endopeptidase enzymes are utilised to break cross linking peptide bonds.

Cross linking of the newly synthesised glycan strands can then occur by a transpeptidation reaction involving transpeptidase enzymes. It is thought that these enzymes are able to recognise the terminal dipeptide of D-alanine. Thus they can remove one of the alanine groups, leaving the normal tetrapeptide and allowing formation of a peptide bond between the now terminal alanine carboxy group and the free amino group on the meso-diaminopimelic acid of next chain. The removal of one of the alanines releases a substantial amount of energy which can be utilised to form this peptide bond.

It is not, perhaps, surprising that the structure and composition of the types of peptidoglycan may have a significant effect on speed and frequency of polarisation responses in bacteria species. They are linear polyelectrolytes which can transmit charge relatively quickly along the length of the bacterial cell, particularly in bacteria where the chains run along the long axis of the cell. Arrangement of peptidoglycan around the girth of bacterial species may have more of an effect in the mechanisms where frequency responses shift the orientation of the cell to be perpendicular to the field, and where capacitive responses of the cell wall are more influential than surface conduction effects.

The degradation of parts of the cell wall by autolytic enzymes are necessary for several purposes, such as allowing the incorporation of newly made peptidoglycan, cell division and separation of daughter cells. The most structurally important, stress bearing portion of the peptidoglycan is deep within the cell wall and its autolysis could be very detrimental. It is normally the outer part of peptidoglycan that is self-degraded (Anderson *et al.*, 1978). Such surface reorganisation creates pits in the wall, resulting in an increased opportunity for counterion access to the cell polymers. Wall turnover depends largely on the culture conditions and growth phase, high rates being found in the exponential phase, though again this can be species related.

Peptidoglycan structure can be modified in several ways, altering the structure and properties of the cell wall. Rogers *et al.* (1980) found amidation of carboxyl groups to be common with D-glutamic acid and meso-diaminopimelic acid, causing a reduction in polymer acidity. In addition the covalent linkage of other polymers e.g. teichoic acids or teichuronic acids to the peptidoglycan of Gram positive cells (or lipoprotein in Gram negatives) is very common. This normally occurs via a phosphodiester, the phosphate contributing an increased negative charge.

Ellwood & Tempest (1969) found the growth environment to significantly influence the proportion of wall linked anionic polymers, such as polysaccharides and teichoic acids. Despite their bonding with peptidoglycan, these polymers do have some mobility and may well contribute to the overall polarisation mechanisms.

2.6 Other Wall Polymers found in Gram Positive Bacteria

2.6.1 Teichoic Acids

These are found in most Gram positive bacteria except species of *Micrococcus* which have a negatively charged membrane associated lipomannan instead (Rogers, 1983). There is some degree of variability in the basic structure of the teichoic acids and different bacterial species may even have more than one type of teichoic acid present within a cell (Hancock, 1991).

Two classifications of teichoic acids have been made, those which are found in the cell wall linked to peptidoglycan and those found linked to the cytoplasmic membrane (commonly known as lipoteichoic acid, LTA).

2.6.1.1 Wall Teichoic Acids

Teichoic acids can account for up to 50 % by weight of bacterial cell walls. Structurally, they are polymers of repeating subunits, normally of glycerol phosphate or ribitol phosphate, having a chain length of up to 35-40 residues (figure 2.8 a-b). Wall polymers are attached to peptidoglycan by phosphodiester linkage groups, covalently bonding the teichoic acid polymers to the 6-carbon of muramic acid in the peptidoglycan backbone.

As previously stated, the polymers have a large negative charge contributed by the phosphate groups, giving them an acid, anionic nature. It is thought to be teichoic acids which mainly cause the overall negative surface charge in Gram positive cells (Hammond *et al.*, 1984). Phosphate groups are fully ionised above pH 2.5 meaning that a teichoic acid chain of 40 polyribitol phosphate or polyglycerol phosphate residues would contain 40 negatively charged

groups, making them extremely important components within the Gram positive cell wall. It is to be noted that these charged polymers within bacterial cell walls would also contribute to the dielectrophoretic response of these cells and determine the nature of the polarisation.

(a)

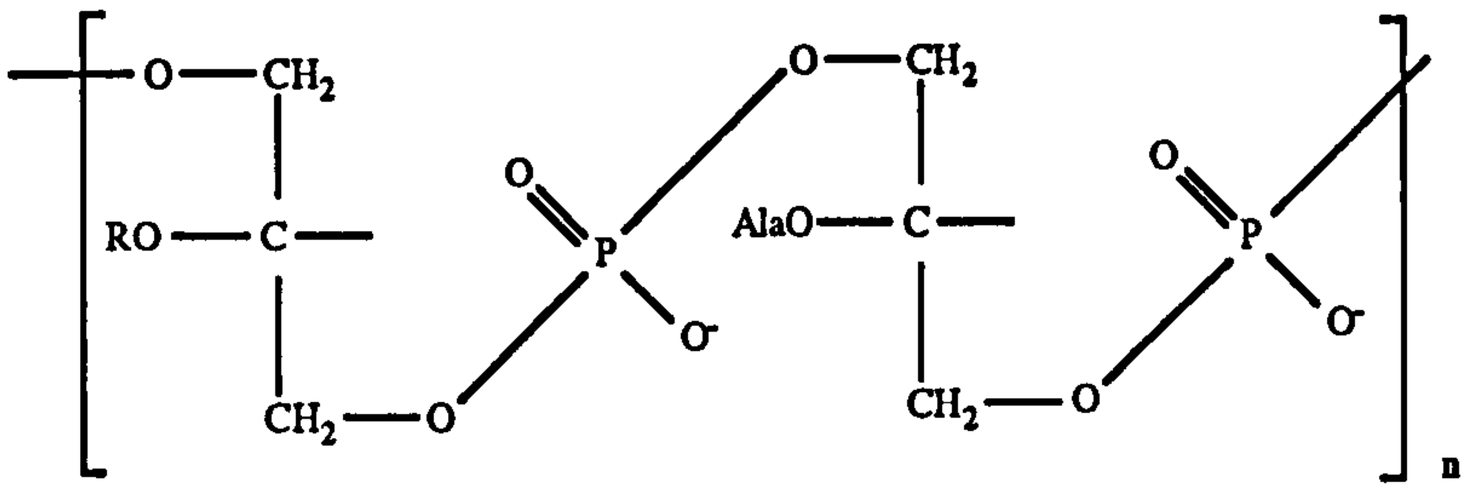

(b)

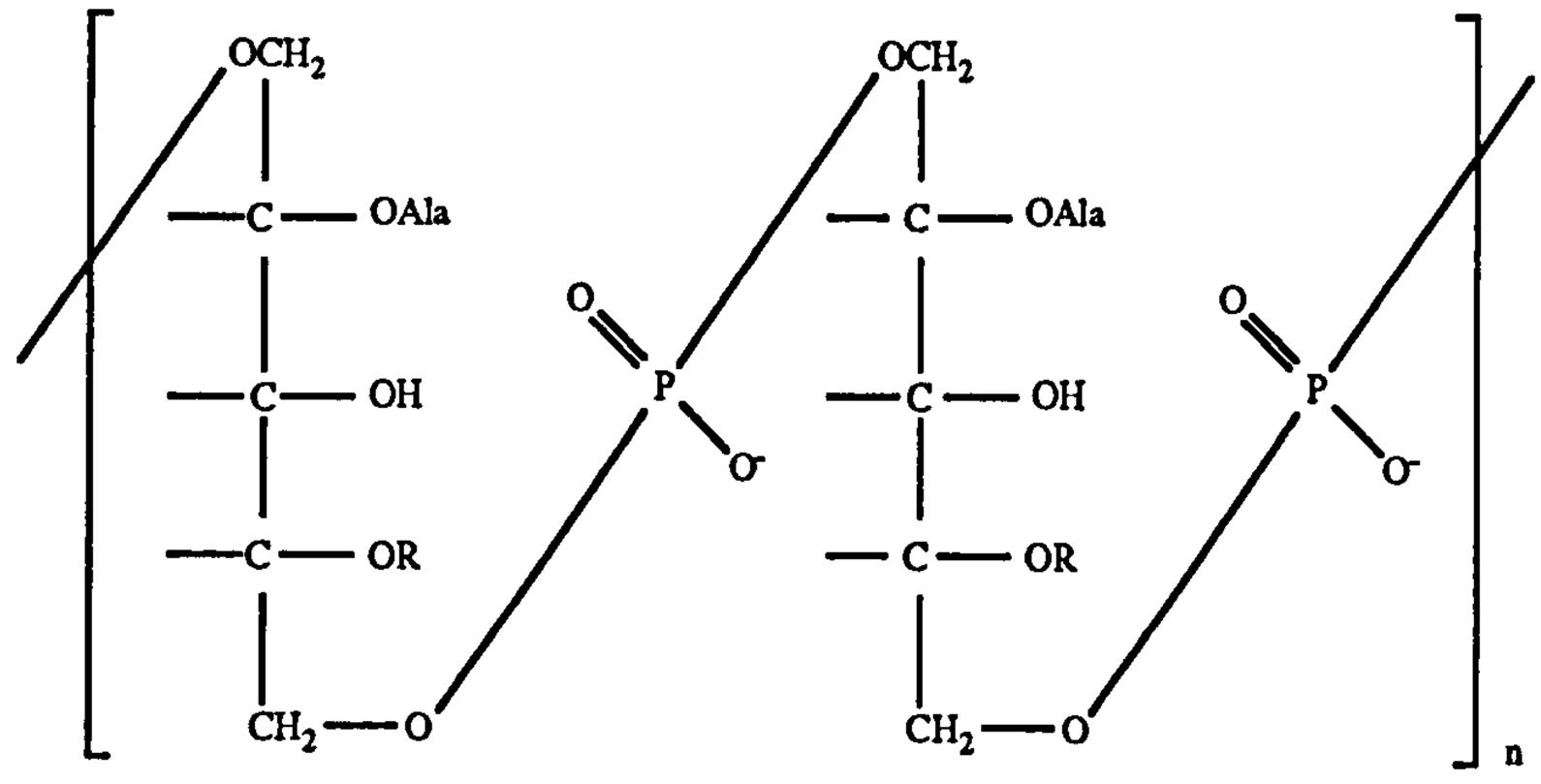

Figure 2.8 : Teichoic acid structures in dissociated form. (a) Glycerol phosphate teichoic acid, (b) Ribitol phosphate teichoic acid.

The ionic charge of these polymers can be regulated by other substituent groups such as D-alanine or sugar molecules. When alanine is present, it is ester linked by its carboxyl group to free hydroxyl groups of the glycerol or ribitol units. Each D-alanine group substituted onto the polymer structure has a free amino group which is protonated at physiological pH. This charge can therefore neutralise the negative charge of an adjacent phosphate group, effectively reducing the negative charge of the teichoic acid polymer, making them critical to the shape and overall structure of the whole bacterial cell (see section 2.6.1.3). Alanine substituents are highly labile and can be easily removed and released into the medium at pH values greater than

7, meaning that the alanylated portion of teichoic acids is considerably lower when grown under alkaline conditions. The effect of culture pH on the D-alanine ester content of lipoteichoic acid has been previously studied in detail in *Staphylococcus aureus* (MacArthur & Archibald, 1984). In addition to an increase in cell surface negative charge by loss of alanine constituents, these groups are also thought to assist in the movement of ions through the cell wall (section 2.6.1.2), with the consequence of a much slower speed of ion conduction related polarisation in response to applied non-uniform electric fields upon release. Once again this demonstrates the significant controlling effect exerted by the nature of the growth medium and the nature of the local environmental conditions.

2.6.1.2 Function of Teichoic Acids

The structure of the teichoic acids, containing many equally spaced phosphate groups means they have a high affinity for divalent cations.

Ellwood & Tempest (1969) found that Gram positive bacteria, when grown in limiting magnesium conditions or in high concentrations of competing ions, contained much teichoic acid in the cell wall (presumably due to their higher affinity for magnesium ions) enabling them to sequester Mg^{2+} ions even when the ions were present in low concentrations. Levels of magnesium binding are thought to be similar in the presence of sodium or potassium cations for this reason, though is reduced by competition with calcium ions (Duckworth, 1977). These ionic exchange and competition processes are important to the dielectrophoretic responses since these ion types will have different mobilities and ionic radii, giving differential movement of particular ions through the cell wall polymeric material. Teichoic acid bound ions will also have a different speed of movement, compared to the freely mobile ionic phase, also influencing polarisation.

Upon switching to phosphate limiting conditions, the teichoic acids are replaced by teichuronic acids which have repeating carboxyl groups as the acidic part of the polymers (Lang *et al*, 1982). Teichuronic acids have less affinity for magnesium ions and so are less necessary under these conditions where magnesium is not limiting. Under these conditions less magnesium ions can bind to the wall polymers, affecting the overall charge on the cell surface and in turn modifying the nature of the cell polarisation and movement of ions through the wall. Growth in phosphate limiting conditions, while causing replacement of wall teichoic acids with teichuronic acids, maintains membrane lipoteichoic acid and this suggests that LTA are probably more essential than wall teichoic acid to cell function.

D-alanine molecules present on the polymers have free amino groups and these have been suggested to contribute to ion movement throughout the cell wall. Magnesium ions, when

interacting with walls lacking alanyl groups are bound to two phosphate groups on the teichoic acid. When alanine is present, its NH_3^+ group neutralises one of the negative phosphate charges as described above and allows only one of the phosphates to interact with the magnesium ions, shifting the position of the cation (Duckworth, 1977). Since the amino group of alanine can neutralise any one of several neighbouring phosphates, the movement of magnesium ions can be directed through the wall to the inner functional membrane on the polymer chain via the phosphate groups (Duckworth, 1977).

The presence of teichoic acids in cells walls affect expansion and contraction of walls under certain ionic and pH conditions resulting from their charged nature. This occurs since the negative charges of phosphated residues can repel each other, stretching the polymer and giving it an elongated appearance.

2.6.1.3 Synthesis of Teichoic Acids

Biosynthesis of these polymers have not been studied in much detail but has been found to again follow an analogous route to that of peptidoglycan, EPS and LPS polymers. Again the undecaprenyl phosphate lipid carrier molecule is involved, thus ensuring that these polymers are produced at the correct time.

Precursor formation, being either CDP-glycerol or CDP-ribitol, occurs in the cytoplasm of the cell by enzyme catalysis of CTP and the polyolphosphates, before assembly in the cytoplasmic membrane and then linkage to the wall peptidoglycan.

The main body of the teichoic acid polymer is then sequentially formed with recirculation of CMP, by addition of the activated nucleotide precursors, transferring phosphorylated glycerol or ribitol to the lipid bound linkage unit. Therefore a chain with a structure such as lipid-P-P-GlcNAc-$(PGly)_3$-$(PRibitol)_{40}$ is produced in this manner with each ribitol unit possessing a phosphate group. The same mechanism is used in the production of polyglycerol teichoic acids.

The complete polymer is then transported across cytoplasmic membrane and covalently attached to the peptidoglycan by a phosphodiester link between the GlcNAc and the muramic acid. Alanyl and glycosyl substituents are likely to be added during this assembly process by the specific enzyme action.

Teichoic acid position in cell walls is uncertain, though an explanation suggested by Duckworth (1977) proposed that peptidoglycan chains lie parallel to the cell surface and teichoic acids are attached to different layers throughout the wall. This produces a cross-linked

peptidoglycan mesh interwoven with other polymers (Hammond *et al.*, 1984). The wall has a very large negative charge from phosphate groups of teichoic acids or carboxyls of teichuronic acids and may also have a large number of negative charges from the uncrosslinked peptides e.g. free carboxyl groups of terminal D-alanine residues of peptidoglycan and the amino acid at the third position. These negatively charged groups tend to have cationic counterions such as sodium or magnesium associated with them. Teichoic acid polymers, being highly charged and having much flexibility, can be modified in arrangement and structure in different ionic environments (Ou & Marquis, 1970). With different ionic strength media or different ionic species present, speed of cell polarisation will be attenuated. These factors have also been documented as leading to a change in wall conformation, making transport of charge along the cell surface different and therefore influencing surface transduction mechanisms.

Frequency dependent capacitance mechanisms will also change with wall thickness and shape. In low ionic strength media, negatively charged centres are spaced regularly along the polymers and tend to repel each other giving extended rod like conformations and lengthening the cell walls (Doyle *et al.*, 1974). Dilute environments containing low concentrations of teichoic acids ionise a second phosphate group on the polymer, increasing the negative charge further. High ionic strengths (e.g. by 1 M NaCl), cause negative charges to be shielded by the high concentrations of cations and suppress ionisation. Therefore the polymers take on more compact nature or random coil arrangement (Doyle *et al.*, 1974). It can be imagined that different ions will shield to varying extents depending upon their valency and size, resulting in a range of wall modifications. Compaction would lead to the cell having smaller volume and may result in a reduced dielectrophoretic force acting on the cell. Shorter, thicker polymeric material would however, probably increase the capacitive response of the cell walls by increasing the distance of the wall over which the field acts.

To produce a large positive dielectrophoretic force, high particle volumes and low ionic strength suspending media are necessary. In the case of Gram positive bacterial cells, this media would produce larger cells and increase dielectrophoretic collection.

2.6.1.4 Lipoteichoic Acids (LTA)

These membrane teichoic acids have a polyglycerophosphate backbone linked by 1,3 phosphodiester bonds, such as that found in wall teichoic acid structure, but is also linked to a glycolipid molecule and bound in the outer part of the cytoplasmic membrane. LTA has a polymeric structure about 25-30 units long and may also have glycosyl and alanyl substituents which have significant influence on the ionic properties of the polymer, as previously discussed with wall teichoic acids.

Once the basic polymer is formed by the above mechanism they are linked to a species dependent glycolipid. With the hydrophobic end linked to a glycolipid and anchored in the cytoplasmic membrane by the fatty acid groups, the hydrophilic end of the molecule is free to extend through the cell wall into the external medium. The co-ordination between wall and membrane teichoic acids may act as a channel for essential divalent ions from the medium to the cytoplasmic membrane.

2.6.2 Teichuronic Acids

As previously stated, phosphate limiting conditions cause replacement of teichoic acids by these teichuronic acids. However, it is not only the level of phosphate in the local environment which influences levels of teichoic acid and teichuronic acid; Mg and Na are also important. Teichuronic acids also hold a negative charge but, unlike the teichoic acids, this is due to carboxyl residues rather than phosphate groups. Polymers of teichuronic acid are also involved in cation provision but are not as effective as independent teichoic acids at acquiring Mg^{2+} ions.

The structures of very few teichuronic acids are known but one component is always a uronic acid such as glucuronic acid or derived from an amino sugar e.g. aminomannuronic acid. Like teichoic acids, they are linear polysaccharides covalently attached to peptidoglycan at one end, though conversely they generally do not contain alanine substituents. The linkage to peptidoglycan may be a direct linkage from the reducing end of the polymer, through a phosphodiester bond to the muramic acid without the bridging sequence (Hancock, 1991).

Teichuronic acids have been found in several genera including *Micrococcus, Staphylococcus* and *Bacillus.* Certain bacteria such as *Micrococcus luteus* and *Bacillus megaterium* produce these polymers in all growth media, being unable to produce wall teichoic acids, whereas *Staphylococcus aureus* is generally unable to produce teichuronic acids at all.

2.7 Cytoplasmic Membrane

Though the cell wall is of a very different nature in many bacterial species, a structure found in both Gram positive and negative cells is the cytoplasmic membrane. The structure of this inner membrane is very different to that of the outer membrane of Gram negative cells. Rogers *et al.* (1980) contrasted cytoplasmic and outer membrane phospholipid compositions, finding a much higher phospholipid content in the cytoplasmic membrane than in the outer membrane. Though this membrane is more typical of a lipid bilayer than the outer membrane, a greater proportion

of PE was found in the outer membrane with more PG and diPG being found in the cytoplasmic membrane.

The cytoplasmic membrane has essentially the same composition in most bacteria, though has different protein content and function. It is metabolically more active than the outer membrane and contains a substantial amount of ATPase. This membrane also has a much greater diversity in protein content than in the outer membrane, contributing 60-70 % of its dry weight. As discussed previously, this insulating membrane has a very fluidic nature allowing easy diffusion of protein molecules, enabling polarisation by physical alignment of these ionised molecules. Diffusion of proteins however, is around 100 times slower than movement of lipid molecules, so even though the proteins have a larger size, they may not polarise as efficiently as lipid molecules. The resistance of this membrane is very great and effectively shields the internal components of the cells from electric fields until high frequencies are utilised.

2.8 Flagella and Fimbriae

Flagella, involved in the motility of bacteria can be up to 20 μm long (12-20 nm diameter), are generally helical in shape and held within the bacteria cell wall or envelope. They consist of polymers of protein subunits known as flagellin and may be governed by growth conditions e.g. pH. Flagella can vary in amino acid composition but predominantly contain aspartic acid and alanine, with moderate amounts of threonine, glutamate and glycine. Ionisation of these amino acids under different conditions can dictate the amount of polarisation of flagellin monomers. Polarisation of the protein monomers could feasibly cause physical orientation of the long flagella in an applied electric field.

Though fimbriae are much shorter than flagella or pili, only being up to 2 μm long, they occur in much larger numbers of up to 400 per cell. Again, their production can vary with growth conditions and even between cells of the same culture, yet when acting together in unison these surface structures can alter the overall polarisation of the cell.

Whenever long surface appendages are present on the surface, either as lipopolysaccharide, capsules or flagella, there is the potential for their structure to be implicated in the movement of charges across the surface and in dipolar rotation. This is due to their elongated appearance which can allow ions to move between the strands and interact with the molecules.

2.9 Overview of Bacterial Structure

Growth conditions have a governing effect upon how all of these polymer types are arranged within the cell and it has been seen that external conditions can alter the distribution of charge in the walls and overall structure, and so influence the polarisation response to an applied electric field. When undertaking experiments to observe the dielectrophoretic collection of bacterial cells, there are many potential variables which exist within normally growing individual bacterial cells. When scaled up to a bacterial concentrations of several million cells in an experimental suspension, there is the potential for many variations in cell structures and cell wall configurations, all interacting differently with the electric field. The many different responses to the field will combine to yield a general spectral trend. When confronted by the nature of this problem with only a single species of bacteria, it can be imagined that there will exist many different permutations of dielectrophoretic frequency spectra for every species in existence and for every possible growth condition. In addition, many microbiological applications for dielectrophoresis require the examination of mixtures of bacterial species, each with their own spectrum. This demonstrates the great diversity of possible frequency dependent responses to non-uniform electric fields.

2.10 Bacterial Surface Charge Characteristics

2.10.1 Measurement of Zeta Potential by Electrokinetic Study (Microelectrophoresis)

2.10.1.1 Background

The zeta potential at the plane of shear of a particle can be indirectly calculated from its electrophoretic mobility as determined by microelectrophoretic measurements. Under the influence of an applied d.c. electric field, particles within a suspension can be induced to move. A layer of bound ions will move with the particle at the plane of shear. The speed of movement of the particle is determined by the potential at this plane, the zeta potential.

Electrophoretic mobility u ($m^2\ V^{-1}\ s^{-1}$) has been defined by James (1991) as linear velocity v ($m\ s^{-1}$) per unit field gradient X ($V\ m^{-1}$) :

$$u = v/X \tag{2.1}$$

Three equations modelling the mobility of particles (Smoluchowski, 1921; Debye & Hückel, 1924; Henry, 1931) have been utilised in describing zeta potentials. However, the equations of Debye-Hückel and Smoluchowski are limited to specific ranges of ionic strength and particle sizes and only the equation of Henry is applicable to all conditions of electrophoretic mobility :

$$u = [D\zeta/6\pi\,\eta]\, f(\kappa a) \qquad (2.2)$$

where ζ is the zeta potential, D and η are the dielectric constant and dynamic viscosity of the suspension medium, $f(\kappa a)$ represents a power series of κa and a is the radius of curvature of the particle under study.

The electrophoretic mobility is thus related to several factors including the zeta potential, medium dielectric constant, particle size and to the Debye-Hückel screening length (λ_D).

2.10.1.2 The Zeta Potential of Bacterial Cells

Many studies examining the zeta potential of bacterial cells have been completed, often involving the selective treatment of cells to disturb and influence their mobility.

Most microbial cells have fixed ionic groups (e.g. amino, carboxyl, phosphate) in their outer layers, the degree of their ionisation varying as a function of pH. Decreases in ionic strength have been found to increase the thickness of the ionic atmosphere, which results in less screening of the surface charged groups. This leads to a reduction in the counterion presence and ionic groups further away from the surface become exposed, so contributing to the total surface charge. Changes in ionic strength result in groups at different levels on the cell surface contributing to the charge and may also cause changes in the conformation of certain molecules making up the outer layers of the cell.

Electrophoretic mobility measurements, though they can give an idea of the relative surface charges of bacterial cells, do not give any information about the location about the various charged groups involved.

Due to the presence of these ionic layers surrounding cells, a surface conductivity mechanism can be created. This surface conductivity has been shown to play an important role in the polarisation of cells in dielectrophoretic motion. This may also bring about a reduction in the electrophoretic mobility by causing a short circuiting mechanism, though this is not considered to be a major source of error (James, 1991).

2.10.1.3 The Cell Surface

The exact location of the cell surface has long been a topic of debate and can be seen to exist at different positions depending on the methods used to examine it. Normal light microscopy techniques would probably identify the surface as a flat plane bounding the cell from the surrounding media, being complicated by capsules and similar layers (Hancock, 1991). Electron microscopy demonstrates more detailed irregular structures extending from the cell and may pinpoint the surface in more detail. However, the open meshwork structures of many species also compounds the problem. Measurement by microelectrophoretic methods is dependent upon the ionic strength of the medium and can extend 1-2 nm from the outermost ionic groups, whereas more invasive techniques such as X-ray photoelectron spectroscopy (XPS) can look at the first few nanometres inside the cell and identify elemental composition (Mozes *et al.*, 1988).

2.10.1.4 Surface Characteristics of Bacterial Cells Influencing Electrophoretic Mobility

The surface charge of bacterial cells is determined by the density and nature of ionic groups and in turn, this is determined by the nature of the suspending medium and the morphology of the cell surface. Changes in the surface properties can be related to changes in electrophoretic mobility and would also be likely to result in shifts in dielectrophoretic frequency spectral form.

Increases in ionic strength of the suspending medium have already been shown to result in changes to zeta potential, causing it to become less negative and reducing the screening length by a compression of the double layer. This overcomes the repulsion between the negatively charged particles and can lead to an aggregation at very high ionic strengths as short range attractive Van der Waals forces come into play. This mechanism is commonly known as 'salting out'.

It is known that multivalent ions bring about this decrease in negativity of zeta potential more rapidly and thus decreases mobility. Higher concentrations of electrolytes are needed with monovalent ions to bring about the decrease to a zero zeta potential, whereas high concentrations of multivalent ions can cause a charge reversal and positive electrophoretic mobility. It was found using *K. aerogenes* that the anionic part of the salt solutions were much less important than the concentration of cations, since different anions resulted in identical mobility curves (Gittens, 1962). This also showed that there was no specific ion adsorption.

Titration curves of pH (which affect electrophoretic mobility values) have helped to characterise the nature of ionic surface groups by relating them to pK values. With one type of surface anion present e.g. carboxyl groups, a simple pH-mobility curve is found. At low pH values, the groups are protonated giving little net charge. Increasing pH causes dissociation of the weak acids giving an increase in mobility to a plateau value. Gittens & James (1963) found surface pK values of *K. aerogenes* corresponding to the presence of carboxyl groups. This anion was also found exclusively on the surface of *E. coli*, giving pK values of 2.9 (Davies *et al.*, 1956).

As the degree of dissociation increases, the surface potential becomes more negative and mobility becomes more rapid. Therefore, pH values above the pK of the groups would cause an increase in these dissociated forms and an increased negative mobility.

Many bacterial species have mixed surface groups e.g. amino, carboxyl, phosphate groups. These surfaces are generally positively charged at low pH due to NH_3^+ ionic groups. As the pH increases, the cells become more negatively charged as protons are sequentially lost from carboxyl and phosphate groups, reaching a plateau at around pH 6. Therefore at physiological pH values the surface will exhibit a negative charge. There is a further increase in negative mobility due to the loss of the proton from the amino groups at greater than pH 9. Studies using XPS have shown that increasing amounts of phosphate significantly increases negative mobility and is thought to be a major component of the surface charge density.

Due to the effect of surface morphology, different surface groups are able become exposed meaning different cultural conditions will influence the pH-mobility curve. To examine the ionic composition of cell surfaces by electrophoretic mobility studies it is first necessary to standardise running conditions and bacterial growth conditions, since variations have an effect on cell size, structure and composition. Only then can specific treatments be related to modifications of ionic atmosphere. Differences have been related to production or exposure of hydrophobic or hydrophilic moieties or to the presence of plasmids which allow expression of fimbriae or other surface components.

2.10.2 Hydrophobicity

An alternative measure of surface characteristics is the assessment of cellular hydrophobicity. It may be expected that a surface displaying a high proportion of charged polar molecules would undergo a greater interaction with water molecules compared to non-polar surfaces. The lack of an attraction between a molecule, or particle, and water is termed *hydrophobicity*. Its main function is to remove the film of water between two surfaces and so allow short range interactions to occur.

This feature of the microbial cell surface has significant importance in determining adhesion properties of bacterial cells e.g. in biofilms and in the adherance of pathogenic bacteria to epithelial cells.

2.10.2.1 Methods of Measuring Hydrophobicity

Many methods of measuring the extent of bacterial hydrophobicity have been described which fall into two categories, those which measure the hydrophobicity of the whole cell, and those which can be brought about by hydrophobic areas on the surface even though the remainder of the cell may be relatively hydrophilic (Rosenberg & Doyle, 1990; Van der Mei *et al.*, 1991)(table 2.6). The wide diversity of techniques are subject to fundamental difficulties and so can produce a range of differing results.

Method	Comment
Contact Angle Measurement Generally a bacterial suspension filtered, partially dried and a small water droplet placed on the lawn. Contact angle, θ, measured by : $\theta = 2 \tan^{-1} (2h/b)$ where h=height and b=base width of the droplet. Greater hydrophobicities found with greater angles. Surface free energies also found.	Problems with liquid purity, even distilled or demineralised water. Errors found in surface tensions and drying procedure. Disagreement over technical aspects. Fate of appendages during drying stage unclear and may affect their normal configuration.
Microbial Adhesion to Hydrocarbons (MATH) Based on partitioning of cells between immiscible hydrocarbon-aqueous system. Hydrophobic cells adhere to hydrocarbon layer, hydrophilic strains found in aqueous phase after mixing. Hydrocarbon layered over aqueous suspension of cells and vortexed. Layers allowed to separate and O.D. of aqueous part measured before and after mixing. Hydrophobicity expressed as a percentage.	Vessels need to be identical and clean since adherance to vessel can occur. Care to avoid attachment of hydrocarbon droplets to cuvette wall. Ionic strength, vortexing time, cell density, composition and pH of buffer, hydrocarbon type, volume etc. can cause variability. Hydrophobicity can be caused by only part of the cell. Raised ionic strength can help separate weakly hydrophilic bacteria by reducing electrostatic interactions.

Kinetic MATH test and other partitioning tests Based on above method. Measures successive decrease in O.D. (compared to initial) with increasing vortex times up to 60 s using different volumes of hexadecane. Slope of removal used to plot rate of adhesion (removal coefficient).	Back extrapolation to y intercept (hydrocarbon volume near zero) often gives positive results. Separation of components dependent on temperature and concentration. Is more quantitative method than above. Experiments can be done with other immiscible solutions e.g. dextran and PEG (hydrophobic bacteria partition in the PEG, hydrophilic in dextran).
Hydrophobic Interaction Chromatography Cells in buffer applied to columns of hydrophobic Sepharose beads and % of cells eluted by various agents found. Expressed as hydrophobic index e.g. $HI = \frac{(\%\ \text{control eluted} - \%\ \text{octyl eluted})}{(\%\ \text{control eluted})}$ Hydrophobic bacteria bound stronger to the hydrophobic beads and give high (near 1) HI values.	Dependent upon the type of buffer composition, temperature, nature of the hydrophobic ligand and density in matrix, pH of eluent (low pH eluent gives high amounts of adsorption in the column)
Salt Aggregation Test Dilutions of ammonium sulphate (4.0-0 M) made in sodium phosphate buffer pH 6.8 (0.002M). Bacteria mixed with equal volumes of each solution. Minimal concentration found at which aggregation occurs. Hydrophobic bacteria clump at lower salt concentrations. Higher concentrations cause loss of electrostatic stabilisation and allow Van der Waals forces to cause aggregation.	Dependent on cell density, type of ammonium salt, pH, temperature and duration of mixing

Table 2.6 : Methods of measuring bacterial cell hydrophobicity.

Hydrophobicity techniques all measure some parameter of bacterial adhesion however, there is little correlation between all of the tests described.

2.10.2.2 Correlation Between Zeta Potential and Hydrophobicity Measurements

It may be expected that there should be a inverse relationship between the surface charge and hydrophobicity. Increased presence of charged polar molecules favours interactions with water molecules through hydrogen bonding and should lead to a reduction in hydrophobicity; it has been found that a reduction of negative charges increases the hydrophobicity (Mozes & Rouxhet, 1990). Techniques for measuring the surface charges of cells do not provide any details about the distribution of the groups over the cell surface. Electrophoretic mobility measures the net charge of the whole cell and therefore the cell may have little or no charge yet may be covered by equal numbers of many positive and negative groups, all of which will lead to a reduction of the hydrophobic effect.

The bacterial cell surface does not exist solely as a hydrophilic or hydrophobic material and should be considered as a mixture of groups, with charged molecules interspersed with regions of apolar groups. Indeed, Marshall & Cruikshank (1973) showed that some bacteria are only hydrophobic at one end of the cell and adhere by attachment through one pole. The hydrophobicity of an organism may depend on the surface exposure of lipophilic components and as mentioned, this exposure in turn can be regulated by the nature of the ionic atmosphere.

The measurement of hydrophobicity is often influenced by electrostatic interactions determined by the potential and thickness of the diffuse layer and is affected by variations of pH and ionic strength. Hexadecane droplets have actually been found to have a negative charge in aqueous suspension, so adhesion does not solely measure hydrophobicity of a cell but also a degree of its surface charge. Reduction of electrostatic interactions by adjusting conditions to the isoelectric point of the cells or by compaction of the ion atmosphere by increased electrolyte concentration causes the zeta potential to become much reduced. Decreases in electrostatic interactions thus allow expression of true hydrophobic interactions.

Hydrophobicity and zeta potential are both indications of the composition and structure of cell surface. Van der Mei *et al.* (1993) conducted experiments to examine the relationships between zeta potential and hydrophobicity as measured by the kinetic MATH test at a range of pH values and used XPS to study the elemental structure of several strains of *Streptococci.* The hydrophobicity was found to generally be greatest near the isoelectric point of the cells when electrostatic interactions were absent. However, very hydrophilic strains were pH independent. This is due to the forces between the cells and the water phase being significantly greater than those involved in hydrophobic attractions, therefore they stay in the aqueous layer irrespective of the pH. By examination of the surface composition, these strains generally had a low N:C elemental ratio, though high isoelectric points of between pH 3 and 5 suggested they should be

rich in protein components. Both increased hydrophobicity and isoelectric points were associated with increasing N:C and decreasing O:C ratios. This agrees with the findings of Mozes & Rouxhet (1990) who described inverse correlations of hydrophobicity with surface oxygen concentration. Hydrophobicity was also correlated with the surface carbon found in the form of hydrocarbon such as protein, phospholipid, lipoprotein or lipopolysaccharide.

Bacterial cells have been found to be more hydrophilic with greater N:P ratios (however, yeasts were more hydrophobic) (Mozes *et al*, 1988; Mozes & Rouxhet, 1990). This correlation may be due to bacterial nitrogen being present in various surface groups, many of which are polar, whilst yeast nitrogen is found mainly as protein.

2.10.3 Factors Affecting Hydrophobicity and Zeta Potential

Electrophoretic mobility has been show to become affected by factors such as surface potential, cell size and shape, ionic strength, pH, temperature and medium viscosity. Since the majority of these factors are fixed during experiments changes in electrophoretic mobility can be attributed to variations in cell size, shape or zeta potential (Gilbert *et al.*, 1991a). Experiments have been conducted to examine changes in electrophoretic mobility following specific chemical treatments. Often anionic surfactants are used to detect lipidic components of a surface, where the nonpolar moieties of the surfactant become bound to the lipid and result in increases in mobility by the raised negative charge (Dyar, 1948). Substitution of amino groups by chemicals such as p-toluenesulphoyl chloride also cause a higher negative charge.

2.10.3.1 Effect of Growth Source

Van der Mei *et al.* (1993) found that cells became more hydrophilic when grown with sucrose as a carbon and energy source compared with growth on glucose or lactose. This correlated with low N:C and O:C surface ratios after sucrose growth, and lowest isoelectric points of cell growth on glucose.

Often bacteria undergo changes in size and shape in relation to nutrient availability. For example, cells often become smaller and more spherical when starved (Rosenberg & Sar, 1990). In addition, increases in both hydrophobicity and surface charge have been noted upon starvation, possibly caused by a reduction in the proportion of charged groups on the surface (Bar-Or, 1990). Increases in hydrophobicity were also found where the available nutrients were provided to cells as solid media (Wadström, 1990).

2.10.3.2 Effect of Growth Phase

There have been discrepancies between hydrophobicity measurements relating to the phase of cell culture growth. Wadström (1990) found that cells in exponential phase were more hydrophobic than stationary phase cells. With the species examined by Savoia *et al.* (1990) using the MATH test, and *E. coli* and *S. epidermidis* studied by Gilbert *et al.* (1991b), the converse was found to be true with cells becoming more hydrophilic during periods of active growth. However, this may also have been affected by electrostatic interactions as previously described.

2.10.3.3 Temperature

Hydrophobicity has been found to be sensitive to heating at 80-100 °C and to protease treatment (Wadström, 1990). However, culture growth at 20 or 42 °C compared to 37 °C did not yield significant differences in hydrophobicity.

2.10.3.4 Antibiotic Effects

The resistance of cells to various antibacterial agents such as antibiotics, often lead to changes in surface properties. Giordano *et al.* (1993) showed differences in outer membrane protein profiles and LPS after exposure of *Pseudomonas aeruginosa* to even sub MIC levels of antibiotics such as difluoroquinolone, aztreonam and netilmicin, often accompanied by increased resistance.

Dealler (1991) also examined the effect of exposure of bacterial species to certain antibiotics. It was suggested that exposure, even to sub-MIC levels, modifies bacterial surface characteristics causing a shift in cell zeta potential from negative to positive values before any physical cell death was observed. The cause was proposed to be a result of transmembrane potential changes affecting zeta potential.

The adhesion of bacteria to epithelial cells are particularly important in pathogenic infections and are brought about by non-specific attractions between the hydrophobic moieties on both host and microbial surface, causing attraction by Van der Waals forces. Often antibiotics are administered to combat infection and even when they are reduced to sub-inhibitory levels they have still been found to have an action by reducing adhesion of bacterial cells by decreasing hydrophobicity (Savoia *et al.*, 1990; McKenney *et al.*, 1994). Antibiotic exposure may alter the structures responsible for initial attachment or prevent the interaction between specialised molecules on surfaces.

Antibiotics which affect cell wall synthesis (benzylpenicillin), protein synthesis (erythromycin) and nucleic acid synthesis (rifampin and nalidixic acid) all caused decreases in the hydrophobicity of *Staph. aureus*. This is due to their effect on surface protein regulatory mechanisms and possibly to limitation of the adhesion properties exhibited by basic or non-polar amino acids such as lysine, leucine and isoleucine (Wadström, 1990).

Studies on sub-MIC antibiotic effects showed increased negative charge and increased hydrophobicity with quinolone antibiotics accompanied by loss of fimbriation (Loubeyre, 1993). The chelation of Mg ions could also give rise to the fimbriae loss by destabilisation of the membrane.

2.10.3.5 Species

The response of different bacterial species is known to be very diverse in practically all types of experiments due to their different compositions and structures (table 2.7). Electrophoretic mobility and hydrophobicity measurements are no exception.

Species	Charge/hydrophobicity	Reference
Campylobacter jejuni	highly negatively charged surface, weakly hydrophobic	
Escherichia coli	low hydrophobicity	Savoia *et al.*, 1990
Klebsiella pneumoniae	very hydrophilic	Savoia *et al.*, 1990
Proteus spp.	very hydrophobic	
Staphylococcus aureus and other coagulase negative staphylococci	high negative surface charge	Wadström, 1990
Thermophilic dairy streptococci spp.	hydrophilic and slightly negatively charged	Van der Mei *et al.*, 1993

Table 2.7 : Results of hydrophobicity and charge measurements with several bacterial species obtained by a variety of methods.

2.10.3.6 Presence of Surface Appendages

Cell to cell contact is facilitated by a displacement of the surrounding double layers and water shells, allowing short range attractive forces to come into action (Stratford & Wilson, 1990), though this is opposed by the electrostatic charge of the cells and stearic hindrances by surface molecules such as glycoproteins (Greig & Jones, 1976). Many of these surface components also contribute to the cellular hydrophobic effect (Hogg & Manning, 1987). Proteins and amphipathic molecules, like lipoteichoic acids or LPS, can inhibit hydrophobic interaction and so help to evade adhesion processes such as phagocytosis. Fimbriae or fibrils are also thought to have an influence.

Fimbriae

Elongated structures have a tip charge which require less energy to penetrate the repulsion field surrounding cells, thus minimising the repelling force between surfaces (Stratford & Wilson, 1990). Therefore, cells which possess fimbriae may have increased hydrophobicity. Irvin (1990) found bacterial pilins to be fairly hydrophobic (30 % of the pilin protein due to hydrophobic amino acids) and that surface hydrophobicity of cells increases upon expression of fimbriae.

When fimbriae are present with a capsule layer on the surface of cells, the electrophoretic mobility has been found to be relatively unchanged (Richmond & Fisher, 1973). Capsulated organisms have a high negative charge due to the presence of glucuronic acids and negative charges in the capsular material which completely overrides any effect due to fimbriae.

Capsular Layers

The presence of capsule reduces the adhesion to hydrocarbons giving hydrophilic characteristics. Electrophoretic mobility of *Aerobacter aerogenes* was found to increase to a maximum during the early exponential phase and then become constant in the stationary phase. This has been attributed to changes in capsule size (Plummer & James, 1961). The movement of capsulated cells indicated a simple carboxyl surface and an absence of amino groups and lipid.

Bayer & Sloyer (1988) looked at the effect of capsular antigens (K1, K29 and K30) and the presence of O antigen (O9) and variety of rough LPS strains on the mobility of *E. coli* . Between pH 6 and 7, the capsules showed a negative charge, with K1 (sialic acid) being the

strongest, followed by K29 and then K30. Presence or absence of the O9 antigen (LPS) had no effect on the charge of capsule-minus strains.

Surface Polymers

The high negative surface charge of species of *Staph. aureus* has been related to the wall polymers such as ribitol and glycerol teichoic acids (Wadström, 1990) as described in section 2.6.1.1. The pH-mobility curve of *Staph. aureus* was found to be non-sigmoid in shape with a maximum value at pH 4-5. When teichoic acid was removed from the surface, this peak was removed. The unusual shape of the curve was thought to be due to the pH dependent change in the configuration of surface teichoic acid molecules.

It is not known, however, whether lipoteichoic acids can be transported to the surface and expose their fatty acids. Though these parts of the cell wall have been shown to be important in surface charge, the mobility of spheroplasts have surprisingly been found to be identical with those of normal cells.

Dickson & Siragusa (1994) performed comparisons of surface charge and hydrophobicity for rough and smooth strains of *Listeria*. They found that the rough strains had both higher negative cell surface charge and hydrophobicity measurements compared with smooth strains. They attributed this to a lack of specific proteins in the cell wall.

Protein Components

Hydrated proteins interact with several water molecules, mainly at their surfaces. However, the amount of water bound to the protein surface is dependent upon the nature of the amino acid composition. Ionic amino acids can bind up to 6 water molecules per residue, compared with about one molecule per polar amino acid residue, whereas hydrophobic amino acids do not bind any water molecules. Therefore, protein composition can affect the degree of hydration, hydrophobicity, surface charge and can also determine dielectrophoretic polarisation responses. Water molecules have a rotational relaxation time of 2-3 ps, so greater hydration can increase the speed of polarisation compared to hydrophobic proteins, due to the high presence of rapidly relaxing water molecules. Increasing buffer salt concentrations generally result in increased salt binding. This results in less water being bound to the protein and causes an apparent increase in the hydrophobicity. However, increased salt concentration also modifies the bulk water structure by altering the H bonding.

2.11 Antibiotics

Antimicrobial agents can be divided into two groups, those which are produced by other micro-organisms (usually termed antibiotics), and those which are synthetic.

Antibiotics are substances produced by micro-organisms which are able to inhibit other micro-organisms (Tortora *et al.*, 1995). Though normally they are naturally produced compounds, the term is now often used to include semi or wholly synthetic compounds.

Since the discovery of penicillin, a large number of different antibiotics have been studied and research continues to find and produce new and more effective examples. Many antibiotics commonly used for clinical applications are modified versions of those produced by micro-organisms in order to improve their potency and efficacy.

Most clinical antibiotics in use today originate from either *Streptomyces* species, *Bacillus* species and the fungi *Penicillium* and *Cephalosporium* (Bowman & Rand, 1980). A number of common antibiotics are shown in table 2.8.

Antibiotic group	Example	Mode of action
Carbapenems	imipenem	Cell wall synthesis inhibition.
Cephalosporins	cefotaxime, cephalexin	Cell wall synthesis inhibition.
Glycopeptides	vancomycin	Cell wall synthesis inhibition
Penicillins	penicillin G	Cell wall synthesis inhibition
Semi-synthetic penicillins	ampicillin, methicillin, oxacillin	Cell wall synthesis inhibition
Polypeptides	bacitracin	Cell wall synthesis inhibition
	polymixin B	Injury to membranes
Quinolones	nalidixic acid	Inhibition of DNA replication
Rifamycins	rifampicin	Inhibition of RNA synthesis
Aminoglycosides	streptomycin, gentamicin	Protein synthesis inhibition
Chloramphenicol		Protein synthesis inhibition
Macrolides	erythromycin	Protein synthesis inhibition
Tetracyclines	tetracycline, chlortetracycline	Protein synthesis inhibition
Antifolates	sulphanilamide, trimethoprim	Inhibit folate synthesis

Table 2.8 : Mechanisms of action of some common antibiotics.

2.11.1 Modes of Action of Antibiotics

Antibiotics can act to either cause bacterial cell death (bactericidal) or inhibit further bacterial growth (bacteriostatic). There are several mechanisms of action of common antibiotics :

2.11.1.1 Inhibition of Cell Wall Synthesis

Interference during peptidoglycan assembly can occur during the formation of the linear strands or during the final cross-linking between the strands. Certain antibiotics (e.g. bacitracin) act by preventing the dephosphorylation of lipid pyrophosphate to lipid phosphate in the peptidoglycan synthesis (section 2.5.2.4). Others (e.g. vancomycin), prevent strand formation by inhibiting the separation of the intermediates from the membrane bound lipid and interrupting cell wall synthesis. The β-lactam antibiotics (penicillins and cephalosporins) act in a manner which prevents the final transpeptidation step. Penicillins bind to the penicillin binding proteins (PBP) on the cytoplasmic membrane and, due to their structural similarity to the strand alanine dipeptides, inactivate the transpeptidase enzymes and prevent the formation of the peptide bond, so inhibiting cross linking of the peptidoglycan strands. An example of a semi-synthetic penicillin, ampicillin, is shown in figure 2.9. Carbapenem antibiotics also possess a β-lactam ring and effectively inhibit cell wall synthesis (Tortora *et al.*, 1995).

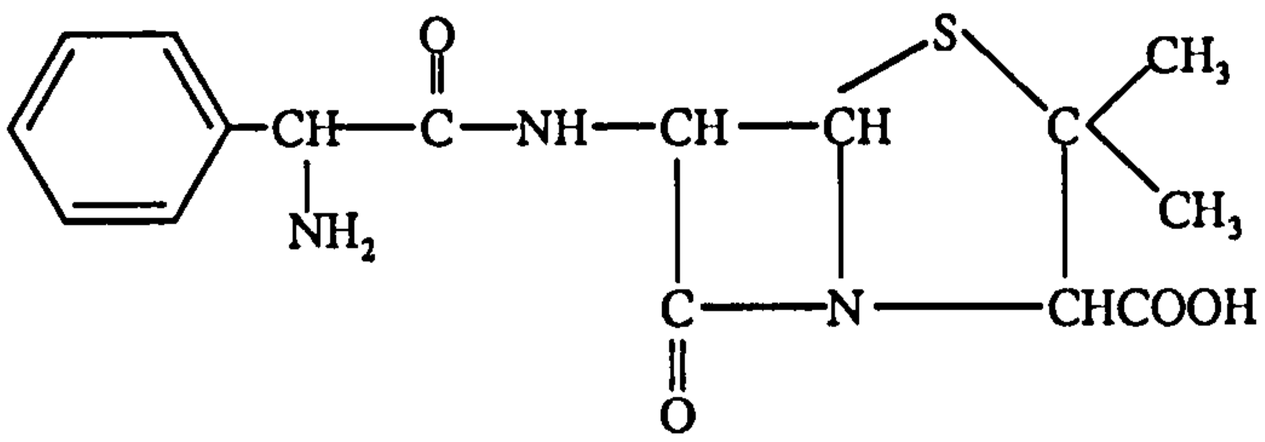

Figure 2.9 : Structure of ampicillin.

2.11.1.2 Inhibition of Protein Synthesis

Protein synthesis at the 70S procaryotic ribosomes is the target site for a range of antibiotics. As well as in bacteria, 70S ribosomes are also present in eucaryotic mitochondria. Therefore, toxicity to host cells may occur with some antibiotics. Generally, antibiotics which inhibit protein synthesis at the ribosomes of bacterial cells do so bacteriostatically. One exception to

this is are the aminoglycosides which do result in the death of the cells (Edwards, 1980). Often antibiotics against protein synthesis can be classified by which ribosomal subunit their action is directed upon. Such inhibition may be active against protein synthesis initiation, amino acyl tRNA binding, translocation and elongation of the peptide chain or by inhibition of peptide bond formation.

The aminoglycosides attach to and inhibit the function of the 30S ribosomal subunit. One of the most studied aminoglycosides, streptomycin, has been found to have several effects which ultimately lead to cell death. Its action on protein synthesis has been found to involve interference with the binding of formylmethionyl-tRNA (preventing correct protein synthesis initiation) and also the misreading of the mRNA. The major site of streptomycin action is the S12 protein in the 30S ribosomal subunit. Tetracyclines also act on the 30S subunits, preventing binding of the amino acyl tRNA molecules to the ribosome acceptor (A) binding site.

Several other antibiotics have inhibitory effects on the 50S ribosomal subunit. One such antibiotic is chloramphenicol. The D-threo isomer of chloramphenicol (figure 2.10) exerts its inhibitory activity against the 50S ribosomal subunit by preventing peptide bond formation between amino acids, which occurs by the peptidyl transferase reaction (Edwards, 1980). The action is thought to be due to a distortion of the subunit which causes a mis-orientation of the tRNA and amino acid. Macrolide antibiotics (erythromycin) have an activity at the same subunit but their effect is to prevent translocation of the nascent polypeptide chain from one binding site to the next, therefore preventing elongation of the chain (Franklin & Snow, 1975; Edwards, 1980).

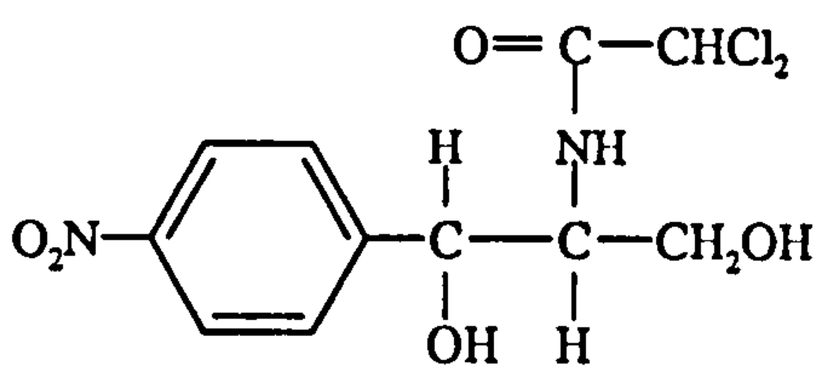

Figure 2.10 : Structure of chloramphenicol.

2.11.1.3 Injury to Membranes

Membrane active antibiotics have been classified into three groups : those which cause a disorganisation of the membrane, those which alter the membrane permeability, and those which affect the membrane enzyme systems. The polymixins e.g. polymixin B as outlined in table 2.8, are specific to Gram negative cells (Edwards, 1980). The activity of these polypeptide antibiotics relies on binding of the structure to membrane phospholipids (possibly by interaction of the lipid portion of the antibiotic with the non-polar region of the membranes and binding of the polar heptapeptide with the polar region of the phospholipid). Their polycationic structure causes displacement of membrane-stabilising divalent cations and so disrupts the membrane integrity causing rapid loss of small molecules, including nucleotides, from the cells (Tortora *et al.*, 1995).

Similar antibiotic activities which change the permeability of the membranes, e.g. by gramicidins or valinomycin, can cause rapid and significant loss of ions and metabolites from the cells and eliminate the selective nature of the cell structure.

2.11.1.4 Inhibition of Nucleic Acid Replication and Transcription

Several antibiotics have an inhibitory activity against the nucleic acid replication steps of bacterial cells. They can generally be classified by the nature of their action. Some affect the nucleotide biosynthesis (e.g. antifolate drugs), others bind to DNA and prevent replication and transcription (e.g. mitomycin C, actinomycin D), and still others have activity against replication and transcription enzymes (e.g. rifampicin, nalidixic acid). Rifampicin specifically inhibits the initiation of DNA transcription. It does not prevent initial binding of RNA polymerase to the DNA template but interferes with the formation of the initial phosphodiester bond in the RNA chain. Nalidixic acid was the first quinolone antimicrobial and led to development of the fluoroquinolones (including norfloxacin and ciprofloxacin), which also target DNA gyrase (Tortora *et al.*, 1995). This antibiotic is a synthetic antimicrobial which inhibits bacterial DNA replication by targeting a subunit of the enzyme DNA gyrase necessary for the replication of bacterial chromosomes. The structure of nalidixic acid is shown in figure 2.11.

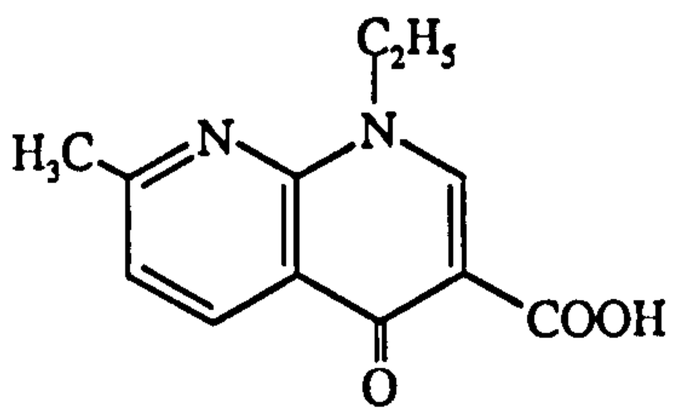

Figure 2.11 : Structure of nalidixic acid.

2.11.2 Entry of Antibiotics into Bacterial Cells

In order for an antibiotic to reach its target site, it is often necessary for it to be transported throughout the cell. The different structure of Gram positive and Gram negative cell envelopes is the basis of the differential specificity of some antibiotics. The entry of antibiotics across the outer membrane is achieved through passive diffusion or self-promoted uptake (Russell & Chopra, 1990a). The passive entry of the molecules through the outer membrane has been proposed to occur through the large number of water filled porin proteins expressed in the membrane (Hancock & Bell, 1988). As mentioned earlier, the porins OmpC and OmpF act as non-specific transmembrane channels for hydrophilic molecules, having an exclusion limit of 600-700 Da. Since the majority of antibiotics have molecular weights of below 1000 (Chopra & Ball, 1982) it is possibly more likely that the presence of these porins can easily convey passage of the antibiotics by simple diffusion processes, making it unnecessary for large amounts of binding to occur. Indeed, the low number of porins present in the outer membrane is likely to be one of the antibiotic resistance mechanisms found in *Ps. aeruginosa*. Porin based diffusion pathways have been proposed for many types of antibiotic including β-lactams, chloramphenicol, tetracyclines and a variety of quinolones. Self-promoted uptake involves the destabilisation and disorganisation of the outer membrane. Hancock & Bell (1988) described the self promoted uptake mechanisms found with certain polycationic antibiotics. As discussed earlier, the LPS molecules of Gram negative cells are stabilised by divalent ions such as Mg^{2+} or Ca^{2+}. These ions can be displaced by the polycationic antibiotics such as polymixin and aminoglycosides, or other permeabilisers, and act as the initiation site for the self-promoted antibiotic uptake through the disruption of the membrane structure. Recent work has suggested that quinolones may not utilise the self-promoted uptake pathway (Marshall & Piddock, 1994).

Passage of antibiotics to target sites within the cytoplasm must be preceded by the crossing of the cytoplasmic membrane. Antibiotics usually cross the cytoplasmic membrane of bacterial

cells by passive diffusion or by active transport mechanisms which derive energy from ATP or the proton motive force (pmf). The passage of hydrophobic antibiotics (e.g. nalidixic acid, trimethoprim, rifampicin), which have difficulty penetrating the outer membrane, generally use the passive mechanism across the cytoplasmic membrane. Active transport usually can only occur when the drug is similar in structure to a naturally occurring molecule and is able to interact with the normal transport carrier (Russell & Chopra, 1990a). With several antibiotics, such as streptomycin and tetracycline, the process is an energy-dependent active transport mechanism.

2.11.3 Resistance

Resistance to antibiotics may be either natural or acquired. A common intrinsic means of resistance is the permeability barrier of the Gram negative outer membrane to some large or hydrophobic antimicrobial molecules (e.g. macrolides and hydrophobic β-lactams) which are unable to diffuse through the porins (Nikaido, 1989). Acquired resistance is based on either mutations in chromosomal genes or from the possession of extrachromosomal DNA (plasmids or transposons) which encode products conferring resistance (Russell & Chopra, 1990b).

2.11.3.1 Common Modes of Resistance

There are several ways in which resistance is achieved by microbial cells. These are outlined in table 2.9.

The majority of these mechanisms are caused by the inclusion of extrachromosomal plasmids, known as R factors, containing genes which code for cellular changes allowing a resistance mechanism to develop. These plasmids are easily transferred between cells in a population (by conjugation) and may often contain genes for resistance against several antibiotics.

2.11.4 Effects of Sub-Inhibitory Levels of Antibiotics on Bacterial Cells

While the dosage of antibiotics in clinical use is determined on the basis of inhibition of bacterial growth *in vitro*, antibiotics are known to still have significant effects on the pathogenicity of bacterial cells even at subinhibitory concentrations.

Several studies and reviews on the action of sub-MIC levels of antibiotics have been published (Lorian, 1980; Lorian, 1985; Chopra & Linton, 1986; Savoia *et al.*, 1990; Jacques *et al.*, 1991; Loubeyre *et al.*, 1993). The most common effect is the changes in cell morphology produced by these sub-MIC levels, resulting in filamentous cells, oval cells or cells with irregular shapes in Gram negative species, and cells with wall thickening and abnormal sizes in Gram positive

species. Additional effects have been observed on the adhesion, surface charge and hydrophobicity of sub-MIC treated cells. Each of these responses are likely to have pronounced effects on the dielectrophoretic polarisation mechanisms and consequent DEP collection.

Mode of resistance	Comment
Drug inactivation	Commonly occurs when β-lactam antibiotics are used. β-lactamase enzymes synthesised by resistant micro-organisms and cleave a covalent bond in the β-lactam ring (Tortora *et al.*, 1995). Chloramphenicol inactivated by chloramphenicol transacetylase production in resistant cells (donates an acetyl group from acetyl-CoA to the antibiotic molecule).
Prevention of access to the target site	Can include permeability differences and active efflux mechanisms which prevent build up of inhibitor concentration within the cell. The Gram negative outer membrane confers resistance against antibiotics which are unable to penetrate it effectively.
Alteration of the target site	Changes in specific target site may make the drug unable to act. A single enzyme mutation in bacterial folic acid pathway may decrease sulphonamide affinity and increase activity of the normal substrate, *p*-amino benzoic acid, conferring resistance.
Bypassing the target metabolic step	Gram negative bacteria are more resistant to β-lactam antibiotics, as they possess little peptidoglycan. Gram positive cells which have large amounts of peptidoglycan are therefore more sensitive. Some microbes e.g. Mycoplasmas do not synthesise peptidoglycan and therefore are resistant to β-lactam antibiotics.
Overproduction of an inhibited enzyme	Trimethoprim attacks the dihydrofolate reductase enzyme in the folic acid synthetic pathway. Resistant cells produce this enzyme plus a modified version with a lower affinity for trimethoprim, which therefore allows sufficient folic acid production.

Table 2.9 : Common resistance mechanisms in bacteria.

2.12 Research Objectives

The fundamental aims of the research in this thesis are both to continue the development of an image analysed dielectrophoretic system and to use this equipment to assess the dielectrophoretic responses of bacterial cells following surface and cell wall treatments.

These investigations included:

- Examination of experimental variations and compilation of standardised conditions and parameters for dielectrophoretic experiments to allow detailed comparison of DEP spectra and attempt to ensure their reproducibility.

- Investigation of *Klebsiella* EPS modifications upon the dielectrophoretic frequency spectrum by alteration of C:N ratio within the growth medium. The effect of mutagenesis to remove ability for EPS production on the frequency spectrum will be investigated.

- Investigation of changes in DEP collection following treatment of cells with antibiotics to affect size, shape and wall thickness. This will involve the use of antibiotics effective against cell wall synthesis, protein synthesis and DNA replication at doses ranging from sub-MIC values to inhibitory concentrations.

- Exposure of EDTA treated *E. coli* cells to lysozyme in order to induce the formation of spheroplasts, to assess the effect of peptidoglycan degradation on the dielectrophoretic spectrum.

- To investigate the effectiveness of the image analysed dielectrophoretic system as a device for the selective counting of bacterial cells and other particles.

Chapter 3 : Materials and Methods

3.1 The Dielectrophoretic System

3.1.1 Electrode Manufacture

3.1.1.1 Electrode Deposition

The microelectrode structures used in the experiments were manufactured by photolithographic techniques in the clean room of the Department of Electronics, University of York as a modification to the method of Price *et al.* (1988).

Super premium microscope slides (BDH, UK) were scoured with mechanical abrasive and stored in filtered deionised water until required. Each slide was then washed in boiling acetone before being blown dry with N_2 gas.

Aluminium metal was evaporated onto the surface of the slides to give a thickness of 1000 Å. Photoresist (Shipley 1400-27) was filtered through a syringe filter unit (0.22 µm pore GVHP filter, Millipore), applied to the surface of the slides and spun at 1500 rpm for 30 s using a photoresist spinner (Headway Research Inc., Texas) to give a uniform layer of resist. The slides were heated for 1 min at 95 °C prior to UV exposure.

To create the electrode structures, a previously designed electrode mask was aligned over a slide and exposed to UV light (365 nm) for 7 s. The resist was developed with MF 319 developer (Ciba-Geigy) and the slide baked for 15 min at 95 °C.

Aluminium not overlaid with exposed photoresist was etched away by immersion of the slide in a 1:1:1 solution of nitric acid, glacial acetic acid and orthophosphoric acid. Remaining photoresist was then removed using boiling acetone, leaving behind the aluminium electrode arrangement.

An adhesion promoter (1:1:98 v/v/v, deionised water:Selectiplast HTR AP3:isopropyl alcohol) was applied to the slides and spun at 1500 rpm for 15 s and then baked for 1 min at 95 °C. Further photoresist (Selectilux HTR 3-200, Ciba Geigy) was spun onto the slide at 550 rpm for 15 s, followed by baking at 95 °C for 35 min.

UV exposure was then carried out for 1 min 45 s through a second mask designed for making a channel arrangement. Developing of the resist in Selectiplast HTR D-2 (Ciba Geigy) was followed by a rinse in isopropyl alcohol, drying with N_2 and a final bake at 150 °C for 80 min.

The electrode structures created were parallel bars each of 50 µm width, separated by gaps of 5 µm. The thickness of the electrodes (1000 Å) enabled a non-uniform field to exist between the electrodes.

3.1.1.2 Chamber Assembly

A chamber was mounted over the top of the slide to allow a continuous recirculation of the particle suspension over the electrodes (Betts & Hawkes, 1994). This was achieved by a modification to the method described in Archer *et al.* (1993a), in that a glass cover was used to improve optical quality over that found with lower grade perspex. The glass allowed a closer working distance and better microscope resolution.

Strips of double sided sticky tape were placed over the top of the electrode photoresist channel, in order to accentuate channel depth. A standard microscope slide (Chance Propper Ltd, England) was cut lengthwise in half (76 mm x 13 mm x 1 mm) and stuck to the tape constituting the cover of the channel. Holes (3.5 mm diameter) were also drilled through this glass plate and lengths of vinyl tubing (1.5 mm I.D., 2.1 mm O.D.) were attached through perspex blocks, allowing circulation of the suspension through the chamber. The assembly was then secured with adhesive (Araldite Rapid epoxy) to give a watertight seal. Channel depth in the chamber was measured as approximately 150 µm.

Wires were used to connect the electrodes to the function generator. To ensure a good electrical contact, silver paint (Agar Scientific) was used to bind the wires to the electrode tabs and secured with epoxy adhesive.

3.1.2 System Set-Up

3.1.2.1 Spectrophotometer Method

As previously described by Hawkes *et al.* (1993), the electrode chamber was placed on its side and attached to a support in the light beam of a spectrophotometer (LKB Ultrospec II). The electrodes were positioned such that the beam passed through the chamber immediately downstream of the electrode bars. This prevented any obscuring of collection by the electrodes. As particles passed through the light beam, a continuous measurement of absorbance could be achieved. Absorbance data was collected via an analogue : digital converter and continually

recorded by the central computer. A trace showing changes in particle concentration over the time course of the experiment was produced.

The particle suspensions used in the experiments (see section 3.1.3) were recirculated through the chamber and ancillary equipment by a peristaltic pump (Gilson Minipuls-3) operating at a range of flow rates from 0.02 $ml.min^{-1}.rpm^{-1}$ up to a maximum of 0.96 $ml.min^{-1}$. The suspension was continuously recirculated by the pump via tubes entering and leaving the spectrophotometer, moving particles from a sample reservoir, through the electrode chamber and finally returning to the reservoir. Conductivity and temperature were also continuously monitored with a flow-through conductivity probe (RE3877Tx, EDT Instruments). This information was directly transferred to the central computer during experiments. A secondary function of the pump was to bubble air through the suspension in the reservoir to keep the particles from settling and facilitating efficient mixing, maintaining a homogeneous suspension.

The electrode wires were electrically connected by coaxial cable to a function generator (Hewlett Packard 8116A), which was used to create an electric field of desired frequency and strength between the electrodes. This was computer controlled via a Hewlett Packard Interface Bus HP 82335A. A 50 Ω shunt allowed constant output from the generator.

Control of the equipment, data recording and data analysis, were all performed by the central computer (AST Bravo 486) using in-house experimental software programs. Using these, it was possible to obtain results from incremented frequency, voltage, pump speed or duration of applied field values and to perform repeated field applications under defined conditions.

3.1.2.2 Image Analysed Dielectrophoresis

An additional method of quantifying dielectrophoretic collection by image analysis was also used. This has been described previously by Archer *et al.* (1993a) and Quinn *et al.* (1995). The system is shown diagramatically in figure 3.1.

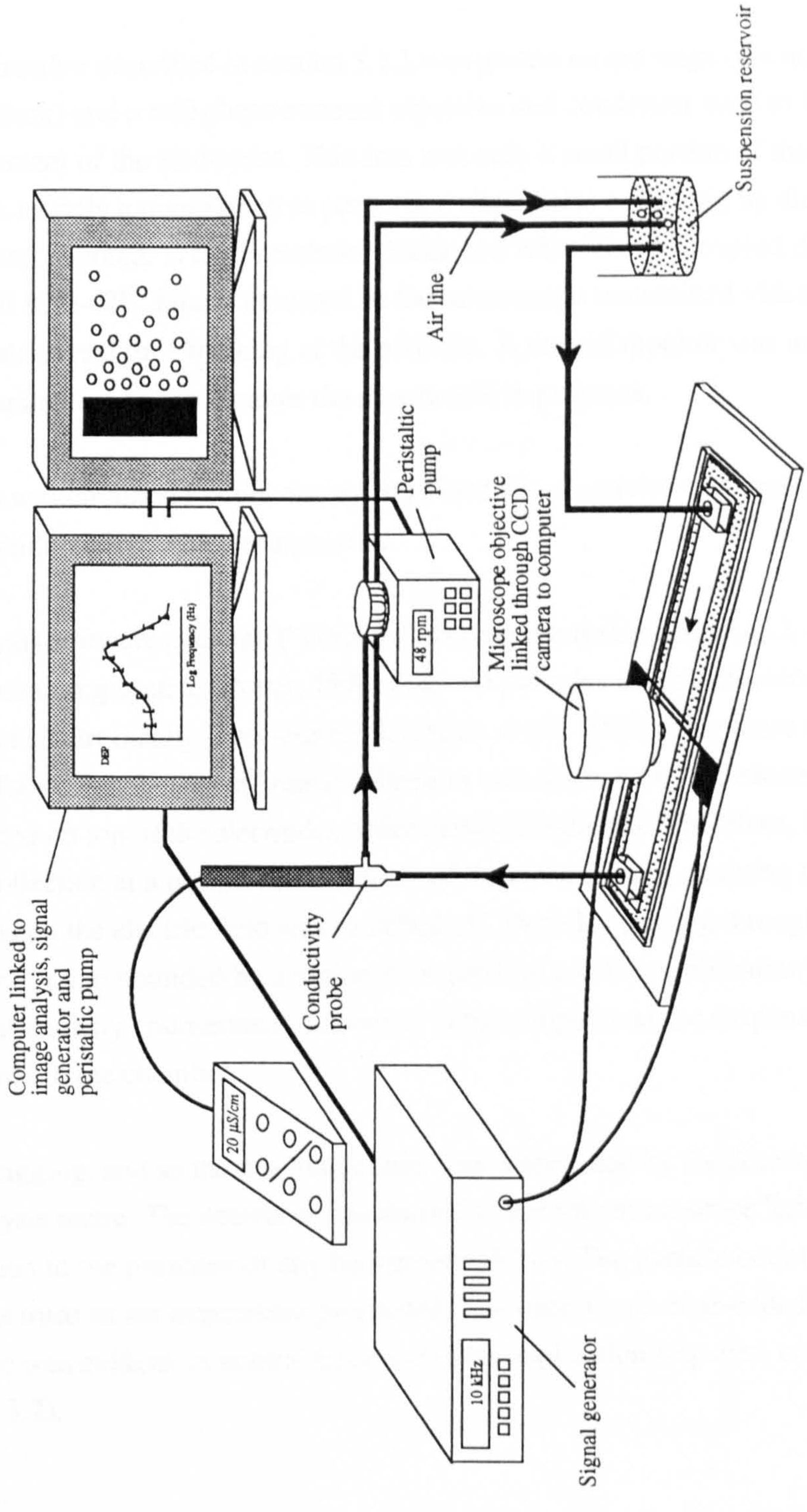

Figure 3.1 : Image analysed dielectrophoretic system.

The electrode chamber described in section 3.1.1 was placed on the stage of a microscope (Labophot-2, Nikon) and a x40 phase contrast objective and condenser used to focus on an area just downstream of the electrodes. This area was only a small portion of the overall electrode length, so only a representative proportion of particles collecting by dielectrophoresis were observed and counted. A high resolution black and white charge coupled device (CCD) camera (Ikegami ICD-42E, Japan) mounted on the microscope transmitted video images to a monitor and enabled real time tracking of the particles. A second monitor was used to display experimental parameters and to monitor the experiment in progress.

The suspension was circulated as previously described. Conductivity was again measured by a flow-through conductivity probe arrangement.

An image analysis software package ("Domino", Perceptive Instruments Ltd.), modified from a rapid colony counting system (Pover, 1990) detected particles using differences in contrast and tagged them electronically. Previous work (Quinn *et al.*, 1995) using these microelectrode arrangements, found that dielectrophoretic collection was obscured by the electrodes and that particles collected on top of the electrodes under certain conditions. Therefore, it was decided to enumerate collection at a position downstream of the electrodes by counting the package of cells released when the electric field was switched off. Particles passing through a previously defined counting frame bounded by a region 8800 μm^2 (at a x40 magnification), could be tagged and continuously enumerated (4 counts.s^{-1}) by computer as the suspension was recirculated through the chamber.

The extent of tagging, and so the resulting count, was determined by the detection level set in the image analysis menu. The detection was also influenced by microscope light levels and focus, in addition to the presence of any background debris. The particle count was displayed as a continuous trace as the experiment proceeded. The trace was colour-coded so that each part of the sequence was evident. A normal trace and pulse application sequence consisted of four stages (figure 3.2).

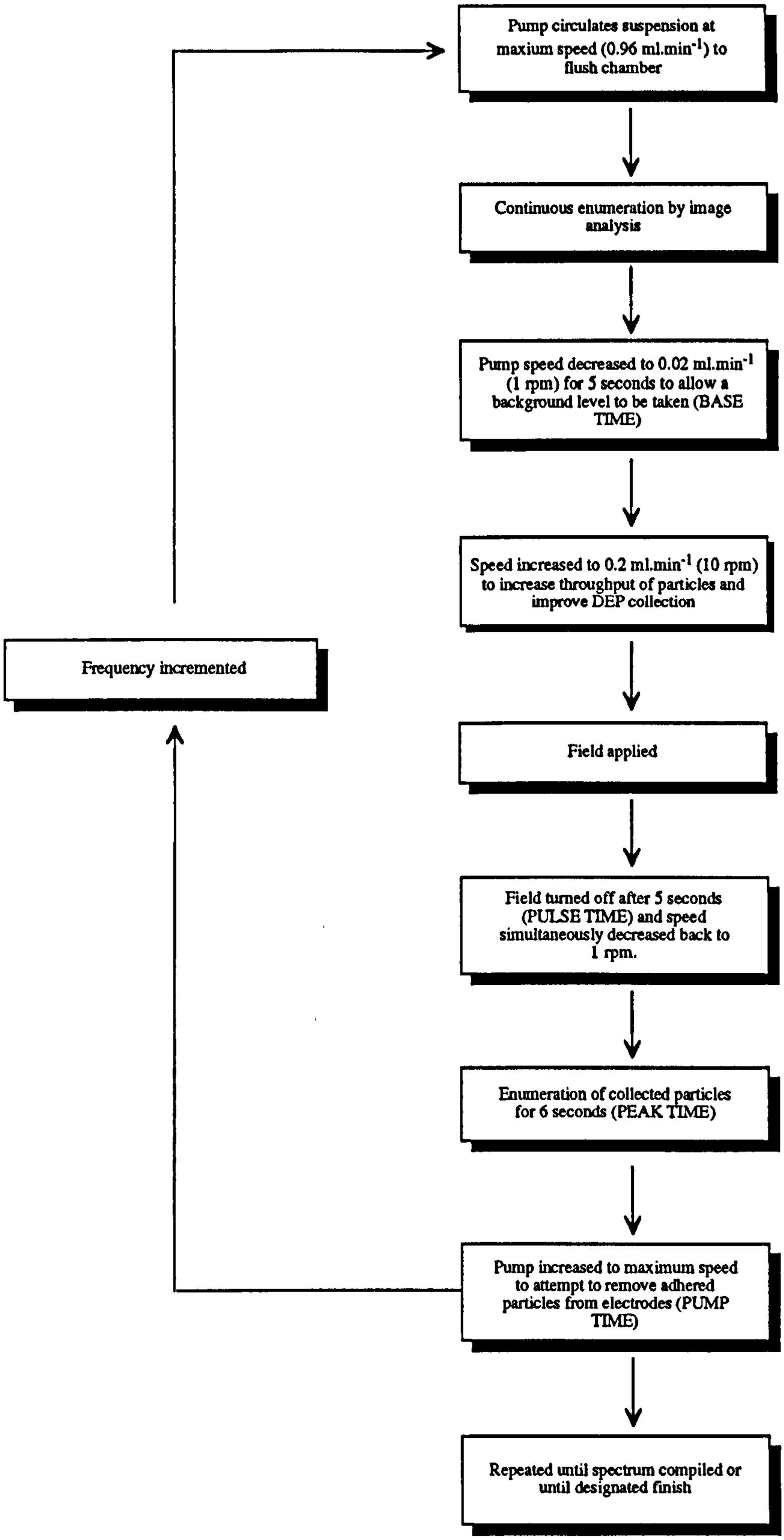

Figure 3.2 : Typical trace and pulse application sequence.

- A background count of the normal particle level passing through the chamber was taken, typically at a pump speed of 1 rpm (0.02 ml.min^{-1}) and 5 s. This period was referred to as the *Base Time*.

- The electric field was applied to the electrodes of the desired frequency, voltage and duration and the pump speed increased to 10 rpm. This period was referred to as the *Pulse Time*.

- The field was turned off and pump again slowed to 1 rpm, where the particles were released from the electrodes and enumerated. This period was referred to as the *Peak Time*.

- The pump was increased to its maximum speed and used to flush through the electrodes to attempt to remove any particles remaining on the electrode surface. This period was referred to as the *Pump Time*.

The number of particles collected was automatically calculated by subtraction of the baseline count (from the Base Time) from the total peak count (from the Peak Time). By this method, any background debris was also accounted for and subtracted from the particle count.
This was important since particles often remain adhered to the electrodes and background after the field was removed, even after rapid flushing.

Parameters were set at their optimum values by observing the trace, e.g. if the peak time was too short and the maximum particle count was not being recorded, this would be apparent.

Three general counting techniques were available for use within the image analysis : full count, downward points count and area count. Each of these could be set with the controlling software. Each of the methods have both advantages and disadvantages to their application which are demonstrated in figure 3.3.

Full Count	Downward points count	Area count
Method : Counts individual particles which have been computer tagged	Method : Tags and counts southern-most points of particles	Method : Counts number of pixels present in an object
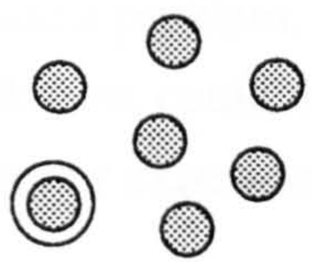	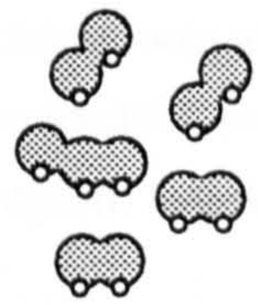	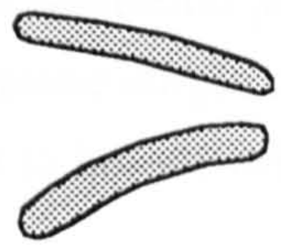
Advantage : Counts individual particles so is accurate	Advantage : Can distinguish single particles in close proximity and count them as individuals	Advantage : Is useful when elongated particles are present. Will show differences when comparing with smaller particles
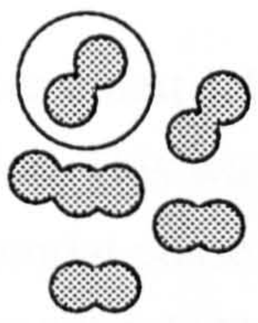	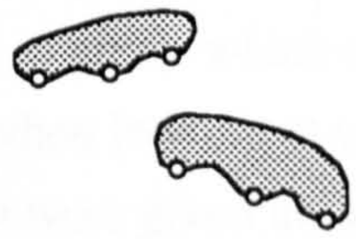	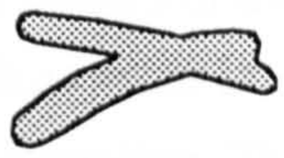
Disadvantage : Particles in close proximity tagged as one particle and count therefore underestimated in high concentrations or where cells clump	Disadvantage : Single cells which are uneven in shape may be counted as more than one particle	Disadvantage : Particles in close proximity tagged as a single particle. Mutual areas of overlapping cells will only be counted once meaning large areas will not be counted. In addition this method is easily influenced by changes in microscope focus, light levels, detection etc.

Note : Circled areas are examples of those counted by the image anaysis

Figure 3.3 : Image analysis detection methods.

Routine experiments were generally operated using the full count method. The full count labelled each particle and counted each tag individually. However, if two particles were close together they could have been given the same tag, so multiple particles might have been counted as one, leading to an underestimation of the dielectrophoretic collection. This may not have been such a significant difference in routine experiments but could have become very important when using high concentrations of cells, or elongated cells, in which there was a higher probability of them coming into close contact. As the number of particles released from the electrodes increased, the probability of this merging increased. Therefore the increase in actual particle concentration was matched by the merging effect, causing a plateau of observed collection. At suspension concentrations or collection efficiencies where this might have become a problem, a pulse length experiment was also run. The detection saturation point, at the plateau, could then be found and provided the collection with the 5 s pulse length used in frequency experiments was not in this region, saturation was deemed not to be occurring.

The downward points count enumerated the most extreme points of the particles. Therefore, groups of particles would have several downward points, allowing them to be distinguished. However this also had a drawback in that individual particles could have been of a non-uniform shape, possibly leading to multiple counts being made for a single particle.

The area count calculated the number of pixels which made up the tagged images of the particles. This was of particular use when looking at very long cells, such as those in exponential phase of growth or which were given treatments leading to elongation. This also had the advantage that it could be used when particles were tending to clump or when high concentrations of particles were used which were in close contact. Disadvantages of this method, were that the tagging for the area count was very dependent upon the level of detection, and so it was important to keep light levels and microscope focus consistent when this counting method was used. In addition, the count could have a tendency to underestimation, especially when cells overlapped or with groups of cells, since they shared common pixels.

Count measurements were converted into a form which could then be displayed, or transferred to spreadsheet or statistical analysis packages. The results of the dielectrophoresis experiments were also automatically transferred to a graph producing software package ("FigP", Biosoft, U.K.).

3.2 Sample Preparation

3.2.1 Latex Particles

Stock suspensions of polystyrene latex beads were obtained as suspensions in distilled water at concentrations of 1.8×10^{10} particles.ml^{-1} (Interfacial Dynamics Corporation, USA). These particles were available in a variety of sizes and with different functional groups attached to the surface having a range of charge densities. The particles normally used for DEP experiments were 2.04 μm in diameter and had sulphate groups chemically bonded to the surface with a total charge density of 7.1 μC.cm^{-2}, with an area of 225 Å^2/charge group.

For standard experiments, a clean glass sample bottle was repeatedly washed in deionised water (Purite) to remove any residues which could alter conductivity of the suspension. A 12 μl sample of the latex stock suspension was then added to 10 ml of deionised water in the sample bottle. This was well mixed and gave a final concentration of approximately 2×10^7 particles.ml^{-1}. Precise concentration was determined by haemacytometer counts.

3.2.2 Bacterial Maintenance

Bacterial species used in experiments conducted in this thesis were :

Enterobacter cloacae (laboratory strain) (30 °C)
Escherichia coli 10418 (NCTC)(37 °C)
Escherichia coli 8114 (NCIMB)(37 °C)
Escherichia coli 39323 (clinical isolate, York District Hospital)(37 °C)
Escherichia coli R35258 (clinical isolate, York District Hospital)(37 °C)
Klebsiella aerogenes 9527 (EPS+) (NCIMB)(30 °C)
Klebsiella aerogenes 9528 (EPS-) (NCIMB)(30 °C)
Klebsiella (Enterobacter) aerogenes (clinical isolate, York District Hospital)(37 °C)
Klebsiella (Enterobacter) aerogenes A1(Sl) (Prof. Ian Sutherland, Edinburgh)(30 °C)
Klebsiella (Enterobacter) aerogenes 87(Sl) (Prof. Ian Sutherland, Edinburgh)(30 °C)
Klebsiella (Enterobacter) aerogenes A4O31 (Prof. Ian Sutherland, Edinburgh)(30 °C)
Klebsiella (Enterobacter) aerogenes A4CRO (Prof. Ian Sutherland, Edinburgh)(30 °C)
Klebsiella (Enterobacter) aerogenes A4CR-TS (Prof. Ian Sutherland, Edinburgh)(30 °C)
Klebsiella oxytoca 1004 (NCFB)(30 °C)
Pseudomonas aeruginosa 10662 (NCTC)(37 °C)
Salmonella enteritidis (clinical isolate, York District Hospital)(37 °C)
Serratia marcescens (laboratory strain)(30 °C)
Shigella sonnei (clinical isolate, York District Hospital)(37 °C)

Bacillus cereus (laboratory strain)(30 °C)
Bacillus globigii (Yorkshire Water plc., U.K.)(30 °C)
Bacillus subtilis 10106 trpC2 (NCIMB)(30 °C)
Micrococcus lysodeikticus (Sigma, U.K., freeze dried culture)(30 °C)
Staphylococcus aureus 6571 (NCIMB)(30 °C)
Staphylococcus aureus (clinical isolate, York District Hospital)(37 °C)
Streptococcus faecalis (laboratory strain)(37 °C)

NCIMB : National Collections of Industrial and Marine Bacteria (Aberdeen, U.K.)
NCTC : National Collection of Type Cultures (Public Health Laboratory Services, London, U.K.)
NCFB : National Collection of Food Bacteria (AFRC Institute of Food Research, Reading, U.K.)

All cultures except the *Klebsiella* strains were maintained by growth at their optimum temperatures (shown above, in parentheses) on nutrient agar (Oxoid, U.K.) plates, and on bacterial preservative beads. Nutrient agar, supplemented with 1 % glucose, was used as the solid growth medium for the *Klebsiella* strains.

Bacteria were routinely subcultured and Gram stained to assess purity. Identity of Gram negative species were regularly confirmed using API20E identification strips (BioMerieux, U.K.).

3.2.3 Scanning Electron Microscopy

Samples of several of the bacterial species used were examined by electron microscopy to observe general cell size and structure. This was of benefit to provide explanations for observed results using these species.

Nutrient broth cultures of *Staph. aureus, B. subtilis, E. coli* 10418 and *Ent. cloacae* were grown overnight at optimum temperatures, with shaking. From each flask a 25 ml volume was removed and harvested by centrifugation (Mistral High Speed 18) at 10 000 rpm for 10 min. The pellet was washed in phosphate buffered saline (PBS) and then fixed by resuspension in 1 ml 3 % SEM quality glutaraldehyde (Agar Scientific, U.K.) in an Eppendorf tube. Fixation was allowed to proceed for 30 min. The Eppendorf tubes were microcentrifuged at 6500 rpm and the pelleted cells washed several times in distilled water. The cells were resuspended in 1 ml 50 % acetone, left for 5 min and then harvested by microcentrifugation. This dehydration procedure was repeated through a series of 70 %, 90 % and 100 % acetone respectively. The cells were finally resuspended in 1 ml 100 % acetone. Vellum tissue envelopes were prepared

and filled with the 100 % acetone cell suspensions. The cells were then Critical Point Dried before being sprinkled onto aluminium stubs, covered with a layer of Sellotape glue, gold sputter coated and examined by SEM (Hitachi S2400) at an accelerating voltage of 8 kV.

The results of the electron microscopy can be found in Appendix 5.

3.2.4 Bacterial Suspensions for Spectrophotometric Use

For efficient quantification of dielectrophoretic collection using the spectrophotometer system, high cell concentrations were necessary. Bacterial cells used in positive DEP experiments needed to be suspended in low ionic strength medium such as deionised water. A washing procedure to remove growth media was used to prepare the samples.

A 100 ml volume of sterile broth culture medium (normally Nutrient Broth, Oxoid) was inoculated with the organism and grown overnight with shaking at the optimum temperature for growth (usually 37 °C). The culture was harvested after 16 h by centrifugation at 10 000 rpm (MSE High Speed 18), washed in 50 ml 0.1 M KCl, followed by further centrifugation, and then with at least three changes of deionised water. The centrifuged pellet was then resuspended in 25 ml deionised water and a volume of 10-15 ml placed in a sample bottle for use in experiments.

3.2.5 Small Scale Bacterial Preparation for Image Analysis

An overnight culture of the organism was made in nutrient broth as above and a 1-2 ml sample taken from the culture in a sterile syringe. The bacteria were filtered through a sterile 0.2 μm pore syringe filter (Minisart, Sartorius) and backwashed with deionised water to resuspend the bacterial cells. This process was repeated a minimum of five times to remove the growth media and reduce the conductivity of the suspending medium. The sample was resuspended in deionised water and adjusted to the desired concentration. Suspensions used for image analysed dielectrophoretic experiments were made so they normally had an $O.D._{510}$ in the region of 0.11 Absorbance Units.

3.2.6 Sample Viability

It has been shown previously that differences in dielectrophoretic frequency spectra exist between viable and non-viable cells (Crane & Pohl, 1968) and this has been exploited for separation purposes (Pohl & Hawk, 1966). To obtain consistent spectra, it was necessary to establish whether there was a significant decrease in viability over the course of a standard

experimental period due to the physical action of the circulating system and presence of the dilute environment, i.e. deionised water.

An overnight culture of *Staph. aureus* was made in nutrient broth and a suspension prepared by the filtration method in the same way as for image analysed dielectrophoresis. A 1 ml sample was taken from the suspension and used to perform viable counts, by decimal dilution in sterile Ringers solution and plate counts on nutrient agar. This was taken to be time T_0, constituting the initial control viable cell concentration.

The suspension was then circulated around the system as previously described, at the maximum pump speed (0.96 $ml.min^{-1}$). Air was continually bubbled through the suspension to keep the cells from settling. At 15 min intervals, aliquots were removed from the reservoir, for a circulation period of 3 h. Viable counts were performed on the samples with incubation at 37 °C overnight. Colony counts were plotted against circulation time to show the viability of the cells over the experimental period. This procedure was also repeated for a Gram negative species, *Shig. sonnei.*

3.3 Standardisation of Experiments

3.3.1 Standardisation of Dielectrophoretic Parameters

A major consideration when performing dielectrophoretic experiments was the number of system and biological variables. The dielectrophoretic response to non-uniform electric fields is known to vary considerably under different experimental conditions (Pohl, 1978). To compare spectra produced by these methods, it was therefore necessary to implement a set of standardised conditions under which to run experiments. Parameters were chosen as a consequence of results found experimentally as described in later sections. These values were found to produce good levels of dielectrophoretic collection or spectral definition for the particles examined.

Selected experimental values are set out in table 3.1.

Parameter		Experimental Value
Voltage		
	Spectrophotometer	16 V peak-peak r.m.s., sinusoidal voltage
	Image Analysis	12 V peak-peak r.m.s., sinusoidal voltage
Conductivity		
	Latex particles	4.45-4.5 $\mu S.cm^{-1}$
	Bacterial cells (Spectrophotometer Method)	45-50 $\mu S.cm^{-1}$
	Bacterial cells (Image Analysis Method)	24-30 $\mu S.cm^{-1}$
Frequency Range		1 kHz-50 MHz
Pulse Length		5 s
Pump Speed		Release speed 1 rpm (0.02 $ml.min^{-1}$)
		Collection speed 10 rpm (0.2 $ml.min^{-1}$)
		Flush speed 48 rpm (0.96 $ml.min^{-1}$)
Spectrophotometer Wavelength		525 nm
Base Time		5 s
Pulse Time		5 s
Peak Time		6 s
Pump Time		5 s
Normal Particle Concentration		
	Latex suspension	12 µl stock in 10 ml deionised water
	Bacterial suspensions	Final $O.D._{510} \approx 0.11$

Table 3.1 : Standard parameters used in dielectrophoretic experiments.

Other considerations were :

- The necessity for constant microscope focus and light levels. Therefore removal of the electrode chamber for storage was undertaken without disturbance of the microscope set up.

- Use of an inverted image analysis detection mode for latex particles. Normal image analysis detects dark areas on a lighter background. However, due to their white colouration, latex particles could not be tagged by the normal method. Inverted mode produces a negative image, making the latex particles darker than the background.

3.3.2 Standardisation of Particle Concentration

The extent of dielectrophoretic collection was known to be dependent upon the concentration of particles in the suspension. As may be expected, higher concentrations of particles present in the suspending medium allow a larger number of particles to be influenced by the electric field and migrate under its action, thus increasing dielectrophoretic collection. The level of collection over the frequency range would increase relative to that exhibited by lower particle concentrations. To compare the spectra taken on different occasions, it was also necessary to maintain the particle concentration, or be able to account for spectral differences.

The dielectrophoretic force is affected by volume and other particle characteristics. It will therefore have different strengths for diverse particle types and it is also desirable to compare and contrast the extent of this force for the different particles. By performing these experiments at similar concentrations, or by at least knowing the concentration, the relative collection per concentration unit can be calculated.

3.3.3 Correlations of Particle Concentration

Experiments undertaken initially with bacterial cells used changes in optical density of the suspension as a measure of changes in particle concentration. The optical density of each bacterial species (including *E. coli* 10418, *Ent. cloacae*, *Staph. aureus*, *Ps. aeruginosa* and *B. subtilis*) was correlated against total count or viable count.

A stock suspension of pure bacteria was made in deionised water. Dilutions of this stock were further made in deionised water, the optical density of each suspension being measured as absorbance at 510 nm and 600 nm using an LKB Ultrospec II spectrophotometer. Due to typical experimental absorbances being around 0.11 Absorbance Units, these correlations were only carried out with suspensions having O.D. less than 0.15-0.2 Absorbance Units.

The viable count of each suspension was then assessed by serially diluting in quarter strength Ringer solution (Oxoid), plating onto nutrient agar (Oxoid) and incubating at 37 °C for 24 h. Total counts were also performed using a 0.02 mm deep bacterial counting chamber (Thoma, Weber Scientific International Ltd).

Optical density was then correlated as linear regressions with total or viable counts. The optical density of latex particle suspensions was also correlated against haemacytometer counts in a similar manner.

3.3.4 Electrode Calibration

Though experimental parameters such as voltage, pulse duration, conductivity and growth conditions could be standardised, the efficiency of the electrodes could vary on a day to day basis, due to factors such as build up of biofilm or oxide layers. To assess the extent of this fluctuation, a calibration step was performed prior to each dielectrophoresis experiment using latex particles, which do not have the variations associated with growth.

A suspension of latex particles was prepared in deionised water as previously described in section 3.2.1. This suspension was circulated and a field of 10 kHz frequency and 12 V applied 30 times. Dielectrophoretic collection was quantified and the mean value found. The amount of DEP collection per unit of particle concentration was obtained on a daily basis.

3.4 Dielectrophoretic Experiments

3.4.1 General Spectra

Suspensions of the particles under study were prepared as described in section 3.2. These were circulated through the electrode chamber and around the system. The conductivity of the suspension was measured and adjusted to the standardised value. Conductivity was increased by slow addition of microlitre volumes of a 0.1 M KCl solution. Decreases in conductivity were produced by repeating the preparation step or by further washing of the suspensions in deionised water. All experiments were performed in an air conditioned laboratory at a temperature of 21 °C.

3.4.1.1 Spectrophotometer Spectra

The suspension was circulated through the system and a wavelength of 525 nm selected on the spectrophotometer. After allowing time for equilibration of the cell suspension and stabilisation of initial conductivity parameters the dielectrophoretic cycle was begun in a similar manner to that previously shown in figure 3.2.

The absorbance of the normal circulating background level was subtracted from the absorbance peak caused by release from the electrodes of the package of previously collected particles at each frequency. This gave a measure of the amount of particles collected at each frequency and was plotted as a spectrum. A spectrum was obtained in this manner for frequencies between 1 kHz and 50 MHz. Spectra were obtained for latex particles and for bacterial species *Ps. aeruginosa, E. coli* 8114, *Ent. cloacae* and *B. subtilis*.

3.4.1.2 Image Analysis Spectra

Bacterial suspensions were circulated and an electric field of set frequency applied to the electrodes. Image analysis was used to detect the number of particles released from the electrodes after the field was turned off and the background level was subtracted to give the net amount of collection at each frequency.

Frequency dependent dielectrophoretic spectra were obtained for latex particles and the bacterial species, *B. subtilis, Staph. aureus, E. coli* 10418, *Ps. aeruginosa, Ent. cloacae* and *Serr. marcescens,* by either full count or downward points count methods to compare with results from the spectrophotometric method.

3.4.2 Pulse Length

3.4.2.1 General Trends

The circulating suspension was also exposed to electric fields of increasing duration. Cycles were performed where the pulse length was increased with fixed field frequency.

A latex particle suspension was prepared as in section 3.2.1. A field of 10 kHz was applied to the electrodes for 1 s. The amount of dielectrophoretic collection (quantified by image analysis) in this time was calculated and recorded. The cycle was repeated with pulse lengths being incremented up to a maximum of 30 s. The amount of collection for each pulse duration was plotted.

This procedure was repeated for *Ps. aeruginosa, Serr. marcescens, Ent. cloacae* , *E. coli* 39323 (clinical isolate) and *E. coli* 10418 bacterial species. The bacterial suspensions were circulated through the chamber and subjected to a field of 1 MHz frequency and 1 s duration. After determining the amount of dielectrophoretic collection up to a duration of 30 s, the data was plotted.

In each case, however, the frequency of the field was first chosen by running frequency spectra of the suspensions as in section 3.4.1. The frequencies chosen were those giving maximum levels of dielectrophoretic collection.

These experiments were of importance since they could be used to determine whether a level of detection or electrode saturation had been reached under normal operating conditions, as described in section 3.1.2.2.

3.4.2.2 Effect of Increasing Pulse Length on Frequency Spectra

Mean dielectrophoretic frequency spectra were produced for *E. coli* 10418 as described above, using a pulse duration of 5 s. This was repeated with the same suspension and conductivity using pulse lengths of 10, 15 and 30 s, observing any differences in collection efficiency at each frequency. Similar experiments were repeated for other bacterial species.

3.4.2.3 Pulse Length at Different Frequencies

To examine the relationship between pulse length and frequency dependent DEP collection in more detail, experiments were performed using *E. coli* 10418 to observe the effect of pulse length increases at specific frequencies.

An *E. coli* suspension was prepared for image analysed dielectrophoretic experiments. A mean pulse length graph, varying from 1-30 s, was obtained as described previously at a 1 kHz frequency. This was repeated for 10 kHz, 100 kHz, 1 MHz and 10 MHz frequencies.

3.4.3 Voltage

Since field strength is an important determinant of DEP collection voltage is a critical parameter and significantly affects the size of the dielectrophoretic force.

A suspension of *Ps. aeruginosa* 10662 was prepared and circulated through the system. A field of 1 MHz was applied at a voltage of 1 V r.m.s. (over a 5 μm electrode gap). The amount of dielectrophoretic collection was quantified by the full count method. The voltage was stepped up at 1 V intervals, to a maximum of 16 V r.m.s., and the amount of collection found at each voltage. This data was then plotted.

3.4.4 Pump Speed

By varying the speed of the pump during the application of the field, more cells or particles could be brought into the area of effective field. To examine this relationship, a bacterial suspension of *Ps. aeruginosa* 10662 was used.

The controlling program was able to vary the pump speed via parameters input into the main set-up menu. Pump speed was adjusted to circulate at 1 rpm when the field (10 V, 5 s, 1 MHz) was applied, the collected cells being quantified by image analysis. Subsequent cycles had successively incremented pump speeds up to 25 rpm. This range was repeated five times and a

mean collection obtained for each speed. Release and flush speeds were kept at the standard values set out in table 3.1.

3.4.5 Multiple Pulse Applications

Using a suspension of latex particles, an electric field of 10 kHz, 5 s duration and 12 V r.m.s. was applied to the electrodes. The amount of collection was established and the cycle repeated 30 times to obtain a mean level of collection. This data was then plotted.

Since there is a general circulating background level of latex particles, the multiple pulse application program was used to obtain a mean level using the same conditions but without the function generator linked to the electrodes. This gave an idea of the amount of background noise which could be attributed to debris or biofilm adhered to the chamber and unaffected by dielectrophoretic collection.

3.4.6 Effect of Increasing Suspension Conductivity

3.4.6.1 General Trends

To examine the effect of conductivity on the frequency spectra of bacteria, a suspension of *E. coli* 8114 was prepared for image analysed dielectrophoretic experiments (section 3.2.5) and circulated through the electrode chamber.

Frequency spectra were run with the suspension using the standard parameters. The conductivity was increased by addition of a small volumes of 0.1 M KCl, and the experiment repeated using identical experimental parameters. The addition of KCl was small (10-100 µl) and was not expected to influence the particle concentration by a significant amount. The mean frequency spectra obtained were then compared. The experiment was repeated for *Ent. cloacae*.

3.4.6.2 Effect of Increasing Conductivity on Frequency Collection

A suspension of *E. coli* 10418 was prepared in deionised water and circulated through the image analysed dielectrophoretic system. Using the multiple pulse application program, 30 repeat measurements of collection were made at each of several frequencies (1 kHz, 10 kHz, 100 kHz, 1 MHz and 10 MHz) and a mean level of collection found for each. This procedure was repeated using the same suspension at three conductivities, increased by addition of microlitre volumes of KCl, and mean collection levels found at each frequency. Therefore, the relative effect of conductivity could be seen for each frequency.

3.4.7 Effect of Increasing Particle Concentration

3.4.7.1 General Trends

It was expected that increasing the particle concentration of a suspension would proportionally increase the level of dielectrophoretic collection (up to an electrode saturation level), since more particles would be moving into the effective field strength region where the DEP force is able to overcome the force of the suspension flow.

A stock suspension of *E. coli* 39323 was prepared in deionised water as previously described. From this stock, samples were taken and further diluted with quantities of deionised water. The optical density was measured at 600 nm (LKB Ultrospec II) blanked against deionised water. A 1 ml sample was taken from each suspension and viable counts conducted as described in section 3.3.3. Each sample in turn was circulated through the electrode chamber, the conductivity adjusted to the same levels, and dielectrophoretic frequency spectra obtained for each, using identical experimental parameters. Dielectrophoretic collection levels were then compared.

3.4.7.2 Normalisation Experiments

One of the problems with standardisation was the effect of particle concentration on the level of dielectrophoretic collection. Dielectrophoretic spectrum experiments were performed on several suspension concentrations using the full count detection method. The relative levels of collection were then examined and mathematical manipulation employed to normalise the levels to the same particle concentrations.

An experiment was performed as previously described in section 3.4.7.1 and the particle concentrations of the suspensions found by total count methods (i.e. microscopic counts)(section 3.3.3). The frequency spectra obtained were normalised by mathematical conversion to the same particle concentration. Normalisation of the spectra was performed by multiplication of the collection at each frequency point on the spectra by $\frac{C_0}{C}$ where C was the suspension concentration, and C_0 was the concentration to which it was normalised.

i.e. supposing the greatest suspension concentration to be 12×10^7 cells.ml^{-1}, normalisation of a spectrum produced by a 4×10^7 cells.ml^{-1} suspension could be achieved by multiplication of each point on the spectrum by $\frac{12 \times 10^7}{4 \times 10^7}$ i.e. by a factor of 3.

The levels of hypothetical collection were then compared to assess the degree of similarity between the adjusted spectra. Under ideal conditions, after normalisation for concentration, the collection levels would be identical for each frequency, assuming all other factors had been standardised.

A pulse length graph (section 3.4.2) was obtained using the greatest suspension concentration to ensure saturation was not occurring.

3.4.8 Effect of Particle Size

From the dielectrophoretic force equation, $\mathbf{F} = \mathbf{P}v\ (\mathbf{E}.\nabla)\ \mathbf{E}$, the volume of the particle has been demonstrated to be of significance in determining the size of the force. Experiments were undertaken to correlate the size of several particle types with the level of dielectrophoretic collection, a measure of the magnitude of the force.

Suspensions of polystyrene latex spheres (2.07, 2.40 and 2.75 µm diameters)(Interfacial Dynamics Corporation, IDC) were made in the normal way. The concentrations were adjusted to 5×10^7 particles.ml^{-1}, on the basis of concentration values of the stock suspensions provided by IDC.

Frequency spectra were obtained for each particle suspension to correlate with particle volume.

With the largest latex volume, a saturation of the detection field may have become problematic. A pulse length graph was run with this suspension (as detailed in section 3.4.2) to ensure saturation was not occurring under the conditions used for the frequency spectrum.

3.4.9 Effect of Resistance Shunt Movement

Connection of the electrode wires to the function generator was through a 50 Ω resistance shunt. This had the effect of stabilising the output voltage and halving its value i.e. a 24 V peak-peak voltage would be reduced to a stable 12 V peak-peak by the presence of the shunt.

Early experiments by Brown A.P. & Archer G.P. (1992) (Unpublished Data) using the spectrophotometric system suggested that movement of the shunt position had a differential effect on the DEP collection of Gram positive and Gram negative cells. It was found that when the shunt was placed at the output of the function generator (i.e. before the connecting coaxial cable) a peak of dielectrophoretic collection was recorded at around a 10 MHz frequency with Gram positive cells (such as *Streptococcus faecalis*), though not with Gram negative *E. coli*. This effect was not seen when the shunt was placed at the end of the coaxial cable closest to the

electrodes. Pathogenic organisms may be either Gram positive or Gram negative. Many infections are caused predominantly by one or other of these types. Therefore, for clinical applications of dielectrophoresis it would be desirable to separate Gram positive cells from Gram negative cells to aid identification.

To further investigate this effect, an overnight culture of *B. subtilis* 10106 trpC2 was made in nutrient broth and incubated with shaking at 30 °C. A suspension was made in the manner described in section 4.1.3.3, and circulated around the dielectrophoretic equipment. The conductivity was adjusted by addition of dilute KCl and frequency spectra obtained. Parameters of 12 V and 5 s duration were used over the frequency range. Initially the shunt was placed at the end of the coaxial cable nearest to the electrodes and a mean spectrum obtained. The experiment was repeated under the same conditions with the shunt moved to the opposite end of the cable, nearest to the function generator output port. This was repeated with *Ent. cloacae*, *Strep. faecalis* and *E. coli* 10418 using either image analysed or spectrophotometric methods. An experiment was also conducted to measure the voltage in the cable by an oscilloscope. The output was compared with the shunt placed at each end.

3.4.10 Position of Dielectrophoretic Collection

It has been shown that the position of collection upon the electrodes varies depending upon the nature of the dielectrophoretic collection (Pethig *et al.*, 1992; Quinn, 1995). Archer *et al.* (1995) also commented that mathematical modelling had been used to propose areas on similar microelectrode structures where positive or negative dielectrophoresis may be predominant. Positive dielectrophoresis was thought to occur generally at regions of high field intensity at the electrode edges, compared with low intensity regions for negative dielectrophoresis on top of electrodes.

A culture of *E. coli* 10418 was prepared in deionised water as previously described. The electrodes were placed under the microscope objective and 6 regions of collection designated as shown in figure 3.4 and labelled according to the proposed nature of the dielectrophoretic force in these regions. By application of electric fields over the frequency range, dielectrophoretic collection was observed microscopically and the regions of collection identified at each frequency.

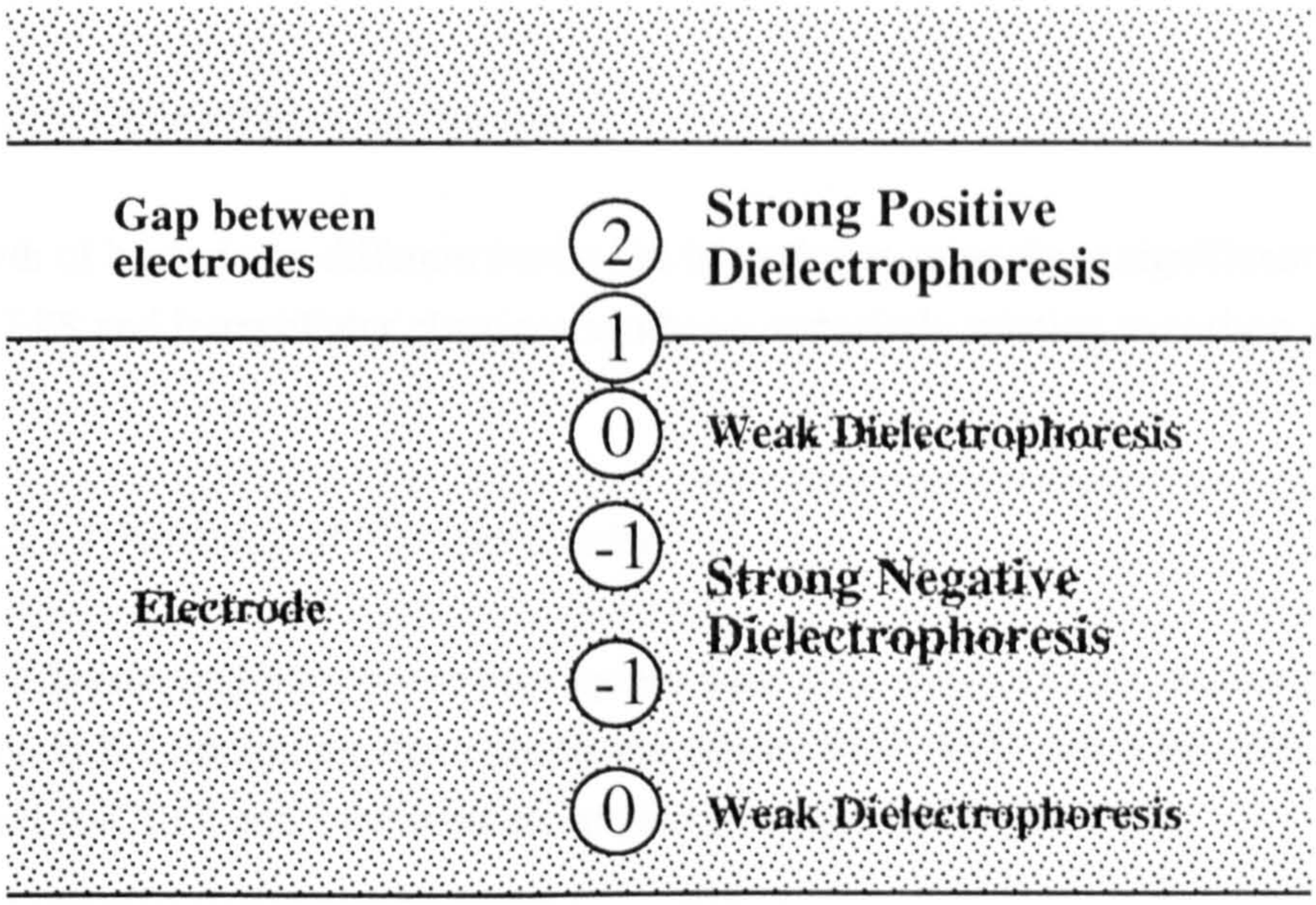

Figure 3.4 : Positive and negative dielectrophoresis areas designated on the microelectrodes.

Samples of the *E. coli* culture were also prepared by filtration and resuspension in 0.5 M sucrose and in 280 mM mannitol, compared to deionised water. The media have different permittivity and viscosity values and are likely to influence the nature of the dielectrophoretic effect. In addition, their osmotic properties may also cause variation in the cells and so change their dielectrophoretic response. Conductivity values were adjusted to be identical in each suspension and the regions of collection compared.

Frequency dependent dielectrophoretic spectra were also obtained for the same suspensions using the image analysis system (section 3.4.1).

3.4.11 Effect of Shaking Cultures of Bacteria

Two *Ps. aeruginosa* cultures were grown at 37 °C for 16 h, one with shaking at 170 rpm, the other stationary. Both were prepared for DEP as normal and their dielectrophoretic spectra compared, with experimental parameters 12 V and 5 s pulse duration. The conductivity of both suspensions was adjusted as necessary to give identical measurements and enumerated by total count to account for cell concentration differences.

3.5 Exopolysaccharide Studies

3.5.1 General Dielectrophoretic Spectra

The growth of bacteria on different media has been shown to produce significant changes in the extent of EPS and intracellular glycogen synthesis, especially relating to carbon and nitrogen sources.

3.5.1.1 Variation of Nitrogen Source

Strains of *Klebsiella (Enterobacter) aerogenes* were obtained from Prof. Sutherland (Edinburgh University, U.K.), including slime producing strains 87Sl, A1Sl and A3Sl; EPS- strains A4O31 and A4CRO; and a temperature sensitive mutant A4CR-TS.

Four flasks of *Klebsiella* medium (KM) (Appendix 3), supplemented with 1 % glucose (sterilised and added separately), were prepared. Two of the flasks contained medium with 1 % casamino acids as an undefined nitrogen source, the others having 0.5 % ammonium sulphate (De Souza & Sutherland, 1994). Cultures of *Kl. aerogenes* 87Sl and A4O31 were made in each medium by overnight incubation at 30 °C with rapid orbital shaking at 220 rpm. A sample from each flask was removed, washed and prepared for dielectrophoretic experiments. Standard frequency spectra were obtained using image analysed DEP for each sample from both medium types, using parameters of 12 V and 5 s pulse duration. The mean spectral form was examined and related to growth medium effects, caused by differing nitrogen sources.

3.5.1.2 Glucose Concentration

Strains of *Kl. aerogenes* 9527 (EPS producing strain) and 9528 (non EPS producing strain) were obtained from the NCTC Culture Collection. Each strain was inoculated into each of three flasks of KM containing 1 % casamino acids and varying concentrations of glucose, 0.5 %, 1 % and 2 % (autoclaved separately). The flasks were incubated at 30 °C overnight and then a sample from each flask prepared for dielectrophoresis.

Dielectrophoretic spectra were obtained for both strains in all three media using standard experimental parameters and related to glucose content in the growth medium. Total counts were also performed on the samples to account for any variation in collection due to concentration.

Osmolarity of the three media was measured after calibration with 400 mOsm.kg^{-1} NaCl (1.26 % w/v) and distilled water, to account for possible variation due to osmotic shrinkage.

3.5.2 Growth Curves

Flasks of KM containing 1 % casamino acids and glucose concentrations 0.5 %, 1 %, 2 % and 5 %, were inoculated with *Kl. aerogenes* 9527 and 9528 and incubated overnight with shaking. Fresh prewarmed flasks of the same media were then inoculated with 1 ml volumes of the overnight cultures and incubated at 30 °C with shaking. Therefore, the inoculum size into each medium was identical for each strain. At 1 h intervals, samples of the growth were removed from the flasks and their optical density read at 510 nm, blanked against samples of uninoculated broth. Incubation was continued for 24 h and growth curves of the two species at each concentration of glucose plotted.

3.5.3 EPS Visualisation

3.5.3.1 India Ink Method (Duguid, 1951)

A loopful of each *Klebsiella* strain bacterial culture (from either broth or solid medium) was mixed with a drop of India Ink and a drop of 20 % glucose solution on a microscope slide. A cover slip was placed over the suspension and blotted to remove excess liquid. The slides were then examined by oil immersion phase-contrast microscopy. Capsulate cells appeared to have haloes, excluding the colloidal ink.

3.5.3.2 Transmission Electron Microscopy

For visualisation of capsules by electron microscopy it was necessary to try to stabilise the capsule to prevent dehydration by the electron microscopy vacuum. The ruthenium red method used here was thought to act by stabilising the EPS and providing an electron dense layer for visualisation by electron microscopy (Handley, 1991).

Cultures of *Kl. oxytoca* (considered to be a capsule producer), were grown overnight in nutrient broth. A 30 ml volume of culture was harvested by centrifugation and the cells washed with sterile distilled water (PBS blocks the reaction with ruthenium red).

The washed cells were then resuspended in an Eppendorf tube in a pre-staining fixative (Appendix 3).

After 1 h in this solution at room temperature, the cells were harvested and washed by 3 changes of 1 ml 0.2 M cacodylate buffer. They were then resuspended and left for 3 h in a staining solution (Appendix 3).

The cells were then washed 3 times in distilled water prior to dehydration by ethanol series. Following embedding and sectioning, the cells were examined by transmission electron microscopy, using a JEOL 1200EX at an operating voltage of 80 kV.

3.5.4 *Klebsiella* Mutagenesis

Mutation was undertaken as a slight modification from the method of Allison & Sutherland (1987), as determined by the optimum mutation conditions found by Adelberg *et al.* (1965).

3.5.4.1 Growth of Organisms

Kl. aerogenes slime producing strains 87Sl (Serotype 8) and A1Sl (Serotype 1) were grown overnight at 30 °C in KM containing 1 % glucose. Fresh flasks of prewarmed media were inoculated with 3 ml of the overnight cultures and grown to exponential phase monitored by optical density measurements ($O.D._{510} \approx 0.5$).

3.5.4.2 Mutagenesis

The exponential phase cells were harvested by centrifugation at 10 000 rpm (MSE High Speed 18) and washed in phosphate buffered saline (PBS)(Appendix 3). These cells were then resuspended in 50 ml sterile 0.1 M phosphate buffer (pH 6.0) (Appendix 3) containing 150 $\mu g.ml^{-1}$ syringe filtered (0.2 µm pore size, Minisart filters, Sartorius) N-methyl-N'-nitro-N-nitrosoguanidine (NTG)(Sigma). The NTG was also streaked onto nutrient agar to ensure sterility.

The suspension was incubated at 30 °C for 1 h to allow mutation to occur. The cells were harvested by centrifugation at 10 000 rpm, washed in PBS and used to inoculate a fresh flask of KM (containing 1 % glucose) to allow multiplication of mutated cells. After overnight incubation, the culture was decimally diluted and plated onto plates of nutrient agar containing 1 % glucose. Colonies with differences in observed morphology, such as rough or non-glossy appearance were picked off the plates and further purified on streak plates. Upon purification, their identity was confirmed by Gram staining (Appendix 4), microscopic observation and the utilisation of API20E identification strips.

3.5.4.3 Spectrum Production

The mutants produced in section 3.5.4.2 and their parent strains were grown in KM containing 1 % glucose and 1 % casamino acids for up to 22 h at 30 °C. A sample of each strain was then removed and prepared for dielectrophoretic experiments, as in section 3.2.5, to compare their frequency responses to an applied electric field. Standard DEP frequency spectra were obtained, as in section 3.3.1, using the full count method of image analysis. Pulse length experiments were also undertaken to ensure saturation was not occurring.

3.5.5 Estimation of Exopolysaccharide

Experiments were performed to assess the respective EPS production of *Kl. aerogenes* 87Sl, A1Sl strains and their respective mutants 22(87Sl), 9(A1Sl) and 14(A1Sl) under identical incubation conditions.

Extracellular polysaccharide was quantified by the method described by Hancock & Poxton (1988). All glassware used in the experiment was first thoroughly cleaned (Decon 90), rinsed well in distilled water and then with analytical grade acetone to remove any residue which could influence quantification.

Overnight cultures of the strains were made in KM containing 1 % glucose and incubated at 30 °C. Each broth culture was first centrifuged for 10 min at 10 000 rpm (MSE High Speed 18) to remove cells. A 20 ml aliquot of the supernatant was then removed and 80 ml ice-cold acetone added to precipitate the EPS. Precipitation was continued at 4 °C for 18 h, resulting in deposition of EPS as a white solid. This was removed by low speed centrifugation at 3000 rpm for 10 min. The supernatant was then decanted and the residue washed three times in acetone. Following washing of the sample, the precipitate was resuspended in 5 ml of sterile distilled water before being dried and weighed.

3.6 Measurement of Hydrophobicity

3.6.1 Growth Temperature Effects on Hydrophobicity

3.6.1.1 Growth of Organisms

Overnight cultures of *E. coli* clinical isolate 39323 and *B. subtilis* 10106 trpC2 were grown in nutrient broth and incubated with shaking at both 30 °C and 37 °C. Measurement of the cell hydrophobicity was then made as in section 3.6.3.

3.6.2 Effects of Growth Phase on Hydrophobicity

3.6.2.1 Growth of Organisms

Overnight cultures of *E. coli* 10418 were grown in nutrient broth at 37 °C. A 2 ml sample of this culture was inoculated into a fresh flask of prewarmed broth and incubated. At hourly intervals, samples were taken, the $O.D._{510}$ measured and a growth curve progressively plotted. By examination of this graph, the exponential period of culture growth was determined. A sample of the culture was immediately taken and prepared under ice-cold conditions to prevent further growth. In a similar way, a sample was taken from the stationary phase of growth and prepared for hydrophobicity measurement (section 3.6.3). Samples taken from these stages of growth were also immediately prepared, as in section 3.2.5, and used to produce image analysed dielectrophoretic spectra.

3.6.3 Hydrophobicity Measurement

Hydrophobicity was measured according to the method of Van der Mei *et al.* (1993). Aliquots of the broth cultures were harvested by micro-centrifugation at 6500 rpm (MSE) and washed several times with deionised water to remove traces of media. The pellets of cells were then resuspended in 0.1 M phosphate buffer (Appendix 3) which had been adjusted to a range of pH values between 2 and 9 by dropwise addition of 1 M KOH or 1 M HCl. The suspension concentration was adjusted to give an approximate $O.D._{600}$ of between 0.4-0.6 Absorbance Units, and this was recorded as A_0. A 3 ml volume was taken from each sample and 150 µl n-hexadecane (Sigma) layered over the top. The samples were vigorously vortex mixed for 10 s and then allowed to settle for a period of 20 min. After this time, the absorbance of the aqueous phase was again measured and recorded as A_t. This procedure of agitation, followed by settling was repeated until a total vortex time of 60 s had been achieved. The relative

adhesion of the cells to hexadecane in each buffer was calculated after each period of settling and expressed as :

$$\log\left(\frac{A_t}{A_0}\times 100\right)$$

The initial rate of adhesion at each pH was also calculated by measuring the decrease in absorbance over the time period.

3.7 Antibiotic Assays

Experiments were undertaken to evaluate the relative sensitivity of test organisms to each of three antibiotics and to determine Minimum Inhibitory Concentration (MIC) values. Antibiotic sensitivity tests were carried out according to the Stokes' method, as described by the British Society for Antimicrobial Chemotherapy Working Party (1991).

3.7.1 Organisms and Antibiotics Tested

Bacterial strains, *E. coli* 8114, *E. coli* 39323, *E. coli* R35258 and *Ent. cloacae* were tested for their resistance against nalidixic acid and ampicillin, compared to that of an antibiotic sensitive control strain *E. coli* 10418.

Gram positive strains, *B. subtilis* 10106 trpC2 and *B. cereus* were tested for their resistance to chloramphenicol, compared to that of the sensitive control strain *Staph. aureus* 6571.

3.7.2 Sensitivity Testing

3.7.2.1 Inoculation of the Assay Plates

Stock solutions of nalidixic acid, ampicillin and chloramphenicol antibiotics (Sigma) were made in sterile deionised water at concentrations of 1000 $\mu g.ml^{-1}$ for the former two, and 10 $mg.ml^{-1}$ for the latter. In the case of nalidixic acid, however, a drop of concentrated ammonia solution was also added to enable more efficient dissolution. The stock solutions were dispensed into Eppendorf tubes and stored at -70 °C prior to use.

Doubling dilutions of the stock solutions were made in sterile deionised water, giving final concentration ranges of 20-320 $\mu g.ml^{-1}$ for nalidixic acid and ampicillin, and 3.125-50 $\mu g.ml^{-1}$ for chloramphenicol.

For each bacterial species to be tested, an isolated colony was picked from a nutrient plate (used to maintain the cultures, section 3.2.2) and emulsified in 2 ml of a sterile 1 % aqueous solution of bacteriological peptone (Oxoid)(York District Hospital, 1994).

A rotary plating apparatus was manufactured by the adherance of a plastic Petri-dish lid to a slowly rotating drill (Harrison, 1994). This allowed an agar plate to be spirally inoculated by dragging a seeded swab radially from the centre of the plate as the drill rotated, enabling rapid and reproducible inoculation procedures.

A sterile swab was immersed in one of the prepared bacterial suspensions and the excess removed by rolling the swab against the side of the container. This procedure allowed formation of semi-confluent growth of the organisms following incubation. The inoculum was applied to an agar plate of Diagnostic Sensitivity Test Agar (Oxoid) using the rotary plating technique. For each assay, the control (antibiotic sensitive) organism was applied to the centre of the plate and the test organism to the outer regions of the plate. This allowed direct comparison of the effect of antibiotic on the two organisms. Once the plate had been seeded with the bacteria, the antibiotic could then be applied.

Sterile antibiotic assay discs (6 mm diameter, Whatman) were immersed in the antibiotic dilution under examination using sterile forceps. Excess antibiotic was removed by blotting onto filter paper and the disc placed onto the plate between the control and test species, as shown in figure 3.5. This was repeated for all antibiotics and dilutions, and with a sterile water control.

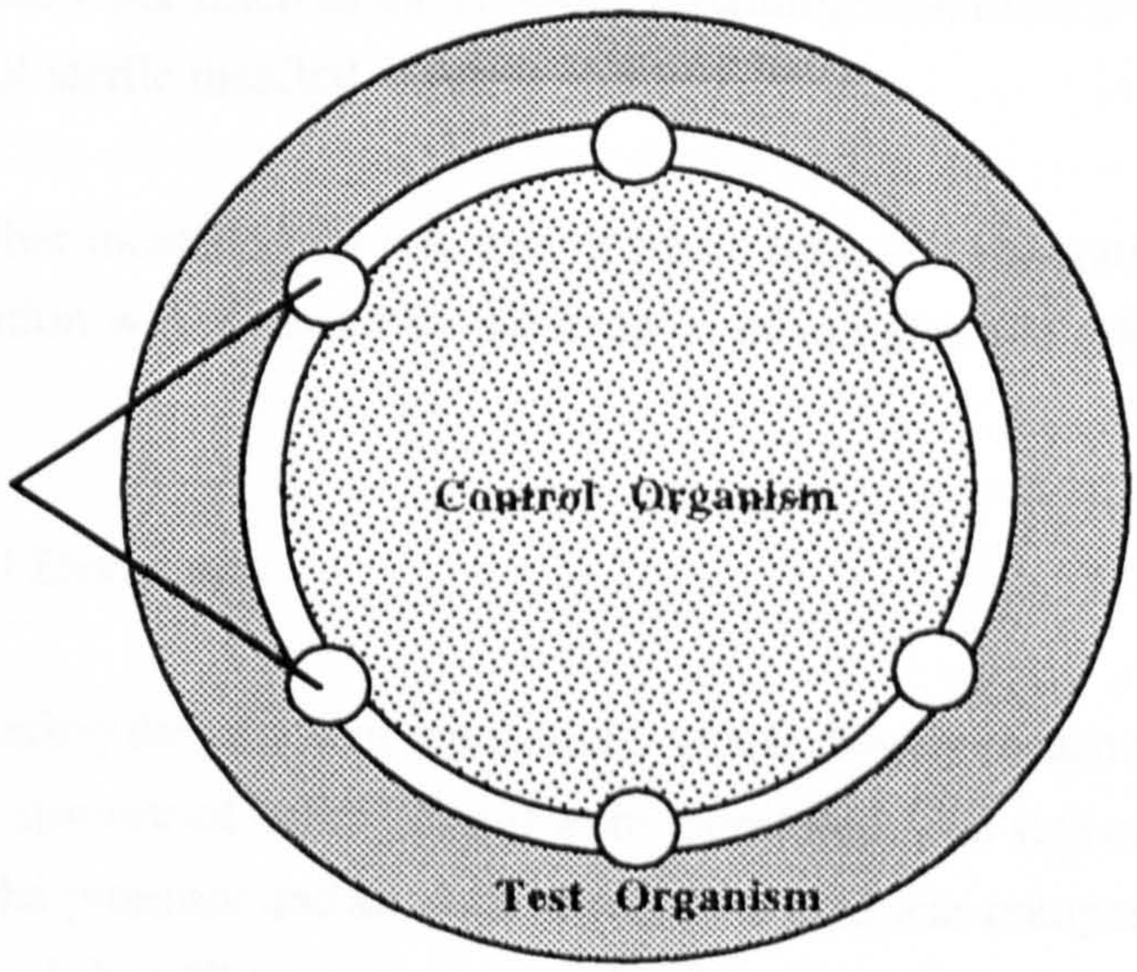

Figure 3.5 : Inoculation of an antibiotic assay plate.

Following overnight incubation at the optimum bacterial growth temperatures (section 3.2.2), the zones of inhibition for control and test organisms were measured. The minimum concentration of antibiotic which still produced inhibition of bacterial growth (MIC) and relative antibiotic sensitivities were assessed.

3.8 Elongation by Nalidixic Acid Treatment

3.8.1 Antibiotic Treatment

The elongation of bacterial cells by nalidixic acid was achieved by the method of Singh *et al.* (1989). Overnight cultures of *E. coli* 10418, *E. coli* (clinical isolate 39323) and *E. coli* 8114 were prepared in nutrient broth and incubated at 37 °C. A 1 ml aliquot was then used to inoculate a further flask of pre-warmed broth. At hourly intervals, samples were removed, the optical density measured and the initial stages of a growth curve plotted. Once the cultures had reached the exponential stage of growth they were harvested by centrifugation at 10 000 rpm (MSE High Speed 18) and washed in sterile PBS (Appendix 3). The pellet was resuspended in 10 ml of PBS. One ml samples containing approximately 10^{10} cells.ml^{-1} were then used to inoculate each of two flasks. In the first flask was a sterile 100 ml PBS solution containing yeast extract (0.03 %) and casamino acids (0.3 %) present with nalidixic acid (Sigma) (Appendix 3). This antibiotic was first made as a separate 1 mg.ml^{-1} aqueous solution (dissolution was assisted by addition of 1 drop concentrated ammonia solution), filter sterilised (0.2 µm pore, Minisart, Sartorius) and then added to the flask to give a final concentration of 10 µg.ml^{-1}. The second flask acted as the control, containing no nalidixic acid, being replaced by an equal volume of sterile distilled water.

Both flasks were further incubated for 6 h, during which time cell elongation without division occurred. The elongation was observed by the removal of samples and microscopic examination.

3.8.2 Monitoring Cell Elongation

At regular intervals during the period of incubation, optical density measurements and total counts in presence or absence of nalidixic acid were monitored. The size of the cells over the incubation period in the presence and absence of nalidixic acid was compared by microscopic observation. Samples of the culture were removed at 30 min periods, harvested by microcentrifugation at 6500 rpm, washed and immediately fixed and Gram stained. A

calibrated eye piece graticule was used to examine the relative cell sizes throughout the incubation.

Samples of nalidixic acid elongated *E. coli* 10418 were also prepared for scanning electron microscopy examination at the end of the incubation period. The procedure was as described in section 3.2.3.

3.8.3 Dielectrophoretic Experiments

Following the 6 h incubation period, samples were removed from the cultures and prepared for dielectrophoretic experiments, as described in section 3.2. Frequency spectra were run for both nalidixic acid treated and untreated cells, using both spectrophotometric and image analysed dielectrophoretic procedures. Both full count and area counts methods were used with the image analysis technique.

Total and viable counts were made on both suspensions to attempt to normalise the resulting spectra and account for any differences in cell concentration.

3.9 Ampicillin Treatment

The effects of sub-inhibitory concentrations of penicillins, and specifically ampicillin, have been examined previously. It has been found that treatment of cells with ampicillin led to alterations in the cell wall structure in both Gram positive and negative species and to bulge formation within the cells. In addition, marked cell elongation was also observed at concentrations of 2 and 20 $\mu g.ml^{-1}$ (Perkins & Miller, 1973). As discussed in section 2.11, ampicillin has its target site within the peptidoglycan structure of the cell wall, preventing transpeptidation and leading to abnormal wall structure.

It was proposed that such treatment of cell walls may have a significant effect on the resulting dielectrophoretic spectrum, by both the changes in cell wall and by bulge formation as well as elongation effects on cell shape and size.

3.9.1 Antibiotic Treatment

Essentially a modified method of Perkins & Miller (1973) and Burdett & Murray (1974) was used to cause modifications to the cells by ampicillin treatment. An overnight culture of *E. coli* 10418 was prepared in sterile nutrient broth by incubation at 37 °C with shaking. A 2 ml aliquot of the culture was removed and used to inoculate a flask of fresh sterile prewarmed

nutrient broth. At hourly intervals, samples were removed, the optical density measured and initial stages of a growth curve plotted. Once the culture had reached the exponential stage of growth, it was harvested by centrifugation at 10 000 rpm (MSE High Speed 18) and washed in sterile 0.5 M sucrose solution. The pellet was resuspended in 100 ml of fresh sterile pre-warmed nutrient broth. The suspension was then split into two equal portions of 50 ml and added to each of two flasks. One of the flasks contained 49 ml of sterile pre-warmed nutrient broth and 1 ml of a sterile syringe filtered aqueous solution of ampicillin (1 $mg.ml^{-1}$ sodium salt, Sigma), therefore giving a 100 ml total volume containing a final antibiotic concentration of 10 $\mu g.ml^{-1}$ and approximately 5×10^8 $cells.ml^{-1}$. The second flask contained similar components but the 1 ml of antibiotic solution was replaced with an equal volume of sterile distilled water.

The flasks were incubated at 37 °C for 3 h, allowing the antibiotic to act on the exponentially growing bacterial cell walls. During the incubation, the absorbance at 510 nm was monitored.

Following incubation, samples were removed and prepared for dielectrophoresis experiments as described in section 3.2.5. Instead of washing in deionised water, however, the samples were prepared by washing and resuspending in a 0.5 M sucrose solution. This was undertaken to avoid possible osmotic lysis caused by the sensitivity produced by ampicillin mediated cell wall inhibition. In addition, samples from both control and treated cultures were removed and their respective morphologies examined by phase contrast microscopy.

The image analysed dielectrophoretic counting method was utilised to produce frequency spectra for both the control and antibiotic treated cells. The experiment was performed using the standard parameters outlined in table 3.1. Total counts were also found for both samples.

3.10 Cell Wall Thickening

3.10.1 Cell Wall Thickening by Tryptophan Absence

It was previously observed that exposure of *B. subtilis* to conditions of unbalanced growth caused by inhibition of protein synthesis mechanisms resulted in a notable thickening of the cell wall (Hughes *et al.*, 1970). This increase in wall thickness was previously observed when a strain of this species, which had a necessity for tryptophan, was grown in a medium lacking this amino acid. Experiments were undertaken to attempt to thicken the cell wall of this strain in a similar manner to observe whether any differences were observed in the subsequent dielectrophoretic experiments.

An overnight broth culture of *B. subtilis* trpC2 was made by incubation at 35 °C in the growth medium described by Hughes *et al.* (1970)(Appendix 3). A 1 ml sample was used to inoculate a further 500 ml volume of pre-warmed broth. This was incubated and grown to mid-exponential phase as determined by optical density ($O.D._{675}$ 0.5). The cells were harvested by centrifugation at 10 000 rpm, washed in warmed (35 °C) 0.1 M sodium phosphate buffer (pH 7.0) (Appendix 3) and resuspended in 50 ml of the same buffer.

Twenty-five ml volumes were then added to each of two flasks containing 5 ml filter sterilised "wall medium" (Appendix 3), one a control containing tryptophan, the other lacking this essential amino acid. Samples were taken from these flasks and prepared for dielectrophoretic experiments (section 3.2.5).

The cultures were then shaken at 35 °C for 240 min, and further samples taken to dielectrophoretically compare with the control cells prior to incubation. Samples were also taken during the incubation to assess O.D. and also for viable counting procedures to monitor the viability and concentration of the cell cultures.

3.10.2 Cell Wall Thickening by Chloramphenicol Treatment

3.10.2.1 Antibiotic Treatment

Unbalanced cell growth caused by interruption of protein synthesis could also be brought about by antibiotic inhibition of the process, resulting in a similar cessation of cell growth without affecting cell wall synthetic mechanisms (Hughes *et al.*, 1970; Chung 1971; 1973). Increases of 2-3 fold in peptidoglycan thickness have been produced by this treatment on Gram positive *B. subtilis* and *B. cereus* cells.

The chloramphenicol treatment was undertaken as a modification to the methods of Hughes *et al.* (1970) and Chung (1973). Essentially, an overnight culture of *B. subtilis* trpC2 was made in nutrient broth by incubation with shaking at 35 °C. A 1 ml aliquot was taken to inoculate a fresh culture of broth. This culture was grown into mid-exponential phase monitored by O.D. readings taken at hourly intervals. After this period, the culture was harvested by centrifugation at 10 000 rpm, washed in PBS and resuspended in a 10 ml volume of sterile nutrient broth. The suspension was split into two equal portions and added to each of two sterile 150 ml flasks containing 44 ml of sterile prewarmed nutrient broth. To one of the flasks was added a 1 ml volume of syringe filtered (0.2 μm pore) aqueous chloramphenicol solution (2.5 $mg.ml^{-1}$, Sigma) to give a final concentration of 50 $\mu g.ml^{-1}$ in a 50 ml total volume. To the other flask was added a 1 ml volume of sterile distilled water.

The cultures were incubated for a 4 h period and the absorbance monitored throughout this time.

Following the incubation period, samples were removed from each culture and prepared for dielectrophoretic experiments, as in section 3.2.5. Viable counts were also performed as previously described.

In addition, samples were removed and prepared for electron microscopy to examine the extent of wall thickening.

3.10.2.2 Electron Microscopy Preparation

One ml samples were removed from each of the two cultures, placed in micro-centrifuge tubes and spun at 6500 rpm. The pellets were washed in PBS and spun a further 3 times, and then finally resuspended in 0.5 % glutaraldehyde and allowed to fix overnight. The samples were then washed a further two times in PBS to remove the glutaraldehyde.

The cells were embedded in agar blocks, fixed in 1 % osmium tetroxide (in 100 mM phosphate buffer, pH 7)(Appendix 3) and dehydrated in an alcohol series. The samples were then embedded in resin and sectioned. The sections were stained with uranyl acetate and examined by transmission electron microscopy (JEOL 1200EX) at an accelerating voltage of 100 kV.

3.11 Spheroplast Formation

An overnight culture of *E. coli* (clinical isolate 39323) was prepared in nutrient broth at 37 °C. A 50 ml volume of the culture was then harvested by centrifugation at 10 000 rpm at 4 °C and washed three times in 0.5 M sucrose. The cells were resuspended in 20 ml 0.5 M sucrose and stored on ice. The suspension was divided equally between a spheroplasting medium consisting of Tris buffer (1 ml 0.1 M, pH 7.6), EDTA (1 ml 0.25 M) and lysozyme (1 ml, 1 $mg.ml^{-1}$), and a control medium with similar constituents, though replacing the lysozyme with sucrose (1 ml, 0.5 M). Spheroplasting was continued by lysozyme action on ice for 10 min. The suspensions were centrifuged at 4 °C and the supernatant discarded. Following washing in 0.5 M sucrose, the cells and spheroplasts were resuspended in sucrose, adjusted to similar absorbance values and prepared for dielectrophoresis. A sucrose solution (0.5 M) was used to prepare the control cells and spheroplasts to prevent osmotic lysis.

The extent of spheroplasting was assessed by observation with phase-contrast microscopy, where the presence of spherical bodies rather than the usual rod-shaped cells indicated

spheroplast formation. Viable counts were also performed on the samples as previously described.

Dielectrophoretic spectra were obtained using the image analysed DEP system and the results from the control and spheroplasts compared.

3.12 Dielectrophoretic Counting

As particle concentration in a circulating suspension increases, the extent of dielectrophoretic collection increases accordingly. By producing a calibration line from known concentrations of particles, it should have been possible to estimate the concentration of similar particles in an unknown suspension by the amount of dielectrophoretic collection. Experiments were conducted to produce such calibration lines and to assess the reproducibility of the method.

3.12.1 Latex Counting Experiments

3.12.1.1 Latex Calibration Line

Suspensions of latex were prepared, as described in section 3.2.1. Volumes of latex stock suspension varying from 1.5 µl to 15 µl were added to 10 ml volumes of deionised water. Each suspension was prepared for dielectrophoretic experiments and circulated through the system. The conductivity was adjusted to around 4.5-5.0 $\mu S.cm^{-1}$ by addition of microlitre volumes of 0.1 M KCl. Upon stabilisation of the conductivity and temperature, an electric field of 10 kHz, 12 V and 5 s duration was applied to the electrodes. The extent of dielectrophoretic collection was assessed using the full count method and the cycle repeated 30 times with the same parameters using the multiple reading program. This gave a mean collection value of the suspension at 10 kHz. After rinsing the tubing by elution with deionised water, the procedure was repeated for the other concentrations of latex and mean collection levels found.

The particle concentration of the suspensions were found by haemacytometer enumeration and correlated against dielectrophoretic collection.

3.12.1.2 Latex Enumeration Trial

After construction of a calibration line of DEP collection against particle concentration, it should be possible to run an unknown concentration of the particle under study and quantify it by the extent of dielectrophoretic collection.

Three latex suspensions were prepared by adding 14 µl, 22 µl and 29 µl of latex stock suspension to 10 ml volumes of deionised water. Each suspension was dielectrophorised after conductivity adjustment, by running 30 repeat measurements at 10 kHz, 12 V and 5 s duration. Each suspension was then quantified by haemacytometer count and a calibration line constructed.

A latex suspension of unknown concentration (within the working range of the system) was prepared in a similar way by a colleague, and run in the system under identical conditions. The conductivity was adjusted to be identical to the known suspensions and a mean dielectrophoretic collection level obtained by 30 repeat pulse applications at 10 kHz, as previously described. Prior to the plotting of the dielectrophoretic count, the unknown latex suspension was enumerated by haemacytometer count.

The level of collection of the unknown was then found and its actual concentration compared to the concentration predicted by the calibration line.

3.12.1.3 Correlation of Counting Methods

As described in section 3.1.2.2, there are three methods of particle enumeration by image analysis, full count, downward points count and area count. The most commonly used methods were the full count and downward points count. Experiments were performed using latex suspensions to compare the level of collection enumerated by both of these methods.

Latex suspensions at a range of concentrations were prepared as above and their conductivities adjusted to be the same. Each suspension in turn was dielectrophorised by 30 repeat pulse applications at 10 kHz, 12 V and 5 s duration. The collection of each suspension was enumerated by both full count and then downward points counting methods.

The level of collection detected by each method was then correlated for each suspension concentration.

3.12.2 Bacterial Counting Experiments

3.12.2.1 Calibration Lines of Pure Bacterial Suspensions

Bacterial suspensions with differing concentrations were made by preparation of a pure stock suspension, as in section 3.2.5, and diluting samples with varying amounts of deionised water. The suspension concentrations were determined by either optical density, total or viable counts. The mean level of dielectrophoretic collection of each suspension at 1 MHz, 12 V and

5 s pulse duration was assessed by 30 repeat applications of the electric field. A calibration line was produced by correlating the concentration against dielectrophoretic collection. This procedure was undertaken for pure suspensions of *E. coli* 39323, *B. subtilis* 10106 and *Serr. marcescens*, with calibration lines being produced for each.

3.12.2.2 Calibration Line for Simple Mixtures of Two Bacterial Species

Further studies on calibration lines by dielectrophoresis were undertaken to establish whether there was any interference between species in a bacterial mix.

Suspensions of *E. coli* 39323 and *B. subtilis* 10106 were made as previously described and their absorbance values adjusted to give similar cell counts, as determined by particle correlations performed in section 3.3.3 The suspensions were then added in a 50:50 mixture of cell suspensions. Aliquots of this stock suspension mix were diluted with varying volumes of deionised water, resulting in several suspensions of different concentrations. The absorbance of each suspension was measured and the samples then examined dielectrophoretically. Thirty repeat 1 MHz pulse applications of 5 s duration were applied to each suspension and the level of collection recorded. The absorbance of each sample was then correlated with mean dielectrophoretic collection.

3.12.2.3 Multiple Mixtures of Bacterial Species

Cultures of *S. enteritidis, Ent. cloacae, E. coli* 39323 and *Ps. aeruginosa* were grown at their optimum temperatures and stock suspensions prepared (section 3.2.5). Total counts were determined for each and volumes of the suspensions added together in amounts such that the concentrations of each species in the mix were equal. Dilutions of the stock mix suspension were then made and samples dielectrophorised by 30 repeat pulses at 1 MHz frequency at identical conductivity values. The mean level of collection was correlated against the suspension concentration as measured by total count. This procedure was repeated in an identical manner using a mixture of *B. globigii, Serr. marcescens* and *B. subtilis* and also with a mixture of *Ps. aeruginosa, Staph. aureus, S. enteritidis* and *Ent. aerogenes* (clinical isolate).

Chapter 4 : Results and Discussion

4.1 Preliminary Experiments

4.1.1 Sample Viability

Figure 4.1 shows the changes in viability of *Staph. aureus* and *Shig. sonnei* over the experimental period. For *Staph. aureus* the viable count of cells in the suspension remained relatively constant at approximately 150 x 10^6 cfu.ml^{-1} over the time course. The Gram negative species was slightly different and some decreases in viable cell concentration were observed especially within the first hour of recirculation. At time T_0 the concentration was approximately 510 x 10^6 cfu.ml^{-1}, dropping to 300 x 10^6 cfu.ml^{-1} after the first hour. The viable count remained more constant for the next hour, after which, the count was very variable. Since shifts in population are unlikely to occur this rapidly, it is more probable that errors were due to some irregular flow within the recirculation causing variations in the counts observed.

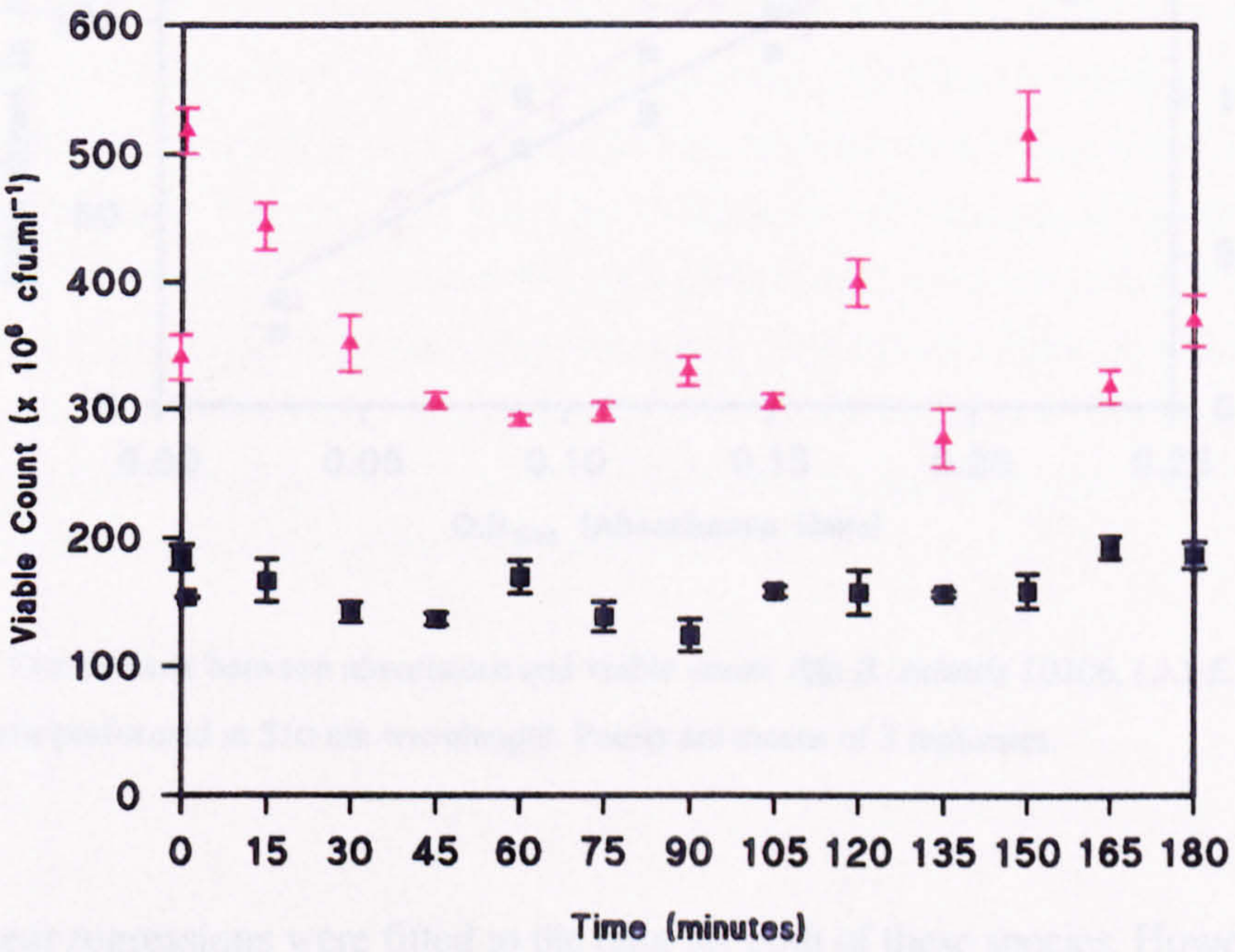

Figure 4.1 : Viability of two bacterial species after recirculation in de-ionised water over a period of 3 h. (■) *Staph. aureus*, (▲) *Shig. sonnei*. Each point is the mean plus standard error of three replicate plate counts.

It is possible that Gram negative species are more susceptible to the effects of low ionic strength media. This result was somewhat unexpected due to the nature of the Gram negative cells which are generally more tolerant to extreme conditions than Gram positive species.

4.1.2 Standardisation of Experiments

4.1.2.1 Correlations of Particle Concentration

Correlations between viable cell concentration and absorbance values for *E. coli* 10418 and *B. subtilis* are shown in figure 4.2 .

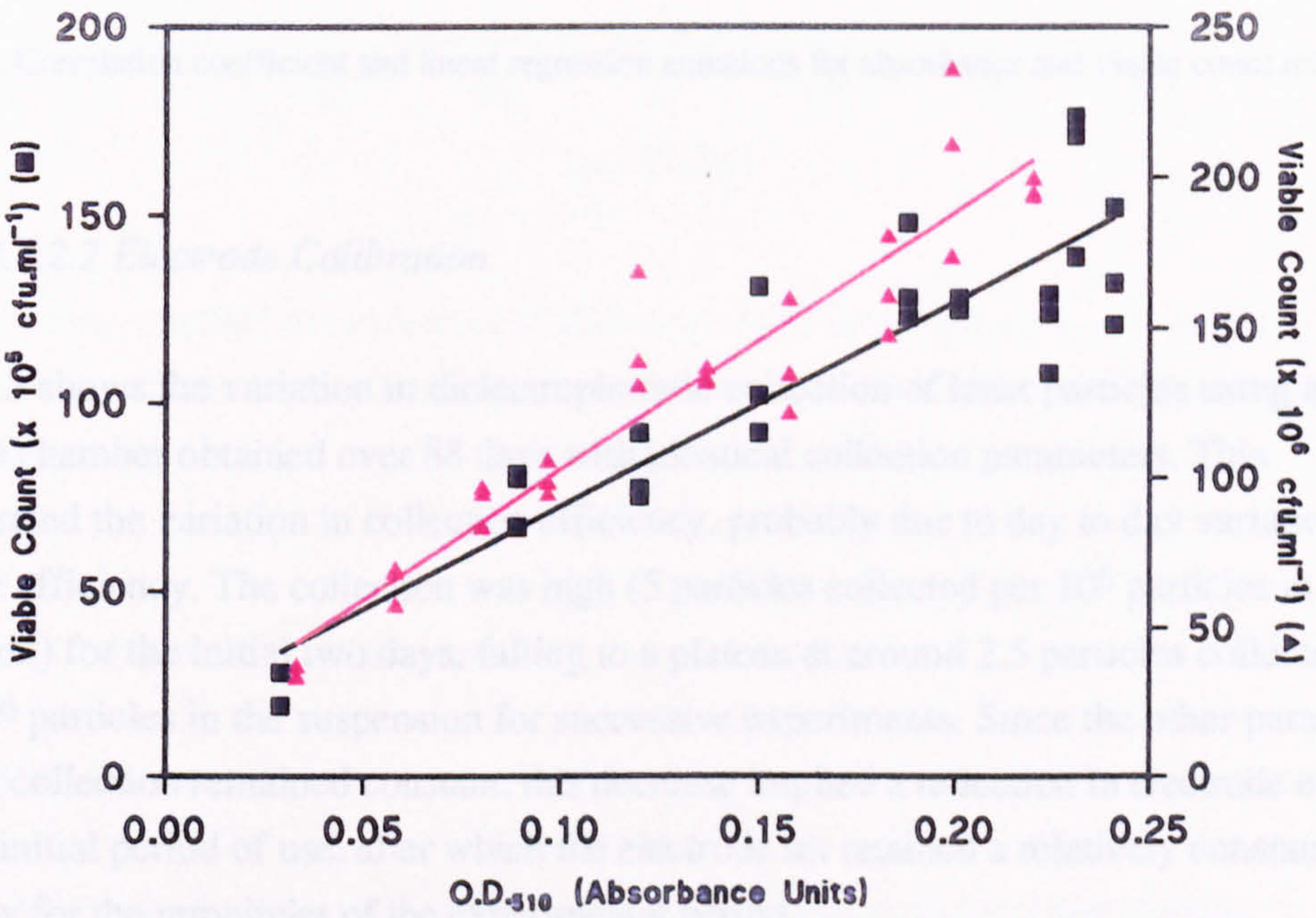

Figure 4.2 : Correlations between absorbance and viable count. (■) *B. subtilis* 10106, (▲) *E. coli* 10418. Measurements performed at 510 nm wavelength. Points are means of 3 replicates.

Good linear regressions were fitted to the data for both of these species. However, there was more than an order of magnitude difference between viable counts of the two species, the *E. coli* having greater numbers of viable cells for the same absorbance values.

Correlation coefficients and regression equations for these and other species are shown in table 4.1. The correlations for each of these particles was very good and so over the concentrations examined the relationships could be used to determine concentration (viable count) of bacterial

suspensions from their optical density measurements and to allow adjustment of the absorbance by dilution to achieve the required cell concentrations.

Particles	Correlation, r	Regression Equation
Latex	0.997	y = 55.87x - 1.397
E. coli 10418	0.946	y = 859.15x + 16.48
Ent. cloacae	0.962	y = 1459.56x + 10.37
Ps. aeruginosa	0.818	y = 1300.89x + 28.87
B. subtilis	0.915	y = 54.58x + 1.78
Staph. aureus	0.869	y = 302.11x - 0.39

y is the cell or particle concentration (x 10^6 particles.ml^{-1}) and x is the absorbance value (Absorbance Units @ 510 nm).

Table 4.1 : Correlation coefficient and linear regression equations for absorbance and viable count relationships.

4.1.2.2 Electrode Calibration

Figure 4.3 shows the variation in dielectrophoretic collection of latex particles using a single electrode chamber obtained over 88 days with identical collection parameters. This demonstrated the variation in collection efficiency, probably due to day to day variation in the electrode efficiency. The collection was high (5 particles collected per 10^6 particles in suspension) for the initial two days, falling to a plateau at around 2.5 particles collected for every 10^6 particles in the suspension for successive experiments. Since the other parameters affecting collection remained constant, this decrease implied a reduction in electrode efficiency over the initial period of use, after which the electrode set retained a relatively constant efficiency for the remainder of the experimental period.

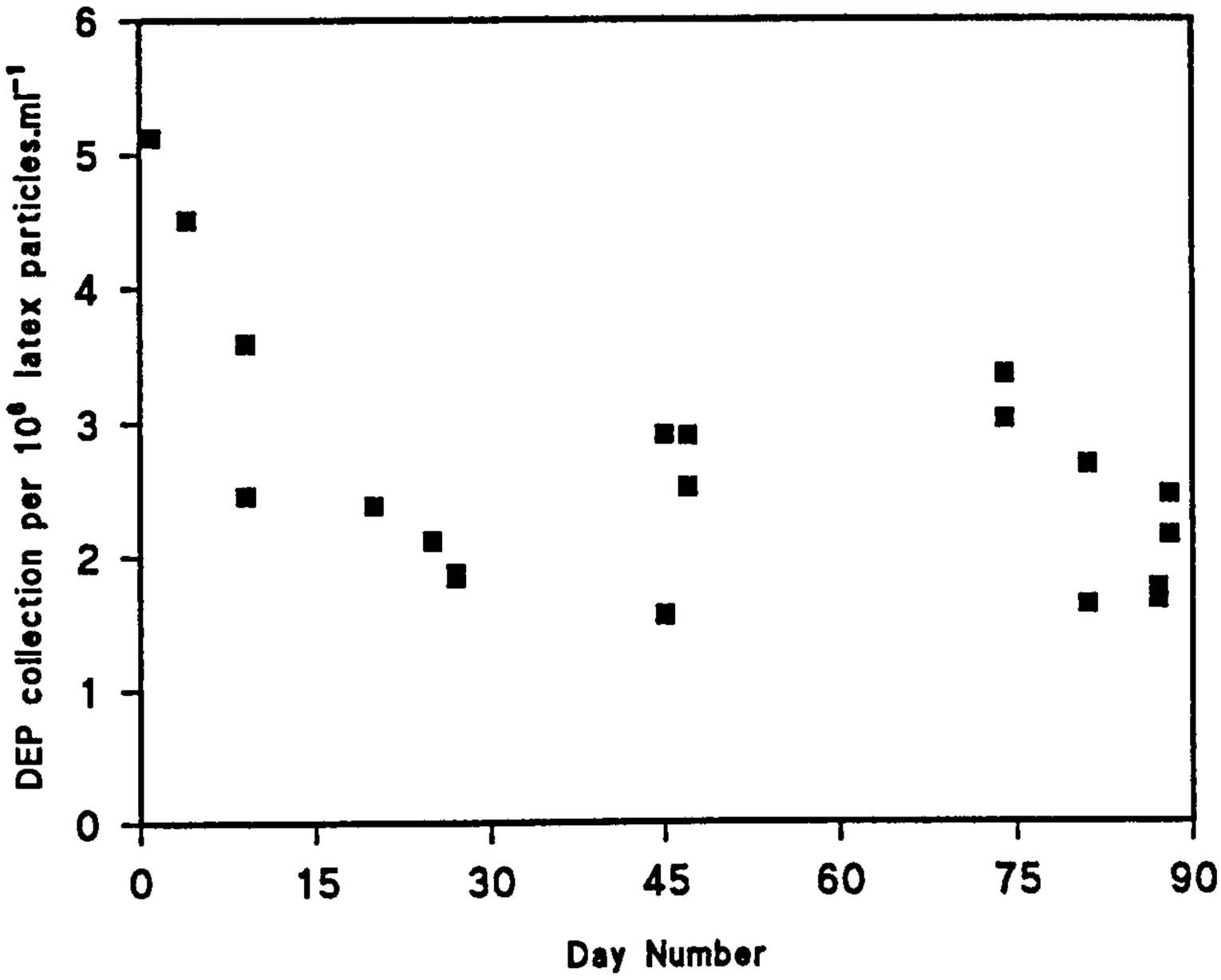

Figure 4.3 : Changes in daily dielectrophoretic (DEP) collection of latex suspensions over an 88 day period. Points are means of 30 repeated pulse applications at 10 kHz with 5 s duration and 12 V pk-pk, 4.5 $\mu S.cm^{-1}$. Full count detection.

4.2 Dielectrophoretic Experiments

4.2.1 General Spectra

4.2.1.1 Spectra Obtained Using the Spectrophotometric Detection System

Several frequency dependent spectra of both Gram positive and Gram negative bacterial species are presented in figure 4.4. The spectra were run with identical experimental parameters and conductivity values. Each spectrum has large regions of good dielectrophoretic collection over the whole frequency range examined.

The individual spectra of each bacterial species have very distinctive and specific frequency characteristics unique to their species. Conclusive differences between the spectra of the Gram positive and negative classification groups were difficult to identify and all of the species appeared to collect well over the frequency range. Most of the species showed a maximum collection in the 1 MHz region though the Gram positive *B. subtilis* had its maximum at a somewhat lower frequency (200 kHz). It was notable also, that the dielectrophoretic collection

of this Gram positive species was greater at the lower frequencies and appeared to decline much more rapidly than the Gram negative species at the higher frequencies in excess of 1 MHz.

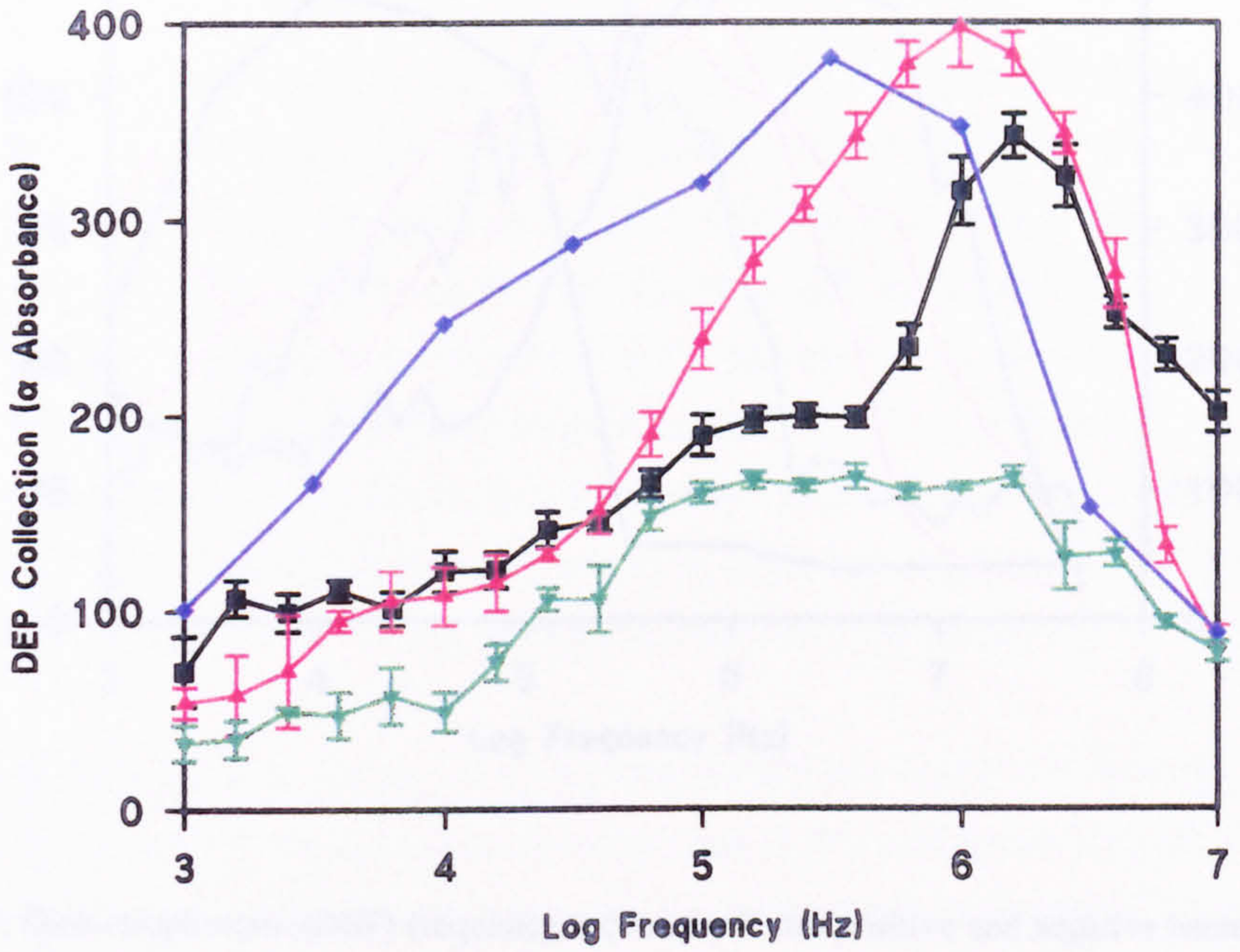

Figure 4.4 : Dielectrophoretic (DEP) frequency spectra for Gram positive and negative bacterial species using the spectrophotometer method of detection. (■) *E. coli* 8114, (▼) *Ps. aeruginosa*, (▲) *Ent. cloacae*, (◆) *B. subtilis*. Conditions : 10 s pulse, 16 V pk-pk, 47.8-63.8 $\mu S.cm^{-1}$. Points are means plus standard error of 5 replicate spectra.

The three Gram negative species also demonstrated unique differences in frequency response due to their particular structure and size. The level of collection of *Ps. aeruginosa* was significantly lower than all of the other species over the frequency range and had a plateau region between 100 kHz and 1 MHz. Both *Ent. cloacae* and *E. coli* had similar levels of collection at frequencies up to 100 kHz. Above this, *Ent. cloacae* began to collect significantly better up to its maximum, while *E. coli* reached a further plateau of collection and only after 400 kHz did collection rise dramatically.

4.2.1.2 Spectra Obtained Using the Image Analysis Detection System

Frequency spectra obtained for several bacterial species using the image analysed detection system are shown in figure 4.5.

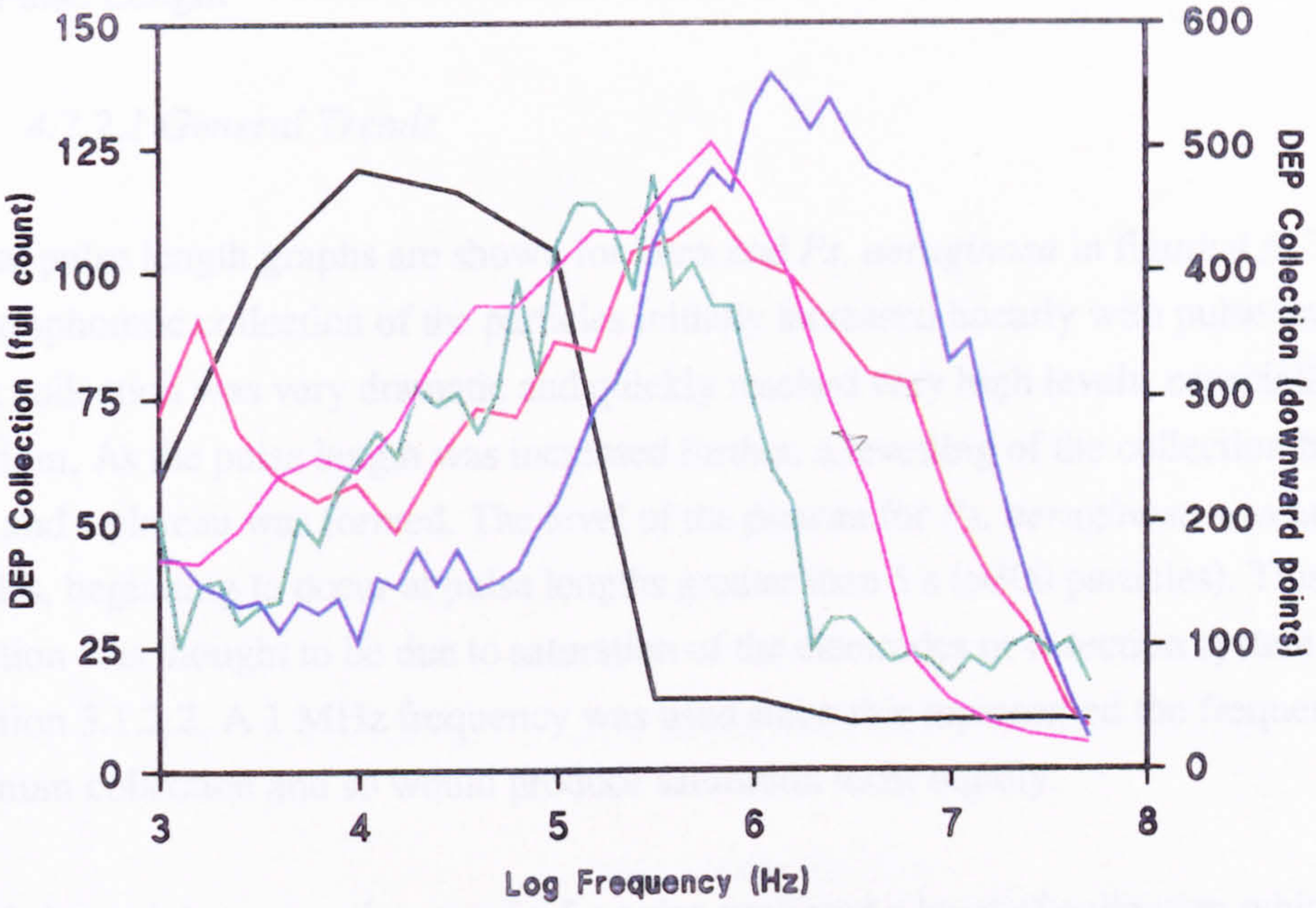

Figure 4.5 : Dielectrophoretic (DEP) frequency spectra for Gram positive and negative bacterial species using the image analysis method of detection. (—) 2.07 μm diameter latex, (—) *B. subtilis*, (---) *Staph. aureus*, (—) *E. coli* 10418, (—) *Serr. marcescens*. Conditions : 5 s pulse, 12 V pk-pk, 24.5 μS.cm^{-1} (bacteria), 4.5 μS.cm^{-1} (latex). Points are means plus standard error of 5 replicate spectra, datapoints not shown for clarity. Latex particles measured by full count method, bacterial species measured by downward points count.

It can be observed that there exist very great differences in the spectra even with species of the same Gram staining properties. Latex had a very characteristic spectrum, collecting very well at low frequencies, but displaying negligible collection at frequencies above 500 kHz. Again, the Gram positive species tended to exhibit relatively good collection in the lower frequency range (below 100 kHz) compared to the Gram negative cells. In addition, the collection again declined very rapidly after the 1 MHz peak frequency in the Gram positive species, while the Gram negative cells still maintained good dielectrophoretic collection.

In the bacterial species other than *Staph. aureus*, the peak collection frequency occurred at around 1 MHz, while in this Gram positive organism, the peak occurred at a lower frequency of 200-300 kHz. The spectra for *B. subtilis* obtained with both spectrophotometric and image analysed DEP detection systems were very similar over the whole frequency range.

4.2.2 Pulse Length

4.2.2.1 General Trends

Typical pulse length graphs are shown for latex and *Ps. aeruginosa* in figure 4.6. The dielectrophoretic collection of the particles initially increased linearly with pulse length. This rise in collection was very dramatic and quickly reached very high levels, especially with the bacterium. As the pulse length was increased further, a levelling of the collection began to occur and a plateau was formed. The level of the plateau for *Ps. aeruginosa* was at around 575 particles, beginning to occur at pulse lengths greater than 5 s (>300 particles). This levelling of collection was thought to be due to saturation of the electrodes or detection system as described in section 3.1.2.2. A 1 MHz frequency was used since this represented the frequency of maximum collection and so would produce saturation most rapidly.

For this bacterial species, the use of a 5 s pulse produced a level of collection which was still in the linear region and so would not cause saturation at this collection frequency. A pulse of this duration could be used for obtaining frequency spectra since there would be no moderation of the collection by saturation and a true spectrum would be produced. The use of a 30 s pulse would produce some saturation, so a resulting frequency spectrum produced with 30 s pulse applications would cause collection at 1 MHz to be limited at a level of 575 particles, since no additional particles would be collected or detected.

The pulse length graph for the polystyrene latex was linear in form at lower pulse lengths and saturation did not begin to occur until after around 25 s, when 500 particles had collected. In this case the frequency used was 10 kHz, the frequency of maximum collection for latex (figure 4.5). The electrodes were not filled as quickly with this particle type as with the *Ps. aeruginosa*, possibly due to a lesser degree of polarisation with the latex.

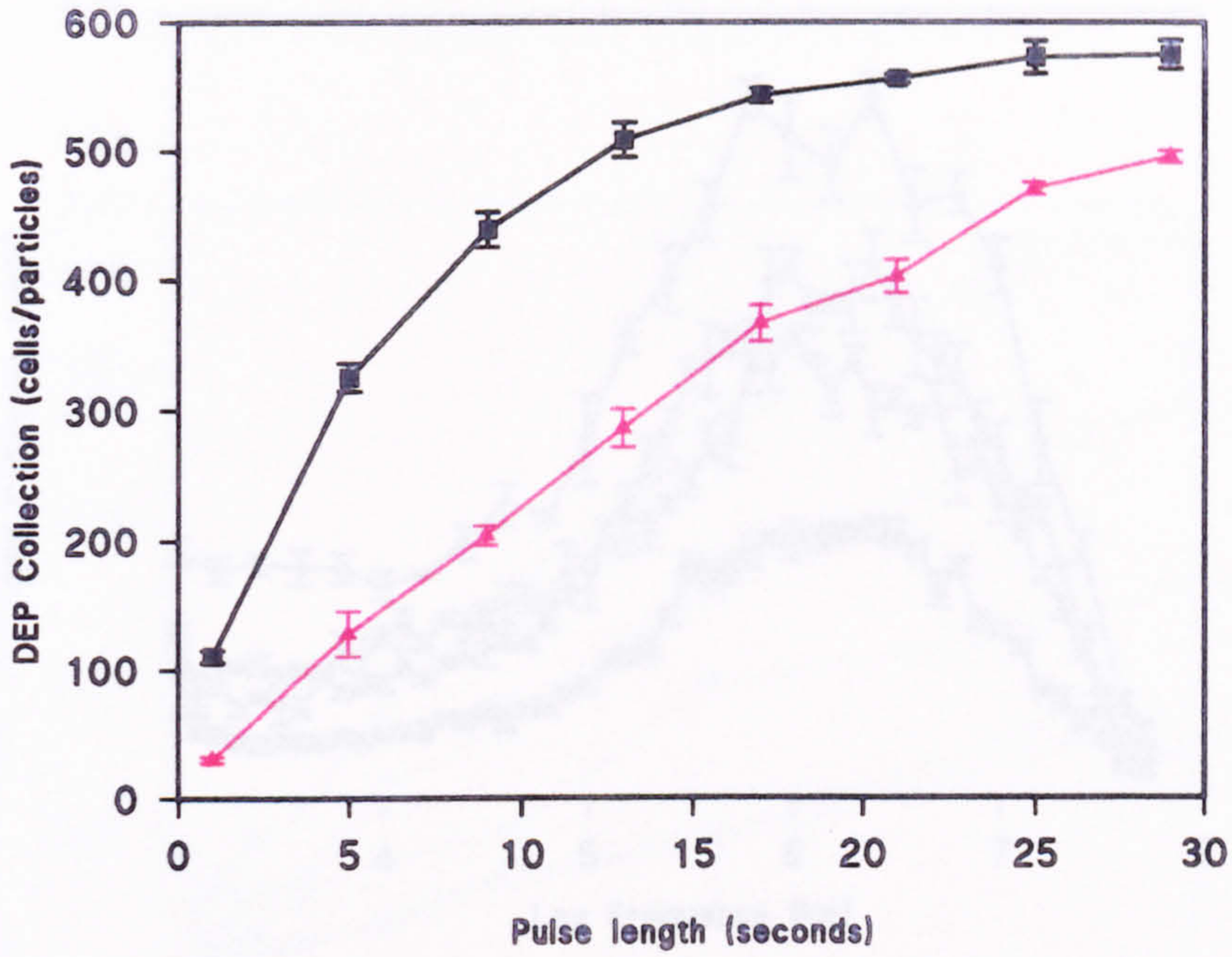

Figure 4.6 : Pulse length graphs of dielectrophoretic (DEP) collection for (■) *Ps. aeruginosa* and for (▲) polystyrene latex particles. Conditions : Full count detection, 12 V pk-pk, 4.45 μS.cm^{-1} (latex), 24.5 μS.cm^{-1} (*Ps. aeruginosa*), 10^4 Hz (latex), 10^6 Hz (*Ps. aeruginosa*). Graphs are means plus standard error of 4 replicate runs.

The small size of the error bars demonstrated the reproducibility of this relationship. Similar results were obtained with other bacterial species. Typically a pulse length of 5 s was subsequently used for dielectrophoretic experiments, since this rarely produced saturation with concentrations normally used and was also seen to produce a substantial collection level.

4.2.2.2 Effect of Pulse Length on Frequency Spectra

Spectra showing the effect of increasing pulse length on *E. coli* dielectrophoretic collection are presented in figure 4.7. The spectra were performed at the same conductivity values and used the same experimental parameters. The image analysis downward points count was used in these experiments, resulting in greater counts (section 3.1.2.2). A typical frequency spectrum for *E. coli* 10418 is shown, with a peak maximum at 1 MHz frequency. As the pulse length was increased from 5 s there was a longer period of time over which collection was able to occur.

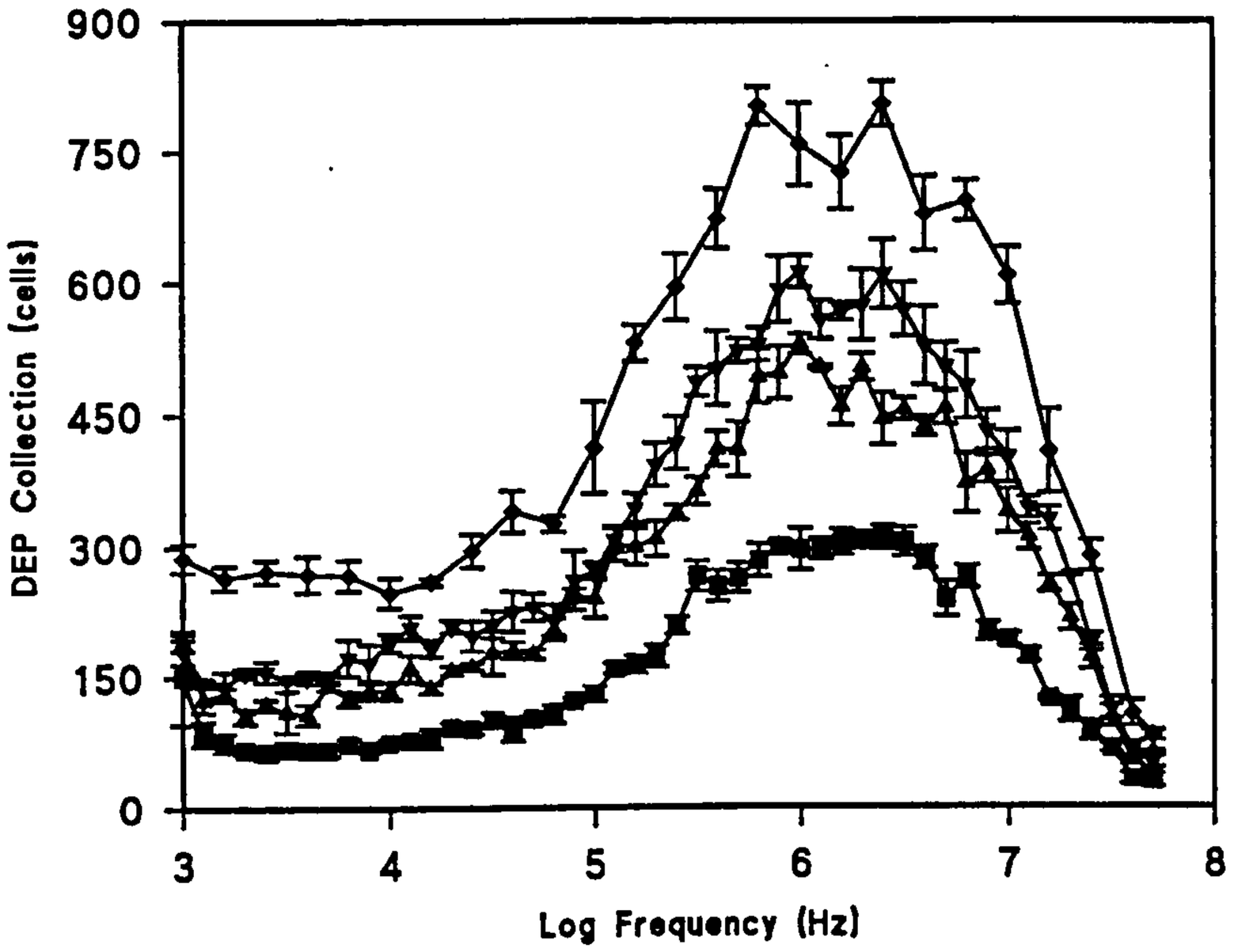

Figure 4.7 : Effect of increasing pulse length on the dielectrophoretic (DEP) spectrum of *E. coli* 10418. (■) 5 s pulse, (▲) 10 s pulse, (▼) 15 s pulse, (◆) 30 s pulse. Conditions : Downward points count detection, 10 V, 33.0-34.8 $\mu S.cm^{-1}$. Points are means plus standard error of 5 replicate spectra.

Though the pulse lengths used were increased from 5 s to 30 s duration, the basic form of each spectrum remained consistent. The increased pulse length, however, had the effect of accentuating peak collection values on the spectrum until saturation point began to occur, due to the increased time available for collection. Frequencies at which particles collected less well would not have increased their collection by a significant amount during the greater pulse lengths when compared to the more efficient frequencies.

Assuming a linear relationship between pulse length and dielectrophoretic collection, the collection of around 300 particles at 1 MHz with the 5 s pulse in figure 4.7, was expected to increase to 600 particles with a 10 s pulse duration. However a level of only 450-500 particles was attained.

4.2.2.3 Pulse Length at Different Frequencies

The effect of pulse length on collection of *E. coli* at each of several frequencies is shown in figure 4.8. The maximum level of collection was observed at 1 MHz, as previously noted from figure 4.7. Each frequencies showed a region of good linearity for a portion of the curves. The frequencies 1 kHz, 10 kHz and 100 kHz had a lower collection and did not appear to become

saturated even with 30 s pulse lengths, with linearity being maintained. At 1 MHz and 10 MHz there was some deviation from linearity after 10 and 15 s respectively.

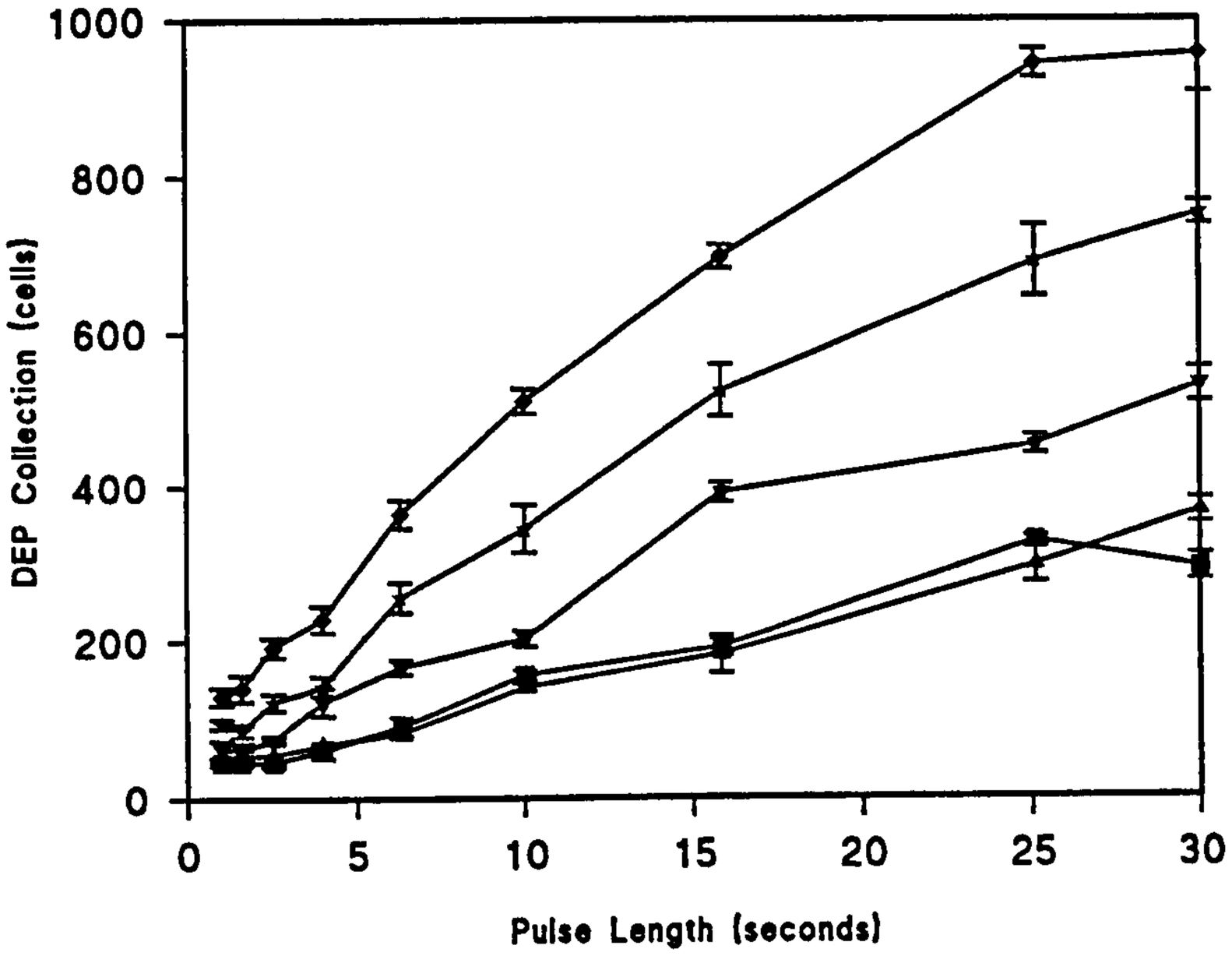

Figure 4.8 : Effect of increasing pulse length on dielectrophoretic (DEP) collection of *E. coli* 10418 at different frequencies. (■) 1 kHz, (▲) 10 kHz, (▼) 100 kHz, (♦) 1 MHz, (★) 10 MHz. Conditions : Downward points count detection, 10 V pk-pk, 31.1-34.6 $\mu S.cm^{-1}$. Points are means plus standard error of 3 replicate runs.

4.2.3 Voltage

Figure 4.9 shows the change in dielectrophoretic collection of *Ps. aeruginosa* as the voltage was increased to the maximum capacity of the function generator.

Generally, in agreement with Pohl (1978) and as may be expected, the voltage had a linear relationship with dielectrophoretic collection, i.e. increasing voltage increased collection until saturation of the electrodes or detection system began to occur, causing levelling of collection. In Pohl's system of static dielectrophoresis, this levelling was due to complete removal of cells from the surrounding medium. However, in the system described here this would not occur because the cells were continually replaced due to the constant recirculation of cells around the system.

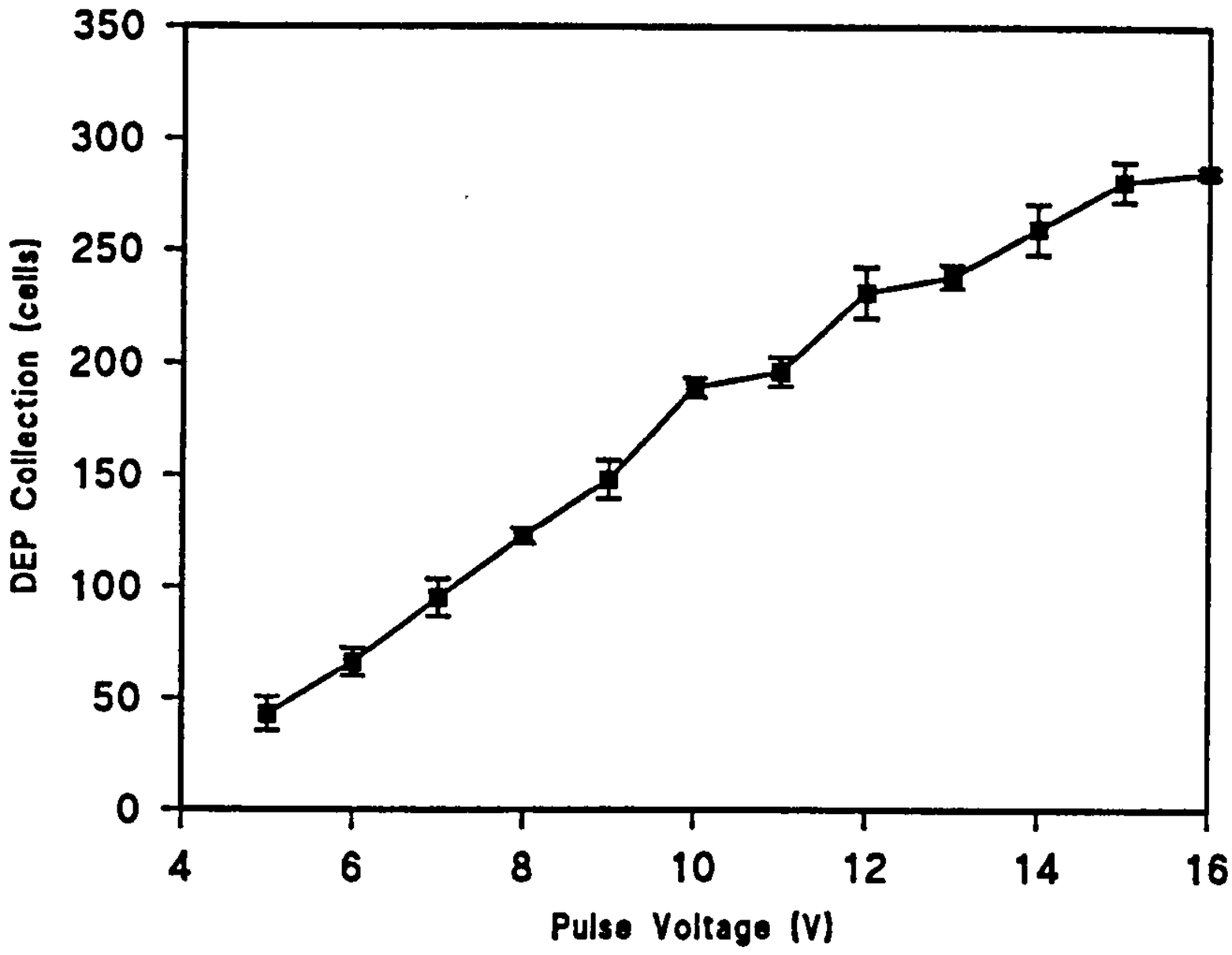

Figure 4.9 : Effect of voltage on dielectrophoretic (DEP) collection of *Ps. aeruginosa* 10662. Conditions : 1 MHz, 5 s pulse, 25.3 $\mu S.cm^{-1}$. Full count detection. Points are means plus standard error of 5 replicate runs.

By examination of figure 4.9, saturation was not obvious, though some levelling of collection may be beginning to occur at higher voltages. This was generally verified by the previously obtained pulse length graph (figure 4.6) which did not appear to undergo significant saturation until greater than around 320 particles had collected.

For standard experiments a voltage of 12 V r.m.s. was used. This was deemed to produce good dielectrophoretic collection but was not sufficiently great to produce major heating effects or electrolytic processes or significant saturation.

4.2.4 Pump Speed

By plotting the amount of collection against the speed of the pump used to circulate the suspension during pulse application, an optimum speed for collection was found. A typical example is shown in figure 4.10 for *Ps. aeruginosa*.

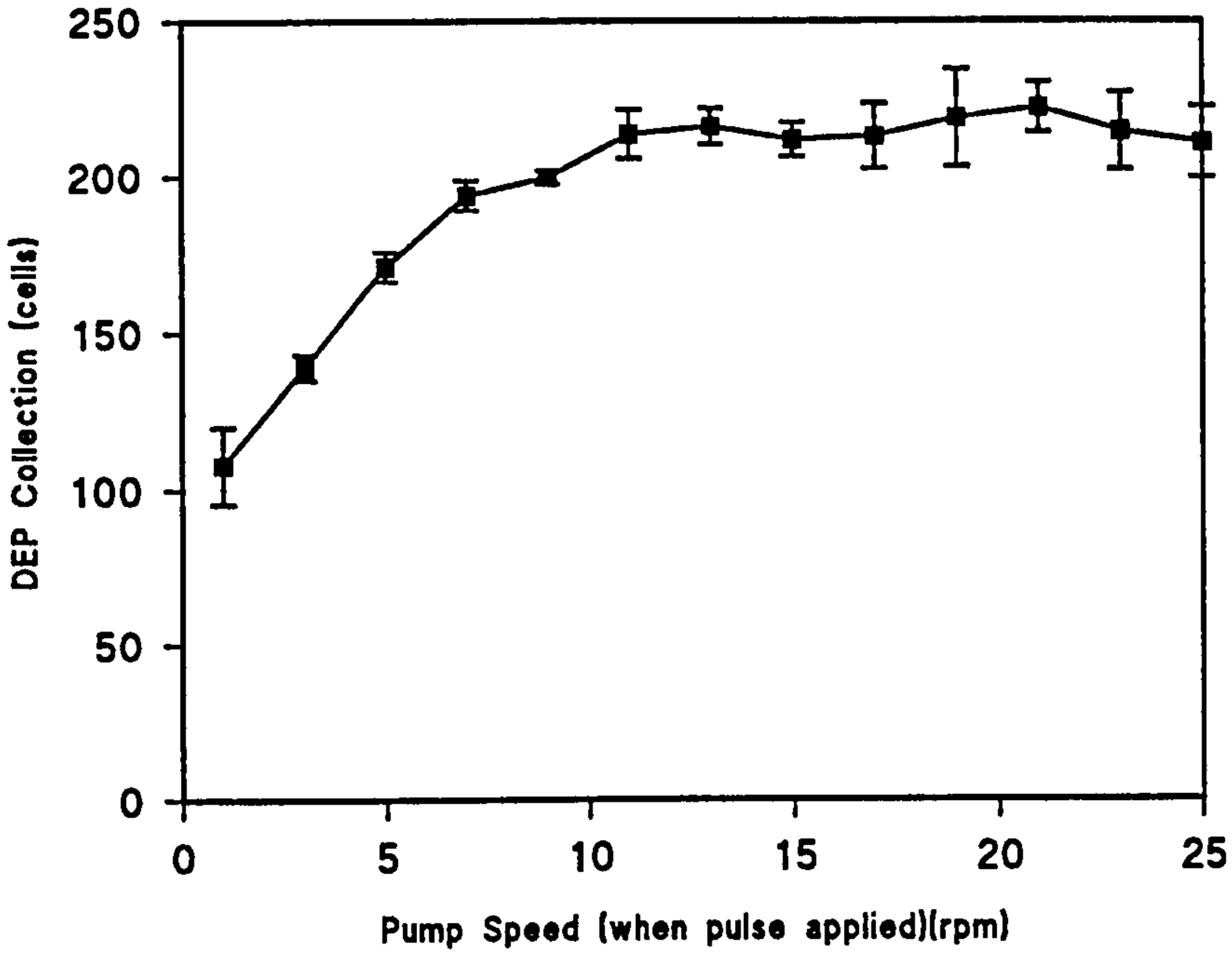

Figure 4.10 : Effect of pump speed on the dielectrophoretic (DEP) collection of *Ps. aeruginosa* 10662. Conditions : 10 V, 5 s pulse, 1 MHz, 24.6 $\mu S.cm^{-1}$. Full count detection. Points are means plus standard error of 5 replicate runs.

Collection increased linearly with pump speed up to a value of 8-10 rpm whereafter there was a plateau of collection (at a level of 215-220 particles) at greater speeds. The increase in speed while the field was applied caused greater numbers of cells to be brought into the effective field for collection and into contact with the electrodes. From previous experiments (figure 4.6) saturation should not have begun until >300 *Ps. aeruginosa* cells had collected. Since the plateau value found here was much lower, it was more likely that the levelling was due to the increased speeds during collection. For *Ps. aeruginosa*, the optimum pump speed for collection was at approximately 10-11 rpm, producing the maximum number of collected particles. For this reason, this speed was adopted for general use during dielectrophoretic experiments.

4.2.5 Multiple Pulse Applications

The amount of collection obtained for polystyrene latex particles, when identical pulses were applied to the electrodes is shown in figure 4.11. When taken in order of pulse application, it can be seen that there was no trend of collection throughout the experimental period, though initial collection was particularly high. Under ideal conditions the amount of collection should

have been the same for each pulse application, yet there were points which appeared to be significantly higher and lower than the mean collection level of 97.88 (± 4.19) particles.

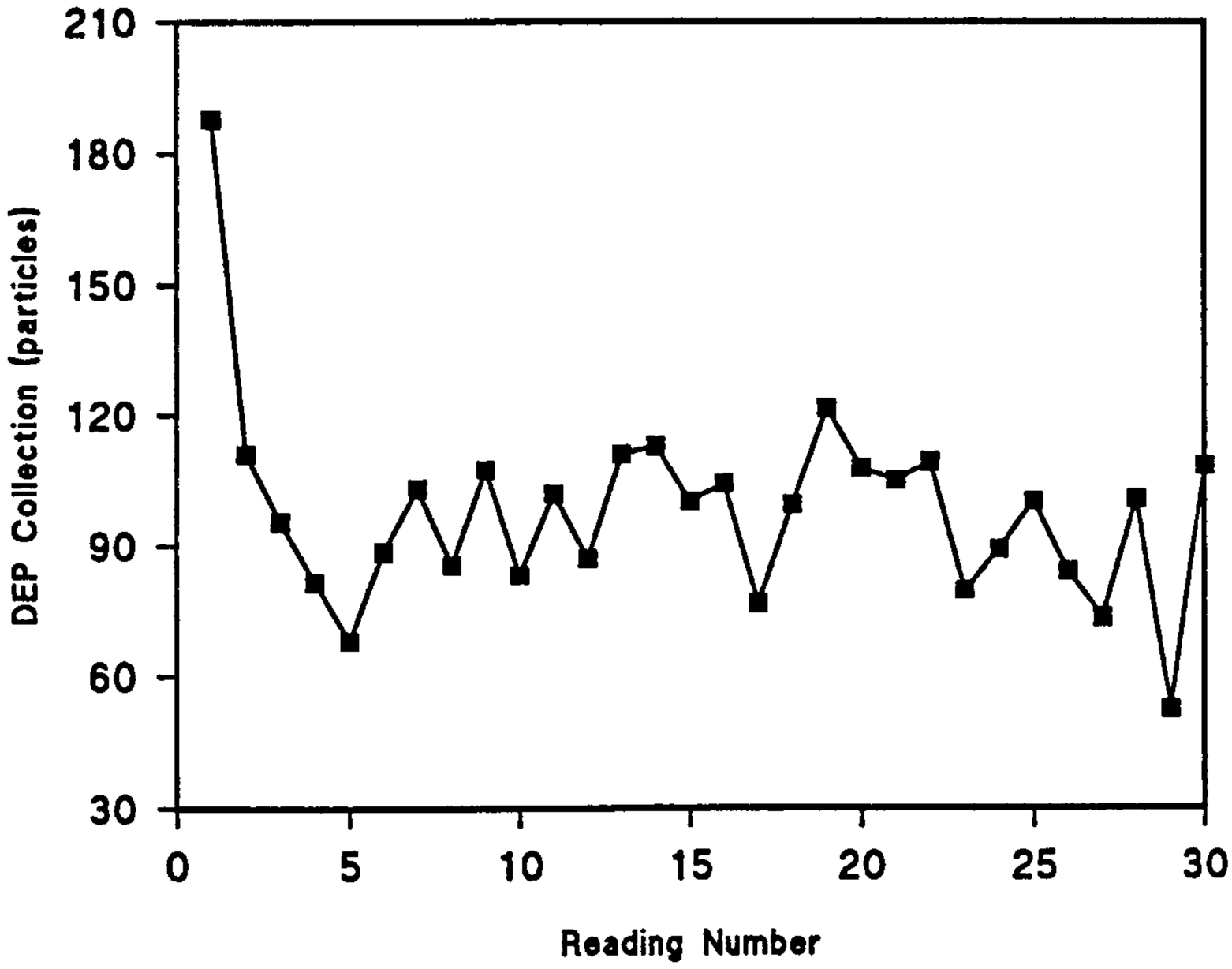

Figure 4.11 : Dielectrophoretic (DEP) collection level of each of thirty repeated pulse applications to a suspension of latex particles. Conditions : 12 V, 10 kHz, 5 s pulse, 4.45 $\mu S.cm^{-1}$. Full count detection.

4.2.6 Effect of Increasing Suspension Conductivity

4.2.6.1 General Trends

Figure 4.12 shows *E. coli* and *Ent. cloacae* bacterial cells collecting over the standard frequency range employed, using a voltage of 10 V and a 5 s pulse duration. As the conductivity was raised from around 18 $\mu S.cm^{-1}$ to 44 $\mu S.cm^{-1}$ the spectral form of *E. coli* became depressed over the whole frequency range, particularly at lower frequencies. It may also be seen that the maximum peak of collection was shifted to higher frequency ranges. At 18 $\mu S.cm^{-1}$, the major collection peak was at around 500 kHz compared to 2 MHz at the higher conductivity.

With *Ent. cloacae*, similar effects were observed as a decrease in peak collection from around 900 particles at just below 100 kHz to little more than 800. The peak became shifted to 1-2 MHz on increasing conductivity values from 22 $\mu S.cm^{-1}$ to 41 $\mu S.cm^{-1}$. This is a common feature to most bacterial species, though some are more conductivity sensitive than others.

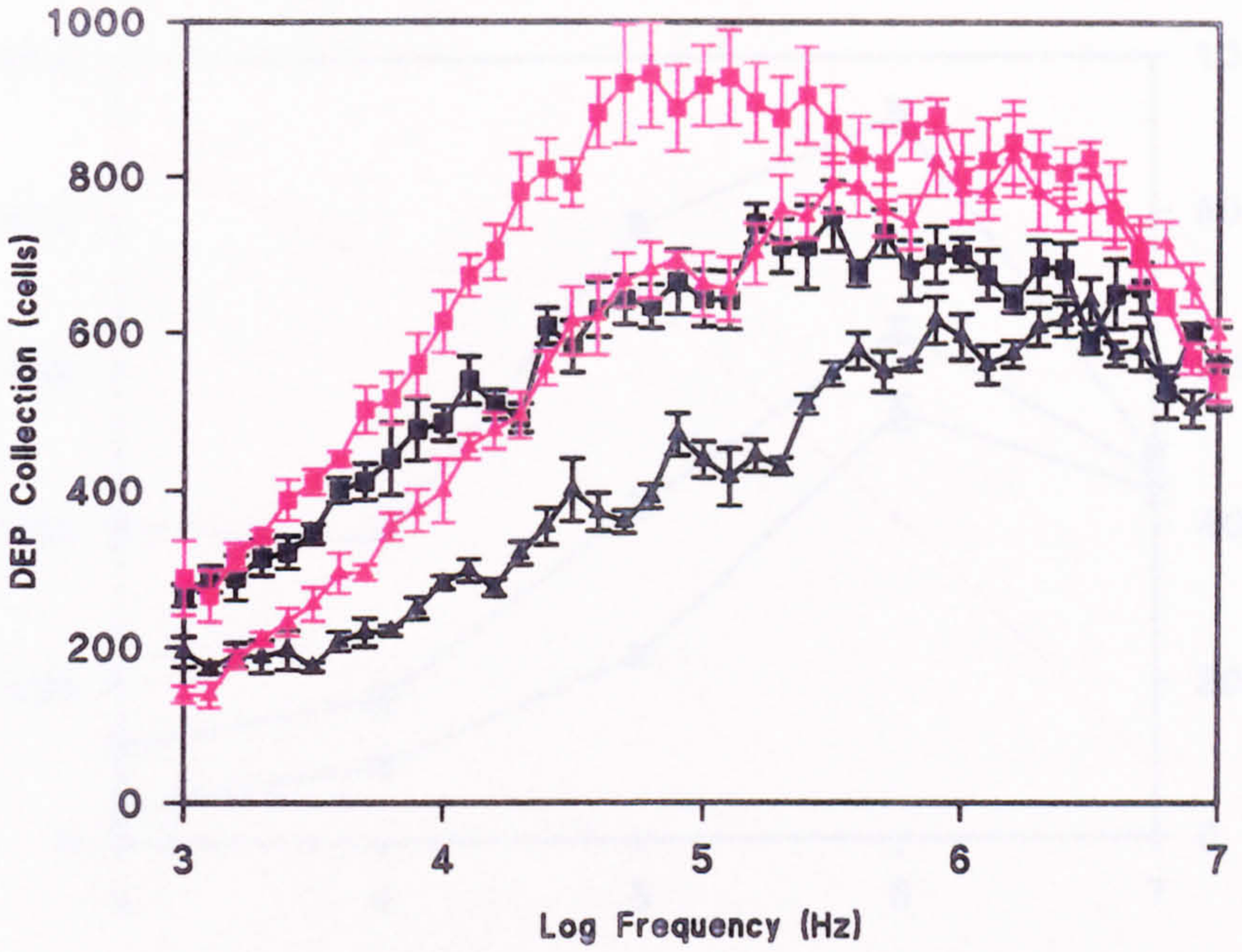

Figure 4.12 : Effect of increasing suspension conductivity on the dielectrophoretic (DEP) collection of two bacterial suspensions. (■) *E. coli* 8114 at 17.47-18.04 μS.cm^{-1}, (▲) *E. coli* 8114 at 43.7-44.2 μS.cm^{-1}, (■) *Ent. cloacae* at 21.8-22.7 μS.cm^{-1}, (▲) *Ent. cloacae* at 40.5-41.5 μS.cm^{-1}. Conditions : 10 V, 5 s pulse. Downward points count detection. Points are means plus standard error of 5 replicate spectra.

Generally the lower frequency regions were more affected by conductivity rises and the peak of collection thus became shifted to higher frequencies as conductivity increased. There was however a simultaneous decrease in overall collection levels, though as can be seen from the spectra, the line of fall off at high frequencies generally remained the same regardless of conductivity.

4.2.6.2 Effect of Increasing Conductivity on Frequency Collection

Figure 4.13 shows the effect of conductivity rises on the dielectrophoretic frequency spectrum in more detail. The increase in conductivity from 14 μS.cm^{-1} to 51 μS.cm^{-1} caused a significant decrease in collection level over the majority of the spectrum. The second axis shows the relative amount of decrease in collection at each frequency, demonstrating that the greatest suppression in collection occurred at lower frequencies, the effect diminishing at higher frequencies. At 10 MHz frequency, the effect of this conductivity increase could be seen to have negligible effect on collection.

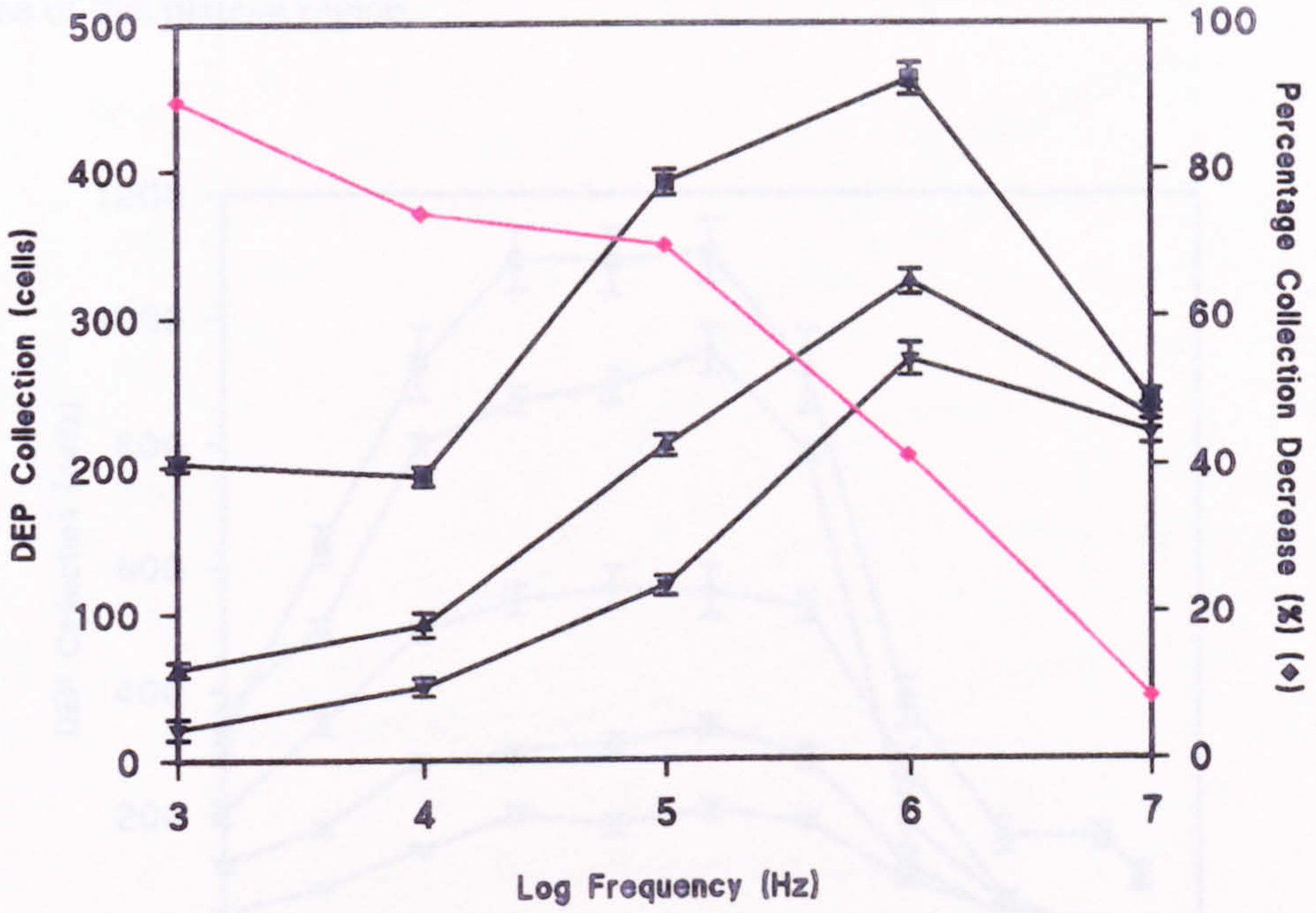

Figure 4.13 : Effect of increasing suspension conductivity on the dielectrophoretic (DEP) collection of *E. coli* 10418 with corresponding percentage decrease in collection caused by the increase. (■) 14.3-14.9 $\mu S.cm^{-1}$, (▲) 30.8-32.7 $\mu S.cm^{-1}$, (▼) 51.6-53.8 $\mu S.cm^{-1}$, (◆) % collection decrease at each frequency. Conditions : 10 V, 5 s pulse. Downward points count detection. Points are means plus standard error of 30 repeat pulse applications.

4.2.7 Effect of Increasing Particle Concentration

4.2.7.1 General Trends

Figure 4.14 shows frequency spectra of suspensions of *E. coli* 39323 having differing concentrations.

Generally, the spectra had very similar form, though the overall peak height of each spectrum was different, collection level rising to correspond with the increased cell concentration. With lower cell concentrations, a less well defined spectrum was produced and the total level of collection was significantly less than the higher concentrations.

The line showing maximum collection was produced from a suspension having $O.D._{600}$ 0.243 (viable cell concentration 5×10^8 $cfu.ml^{-1}$). The frequency of maximum collection had the form of a plateau covering the frequency range of 35-350 kHz, detecting almost 1100 cells. This was a very high level of collection for bacterial cells due to the suspension having such a high

cell concentration and would likely have resulted in saturation effects, possibly explaining the presence of this plateau region.

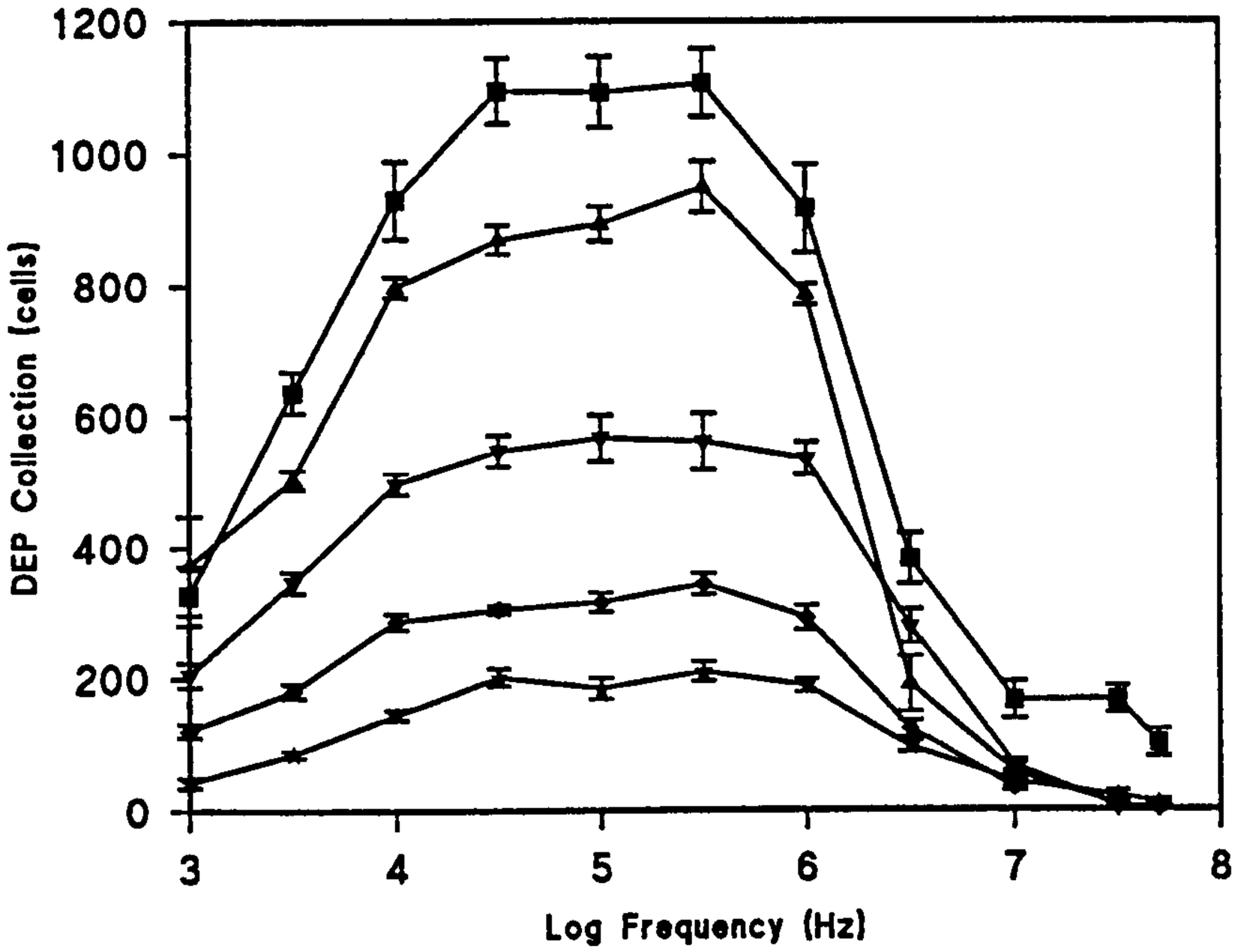

Figure 4.14 : Effect of cell concentration on the dielectrophoretic (DEP) spectrum of *E. coli* 39323. (■) $O.D._{600}$ 0.243, (▲) $O.D._{600}$ 0.169, (▼) $O.D._{600}$ 0.117, (◆) $O.D._{600}$ 0.089, (★) $O.D._{600}$ 0.057. Conditions : 10 V, 5 s pulse, 27.7-34.7 $\mu S.cm^{-1}$. Downward points count detection. Each point is the mean plus standard error of ten replicate spectra.

The second highest spectrum had a mean suspension concentration of 2.93×10^8 $cfu.ml^{-1}$ as determined by viable count. The collection of this suspension had the maximum collection point at 300 kHz, detecting a collection level of 900.

The other four spectra, having $O.D._{600}$ values 0.169, 0.117, 0.089 and 0.057 had mean viable counts 2.93×10^8 $cfu.ml^{-1}$, 1.96×10^8 $cfu.ml^{-1}$, 1.25×10^8 $cfu.ml^{-1}$ and 0.92×10^8 $cfu.ml^{-1}$ respectively.

These spectra were re-drawn, expressing the level of collection at several frequencies as a function of the absorbance value of the suspensions. This is shown in figure 4.15.

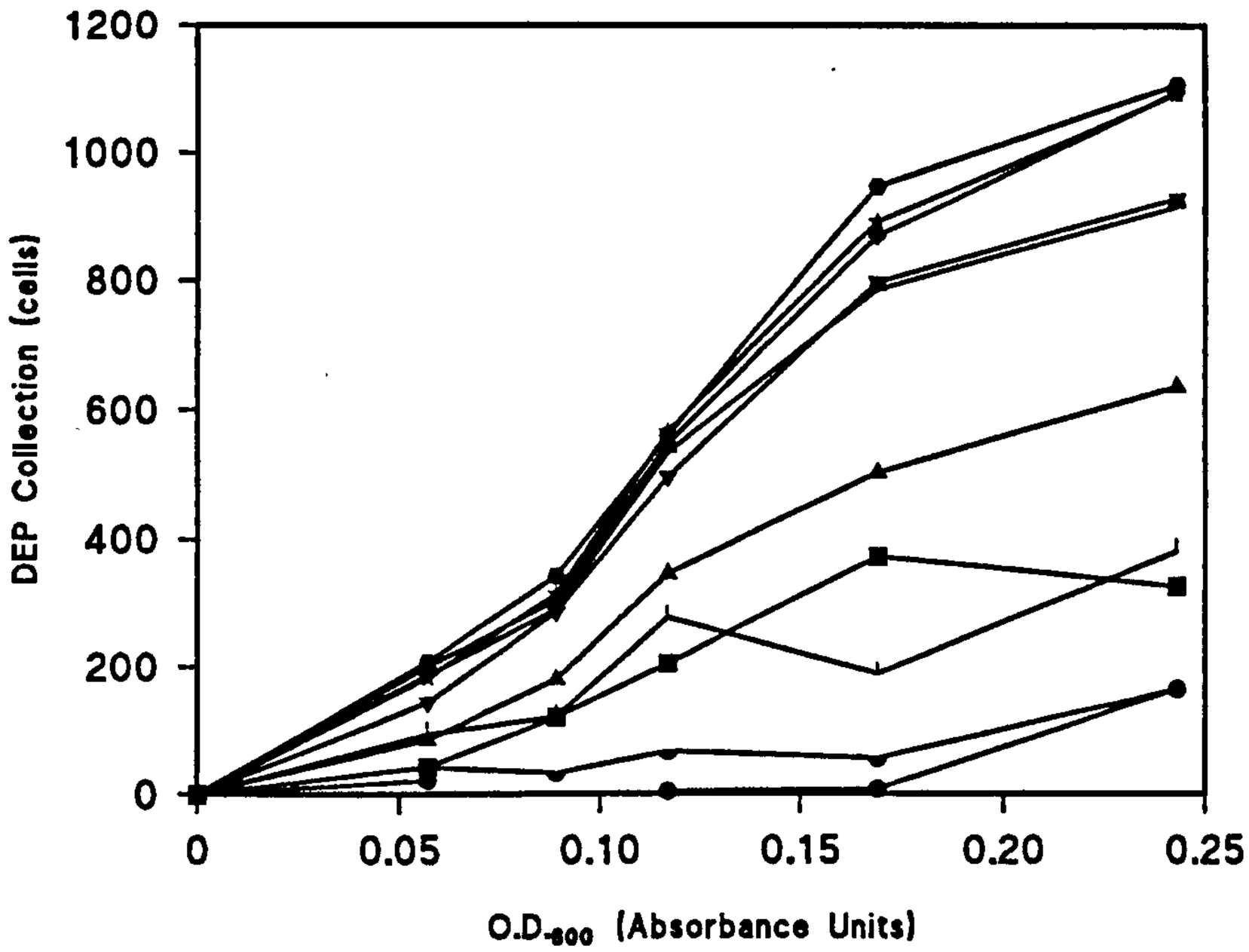

Figure 4.15 : Effect of cell concentration on the dielectrophoretic (DEP) collection of *E. coli* 39323 at each of several frequencies. (■) 10^3, (▲) $10^{3.5}$, (▼) 10^4, (◆) $10^{4.5}$, (★) 10^5, (●) $10^{5.5}$, (⁀) 10^6, (I) $10^{6.5}$, (‿) 10^7, (○) $10^{7.5}$. Each point is the mean of ten replicate spectra; error bars not shown for clarity.

This figure shows that at the frequencies giving greatest collection levels (between 10^4 Hz and 10^6 Hz), the relationships with absorbance produced apparent sigmoidal shaped curves, caused by very low collection with the low O.D suspensions and saturation plateaus at the higher cell concentrations at around 1000 particles detected.

The frequency $10^{3.5}$ Hz showed similar sigmoidal form. Collection at the more extreme frequencies was irregular and also had different gradients to the relationships. Generally, these frequencies had more of a linear form, though their overall collection was significantly reduced.

4.2.7.2 Normalisation Experiments

It would be advantageous to applications of dielectrophoresis if experiments could be performed with non-specific particle concentrations and then to calculate the collection theoretical obtainable with other concentrations. This would allow the facility to input a

suspension, calculate its concentration and manipulate its spectrum to directly compare with other suspensions on a frequency to frequency basis.

Figure 4.16 shows spectra for 5 different concentrations of *E. coli* suspensions. The lowest concentration (having a total count of 5.75×10^7 cells.ml^{-1}) produced little DEP collection, with increasing concentrations collecting successively greater numbers of cells. The greatest suspension concentration had a collection peak at just less than 250 cells, at a frequency of around 600 kHz. The other spectra appeared to have a similar shape, though as in figure 4.14, their collection levels were different. In addition, three of the suspensions (5.75×10^7 cells.ml^{-1}, 8.176×10^7 cells.ml^{-1} and 27.5×10^7 cells.ml^{-1}) had abnormally high collection at the initial frequency of 1 kHz. This has been observed previously and is possibly due to electrode polarisation effects or other anomalies caused by the electrode surface.

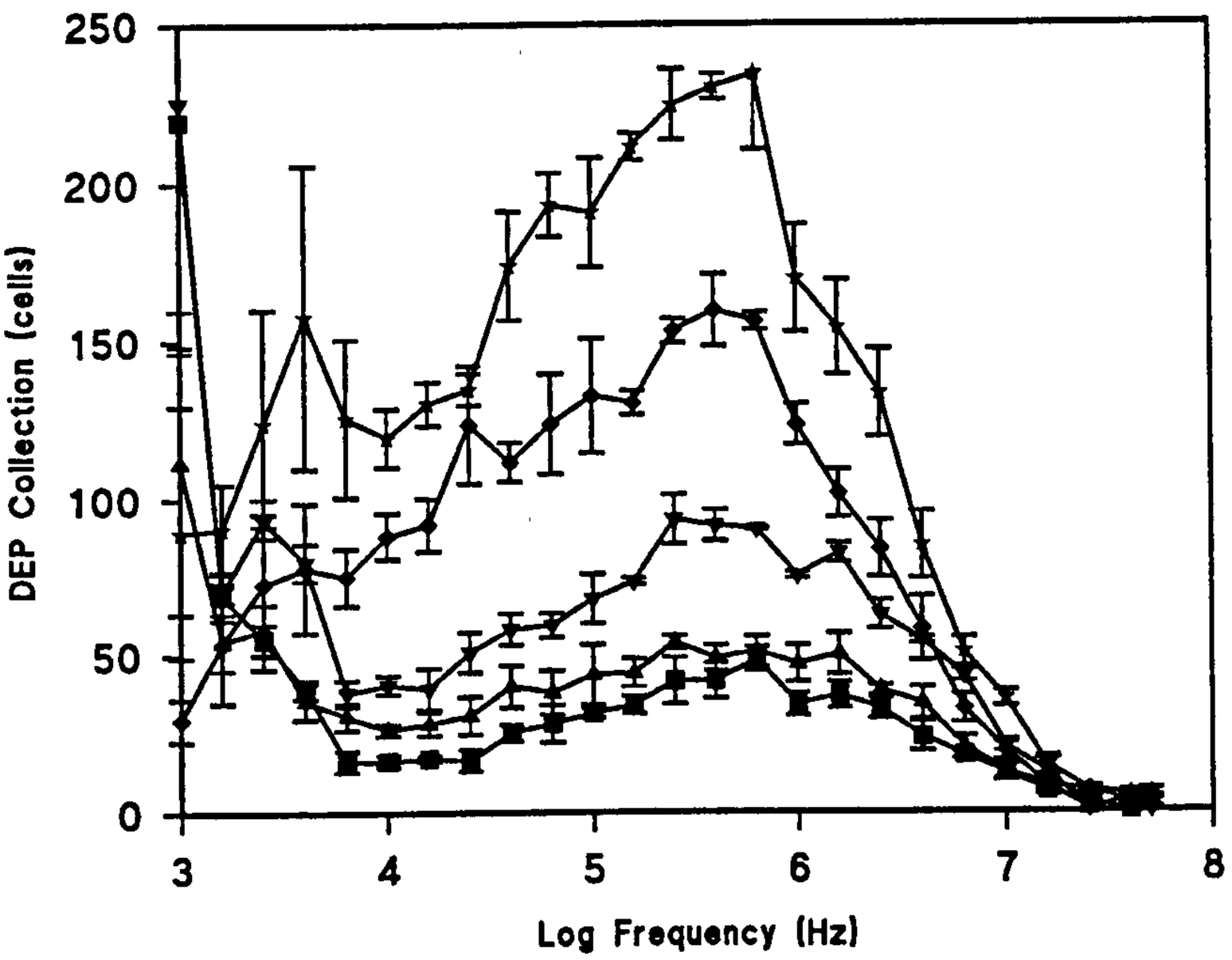

Figure 4.16 : Frequency spectra of *E. coli* showing effect of cell concentration on dielectrophoretic (DEP) collection. (■) 5.75×10^7 cells.ml^{-1}, (▲) 8.176×10^7 cells.ml^{-1}, (▼) 9.063×10^7 cells.ml^{-1}, (◆) 17.96×10^7 cells.ml^{-1}, (★) 27.5×10^7 cells.ml^{-1}. Conditions : 12 V, 5 s pulse, 24.4-24.6 μS.cm^{-1}. Full count detection. Each point is the mean plus standard error of 3 replicate spectra.

The spectra were normalised to the highest concentration (27.5×10^7 cells.ml^{-1}) and each point on the spectra manipulated by simple multiplication according to a linear relationship prediction. According to a linear relationship model between dielectrophoretic collection and cellular concentration the modified spectra should become overlaid and have identical collection.

The manipulated spectra are shown in figure 4.17.

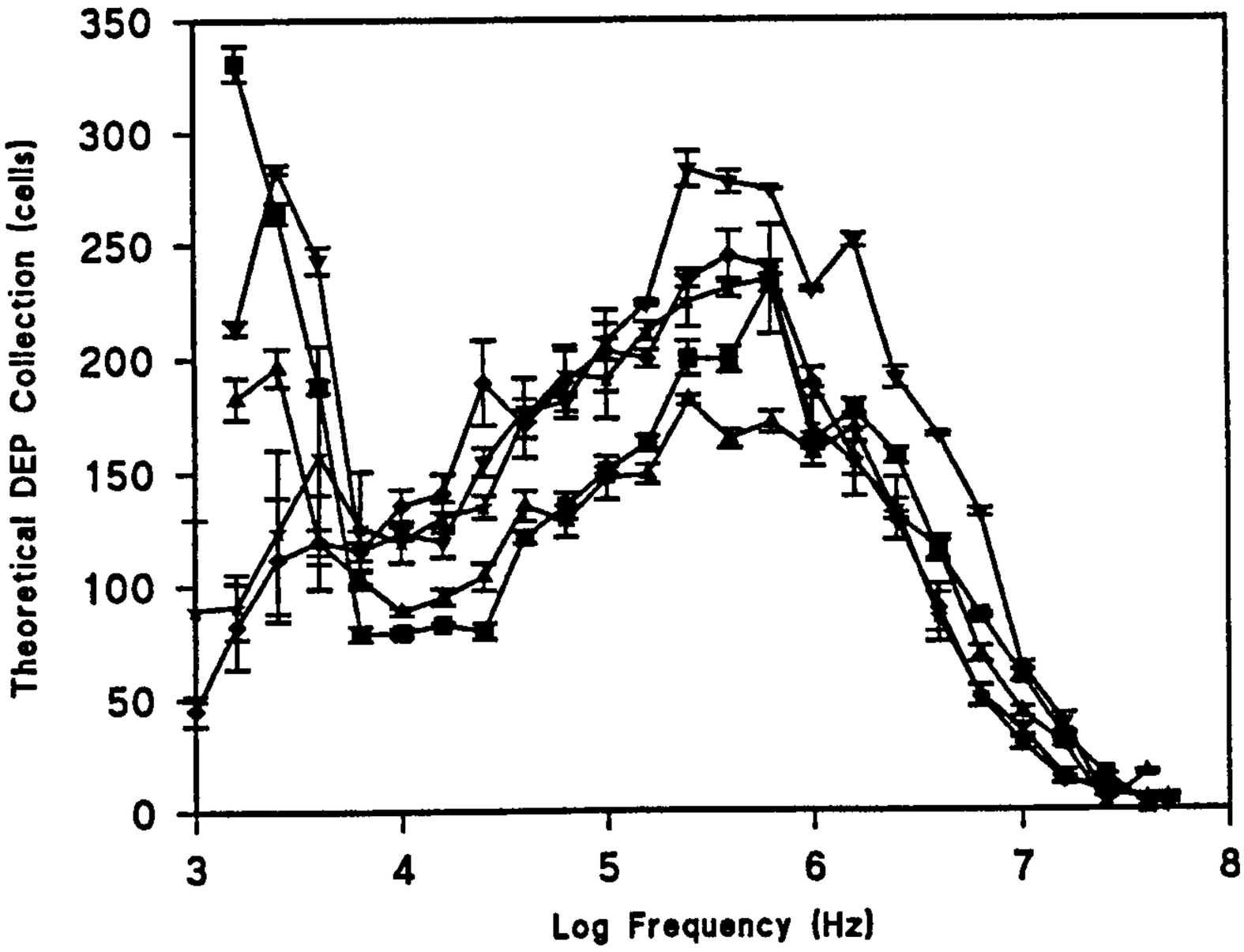

Figure 4.17 : Frequency spectra of *E. coli* after normalisations to a cell concentration of 27.5×10^7 cells.ml^{-1}.

Since doubling the suspension concentration was expected to result in a doubling of the number of cells passing the electrodes, there should have been a similar relationship with the amount of collection. This assumed that there was a linear relationship between concentration and collection, the equation of the line passing through zero (i.e. doubling concentration would double the resulting collection level). If this was the case, the spectra should become overlaid and identical once they had been normalised. As can be seen from figure 4.17, normalisation brought some of the spectra closer together. However, they still appeared to have significant differences between them. In particular, the suspensions with the two lowest cell concentrations were significantly lower than the other spectra. Thus, normalisation by this method did not appear to have been successful. The explanation for this is that the relationship between concentration and collection was not linear, as found in section 4.2.7.1, and so

spectra could not be directly compared by this method. All other parameters were kept identical and so could not be responsible for this discrepancy.

4.2.8 Effect of Particle Size

Figure 4.18 shows the relative dielectrophoretic collection over the frequency range for polystyrene latex of 2.07, 2.40 and 2.75 μm diameters respectively. Experimental parameters were kept constant for the experiments. Only frequencies between 1 kHz and 1 MHz are shown as collection of the latex particle types examined did not occur at frequencies greater than 1 MHz. The general form of the spectra had a plateau of maximum collection between frequencies of 1 kHz and 30 kHz, decreasing in level after this frequency. The error bars on the spectra were quite large, and this was thought to be due to the effects of the slight increases in conductivity over the course of the experiment which resulted in a gradual lowering of spectrum height (section 4.2.6). This conductivity increase may have been due to shearing of the sulphate groups present on the surface during the experiment.

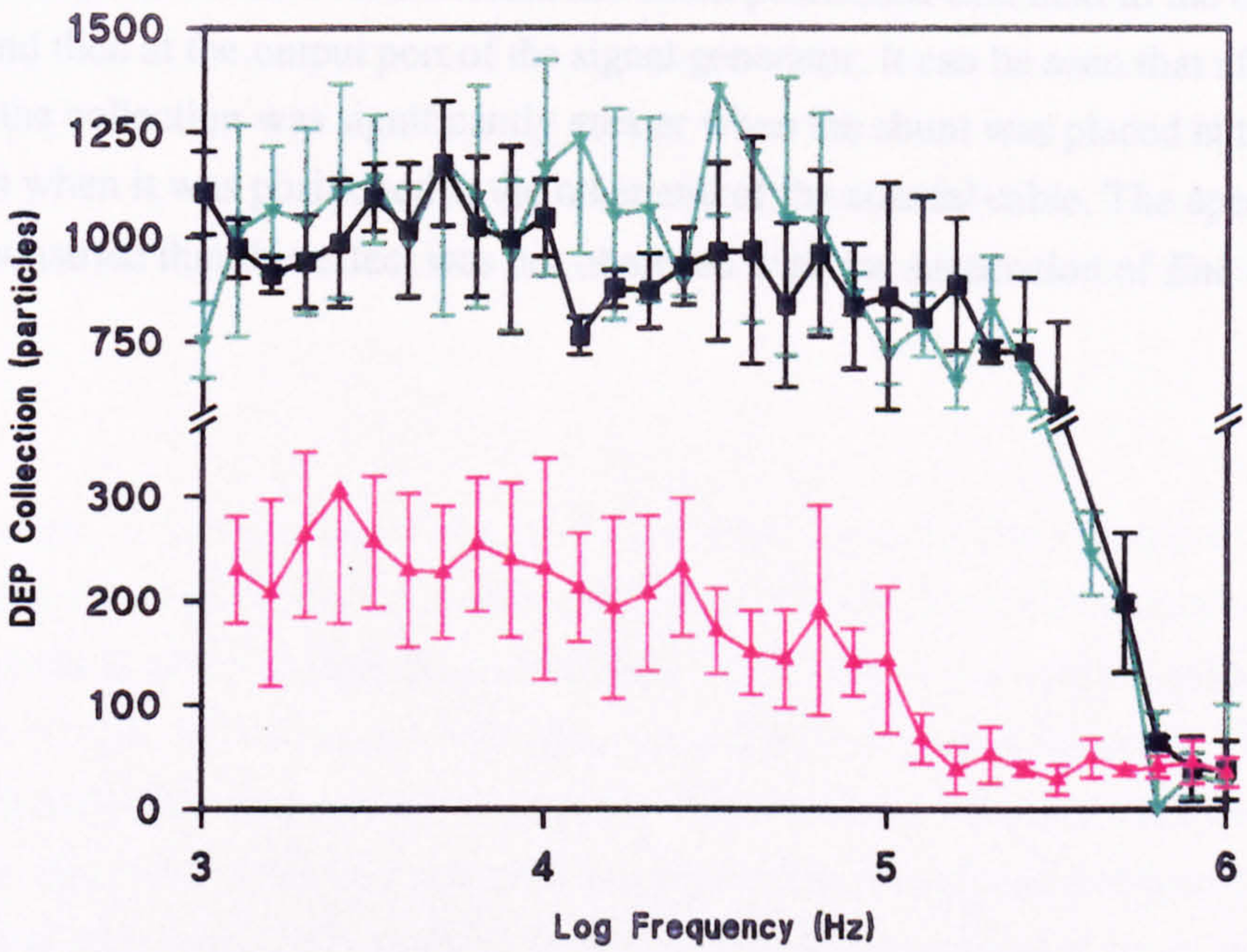

Figure 4.18 : Effect of particle size on the dielectrophoretic (DEP) frequency spectrum of polystyrene latex particle suspensions. (■) 2.07 μm diameter, (▲) 2.40 μm diameter, (▼) 2.75 μm diameter. Conditions : 10 V, 5 s pulse, 5 x 10^7 particles.ml^{-1}, 5.00-5.89 μS.cm^{-1}. Points are means plus standard errors of 5 replicate spectra. Downward points count detection.

Both particles of 2.07 µm and 2.75 µm diameters had very similar levels of dielectrophoretic collection over the majority of the frequency range, and the error bars of five repeated spectra showed no significant difference between the two. However, when they were compared with the collection of the 2.40 µm latex particles, they demonstrated much higher general collection over the frequency range. This was unexpected due to the relationship between particle volume and increasing dielectrophoretic force (equation 1.6), and will be discussed in great detail in section 4.4.8. The shape of the spectrum of 2.40 µm latex was again very similar in form to the other two particle sizes, though had a significantly reduced overall collection. A maximum level of 300 counts (as measured by the downward points count detection method) was obtained with this particle size compared with 1000-1200 counts for the two previously described.

4.2.9 Effect of Resistance Shunt Position

Figure 4.19 shows a typical *B. subtilis* spectrum conducted using the same bacterial suspension and conditions, with the resistance shunt positioned first next to the electrode chamber, and then at the output port of the signal generator. It can be seen that after 10 MHz frequency, the collection was significantly greater when the shunt was placed at the generator output, than when it was positioned at the other end of the coaxial cable. The spectra also shown demonstrate that this effect was not observed with the suspension of *Ent. cloacae*.

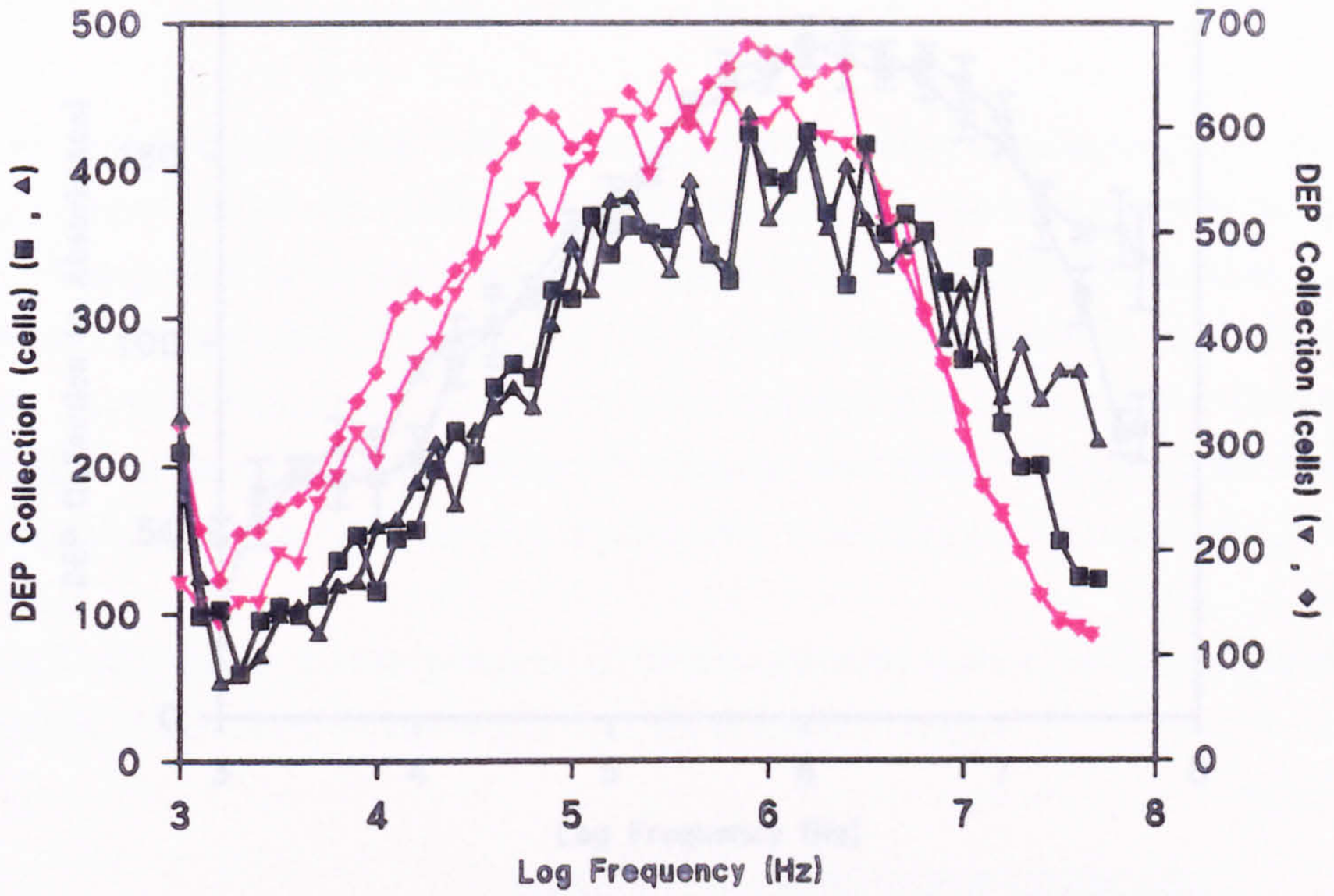

Figure 4.19 : Effect of resistance shunt position on the dielectrophoretic (DEP) collection of bacterial species. (■) *B. subtilis* with shunt next to electrodes, (▲) *B. subtilis* with shunt at signal generator output port, (▼) *Ent. cloacae* with shunt next to electrodes, (◆) *Ent. cloacae* with shunt at signal generator output port. Conditions : 10 V, 5 s pulse, 46.5-48.6 $\mu S.cm^{-1}$ (*B. subtilis*), 25.9-26.4 $\mu S.cm^{-1}$ (*Ent. cloacae*). Downward points count detection method. Each point is the mean plus standard error of 5 replicate spectra.

Again in figure 4.20 the effect was seen to be present using the Gram positive *Strep. faecalis* species, using the spectrophotometric method. In each case, there was an increase in the dielectrophoretic effect at high frequencies when the shunt was positioned at the signal generator, though this effect was only observed with Gram positive species. There was no increase in collection with any of the species when the shunt was positioned nearer to the electrodes. Since the effect was observed using both image analysed and spectrophotometric methods and only with Gram positive species, it was not considered to be an artefact due to any electrical interference. To further investigate the effect, an oscilloscope was connected to monitor the voltage output from the generator over a range of frequencies when the shunt was moved. Figure 4.21 shows that when the frequency was raised above 10 MHz, the applied voltage of 12 V no longer remained stable. When the coaxial cable was connected with the shunt next to the oscilloscope, the voltage began to drop slightly. With the shunt placed at the opposite end of the cable, nearest the output port of the signal generator, it was observed that there was a substantial increase in voltage as the frequency was increased. This reached a final level at 50 MHz which was 175 % greater than the input voltage.

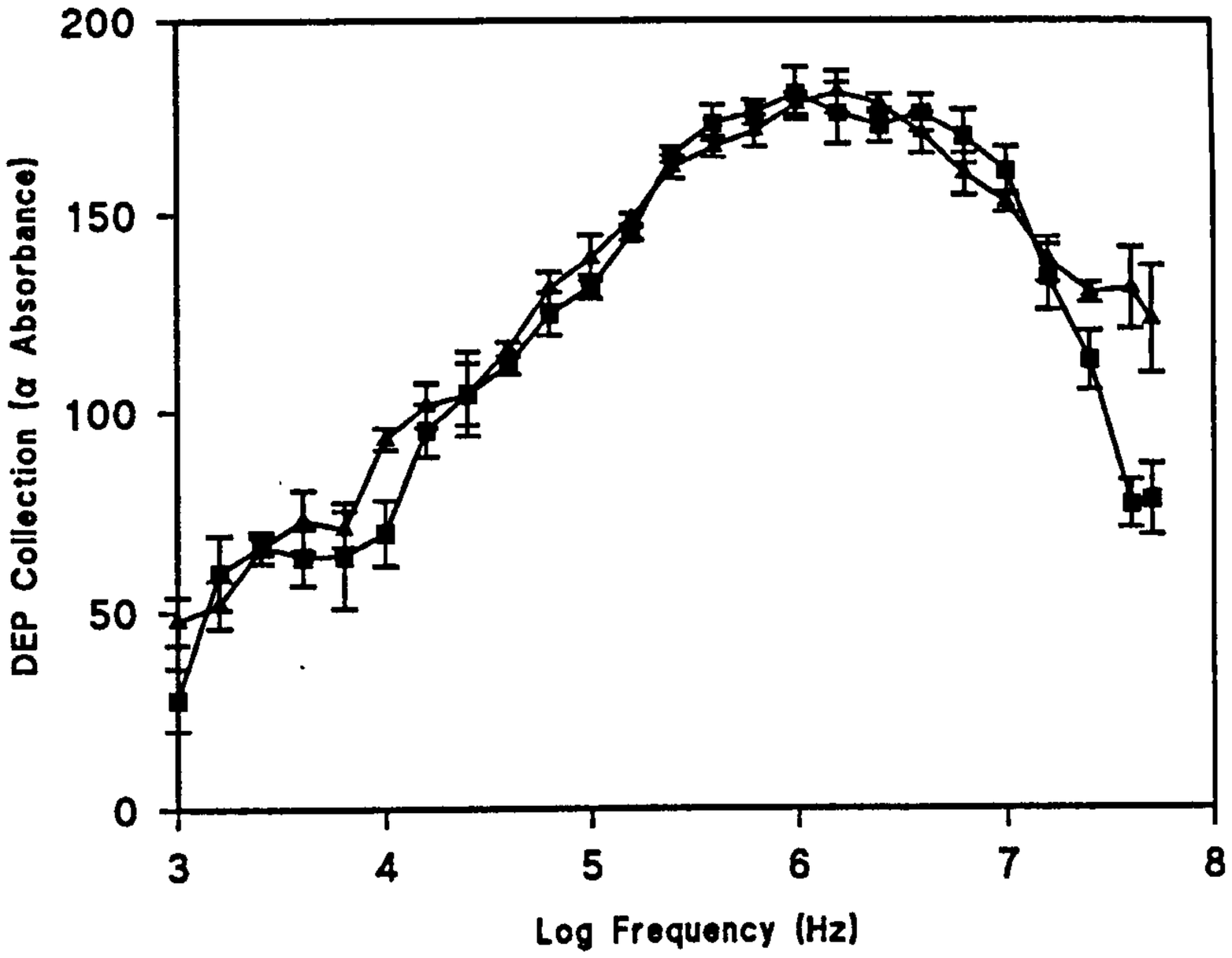

Figure 4.20 : Effect of resistance shunt movement on the dielectrophoretic (DEP) collection of *Strep. faecalis.* (■) shunt next to electrodes, (▲) shunt at the signal generator output port. Conditions : 12 V, 5 s pulse, 46.5-48.6 $\mu S.cm^{-1}$. Spectrophotometric method of detection. Each point is the mean plus standard error of 5 replicate spectra.

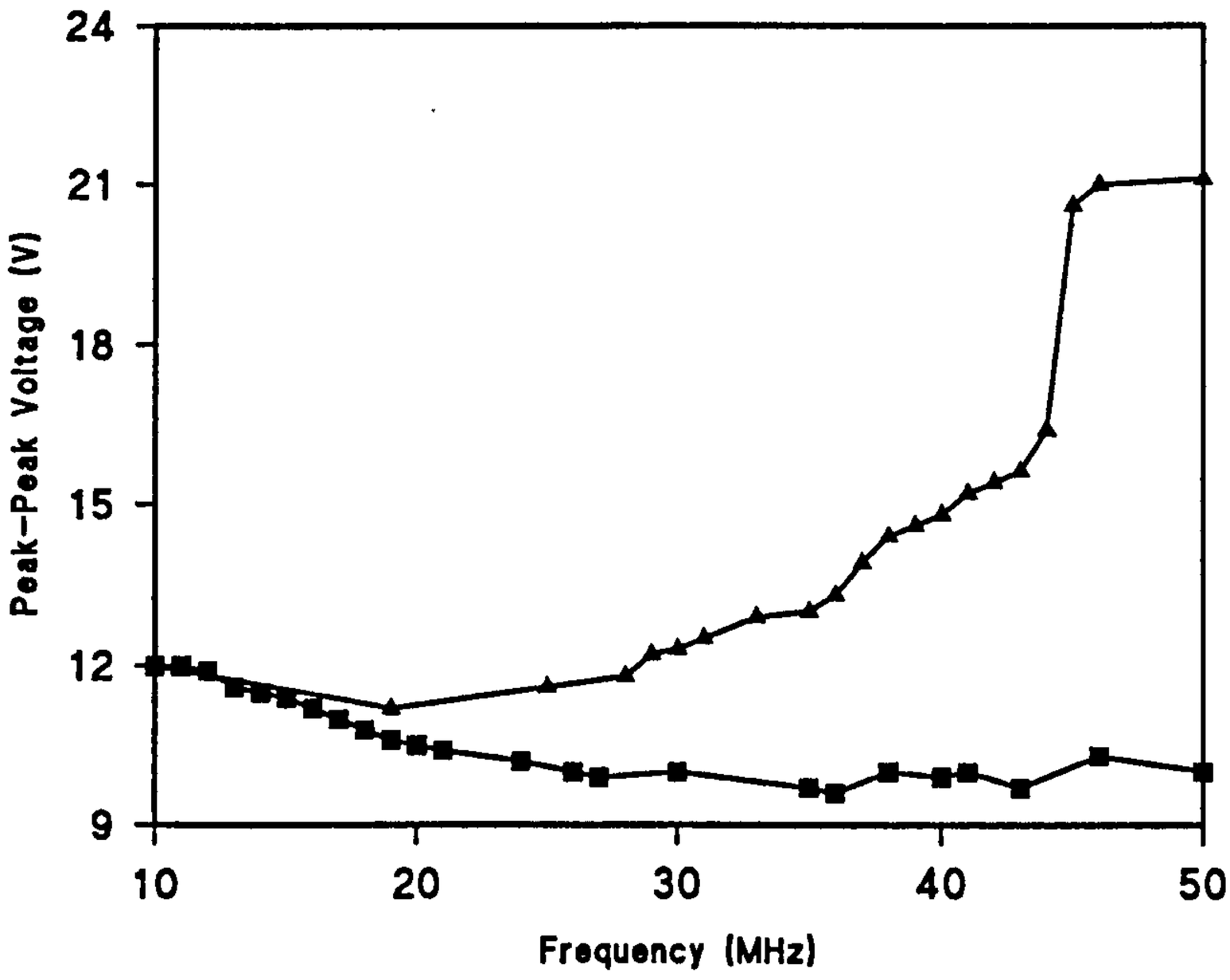

Figure 4.21 : Effect of resistance shunt movement on the voltage output received by the electrodes. (■) Shunt next to electrodes, (▲) Shunt at signal generator output port.

4.2.10 Position of Dielectrophoretic Collection on Electrodes

Pethig *et al.* (1992) and Quinn (1995) showed that the position of dielectrophoretic collection upon electrodes was related to the nature of the dielectrophoretic response, whether positive or negative forces were occurring. It was demonstrated that negative DEP collection predominantly occurred in the regions of low field intensity (proposed to be on the top of, or between, electrode structures). As the frequency was altered to allow positive dielectrophoresis to become more favourable, the position of collection moved successively closer to the edge of electrodes where higher field intensity regions were more likely to be encountered.

Figure 4.22 shows the relative positions of dielectrophoretic collection at the electrodes for suspensions of cells in different media over the frequency range.

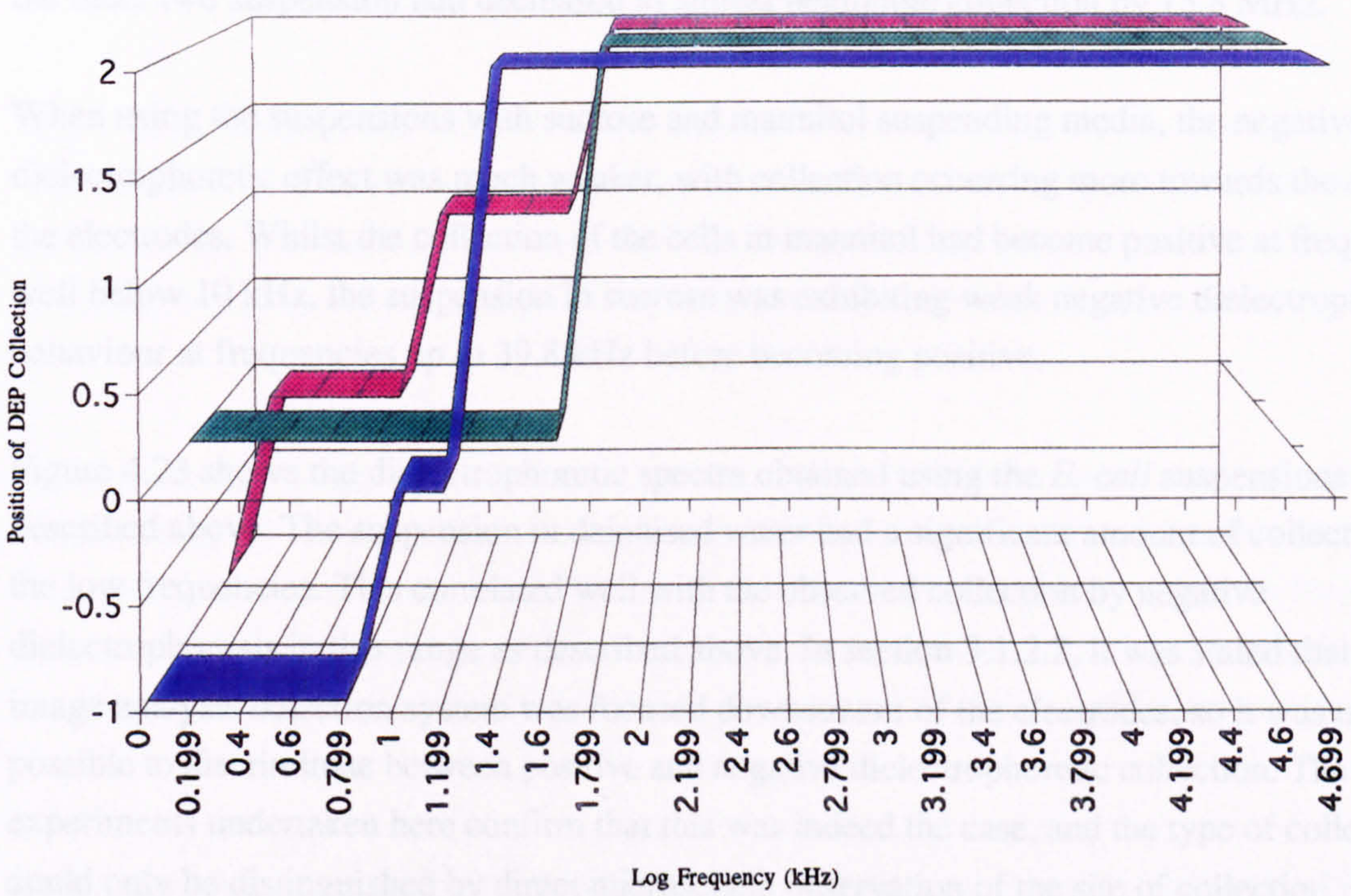

Figure 4.22 : Position of dielectrophoretic (DEP) collection of *E. coli* on electrodes when suspended in a variety of media. (■) Deionised water, (■) 0.5 M sucrose, (■) 280 mM mannitol.

It can be seen that each of the different media resulted in collection on top of the electrode bars at lower frequencies. Using mathematical modelling, this location was shown to have significantly lower field intensity regions and was a position for the occurrence of negative

dielectrophoresis. As the applied frequency was increased, the repulsive dielectrophoretic force became successively weaker and cells moved to designated greater field intensity regions as positive dielectrophoretic action was thought to dominate. With the cells suspended in deionised water, the cells were subject to a very strong negative dielectrophoretic effect for frequencies up to 6.3 kHz. The transition for the dielectrophoretic force to become positive was considered to be completed by 25 kHz, passing through theoretically proposed areas of weak negative dielectrophoretic collection.

This classification of collection area into positive and negative DEP gave no conception of the degree of dielectrophoretic collection, but was observed microscopically, with maximum negative dielectrophoresis occurring at the lowest frequencies (1 kHz and 1.58 kHz) and the peak of positive DEP being at 1 MHz and 1.58 MHz in each case, becoming weaker at frequencies greater than 2.51 MHz. It was, however, observed that there was still quite strong positive dielectrophoretic collection with the sucrose suspension right up to 25.1 MHz, when the other two suspension had decreased to almost negligible collection by 15.8 MHz.

When using the suspensions with sucrose and mannitol suspending media, the negative dielectrophoretic effect was much weaker, with collection occurring more towards the edges of the electrodes. Whilst the collection of the cells in mannitol had become positive at frequencies well below 10 kHz, the suspension in sucrose was exhibiting weak negative dielectrophoretic behaviour at frequencies up to 39.8 kHz before becoming positive.

Figure 4.23 shows the dielectrophoretic spectra obtained using the *E. coli* suspensions described above. The suspension in deionised water had a significant amount of collection at the low frequencies. This correlated well with the observed collection by negative dielectrophoresis in this range as described above. In section 3.1.2.2, it was stated that the image analysis detection system was focused downstream of the electrodes, so it was not possible to discriminate between positive and negative dielectrophoretic collection. The experiments undertaken here confirm that this was indeed the case, and the type of collection could only be distinguished by direct microscopic observation of the site of collection.

Neither of the suspensions made in sucrose or mannitol had significant levels of collection at lower frequencies, also verifying the observed results of very weak levels of negative dielectrophoresis which could be easily overcome by the flow of the suspension during field application.

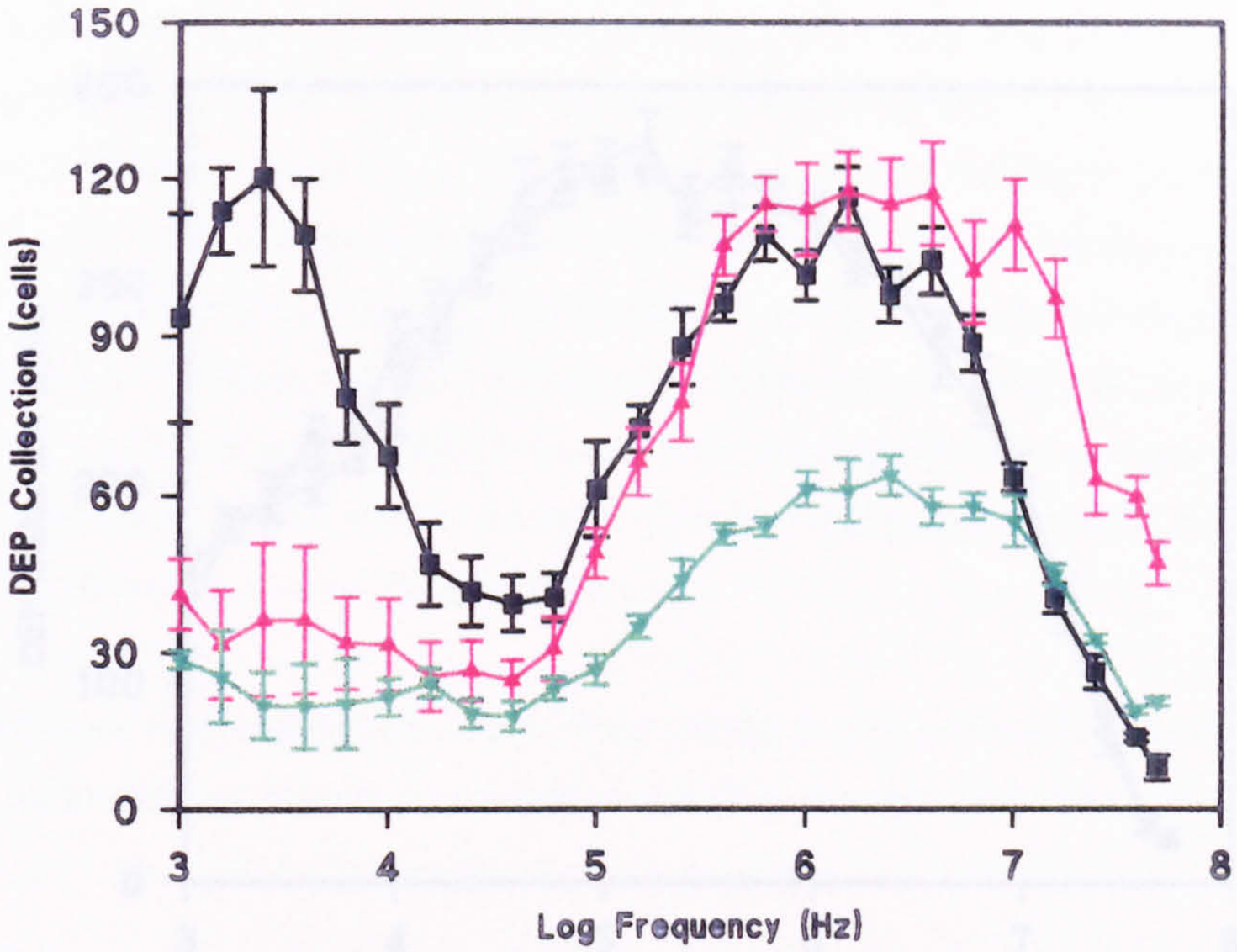

Figure 4.23 : Dielectrophoretic (DEP) frequency spectra of *E. coli* when suspended in a variety of media. (■) Deionised water, (▲) 0.5 M sucrose, (▼) 280 mM mannitol. Conditions : 12 V, 5 s pulse, 24.5 μS.cm^{-1}. Total counts : 26.125 x 10^7 cells.ml^{-1} (deionised water), 32.04 x 10^7 cells.ml^{-1} (sucrose), 20.66 x 10^7 cells.ml^{-1} (mannitol). Full count method. Each point is the mean plus standard error of 5 replicate spectra.

The collection produced with each of the suspensions had similar maxima of collection in the MHz range. However, it may be seen that the collection of both the sucrose and mannitol suspensions at greater than 100 kHz had been shifted to higher frequencies with respect to the deionised water suspension. This was especially noticeable with the sucrose suspension which still had a sizeable amount of collection at greater than 10 MHz (as observed microscopically above).

The low level of collection found with the mannitol suspension was most likely to be due to the lower cell concentration as determined by the total count.

4.2.11 Effect of Shaking Cultures of Bacteria

In trial experiments it was noticed that an unshaken culture of *Ps. aeruginosa* 10662 produced cells which appeared to be slightly larger and less motile than those found with a shaken culture. Spectra were obtained with cells which had been either shaken or unshaken for 16 h and these are shown in figure 4.24.

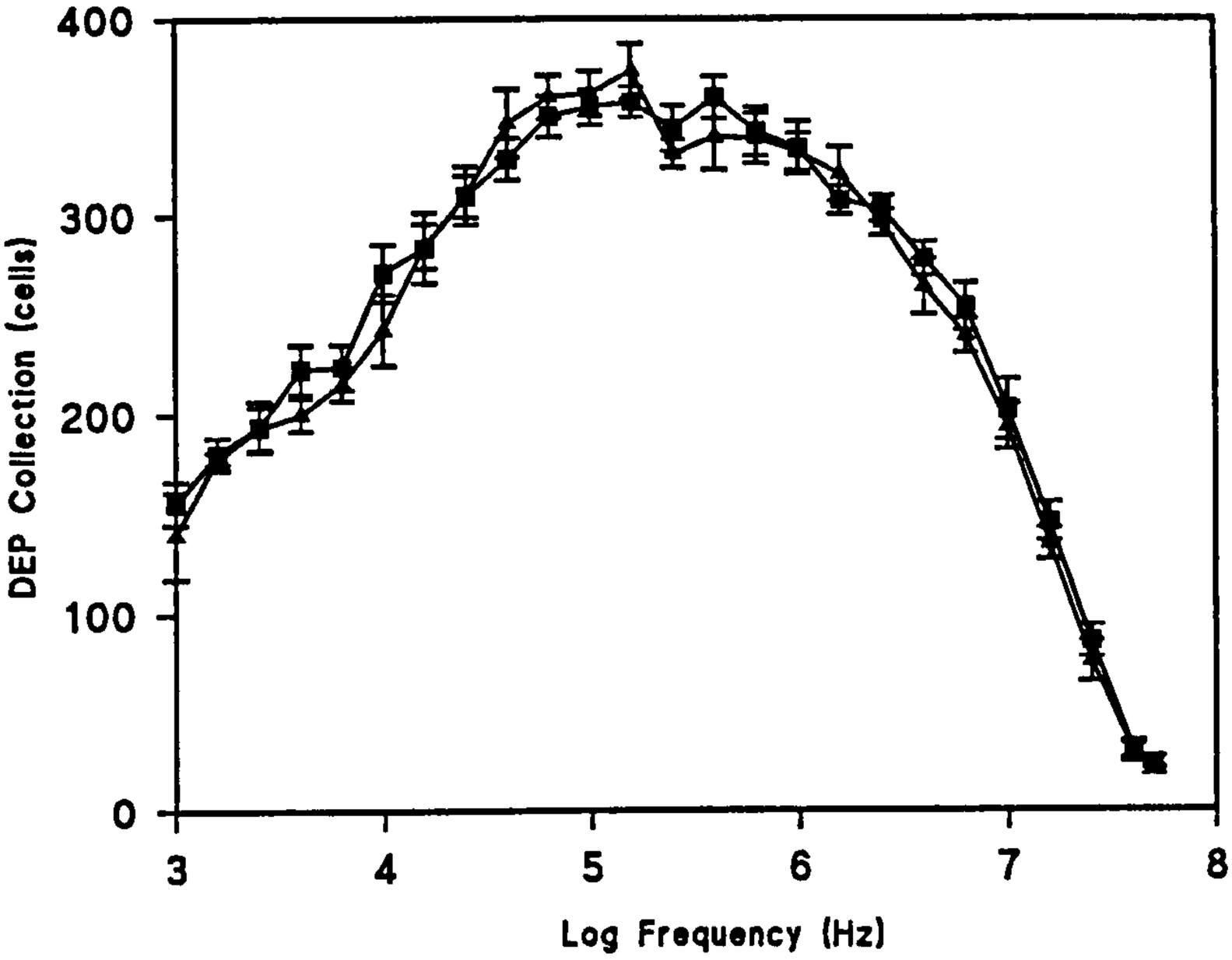

Figure 4.24 : Effect of shaking during culture growth of *Ps. aeruginosa* 10662 on the subsequent dielectrophoretic (DEP) frequency spectra. (■) Unshaken broth culture, (▲) Shaken broth culture. Total counts : 26.9 x 10^7 cells.ml^{-1} (unshaken), 27.375 x 10^7 cells.ml^{-1} (shaken).

The collection of the two suspensions (which had been adjusted to similar concentrations) did not appear to have any significant differences over the whole frequency range and had almost identical spectra. Thus the influence of shaking on the dielectrophoretic collection of bacterial cells within a broth culture, for this species, appeared to be negligible.

4.3 Discussion of Preliminary Dielectrophoretic and Standardisation Experiments

4.3.1 Sample Viability

Studies on the survival of many bacterial species within dilute environments such as distilled or lake water have been examined, especially in work by Sjogren & Gibson (1981). They concluded that the survival of different species of Gram negative genera was often related to the levels of ribonuclease and ATPase within the cells. This enabled conversion of internal cellular components into resources which could enable survival for elongated periods of time. Survival was predominantly found with species of bacteria related to *Klebsiella*. *E. coli* was found to

have low levels of ribonuclease and ATPase, making it susceptible to large viability losses after 24 h in distilled water. The results described in section 4.1.1 may also be possible to attribute to similar explanations. Since *Shig. sonnei* is very closely related to *E. coli* it may undergo similar losses in viability, even though its presence in deionised water for the duration of the experiment was only for a short period of time lasting only 3 h. The continuous flow dielectrophoresis moves bacterial cells at high speeds, compared with that experienced in stagnant lake water. Therefore, the shear forces and impact during recirculation may also be a contributory factor. However, this continuously recirculating system has been used in experiments with more fragile porcine sperm cells with no significant short term loss in viability due to the recirculation (Betts, 1995b).

Though the content of ribonuclease and ATPase within *Staph. aureus* is unknown, its stability in deionised water did not present a problem in viability changes in dielectrophoretic experiments.

Even though typical dielectrophoretic experiments have normally been performed over short timescales of less than 2 h, the results of Sjogren & Gibson (1981) found that even with this short period of time in dilute media, species such as *Flavobacterium* and especially *Alcaligenes* underwent significant losses in viability of up to 80 %. Since the dielectrophoretic spectra of bacterial species have been shown to be drastically altered by changes in viability status, the spectra of such species, when obtained with a deionised water suspension, should be obtained very rapidly and examined with caution. It is suggested that, when examining newly acquired strains of bacteria, their viability in deionised water be assessed. Alternatively future bacterial suspensions could be made, as in experiments performed by Pethig *et al.* (1992), in iso-osmotic mannitol or sugar solutions to maintain viability.

4.3.2 Standardisation of Experiments

One of the most prominent requirements for assessing and comparing scientific results from one experiment to the next is the necessity for standardised procedures and parameters. Dielectrophoresis is no exception. One of the major advantages of dielectrophoresis is the ability to discriminate and identify particle or cell types by spectral analysis. However, these spectra are, as demonstrated in the experiments described, subject to variation depending upon the experimental conditions. To be able to compare particle spectra to previously obtained results or even to compare treated samples with controls, the effects of these procedural variations must be accounted for or removed from the investigation.

4.3.2.1 Correlations of Particle Concentration

Absorbance has been used in many experiments due to the ability of rapidly processing a sample for dielectrophoretic experiments, important for the many possible industrial and clinical applications of dielectrophoresis. Since different particle types have different polarisabilities, the extent of the dielectrophoretic force will vary causing different levels of particle collection. Therefore to compare the resultant spectra of samples, particle concentrations ideally need to be identical to be able to attribute the level of particle collection to the polarisability of the particle rather than its concentration. Previously defined correlations between absorbance and actual cell concentrations make it possible to quickly adjust the concentration to run at comparable levels.

This method has many inherent difficulties since many of the particle types have vastly different sizes and therefore the same absorbance values are represented by very different particle concentrations. By adjustment of the cell concentrations to be equal, the collection could, in theory, be directly compared. However, the very different cell sizes result in image analysis detection problems since large concentrations of cells such as *B. subtilis* or elongated cells (as discussed in section 3.1.2.2) lead to saturation of the image analysis frame. The selected cell concentration would thus need to be low to prevent saturation, but such low concentrations for smaller cells such as *E. coli* would cause only minimal amounts of dielectrophoretic collection due to its lower extent of polarisation.

Adjustment of particle concentration by absorbance readings is more prone to errors when groups of particles or filamentous bacterial species are under examination. Often species such as *B. cereus* divide to form chains of cells which can form visible particulate aggregations in suspension. The observed low correlation values of *Ps. aeruginosa* and *Staph. aureus* may be due to such cellular properties. The former was highly motile and this may have caused errors in the reading of absorbance values. The latter forms tight clusters of cells which may not have become completely separated during the experiment. Therefore both absorbance values may be erroneous. Viable count procedures may have also resulted in several of these cells forming single colonies on the agar surface causing anomalies in the counting procedure. Nevertheless, it is considered that these relationships will have sufficient correlation to enable a simple concentration range to be found for the dielectrophoretic experiments. The amount of error by this method may be compensated by the greater speed of sample preparation possible when using absorbance methods rather that adjusting concentration by way of the more laborious counting chamber.

Since any cell population is made up of a proportion of non-viable or non-culturable cells, the viable count (as determined by growth on solid media), represents only a proportion of the total cell count. Both viable and non-viable cells collect by dielectrophoresis so a total cell count would be the most appropriate method of measuring concentration. However, this method is more time consuming to perform on a daily basis and absorbance gives an accurate indication of the concentration for use in adjusting the range of cell concentrations.

4.3.2.2 Electrode Calibration

The possible effect of electrode variations have made it necessary to implement a stage of electrode calibration before use of the experimental system.

Due to the small scale nature of electrode manufacture for dielectrophoretic experiments, variations such as uneven electrode edges caused by the anisotropic acid etching or different thicknesses of evaporated metal can alter edge effects and field non-uniformity, resulting in differences in dielectrophoretic collection between sets of electrodes. Calibration of these electrodes to examine these variations has become necessary. In the future, however, electrodes are likely to become mass produced by automated methods and so will be much more consistent in electrical character, facilitating a more simple calibration regime.

Electrode surfaces are known to become contaminated with various substances which can reduce the electric field strength. Often, the contact of metal surfaces with water and air can result in the formation of oxide layers. Oxides are more insulating than the electrodes and can reduce the effective field produced by the electrodes. Presence of thicker oxide layers would reduce collection proportionately.

The use of abiotic polystyrene latex spheres which do not have the variations associated with growth of biological cells are often used in the calibration of many types of equipment e.g. flow cytometer. These particles should collect reproducibly under controlled conditions and so are ideal for use as a dielectrophoretic calibration sample.

The decrease in collection level during the first two days for the electrodes examined could be indicative of the build-up of debris which moderated the electric field strength. When particles come into contact with the electrodes the water layer separating the surfaces becomes displaced and allows short range Van der Waals interactions or other adherance mechanisms to occur. Therefore, dielectrophoretic collection which bring particles close to electrodes often results in the retention of the particles at the electrodes even after flushing by the use of high pump speeds. The formation of this layer limits the amount of further physical contact of particles with the electrodes. After this initial sticking, the adherence of additional particles became

reduced and the level of collection remained relatively constant for the remainder of the 88 day period. Biological material such as build-up of microbial biofilm would have a similar effect to that described above (especially problematic cells having associated EPS). Due to the variability of collection of these latex particles even on a daily basis, an appraisal of the performance of the calibration would be necessary (with mathematical compensation for electrode quality) until electrode variability could be significantly reduced.

An associated problem was the adherance of particles in the areas downstream of the electrode bars. Whilst this did not directly influence the electrodes or the extent of dielectrophoretic collection, it caused difficulties with the image analysed detection of collection following particle release. The sticking of particles caused them to be detected as a background during the baseline count. This background was subtracted from the peak by the computer software after each applied pulse. However, when large numbers of particles were stuck in the background, particles passing through the counting frame after release from the electrodes came into close contact with these adhered particles. This resulted in a detection of several particles as a single particle (as in section 3.1.2.2) and consequently dielectrophoretic collection was underestimated, reducing effectivity of the electrodes. To remove these adhered background particles and prolong electrode life, cleaning was attempted with a variety of detergents and disinfectants. This was unsuccessful and generally cleaning was routinely performed by forcing deionised water through the chamber with a syringe to attempt to remove the particles. Storage under refrigerated conditions and in the dark minimised deterioration. However, when background contamination was considered to be too great, the electrodes were discarded.

Becker *et al.* (1994) coated their electrode structures with a bovine serum albumin (BSA) solution to reduce adherance of cells. However BSA is a protein material, also having associated water structure which would also moderate the electric field and become polarised by it. Though it is perhaps better to have a more uniform covering of constant presence modifying the electric field effects, the protein structure could also be affected by the great heating effects at the electrode surface potentially resulting in a denaturation and different response to the native BSA properties of the initial covering. Perhaps a more efficient material would be a polymeric coating such as a sialysing agent or polyvinylalcohol (PVA). As a further step, a thin covering of a dielectric layer such as silicon dioxide or silicon nitrile has been investigated (Milner K.R, Brown A.P., Allsopp D.W.E., Betts W.B. & Goodall D.M., 1995 (Unpublished Data); Schnelle *et al.*, 1996). This helps to prevent debris buildup during experiments and allows harsh cleaning agents such as strong acids or alkalis to be used after a set of experiments without damage to electrodes. These dielectric materials are also effective in preventing electrode polarisation (e.g. platinum black) as discussed below since the cell suspension is not in direct contact with the electrode. The use of more chemically resistant metals such as gold as the electrode material could also allow more efficient cleaning regimes.

4.3.2.3 Electrode Polarisation

Electrode polarisation occurs when a metal electrode is placed in a solution or cell suspension, and is manifest as a d.c. potential at the interface of the two materials (Schwan, 1966). This acts as in impedance and causes the current and voltage to be out-of-phase especially at low a.c. frequencies, below 10 kHz resulting in anomalous dielectrophoretic collection. The electrode polarisation effects depend greatly on the size and nature of the electrodes and of the suspension, being greater with high conductivity samples. Therefore DEP, using such low conductivity suspensions, will have an electrode polarisation effect which is greatly reduced. The effect can be further reduced by the use of a platinum black coating over the electrodes which can reduce the polarisation impedance by up to four orders of magnitude (Schwan, 1966).

4.4 Dielectrophoretic Experiments

4.4.1 General Spectra

4.4.1.1 General Comments

The most outstanding feature of the dielectrophoretic frequency spectrum measurement was the very different spectra obtained even with what are often considered closely related bacterial species. The use of standardised conditions for running experiments makes it easier to attribute particular characteristics of spectra and allow comparison.

The use of this continuous dielectrophoretic system has great advantages over the static systems used by many other workers. The spectra shown in the figures were normally produced within 10 min, allowing rapid and reproducible analyses of samples. On occasion, there was a successive lowering of repeated spectra over time. It was possible that this decrease could have been as a result of irreversible changes in cell structure following polarisation by the dielectrophoretic force reducing further susceptance to polarisation on the next pass. However, since much less than 0.1 % of the suspension actually is collected by the microelectrodes during a typical spectrum, the probability of permanent damage being caused to a substantial proportion of the suspension is very small. Thus reduction in cell collection is more likely to be due to reduction in polarisability caused by other mechanisms such as conductivity increase or the effect of prolonged exposure to the low ionic strength environment. Conductivity effects will be discussed further in section 4.4.6. Inoue *et al.* (1988) also observed a successive lowering of spectra with time for a suspension of *Micrococcus lysodeikticus* over the

frequency range (10 Hz to 1 MHz). This occurred particularly at the lower frequencies due to release of ions from the cell interior into bulk solution, lowering particle polarisability. Generally, however, experimental conditions were sufficiently consistent to express the data as means (plus error bars) of the repeated spectral datapoints.

The dielectrophoretic spectra of the bacterial species examined were very different, each having a unique frequency response of the range. This was not unexpected since the many polarisation mechanisms exhibited by different bacteria allow for a wide range of frequency responses. Often surface characteristics of the cells determine the major frequency responses especially at frequencies below 1 MHz. Similar species of bacteria were expected to have spectra which were more similar in form, and general trends for Gram positive and Gram negative groups were anticipated. However, differences between the spectra of the Gram positive and negative classification groups were difficult to isolate from the major spectral differences between species.

The occurrence of the *B. subtilis* and *Staph. aureus* maxima at frequencies below the usual Gram negative peak of 1 MHz could be related to the overall Gram positive wall structure. It is well documented that membranes undergo capacitive mechanisms in the MHz region (Pohl, 1978; Pethig, 1979) and the presence of the outer membrane in Gram negative species may shield other responses and make this the predominant response at the higher frequencies. Since Gram positive cells do not possess an outer membranous structure, their response is more related to their cell walls and polymeric material. Experiments to induce thickening of the cell walls were undertaken to study this response in more detail (see section 3.10).

It is possible that one of the major factors in the dielectrophoretic response of Gram positive species is the degree of cross linking between cell wall polymers. The low frequency portion of the dielectrophoretic frequency spectrum for cells is considered to be a result of surface conductivity effects. Therefore in Gram positive cells the ease of movement of mobile charges through the cell wall will be more efficient in more open networks of cell wall polymers. It might be expected that cell walls with a great deal of cross linking obstruct the passage of charges, producing a slower polarisation response at these lower frequencies. By examination of figure 4.5, *Staph. aureus*, which has a cross linking index of 93.5 % (table 2.5) i.e. a large amount of cross linking, the low frequency region of its spectrum has very little collection. This possible explanation of spectral form is further consolidated by examination of the DEP spectrum of *B. subtilis* which collects well at lower frequencies. This species of Gram positive bacteria has a much lower level of cross linking (41 %) allowing more rapid passage of charges through the wall and more efficient polarisation at lower frequencies, resulting in an increased DEP collection. Further work is needed to examine this possible explanation of Gram positive

spectra. Similar explanations may be anticipated with Gram negative cells, where the protein content of the outer membrane may play a similar role in polarisation efficiency.

The rate of decrease in collection after the peak frequency could potentially be used as a method to discriminate between Gram positive and Gram negative species. The Gram negative species studied all appeared to exhibit a less rapid decline in collection than the Gram positive cells. In contrast to the polystyrene latex, bacterial cells have a much wider frequency range of dielectrophoretic collection, collecting at all frequencies between 1 kHz and 50 MHz. This is known to be due to the multi-component structure of bacterial cells, each of which can have very different frequency dependent polarisation mechanisms (Chen, 1972; Pohl, 1979; Pethig, 1979). Polystyrene latex particles have a much more homogeneous nature, resulting in fewer polarisation mechanisms and thus their dielectrophoretic collection occurs over a narrower frequency range. The main dispersions associated with polystyrene latex particles have been attributed to surface ionic conductivity effects related to the ionic double layer surrounding the particles, having low relaxation frequencies (Pethig, 1979).

There were inadequacies in the detection system which, although produced very rapid and accurate particle counts, did not allow for discrimination between positive and negative dielectrophoretic collection.

4.4.1.2 Detection of Negative Dielectrophoresis

Negative dielectrophoresis, caused by a greater polarisability of the suspending medium than that of the suspended cells, results in a repulsion of cells to areas of low potential energy, where the field intensity is at a minimum i.e. in certain areas between electrodes or on top of electrodes. When the field is turned off, these cells are released from the potential energy wells. Cells passing through the light beam or image analysis detection frame cause an increase in count. This increase, however, does not give any idea of spatial distribution of the cell collection which has occurred. Therefore collection could occur equally by positive dielectrophoresis at electrode edges or by negative electrodes in between electrodes or on electrode surfaces as in figure 3.4 and still produce an identical dielectrophoretic count.

The use of both spectrophotometric and image analysed detection methods measured release of cells downstream to prevent obstruction by the electrode presence. It was not possible to directly observe whether dielectrophoresis was positive or negative during the course of an experiment. Therefore, when the collected cells were released from the electrodes and passed through the detection window, particles collected by positive dielectrophoresis could not be discriminated from those collected by negative dielectrophoresis as all released cells were quantified together.

Weak dielectrophoretic forces, for instance as a negative force changes to a positive force, will possibly be overcome by the flow force meaning there is little overall collection. However, very strong positive or negative dielectrophoretic forces are sufficient to hold cells at the electrodes until the applied field is turned off. In some cases, it was possible to implicate negative dielectrophoresis in some of the spectra. Often, high collection at low frequencies (typically below 10 kHz) was observed on top of the electrode surfaces, described by Quinn (1995) to be due to negative dielectrophoretic effects. This was normally associated with reduced collection at frequencies in the 10 kHz region, followed by a further rise in collection as positive dielectrophoresis began to dominate the response (as shown in figure 4.23).

4.4.2 Pulse Length

4.4.2.1 General Trends

The pulse length graphs for latex and for *Ps. aeruginosa* had similar form, increasing with pulse length up to an asymptotic plateau. The asymptote level of collection should not be dependent upon the concentration of suspension used for the experiment (though the time taken to reach the plateau will vary with concentration). It is, however, dependent upon the size of the cells, saturation occurring at lower levels with larger particles. The plateau level is determined by the area of electrode available for DEP collection and by the size of the detection area, as well as the level of background debris (as discussed in section 4.3.2.2). It should be stressed however that these levels are specific for the conditions used in this experiment. Variations in light levels, focus, electrode efficiency and detection etc. will result in modifications to particle detection saturation point being reached after different times.

The gradient of the two pulse length graphs (figure 4.6) are very different, the smaller bacterium reaching saturation at much lower pulse lengths than the latex. As well as being related to the concentration of the particles, the rate of collection may also be related to the size of the particles. The very good collection of bacterial cells at short pulse lengths may be due to a co-operative effect which will be explored in greater detail in section 4.4.7. In essence, initial cell collection could cause a further distortion of the electric field making it even more non-uniform. Additional particles could be then attracted due to increased field non-uniformity.

The polystyrene latex particles were not observed to have the same degree of co-operativity and the initial part of the curve was approximately linear with pulse length. Aggregation of field lines will be relatively greater when created by smaller particles since the area over which the field lines are spread is much smaller than with larger particles (figure 4.25). This causes a larger density of field lines at the poles of bacterial cells compared to that around bigger latex

particles. Therefore additional particles could be more easily attracted to these smaller particles, making the co-operative effect more significant in smaller bacterial cells.

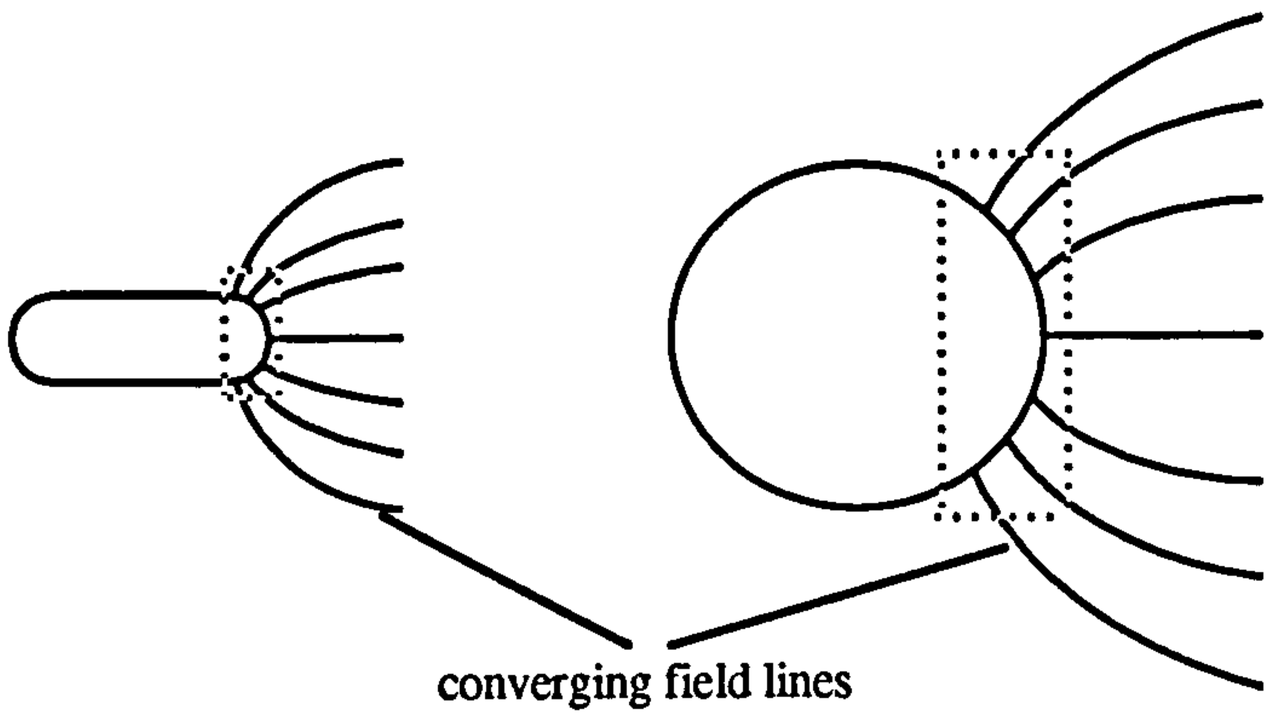

Figure 4.25 : Aggregation of field lines with different particle sizes.

4.4.2.2 Effect of Pulse Length at Different Frequencies

It was initially expected that since the experiment utilised continuous dielectrophoretic processes, that doubling the pulse length should have caused a doubling of the extent of collection until saturation became limiting. The spectrum using 30 s pulse duration became limited by saturation since collection was not as great as expected in the MHz region in figure 4.7. From the pulse length graphs for *E. coli* (figure 4.8), saturation began to occur after a cell collection level of 500. Detection of additional particles was possible up to a detection of 1000 from the downward points count, though was not as efficient as at lower pulse lengths as demonstrated by the levelling effect. Thus the spectrum observed in figure 4.7 for the 30 s pulse length was becoming saturated and further increases in pulse length would have been unlikely to yield collection greater than 1000. During the course of these experiments it became apparent that it was necessary to conduct pulse length experiments in parallel, in future experiments, to ensure that this saturation effect was not occurring and limiting the degree of collection.

By examination of the pulse length graphs obtained with *E. coli* lower pulse durations were seen to have linear regions, which, if extrapolated to very small pulse lengths appeared to still produce moderate collection levels. The image analysis detection (i.e. background noise) was not the cause of such high levels, implying that there was a very rapid increase in collection during the first second of field application. This rapid increase was predicted to be caused by the mutual dielectrophoretic co-operative effect.

4.4.3 Voltage

The dielectrophoretic force is proportional to the size of the electric field and is thus related to the voltage. Collection increased linearly with the size of the applied voltage over the range examined. Fields of 16 V across a 5 μm gap between electrode bars resulted in a collection of 300 particles. Though this voltage was the maximum output of the signal generator used in these experiments a theoretical further voltage increase should have caused further dielectrophoretic collection. Again this collection would be limited by saturation of electrodes or detection system. The saturation level with *Ps. aeruginosa* was found in section 4.2.2.1 to begin at around 300 particles, meaning that 16 V was around the maximum voltage possible to use before collection became limited. A standard voltage of 12 V was used in normal dielectrophoretic experiments to avoid this saturation problem.

At low voltages, it was seen that collection of bacterial cells did not occur until the voltage had been increased to above 3 V. These low voltages cause weak polarisation of the cells and so the flow of the suspension easily removed the cells from the electrodes. It was only as the voltage was increased sufficiently for the dielectrophoretic force to overcome the hydrodynamic forces of the suspension that collection began to occur. Indeed, this "threshold" voltage needed to initiate collection could be used to give an idea of the size of the dielectrophoretic force. Similar balancing of forces has been used previously to calculate the size of the dielectrophoretic force for particular particle types. Dielectrophoretic levitation (Crane & Pohl, 1977) used the balancing of dielectrophoretic force and gravitational forces in this manner.

4.4.4 Pump Speed

Optimisation of pump speeds during pulse application enabled more efficient collection, especially when using suspensions of low particle concentration. Increased pump speeds brought more particles into the vicinity of effective field surrounding the electrodes allowing potential collection. Conversely, very high pump speeds also had the effect of overcoming the dielectrophoretic force and stripping the particles from the electrodes. The range of pump speeds applied to the suspension of *Ps. aeruginosa* showed the speed producing maximum level of collection was at around 10 rpm. Pump speeds below this value produced lower levels of collection since fewer particles were made available for collection. Increasing the speed past 10 rpm did not further increase the level of cells collected since the flow of suspension was beginning to overcome the force of DEP. At pump speeds greater than those examined experimentally, the level of collection would be expected to become reduced as the flow force became even greater.

This optimum may not be identical for all organisms, being dependent upon size, shape and probably also the motility of the organism. It is also likely to be related to the cellular concentration of the suspension since different concentrations would result in different amounts of cells being brought into the effective field and increasing the effective field non-uniformity. Due to the size of the forces on the particles, this relationship would be expected to be altered by use of particles of different diameters, the stripping of larger particles from the electrodes occurring at lower pump speeds.

Two other points were provided by this experimental data :

- This method could be used to predict the relative size of the dielectrophoretic force by balancing the force of collection with the hydrodynamic force of the suspension produced by different pump speeds (as with the balancing of voltage and flow rate). Similar experiments have been undertaken in this manner, relating the trajectory of particles to the size of the dielectrophoretic force

- Field application while the pump was stopped (i.e. pump speed of zero) resulted in a collection of greater than 100 particles. While there will still be some residual flow of suspension remaining from the baseline reading (*Base Time*), the field extends several microns into the medium causing attraction of particles to the electrodes even in absence of flow as in static dielectrophoretic systems.

The speed upon release is also an important factor, since low flow rates may not bring all of the released particles into the counting frame during the *Peak Time*, resulting in underestimation of collection. Very high release speeds will pass the particles through the frame too quickly such that the image analysis system will not be able to count the particles efficiently.

4.4.5 Multiple Pulse Applications

Repeat pulse applications were used to obtain mean collection levels for a particular suspension, initially for calibration purposes. The random nature of the levels of collection demonstrate that each field application is unaffected by the preceding pulse and the level of collection is determined by the number of particles passing the electrodes during the application of the field and by their relative proximity to the electrode surface.

The presence of anomalous points could indicate potential inhomogeneities in the suspension. Clumps of particles passing through the detection frame may result in a great amount of detection noise and unrepresentative levels of enumeration. Alternatively clumps of material may block the electrode surface to other cells, leading to very low levels of overall collection.

This type of problem is only transient and would be cleared upon flushing for the next applied field.

The more long term problem of particle sticking has already been discussed (section 4.3.2.2). Often, the first few pulse applications resulted in much reduced levels of collection and this was deemed to be caused by the initial adherance of particles upon the electrode surface which were not released upon field cessation. Once the electrodes had acquired a coating of particles the collection level became relatively constant for the remaining pulses. Nevertheless, these significantly higher or lower points can greatly bias the mean of the collection level. Generally, however, the level of collection is quite reproducible from one pulse to the next and the error is generally small.

As detailed earlier, the level of collection is dependent upon many factors relating to the particle under examination and experimental parameters. Under ideal conditions, this level of collection would have been highly reproducible from one day to the next. Ideal conditions are, however, somewhat different to the reality of the situation, further emphasising the need for electrode calibration.

4.4.6 Effect of Increasing Suspension Conductivity

The basis of the conductivity effect was introduced in section 1.1.4.2. Dielectrophoresis occurs due to relative differences in the dielectric properties (conductivity and permittivity) of the particles and suspending medium. Collection at the electrode edges (positive DEP), the phenomenon examined here, is brought about by having a greater particle polarisability than that produced by the medium.

As medium conductivity was increased, the level of cell collection, especially at these lower frequencies began to decrease. This caused the onset of positive dielectrophoretic collection to occur at increasingly higher frequencies. Increased ionic strength resulted in enhanced polarisability of the medium making it more difficult for the particle polarisability to exceed that of the medium. Since conductivity contributions to polarisability become less significant at higher frequencies due to the inefficiency of surface movement of charge, effects of conductivity increase are more noticeable at the lower frequency range.

Over the frequency range, different polarisation mechanisms influence particle polarisability. At lower frequencies, the polarisation was mainly caused by surface conduction effects and so became reduced when the ionic strength of the medium increased. Only at higher frequencies did other, more effective mechanisms begin to occur. As medium conductivity was increased,

progressively higher frequencies were necessary before the particle polarisation became sufficient to display a high level of positive dielectrophoretic collection.

This decrease in collection at the lower frequencies was observed with both *E. coli* and *Ent. cloacae*, with very little effect at the high frequency range.

This frequency related effect was further demonstrated with the highest percentage of collection decrease visible at the lower frequencies, caused by raised conductivity. At frequencies around 10 MHz, there was found to be negligible decrease in collection caused by conductivity rises.

As medium conductivity increases further, particles find it more difficult to exceed the polarisability of the medium (even at higher frequencies), so the positive dielectrophoretic force becomes reduced. Very high conductivity results in negative dielectrophoresis. This was also shown by Price *et al.* (1988) where *M. lysodeikticus* produced negative dielectrophoretic forces at medium conductivities in excess of 2000 $\mu S.cm^{-1}$. The point at which negative dielectrophoresis becomes predominant is dictated by the actual particle conductivity characteristics. Different cell types have been found to have a variety of conductivity values and a list of these, found by a mathematical method by Markx *et al.* (1994), is shown in table 4.2.

Species	Frequency	Conductivity ($\mu S.cm^{-1}$)
Bacillus megaterium	10 kHz	888±39
Bacillus subtilis	10 kHz	935±96
Enterococcus faecalis	10 kHz	230±21
Erwinia carotovora	10 kHz	20±9
Escherichia coli	100 kHz	412±25
Klebsiella rubiacearum	10 kHz	513±102
Micrococcus lysodeikticus	15 kHz	1557±116
Pseudomonas putida	10 kHz	195±14
Saccharomyces cerevisiae	10 kHz	10

Table 4.2 : Particle conductivity values found by mathematical methods. Modified from Markx *et al.* (1994)

Different particle types have different sensitivities to conductivity increases. The above values have been utilised in the separation of two micro-organism types, by manipulating medium conductivity values to be between the conductivity values of the particles. The medium conductivity was then both less than and greater than the conductivities of the particles. The two particle types therefore moved to electrodes by positive dielectrophoresis in the former and away from the electrodes by negative dielectrophoresis in the latter case.

In comparison with bacteria, the conductivity of latex particles was lower, hence the reason for the utilisation of such low suspension conductivity values. Collection of latex particles was significantly depressed by even a conductivity rise of only 1 or 2 $\mu S.cm^{-1}$. Conductivities comparable to those used in bacterial experiments (25 $\mu S.cm^{-1}$) resulted in negligible positive dielectrophoretic collection.

4.4.7 Effect of Increasing Particle Concentration

4.4.7.1 General Trends

As with the pulse length experiments, the number of particles passing the electrodes contributes to increased levels of dielectrophoretic collection. The number of particles passing the electrodes during the pulse application can be expressed as N, where

$$N = f.c.t \qquad (4.1)$$

(f = flow rate, $ml.s^{-1}$; c = particle concentration, $particle.ml^{-1}$; t = pulse length, s).

Increased particle concentrations generally enhance the level of DEP collection under conditions where the dielectrophoretic force results in some particle collection. The level of collection in the spectra obtained for *E. coli* increased with greater particle concentrations. This rise in collection was again limited at higher particle concentrations corresponding to saturation effects. This was more effectively shown by figure 4.15 where levelling of the dielectrophoretic collection was observed at concentrations with O.D. in excess of 0.16 (corresponding to a viable count of around 3.2×10^8 $cfu.ml^{-1}$) using the more efficient collection frequencies.

Work performed by Pohl (1978) on the relationship of dielectrophoretic collection with concentration found linear responses using a static pin-pin dielectrophoretic system. However, even with this system, low concentrations resulted in appreciably high levels of collection and did not tend towards zero as concentration was decreased to zero. This also demonstrates that the co-operative effect of dielectrophoretic pearl chain formation may have caused more pronounced yield.

A continuous DEP system examined by Pohl (1978) did actually show maximum DEP collection rate for silica within the first minute (of a 10 min period) of field application, the rate of collection decreasing after this time. However, this observation received little comment. The subsequent measurement of DEP collection by "yield" (average pearl chain length after a set

time period) was normally quantified after periods of around 1 min. In these cases any co-operative collection would probably have already occurred. The image analysed continuous system used in the results presented here is much more accurate and allows these events to be observed.

DEP collection with the system described in this thesis followed a sigmoidal curve with increasing cell concentrations. The lower concentration ranges were expected to have a linear relationship with collection due to the linear relationship with numbers of particles passing the electrodes. On further analysis, concentration may be found to undergo a co-operative effect.

4.4.7.2 Co-operative Effect of Dielectrophoretic Collection

For a suspension of cells having low concentration, dielectrophoretic collection would be initially very low since only relatively small numbers of particles would be passing the electrodes and available for collection. The nature of mutual dielectrophoresis, as described by Pohl (1978), is caused by a particle which has become polarised by the non-uniform field producing a greater distortion in field lines such that additional particles are attracted to these secondary effects of non-uniformity. A similar case occurs at the electrode surfaces producing the observed pearl chains. Thus it is logical that the first cells collected at the electrodes will distort the field sufficiently to attract additional cells. The increased level of collected cells will then cause more substantial non-uniform effects producing such a strong effect that an even greater number of cells are collected. This co-operative effect would increase collection at an exponential rate until limited by effects of saturation or detection, or by the number of cells passing into the vicinity of the effective field.

The nature of co-operativity during an experiment is very dependent upon the size of the particles under study (as described in section 4.4.2.1) but also upon the other experimental parameters such as pump speed, pulse length and concentration, all of which influence the size of the mutual dielectrophoretic force.

Nevertheless, there appears to be an almost linear region within the curve relating collection to the suspension concentration. This has a notable significance which should perhaps be elucidated at this point. Relationships between particle concentration and the corresponding dielectrophoretic collection at a particular frequency can be used for quantification purposes. A calibration line, whether linear or sigmoidal, produced by suspensions of known concentrations could theoretically be used to estimate cell concentrations within unknown suspensions. Since image analysis techniques count a proportion of cells passing through the chamber this detection method alone could be used in this capacity. Dielectrophoresis, though, has additional benefits. Previous experiments shown in section 4.2.1 demonstrated the ability

to discriminate dielectrophoretically between different cell types. This selectivity shows the possibility of manipulating the collection parameters to collect one specific cell type. The selective nature of dielectrophoresis can be coupled with this potential quantification system to enable selective enumeration of different species within mixed population suspension of unknown concentration purely by their observed levels of dielectrophoretic collection.

4.4.7.3 Normalisation Experiments

Mathematical manipulations of spectra (figure 4.17) were performed to show theoretical collection levels at identical concentrations. Following this normalisation, level of collection was found still to be significantly different. As previously discussed, linear normalisations were found to be inappropriate for mathematical manipulation of data. This was due to the existence of sigmoidal relationships between particle concentration and dielectrophoretic collection.

The sigmoidal relationship between concentration and collection explains the lower level of normalised collection found with the two suspensions of lowest original concentration found in figure 4.17. These suspensions had viable cell counts of 5.75×10^7 cells.ml^{-1} and 8.176×10^7 cells.ml^{-1}, which, by comparison with figure 4.15, were still in the lag part of the exponential co-operative curve. Linear normalisations predicted a much slower increase in collection with greater cell concentrations than actually found by the co-operative effect. Thus the predicted level of collection for the normalised concentrations was significantly lower than that found experimentally.

To make accurate mathematical predictions on the extent of collection of different cell concentrations, normalisation should be carried out according to a sigmoidal relationship. However, this makes normalisation much more difficult to perform since each frequency will have a different rate of exponential rise in collection with each concentration, resulting in different levels of collection increase for each frequency. If the relationships were linear at all frequencies of the spectrum (until saturation point), a simple multiplication step would be able to account for concentration differences, altering collection at the same rate for each frequency.

However, the complex nature of the existing relationships make it very difficult to normalise spectra to account for differences in concentrations. Each particle and cell type would be likely to show different rates of co-operative effects. The amount of co-operativity would be different over a range of frequencies, influencing the level of collection for a given concentration.

To utilise sigmoidal equations to normalise spectra, the relationships would first need to be found for each frequency of the spectrum so that the equation of the relationship could be used

in subsequent experiments. These equations would also be expected to vary greatly with changes in experimental conditions and parameters, necessitating derivation for an infinite number of conditions.

4.4.8 Effect of Particle Size

Dielectrophoretic force has been shown to increase with volume. From this theory it might be expected that particles of 2.75 μm diameter would have demonstrated the maximum level of collection, with the 2.07 μm size having the lowest collection, relative to their volume ratios. The results, however, do not agree with this suggestion.

The volume ratios of the particles 2.07 : 2.40 : 2.75 were 1 : 1.56: 2.34, implying that the 2.75 μm particles should collect more than double that of 2.07 μm particles. This discrepancy with actual collection level may be attributable to charge density differences on the surfaces of the particles. Chemical analyses provided with the particles (table 5.4) showed that the charge densities were comparable with the 2.07 μm and 2.75 μm diameter particles, though much reduced in the 2.40 μm particles.

Diameter (μm)	Lot No.	Surface charge density ($\mu C.cm^{-2}$)	Area per charge group ($Å^2.charge\ group^{-1}$)	Stock particle concentration
2.04	5-376-46	7.1	225	$1.8 \times 10^{10}.ml^{-1}$
2.07	10-367-23	7.94	202	$1.7 \times 10^{10}.ml^{-1}$
2.40	2-64-48	2.82	567	$1.1 \times 10^{10}.ml^{-1}$
2.75	10-295-22	9.83	163	$7.4 \times 10^{9}.ml^{-1}$

Table 4.3 : Surface charge characteristics of polystyrene latex particles (Interfacial Dynamics Corporation).

The results obtained suggest that polarisation and dielectrophoretic force is related more to charge density than to volume. The highest charge density was for 2.75 μm diameter particles, followed by 2.07 μm and then 2.40 μm, correlating with the overall levels of dielectrophoretic collection and explaining why the 2.40 μm diameter particles do not collect as well as the smaller 2.07 μm size.

The underlying explanation lies in the concept that greater charge densities on the particle surface lead to greater density of counterions in the double layers. Polarisation at lower frequencies, as seen with latex particles is related to surface conductivity effects and charge hopping within the ion cloud. Greater ion density in this region will result in a larger movement of ions in response to the electric field. This very large bulk movement causes a significant

polarisation mechanism at these frequencies and causes a greater degree of dielectrophoretic movement and hence collection. A greater charge density and thus smaller area per charge group causes overlapping of potential energy wells, enabling easier movement of counterions and more rapid charge hopping effects. In addition, the greater charge density gives more available sites for mobile counterions to occupy during the 'hopping' process.

However, even though the 2.75 μm diameter particles have a much greater charge density and volume, their dielectrophoretic collection is not significantly greater than the 2.07 μm particles. In addition, the conductivity of the 2.07 μm suspension is slightly higher than the other suspensions, theoretically decreasing its collection. Flow forces on the particles also need to be taken into consideration, possibly explaining the lesser collection of the 2.75 μm diameter particles, due to the increased pressure on the greater surface area of the particles.

4.4.9 Effect of Resistance Shunt Position

Early dielectrophoretic experiments, which first observed a peak in dielectrophoretic collection at frequencies greater than 10 MHz with certain Gram positive cell species, were initially attributed to artefactual results. It was originally suspected that the effect may have been caused by interference with the detection signal when the resistance shunt was repositioned. However, the overall effect appears to exclusively influence the degree of dielectrophoretic collection of Gram positive cells, whilst having no effect on Gram negative species. The additional results obtained here now suggest that these are true effects and the nature of the electrical basis has been studied in more detail.

It is suggested that this result is caused by transmission line effects brought about by a mismatching of the impedances within the system. This mismatching could have led to reflection of the signal and possible phase interferences when the cable was unmatched (Horowitz & Hill, 1989) i.e. when the shunt was positioned by the generator output. The effect is also known to be determined by the electrical length of the cable, governing the degree of interference and so the ultimate voltage delivered to the electrodes. When the shunt was at the other end, the signal was modified and stabilised by the 50 Ω resistance which had significantly better matching properties. The results obtained in figure 4.21 by oscilloscope measurements of output voltage show the very great differences in voltage across the electrodes caused by shunt movement.

The explanation of the exclusive influence of these voltage changes on Gram positive cells but not on Gram negative cells is still incomplete. The effect could be related to the Gram positive cell structure which may be more dramatically affected by the increased voltage. Alternatively, it may be explained by a more simplistic scenario in which Gram negative cells may have a

spectrum with zero collection at these high frequencies, whilst Gram positive cells may still undergo some degree of positive dielectrophoresis which can be greatly increased by the raised voltage.

While either or both suggestions may be involved, the real implications of this occurrence should not be overlooked. In many applications, one or other of the Gram classifications are more desirable for study or separation. This phenomenon offers significant potential for fundamental separation or classification of bacterial populations on an almost real-time basis. By examination of the degree of dielectrophoretic collection when a resistance shunt is placed at the output of the signal generator, Gram positive cells might easily be discriminated and separated from their Gram negative counterparts within a mixed population.

4.4.10 Position of Dielectrophoretic Collection

The nature of the suspending medium is important in determining the overall dielectrophoretic movement of particles. Since dielectrophoresis is related to the relative polarisability of both particle and medium, negative dielectrophoresis should be more prevalent in media with greater polarisability. As explained earlier, the negative dielectrophoretic effect is generally more predominant at lower frequencies since more efficient polarisation mechanisms do not come into action until higher frequencies are reached.

A medium such as deionised water will require a particle with a very great polarity to bring about positive dielectrophoresis due to its own polar nature and presence of permanent dipoles within the water molecules. Therefore, in comparison to the less easily polarisable medium of sucrose and mannitol, the size of the negative dielectrophoretic force on the particles was considerably greater. Position of particle collection was therefore found in proposed areas of negative dielectrophoresis for greater frequency ranges with the deionised water.

The collection produced with each of the suspensions had similar maxima of collection in the MHz range. However, it was seen that the collection of both the sucrose and mannitol suspensions at greater than 100 kHz became shifted to higher frequencies with respect to the deionised water suspension. This was especially noticeable with the sucrose suspension which still had a sizeable amount of collection at greater than 10 MHz (as observed microscopically above). It is considered likely that this may be due to the lower relative permittivities of these media. At the higher frequencies where cell polarisation normally becomes more difficult, the cells will still be more polarisable than the sucrose and mannitol, resulting in a greater level of positive dielectrophoretic collection than with the more polar deionised water. The low viscosity and highly polar nature of the water allows ease of repolarisation right up to a frequency of 17 GHz before relaxation occurs (Bone & Zaba, 1992).

The viscosity of the respective media will also have an effect in retarding the movement of particles throughout the liquid, probably leading to a much lesser dielectrophoretic collection (whether positive or negative) at higher viscosities. This demonstrates that the nature of the medium can be effective in determining the size and direction of the dielectrophoretic force and can ultimately be used in the physical separation of particles having different relative polarisabilities as shown by Markx *et al.* (1994).

At increased viscosities, the orientation of water dipoles also becomes harder. Therefore the liquid polarisation becomes slower meaning that cell polarisation will be much more efficient relative to the medium. As the frequency increases, the medium is less able to become polarised, allowing positive dielectrophoresis of the cells to occur at even higher frequencies.

4.4.11 Effect of Shaking Cultures of Bacteria

The shaking of the bacterial broth culture did not influence the dielectrophoretic spectrum. *Ps. aeruginosa* is a strict aerobe, requiring non-limiting conditions of oxygenation to grow. It was therefore expected that the growth rate of the cells would be considerably reduced in the stationary culture. Changes in growth rate of the cells would have thus been expected to result in differences in frequency response, as compared with the growth phase hydrophobicity experiments.

It may have been possible that sufficient gas exchange was possible within the non-shaken culture to sustain normal *Pseudomonas* growth though the dissolved oxygen level was expected to have been significantly reduced compared to the vigorously shaken flask. Ingraham *et al.* (1983) described work stating that the oxygen consumption was not significantly influenced by the growth rate of *E. coli* batch cultures, so perhaps this has similar consequences with *Ps. aeruginosa* indicating that the growth of the two cultures (which may have had different growth rates) consumed comparable levels of oxygen assuming the stationary cultures were non-limited.

4.5 Exopolysaccharide Studies

4.5.1 Dielectrophoretic Spectra

4.5.1.1 Variation of Nitrogen Source

The two bacterial types A4O31 and 87Sl are both related strains of serotype 8 of *Kl. aerogenes*, the former being an EPS- mutant while the latter is a slime producing strain. Spectra showing differences in dielectrophoretic collection over the applied frequency range are shown in figure 4.26.

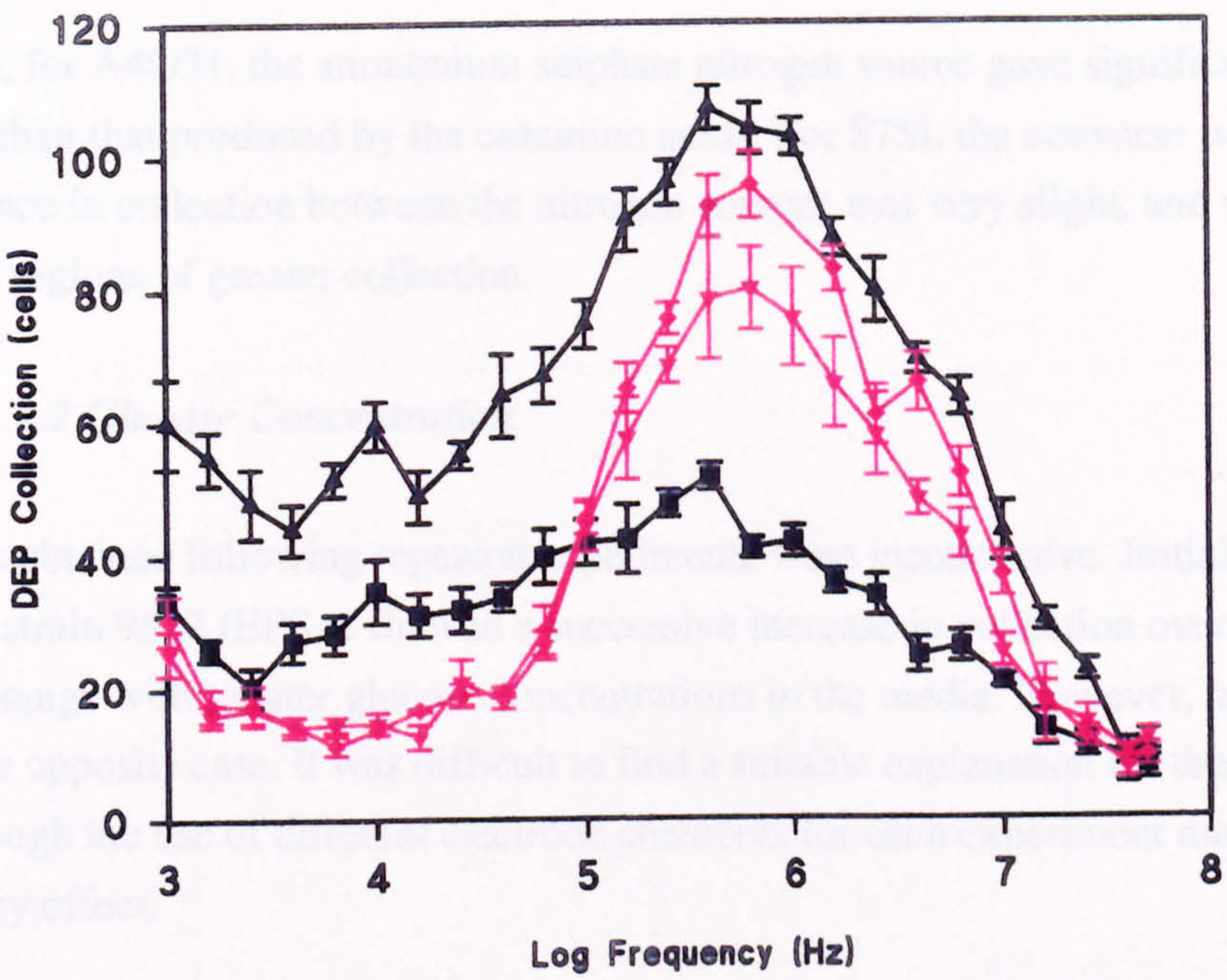

Figure 4.26 : Effect of growth in different nitrogen sources on the dielectrophoretic (DEP) frequency spectra of two related strains of *Klebsiella aerogenes*. (■) *Kl. aerogenes* A4O31 grown in 1 % casamino acids, (▲) *Kl. aerogenes* A4O31 grown in 0.5 % $(NH_4)_2SO_4$, (◆) *Kl. aerogenes* 87Sl grown in 1 % casamino acids, (▼) *Kl. aerogenes* 87Sl grown in 0.5 % $(NH_4)_2SO_4$. Conditions : 12 V, 5 s pulse, 24.5-24.6 $\mu S.cm^{-1}$. Full count detection method. Each point is the mean plus standard error of 5 spectra.

The spectra obtained from the two organisms had differences over the frequency range. The collection of A4O31 occurred over the whole frequency range giving moderate collection even at low frequency values. Indeed, there appeared to be some significant collection at the 10 kHz frequency when grown on both nitrogen sources. The other strain, while related, had a

somewhat different spectrum, giving positive dielectrophoretic collection over a much narrower frequency range with the onset at around 30 kHz. The peak collection occurred at around 650 kHz for the 87Sl strain but appeared to be at slightly lower frequency values with A4O31. Since both strains are of the same original serotype, they might be expected to have had similar spectra. As this was not the case, the more widespread frequency response and increased collection at lower frequencies could have been indicative of different cellular structure in the mutant O-strain.

Whilst the peak collection level of 87Sl grown on casamino acids was much greater than that of A4O31 (collecting almost double that of A4O31), growth on ammonium sulphate led to approximately 35 % greater collection level with the non-EPS producer (A4O31) than with the slime producer.

In addition, for A4O31, the ammonium sulphate nitrogen source gave significantly greater collection than that produced by the casamino acids. For 87Sl, the converse was true, though the difference in collection between the nitrogen sources was very slight, and was apparent only in the regions of greater collection.

4.5.1.2 Glucose Concentration

The results obtained following repeated experiments were inconclusive. Initial spectra of *Klebsiella* strain 9527 (EPS+) showed a successive increase in collection over the whole frequency range with greater glucose concentrations in the media. However, later experiments showed the opposite case. It was difficult to find a suitable explanation for these different results, though the use of different electrode chambers for each experiment may have had a contributory effect.

The spectra of the EPS+ strain for the later experiments are shown in figure 4.27, along with the non-EPS producing strain. Increasing concentrations of glucose resulted in a general decrease in collection level over the frequency range. In 0.5 % glucose, a peak collection level of approximately 310 cells was realised, falling to around 270 after growth in 2 % glucose. The spectral form of this capsulated strain of *Klebsiella aerogenes* had more similarity with the EPS- strain A4O31 shown in figure 4.26 above with collection occurring well over the whole frequency range, while the non-capsulated strain (9528) of figure 4.27 was similar to the slime producer 87Sl.

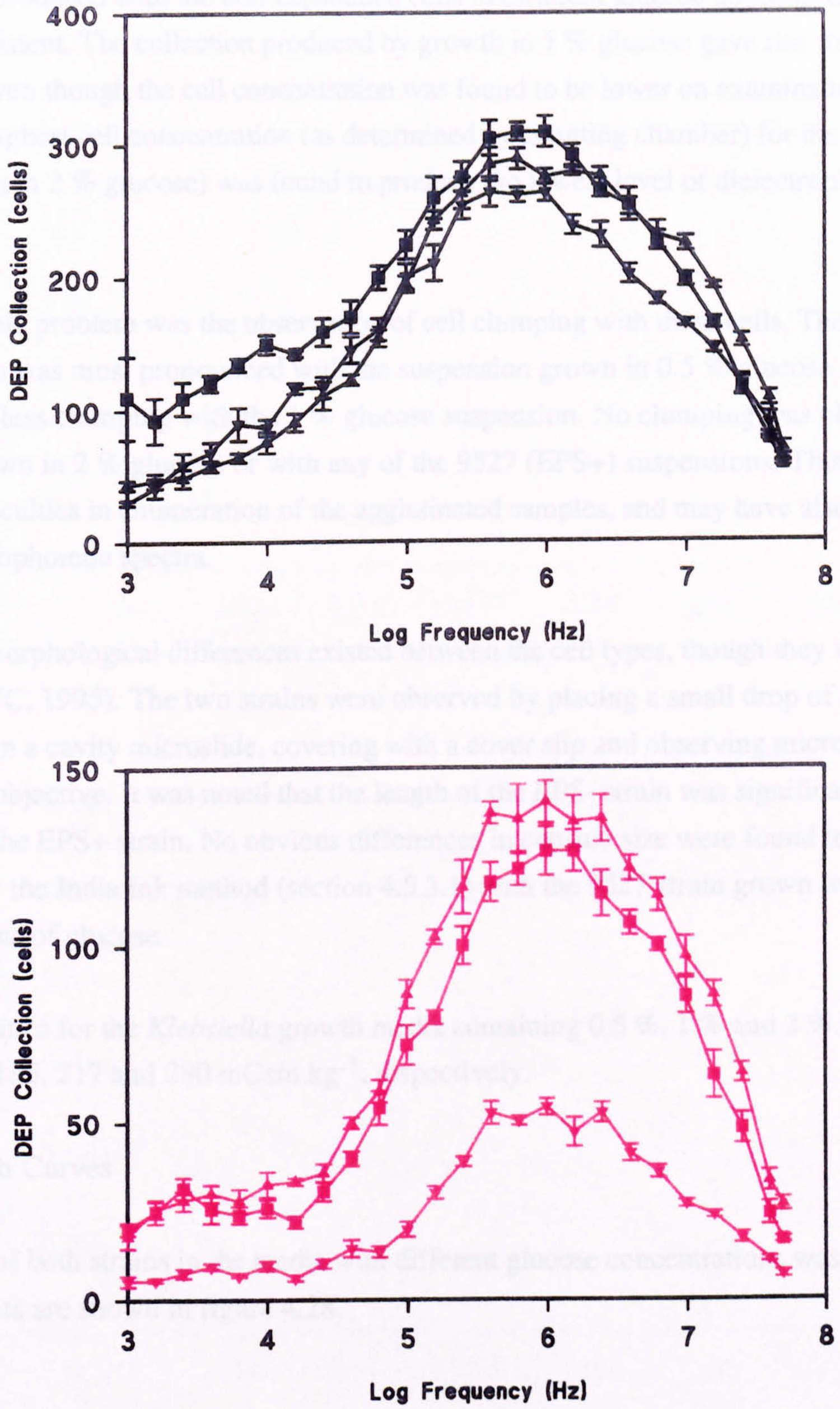

Figure 4.27 : Effect of growth in increasing medium glucose concentrations upon the dielectrophoretic (DEP) frequency spectra of *Klebsiella aerogenes* strains. Strain 9527 (EPS+) grown in (■) 0.5 % glucose, (▲) 1 % glucose and (▼) 2 % glucose, respectively. Strain 9528 (EPS-) grown in (■) 0.5 % glucose, (▲) 1 % glucose and (▼) 2 % glucose, respectively. Conditions : 12 V, 5 s pulse, 24.3-25.3 μS.cm^{-1}. Full count detection method. Each point is the mean plus standard error of 5 replicate spectra.

The spectra produced with the non-capsulated cells in different glucose concentrations were again inconsistent. The collection produced by growth in 1 % glucose gave rise to the greatest collection, even though the cell concentration was found to be lower on examination by total count. The highest cell concentration (as determined by counting chamber) for the acapsulate strain (grown in 2 % glucose) was found to produce the lowest level of dielectrophoretic collection.

One noticeable problem was the observation of cell clumping with these cells. The agglutination was most pronounced with the suspension grown in 0.5 % glucose media, followed by less clumping with the 1 % glucose suspension. No clumping was obvious with the cells grown in 2 % glucose or with any of the 9527 (EPS+) suspensions. This caused obvious difficulties in enumeration of the agglutinated samples, and may have also influenced their dielectrophoretic spectra.

Additional morphological differences existed between the cell types, though they were related strains (NCTC, 1995). The two strains were observed by placing a small drop of each suspension on a cavity microslide, covering with a cover slip and observing microscopically using a x40 objective. It was noted that the length of the EPS- strain was significantly greater than that of the EPS+ strain. No obvious differences in capsule size were found to exist when examined by the India Ink method (section 4.5.3.1) with the 9527 strain grown with differing concentrations of glucose.

The osmolarities for the *Klebsiella* growth media containing 0.5 %, 1 % and 2 % glucose were found to be 185, 217 and 280 $mOsm.kg^{-1}$, respectively.

4.5.2 Growth Curves

The growth of both strains in the media with different glucose concentrations was monitored and the results are shown in figure 4.28.

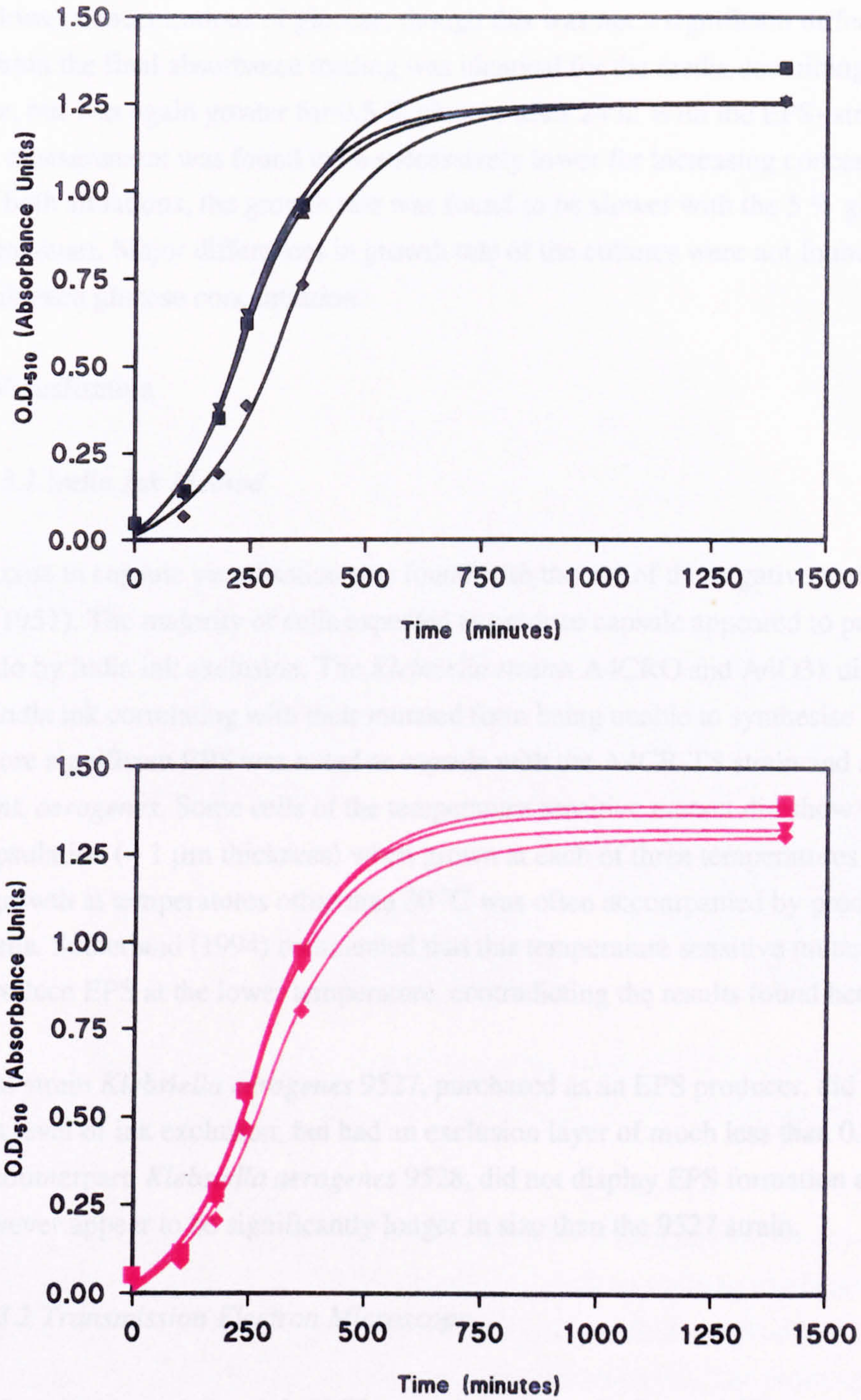

Figure 4.28 : Growth curves of *Klebsiella aerogenes* strains in media containing differing glucose concentrations. Strain 9527 (EPS+) grown in (■) 0.5 % glucose, (▲) 1 % glucose, (▼) 2 % glucose and (◆) 5 % glucose, respectively. Strain 9528 (EPS-) grown in (■) 0.5 % glucose, (▲) 1 % glucose, (▼) 2 % glucose and (◆) 5 % glucose, respectively. Smoothed curves were fitted to the data.

With both strains a slight increase in the rate of culture growth was found with media containing lower concentrations of glucose, though this was not a significant difference. For the EPS+ strain the final absorbance reading was identical for the media containing 1, 2 and 5 % glucose, but was again greater for 0.5 % glucose after 24 h. With the EPS- strain, the final absorbance measurement was found to be successively lower for increasing concentrations of glucose. In both situations, the growth rate was found to be slower with the 5 % glucose containing medium. Major differences in growth rate of the cultures were not found in either strain or with each glucose concentration.

4.5.3 EPS Visualisation

4.5.3.1 India Ink Method

Limited success in capsule visualisation was found with the use of the negative staining method of Duguid (1951). The majority of cells expected to produce capsule appeared to produce only a limited halo by India ink exclusion. The *Klebsiella* strains A4CRO and A4O31 did not appear to exclude India ink correlating with their mutated form being unable to synthesise EPS material. More significant EPS was noted as capsule with the A4CR-TS strain and a clinical isolate of *Ent. aerogenes*. Some cells of the temperature sensitive mutant did show moderate to heavy encapsulation (≈ 1 μm thickness) when grown at each of three temperatures 20, 30 and 37 °C, but growth at temperatures other than 30 °C was often accompanied by production of very long cells. Sutherland (1994) commented that this temperature sensitive mutant was unable to produce EPS at the lower temperature, contradicting the results found here.

The bacterial strain *Klebsiella aerogenes* 9527, purchased as an EPS producer, did not produce a significant level of ink exclusion, but had an exclusion layer of much less than 0.25 μm. Its acapsulate counterpart, *Klebsiella aerogenes* 9528, did not display EPS formation as expected, but did, however appear to be significantly longer in size than the 9527 strain.

4.5.3.2 Transmission Electron Microscopy

A transmission electron micrograph of *Kl. oxytoca* is shown in figure 4.29.

The most notable feature of the cells in the micrograph are the dense bundles surrounding the outer membrane. This material on the surface of the cell sections can be visualised as having a fibrous nature. This layer, however, was much thinner than that expected from capsular structures, extending only 50 nm from the cell surface. Some additional material may be

observed at the top of the centre cell section. However, this may simply be the result of an incomplete section, allowing visualisation of the material on the surface of the pole.

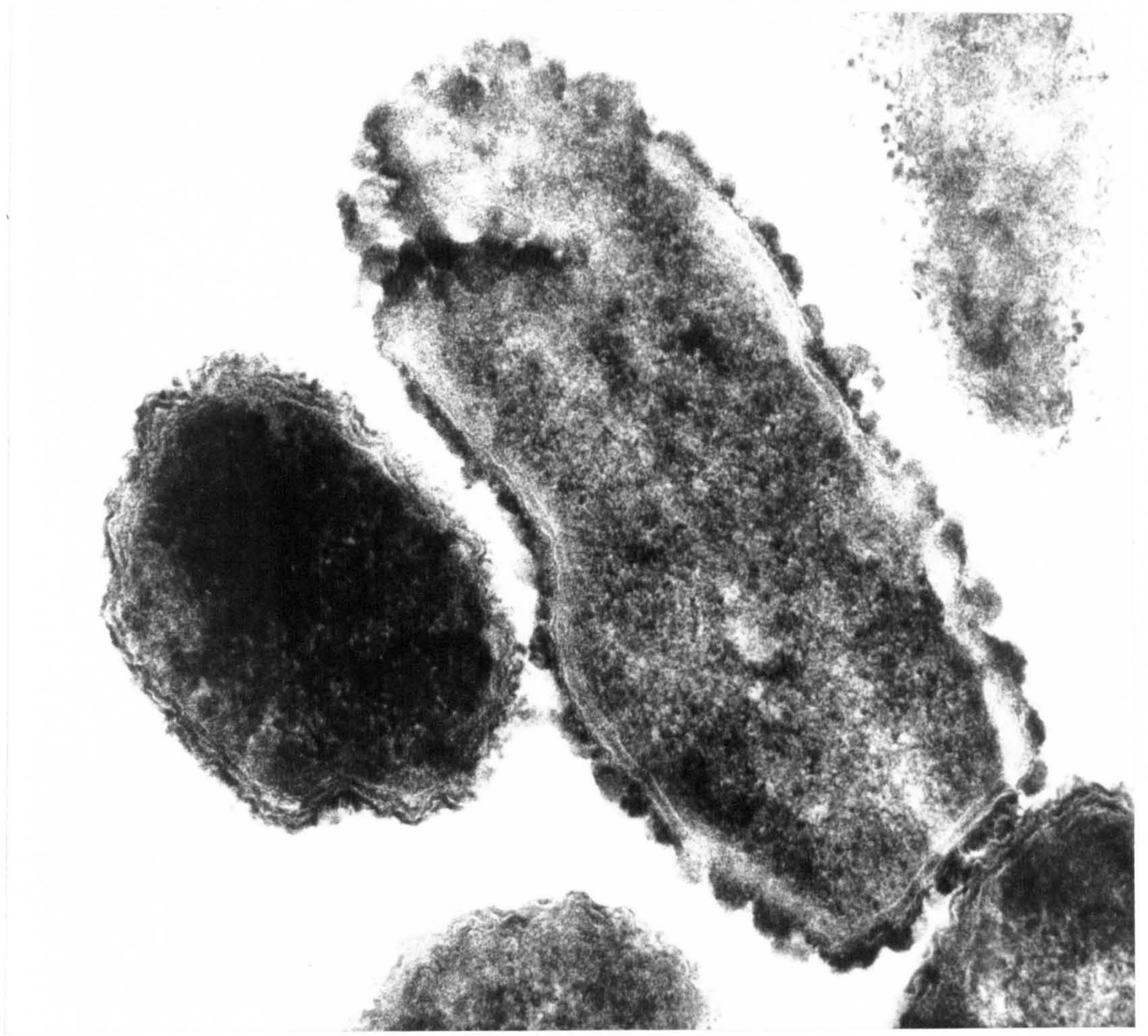

Figure 4.29 : Transmission electron micrograph of longitudinal section of a *Klebsiella oxytoca* cell demonstrating a ruthenium red staining layer. Accelerating voltage 80 kV, x 40,000 magnification. Scale : 20 mm = 200 nm.

Another interesting feature of this section is the general Gram negative cell structure including the clearly visibly 'double track' structure of the cell wall, comprising the dense peptidoglycan layer separating two membranes, the inner cytoplasmic membrane and outer membrane (seen in the figure as a dark area bounded by two white lined membranes). The dense cytoplasmic material is also clearly visible.

4.5.4 *Klebsiella* Mutagenesis

Mutagenesis resulted in the isolation of 30 mutants on the basis of different colony morphology or colour from the parent strains, 87Sl and A1Sl. Photographs of the slime producing strain 87Sl and its rough mutant 22 can be seen in figure 4.30. The obvious differences in colony

morphology can be seen, with the mutant having a very irregular colony edge and being non-mucoid.

Figure 4.30 : Colony morphologies of the slime producing strain, 87S1 and its mutant 22. Parent strain shown on the left of the photograph, mutated form on the right.

The majority of these mutants were produced from the A1S1 parent. The mutants were purified and Gram stained for further investigation and to confirm their identity. Ten of them were kept for further study. The nature of the mutations are outlined in table 4.4.

Mutant	Number	Colony Aberration	Microscopic Characteristics
A1Sl	**Parent**		
	1	Non-mucoid, white colour	As parent
	4	Non-mucoid, undulate colony	As parent
	9	Small, glossy, individual colonies	Short Gram negative rods
	14	Non-mucoid, rough colony with darker centre	Gram negative rod as parent, though some very long cells also present
	15	Very rough edge, slightly mucoid	Very short Gram negative rods with some very long
	25	White, non-glossy colony	As parent
	27	White, non-glossy colony	As parent
	29	Very mucoid growth (greater than parent)	As parent
87Sl	**Parent**		
	20	Non-mucoid, rough colony with darker centre	As parent
	22	Rough edge	As parent

Table 4.4 : Colony morphology and microscopic characteristics of mutated strains produced from *Klebsiella aerogenes* slime producing parents.

Three of these mutants, 9, 14 and 22 were selected for use with dielectrophoretic experiments and thus were maintained for further study. Their identity was confirmed using the API20E identification system, as were their parent strains. All strains were positively confirmed by this method, as *Klebsiella* to an accuracy of 97.8 %.

The spectra of the parent slime producing strains are shown in figure 4.31. A typical spectrum of 87Sl has been discussed previously in section 4.5.1.1 and again had similar form and low level of collection. The spectrum of A1Sl appeared to have a greater level of collection that the 87Sl strain, especially at frequencies greater than 300 kHz but most noticeably at frequencies greater than 1 MHz.

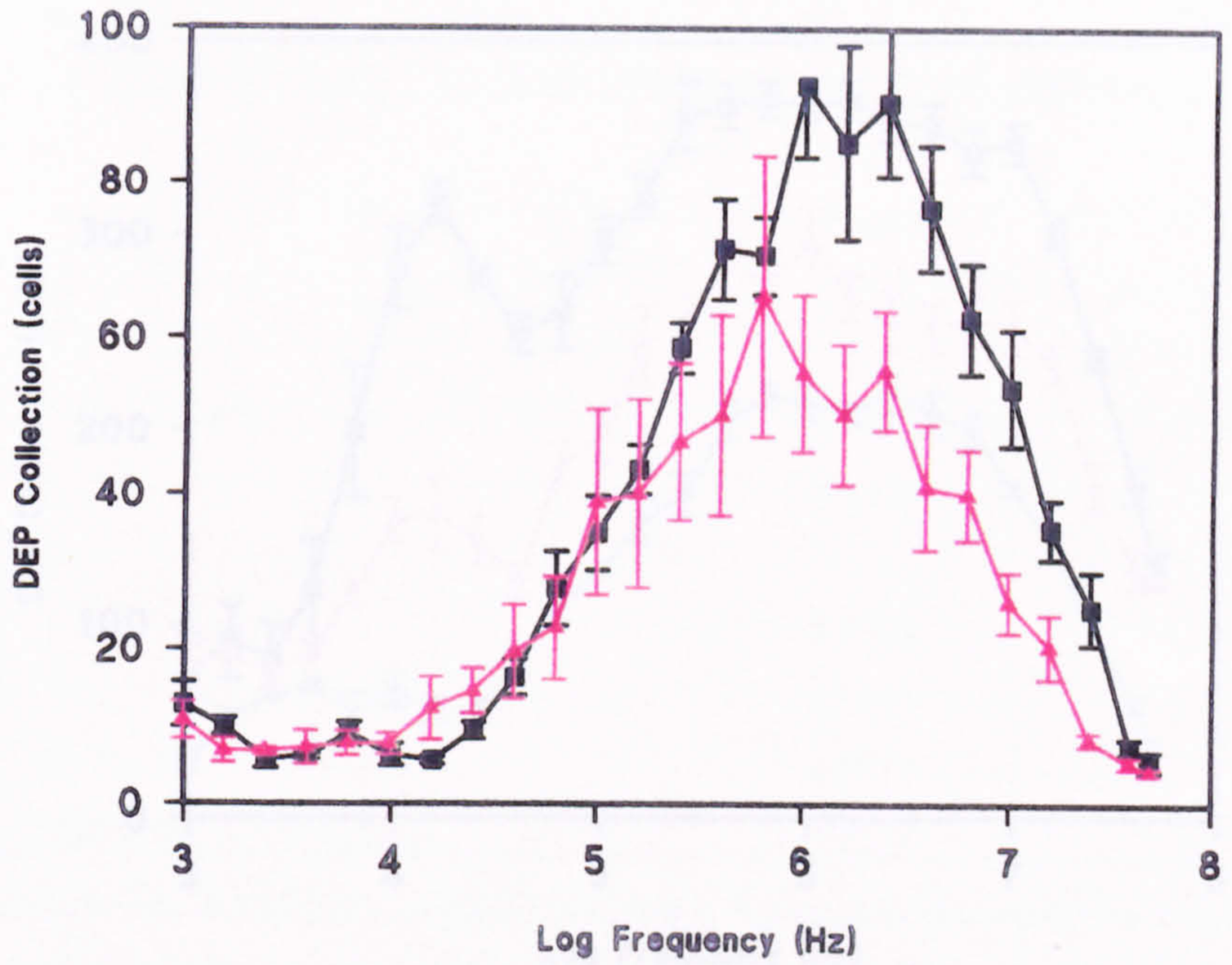

Figure 4.31 : Dielectrophoretic (DEP) frequency spectra of slime producing parent strains of *Klebsiella aerogenes*. (■) A1Sl, (▲) 87Sl. Conditions : 12 V, 5 s pulse, 24.4-26.9 μS.cm^{-1}. 15.563 x 10^7 cells.ml^{-1} (87Sl), 19.75 x 10^7 cells.ml^{-1} (A1Sl). Full count detection method. Each point is the mean plus standard error of 5 replicate spectra.

The peak collection frequency of A1Sl also appeared to occur at a higher values than 87Sl (which was higher than A4O31, section 4.5.1.1), and was seen at 1 MHz and greater. The associated mutant strains were also very different in spectral form (figure 4.32).

A notable feature was the greater overall level of collection of the mutants at all frequencies compared to that of the parent strains. While mutant 22 kept a similar form to the parent 87Sl, the mutants of A1Sl were significantly different to their parent.

Both mutants 9 and 14 had similar spectra to each other, even though their mutations produced different morphologies. Both had significant dielectrophoretic collections in the region of 10 kHz with a flattened region from 500 kHz, unlike their parent. These mutants still showed collection of many cells up to frequencies of 10 MHz, while the majority of other cell types studied (including A1Sl) had almost negligible collection at this frequency. The peak at 10 kHz was comparable to the similar peak observed with the A4O31 mutant strain examined in section 4.5.1.1.

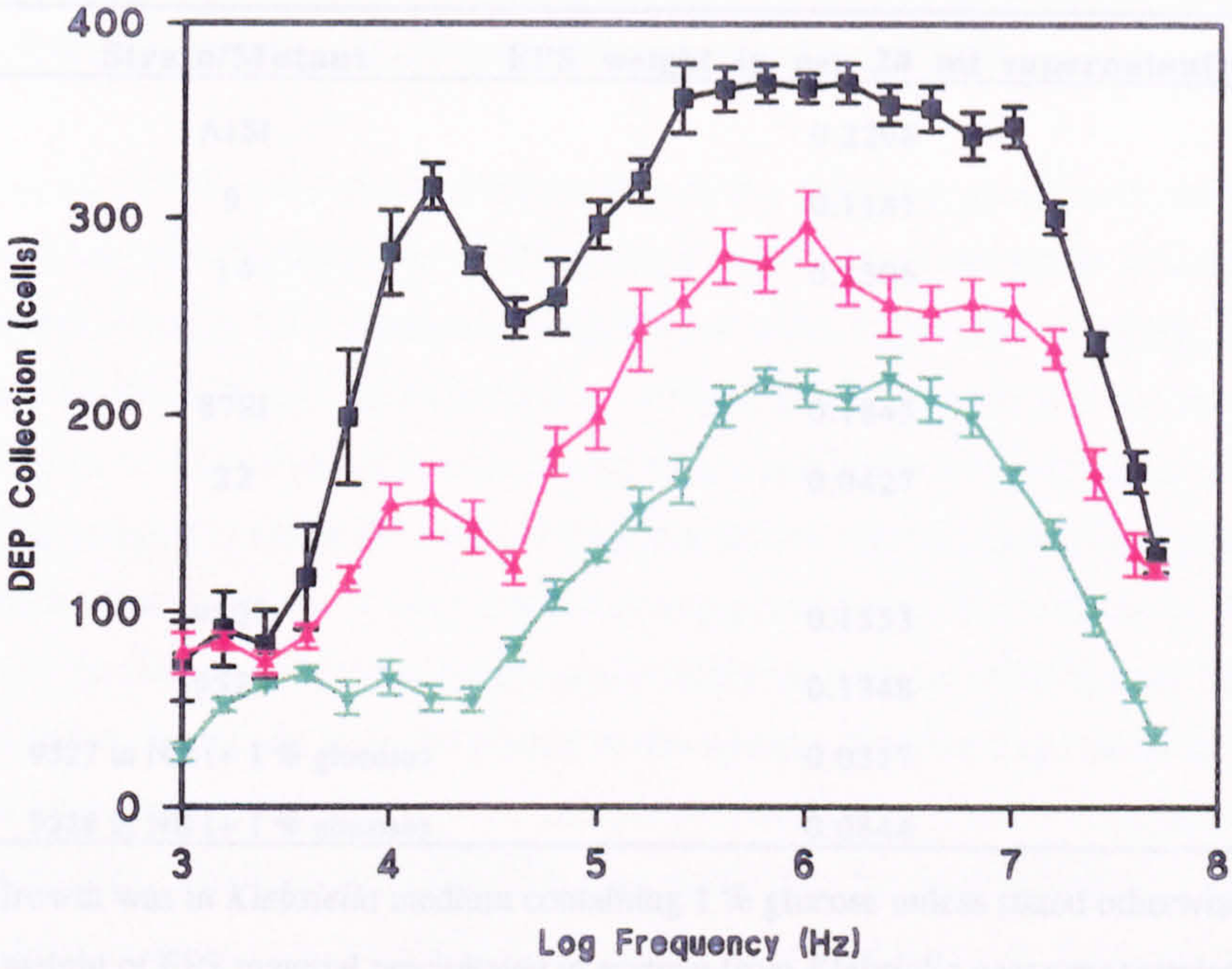

Figure 4.32 : Dielectrophoretic (DEP) frequency spectra of mutants of *Klebsiella aerogenes*. (■) Mutant 9 (A1Sl), (▲) Mutant 14 (A1Sl), (▼) Mutant 22 (87Sl). Conditions : 12 V, 5 s pulse, 24.5-25.4 μS.cm^{-1}. 20.125 x 10^7 cells.ml^{-1} (Mutant 9), 17.75 x 10^7 cells.ml^{-1} (Mutant 14), 15.75 x 10^7 cells.ml^{-1} (Mutant 22). Full count detection method. Each point is the mean plus standard error of 5 replicate spectra.

4.5.5 Estimation of Exopolysaccharide

The dry weight of EPS material extracted from the *Klebsiella* strains and mutants are as detailed in table 4.5.

Generally the weight of EPS produced by the slime producing strains was much greater than that produced by the mutants following the treatments described in section 3.5.4.2. As expected the strain A1Sl, which produced copious amounts of slime in the *Klebsiella* medium, had the greatest dry weight of EPS, producing almost double the material found with its mutant 9.

The results found with the *Klebsiella* strains 9527 and 9528 were conflicting. While the encapsulated strain produced more material than the EPS- strain when grown in *Klebsiella* medium, the precipitated material produced in nutrient broth was much lower in weight, even with the EPS producing strain.

Strain/Mutant	EPS weight (g per 20 ml supernatant)
A1S1	0.2298
9	0.1181
14	0.1306
87S1	0.1845
22	0.0427
9527	0.1553
9528	0.1348
9527 in NB (+ 1 % glucose)	0.0317
9528 in NB (+ 1 % glucose)	0.0844

Growth was in *Klebsiella* medium containing 1 % glucose unless stated otherwise.

Table 4.5 : Dry weight of EPS material precipitated in acetone from *Klebsiella aerogenes* strains.

4.6 Discussion of Exopolysaccharide Investigations

4.6.1 Variation of Nitrogen Source

The conditions for optimal production of EPS material have been described previously, in section 2.2.5. Generally, high C:N ratios are associated with significant production. The level of nitrogen in the growth medium can have very great influence on EPS levels secreted. Though the nitrogen levels used in these experiments were non-limiting, it has been commented that the source of nitrogen, whether synthetic (ammonium sulphate) or semisynthetic (casamino acids), could also affect the level of EPS produced (De Souza & Sutherland, 1994). These sources, even under non-limiting conditions produced substantial EPS.

After incubation of the slime producing strain 87S1 in media containing ammonium sulphate or casamino acids, it was found that the semisynthetic nitrogen source produced copious amounts of gelatinous slime, while the synthetic source produced only moderate amounts. The slime was found to be very viscous and necessitated the use of a centrifuge to obtain cell samples for use in dielectrophoretic experiments. It has previously been noted that the forces involved in centrifugation can be sufficient to disrupt cell surfaces and elicit the release of LPS material into

the medium (Gilbert *et al.*, 1991c). Loss of LPS would undoubtedly affect cell surface charge and the movement of ions over the surface. To control this, slime producing cells grown in ammonium sulphate were also centrifuged under identical conditions.

Fomchenkov *et al.* (1979) paid particular attention to the washing procedure used in preparation of their cells, finding that washing steps caused some decrease in collection at lower frequencies, though this became less significant with additional washing. It is probable that a great deal of the EPS and associated ions would have been removed by similar washing procedures used here. However, it is considered that a sufficient proportion of the EPS produced would remain to elicit the desired response to the electric field. EPS also has a continuous production for a short time after washing procedures. Nevertheless, the washing procedure could produce anomalous results since different extents of EPS may be removed making it difficult to highlight specific trends in the spectra. Further experimental research would need to be conducted in this area of sample preparation to ensure conclusive and representative results. The removal of EPS by washing may be responsible to a certain extent, for the similarities in spectrum for strain 87Sl in both nitrogen sources. Remaining EPS material produced in the casamino acids medium, being much more viscous, may remain adhered to the cell surface and cause the observed increase in collection at the peak frequencies.

The presence of EPS material on the surface of the cells could potentially increase the overall polarisation of the cell. The composition of EPS material can comprise up to 99 % water, which is effectively bound to the surface. This bound water layer, in a similar manner to the water of hydration surrounding globular proteins (Bone & Zaba, 1992), polarises and relaxes along with the cell. Water molecules have a greater polarisability (with relaxation around 20 GHz) than many of the larger molecules composing the cell and so can increase the effective polarisability of the cell, over that of a cell not bearing an EPS layer. This water will also increase the effective cell volume and thus increase the dielectrophoretic force upon the particle. The polysaccharide nature of the EPS may also possess many permanent and inducible dipoles which would exacerbate any polarisation mechanisms.

The exopolysaccharide polymers produced as slime are not physically bound to the cell surface. Polarisation of these molecules by the applied field by dipolar rotation mechanisms may be much greater than with the fixed polysaccharide molecules. EPS polysaccharide chains can possess many ionic charges along their length which give rise to sizeable dipole moments. Free polymers, as slime, are able to fully orientate themselves along field lines making their maximum contribution to cell polarisation and dielectrophoretic collection. Fixed polymers as discrete capsular material would be restricted in their orientation by the adhesion to the cell surface. Thus they would contribute significantly less towards the overall polarisability of the cell (figure 4.33). In addition, the charged slime polymers may be able to physically move,

along with associated water molecules, creating a larger charge density in certain regions of the cell, promoting dielectrophoretic collection. Therefore, the increased production of slime in the semisynthetic casamino acids medium is likely to induce increased dielectrophoretic collection as a result.

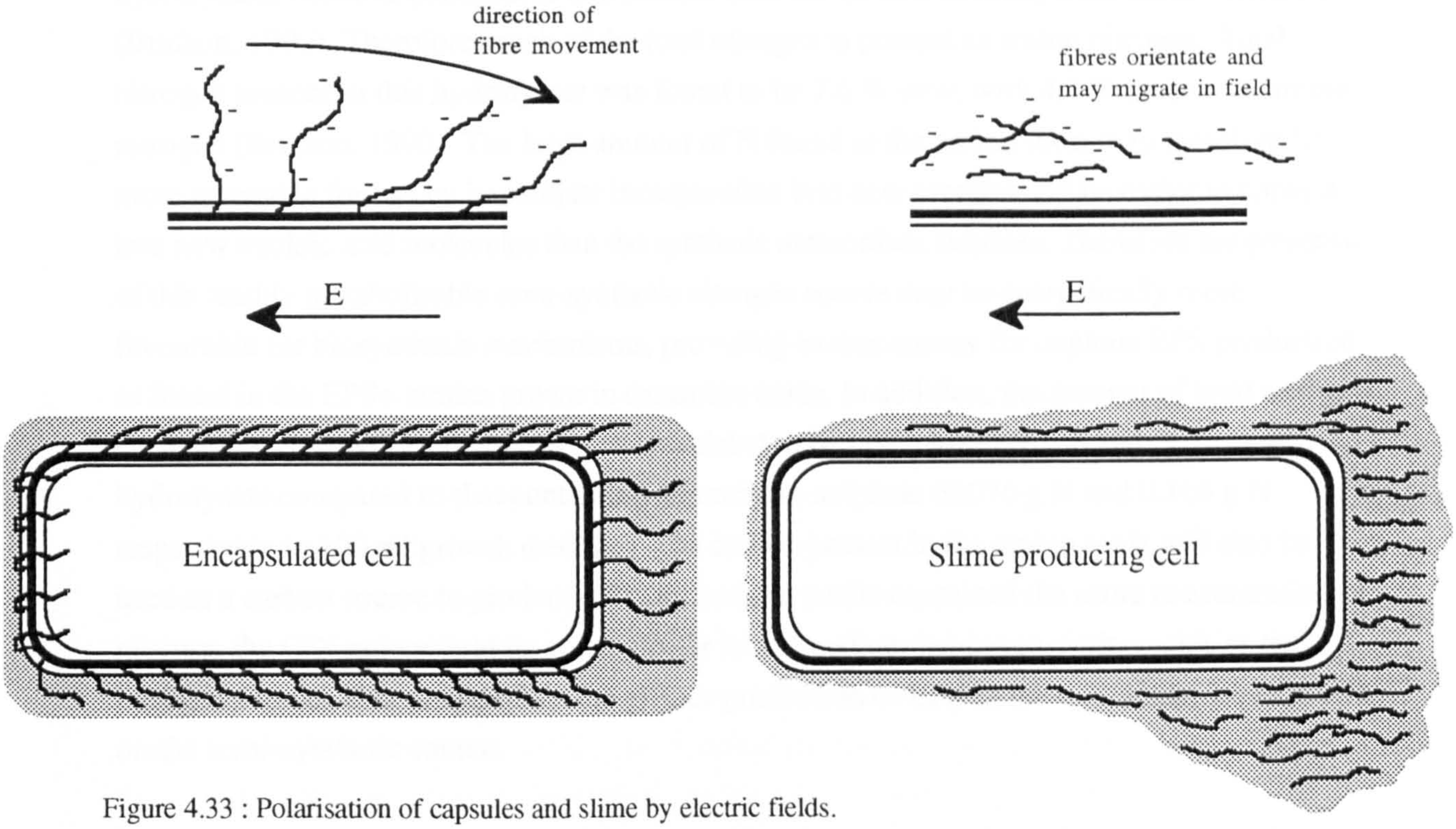

Figure 4.33 : Polarisation of capsules and slime by electric fields.

Since EPS production for a particular strain is identical in composition, it is unlikely that the differences in DEP collection are caused by structural differences in the EPS related to the different growth sources.

If, however, the effect of nitrogen source was solely to affect the level of EPS production, it might be expected that the A4O31 (EPS-) strain would give identical spectra after incubation in both nitrogen sources. As this is clearly not the case, it is anticipated that the different nitrogen sources also produce differences in cell structure accounting for the great differences in spectra between the A4O31 cells grown in $(NH_4)_2SO_4$ and those grown in casamino acids. Though again, if the nitrogen sources caused such changes in EPS- strains, it is possible that the differences seen with the 87Sl strain is not due to EPS differences, but to structural and morphological effects. Once again, the nature of bacterial growth makes it very difficult to attribute spectral changes to a single source.

The differences in spectra may be caused by the nature of the medium rather than the actual content of nitrogen which is utilisable.

Casamino acids are a crude hydrolysate of protein and contain a mixture of many components, including a mixture many unspecified amino acids. Generally the similar casein derived hydrolysates contains phosphorus and sodium chloride as well as many trace metal elements (Bridson, 1990). Therefore much of the total nitrogen is present as amino nitrogen. Total nitrogen present in this hydrolysate was found to be 7.6 % w/w, with 4.9 % present as amino nitrogen (Bridson, 1990). The large amount of N found in the amino form may therefore be more amenable for use by immediate incorporation into new proteins and be easier to convert into new nucleic acid molecules than the synthetic ammonium sulphate. Therefore the presence of this readily metabolisable semi-synthetic nitrogen source may be energetically more favourable for biosynthetic mechanisms, providing excess energy for copious EPS production as found in the EPS+ strains grown in casamino acids. In addition, the amount of total nitrogen present in the growth medium has been calculated to be much lower in medium with casein hydrolysate compared to that containing ammonium sulphate (0.076 g N and 0.106 g N respectively in 100 ml growth medium). The carbon present in the amino acids will also be used as a carbon source to produce EPS. Since both media contained the same concentration of glucose, the C:N ratio would be much greater in the medium having casamino acids as the nitrogen source. This may explain the greater production of EPS in the 87Sl strain when grown on the semi-synthetic source.

However, this does not explain the increased collection of the EPS- strain when grown in the synthetic ($(NH_4)_2SO_4$) nitrogen source. An alternative explanation is that the observed spectra are related, not to EPS differences but to cell growth and surface structural charges.

Though the nitrogen is unlikely to be limiting in either medium, the greater level in the media containing ammonium sulphate will probably result in much better cell growth. In the EPS- strain, none of the carbon source would be used for EPS production, enabling cell division and growth to be much more efficient. Since the O.D. of the samples used for dielectrophoretic experiments were identical, small differences in cell size may have caused the samples to have slightly different cell concentrations. Actual cell numbers were found quantitatively using counting chamber methods in later experiments. In this instance it may have been possible that the faster growth of A4O31 on ammonium sulphate may have produced cells which were slightly smaller and more rapidly dividing, producing greater cell concentrations per O.D. unit compared to the sample grown in casamino acids. This may have resulted in the dielectrophoretic count being much greater, as discussed in section 4.4.7.

The greater nitrogen levels in the ammonium sulphate sample may have also caused rapid production of proteins expressed in the outer membrane of the cells. As discussed earlier, the protein content of the outer membrane may have significant effect on the polarisation of cells, potentially causing increased dielectrophoretic collection. These surface changes may be masked in the EPS+ strain by the presence of the slime surrounding these cells, so not directly accessible by the electric field.

4.6.2 Glucose Concentration

The different responses in successive experiments of *Klebsiella* cells after growth on different concentrations of glucose medium is difficult to explain, other than by experimental differences such as the washing procedure or electrode changes or by differences in EPS production by the 9527 (EPS+) strain. It was expected that the presence of additional glucose in the growth medium would have caused large changes in the level of EPS expression by the cells and so increased DEP collection levels. This was observed with an initial experiment (results not shown), demonstrating that the cells theoretically having a larger polymeric capsule layer with its associated water was better polarised by the applied electric field as discussed above. However, the bound nature of the capsular layer, and the very small size as found by India Ink exclusion methods (section 4.5.3.1) would be likely to have only a small effect on increasing polarisation and DEP collection, and indeed the effect on dielectrophoretic frequency spectra was very small for *K. aerogenes* 9527 in the initial experiment, causing slight increases over the whole frequency range. In the experiments conducted where the nitrogen source was varied it was clear to see the amount of EPS produced as slime and be able to correlate with growth conditions. Here, the use of a capsulate strain with very little EPS production made it very difficult to observe any changes in capsule production by the India Ink method of visualisation.

Later experiments showed opposite trends for the EPS producing strain, greater levels of glucose in the medium suppressing dielectrophoretic collection in the 9527 strain. This could not be attributed to differences in cell number, since identical concentrations of cells were present in each of the EPS+ samples as determined by total counts.

The overall level of collection for the capsule producing strain was much greater than that for the acapsulate strain and this can be attributed to the differences in cell size as found microscopically and thus cell concentration. Since the cells were prepared for dielectrophoretic experiments according to O.D., the sample of smaller EPS+ cells would have contained a greater concentration of cells

A possible explanation for the lower collection levels with cells grown in the 2 % glucose medium may be related to the differences in osmolarity between the media. Lohia *et al.* (1985)

found the osmolarity of the growth medium to affect the structure of the cells, producing cells with wavy outer membrane structure in the high osmolarity medium. Transfer of cells from low osmolarity growth medium to high osmolarity produced the same wavy structure within 15 min and transfer of cells from high osmolarity medium to distilled water caused rapid lysis in *V. cholerae*. However, they found very little difference in outer membrane constituents, either quantitatively or qualitatively, in *Vibrio cholerae* cells grown in medium of high (390 $mOsm.kg^{-1}$) and low osmolarity (137 $mOsm.kg^{-1}$). It might be expected that similar results might be found with the *Klebsiella* cells studied here.

The growth of *Klebsiella* in media of different osmolarity will probably alter the cell structure. Though the differences in osmolarity between the media may not appear very great (185 $mOsm.kg^{-1}$ and 280 $mOsm.kg^{-1}$ in 0.5 % and 2 % glucose respectively), the effect upon cells may be important. The internal osmolarity of *Streptococcus faecalis* and *Micrococcus lysodeikticus* were predicted to be 470 and 270 $mOsm.kg^{-1}$ respectively (Marquis & Carstensen, 1973) and similar values may be found for *Klebsiella*. The growth of cells in the high osmolarity medium (2 % glucose) may therefore cause plasmolysis and osmotic destabilisation, possibly brought about by some loss of divalent ions. This may affect the response of cells when used for dielectrophoretic experiments. When placed back into deionised water, it will take time to return to normal and may result in the loss of ions from the cells during the washing procedure due to membrane disruption. This may reduce the overall polarisability of the cells and so reduce dielectrophoretic collection as observed. Further work could be done to examine the structure of these cell types by electron microscopy, both after growth in each of the media and following the washing and preparation procedure. The integrity of the cells and contents could then be assessed.

A possible better way of varying the C:N ratio would have been to vary the concentration of the nitrogen source while keeping the glucose concentration the same in each case. This would be more likely to keep the osmolarity the same and avoid any changes to cell structure.

The observed clumping with cells grown in media containing 0.5 % and 1 % glucose may also be due to osmotic effects as cells are changed from the growth medium to deionised water. However, growth medium containing 1 % glucose has been used as a standard medium for growth of several *Klebsiella* strains and clumping has not previously been observed. The autoagglutination may be related to the nature of the mutation which makes strain 9528 acapsulate or to the larger cell size compared with strain 9527. An alternative explanation may be that the hydrophobicity of the cells may change when grown in the different media.

Hydrophobicity has been found to be closely related to the composition of growth medium as well as other cultural effects (Horská *et al.*, 1993), and has also been correlated with the type

of carbon source within the growth medium (Van der Mei *et al.*, 1993). If growth in low glucose concentrations resulted in increased hydrophobicity the water layer separating cells would be more easily repelled predisposing the agglutination of cells by allowing short range Van der Waals forces to become more active (Stratford & Wilson, 1990). This might be brought about by loss of surface charge, possibly by a depletion of surface molecules such as LPS or proteins. Bar-Or (1990) showed increases in hydrophobicity with starvation, and this may be a similar effect found here with lower concentrations of glucose, which leads to a coagulation of the cells. The composition of the surface of cells grown in different concentrations of glucose could be examined to assess the molecules present.

4.6.3 Growth Curves

The growth curves of both the EPS+ve and EPS-ve strains were found to have important similarities. In both cases, the lower concentrations of glucose showed slightly faster growth rates. The most likely explanation for the slower rate of growth and lower final absorbance values is probably the influence of the osmotic conditions as described above. Growth in successively increasing glucose concentrations raised the osmolarity to which the cells were exposed. This would result in different degrees of turgor or plasmolysis in each medium, depending on the internal cellular osmolarity. Growth in these media would therefore cause a greater shrinkage of the cell structure at higher glucose concentrations. Since the growth curve was measured by O.D. readings, the size of cells would have an influence on the amount of light absorbance, less shrinkage producing increased absorbance levels. This accounts for the similar effect observed with the EPS- strain, thus eliminating any effect due to capsule production.

It would have been expected that if capsule production had been greater in the cultures containing more glucose, the increase in absorbance should have been more rapid compared with the EPS- strain. This was not observed. As found in section 4.5.3.1, the amount of capsule production with the 9527 strain was barely visible under microscopic examination. Therefore it was likely that any changes in EPS production would be slight and masked by the changes in the cell absorbances.

Another possible explanation of lower O.D. values with the greater glucose concentration is related to the rapid production of metabolic waste products, resulting in slower culture growth. However, this is considered to be unlikely since the decreased growth rate was observed immediately following inoculation with the highest glucose concentration. In this situation, waste products would be unlikely to have accumulation during this short time, whereas almost immediate plasmolysis effects would be able to occur.

Ideally, viable or total counts should have been performed alongside the absorbance readings. This would have shown conclusively whether the differences in absorbance were due to variations in cell number, or whether they were simply caused by shrinkage of cell volume.

4.6.4 EPS Visualisation

4.6.4.1 India Ink

Visualisation of capsular material was attempted on several occasions and was problematic with many strains. This difficulty continued even when growth from both solid and liquid medium was examined, grown in media having glucose concentrations of up to 5 % w/v.

One of the most extreme difficulties was found when attempting to observe cell associated EPS produced by the slime forming mutants, A1Sl, A3Sl and 87Sl, though this method of Duguid has previously been demonstrated to be applicable to slime producing strains. While EPS production was obvious from the slimed nature of colonies on agar and the viscous nature of liquid culture, individual cells could not be directly visualised by the method to the high slime viscosity.

It was difficult to estimate the size of the EPS material excluding the colloidal ink, as the size was distinctly variable within the samples studied. While some cells demonstrated an exclusion layer of around 1 μm, other cells in the sample did not show the halo. Growth and resuspension of these strains in glucose solutions was undertaken to enable a rehydration of capsule fibres, however, generally limited success was found. In addition, both broth cultures and growth from solid media were used, and both exponential and stationary phase stages of growth. All of these modifications resulted in the same limited success.

It was highly unlikely that each of the *Klebsiella* strains examined by this method would only produce 'microcapsule' material, as the majority of these Gram negative strains are known to produce discrete capsules of a very large size. This method of capsule visualisation has been used successfully by numerous workers even with slime producing strains so it is inexplicable that similar results could not be regularly obtained here. Many alternative methods were discussed by Duguid (1951), but the India ink wet stain was thought to be the most accurate and reproducible.

A possible explanation for the inefficient capsule visualisation may be related to the nature of the ink. Indian Ink is a colloidal material in which the capsule or slime produced by the bacterial cells is supposed to exhibit exclusion of the particulates. Should the ink colloids be of a size that is too small, it may be possible for the capsule to be penetrated. The 'halo',

indicative of capsule presence may therefore not be observed, except in highly viscid capsule structures able to exclude even the smallest particulates.

It is considered that this method, though used successfully in some cases here, requires a great deal of perseverance in order to obtain reproducible preparations. The visualisation of EPS material is known to have many difficulties due to the high water content.

4.6.4.2 Transmission Electron Microscopy

Due to the difficulties encountered with light microscopy of capsule structures, attempts were made to circumvent this by the use of electron microscopic visualisation methods.

The majority of species of *Klebsiella* are known to produce large extents of EPS material, often as discrete capsule layers. The ruthenium red method of staining has previously been used as a method of demonstrating EPS production with the electron microscope (Handley, 1991). However, the electron microscopy of such capsule and EPS material is also known to have major difficulties in stabilisation of this material due to the water content. The major problem associated with electron microscopy of EPS is the dehydration of the material in the high vacuum due to the proportion of water. Ruthenium red has been suggested to stabilise the polysaccharide by its polycationic nature interacting with the negatively charged fibres and thus prevent collapse. This ruthenium red staining as used by Oyston & Handley (1990) for *Bacteroides fragilis* was shown to highlight a 'ruthenium red staining layer' (RRL). This was thought to correspond to the capsule layer.

A similar method of visualisation, using antiserum to stabilise the capsule layer has also been described to produce good visualisation and is commonly referred to as the 'quellung reaction'. Essentially, the capsule material is swelled by the reaction allowing visualisation (Handley, 1991). This method, however, can only accentuate the presence of capsule for examination of EPS presence or absence rather than providing any information about natural EPS size.

The electron microscopy sections obtained here were of *Klebsiella oxytoca*. According to Ørskov (1984) "*Klebsiella oxytoca* strains are encapsulated." However, the micrographs produced showed only a minor covering of fibrous material. This material, stained as an RRL, may be considered to be capsule material though the size was initially expected to be significantly greater than actually found. Sometimes, however, the capsule layer has been known to collapse even when using this stabilising method of ruthenium red, during the fixation, staining and dehydration stages and at present there is no method of determining the amount of shrinkage (Springer & Roth, 1973). The formation of the observed bundles of material (similar to that found by Bayer & Thurow (1977)) are therefore considered to

represent dehydrated EPS polysaccharides, the size of which is comparable to the RRL layers observed with ruthenium red stained sections of capsulated *Leuconostoc mesenteroides* shown by Handley (1991).

However, previous work has also shown non-capsulated strains to cause a similar RRL layer (Oyston & Handley, 1990). It has been proposed that ruthenium red may also stain other polysaccharides such as LPS due to anionic character. These are distinguished from discrete capsule layers on the basis of the size of the RRL. The lipopolysaccharide material can extend up to 20-30 nm from the cell surface as mentioned in section 2.4.3, so any RRL attributable to this polysaccharide is unlikely to exceed this distance from the surface. Since the thickness of the layer here was found to be in excess of 50 nm, it is more likely that true capsular material has been visualised.

4.6.5 *Klebsiella* Mutagenesis

This type of experiment has been undertaken many times by previous workers to produce mutated strains (Poxton & Sutherland, 1976; Allison & Sutherland, 1987). Often such experiments have been designed to produce mutants lacking EPS material. The mutagenesis of *Klebsiella* strains undertaken here was a similar experiment, and produced very important results. Mutagenesis was originally performed to attempt to create identical cell types but which differed in their ability to produce EPS. Enzymatic removal of EPS material was considered to be inappropriate due to the heteropolysaccharide nature of the material which made it difficult to select suitable enzymes for the degradation that would not have an additional effect on the cell surface. The standard application of blending and centrifugation to remove EPS was also considered an unacceptable method due to probable reduction in viability (Sutherland, 1994) which would ultimately affect the dielectrophoretic response.

Mutated cells were isolated by their great differences in colony morphology compared to the parent cells, producing rough, non-glossy colony growth. Microscopic examination also showed some differences in cell morphology. The mutagenesis was not thought to produce a specific mutation in the cells, and many effects on cell composition and structure could result as was seen in the colony and microscopic morphology. Therefore, the effect of these non-specific mutations on dielectrophoretic spectra could have been found to produce many different changes in frequency and collection from one mutant strain to the next. However, the resulting spectra from mutants of the same parent i.e. mutant 9 and mutant 14, were actually found to have close similarities in form. Therefore it is possible that the mutations had some similar effects on cell structure, whether as a directed mutation or as a consequential effect produced from different mutation sites.

Dielectrophoretic experiments performed to compare the frequency responses of the mutants with that of their parents found very large differences. One of the most notable differences between them was the great increase in amount of dielectrophoretic collection over the whole frequency range examined. As with the experiments found with changing glucose concentration and nitrogen source, an increase in collection over the frequency range may be attributable to loss of EPS production. It is uncertain whether the mutation of the slime producing strains caused a loss of EPS function by prevention of synthesis mechanisms or export mechanisms.

As discussed previously, the loss of EPS material in the mutants may uncover the more anionic surfaces of the cells, caused by molecules such as LPS. Thus, the phosphate groups present on the cell surface will be able to interact with the electric field and potentially cause increase in the level of dielectrophoretic collection. This effective increase in negative charge may produce an increase in counterion layer and Debye length, allowing more efficient diffuse atmosphere polarisation at the low frequencies. This would explain the observed increase in collection, with maximum rise in collection occurring at the low frequency range. The differences in collection efficiency between mutants 9 and 14 of the same strain may reflect the degree of loss of EPS production, greater loss of function increasing the level of collection. This also validates the results found that even isogenic strains, such as *Klebsiella aerogenes* 9527 and 9528 and mutants from the same parent can all elicit very different frequency spectra. Thus, any dielectrophoretic spectrum is dependent, not only on growth medium, temperature and DEP experimental parameters but also on the serotype or structure of the organism under test.

Other mutations may involve the actual loss in LPS O-side chain as in 'rough' mutants as shown in figure 2.3. While loss of the side chains and core region may cause a reduction in collection, again due to loss of surface charge, the O-side chains may have other effects on polarisation mechanisms. Their length, penetrating into the medium may interact with counterions, as they move as a consequence of double layer polarisation. Therefore the loss of the O-side chain may facilitate easier movement of charge over the surface, increasing the ability for polarisation and DEP collection. It is known that the extent of O-side chain mutation can vary, producing different 'rough' mutants which would allow different extents of polarisation. It might be expected that greater collection may occur with mutations which cause loss of greater proportions of the O-side chain in this way. However, some slight shift in spectrum may be expected if this were the case, since the more intact LPS would interact more greatly with the counterions, hindering them as they undergo switches in movement as the field reverses. This change in spectrum would only be likely to occur at lower frequencies below 100 kHz since it is these which are related to surface conductivity effects.

The counter-argument is that as more of the LPS is removed by the mutation, less phosphate groups and other anions exist to contribute to the surface charge. Therefore increased mutation of this molecule could cause reduction in the screening length and so less efficient polarisation and collection. The effect of cell concentration was eliminated by examining samples where the total cell count was identical.

The continued collection of the mutants (especially the A1Sl mutants) up to 10 MHz, compared with the parent strains may reflect increased mechanisms related to interfacial polarisation or membrane capacitance, which are thought to be found at these higher frequencies (Pohl, 1978). The plateau levels of the spectra are similarly difficult to explain. They are known not to be due to saturation of electrode or detection levels, since pulse length graphs found no levelling of collection using a 5 s pulse length.

At this stage the effect of the mutation on the cells is inconclusive and may either be solely related to loss of EPS function, to additional LPS modifications, or even other cell composition effects. Serological examinations could be carried out upon the mutants to examine their antigenic characteristic and elucidate whether the K antigens (related to capsule presence) or O antigens (related to LPS presence) are present or absent. Following this further experiment, it may be possible to comment more definitely upon the cause of DEP collection changes following this mutation.

4.6.6 Estimation of Exopolysaccharide

Generally the weight of EPS produced by the slime producing strains was much greater than the mutants produced by the treatments in section 3.5.4. This verified that the mutants had in fact lost the ability to produce EPS material as noted from visual observation of colony morphology. This also showed that the strain A1Sl had produced a 25 % greater level of EPS material that the 87Sl slime producing strain. Therefore loss of this function was likely to produce more significant changes in dielectrophoretic spectrum in the A1Sl strain as observed in figure 4.32. In addition, the greater level of collection, produced by mutant 9 also correlated with minimum EPS production. This has the implication that decreasing EPS production led to increasing dielectrophoretic collection as described above. The similar results found for 87Sl and its mutant could also be explained in this way.

The capsule producer, *Klebsiella aerogenes* 9527 was also known to produce EPS, though not observed using India ink of other visualisation methods. The weights of EPS obtained demonstrate that during cell growth in rich growth medium such as nutrient broth, the production of EPS is less favoured. This agrees with general findings related to EPS formation in that it has greatest levels of synthesis when there is adequate carbon source but when other

nutrients are more limiting. In fact the growth in KM of the 9527 strain produced almost as much EPS material as that found with the slime producer 87Sl.

The greater level of EPS formed by the acapsulate strain (9528) compared to the capsule producer (9527) in nutrient broth is more difficult to understand but may be caused by the experimental error associated with the precipitation, drying and weighing of the low quantities of EPS material in this rich medium. There was a very great difference in EPS production in KM compared with the nutrient broth medium. An increase of around 390 % was found when the capsulated cells were grown in the more minimal medium, again correlating with increased production of EPS in high carbon containing media limited by other nutrients.

4.7 Measurement of Hydrophobicity

4.7.1 Growth Temperature Effects on Hydrophobicity

The relative change in absorbance over time for a pH range can be seen in figure 4.34 for *B. subtilis* grown at 30 °C.

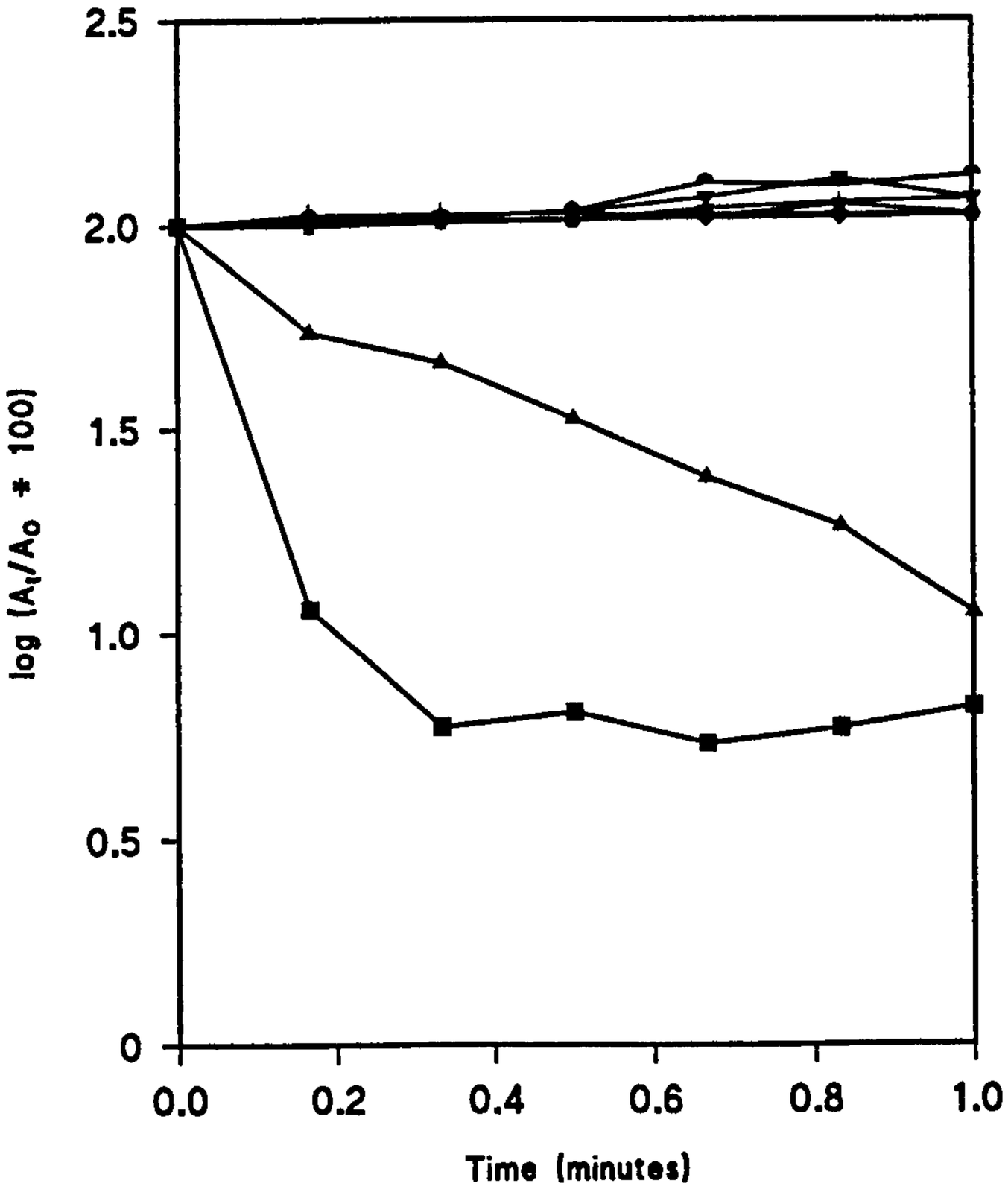

Figure 4.34 : Change in aqueous phase absorbance (at 600 nm) of *B. subtilis* grown at 30 °C with increasing total mixing time with n-hexadecane. (■) pH 2, (▲) pH 3, (▼) pH 4, (◆) pH 5, (★) pH 6, (●), pH 7, (⁀) pH 8, (|) pH 9.

A significant decrease in aqueous phase optical density was noted after 0.3 min for the suspension at pH 2. The suspensions less acidic than pH 3 had negligible adherance to the hexadecane even after 1 min vortexing time. This data was replotted as the initial rate of adhesion and is shown in figure 4.35(a). This clearly shows that the maximum rate, and so the Point of Maximum Hydrophobicity (PMH)(Van der Mei *et al.*, 1993) occurred at pH 2 and reached a value of nearly 6 min^{-1}.

The rates of adhesion are also shown in figure 4.35 for growth of *B. subtilis* at 37 °C, and for *E. coli* at 30 °C and 37 °C.

For *B. subtilis* grown at 37 °C, the PMH, while still at pH 2, became reduced to around 4.2 min^{-1}. The rate of adhesion for *E. coli* was very small at both temperatures but was greatest at pH 2 (0.14 min^{-1}) for the growth temperature at 37 °C.

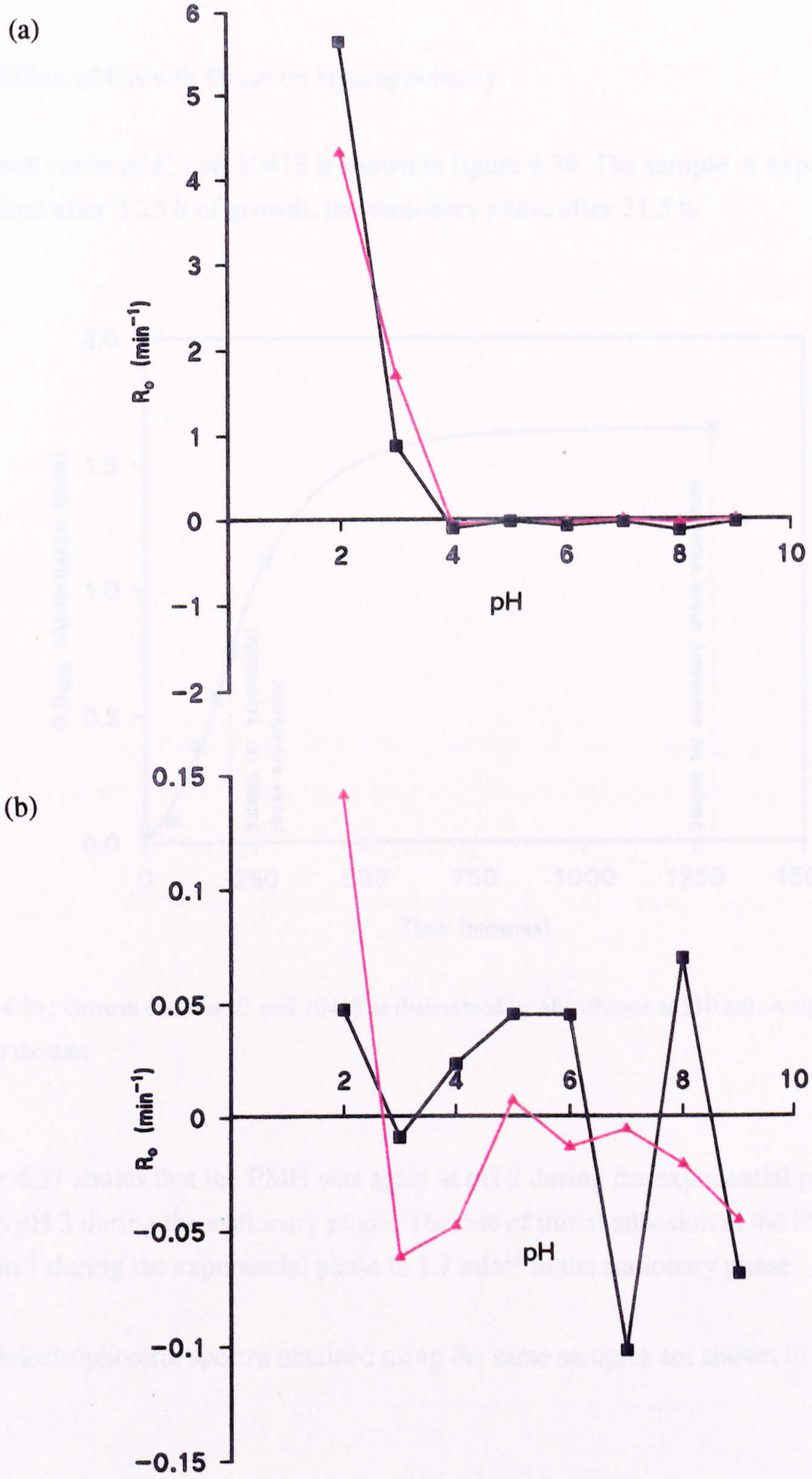

Figure 4.35 : Rate of adhesion of *B. subtilis* and *E. coli* grown at two temperatures to n-hexadecane over a range of pH values. (a) (■) *B. subtilis* after growth at 30 °C, (▲) *B. subtilis* after growth at 37 °C; (b) (■) *E. coli* after growth at 30 °C, (▲) *E. coli* after growth at 37 °C.

4.7.2 Effect of Growth Phase on Hydrophobicity

A growth curve of *E. coli* 10418 is shown in figure 4.36. The sample of exponential growth was taken after 3.25 h of growth, the stationary phase after 21.5 h.

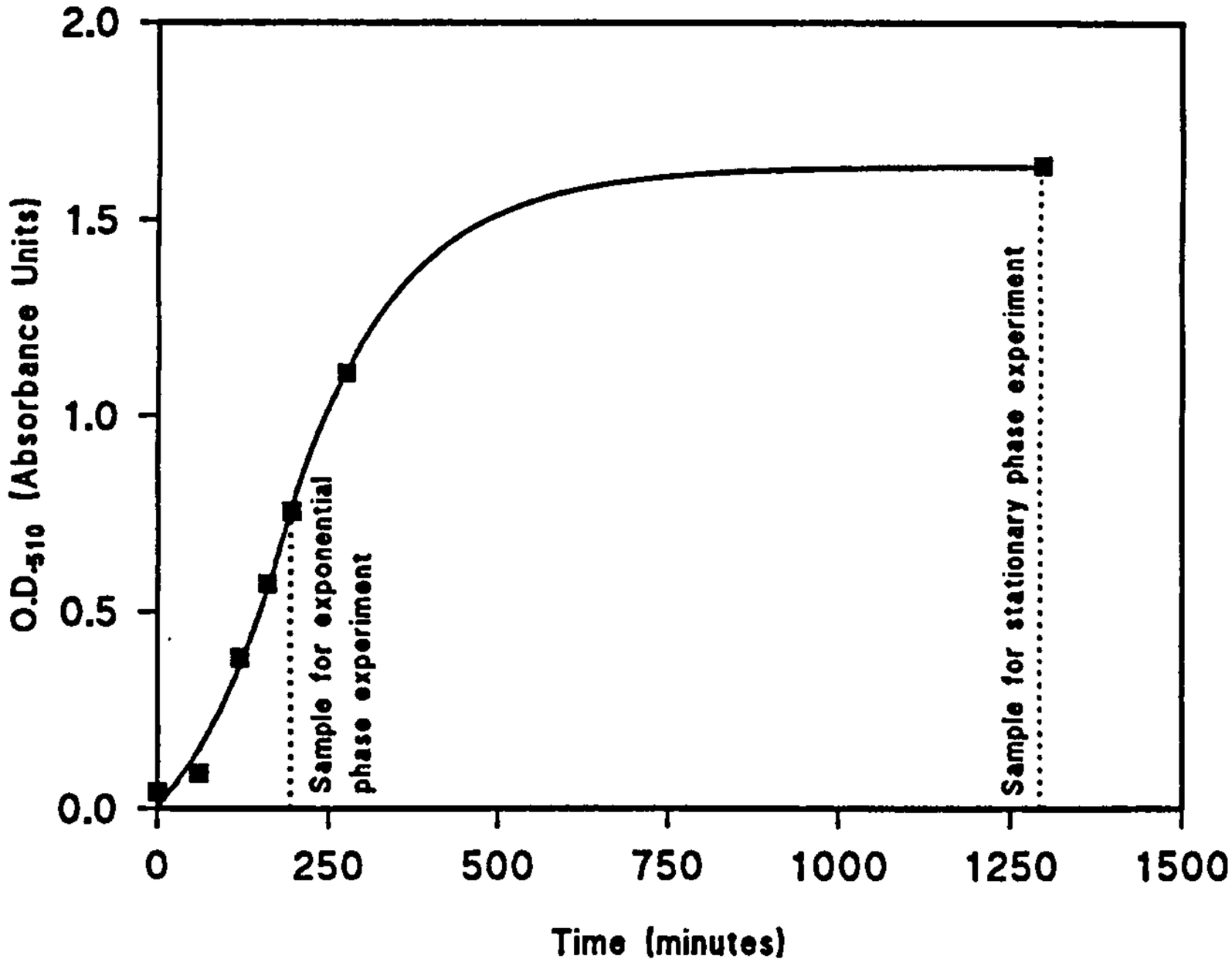

Figure 4.36 : Growth curve of *E. coli* 10418 as determined by absorbance at 510 nm. A sigmoidal curve was fitted to the data.

Figure 4.37 shows that the PMH was again at pH 2 during the exponential phase of growth yet rose to pH 3 during the stationary phase. The rate of initial adhesion at the PMH dropped from 2.4 min^{-1} during the exponential phase to 1.7 min^{-1} in the stationary phase.

The dielectrophoretic spectra obtained using the same samples are shown in figure 4.38.

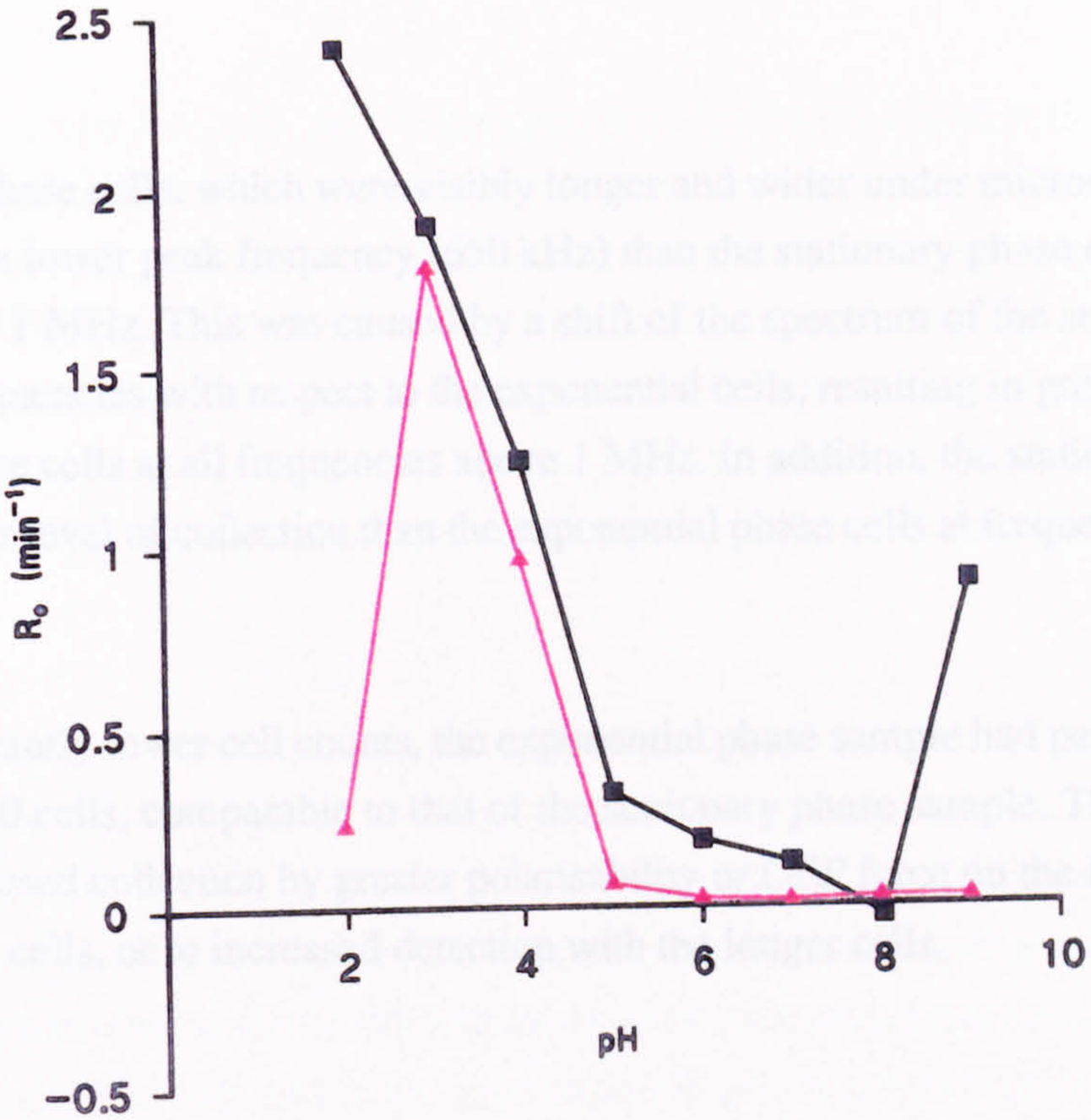

Figure 4.37 : Rate of adhesion of *E. coli* 10418 to n-hexadecane over a range of pH values with samples taken from different stages of growth. (■) Exponential phase cells, (▲) Stationary phase cells.

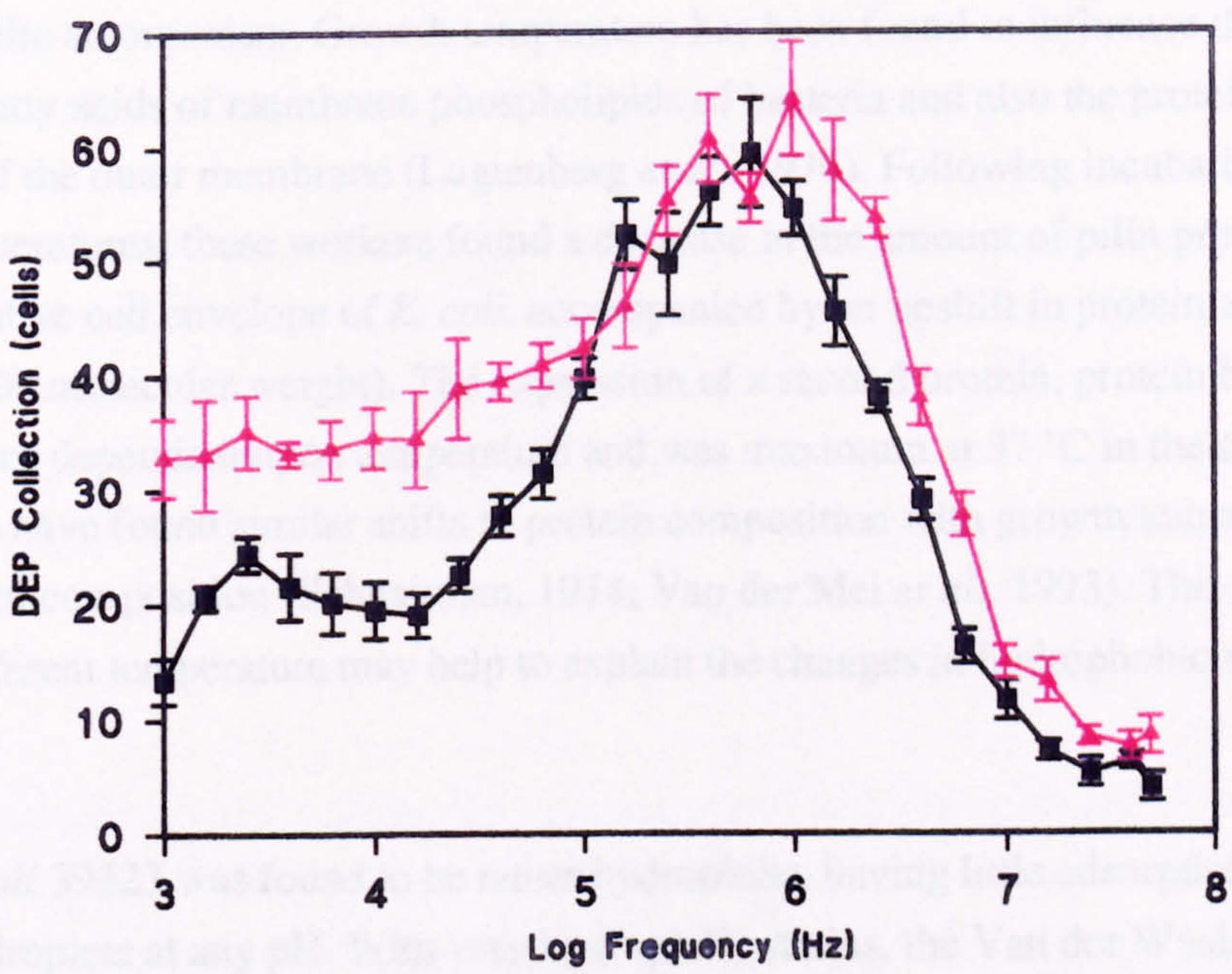

Figure 4.38 : Dielectrophoretic (DEP) spectra of exponential and stationary phase cells of *E. coli* 10418. (■) Exponential phase, (▲) Stationary phase. Conditions : 12 V, 5 s pulse, 24.5 μS.cm^{-1}. 10.3 x 10^7 cells.ml^{-1} (exponential phase), 15.71 x 10^7 cells.ml^{-1} (stationary phase). Full count detection method. Each point is the mean plus standard error of 5 replicate spectra.

The exponential phase cells, which were visibly longer and wider under microscopic examination, had a lower peak frequency (650 kHz) than the stationary phase cells which had a peak frequency of 1 MHz. This was caused by a shift of the spectrum of the stationary phase cells to higher frequencies with respect to the exponential cells, resulting in greater collection of the stationary phase cells at all frequencies above 1 MHz. In addition, the stationary phase cells had a much greater level of collection than the exponential phase cells at frequencies below 100 kHz.

Even with significantly lower cell counts, the exponential phase sample had peak collection levels of around 60 cells, comparable to that of the stationary phase sample. This was probably due to either increased collection by greater polarisability or DEP force on the larger exponential phase cells, or to increased detection with the longer cells.

4.8 Discussion of Hydrophobicity Results

4.8.1 Growth Temperature Effects

Cells generally possess a surface negative charge and typically the greater this negativity, the more hydrophilic an organism. Growth temperature has been found to influence the degree of saturation of fatty acids of membrane phospholipids of bacteria and also the protein composition of the outer membrane (Lugtenberg *et al.*, 1976). Following incubation at increased temperatures, these workers found a decrease in the amount of pilin protein found in the Gram negative cell envelope of *E. coli*, accompanied by an upshift in protein a (a major Omp of 40 KDa molecular weight). The expression of a second protein, protein b, was also found to be very dependent upon temperature and was maximum at 37 °C in the strain studied. Other workers have found similar shifts in protein composition with growth temperature as well as medium composition (Schnaitman, 1974; Van der Mei *et al.*, 1993). This expression of proteins at different temperature may help to explain the changes in hydrophobicity and rate of adsorption.

Escherichia coli 39323 was found to be rather hydrophilic, having little adsorption to the hydrocarbon droplets at any pH. With very hydrophilic strains, the Van der Waals attraction between cells and water is stronger than the electrostatic interaction between cells and hexadecane holding cells in the aqueous phase regardless of pH (Van der Mei *et al.*, 1993). At both temperatures the R_0 was small but increased at pH 2 (0.14 min^{-1}) after growth at 37 °C. This could implicate a change in protein composition. Increased hydrophobicity and isoelectric points have been associated with increasing N:C and decreasing O:C ratios (Van der Mei *et al.*,

1993). This can be correlated with the surface carbon and nitrogen found in the forms of protein, phospholipid, lipoprotein or lipopolysaccharide. Greater N:C ratios may have therefore been associated with the increase in growth temperature. The increased adhesion may therefore be caused by increased expression of amino nitrogen at the higher temperature of 37 °C. This may be likely since this temperature is known to be the optimum for growth of the strain tested and could be expected to have optimum protein production under these conditions. A possible change in protein type expressed could also be responsible for the increased adhesion.

With the *Bacillus* species examined, similar results were found but were more extreme, the optimum growth temperature again increasing adhesion to hydrocarbon. This organism was very hydrophobic at pH 2. There was no apparent shift in the pH of maximum hydrophobicity, possibly indicating there was no change in the type of negatively charged surface molecules. Such changes in molecules would be expected to become protonated and so reach their isoelectric point at different pH values due to variation in pK. The rapid increase in adhesion at pH values below pH 3 could correspond with the protonation of carboxyl groups which have a pK of 2.9. Therefore it may be possible that the increase in hydrophobicity at 30 °C for this species could be due to the increase in the number of such surface groups, since there will be more charged molecules necessary to be protonated to neutralise the surface negative charge. Similar shifts in protein composition may occur with this Gram positive species, though would occur at the cytoplasmic membrane. However, since these groups are unexposed due to the overlaying cell wall, their effect on hydrophobicity is not expected to be significant.

An associated factor may be involved with membrane fluidity. The optimum temperature for growth causes both outer and cytoplasmic membranes to have maximum fluidity due to the greater level of saturated fatty acids. Changes in phospholipid composition may therefore affect the amount of charge on the membrane, caused by the polar head groups. Increase in hydrophobicity may therefore be as a result of increase of charged groups at the optimum growth temperatures i.e. 30 °C in *Bacillus subtilis*. Again this may not cause a noticeable effect on hydrophobicity due to the position of the cytoplasmic membrane.

As a consequence of reduced fluidity, the turnover of cell wall polymers should also have become diminished as carrier lipids are immobilised. Since the majority of wall polymers in both Gram positive and negative cells utilise carrier lipids, synthesis becomes inhibited. This stops further polymers being inserted into the wall. As many of these polymers have a large negative charge, the surface charge of the bacterial cells could become reduced at non-optimum growth temperatures. Such a decrease in charge should therefore result in an increase in hydrophobicity at temperatures below the optimum. However, growth at 30 °C (optimum temperature) produced maximum hydrophobicity in *B. subtilis* compared to 37 °C. This

organism is known to have a large amount of phosphorus present in its cell wall compared to other elements, increasing the negative charge of the cells (Mozes *et al.*, 1988). Therefore at the temperature of 37 °C, the amount of phosphorus deposited in the wall may have become increased.

Further work to examine these effects is necessary, especially relating to the surface and wall elemental composition.

4.8.2 Growth Phase Effects

The PMH was again at low pH values reflecting cell surface composition. This *E. coli* 10418 strain appeared to have a greater level of hydrophobicity than that found in section 4.7.1 for *E. coli* 39323, possibly attributed to the variation in cell composition with different bacterial strains. Differences in charged outer membrane constituents such as a reduction in LPS production may cause such an increase in hydrophobic interaction. Losses in structure of this type could also offer potential explanations for the increased sensitivity of *E. coli* 10418 to access by antibiotics as found in the antibiotic assays (section 4.9).

The most notable differences in hydrophobicity between the exponential phase and stationary phase cells was the observed shift in PMH from pH 2 to pH 3 respectively, with a significant decline in hydrophobicity at pH 2. As discussed above, this may again be a result of surface changes found in different phases of growth. Schnaitman (1974) found a reduction in specific proteins expressed in the outer membrane of *E. coli* when the cells entered the stationary phase. This was accompanied by a switch in the dominant outer membrane protein types, protein 1 being rich in the exponential phase. This result is contrary to those found by Lugtenberg *et al.* (1976) who regarded the outer membrane composition as being largely independent of growth phase. The shift in PMH to higher pH values may be attributable to a reduction in the amount of negative charge groups present on the surface meaning that neutralisation of the negative surface charge may be completed by only a low concentration of protons i.e. higher pH. Alternatively, a switch in chemical composition as cells enter the stationary phase may allow easier protonation at higher pH values.

As found by Wadström (1990), exponential phase cells were found to be more hydrophobic than stationary phase cells. The contrasting results found by Gilbert *et al.* (1991b) with *E. coli* and *Staph. epidermidis* were obtained using the HIC technique, reflecting the lack of correlation between their method and the MATH test used here. Reduction of components, especially protein, during the stationary phase may reduce the N:C ratio in the membranes and so cause the observed decrease in hydrophobicity as described above.

The decline in the rate of adhesion as cells enter the stationary phase found here may also be related to the actual size changes during the growth phase. Larger exponential phase cells only need to possess small amounts of hydrophobic moieties to cause rapid reduction in absorbance measurements within the aqueous phase.

Charge on cell surfaces may not reflect true relative hydrophobicity due to electrostatic interactions. High ionic strength media used for measurement of hydrophobicity causes an increased screening of the surface charge on the cell, so reducing the effect of electrostatic interactions. When cells were resuspended in low ionic strength media for the purposes of dielectrophoretic experiments, the charge on the cells may become more involved.

Experiments undertaken previously by Pohl (1978) found differences in dielectrophoretic collection during different stages of the cell growth cycle for yeast cells. Results shown in section 4.7.2 also show that there are differences between growth stages in bacterial cultures. It has long been known that there are large differences in size between exponential phase and stationary phase cells (Schaechter *et al.*, 1958). These differences in growth phase were found to cause similar shifts in spectrum to lower frequencies with exponential phase cells (from 1 MHz peak frequency to 650 kHz) to those observed with nalidixic acid. This may be related to the increased cell size and will be discussed in detail in section 4.14.3.

The decreased hydrophobicity of the stationary phase cells may be reflected in the increased DEP collection at the lower frequencies below 100 kHz. Such a decrease in hydrophobicity may be associated with an increase in surface charged groups thus increasing the electrical double layers. Therefore at frequencies in which surface conductivity effects are active i.e. 1 kHz to around 100 kHz, the increased counterion layer may be more easily polarised at these frequencies, improving the polarisability of the cells and increasing DEP collection.

As the frequency of collection is increased further, other polarisation mechanisms begin to occur. The larger exponential cells will find it more difficult to remain attracted to the electrodes as the dielectrophoretic force begins to diminish, as the continuous flow forces are more effective on these cells with increased volume. Therefore the collection of the exponential phase cells will become decreased at lower frequencies than found with the stationary phase cells.

To avoid these differences associated with bacterial growth phase, cells were normally prepared for dielectrophoretic experiments after overnight incubation, typically for 16 h. The bacterial species examined here would be in the stationary phase of growth after this time. Similarly Fomchenkov *et al.* (1979) used cells in stationary phase for dielectrophoretic analysis to eliminate the effects associated with growth. Hancock (1991), however, regarded the use of

the exponential phase of growth to be more appropriate for elimination of bacterial phenotypic changes.

Similar experiments would have been useful to examine changes in hydrophobicity and surface charge following EPS treatments and mutagenesis, and also after the antibiotic treatments undertaken. Potential comparisons could have been made with the resulting dielectrophoretic frequency spectra.

4.9 Antibiotic Assays

The relative sensitivities of each bacterial strain to the three antibiotics used are shown in figures 4.39(a-c).

(a)

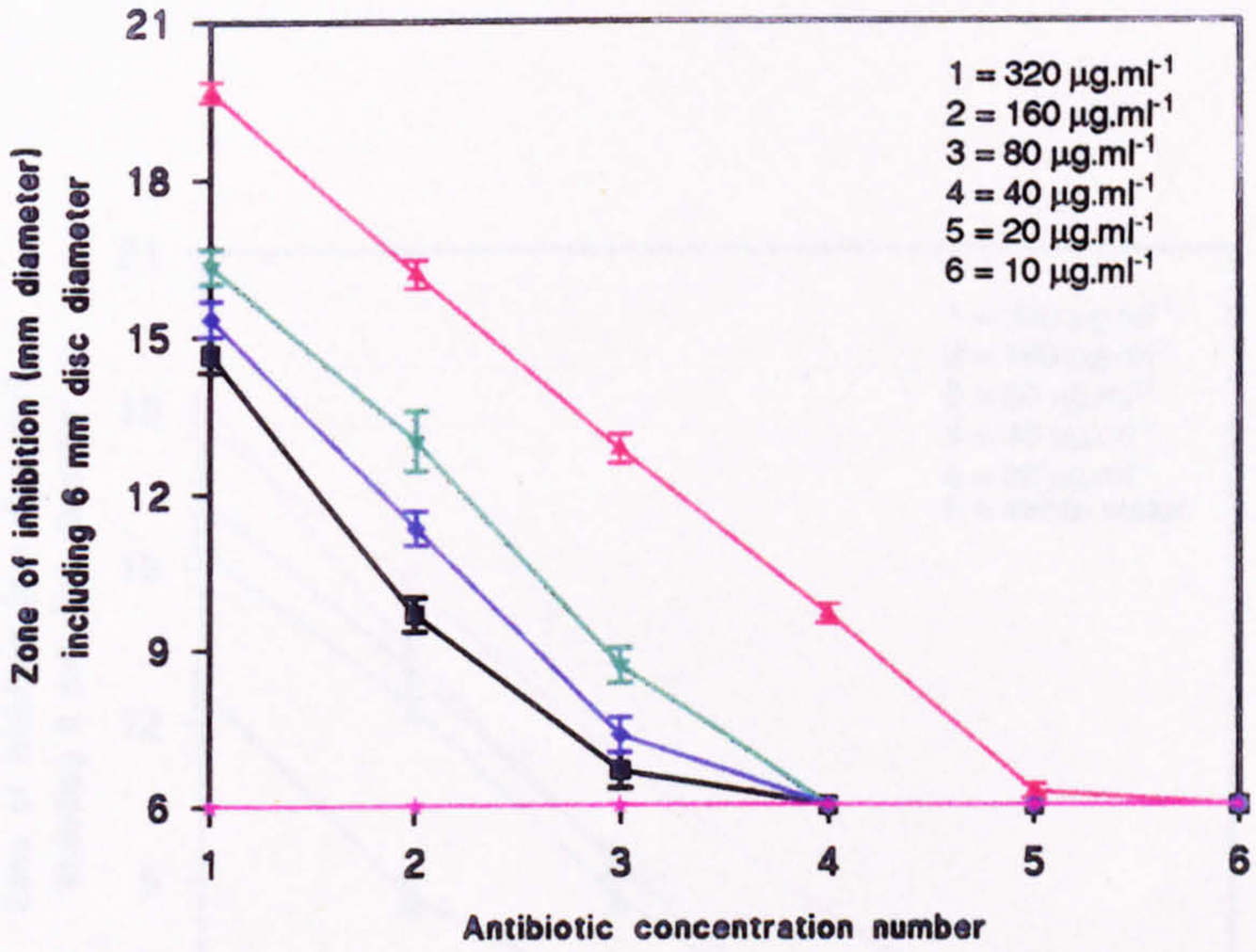

(b)

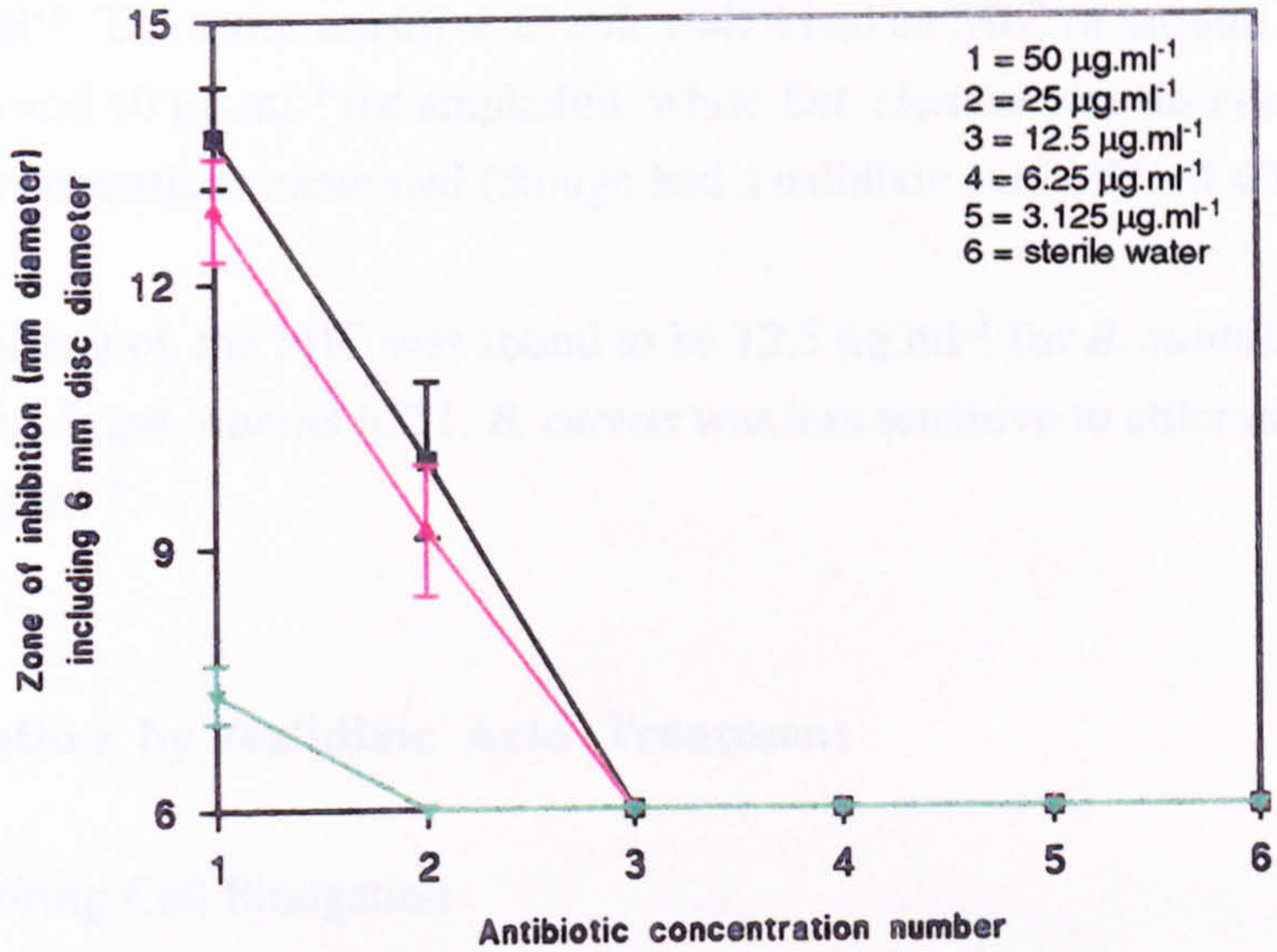

(c)

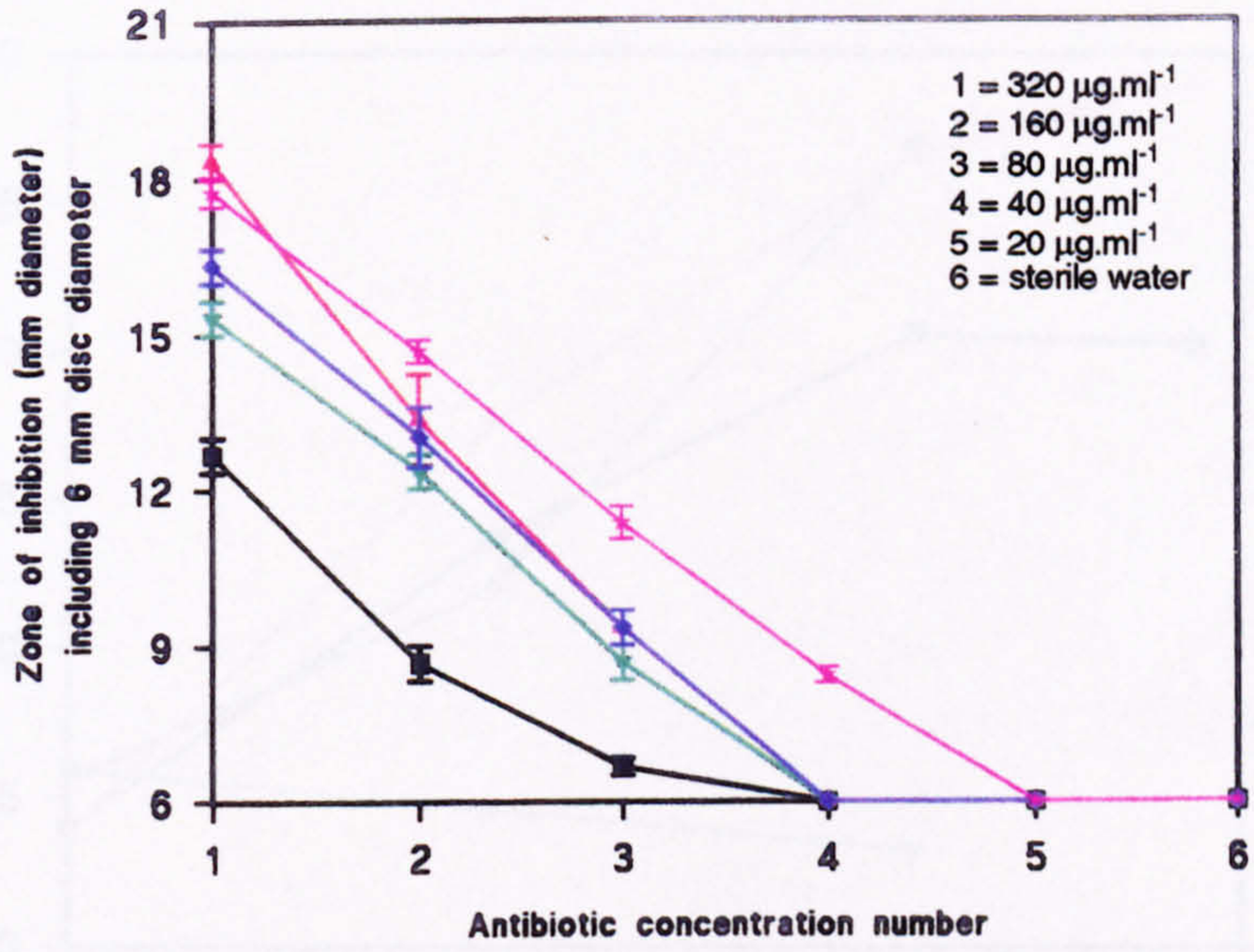

Figure 4.39 : Agar diffusion assays of antibiotic resistance of several Gram positive and negative bacterial species. (a) Ampicillin : (■) *E. coli* 8114, (▲) *E. coli* 10418, (▼) *E. coli* R35258, (◆) *E. coli* 39323, (★) *Ent. cloacae*. (b) Chloramphenicol : (■) *B. subtilis* 10106, (▲) *Staph. aureus* 6571, (▼) *B. cereus*. (c) Nalidixic Acid : (■) *E. coli* 8114, (★) *E. coli* 10418, (▼) *E. coli* R35258, (◆) *E. coli* 39323, (▲) *Ent. cloacae*. Points are means plus standard error of 3 replicates, except *E. coli* 10418 samples, which are means of 12 replicates.

For the antibiotics, ampicillin and nalidixic acid, MIC values for all but two strains were found to be 40 $\mu g.ml^{-1}$. The more sensitive *E. coli* 10418 had an MIC of around 20 $\mu g.ml^{-1}$ for nalidixic acid and 10 $\mu g.ml^{-1}$ for ampicillin, while *Ent. cloacae* was resistant to all of the ampicillin concentrations examined (though had a nalidixic acid MIC of 40 $\mu g.ml^{-1}$).

For chloramphenicol, the MIC was found to be 12.5 $\mu g.ml^{-1}$ for *B. subtilis* 10106 and for the sensitive strain *Staph. aureus* 6571. *B. cereus* was less sensitive to chloramphenicol, having an MIC of 25 $\mu g.ml^{-1}$.

4.10 Elongation by Nalidixic Acid Treatment

4.10.1 Monitoring Cell Elongation

Figure 4.40 demonstrates the effect of nalidixic acid presence in the medium on growth of *E. coli* cells.

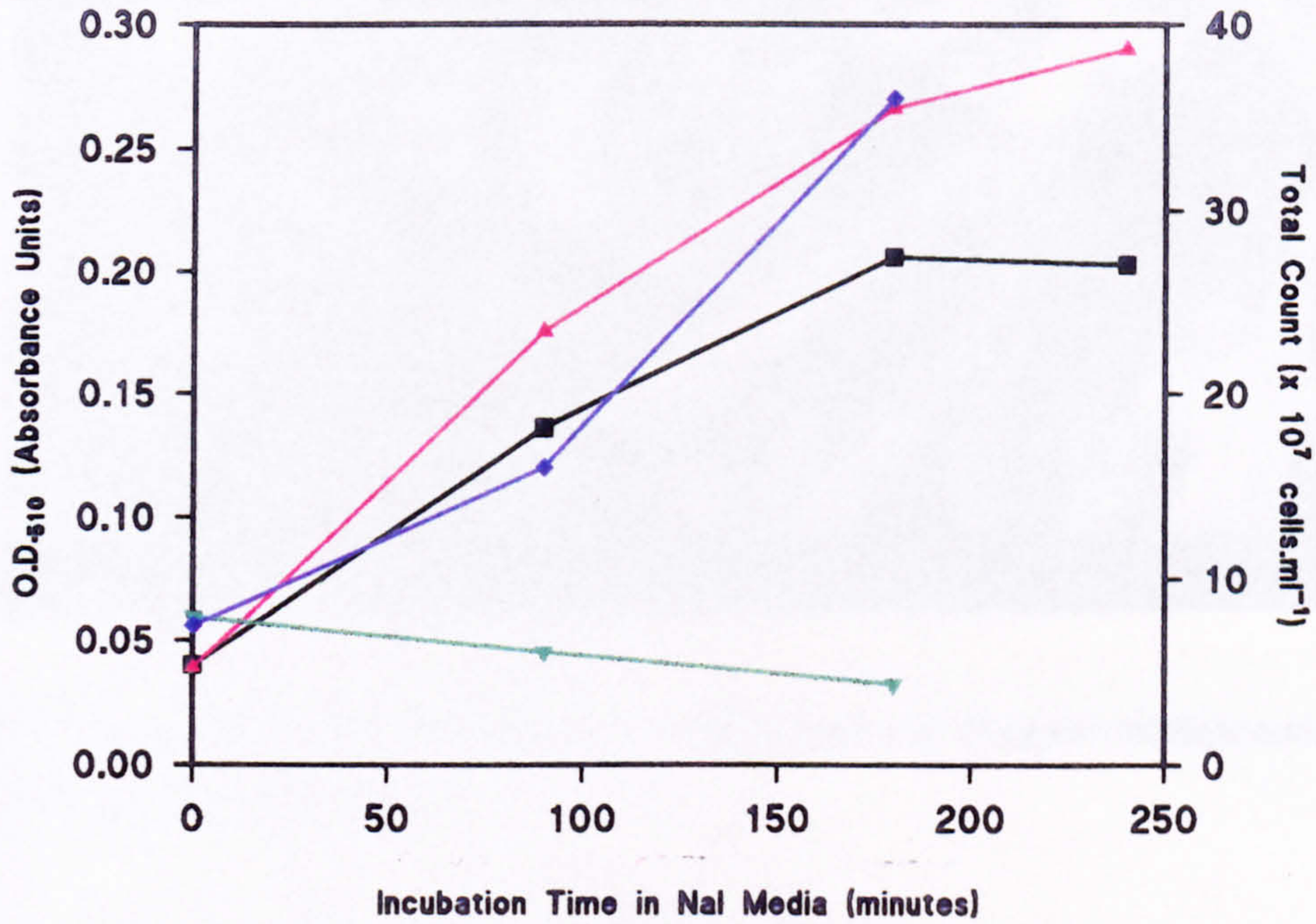

Figure 4.40 : Changes in absorbance and total counts during incubation in nalidixic acid. In presence of 10 $\mu g.ml^{-1}$ nalidixic acid : (■) $O.D._{510}$, (▼) Total count; In absence of nalidixic acid : (▲) $O.D._{510}$, (◆) Total count.

The absorbance of both treated (Nal+) and control (Nal-) suspensions increased over the period of incubation, though there was greater increase in the latter culture. Associated with this increase in O.D. was an increase in the total count of cells in the control. The rise in the O.D. of the culture containing nalidixic acid, however, was accompanied by a fall in total count throughout the incubation. This was caused by a significant elongation of the *E. coli* cells by the antibiotic action, resulting from a cessation of cell division. Therefore while the cell size still increased, there was no division and thus no increase in cell count.

This was verified by the electron micrograph (figure 4.41) which shows the elongated cells having a cell length well in excess of 5 μm, compared to control cells of up to 2 μm lengths (figure A5.1(d)).

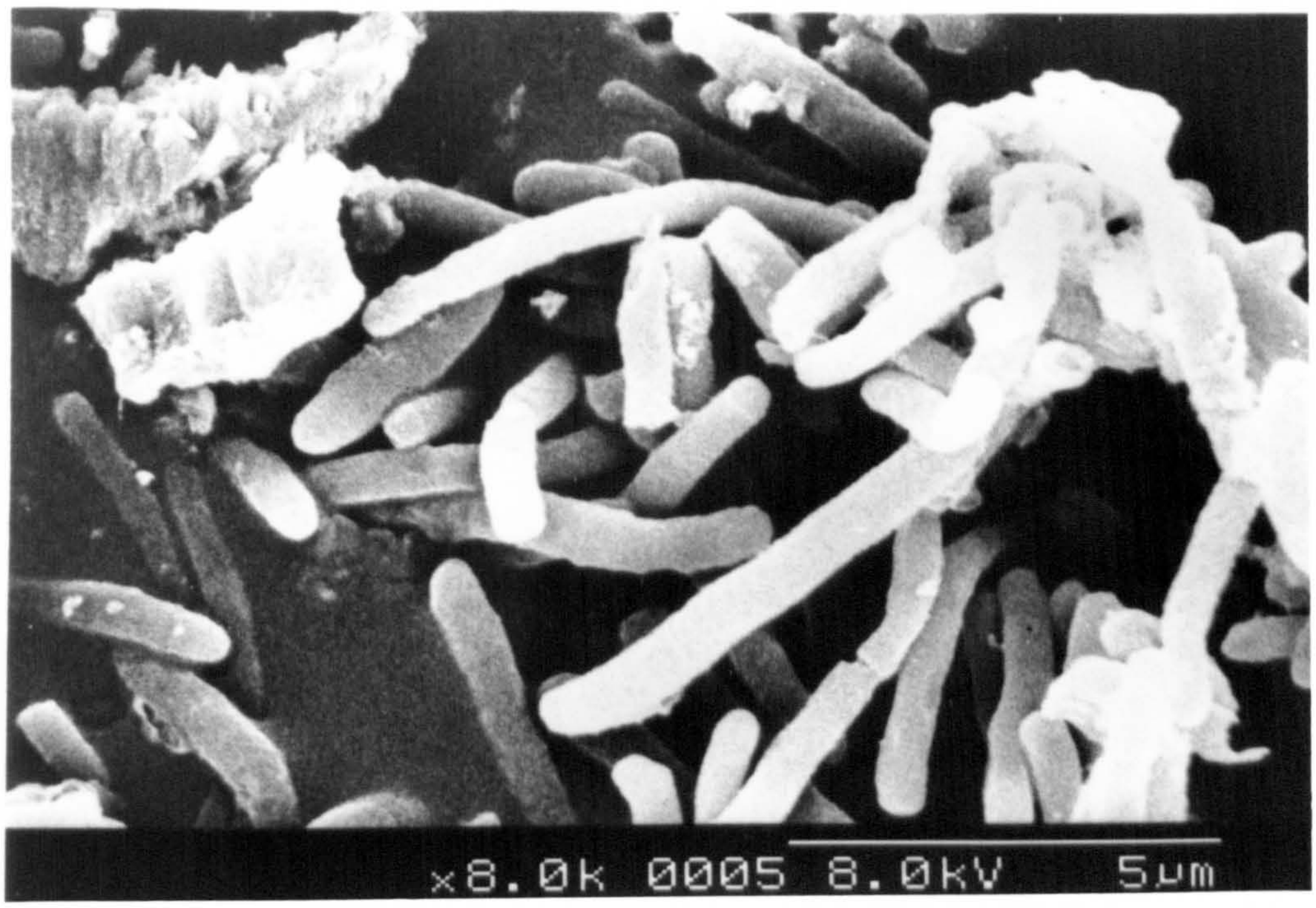

Figure 4.41 : Scanning electron micrograph of *E. coli* 10418 treated with 10 $\mu g.ml^{-1}$ nalidixic acid. Accelerating voltage 8 kV, x 8,000 magnification.

Light microscope observations of Gram stained cultures over the incubation time (figure 4.42) showed even greater length increases of up to 13 μm in the antibiotic treated cells. These results show that in cultures grown in PBS, there was no significant increase in cell length even in the presence of antibiotic. This was expected since there was no carbon and energy source in PBS, meaning that further cell growth would not occur.

(a)

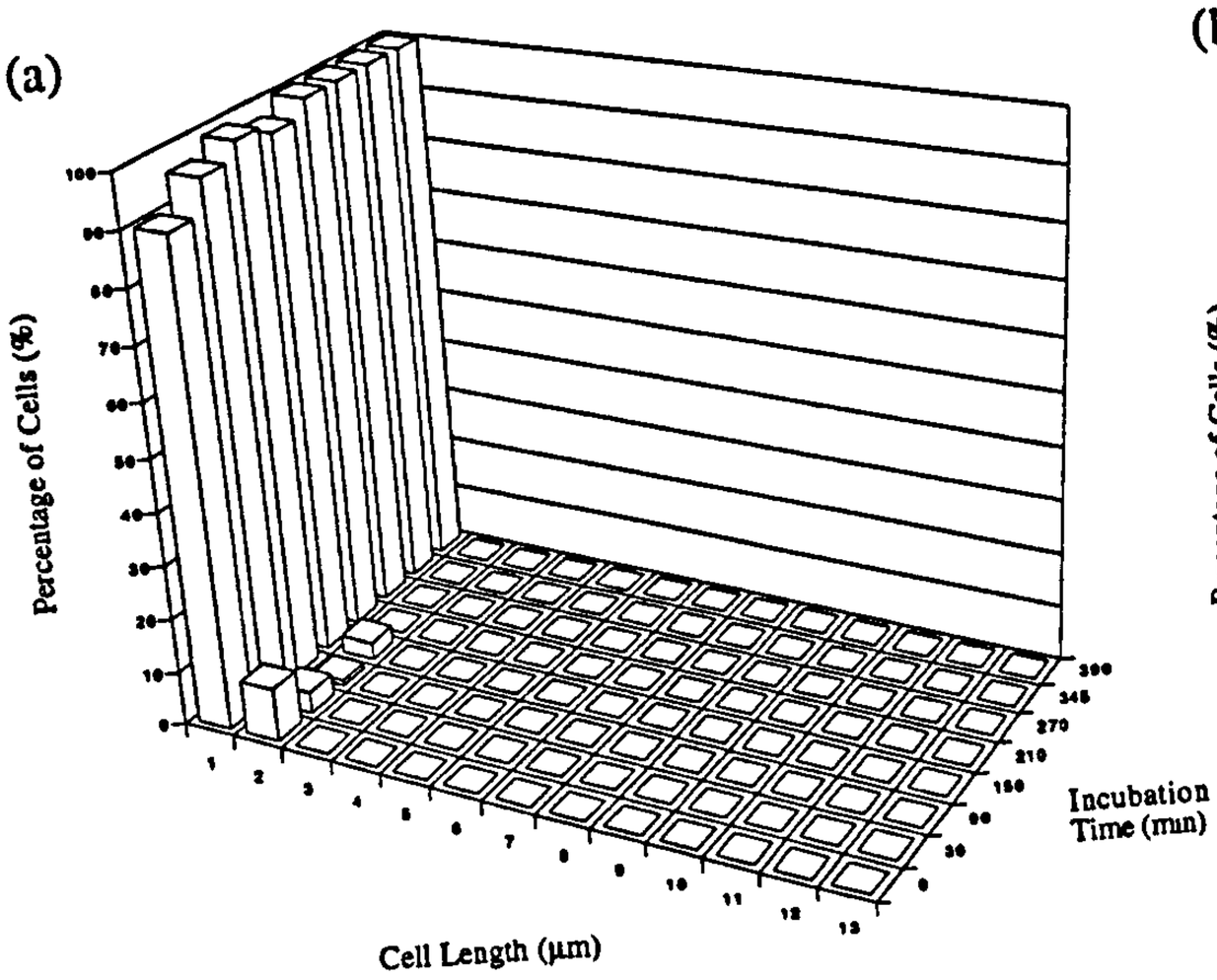
Percentage of Cells (%)
Cell Length (μm)
Incubation Time (min)

(b)

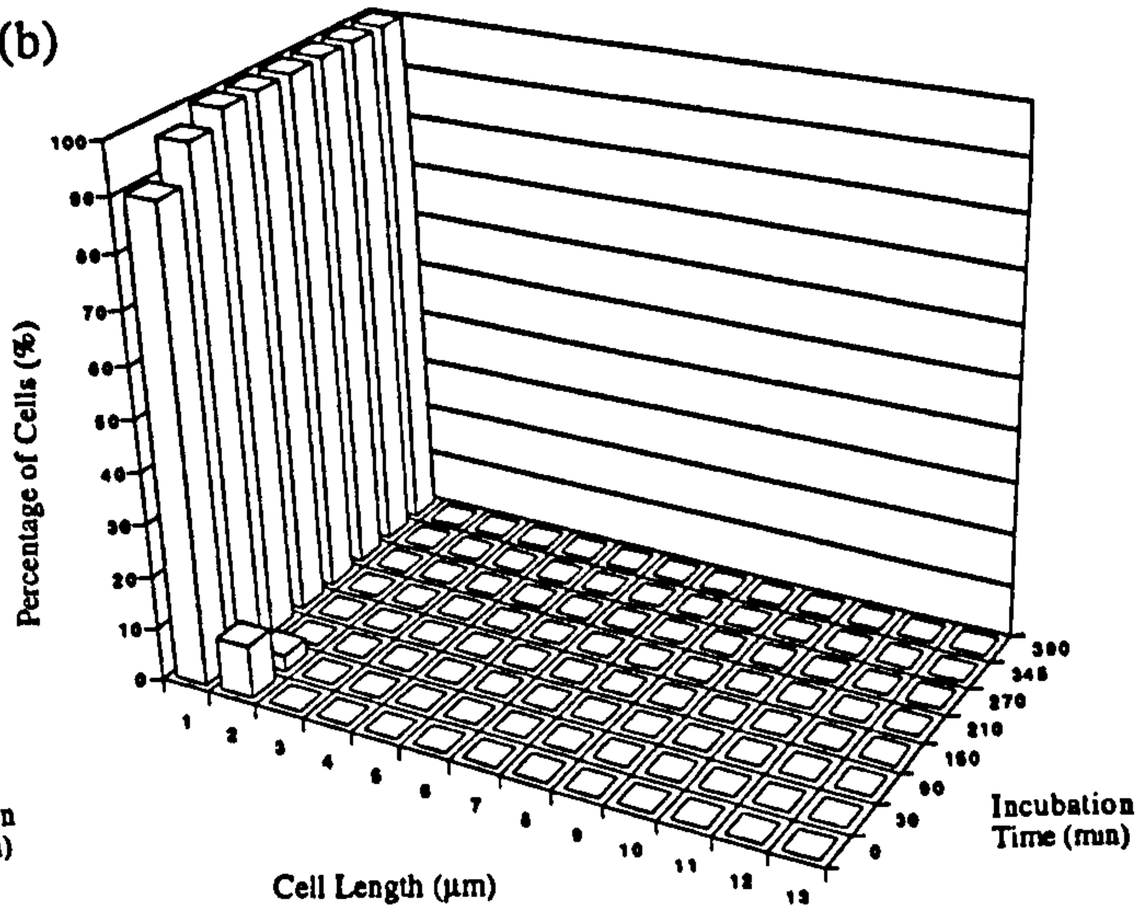
Percentage of Cells (%)
Cell Length (μm)
Incubation Time (min)

(c)

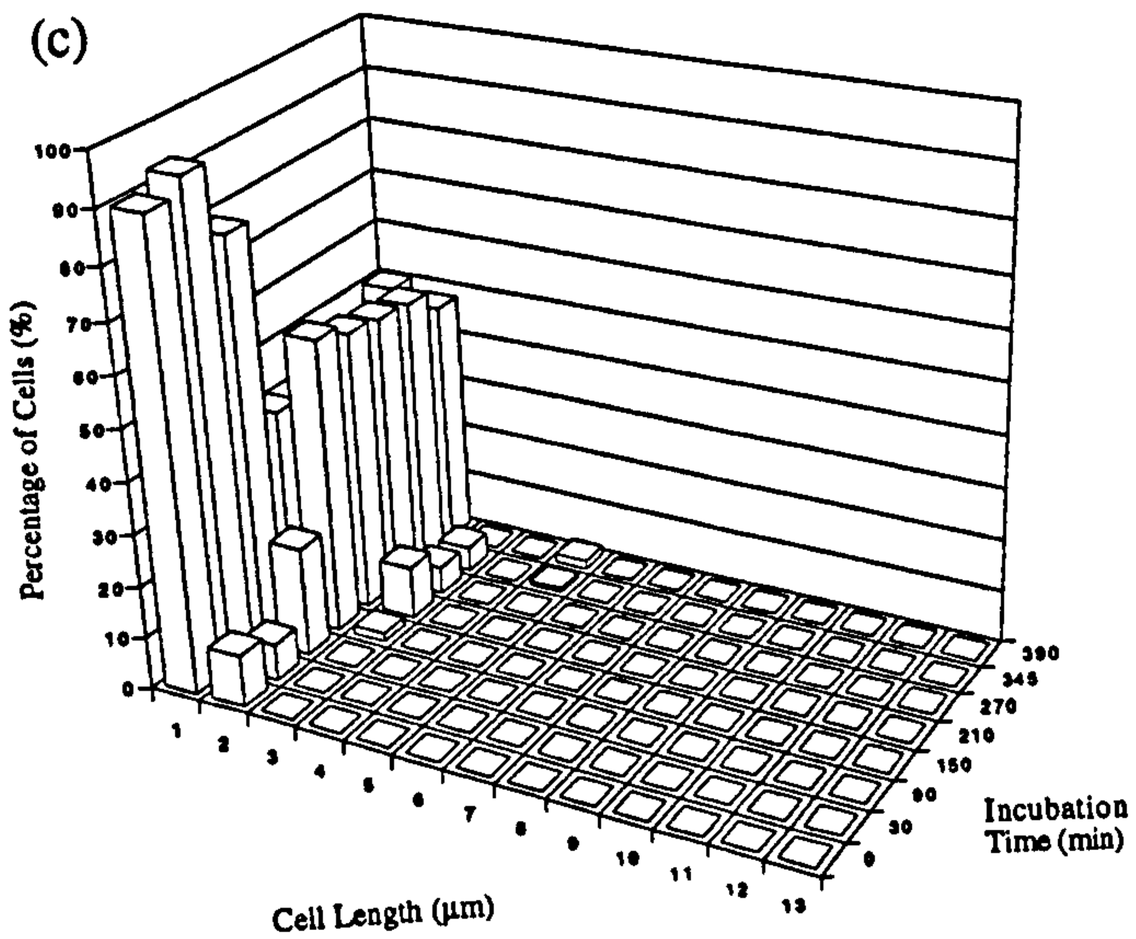
Percentage of Cells (%)
Cell Length (μm)
Incubation Time (min)

(d)

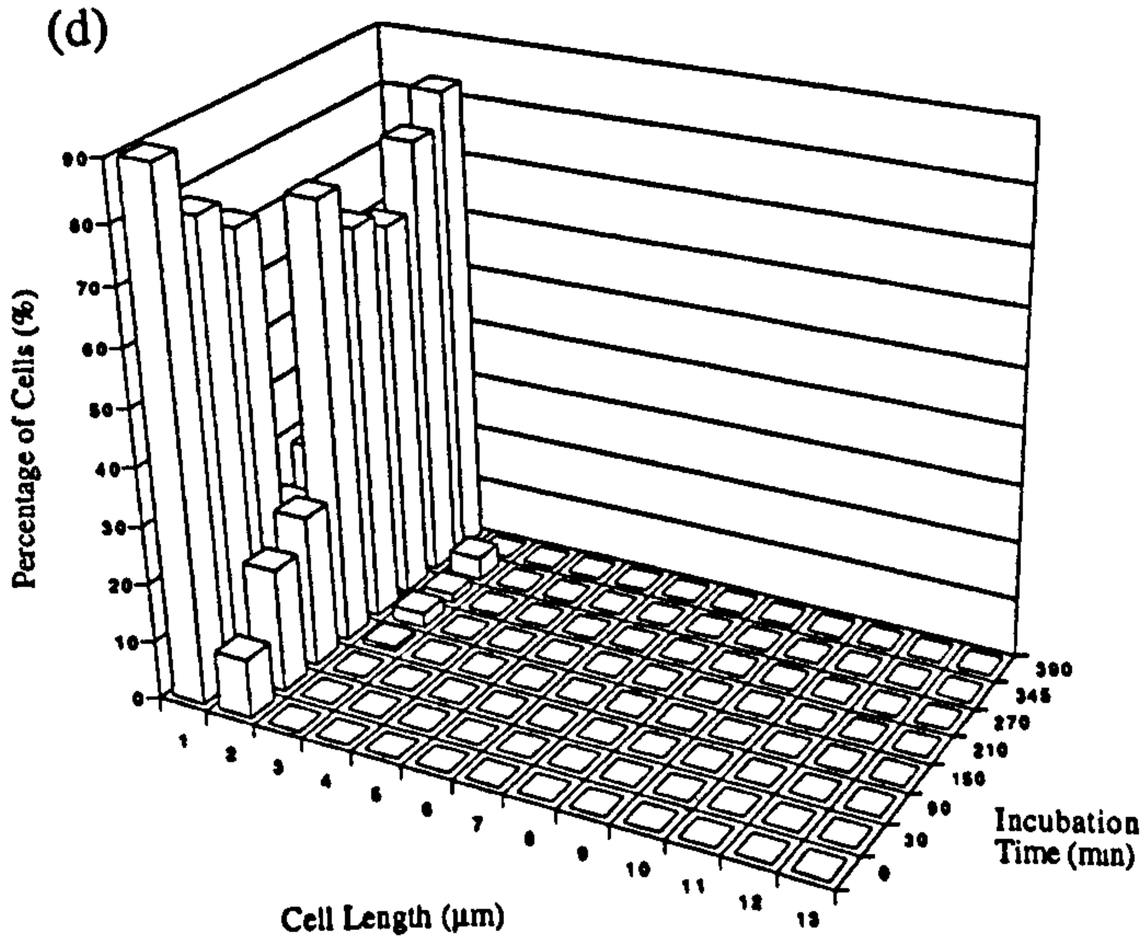
Percentage of Cells (%)
Cell Length (μm)
Incubation Time (min)

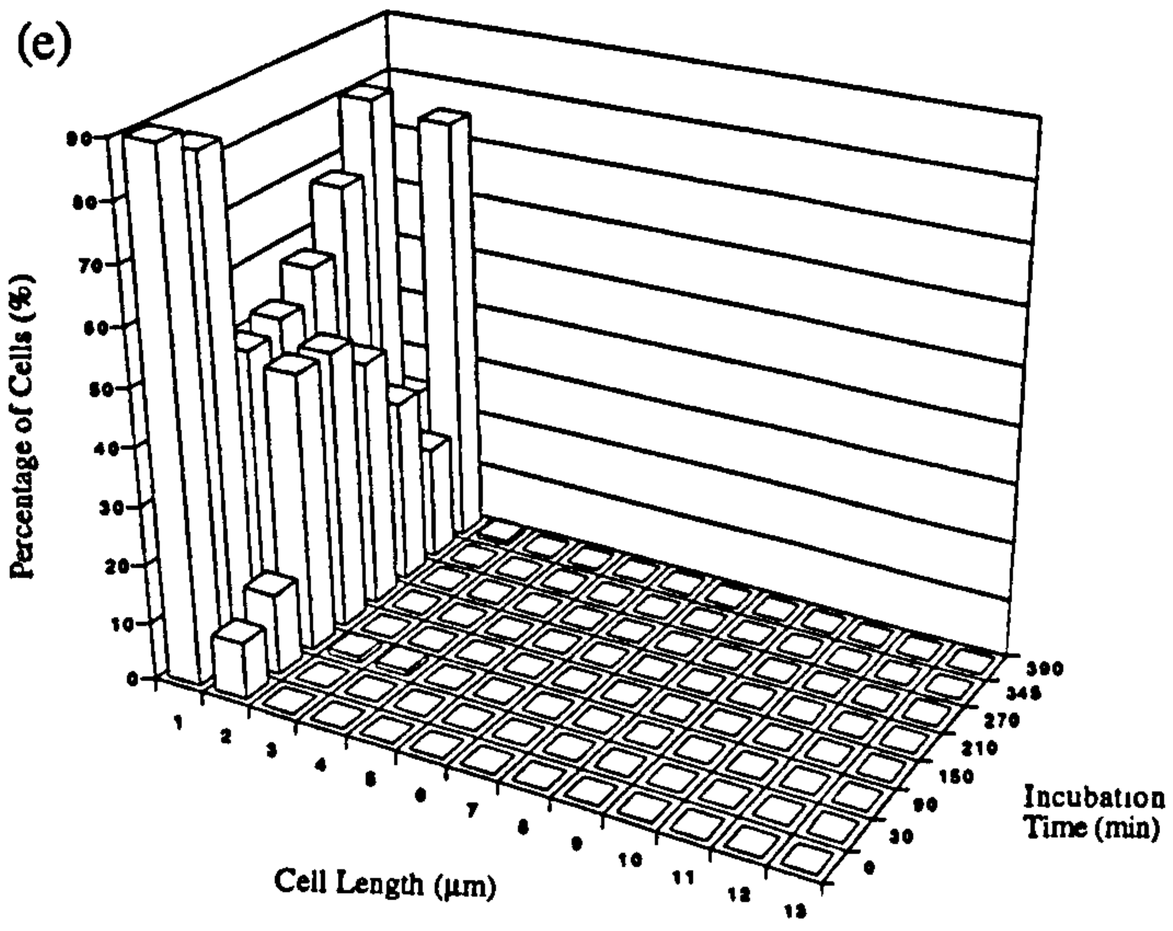

Figure 4.42 : Histograms showing measurement of cell length after increasing incubation time in different growth media with presence or absence of nalidixic acid antibiotic. (a) PBS + 10 $\mu g.ml^{-1}$ nalidixic acid, (b) PBS control, (c) PBS + casamino acids + 10 $\mu g.ml^{-1}$ nalidixic acid, (d) PBS + casamino acids control, (e) PBS + yeast extract + 10 $\mu g.ml^{-1}$ nalidixic acid, (f) PBS + yeast extract control, (g) PBS + yeast extract + casamino acids + 10 $\mu g.ml^{-1}$ nalidixic acid, (h) PBS + yeast extract + casamino acids control.

In cultures containing PBS+casamino acids or PBS+yeast extract, there was an increase in cell size of both treated and control cultures, though this appeared to be more notable when cells were grown with casamino acids as the nutrient source. However, the results show that greater length was attained in the presence of nalidixic acid, producing cells up to 5 μm in length.

Maximum cell elongation was found with cells grown in PBS+yeast extract+casamino acids in the presence of nalidixic acid. After around 200 min incubation, a significant proportion of the cells had elongated and many of them had lengths of 4-5 μm. After 390 min, the range of lengths was much greater, though fewer cells were found with each length. This incubation produced cells of lengths up to 13 μm. In the absence of the antibiotic, only a small increase up to 3 μm cell length was observed, and this may be typical of normal growth.

This elongation was observed with strains of *E. coli* 10418 and 8114, and for *Ent. cloacae* using a 10 $\mu g.ml^{-1}$ concentration of the antibiotic.

4.10.2 Dielectrophoretic Experiments

The results of initial experiments using the spectrophotometric method on nalidixic acid treated *E. coli* cells are shown in figure 4.43. This shows that treatment of the cells with 10 $\mu g.ml^{-1}$ nalidixic acid resulted in a shift of the resultant dielectrophoretic spectrum to lower frequencies. In a control sample not treated with the antibiotic the normal peak at around 2 MHz was found. The treated sample, undertaken under similar conditions produced a maximum peak at 800 kHz, significantly earlier. In addition, the onset of the positive dielectrophoretic peak was at lower frequencies (50 kHz) than in the control sample (100-200 kHz). The overall level of the dielectrophoretic spectra also appeared to be very similar, probably due to the detection system measuring the sample absorbance, which was also related to cell size rather than solely to cell number.

The image analysed dielectrophoretic spectra had a similar appearance to the results obtained spectrophotometrically, though the overall collection level of the treated and untreated samples varied greatly. Figure 4.44 shows spectra of treated and untreated *E. coli* 10418 at the beginning and end of the incubation period. Though the sample concentrations were somewhat different the general spectral form was conserved with the untreated sample and with the T_0 treated sample which was taken from the culture immediately after addition of the antibiotic.

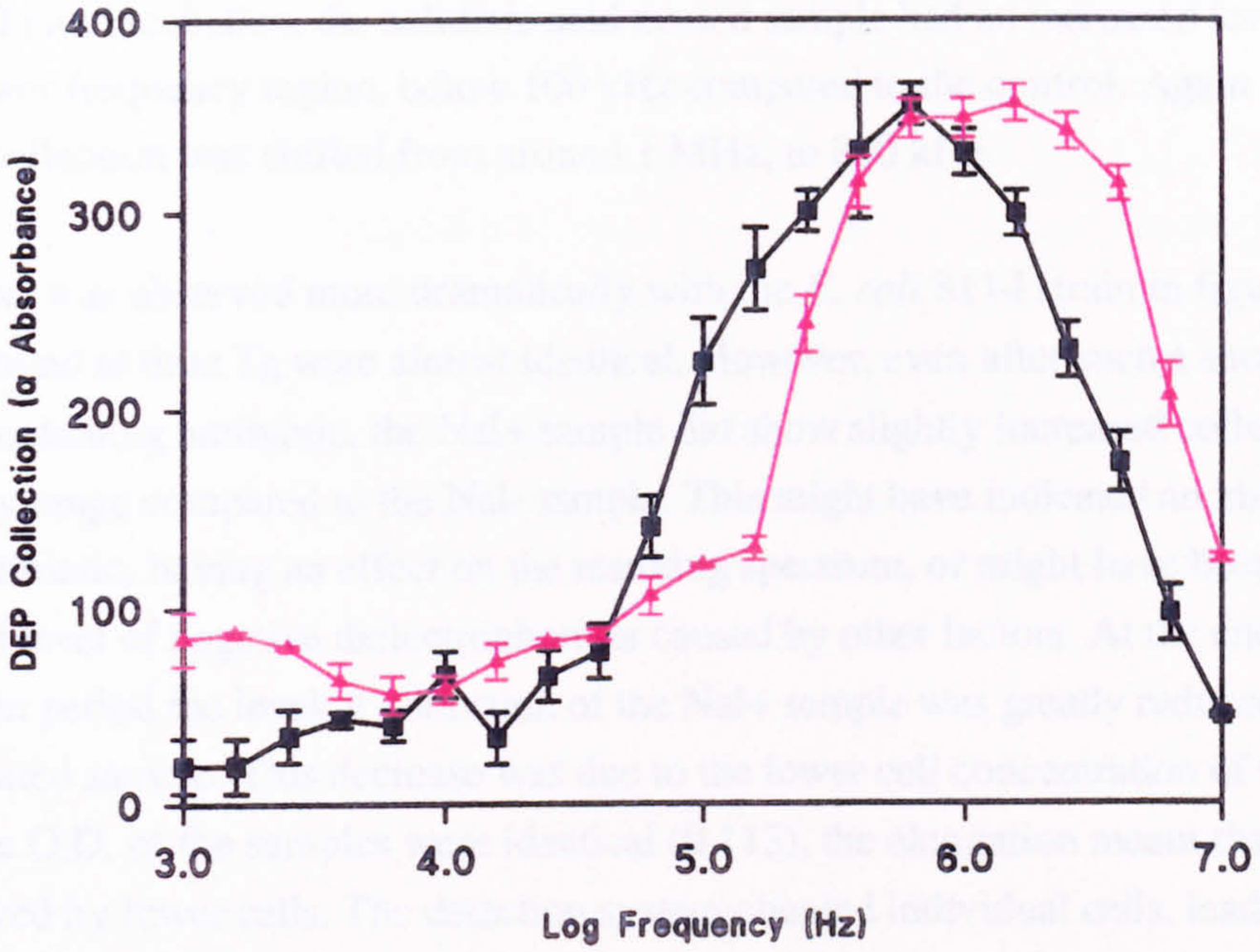

Figure 4.43 : Dielectrophoretic (DEP) spectra of *E. coli* 8114 treated for 240 min with 10 μg.ml^{-1} nalidixic acid. (■) Antibiotic treated cells, (▲) Control cells. Conditions : 16 V, 10 s pulse, 57-65 μS.cm^{-1}. Spectrophotometer detection method, 525 nm wavelength. Each point is the mean plus standard error of 4 replicate spectra.

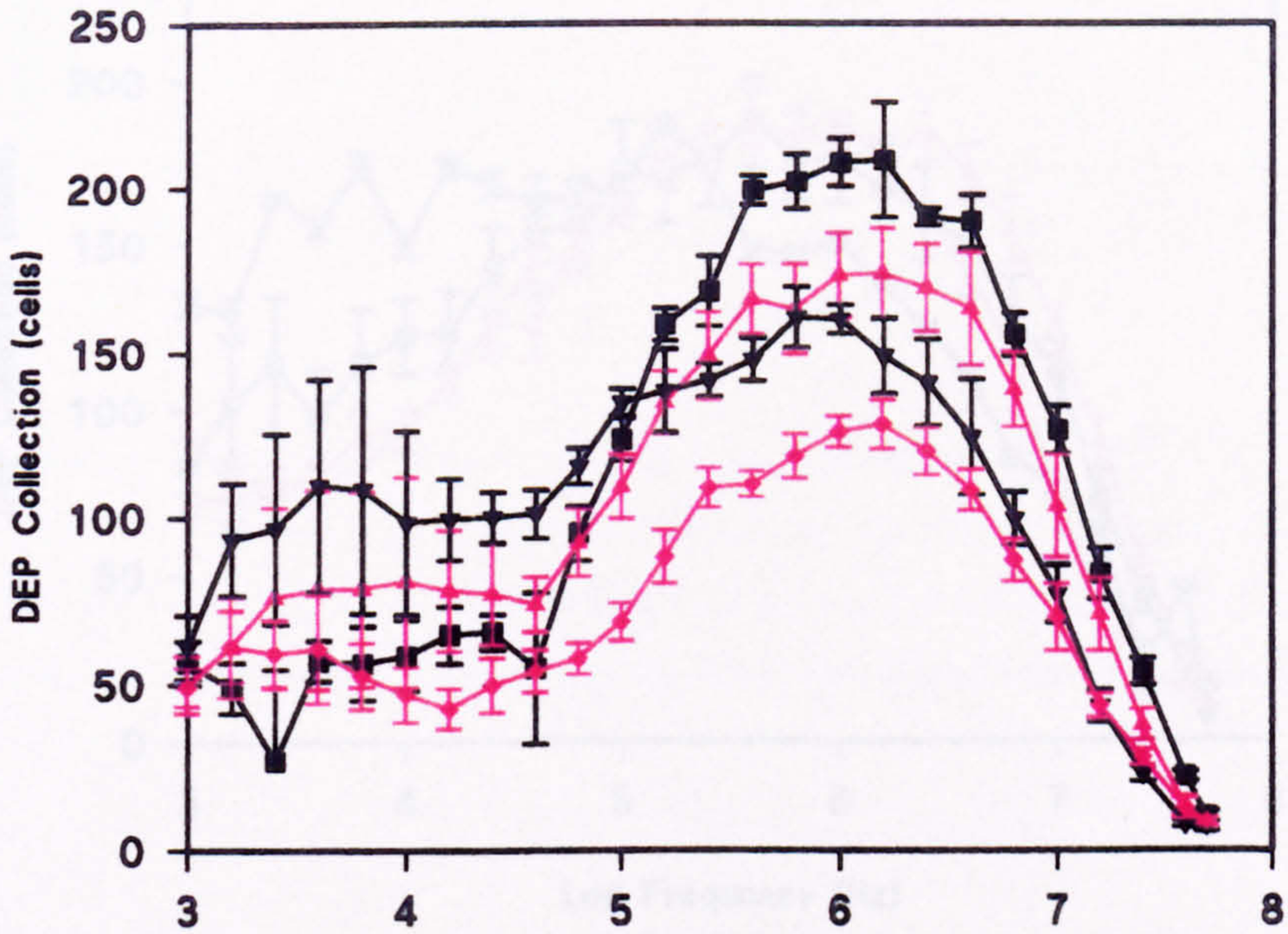

Figure 4.44 : Dielectrophoretic (DEP) spectra of *E. coli* 10418 treated for 270 min with 10 μg.ml^{-1} nalidixic acid. (■) Antibiotic treated cells at time T_0, (▼) Antibiotic treated cells at time T_{270}, (▲) Control cells at time T_0, (◆) Control cells at time T_{270}. Conditions : 12 V, 5 s pulse, 24.5 μS.cm^{-1}. Full count detection method. Each point is the mean plus standard error of 5 replicate spectra.

After 270 min incubation, the nalidixic acid treated sample had an increased level of collection in the lower frequency region, below 100 kHz compared to the control. Again the frequency peak of collection was shifted from around 1 MHz, to 800 kHz.

This effect was observed more dramatically with the *E. coli* 8114 strain in figure 4.45. The spectra found at time T_0 were almost identical. However, even after such a short time in the culture containing antibiotic, the Nal+ sample did show slightly increased collection in the low frequency range compared to the Nal- sample. This might have indicated an immediate binding of the antibiotic, having an effect on the resulting spectrum, or might have been due to an increased level of negative dielectrophoresis caused by other factors. At the end of the incubation period the level of collection of the Nal+ sample was greatly reduced compared to the untreated sample. This decrease was due to the lower cell concentration of the sample. While the O.D. of the samples were identical (0.113), the elongation meant that this O.D. could be achieved by fewer cells. The detection system counted individual cells, leading to a lower level of dielectrophoretic collection for this sample. By mathematical manipulation of the data to make their peak heights the same, the spectral form could be directly compared. Total counts of the samples gave values of 11.66×10^7 cells.ml^{-1} (Nal+, T_0), 6.33×10^7 cells.ml^{-1} (Nal+, T_{240}), 10.375×10^7 cells.ml^{-1} (Nal-, T_0) and 20.04×10^7 cells.ml^{-1} (Nal-, T_{240}).

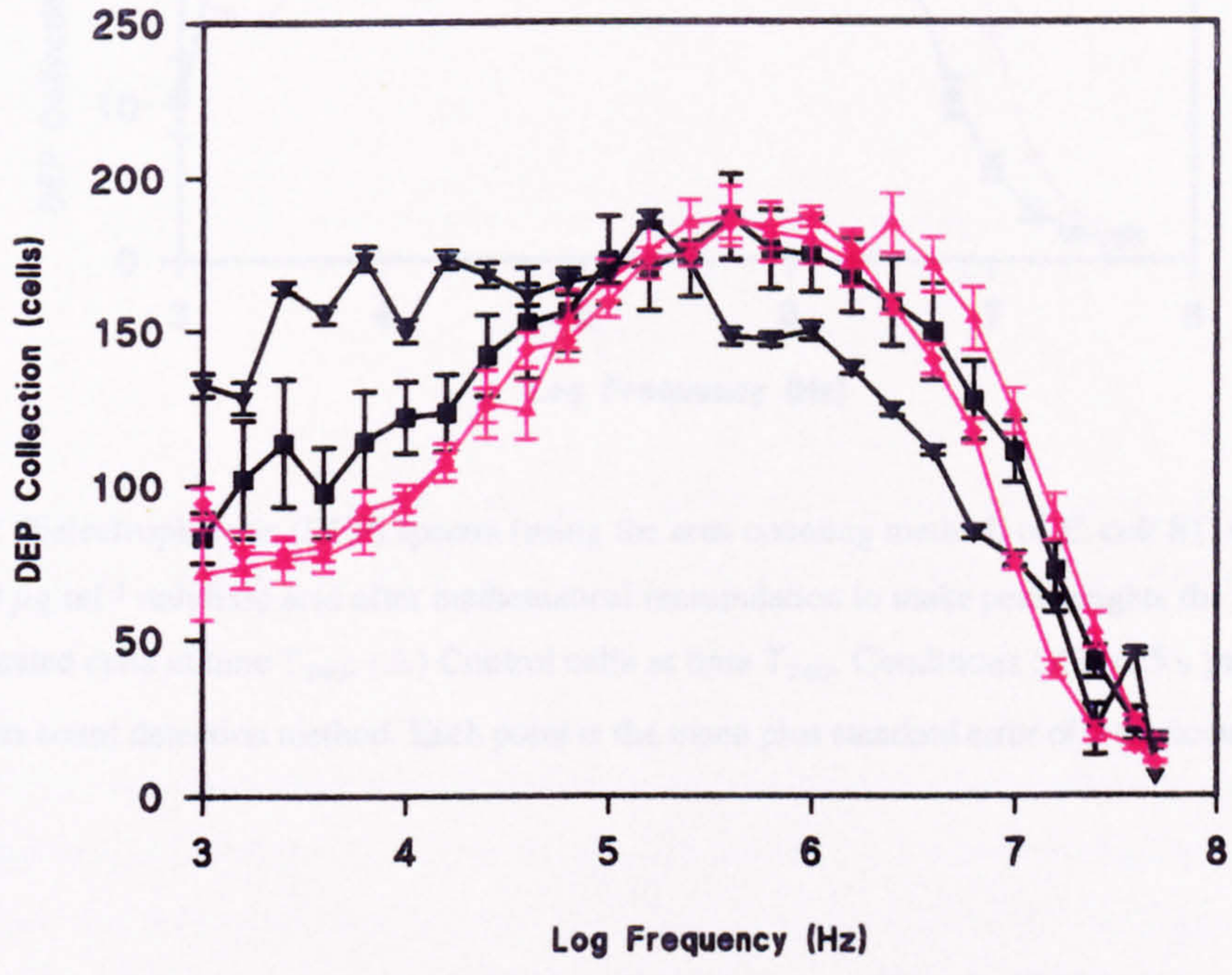

Figure 4.45 : Dielectrophoretic (DEP) spectra of *E. coli* 8114 treated for 240 min with 10 μg.ml^{-1} nalidixic acid after mathematical manipulation to make peak heights the same. (■) Antibiotic treated cells at time T_0, (▼) Antibiotic treated cells at time T_{240}, (▲) Control cells at time T_0, (◆) Control cells at time T_{240}. Conditions : 12 V (pk-pk), 5 s pulse, 24.5-28.1 μS.cm^{-1}. Full count detection method. Each point is the mean plus standard error of 5 replicate spectra.

In an attempt to obviate this problem of elongation reducing the cell count, the image analysis 'Area' detection method was also used with the same samples (figure 4.46). This detection method, however, also had related problems. Though, the cell concentration of the NaI+ sample was much lower than the other samples, the area of cells detected was more than double that of the untreated samples, giving similar comparison difficulties. Again, after multiplication of the datapoints to identical peak heights, the spectral form could be more directly compared. When this normalisation was performed, the same spectral shift was apparent after nalidixic acid treatment. In this case the shift was moved from around 800 kHz-1 MHz to below 100 kHz.

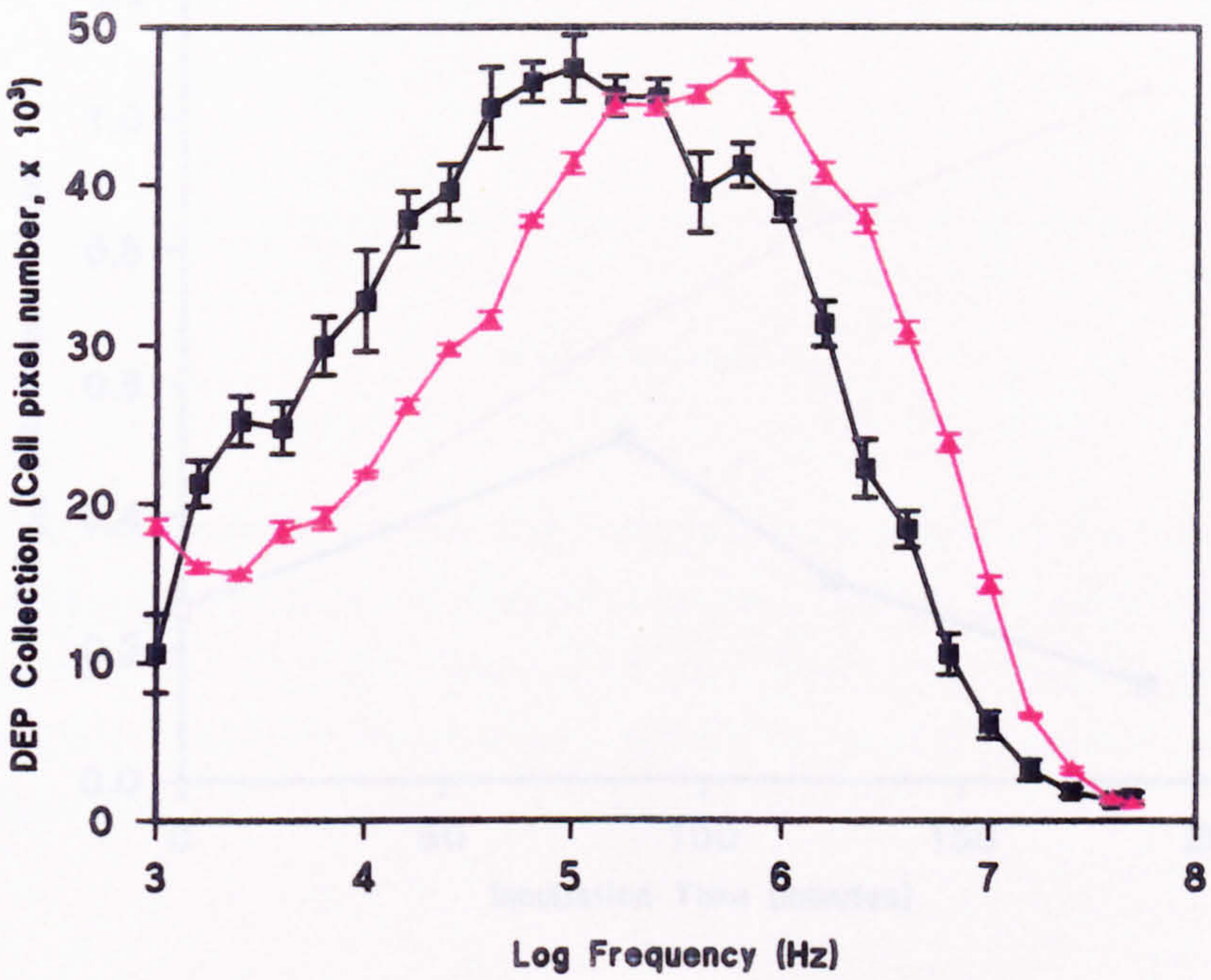

Figure 4.46 : Dielectrophoretic (DEP) spectra (using the area counting method) of *E. coli* 8114 treated for 240 min with 10 μg.ml^{-1} nalidixic acid after mathematical manipulation to make peak heights the same. (■) Antibiotic treated cells at time T_{240}, (▲) Control cells at time T_{240}. Conditions : 12 V, 5 s pulse, 24.5-26.3 μS.cm^{-1}. Area count detection method. Each point is the mean plus standard error of 5 replicate spectra.

Spectra produced in the same way with the clinical isolate *E. coli* 39323 did not show the same frequency shift after antibiotic treatment with 10 mg.ml^{-1} nalidixic acid and both control and treated cell spectra were identical. However, after microscopic examination of the cells, it was noted that elongation had not occurred with this antibiotic concentration. This correlated well with the observation that this strain had a higher MIC value for this antibiotic and was more resistant.

The repeatable nature of this shift, with several different strains also shows that this is a true general effect of *E. coli* and not a characteristic of a particular strain.

4.11 Ampicillin Treatment

The change in absorbance of the *E. coli* cells during incubation in presence or absence of ampicillin are shown in figure 4.47.

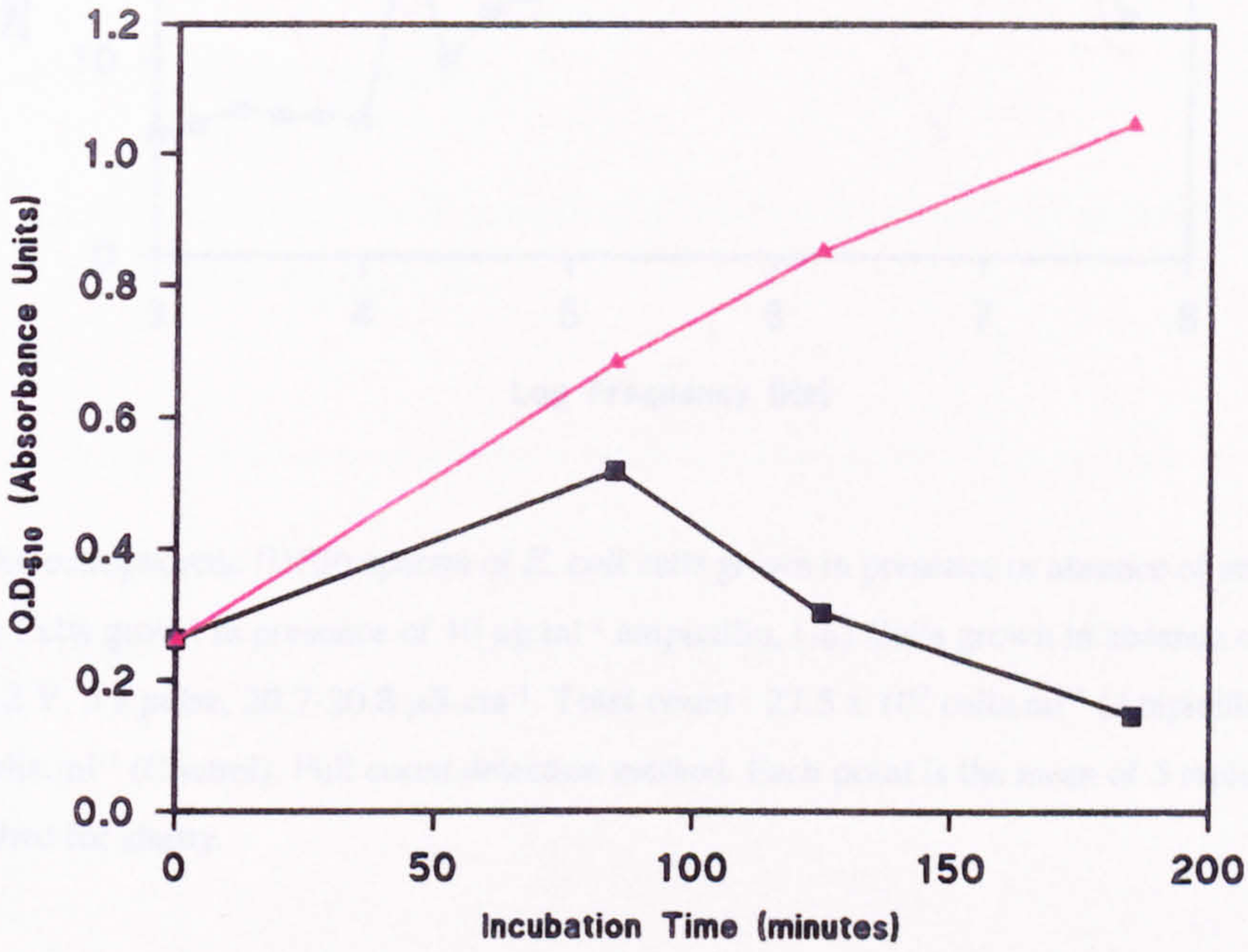

Figure 4.47 : Change in absorbance of *E. coli* 101418 during incubation for 180 min in presence or absence of ampicillin antibiotic. (■) Treated with 10 μg.ml^{-1} ampicillin, (▲) Control sample without ampicillin.

Both samples were observed to undergo an initial increase in optical density as cell growth and division proceeded. After approximately 90 min, however, the sample exposed to ampicillin underwent a dramatic and rapid reduction in O.D. until the end of the incubation period. The O.D. of the control sample continued to rise throughout the duration of the incubation. After microscopic examination of the cultures, the cells treated with ampicillin were found to be significantly elongated by 2-3 times and exhibited typical bulge formation from the sides of the cells. In addition, the broth from these cells had become much more viscous compared to the controls possibly indicating leakage of cytoplasmic contents through the damaged cell walls.

The dielectrophoretic frequency spectra obtained from these samples are shown in figure 4.48.

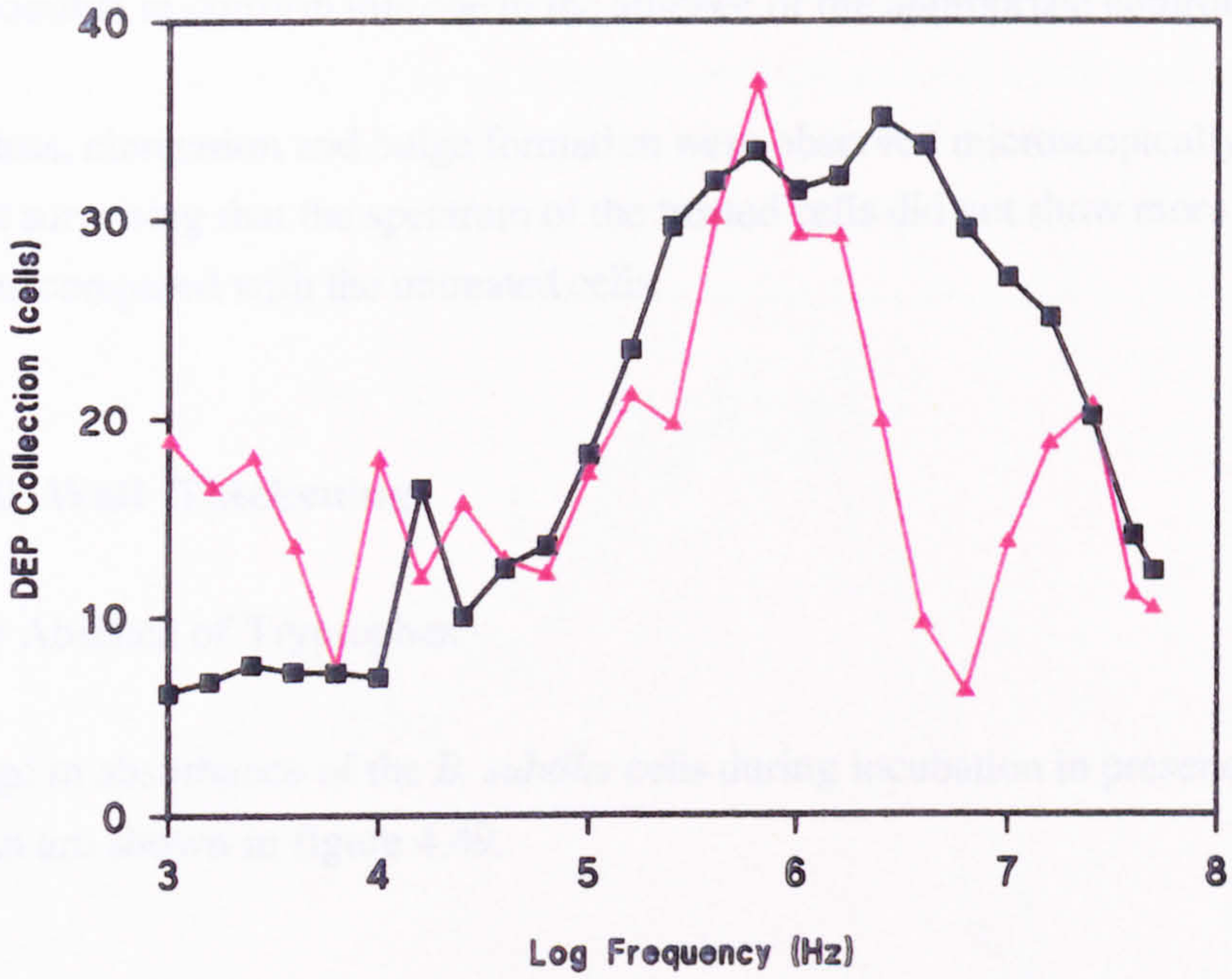

Figure 4.48: Dielectrophoretic (DEP) spectra of *E. coli* cells grown in presence or absence of ampicillin antibiotic. (■) Cells grown in presence of 10 μg.ml^{-1} ampicillin, (▲) Cells grown in absence of antibiotic. Conditions : 12 V, 5 s pulse, 20.7-20.8 μS.cm^{-1}. Total count : 27.5 x 10^7 cells.ml^{-1} (Ampicillin treated), 28.35 x 10^7 cells.ml^{-1} (Control). Full count detection method. Each point is the mean of 5 replicate spectra. Error bars omitted for clarity.

The large degree of error (caused by background noise) within the 5 replicate spectra for the control cells make it difficult to highlight conclusive differences between the two spectra. The spectra of the treated cells were much more reproducible. Possibly the most noticeable difference between the spectra, was the rapid fall of in collection of the control cells in the MHz region, compared to the antibiotic treated cells which still had good collection up to around 4 MHz. The rapid fall off in control cell collection may be considered to be an artefact of spectral noise causing bad collection.

To attempt a possible comparison between antibiotic treated and untreated cells, the spectrum of the same *E. coli* 10418 strain in 0.5 M sucrose of figure 4.23 may be tentatively used as a control, untreated spectrum. This figure shows great similarity in spectrum shape with that of the antibiotic treated cells. Both the control and treated samples showed an increase in dielectrophoretic collection at around 60 kHz and the extended peak collection plateau right up to 5-10 MHz. This was a characteristic of presence of cells in sucrose rather than the usual 1

MHz peak found with deionised water. Generally there did not appear to be a great deal of spectral difference between the antibiotic treated and untreated cells (of figure 4.23), though it was not possible to confirm this due to the absence of the appropriate control.

Nevertheless, elongation and bulge formation were observed microscopically, so it is somewhat surprising that the spectrum of the treated cells did not show more significant differences compared with the untreated cells.

4.12 Cell Wall Thickening

4.12.1 By Absence of Tryptophan

The change in absorbance of the *B. subtilis* cells during incubation in presence or absence of tryptophan are shown in figure 4.49.

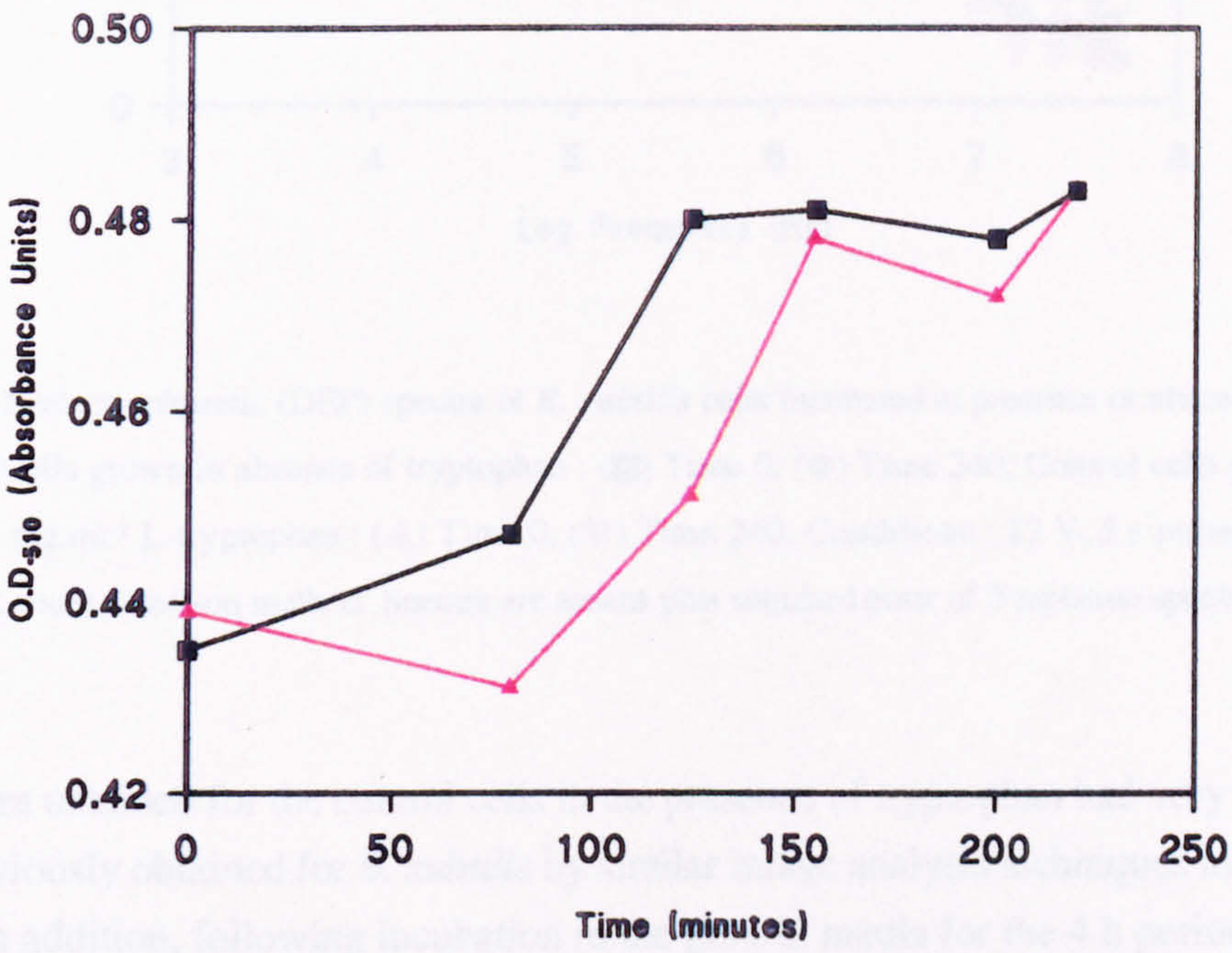

Figure 4.49 : Change in absorbance of *B. subtilis* 10106 during incubation in presence or absence of tryptophan. (■) Cells grown in absence of tryptophan, (▲) Control sample in presence of tryptophan.

Incubation of the cells in presence or absence of tryptophan did not appear to produce significant differences in absorbance measurements. The increase in absorbance in both control and treated cultures was very minor over the incubation period, increasing from only 0.44 to

0.48 Absorbance units. This may be due to the incubation medium consisting of a simple minimal glucose-amino acids-salts mixture.

The dielectrophoretic spectra of these cells grown in presence or absence of tryptophan are shown in figure 4.50.

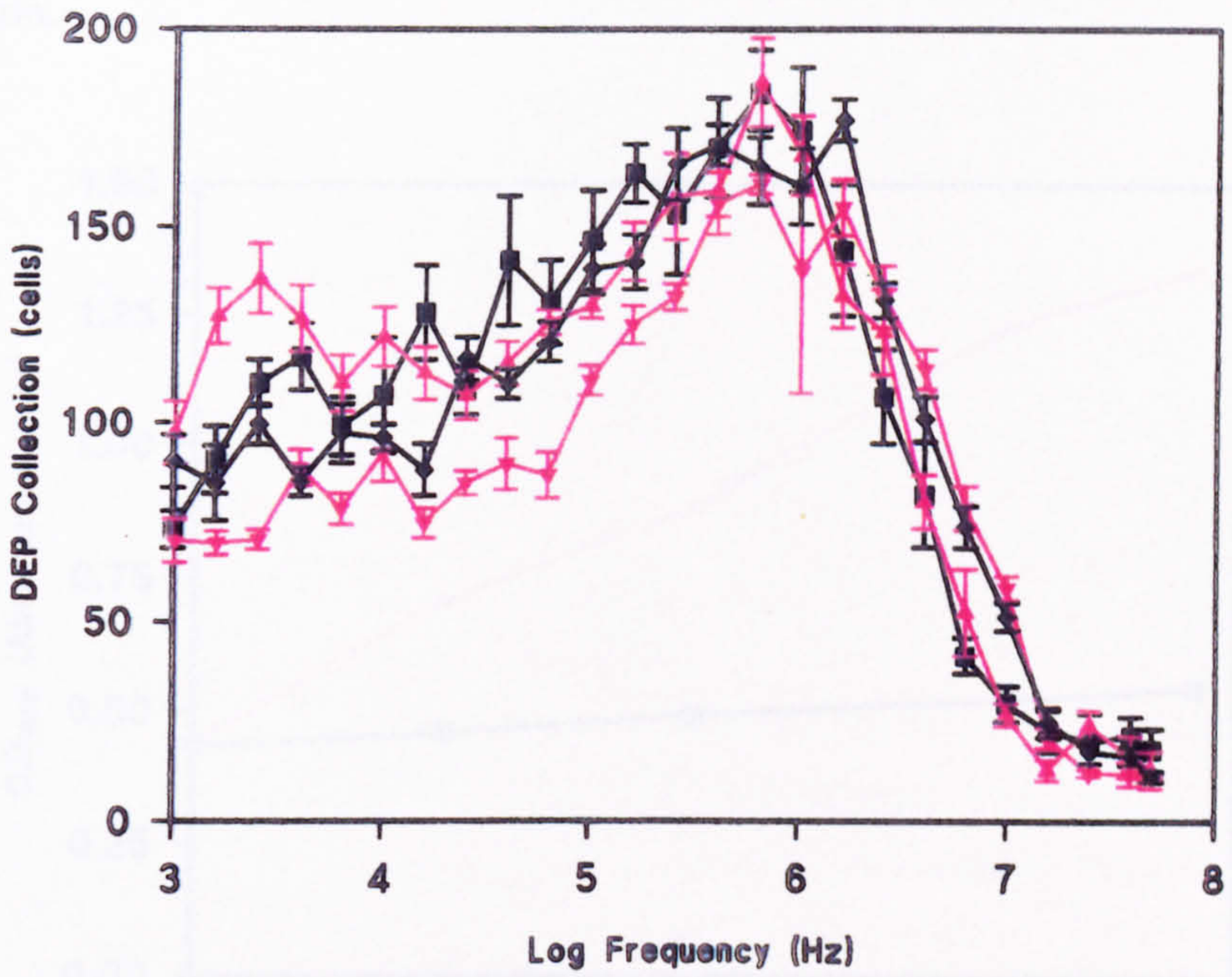

Figure 4.50 : Dielectrophoretic (DEP) spectra of *B. subtilis* cells incubated in presence or absence of tryptophan for 240 min. Cells grown in absence of tryptophan : (■) Time 0, (◆) Time 240; Control cells grown in presence of 1 mg.ml^{-1} L-tryptophan : (▲) Time 0, (▼) Time 240. Conditions : 12 V, 5 s pulse, 24.6-28.3 μS.cm^{-1}. Full count detection method. Spectra are means plus standard error of 5 replicate spectra.

The spectra obtained for the control cells in the presence of tryptophan had very similar form to those previously obtained for *B. subtilis* by similar image analysis techniques in section 4.2.1.2. In addition, following incubation in the growth media for the 4 h period did not appear to have any effect on the spectra obtained, and the form was generally conserved.

The samples incubated in the absence of tryptophan were expected to have an altered spectrum due to proposed wall thickening mechanisms. However, the results obtained in figure 4.50 did not show any significant differences between the cells grown in the presence or absence of tryptophan. The error bars obtained for the spectra, though relatively small, were sufficient that no differences could be attributed to the treatment at any frequency over the range examined.

4.12.2 By Chloramphenicol Presence

In this case, treatment of *B. subtilis* with chloramphenicol antibiotic to attempt to thicken cell walls resulted in a cessation of growth compared to the control sample as demonstrated by the absorbance measurements measured throughout the incubation period (figure 4.51). This effectively shows that the action of the antibiotic on protein synthesis had occurred preventing cell division.

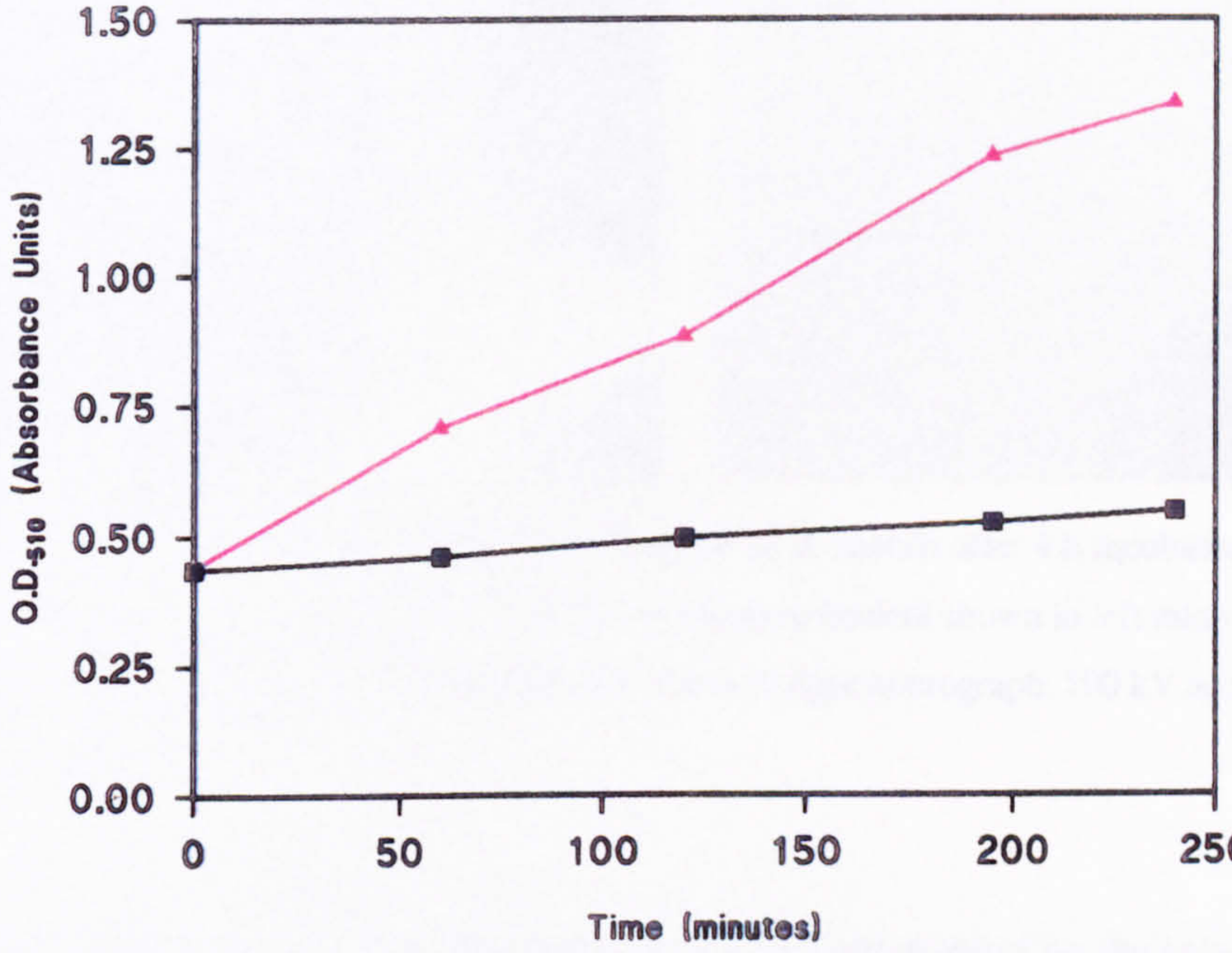

Figure 4.51 : Change in absorbance of *B. subtilis* 10106 during incubation in presence or absence of chloramphenicol at 50 μg.ml^{-1}. (■) Cells grown in presence of antibiotic, (▲) Control sample in absence of antibiotic.

Exposure of *B. subtilis* cells to the antibiotic was also found to be accompanied by significant increases in the cell wall thickness as demonstrated by the electron micrographs shown in figure 4.52.

As can be observed from the micrographs, the walls of the treated cells have become thickened from 28-29 nm in the untreated cells to 57-71 nm after incubation in chloramphenicol. This corresponds to a 2-2.5 fold increase in wall thickness following antibiotic treatment, a similar result to that found by Hughes *et al.* (1970) and Chung (1971; 1973).

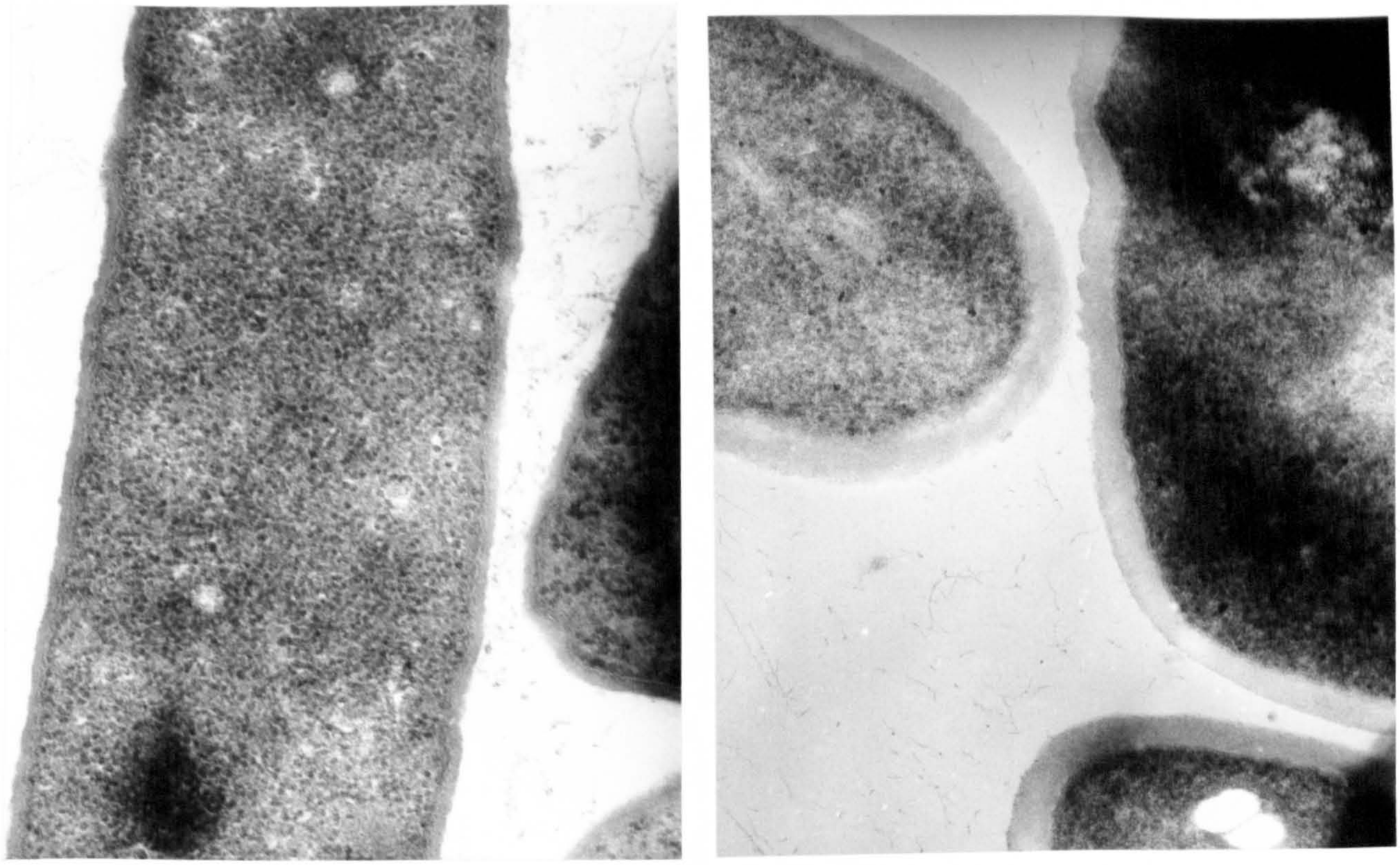

Figure 4.52 : Transmission electron micrographs of sections of *B. subtilis* after 4 h incubation in presence or absence of chloramphenicol. Control cells in absence of chloramphenicol shown in left micrograph; Cells incubated in presence of 50 $\mu g.ml^{-1}$ chloramphenicol shown in right micrograph. 100 kV accelerating voltage. Scale : 14 mm = 200 nm.

The effect of this inhibition of protein synthesis and wall thickening on the subsequent dielectrophoretic spectra is shown in figure 4.53.

Again the spectra of the control *B. subtilis* cells has the same general form as previously shown in figure 4.50, collection increasing steadily up to a maximum peak frequency at 1 MHz. In comparison, the collection of the antibiotic treated cells rose to an initial peak at around 20 kHz and then dropped again to a minimum at approximately 100 kHz, before beginning to increase again. The maximum peak of collection was in a similar frequency region as the control cells (1 MHz). The remainder of the frequency spectrum closely followed that of the untreated cells at frequencies greater than 1 MHz. Thus unlike the tryptophan treatment described above, significant difference in spectra were obtained by this method of protein synthesis inhibition.

In addition, significant differences in viable count were obtained giving 2.59×10^5 $cfu.ml^{-1}$ in chloramphenicol treated cells and 369.3×10^5 $cfu.ml^{-1}$ in the control cells. However, these differences in viable count did not appear to cause changes in the peak collection height of the cells. Chloramphenicol treated cells, however, also appeared to be slightly elongated compared with the control cells upon microscopic examination.

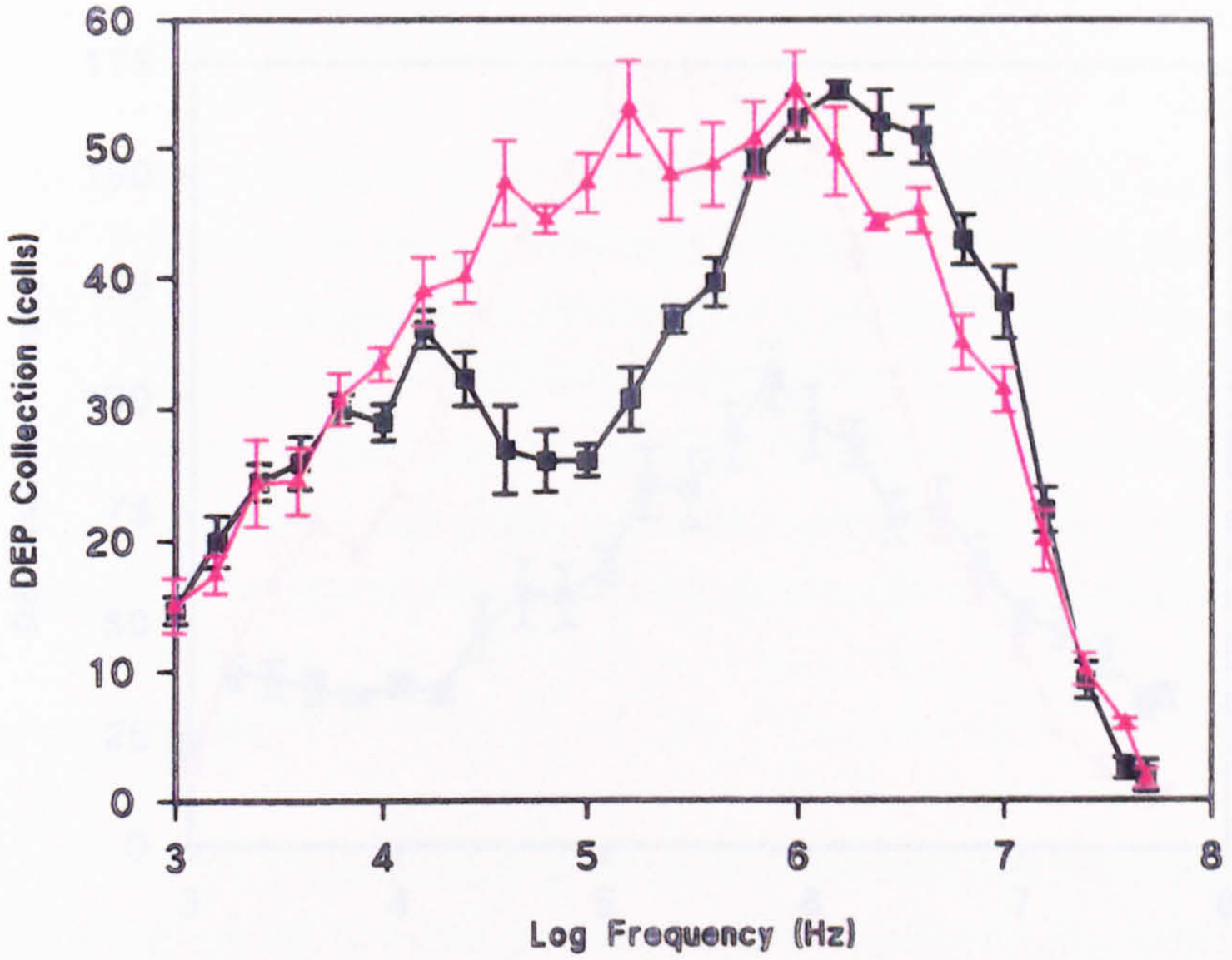

Figure 4.53 : Dielectrophoretic (DEP) spectra of *B. subtilis* cells grown for 4 h in presence of absence of chloramphenicol. (■) Cells grown in presence of 50 μg.ml^{-1} chloramphenicol, (▲) Control cells grown in absence of chloramphenicol. Conditions : 12 V, 5 s pulse, 24.5-24.8 μS.cm^{-1}. Full count detection method. Each spectrum is the mean plus standard error of 5 replicate spectra.

4.13 Spheroplast Formation

Following exposure of the *E. coli* cells to the EDTA and lysozyme for 10 min, microscopic examination demonstrated that spheroplasting was complete after this time. Spherical shaped bodies were observed compared to the rod shaped cells noted in the control sample in absence of lysozyme treatment.

The dielectrophoretic frequency spectra obtained with the samples are shown in figure 4.54. The figure shows significant differences between the control cells and the spheroplasts over the whole frequency range. The DEP collection was much reduced compared to the untreated cells, reaching less than 50 % of the collection shown by the untreated cells at most frequencies. Collection of the spheroplasts exceeded that of the control only at frequencies greater than around 4 MHz. In addition to the reduction in collection of the spheroplasts, the peak frequency also appeared to have undergone a slight shift from around 300-400 kHz to around 800 kHz compared to the untreated cells.

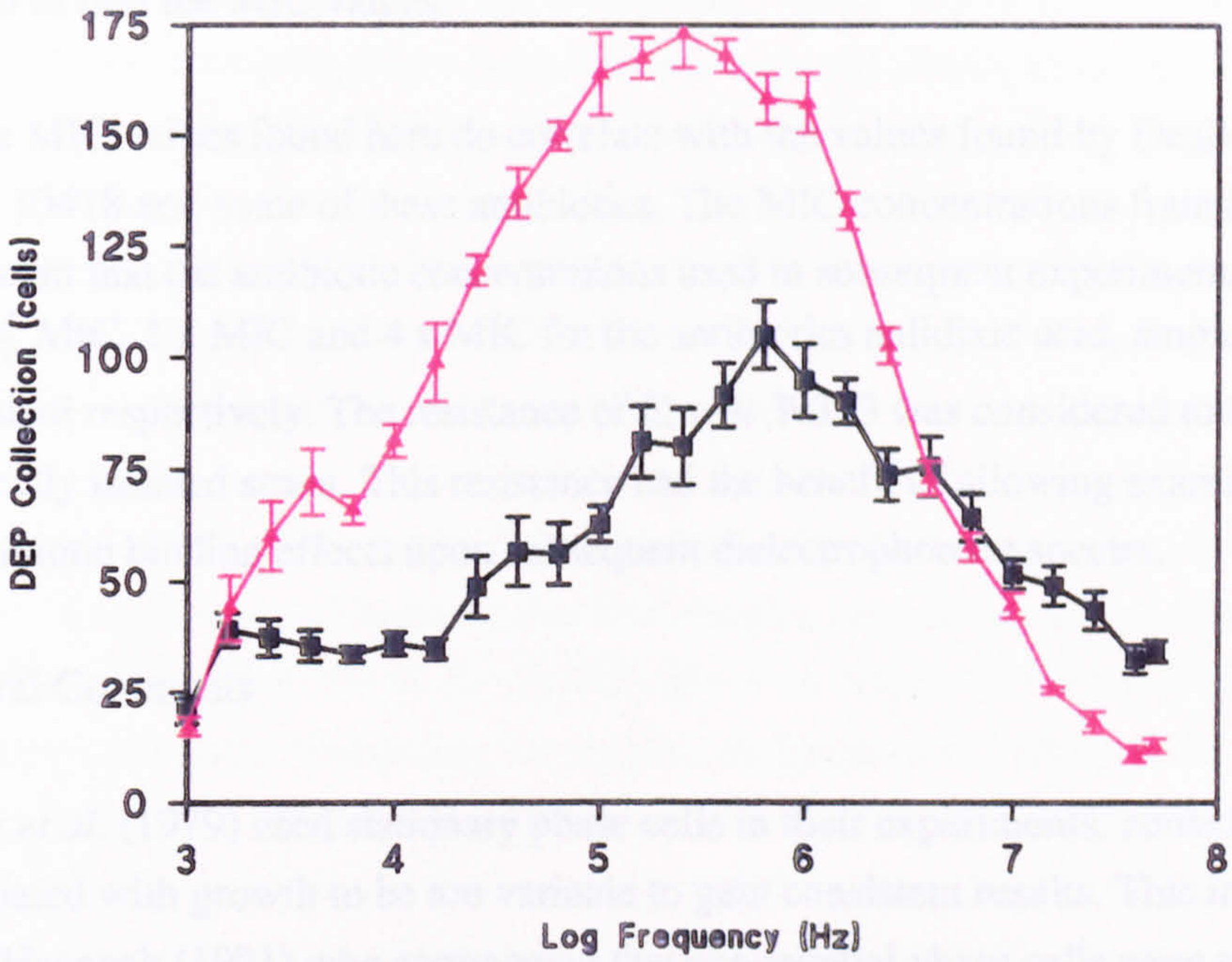

Figure 4.54 : Dielectrophoretic (DEP) frequency spectra obtained for spheroplasts of *E. coli* and a control sample not exposed to lysozyme. (■) Spheroplasts, (▲) Control cells. Conditions : 12 V, 5 s pulse, 24.2-24.3 μS.cm^{-1}. Full count detection method. Each point is the mean plus standard error of 5 replicate spectra.

4.14 Discussion of Antibiotic Treatments and Cell Wall Treatments

4.14.1 Antibiotic Assays

The method used to assess the relative antibiotic sensitivity of the bacterial cells was the Stokes' method. This essentially exposed an organism, known to be sensitive to antibiotic action, to identical antibiotic concentrations as that experienced by an organism under test. A direct comparison of antibiotic sensitivity of the two organisms could then be made. Generally, this method is typically employed to simply classify the sensitivity of a test organism, rather than to obtain MIC values for a particular antibiotic. The results obtained using this method had different MIC levels compared to those quoted by the British Society for Antimicrobial Chemotherapy Working Party (1991), even using identical control organisms (*E. coli* 10418 and *Staph. aureus* 6571). In their experience, these control sensitive organisms were normally inhibited by 2 μg.ml^{-1} concentrations of each of the antibiotics examined here (nalidixic acid, chloramphenicol and ampicillin). The Working Party commented that "there is no standard methodology for MIC tests..." and so the higher level of antibiotics necessary to inhibit the

control species found in experiments described in this thesis, could reflect the different methods used to find the MIC values.

However, the MIC values found here do correlate with the values found by Dealler (1991) using *E. coli* 10418 and some of these antibiotics. The MIC concentrations found for these organisms meant that the antibiotic concentrations used in subsequent experiments were at levels, ¼-½ MIC, 1 x MIC and 4 x MIC for the antibiotics nalidixic acid, ampicillin and chloramphenicol respectively. The resistance of *E. coli* 39323 was considered to be due to it being a clinically isolated strain. This resistance had the benefit of allowing examination of the strain for antibiotic binding effects upon subsequent dielectrophoretic spectra.

4.14.2 General Comments

Fomchenkov *et al.* (1979) used stationary phase cells in their experiments, considering the effects associated with growth to be too variable to gain consistent results. This in conflict with the views of Hancock (1991) who commented that exponential phase cells were much more similar in state of growth than stationary phase cells. Generally, in experiments discussed here, stationary phase cells were used, though this was more to eliminate detection problems associated with studying elongated exponential phase cells. However, antibiotic treatments were conducted by growing cells taken from the exponential phase in growth media containing antibiotics at subinhibitory concentrations for a number of hours. Experiments were undertaken in this way since antibiotic action is known to be proportional to the growth rate of the cells, having significantly less activity on stationary phase cells (phenotypic tolerance)(Tuomanen *et al.*, 1986). Several examinations of the effects of adding antibiotics to washed samples in deionised water upon dielectrophoretic response have been performed (Fomchenkov, 1979; Betts, 1994; Quinn, 1995)

4.14.3 Elongation by Nalidixic Acid Treatment

Nalidixic acid, an 8-aza-4-quinolone, has been used in clinical practice for a number of years, especially in the treatment of urinary tract infections, being more effective against Gram negative cells (Franklin & Snow, 1975). The action of nalidixic acid is against DNA gyrase subunits of bacterial cells, involved in DNA synthesis mechanisms (Hrebenda *et al.*, 1985). DNA gyrase enables replication of the bacterial chromosome by producing a single stranded nick which allows negative supercoiling. This antibiotic has an effect against the gyrase A subunit, stopping DNA replication but only having minor effects against RNA or protein synthesis (Gale *et al.*, 1972). Once inside the cell, the action of nalidixic acid on DNA synthesis elicits the "SOS response" within the cell (Radman, 1975) involving inhibition of septation and initiation of DNA repair activities until the damage has been repaired. An often

noted action of such antibiotics is the elongation or filamentation of cells produced by cessation of cell division processes. This action is predominantly found with low or sub-MIC concentrations of the antibiotic, causing great increases in cell length. Certainly with nalidixic acid, it has been found that for antibiotic induced bactericidal effects, RNA and protein synthesis mechanisms must proceed (Deitz *et al.*, 1966). The inhibition of these processes e.g. by chloramphenicol or nutrient limitation, did not produce the same lethal effects. Indeed, the action of nalidixic acid was found to be reversible, and the effects on DNA synthesis inhibition were removed by washing and resuspension in antibiotic free medium (Goss *et al.*, 1965).

The results found in section 4.9, the MIC for nalidixic acid was found to be either 40 or 20 $\mu g.ml^{-1}$ for the *E. coli* strains. Therefore the filamentation seen in the results of section 4.10.1 was produced by antibiotic levels of $\frac{1}{4}$-$\frac{1}{2}$ MIC levels i.e. well below the level that would produce bactericidal effects. Elongation was applied by Singh *et al.* (1989) to the viable counting of bacterial cells using image analysed epifluorescence microscopy, since elongated cells were considered viable when found to elongate in the presence of 20 $\mu g.ml^{-1}$ nalidixic acid. These workers also measured substantial increases in breadth of cells. In agreement with Singh *et al.* (1989), who found an increase in length of 2-3 times with *E. coli* when compared with control cells, the results found here produced comparable average elongation. In some cases significantly greater cell lengths of up to 13 μm were found. This size increase has been found to diminish as concentrations of the antibiotic became greater (around 20 or 40 $\mu g.ml^{-1}$). Results observed here also found that cell length also became reduced to sizes similar to control cells after longer periods of exposure.

The results of dielectrophoretic experiments showed consistent shifts in spectra to lower frequencies implying a slowing of repolarisation response in higher frequency regions.

While the most noticeable effect of nalidixic acid treatment upon the cells was the very great elongation caused by cessation of cell division, other effects caused by the antibiotic cannot be disregarded.

Experiments with different latex particle sizes (section 4.4.8) showed that there was no distinguishable change in DEP collection with volume, even when volume differences of more than double were used. Rather, in that case, increase in collection was more related to the surface charge density of the particles, masking any possible differences due to size. Though very great differences in cell size existed in the nalidixic acid treated cells, variation in peak height was considered to be more related to detection problems rather than increased DEP due to cell volume. The more notable effect between antibiotic treated and control cells was the shift in peak height to lower frequencies with greater length.

In the wide ranging studies of Pohl (1978) different sized silica particles (down to 0.2 μm diameter) showed similar shifts in frequency in the low frequency range, with smaller particles collecting better at higher frequencies. In contrast to the results obtained here, no discernible changes in collection were found by Pohl in the frequency range greater than 100 kHz. It was commented that this change in low frequency region was due to alterations of surface conduction mechanisms involving both bound and diffuse ion atmospheres, therefore being confined to the low frequency region rather than the interfacial mechanism related higher frequencies. The relaxation times associated with these mechanisms were related to the square of particle radius and were found to become longer with increased radius, shifting the DEP peak to lower frequencies. Additional effects relating to the particle size are described by the often used equation (1.6) which shows that the dielectrophoretic force is greater with increased particle dimensions. As shown with the latex particle experiments however, the overall size is generally overshadowed by the nature of the polarisation mechanism and larger surface conductivity effects.

Similar effects could be in effect with the *E. coli* bacterial cells examined here. The shift in peak frequency occurred with the MHz peak shifting from 2 MHz to 800 kHz. This result is distinct from that obtained by Pohl in that it occurred at much greater frequencies, those which might normally be attributed to interfacial polarisation mechanisms. There might be several explanations for this observed phenomenon.

The first explanation is that the shift may be caused by a surface conductivity modified Maxwell-Wagner polarisation response. Exposure of the bacterial cells to low concentrations of this antibiotic may moderate the surface conductivity response. Nalidixic acid is known to have a negative charge under physiological conditions. It might be expected that binding of this antibiotic to structures in the Gram negative outer cell membrane, while being unfavourable due to the repulsion by the negative electrostatic charge of the cell, may cause a shift in the ability of the surface conductivity to repolarise. The effective increase in surface negative surface charge, or increased co-anion presence within the electric double layer may cause increases in the Debye length and diffuse atmosphere. Polarisation at the lower frequencies may become more efficient, promoted by this surface conductivity enhancement. In addition, adsorption of negatively charged antibiotics may result in the localisation of adjacent counterion potential energy wells and more efficient charge hopping at the lower frequencies. While this explains an increased polarisation response at lower frequencies after antibiotic treatment, it does not explain the observed reduction in collection at 2 MHz following treatment.

This fall off in collection at lower frequencies (in the MHz range) with the treated cells may be more simply due to effective size increase following antibiotic exposure. Generally rod shaped cells were observed to collect by one of the polar regions of the cells even though membrane

capacitance mechanisms are normally favoured at higher frequencies causing an orientation perpendicular to field lines (Pohl, 1978). It has been found that in some cells (*B. subtilis*), the polar end caps possess great amounts of negative charge (Sonnenfeld *et al.*, 1985). Therefore dipole formation will be efficient within these regions, resulting in a predisposition for DEP collection to occur by attraction of these regions overcoming the suspension flow. The hydrodynamic force on the collected cells will be greater in elongated or antibiotic treated cells compared to much smaller control cells. Therefore as frequency increases and sequential polarisation mechanisms cease their contribution, elongated cells or larger particles will undergo rapid decrease in collection, even when the DEP force may be sufficient for smaller control cells to still collect efficiently.

Elongation of the cells may have other effects on surface conductivity. The overall surface area of these antibiotic treated cells will be much greater than that found in the control cells possibly enabling a massive surface conductivity polarisation in the lower frequency range, also resulting in a very large dipole moment since charge density and separation will be greatly increased.

The SOS response of the cells causes an increase in cell size, while preventing cell division. This is produced by the inhibition of the septation step (necessary for cell division). Prevention of this step could have consequences for polarisation mechanisms. The intracellular cytoplasm would remain interconnected within unseparated daughter cells. While this allows ease of charge movement through the cell, it also removes cell wall interfaces at the septa, reducing possible charge build up. This reduction in interfacial polarisation, which is normally thought to dominate responses in the MHz region, could be yet another explanation for the reduction in DEP collection at 2 MHz while not being observed in the control cells.

The small size of this antibiotic and its resultant binding does not seem to be sufficient to cause stearic hindrances against polarisation, but its charge may obstruct the movement of counterions across the cell surface when binding occurs only to a limited extent. However, these explanations are based upon the assumption of antibiotic binding as an intermediate step in the action of the antibiotic.

4.14.3.1 Antibiotic Uptake in Bacterial Cells

One proposed explanation for the effect of antibiotics on the resultant DEP spectra of bacterial cells is that changes may be caused, not by the action of the antibiotic on the cell but rather by the physical binding of antibiotics to the surface of the cells effectively altering the nature of surface. The adhesion of antibiotics to surface receptor groups is generally unlikely to be specific in antibiotics which have an intracellular target site and would probably be due to the

charged forms of antibiotics interacting with countercharges on the outer surface of cells or undergoing chemical bonding. It is possible that the binding of antibiotic structures to the surface would thus be able to influence the relative polarisability of the cell.

Access to the cell interior is not always a binding-mediated process. The entry of quinolones into cells is generally through the porins present in the outer membrane of Gram negative cells and is thus a diffusion controlled process, made easier by the low molecular weight of the antibiotic. Since the action of nalidixic acid is upon the DNA replication process and does not, as described in section 2.11.2, utilise the self-promoted uptake mechanism of entry, it is unlikely that any surface binding of nalidixic acid occurs. This is partly validated by the inactivity of nalidixic acid upon the resistant strain of *E. coli* (clinical isolate 39323) and by the absence of effect upon its spectrum. If the dielectrophoretic spectra shifts after exposure to sub-MIC levels of nalidixic acid had been as a result of non-specific physical binding to the cell surface, it is probable that this similar effect should have been also observed in this resistant strain. Alternatively, the nalidixic acid binding hypothesis could be advocated if the binding of this antibiotic was at specific receptor sites present on the sensitive strains but not on the resistant strain. The hypothesis of antibiotic binding to specific surface epitopes could be tested by the use of radiolabelled antibiotics, the binding of which could be assessed following a washing procedure. This binding effect should also have been observable as an immediate chemical process following inoculation of cells into the antibiotic containing medium. However, the spectrum of the treated cells removed at T_0 was practically identical to the control sample.

Binding of other antibiotics to bacterial cell walls and outer membranes has been previously demonstrated in those which have targets in the peptidoglycan or which penetrate by the self-promoted uptake mechanism as described in section 2.11.2. In the cases of these antibiotic types the binding is highly likely to influence the dielectrophoretic polarisation mechanisms. It is unknown at this stage, however, whether their presence has sufficient effect to be detectable by the current dielectrophoretic system, or indeed whether it will be masked by more predominant effects e.g. the action of the antibiotic on the target site. The dielectrophoretic spectra of treated cells following a washing step (to remove unbound antibiotic) would need to be compared with untreated cells to be able to elucidate the result of binding on DEP.

It is easier to consider the more significant action of the antibiotic on the cell to be responsible for the observed spectral changes. The action of sub-MIC antibiotic levels have been found to have several effects, both on the cell structure and composition and also upon the charge and hydrophobicity of the cell. Giordano *et al.* (1993) showed differences in the proteins and LPS present in the outer membrane after exposure of *Pseudomonas aeruginosa* to even sub MIC levels of antibiotics. The effect of some antibiotics at sub-MIC level caused increases in the

level of OmpF, a transmembrane porin. This would be likely to have a significant influence on the ion passage through the outer membrane making them more permeable and reducing selectivity. This effective short circuit would probably result in the leakage of intracellular ions into the surrounding medium, resulting in an overall lowering of the relative polarisability of the cell compared to the medium and potentially decreasing the level of DEP collection (though this may be compensated by greater DEP collection caused by the relative increase in cell volume of treated cells). This process may be more commonly observed with protein inhibiting antibiotics such as chloramphenicol.

4.14.4 Ampicillin Treatment

Beta lactams have their target at the penicillin binding proteins in the cytoplasmic membrane and therefore do not need mechanisms for crossing this membrane. Many of them are sufficiently hydrophilic for passage through the outer membrane of Gram negative cells to occur by passive transport through the porin molecules.

Ampicillin is monoanionic at neutral pH and therefore its diffusion through the outer membrane is somewhat more hindered compared to neutral antibiotics. This is due to the presence of certain charged amino acid residues in the porin interiors which interact with the molecules as they pass through.

By comparison with the antibiotic assays found in section 4.9, the level of ampicillin used to treat these *E. coli* cells was found to be equal to the MIC value of this organism. It may have been expected that the effect of MIC levels of this antibiotic may have been similar to the response found with nalidixic acid. Both antibiotics caused significant elongation of the bacterial cells, however ampicillin treatment also resulted in bulge formation in the sides of bacterial cells due to a weakening of the cell wall.

Due to the absence of adequate control cells for this antibiotic treated sample, the spectrum of *E. coli* 10418 in 0.5 M sucrose of figure 4.23 will be referred to as a control sample. It must be stressed, however, that this is <u>not</u> the correct control for the antibiotic treatment, though has been run under identical DEP conditions as the antibiotic treated sample. Therefore definite conclusions should not be drawn, though the spectra will be compared to obtain useful information and possible explanations offered to describe the spectra.

As has previously been discussed (section 4.14.3) increases in particle size did not necessarily produce changes in dielectrophoretic spectrum, though shifts to rather lower frequency ranges may be observed. However, cell elongation by ampicillin treatment did not appear to produce such changes in spectrum compared with the control sample. Indeed, the elongation did not

produce any significant changes in spectrum compared to the control at any of the frequencies examined.

The samples were resuspended in 0.5 M sucrose to prevent possible osmotic lysis caused by the observed cell wall weakening as found by bulge formation. As seen by the results in section 4.2.10, the use of sucrose as a suspending medium caused an DEP collection peak plateau to be observed up to frequencies 5-10 MHz. The similar plateau found with ampicillin treated cells may be explained by the same reason, rather than as a direct consequence of the antibiotic action on the cells.

Though cell treatment with ampicillin has been found to cause temporary shifts in zeta potential, this was not considered to be due to antibiotic adsorption (Dealler, 1991), and similarly have not been correlated with changes in dielectrophoretic spectrum. Studies by Fomchenkov *et al.* (1979) found there was no decrease in the polarisability of cells when exposed to penicillin. Similarly, it is unlikely that such a decrease would be found with ampicillin, a related β-lactam.

Ampicillin action is upon the cell wall polymers, preventing the transpeptidation of peptidoglycan strands and bringing about a weakening of the cell wall. Due to the spectral similarity between the treated and control samples, this change in structure (elongation and bulge formation) by MIC levels of ampicillin, though apparently very large upon first examination, may not be significant enough to produce frequency spectrum changes.

Even possible binding to cell outer membrane of the *E. coli* cells did not appear to cause changes in dielectrophoretic spectrum. Such effects were probably overshadowed by more bulk effects, and not detectable by the current system.

4.14.5 Cell Wall Thickening

4.14.5.1 By Absence of Tryptophan

Previous work by Shockman (1965) and Hughes *et al.* (1970) have shown that the growth of cells in media lacking an essential amino acid can produce significant wall thickening due to inhibition of protein synthesis, but continuation of wall polymer synthesis.

Bacillus subtilis trpC2, has a genetic mutation, unable to synthesise this gene product used in the biosynthetic pathway of tryptophan. This amino acid is present in relatively small amounts in typical cells. In *E. coli* B/r cells, tryptophan is only found at levels of 54 $\mu mol.g^{-1}$ dried cells, compared with glycine which is found at 582 $\mu mol.g^{-1}$ dry cells. Absence of tryptophan

from the medium would therefore be likely to prevent synthesis of this amino acid. For protein synthesis to occur properly, it is necessary for all amino acids involved in synthesis of a protein to be present simultaneously (Shockman, 1965). Absence of an amino acid would therefore prevent the synthesis of the protein and so lead to wall thickening.

Due to the similarity in effect between amino acid absence and chloramphenicol treatments on cell wall structure, the resulting dielectrophoretic spectra obtained would be expected to have similarities. However, figure 4.50 showed no real differences between cells grown in absence of tryptophan and those grown in presence of tryptophan. This was a surprising result since cell wall thickening by this method was expected to cause significant changes in frequency spectrum.

One possible explanation for the absence of spectrum changes between treated and control cells is that the treatment may not have been successful in bringing about wall thickening processes in this case, even though the previous experiments of Hughes *et al.* (1970) performed with identical methods and bacterial strains caused increases in wall thickness. Future experiments of this type would need to verify the wall thickening by electron microscopy as in figure 4.52 or by examination of protein synthesis mechanisms to confirm its inhibition. An indication that wall thickening may not have occurred was from the results of the O.D. measurements, taken throughout the incubation in presence/absence of tryptophan. This showed similar increases in O.D. in both the treated and control samples, indicating the growth rate of the treated cells had not become altered compared with the control cells. Normally, inhibition of protein synthesis e.g. by the chloramphenicol treatment in section 4.12.2, caused a reduction in growth rate as cell division became impeded. Thus it may be inferred that the omission of tryptophan did not cause inhibition of protein synthesis.

There may be several ways to explain why wall thickening may have been unsuccessful :

- There may be some carry over of tryptophan from the original growth medium meaning that there was sufficient levels of this amino acid remaining to allow protein synthesis to occur. However, the harvesting and washing procedure prior to inoculation into 'wall thickening medium' makes this unlikely.

- Tryptophan is only normally found in very small levels in some proteins. It may be possible for biosynthesis of necessary proteins to still occur without the need for this amino acid. Gale (1962) found several proteins to be synthesised even in the absence of some common amino acids. This, however, is more unlikely due to the successful thickening of cell walls found by Hughes *et al.* (1970).

- The cells placed into the wall thickening medium may have been in late exponential or early stationary phase of growth. This would mean that the rate of culture growth and cell division would have become much slower, producing a longer lag time, when placed into the wall medium, before exponential growth resumed. Therefore only a few cell cycles would have been able to occur during the 4 h incubation step and so only minor deposition of thickened wall material may have possible. This could have accounted for the similarities in spectra between cells grown in presence and absence of tryptophan.

- Insufficient growth and deposition of wall material may have occurred due to the minimal nature of the wall thickening medium.

Results obtained after successful wall thickening by this method may be expected to have similar traits in dielectrophoretic frequency response to those observed for cells with walls thickened by the chloramphenicol method. Further experiments of this type are required with verification of wall thickening by electron microscopy or by incorporation of radiolabelled peptidoglycan related amino acids.

4.14.5.2 By Chloramphenicol Presence

So far the action of antibiotics discussed has been concerned with Gram negative cells, and specifically *E. coli*. The action of antibiotics on Gram positive cells is also very important. The action of chloramphenicol on the dielectrophoretic spectrum of *B. subtilis* has been found to produce very different spectra to those produced following the action of nalidixic acid.

Chloramphenicol binds mainly to the protein L16 of the 50S ribosome subunit inhibiting peptidyl transferase activity (Chopra & Ball, 1982). Since the target site of this antibiotic is intracellular it also has to overcome much of the cell wall structure. Its passage through the wall of Gram positive cells is probably much easier than in Gram negative cells due to the absence of the outer membrane. Its small size, 323 Da, makes it possible to penetrate the peptidoglycan cell wall without difficulty and this is followed by a passive transport process across the cytoplasmic membrane by its hydrophobic nature. Therefore, it may again be unlikely for any cell wall binding processes to be in action.

The exposure of Gram positive cells to chloramphenicol has been found to increase the thickness of the peptidoglycan cells wall (Hughes *et al.*, 1970; Chung, 1971; 1973). This has been attributed to "unbalanced growth" as defined by Shockman (1965). Inhibition of protein synthesis by the presence of chloramphenicol, or the absence of a nutritionally essential amino acid e.g. tryptophan or valine, can result in a continuance of cell wall synthesis and increased wall thickness while inhibiting protein synthesis. The thickening of the cell wall has been

proposed to be caused by continued deposition of new cell wall material at sites predetermined for cell division. These sites, due to the absence of protein synthesis, do not become divided and continue building up wall polymers thickening the cell wall thickness by 2-3 times. This wall thickening was very obvious from the electron micrographs obtained for cells grown in the presence of this antibiotic. In these experiments, the concentration of chloramphenicol used to treat *B. subtilis* was 4 times greater than the MIC value found for this organism (section 4.9), therefore having significant action upon the protein synthetic mechanisms.

The loss of dielectrophoretic collection of these antibiotic treated cells was in the lower frequency range, implicating cell wall and surface conductivity effects. The increase in cell wall thickness may therefore have had the effect of slowing the movement of charges through the cell wall. The cell wall has been described as containing large amounts of anionic polymers conferred by the teichoic acid proportion. The large negative charge in the wall therefore binds a large amount of positively charged counterions. Depending upon the strength of binding of the counterions, the polarisation of a cell by these conduction mechanisms may become slow as the movement of charge throughout the wall is hindered. Therefore an increase in wall thickness of 2-2.5 times will be predicted to increase the size of the cellular negative charge and its wall since additional anionic polymers will be synthesised. The greater number of negative charges could serve to slow the passage of counterions even further as they pass through the wall in response to the applied electric field. This could result in a reduction in cell polarisability in these lower frequency regions and reduce the level of dielectrophoretic collection as observed in figure 4.53.

Contrary to this explanation, the presence of additional anionic wall polymers could be thought to increase the surface negative charge and thus the surrounding counterion atmosphere. This increase in diffuse layer, which is often involved in low frequency polarisation mechanisms, would therefore be able to contribute more to the polarisation response and increase collection. This contradicts the explanation offered above, as this would cause increases in dielectrophoretic collection in the low frequency range rather than the observed reduction.

Any inhibition of protein synthesis is likely to produce an effect, although not necessarily immediate, on the protein composition of the cell. In Gram positive cells, the electric field can easily penetrate the conducting cell wall until the resistance of the insulating cytoplasmic membrane is encountered. Therefore any changes to the cytoplasmic membrane in Gram positive cells may cause differences to the cell polarisation. There is a great deal of protein material expressed in the envelope of Gram negative cells and within the cytoplasmic membrane of all species. Inhibition and reduction of the overall protein content will be likely to result in modifications to polarisation mechanisms. Proteins are often composed of many charged amino acids and normally possess very large permanent dipole moments. It has often

been commented that these membrane proteins are freely mobile in the phospholipid membranes (Vaz *et al.*, 1984; Kell & Harris, 1985; Harris & Kell, 1985). Their contribution to the overall polarisability by movement in response to applied electric fields could thus be very large, produced by both translational and rotational responses of the globular proteins. Reduction in the amount of protein may therefore significantly reduce the polarisability of cells. Since the movement of proteins in the lipid bilayer is diffusion controlled, the process will be relatively slow, dependent upon the fluidity of the membrane. The relaxation frequencies of membrane proteins can be found to vary significantly depending upon their mobility and distance that the proteins are able to migrate before encountering a barrier (Kell & Harris, 1985). Aqueous suspensions of globular proteins have been found to have relaxation frequencies within a decade of 1 MHz. Typical membrane proteins are regarded as having relaxation frequencies between 2-20 kHz (Kell & Harris, 1985), just below that reduction in collection observed in the spectra of chloramphenicol treated cells, though again this is dependent upon the membrane fluidity and upon the ratio of protein : lipid. Vaz *et al.* (1984) found that increased lipid : protein ratios resulted in more rapid diffusion processes.

Restrictions to the lateral movement of these membrane proteins by barriers are thought to be able to give relaxation frequencies as high as 100 kHz to 10 MHz, critical frequency being inversely proportional to the distance possible to move before encountering a barrier (Kell & Harris, 1985). To give a relaxation frequency of 100 kHz, the proteins may be able to move up to 10 nm before reaching a barrier. This correlates well with the observed frequency at which chloramphenicol treated cells undergo reduction in dielectrophoretic collection. This reduction may therefore be due to a reduction in the amount of protein in the membrane caused by the antibiotic action. The membrane proteins are able to undergo binding and loss of protons and charges from their structure and transfer them tangentially along the membrane. Loss of protein from the membrane would therefore presumably also have the consequence of reducing the amount of sites available for conduction of charges by charge hopping mechanisms.

The rise in DEP collection again after 100 kHz was probably due to the initiation of additional polarisation mechanisms such as the onset of membrane capacitive and Maxwell-Wagner interfacial polarisations.

The exposure of bacterial cells has been found to affect both surface charge and hydrophobicity measurements. Morris & Jennings (1975; 1977) noted a reduction in the polarisation of *E. coli* cells as measured by orientation responses at low frequencies following antibiotic treatment. This reduction was attributed to a neutralisation of the surface negative charge by binding of the antibiotics studied (aminoglycosides, streptomycin and neomycin). Similar work by Fomchenkov *et al.* (1979) also found a decrease in the dielectrophoretic response of *E. coli* after addition of the antibiotics. The antibiotics used were known to bind to the walls and gain

access to cells by the self promoted uptake mechanism, causing cell envelope destabilisation through displacement of surface divalent cations, possibly adding to the polarisability decrease. The further work by Morris & Jennings (1977) showed several different antibiotic types, both charged (positive and negative) and neutral to demonstrate similar effects of rapidly reducing polarisability.

Alternative explanations could have been related to reduction in surface conductivity effects by increased counterion binding by the adsorbed antibiotics, reducing both polarisability and electrophoretic mobility. Dealler (1991) examined the effect of exposure of bacterial species to certain antibiotics. It was suggested that exposure, even to sub-MIC levels, modified bacterial surface characteristics causing a shift in cell zeta potential from negative to positive values before any physical cell death was observed. A separate population of cells with different charge became established after antibiotic exposure, the cause of which was proposed to be a result of transmembrane potential changes affecting zeta potential. It was considered that antibiotic binding would have resulted in an immediate action on cell mobility and zeta potential, compared to the observed changes occurring over a period of around 1 h.

The exposure of bacterial cells to antibiotics, even at sub-MIC levels of antibiotics has generally been shown to reduce adhesion and hydrophobicity properties as previously described (section 2.10.3.4). Future experiments to further study the effects of these antibiotics would be beneficial, particularly to establish possible relationships between frequencies within dielectrophoretic spectra and hydrophobicity. By examination of such frequencies following exposure of cells to antibiotics, it may be possible to assess possible effects on adhesion. Since adhesion to human cells is an important factor in the cause of bacterial infection, this technique may thus enable rapid screening of antibiotics to examine effectivity against disease.

4.14.6 Spheroplast Formation

Pohl (1978) commented on a temporary decline of DEP collection following exposure to 1 mM EDTA, attributed to a chelation of divalent cations from the local environment and destabilisation of the cell outer membrane. The use of EDTA here, was necessary to allow more efficient action of lysozyme by enabling easier penetration of the enzyme through the outer membrane of the Gram negative cells. To eliminate similar effects of reduction in DEP collection of spheroplasts, EDTA was also added to the control cells in equal concentrations. Thus any changes in the dielectrophoretic frequency spectrum should be attributable wholly to the action of lysozyme on the cell wall polymers.

Following exposure of *E. coli* cells to lysozyme in the presence of EDTA, resulting dielectrophoretic spectra were found to have decreased significantly compared to control cells.

This reduction in dielectrophoretic collection of lysozyme treated cells was thus attributed to disintegration of the peptidoglycan wall material produced by the enzymic degradation of the linkage between N-acetylmuramic acid and N-acetylglucosamine units. Around 1000 lysozyme molecules have been found to be sufficient for spheroplast production (Marvin & Witholt, 1987). The procedure used in these experiments produced spherical bodies as determined by phase-contrast microscopy, similar to those found by Birdsell & Cota-Robles (1967). These bodies were considered to be spheroplasts of *E. coli* produced by lysozyme treatment.

As discussed previously, the high dielectric constant of Gram positive cells at low frequencies has been attributed to the cell wall material. The removal of wall material by lysozyme to yield protoplasts was found to cause significant reductions (almost two orders of magnitude) in dielectric constant at frequencies lower than 100 kHz (Einolf & Carstensen, 1969), the β-dispersion being due to the cytoplasmic membrane (Pauly, 1962). The effective conductivity of the cell was also found to be reduced by removal of wall material. This reduction in dielectric characteristics of the bacterial cell would ultimately reduce polarisation and so, positive dielectrophoretic collection at low frequencies as found by Inoue *et al.* (1988). Similar results might have been expected with the Gram negative spheroplasts produced here. However, the outer membrane present on *E. coli* cells possesses very good insulation properties, effectively shielding the interior from the electric field. Only at high frequencies was the membrane expected to become short circuited by the membrane capacitance. Therefore dielectrophoretic observations of changes in wall material would also be unexpected until electric field penetration had occurred.

Nevertheless, a significant decline in DEP collection was observed at these lower frequencies (and indeed, over the whole frequency range studied) thus implicating the permeabilisation of the outer membrane. Following EDTA treatment, the membrane may have become sufficiently injured for the electric field to access the cell interior. Penetration of the electric field into the spheroplast would allow the major contributions of wall conductivity mechanisms to become much more active underneath the membrane. Passage of ions along the peptidoglycan chains within the wall would become a significant polarisation mechanism at these low frequencies. In this case, the loss of cell wall material through the injured membrane would produce a notable change in polarisation mechanisms. The loss of cell wall conductivity and permittivity characteristics by peptidoglycan degradation would therefore be observed as a reduction in polarisability and spheroplast collection.

In addition to the reduction in collection of the spheroplasts, the shift in peak frequency from around 300-400 kHz to around 800 kHz compared to the control cells could also be attributed to the action of lysozyme. Destabilisation of the membrane by EDTA, and the lysozyme effect on the wall material is generally associated with a loss of LPS material and intracellular

components, including many ions. This ion loss would lead to a decline in intracellular conductivity and dramatic inhibition of cell conduction polarisation mechanisms and DEP collection. Similar reductions in ion concentrations within the walls would have similar consequences. Since these conductivity mechanisms are more prevalent at lower frequencies, reduction in the amount of wall polymers and counterions may result in a reduction in polarisation at these frequencies compared to higher frequencies. Thus the shift in peak may be a reduction in low frequency polarisation rather than increased high frequency mechanisms.

LPS loss may also cause reduction in surface charge due to their significantly anionic character. This would be detectable as an increase in zeta potential (i.e. becomes less negative) and so reduction in Debye length of electrical double layers as described in section 2.10.3.6. As a consequence, the diffuse atmosphere would be less influenced by electric fields at low frequencies, causing shifts in collection to higher frequencies in spheroplasts as observed.

As was discussed in section 4.4.1, lesser cross linking or polymer presence may have been expected to allow easier passage of ions through the wall material and increase conductivity polarisations. This, however, was in contradiction of the results obtained here with spheroplasts of *E. coli*, as it was presumably dominated by the more significant loss of charged intracellular and wall components into the medium.

Alternative explanations of the decrease in spheroplast DEP collection may again be related to osmotic effects as discussed earlier, to differences in shape between spheroplast and control cells or the binding of lysozyme within the cell wall.

It may be argued that the overall decrease in spheroplast collection may have been caused, not by the enzymatic effects of lysozyme treatment, but by differences in concentration. However, since a sucrose medium was used to prevent osmotic lysis, differences in viable count were not anticipated. Identical volumes, having the same cell concentration were used as control and lysozyme treated samples to avoid initial variation in concentration. In addition, differences in particle concentration between spheroplast and control cell suspensions do not explain the accompanying shift in frequency response.

4.15 Dielectrophoretic Counting

4.15.1 Pure Suspensions

4.15.1.1 Polystyrene Latex

The relative collection of each concentration of latex is shown in figure 4.55.

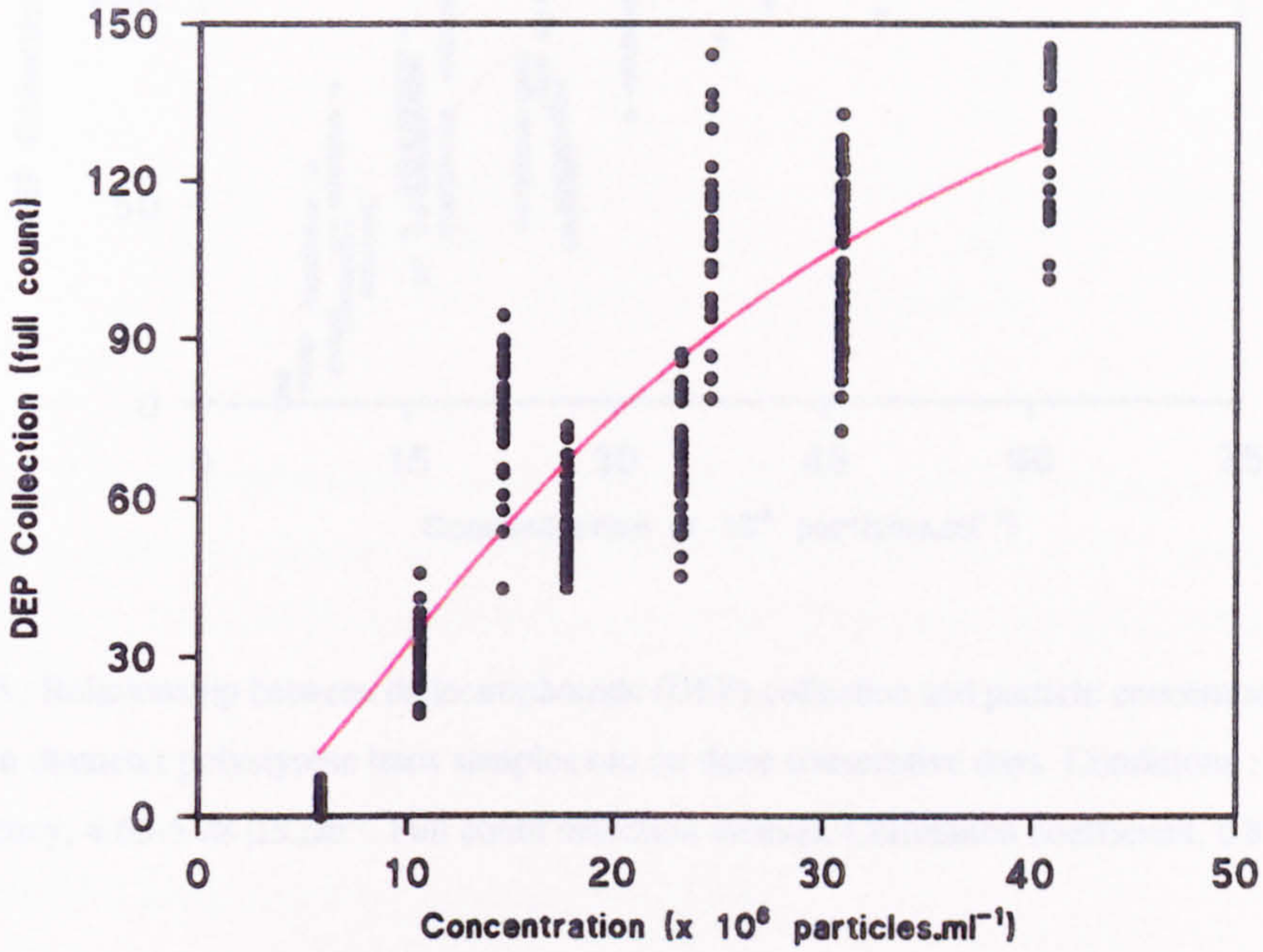

Figure 4.55 : Relationship between dielectrophoretic (DEP) collection and particle concentration in suspension, for 2.04 μm diameter polystyrene latex. Conditions : 12 V, 5 s pulse, 10 kHz frequency, 4.65-5.28 $\mu S.cm^{-1}$. Full count detection method. Correlation coefficient, 0.915.

Experiments were repeated several times for latex particles and a correlation between concentration and collection was found (shown in figure 4.56). The results showed a good correlation between dielectrophoretic collection and suspension concentration within the range of concentrations used. High concentrations of latex showed the same plateau of collection as discussed earlier. The relationship was found to be sigmoidal in shape as discussed earlier, due to the possible co-operative nature of dielectrophoretic collection. The curve, however, does have a linear region at lower particle concentrations which could be used for enumeration of suspensions of unknown concentration by comparison with these previously derived calibration lines. The limit of particle concentration for use of this linear region can be seen to

vary, depending upon the efficiency of the electrodes and collection for a given sample, in addition to other parameters such as conductivity and voltage.

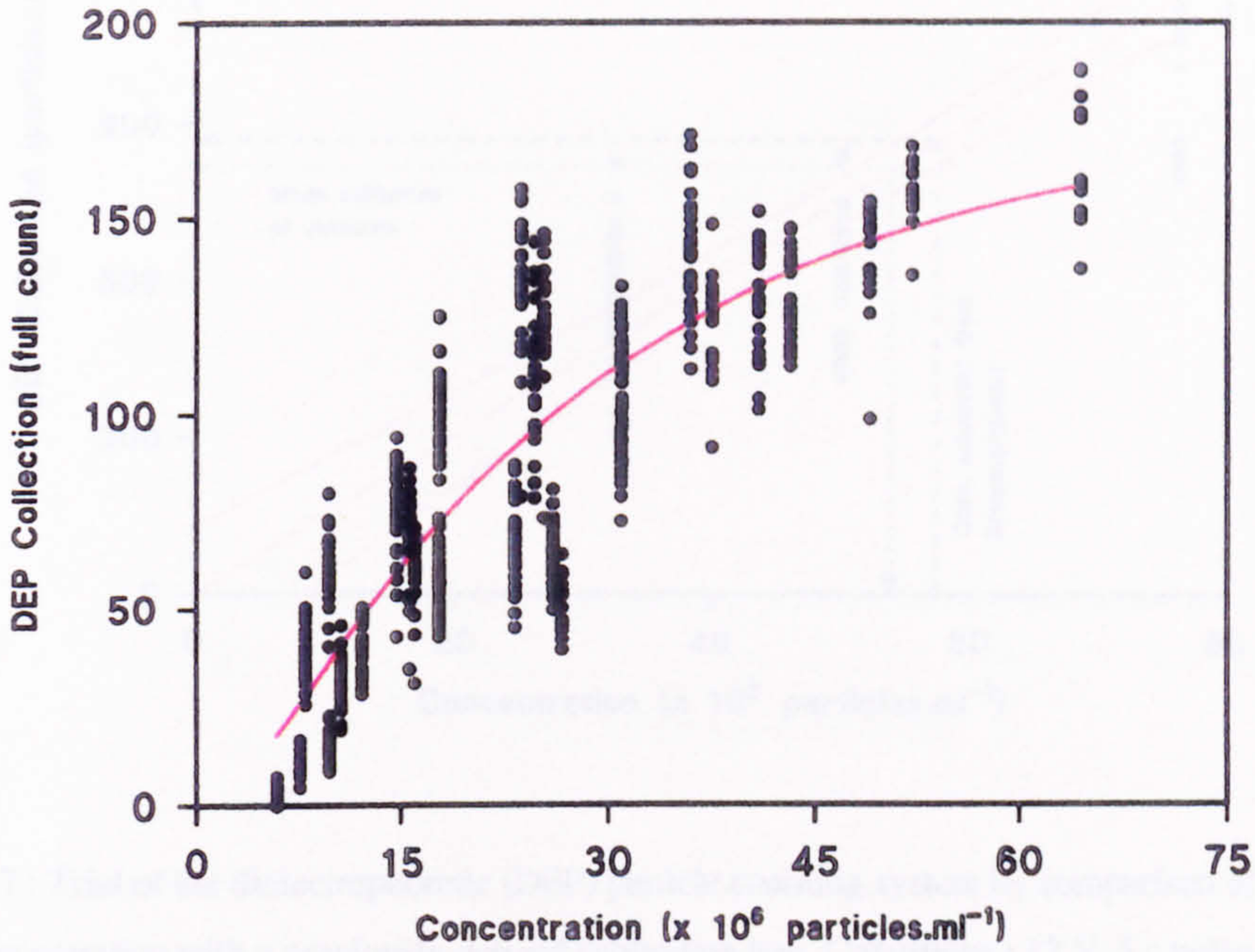

Figure 4.56 : Relationship between dielectrophoretic (DEP) collection and particle concentration in suspension, for 2.04 μm diameter polystyrene latex samples run on three consecutive days. Conditions : 12 V, 5 s pulse, 10 kHz frequency, 4.65-5.28 $\mu S.cm^{-1}$. Full count detection method. Correlation coefficient, 0.873.

4.15.1.2 Estimation of Unknown Concentrations

The relative collection of the three known concentration particle suspensions is shown in figure 4.57. In this instance, the line of best fit through the data points was a simple linear regression as fitted by the FigP software package rather than a sigmoidal curve. The equation of the line, $y = 15.1014x$, which gave a correlation coefficient (r) of 0.84 was used to predict the range of particle concentration (within confidence limits) of the unknown sample by its level of dielectrophoretic collection. The mean concentration found by haemacytometer counts was 57.35×10^6 particles.ml^{-1}.

Calculation of the 95 % confidence interval predicted a particle concentration range of 51.93-56.75 x 10^6 particles.ml^{-1} on the basis of the number of particles collected dielectrophoretically. By comparison with the actual particle concentration of the unknown sample (from haemacytometer counts) the concentration estimated by dielectrophoretic counts was found to be less than 9.5 % different from the actual concentration.

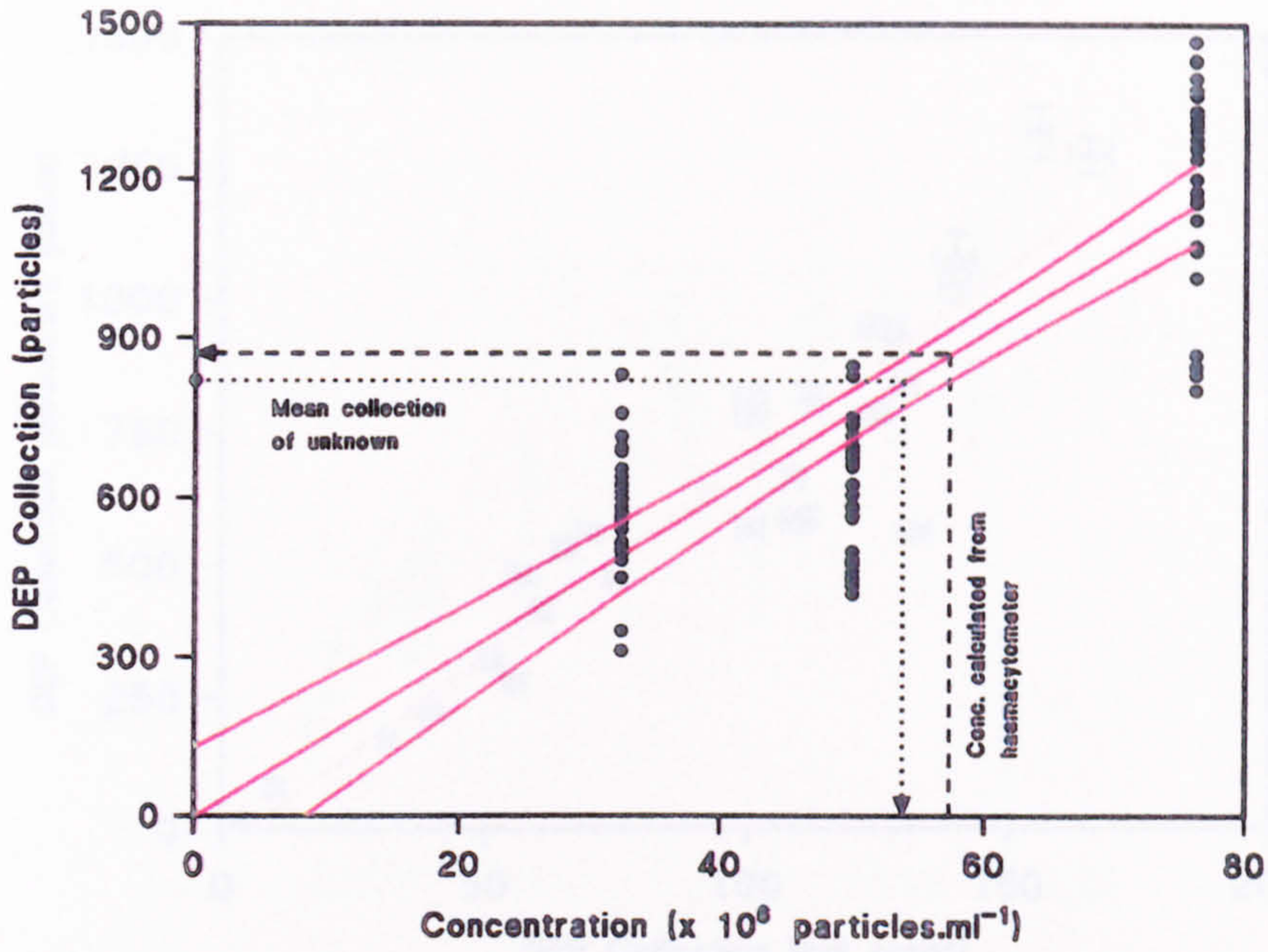

Figure 4.57 : Trial of the dielectrophoretic (DEP) particle counting system by comparison of an unknown sample concentration with a previously derived calibration line. Conditions : 12 V, 5 s pulse, 10 kHz frequency, 4.93-5.11 $\mu S.cm^{-1}$. Downward points count detection method. Correlation coefficient, 0.84. y = 15.1014 [± 0.67 C.I.].

4.15.1.3 Correlation of Counting Methods

The mean collection obtained using the counts were calculated for each suspension. The relationship between the full count and downward points count is shown in figure 4.58.

A linear regression line of equation y = 7.2844x - 41.599 was fitted to the data with a correlation coefficient (r) 0.942. Over the whole range of latex concentrations used, the data fitted very well to a linear relationship. This demonstrated that the downward points count produced a detection which is more than 7 times greater than the full count obtained for a particular suspension.

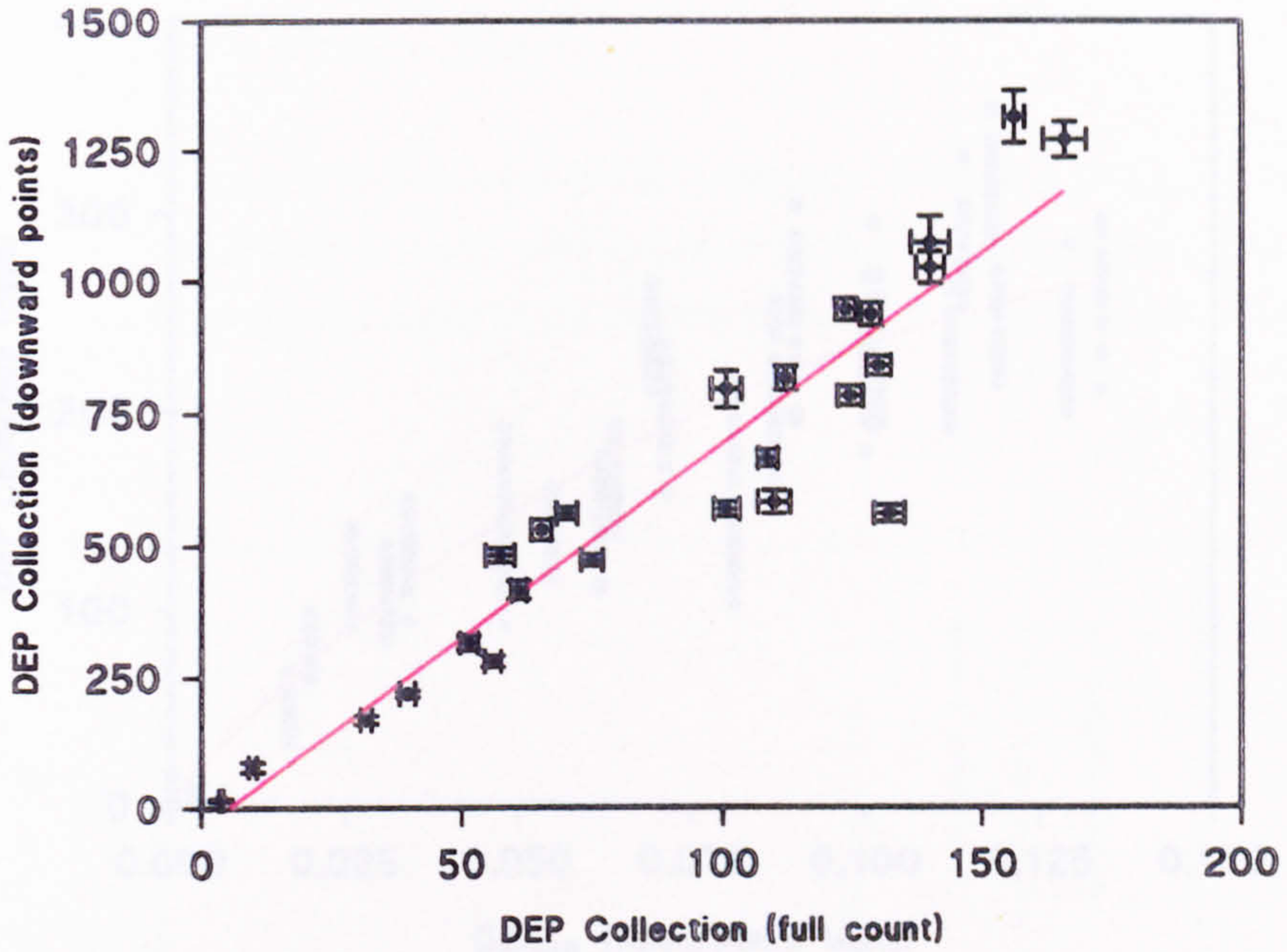

Figure 4.58 : Correlation between dielectrophoretic (DEP) full count and downward points count image analysis detection methods for suspensions of polystyrene latex particles. Conditions : 12 V, 5 s pulse, 10 kHz frequency, 4.65-5.28 $\mu S.cm^{-1}$. Correlation coefficient, 0.942. Each point is the mean plus standard error of 30 repeat pulse applications.

4.15.1.4 Bacterial Cultures

Significant relationships were obtained between the absorbance of a suspension and its dielectrophoretic collection for *E. coli, Serr. marcescens* and *B. subtilis* bacterial species.

A representative relationship is shown in figure 4.59 for two pure suspensions of *E. coli* which were undertaken on two consecutive days.

A sigmoidal curve was fitted to the data and gave a coefficient of correlation of 0.932, indicating a clear relationship between DEP and concentration. Increasing saturation levels can be seen to occur as the cell concentrations are raised. Conductivity variations were minimal throughout the experiments, though the more concentrated suspensions were generally prone to slightly higher conductivity values. This has been attributed to interaction with the medium, causing leakage of ions from bacterial cells (and removal of surface chemical groups from the latex spheres in the above experiments).

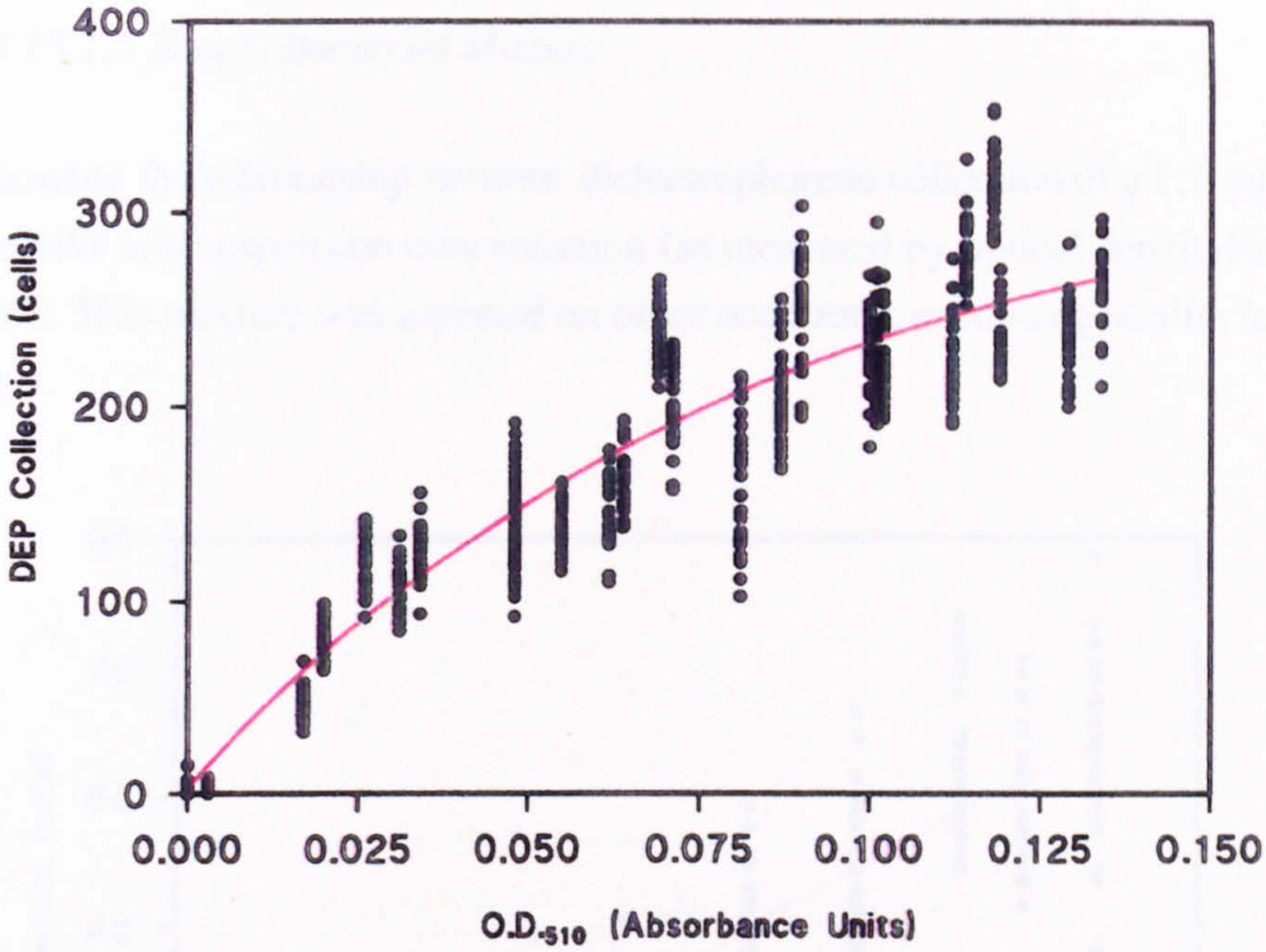

Figure 4.59 : Relationship between dielectrophoretic (DEP) collection and particle concentration in suspension, for *E. coli* 39323 run on two consecutive days. Conditions : 12 V, 5 s pulse, 1 MHz frequency, 24.5-28.5 $\mu S.cm^{-1}$. Full count detection method. Correlation coefficient, 0.932.

Additional correlation data is shown in table 4.6 for the other pure suspensions.

Particle	Correlation coefficient, r
Polystyrene Latex :	
Individual experiments	0.915, 0.925, 0.971
Data plotted together	0.873
Escherichia coli :	
Individual experiments	0.941, 0.945
Data plotted together	0.932
Bacillus subtilis	0.937
Serratia marcescens	0.87

Table 4.6 : Correlation of curves fitted to data of dielectrophoretic collection against particle concentration in pure suspensions.

4.15.1.5 Simple Bacterial Mixture

A plot showing the relationship between dielectrophoretic collection of a 1:1 mixture of *E. coli* and *B. subtilis* and suspension concentration (as measured by optical density) is shown in figure 4.60. This mixture was repeated on other occasions, producing similar levels of correlation.

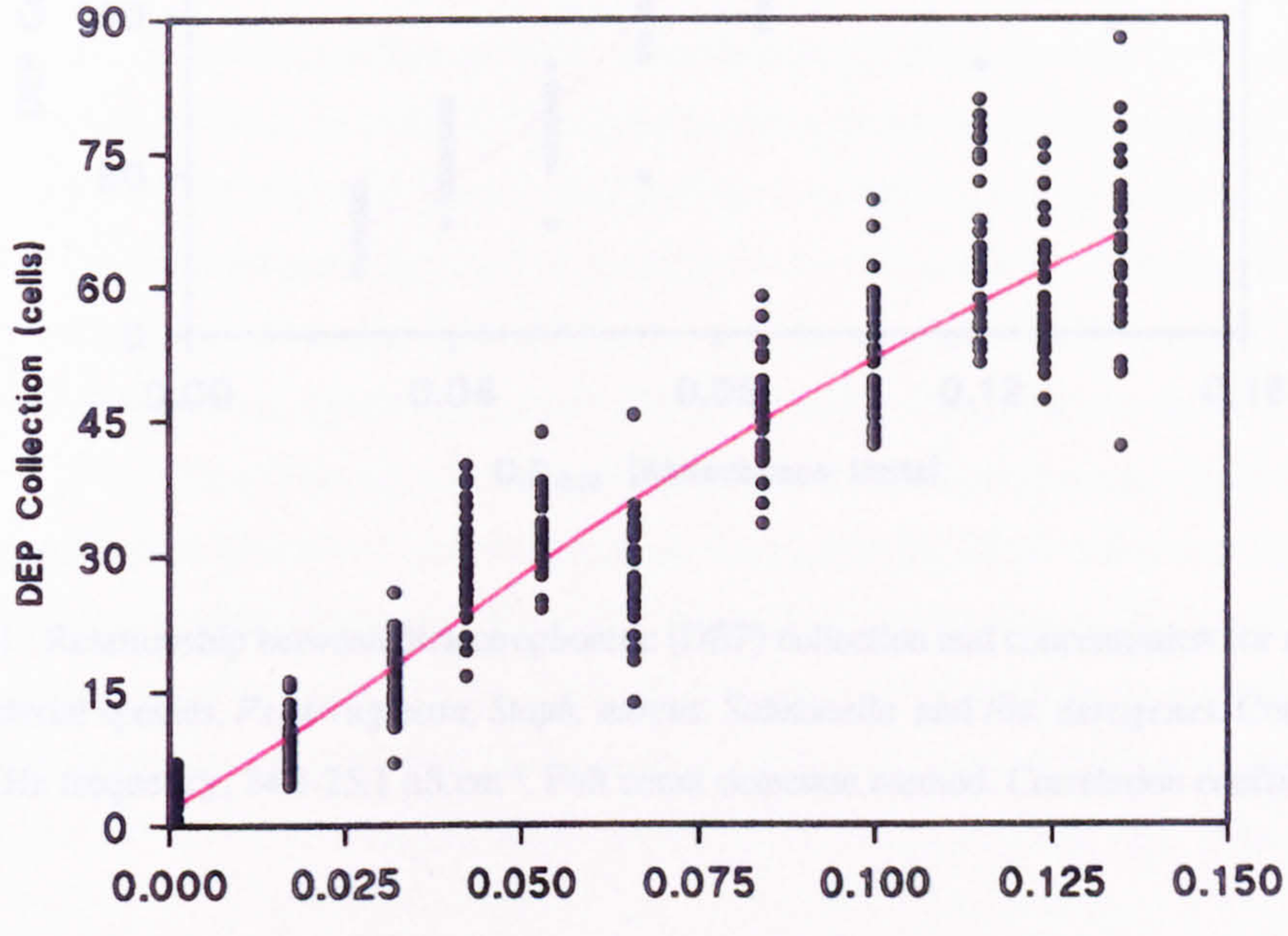

Figure 4.60 : Relationship between dielectrophoretic (DEP) collection and concentration for a mixture of two bacterial species, *E. coli* and *B. subtilis*. Conditions : 12 V, 5 s pulse, 1 MHz frequency, 24.5-25.2 $\mu S.cm^{-1}$. Full count detection method. Correlation coefficient, 0.948.

The data from this mixture of two bacterial species was fitted very well by the curve, producing a coefficient of 0.948. It should be noted that in this case, the best fitting sigmoidal line was reduced to almost a straight line over the concentration range.

4.15.1.6 Complex Mixtures

The relationship between dielectrophoretic collection and concentration (as measured by O.D.) of a mix of *Ps. aeruginosa, Ent. cloacae, E. coli* and *Salmonella* species is shown in figure 4.61.

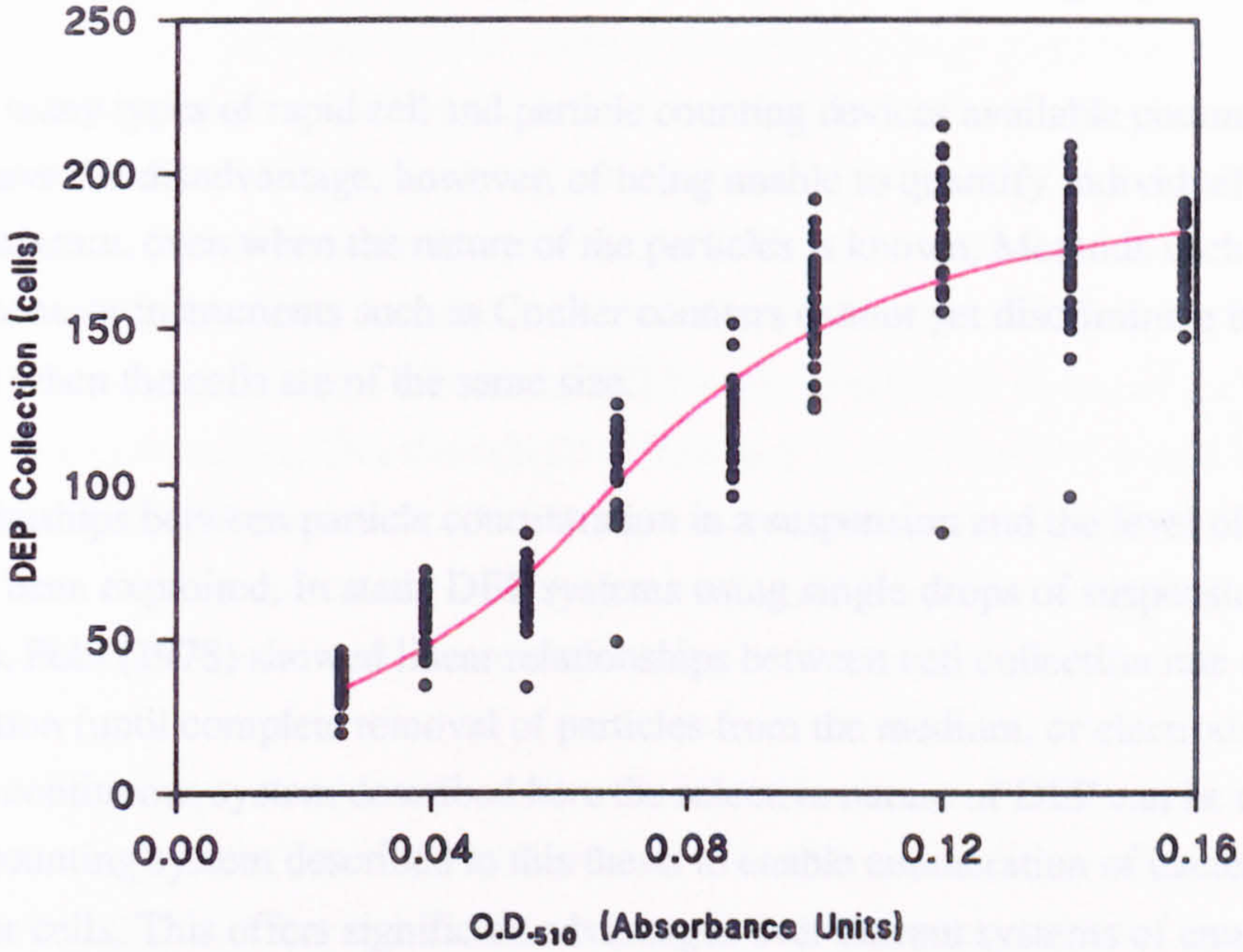

Figure 4.61 : Relationship between dielectrophoretic (DEP) collection and concentration for a complex mixture of four bacterial species, *Ps. aeruginosa, Staph. aureus, Salmonella* and *Ent. aerogenes*. Conditions : 12 V, 5 s pulse, 1 MHz frequency, 24.3-25.1 $\mu S.cm^{-1}$. Full count detection method. Correlation coefficient, 0.957.

A correlation of 0.957 was obtained. With this mixture, a highly sigmoidal curve was produced to fit the data, which was observed to reach the saturation point at concentrations having an $O.D._{510}$ above 0.1 Abs. Units collecting around 150 particles. Other mixtures of species were also run and their correlation coefficients are shown in table 4.7.

Particle	**Correlation coefficient, r**
E. coli/B. subtilis :	
Individual experiments	0.948, 0.905
Data plotted together	0.871
Ps. aeruginosa/Staph. aureus/Salmonella/Ent. aerogenes :	
Individual experiment (correlated against O.D.)	0.957
Individual experiment (correlated against total count)	0.932
Ps. aeruginosa/Ent. cloacae/Salmonella/E. coli	0.942
Serr. marcescens/B. globigii/B. subtilis	0.87

Table 4.7 : Correlation of curves fitted to data of dielectrophoretic collection against particle concentration in suspensions of mixed bacterial species.

4.16 Discussion of the Dielectrophoretic Particle Counting System

There are many types of rapid cell and particle counting devices available commercially. Many of these have the disadvantage, however, of being unable to quantify individual fractions within a mixture, even when the nature of the particles is known. Methods such as impedance measurement, or instruments such as Coulter counters cannot yet discriminate between species, especially when the cells are of the same size.

The relationships between particle concentration in a suspension and the level of DEP collection has never been exploited. In static DEP systems using single drops of suspension over electrodes, Pohl (1978) showed linear relationships between cell collection rate and concentration (until complete removal of particles from the medium, or electrode saturation). Using the continuous system described here the selective nature of DEP can be coupled with the DEP counting system described in this thesis to enable enumeration of bacterial species, particles or cells. This offers significant advantages over current systems of enumeration. Using appropriate calibration lines, the particle concentration of an unknown suspension could be quickly and accurately assessed. The DEP method of particle counting has a further potential benefit in that it could be used to selectively count one type of particle in a mixture of different types. By optimisation of particular frequencies or medium conductivities, specific particle types could be selectively collected as shown by Markx *et al.* (1994), and quantified.

The results described in section 4.15 show similar relationships to those found in the particle concentration experiments of figure 4.15. The reasons for the sigmoidal relationships produced by the data has been discussed previously, due to the co-operative collection and saturation effects. Such sigmoidal curves were produced by both the latex particles and bacterial species examined. However, some of the curves produced, especially figure 4.60 using *E. coli* and *B. subtilis* were approaching a linear relationship between DEP collection and cell concentration. Each of the curves fitted to the samples studied produced very good correlation coefficients with the data. Reproducibility of the relationships was found to be good, since samples run on three consecutive days also produced a good coefficient of correlation ($r = 0.873$) when the data was plotted together. Therefore, it was possible using these lines, to evaluate the concentration of cells or particles within an unknown sample of the same particle by comparison with one of these previously derived lines.

The nature of the sigmoidal relationship between cell or particle concentration and the extent of its collection makes it more difficult to accurately predict the concentration of particles in a sample than would a simple linear relationship. Nevertheless, even a sigmoidal relationship may be used for such purposes provided it is a consistent relationship for a particular set of

conditions. For concentration prediction purposes, the gradient of the slopes within a sigmoidal relationship are very important. A shallow gradient within the exponential phase of the curve would result in small increases in DEP collection caused by large increases in concentration. This could result in inaccuracies of predicted concentration due to any slight variations in the dielectrophoretic collection. The point of saturation is also important and should not be used for predicting concentration as no further increase in DEP occurs even with much greater concentrations of particles in suspension. Should the gradient of the exponential phase of the curve become very steep, large increases in DEP collection would be found for only small increases in concentration. Therefore slight differences in concentration would be easily observed by the great increase in collection, making prediction of a sample concentration much more accurate. For this reason it is advantageous to improve collection by use of optimum experimental conditions for a particular organism.

In section 4.15.1.2, an attempt was made to quantify an unknown concentration of latex particles in a suspension, by comparison with a previously derived calibration line. The calibration line, derived from previously dielectrophorised samples of latex, was used. The 95 % confidence interval of the dielectrophoretic collection predicted a particle concentration range which had a maximum of 9.5 % difference from the haemacytometer count. This estimation was produced from a line created from only three points, so accuracy of prediction could be markedly improved by using more suspensions of latex particles to generate more points on the calibration line. Nevertheless, even with such a basic calibration line a similar degree of accuracy was produced to that found with many existing rapid counting techniques currently in use. A further optimised calibration line could only improve the accuracy. In addition, error involved with haemacytometer or counting chamber estimates would also contribute to this observed difference.

One consideration with this method, is that the unknown sample concentration should be in the region covered by the calibration line, and ideally within the exponential part of the curve. This may cause some difficulties with very concentrated samples, and would necessitate a dilution procedure, possibly by running several samples from a dilution series.

Any variation in experimental condition or efficiency of electrodes would produce differences in the relationship between the particle concentration and the degree of its collection. For instance, changes in sample conductivity would result in a change in collection level. This highlights the need for standardised conditions in dielectrophoretic experiments as discussed earlier. Even under identical conditions of frequency and suspension conductivity, the great diversity of polarisabilities between different particle and cell types leads to many levels of dielectrophoretic yield. This variation in collection and sigmoidal DEP versus concentration curves found with different organisms, dictates that for each organism or mix of organisms

under study, a calibration line must first be derived. This method of dielectrophoretic counting is therefore inappropriate for use with samples in which the type of organism or composition of organisms within a mixture is variable. However, if reproducible samples can be obtained, this method can be reliable. In addition, testing for a particular organism e.g. *E. coli* can in theory be achieved, if the experimental conditions can be manipulated to selectively collect this species for enumeration. However, calibration lines necessary to compare with an unknown sample must be derived previously. To enumerate a single type of organism, conditions must be controlled to collect only that particular organism at the electrodes. Any additional collection by an unspecified particle would influence the count and the predicted concentration. It is therefore anticipated that this application would be most accurate for use on pure culture systems, or importantly, those which have been previously separated using the selectivity properties of dielectrophoretic methods.

Research is ongoing to determine experimental conditions which would selectively collect and separate specific bacterial species for use with this particle counter.

The bacterial suspensions used also showed good correlations between the fitted line and the data shown by the high correlation coefficients, producing similar relationships to that found for latex particles. Both pure cultures and mixed cultures were found to produce similar sigmoidal curves. The existence of such relationships with mixtures of several bacterial species was very encouraging and demonstrates the possibility for use as a bacterial counting system. No interference in collection was found to occur between the organisms, and both the larger Gram positive cells and small Gram negative cells examined within the mixture collected, as observed down the microscope. All of the species were previously found to collect well at the 1 MHz frequency. Therefore the relationship gave an idea of the number of total cells rather than any individual component. However, due to the different extents of collection at the 1 MHz frequency for each organism, some of the species would make more of a contribution to the collection than others. However, by manipulation of the conditions, the system could be made to selectively collect one species.

The relationship between the full count and downward points count was shown to be linear, with a high level of correlation between the methods ($r = 0.942$). This relationship, although expected to remain linear for all particle types, was also expected to have a gradient that was very dependent upon the nature of the particle. Polystyrene latex particles are very uniform, and due to their spherical shape, there should only be one southernmost point at any time. Thus a linear 1:1 relationship between downward points count and full count for latex was expected. This demonstrates the problems associated with the two counting methods, since a much greater downward points count was found compared with the full count. Thus, either the former count overestimates the number of points, or the full count does not count every particle

collected. The downward points count would be expected to decline in accuracy when using bacterial cells, due to increased irregularity of cell shape.

The suspension concentrations used, were quite high since this allowed a reasonably high dielectrophoretic yield to be possible during the short pulse duration. Image analysis, which detects and counts individual particles, is an efficient system for examination of much lower concentrations of cells (even single cells) using this dielectrophoretic counting method and this is currently under investigation. This is of obvious importance to the advancement of microbiological methodology since often only low numbers of bacterial contaminants are present in samples. Image analysed dielectrophoretic counting has the potential to quantify very low concentrations, down to even 1 cell in large quantities of diluent. For instance this counting system could potentially be used for rapidly assessing the coliform content of water samples. The current microbiological standard is set at a level of less than 1 coliform present per 100 ml of water. This count could possibly be performed in a few minutes, compared to most current methods used which can take up to 24 h to evaluate. The DEP technique could dispense with enrichment steps and allow rapid real time analysis of samples.

It is possible to obtain a database of calibration lines for each particle, run over many days, and which could be referred to for enumeration purposes. However as with many techniques, conditions must be identical and calibration is required to ensure electrode efficiency is identical from day to day. Electrodes can incur damage or build up of debris on the surface, thus modifying the non-uniform field produced and so altering DEP collection. This technique could also be used for electrode calibration purposes. Polystyrene latex are abiotic particles which collect reproducibly (see section 4.1.2.2) under identical experimental conditions. Therefore any discrepancies in dielectrophoretic yield using these particles is attributed to electrode anomalies. Changes in electrode efficiency could thus be rectified by increasing the voltage or by mathematical adjustment of dielectrophoretic results of experiments. This system then, is an almost real-time quantification method for particle suspensions offering selectivity while remaining non-invasive and reproducible under standard conditions.

Chapter 5 : General Discussion and Recommendations for Future Work

Following the early work on dielectrophoresis in the 1950s, two comprehensive texts were published, with particular relevance to bacterial cells and their dielectrophoretic collection (Chen, 1972 and Pohl, 1978). The majority of the research undertaken to date has been approached from the point of view of physicists. The work in this thesis takes a biological approach and in particular, examines modifications to standard reference DEP spectra brought about by treatments to, and upon, bacterial cell walls and surfaces. In addition, development and applications of a novel dielectrophoretic counting method have been described which could eventually be of significant benefit to the area of analytical microbiology.

Dielectrophoresis has received publicity due to its wide ranging applications, notably for cell separations and characterisation. Its many potential applications include bacterial identification, microbiological analysis of food and liquids, abstraction of particles from water or from hydrocarbons, cellular viability assessment, separation of cancerous cells from non-cancerous cells, infected blood and urine analysis, clean-up of atmospheric pollution, antibiotic sensitivity assessment and sperm separation, as well as many other enrichment processes.
Dielectrophoretic systems also exist at extremes of size, from large scale grid structures to microelectrodes. Microfabrication techniques are now very much at the forefront of research in this area and work is ongoing to demonstrate dielectrophoresis of viruses and plasmids, as well as linking techniques such as flow cytometry, capillary electrophoresis and polymerase chain reaction (PCR) with dielectrophoresis (Betts *et al.*, 1995; Betts W.B., Allsopp D.W.E., Goodall D.M., Brown A.P. & Milner K.R, 1995 - Unpublished Data).

To begin studying the effects of treatments upon bacterial cell dielectrophoresis, it was first necessary to investigate untreated cells. Upon initial investigation it was found that the majority of dielectrophoretic experiments in the literature, had been undertaken using non-standardised conditions. In order to accurately compare a frequency spectrum of one particular organism to that of another, it is necessary to ensure that both are run under identical conditions. Therefore, in this thesis, an attempt has been made to identify a set of standard conditions under which dielectrophoretic experiments, using the patented continuous flow-through system of Betts & Hawkes (1994), could be run. Preliminary experiments were undertaken using both bacterial cells and abiotic polystyrene latex spheres to optimise the conditions used in typical dielectrophoretic experiments. These experiments have shown linear relationships of DEP collection with voltage and pulse length, and more complex relationships with particle concentration, conductivity, frequency and pump speed using this system. Optimised conditions were found to be attained using a 12 V, 5 s pulse duration, 10 rpm collection speed and a frequency range of 1 kHz to 50 MHz. Ideal conductivities were at 24.5 $\mu S.cm^{-1}$ for

bacteria and 4.45-4.5 $\mu S.cm^{-1}$ for latex, producing good DEP collection and definition of frequency spectra. Particle concentrations used for bacteria were typically at $O.D._{510}$ values of 0.11 Absorbance Units, with latex suspensions being made with 12 µl stock suspension in 10 ml deionised water for frequency spectra experiments.

Other experiments showed that the viability of some bacterial species did not undergo significant declines in viability over a 3 h period in recirculating deionised water (section 4.1.1). However, it was previously observed that some viability is often lost over even short periods in dilute environments. It is therefore advisable to make a thorough study of survival of any organism in deionised water or low ionic strength medium prior to dielectrophoretic experiments. Alternatively, iso-osmotic media could be utilised as previously discussed.

Ever since the introduction of Koch's pour-plate method for assessing viability, the search has been on for a more rapid and equally accurate method to supersede it. The majority of rapid bacteriological tests involve an incubation or pre-enrichment step to obtain large numbers of cells, each having the additional lag time associated with growth. Dielectrophoresis has been shown to be an emerging technology for almost real-time separation and characterisation of particles, obviating the need for lengthy enrichment procedures.

In 1966, Pohl and Hawk showed that viability status had a significant effect on dielectrophoretic spectra, demonstrating dielectrophoretic separation of living and dead yeast. Similar results were found by Hawkes *et al.* (1993) and Quinn *et al.* (1995) using other organisms. When looking at the relationship between the viability of cells and their dielectrophoretic responses, it must be realised that changes in viability can be brought about in a variety of different ways. The use of dielectrophoresis in many experiments (and also in "real world" samples), is likely to encounter samples which might contain substantial proportions of both viable and non-viable cells, and also those with various intermediate states of injury. To identify a particular organism on the basis of its 'fingerprint' spectrum, frequency trends need to be highlighted in order to account for its viability status. Each method of bringing about changes in viability will have a range of actions on the bacterial cell, particularly on wall and surface characteristics, resulting in a diversity of frequency responses upon exposure of the treated cells to non-uniform electric fields. For instance, UV treatment of bacterial DNA will eventually influence the formation of membrane proteins, but this may take much longer to change the dielectrophoretic spectra than a physical treatment of the cell wall itself. Different bacterial species, and even strains of the same species can also possess different cell structures, all of which will affect the dielectrophoretic response. Experiments have been performed on a wide variety of organisms to identify ways in which frequency spectra are altered by different cell structures and treatments. The majority of frequency dependent responses, at least over the frequency range examined here, are related to cell wall and surface responses.

The aim of part of this thesis was to demonstrate the wide diversity of even closely related bacterial cells and the tremendous effects of even minor changes to cells upon their dielectrophoretic response. The basic cell structure and surface chemistry largely determine its electrical properties and thus are determining factors of how a cell reacts to the application of non-uniform electric fields in dielectrophoresis.

Bacterial cells are very complex organisms and their cell structures vary greatly from one species, and even from one cell, to the next. Any process that affects cell structure or size, is likely to influence the dielectrophoretic frequency response. One of the most recurring complications of experiments performed during this work, was the interconnected nature of cell structure biosynthetic mechanisms. Many of the processes of growth have consequential effects upon the composition of the cells under study. This results in difficulties when attempting to employ specific treatments to cells. Experiments undertaken to vary the EPS component of *Klebsiella* met with such difficulties. Variation of growth media, to influence the carbon:nitrogen ratio, determines the level of EPS produced by the cells. However, this has additional effects on the nature of intracellular glycogen storage granules and will also affect the composition of the outer membrane. Even intrinsic effects such as cell growth was found to affect the spectrum. The growth phase of bacterial cells was found to cause shifts in frequency response, exponential phase cells collecting better than stationary phase cells at lower frequencies. This may have been due to the larger cell size of exponential phase cells influencing surface conductivity effects or to modifications to the protein content in the outer membrane of the Gram negative cells.

Similar problems were encountered when using antibiotics to treat the bacterial cells. It is commonly found that antibiotics do not have a single action, and the effect is very much dependent upon the concentration of antibiotic used. Sub-MIC levels of antibiotics were found to have important effects upon reducing adhesion and hydrophobicity, as well as causing changes in the Gram negative outer membrane components of protein and LPS. Low levels of nalidixic acid were shown to elicit a mechanism of significant elongation. Thus any observed effects upon dielectrophoretic frequency spectra, while being due to the action of antibiotic, could be caused by one of a number of reasons. Indeed, the most obvious change e.g. cell elongation, or cell wall thickening, caused by antibiotic action may not responsible for dielectrophoretic effects. Smaller changes such as protein composition may actually account for the observed response. Even the employment of strict control regimes will not necessarily eliminate these interactive effects.

The great number of connected pathways of a response to treatment makes it very difficult to confidently attribute spectral changes. Due to the theoretical basis of many polarisation mechanisms, a number of possibilities exist to explain observed dielectrophoretic changes, often involving both surface charge effects and physiological changes. Indeed, the same effect can be interpreted in several ways. For example, the loss of the LPS components from the surface of Gram negative cells can cause a decrease in negative surface charge and so reduce polarisation by reducing the size of the electrical double layer. Conversely, the same loss of LPS can be thought to improve polarisation by the loss of counterion interaction and hindrance with the negative charges of the polymers resulting in faster charge hopping. Thus the same effect can explain observed results in opposing ways. Indeed, the two opposite explanations may both contribute and interact to give the observed result.

The nature of the growth medium has also previously been found to have major implications with regard to the dielectrophoretic spectra of bacterial cells due to effects upon the cell structure. The protein content of the outer membrane has been found to change in both composition and amount of protein when grown in different media. The teichoic acids present within Gram positive wall structure have also been found to become converted to teichuronic acids during growth under limiting phosphate conditions. Such changes in cell structure will have significant effects upon polarisation mechanisms, particularly surface ion movement and diffuse atmosphere polarisation. This problem is evident even under tightly controlled conditions within a laboratory situation, so will be more exacerbated within "real-world" samples, where bacterial cells will have a wide diversity of growth and nutritional backgrounds. Reproducible spectra for species grown under identical conditions and using the same experimental parameters can be obtained, but to examine a particular trait is very difficult. To attempt identification with these samples is, at best, a very difficult undertaking. A large database of spectra obtained under different conditions would be necessary and possibly the most that could be expected might be a broad classification of cells.

The suspending medium used for dielectrophoretic experiments was also found to be very important in influencing the dielectrophoretic spectrum produced by an organism. Since the frequency response of a cell is a result of the interaction between the dielectric properties of both the cell and the suspending medium, modification of the medium can have very significant effects. The replacement of deionised water with mannitol or sucrose as the suspending medium resulted in shifts of the particle spectrum to greater frequencies. This was thought to be due to the reduced permittivity of these latter two media, enabling the particle permittivity to be in excess at higher frequencies. Deionised water does not undergo relaxation until the much greater frequency of 20 GHz, so is still highly polarisable at a 50 MHz frequency, reducing the excess permittivity of the particle at this frequency. The nature of the suspending medium also

leads to fundamental changes in the bacterial cell structure. The plasmolytic effects of concentrated sugar solutions on bacteria has been discussed previously and is well documented. In deionised water, the negatively charged phosphate groups present on the polymeric cell wall components are less shielded causing a repulsion of fibres and elongation of the cell.

Conductivity effects within the medium were also found to be important. Increasing conductivity caused a decline in collection and shifts in frequency for similar reasons. Higher conductivities were found to decrease the relative polarisability of the particle or cell compared to the medium, so opposing particle collection.

Much theoretical work on dielectrophoresis has been undertaken in an attempt to explain polarisation mechanisms. Experimental work has mainly consisted of associating experimentally determined relaxation times and dielectric behaviour with theoretical models. However, very little experimentation has been performed to prove these mechanisms beyond doubt. Thus the proposed explanations for some of the results obtained here are based solely upon the mechanistic theory proposed by Pohl (1978) and subsequent workers.

Useful future work would be to relate the effects of cell treatments to definite polarisation effects. For instance an alteration of surface conductivity by a treatment could be examined by monitoring surface conductivity using ion-specific microelectrodes or pH dependent fluorophores such as those used by Teissié *et al.* (1985) to observe ion movement over the surface. Such experiments would possibly be facilitated by dielectrophoretic experiments on single cells. It is also of interest to examine whether polarisation of cells can alter localised chemical processes and compartmentalisation. Migration of proteins under the influence of an applied electric field could disturb many specific transport mechanisms. The effect of cell deformation by polarisation may lead to irreversible cell damage, even though loss of viability due to dielectrophoresis has not be observed. Such effects would be very useful to examine for the purposes of clinical applications, especially when using human cells. It would be necessary to maintain complete function in cells such as sperm or bone marrow stem cells after dielectrophoresis if re-implantation of these was required.

Surface conductivity effects have been proposed to occur at low frequencies due to the large pliant response of the electrical double layer. Restrictions were imposed by the available frequency range of the signal generator used and it is recommended that future experiments should be performed over a much greater frequency range, since much of the dielectrophoretic frequency range has not been observed and important responses after treatments could have been easily overlooked. However, problems are associated with the use of lower frequencies, relating to the nature of the microelectrodes used for dielectrophoretic experiments. Using these

conductivities, frequencies lower than 1 kHz have been found to produce electrolytic effects within the medium. This has often resulted in the stripping of the aluminium from the glass substrate. Electrode polarisation effects also become more of a problem at these lower frequencies, therefore requiring other electrode materials. Difficulties such as these could be overcome by the use of the more resistant gold covered titanium electrodes or platinum black coated platinum electrodes.

The effect of electrode variation was also examined in this work and a latex calibration method proposed to attempt to standardise the electrode collection quality. The extent of DEP collection is very much related to particle concentration in the circulating suspension. It was proposed by Archer *et al.* (1993b), that for a continuously recirculating system such as that used here, dielectrophoretic collection had a linear relationship with pulse duration until limited by electrode capacity or other factors, since particles are continuously brought close to the electrodes permitting a rapid attraction. Furthermore, increasing the particle concentration in the circulating suspensions enabled a higher number of particles to pass into the effective field allowing them to become available for dielectrophoretic collection. Dielectrophoretic collection was therefore thought to be largely linearly proportional to particle concentration. The work performed in this thesis further examined the relationship between particle concentration and dielectrophoretic collection and found it to be sigmoidal rather than linear. At low concentrations only a few particles are collected at electrodes. As more cells are collected at increasing concentrations, their presence is likely to further distort the electric field, making it more non-uniform and causing more rapid attraction of additional particles. This co-operative effect accentuates collection until a saturation point is reached. At high concentrations the large DEP collection saturates electrodes and holds other particles further away from them in weaker field strength regions. Here the flow of the suspension can overcome the DEP attractive force and shear particles from the electrodes. This leads to a plateau in collection level. The relationship between collection and concentration was examined in order to assist the development of a potential counting system. The dielectrophoretic system has never before been suggested as a possible counting device, and actually has potential as a selective counter by application of specific conditions to abstract and enumerate particular particles of interest.

The experiments undertaken in this thesis have been bulk effects relating to the dielectrophoretic response of the majority of cells within a suspension. Early work described in the literature using static systems, had measurement of dielectrophoretic yield recorded by manual counting of pearl chain length. The dielectrophoretic collection rate (DCR) was calculated using the number of cells that accumulated per unit of time and per unit length of the electrode.

The implementation of image analysed dielectrophoretic experiments has increased the sensitivity of detection from minimum cell concentration of around 10^7 cells.ml^{-1} to as low as a single cell in a much larger volume. The only limiting factor of the cell concentration analysed is effectively the ability to produce the characteristic dielectrophoretic frequency spectrum. This dielectrophoretic collection makes the assumption that all of the particles are identical, a supposition which is very seldom an accurate depiction of reality. Within a bacterial culture, there are many different stages of cell cycle growth each with a range of sizes and structural characteristics. Thus the dielectrophoretic force may be sufficient to collect cells from each category, yet the actual frequency response of the individual groups may be significantly different. Therefore the sample frequency spectrum may be a composite of many diverse responses. There is no evidence to suggest that the overall frequency spectrum obtained is representative of the most common particle grouping, since it may be greatly influenced by a few 'rogue' frequency responses. Perhaps a more accurate method of assessing the dielectrophoretic response is the examination of individual cells. One could perhaps argue that a spectrum is notionally difficult to obtain using a single particle. However, it is the dielectrophoretic force which determines the degree of collection at any frequency. The size of this force has been found by previous workers using single cells at different frequencies, by looking at cell balancing techniques. For instance, the force can be calculated by minimum field voltage which can suspend a particle against an opposing force of gravity (Crane & Pohl, 1977). Other methods could involve tracing particle trajectories towards an electrode when opposed by a perpendicular suspending medium flow. Using this method, it can be predicted that weaker dielectrophoretic forces will result in a longer parabolic trajectory due to a more significant particle movement in the direction of the flow compared to the component of movement towards the electrode.

More work on trajectories and single cell analyses is encouraged for application purposes since in many cases very small numbers of cells are available for study. For instance, separation of non-cancerous bone marrow stem cells from cancerous cells could be performed on a single cell basis. Only very few non-cancerous stem cells are necessary for re-implantation back into patients following chemotherapy. Conversely, further work on the analysis of large volume samples is also necessary, particularly following the emergence of interest in the examination of water-borne viruses (Sellwood & Wyn-Jones, 1996). It was originally suggested by Chen (1972) that since the dielectrophoretic force is proportional to volume, the collection of small particles such as viruses will be overshadowed by the diffusional forces associated with Brownian motion. Limits for dielectrophoretic collection were proposed to be in the range 0.01-0.1 μm, effectively excluding some viruses. However, recent work by Muller *et al.* (1996a, 1996b) has shown the manipulation of particles of 14 nm in diameter (including viruses) by electric fields, effectively demonstrating the opportunity for future dielectrophoretic applications in virology. As yet, however, viruses remain inadequately studied by

dielectrophoretic experiments, though many new electrode geometries even down to sub-micron dimensions are being manufactured to increase the effective collection of particles.

Though complications with dielectrophoretic experiments have been highlighted in this thesis, many possible applications have also been proposed. A great deal of progress for dielectrophoresis over the next decade is anticipated, especially within the areas of analytical biology and clinical microbiology, as this technique becomes more widely studied.

Appendix 1 : Derivation of Dielectrophoretic Force Equations

When a perfectly insulating particle in a perfectly insulating medium is subjected to an external electric field (E_{ext}), the field is modified and distorted by the particle polarisation, which may be represented as a point dipole at the sphere centre. The field inside the sphere (E_{int}) can be expressed as

$$E_{int} = E_{ext} \frac{3K_m}{K_p + 2K_m}$$

where K_m and K_p are the relative dielectric constants (relative permittivities) of the medium and particle respectively.

Since the dipole per unit volume, **P**, as described previously is

$$\mathbf{P} = \chi_E \, \varepsilon_o \, \mathbf{E}_{int}$$

the induced dipole vector for the whole particle, μ, is equal to **P**v

i.e. $$\mu = \tfrac{4}{3} \pi a^3 \chi_E \, \varepsilon_o \, \mathbf{E}_{int}$$

$$= \tfrac{4}{3} \pi a^3 \chi_E \, \varepsilon_o \frac{3K_m}{K_p + 2K_m} \mathbf{E}_{ext}$$

$$= 4\pi a^3 \, \varepsilon_o \, K_m \frac{K_p - K_m}{K_p + 2K_m} \mathbf{E}_{ext}$$

$$= 4\pi a^3 \, \varepsilon_m \frac{\varepsilon_p - \varepsilon_m}{\varepsilon_p + 2\varepsilon_m} \mathbf{E}_{ext}$$

where K_m and K_p are relative permittivities and ε_m and ε_p are absolute permittivities of the medium and particle respectively.

Appendix 2 : Exopolysaccharide Structures

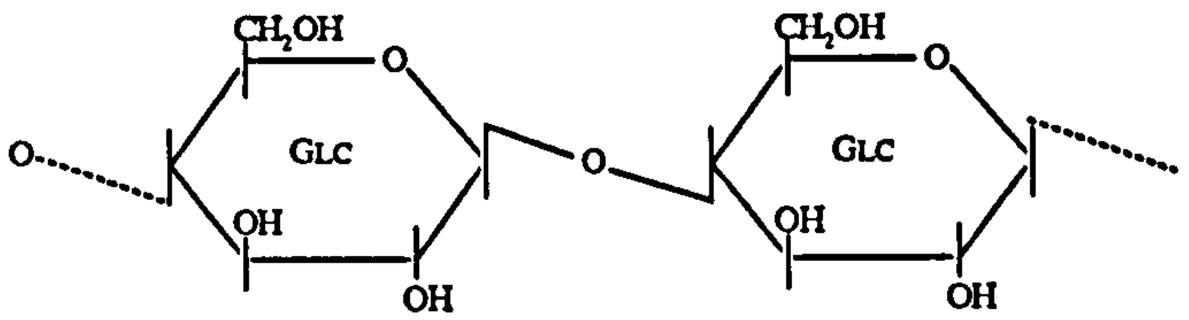

Figure A1.1 : Repeating subunit of cellulose.

Figure A1.2 : Structure of a levan homopolysaccharide.

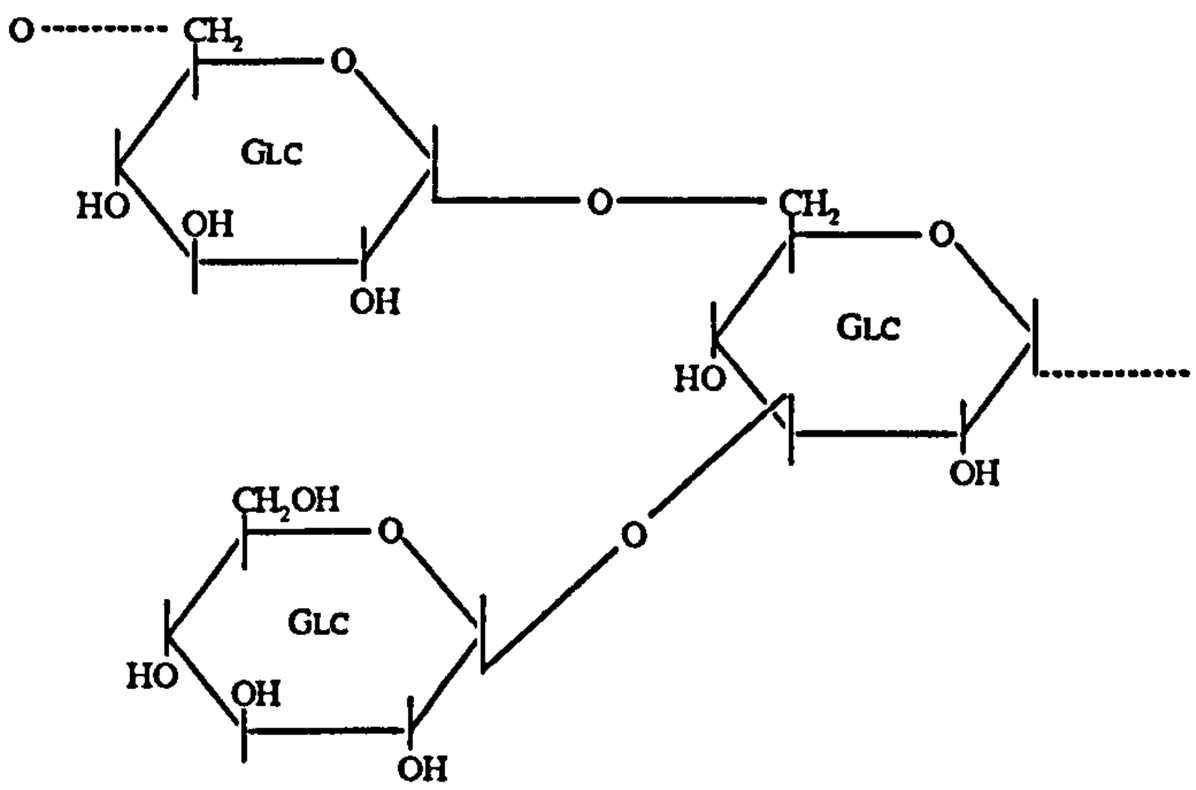

Figure A1.3 : Structure of a dextran homopolysaccharide.

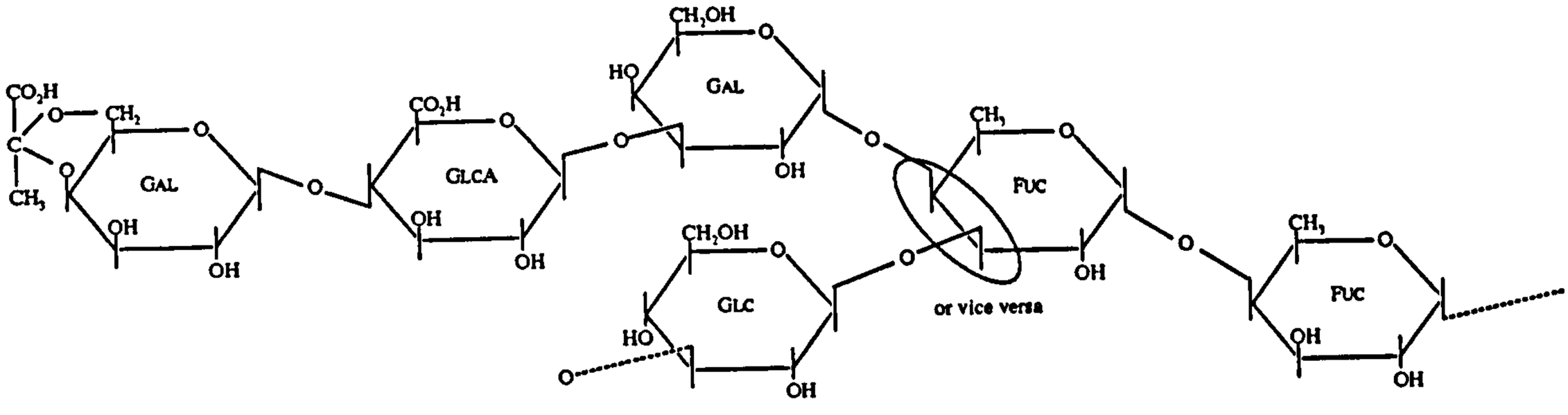

Figure A1.4 : Structure of colanic acid heteropolysaccharide.

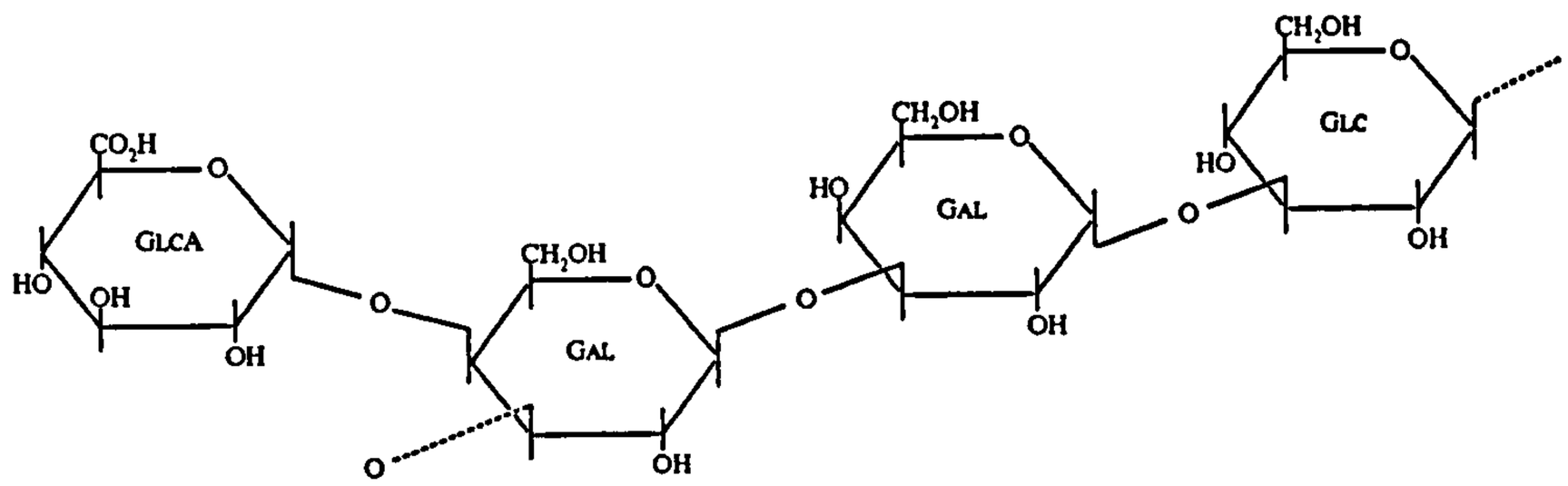

Figure A1.5 : Structure of *Klebsiella* Type 8 heteropolysaccharide.

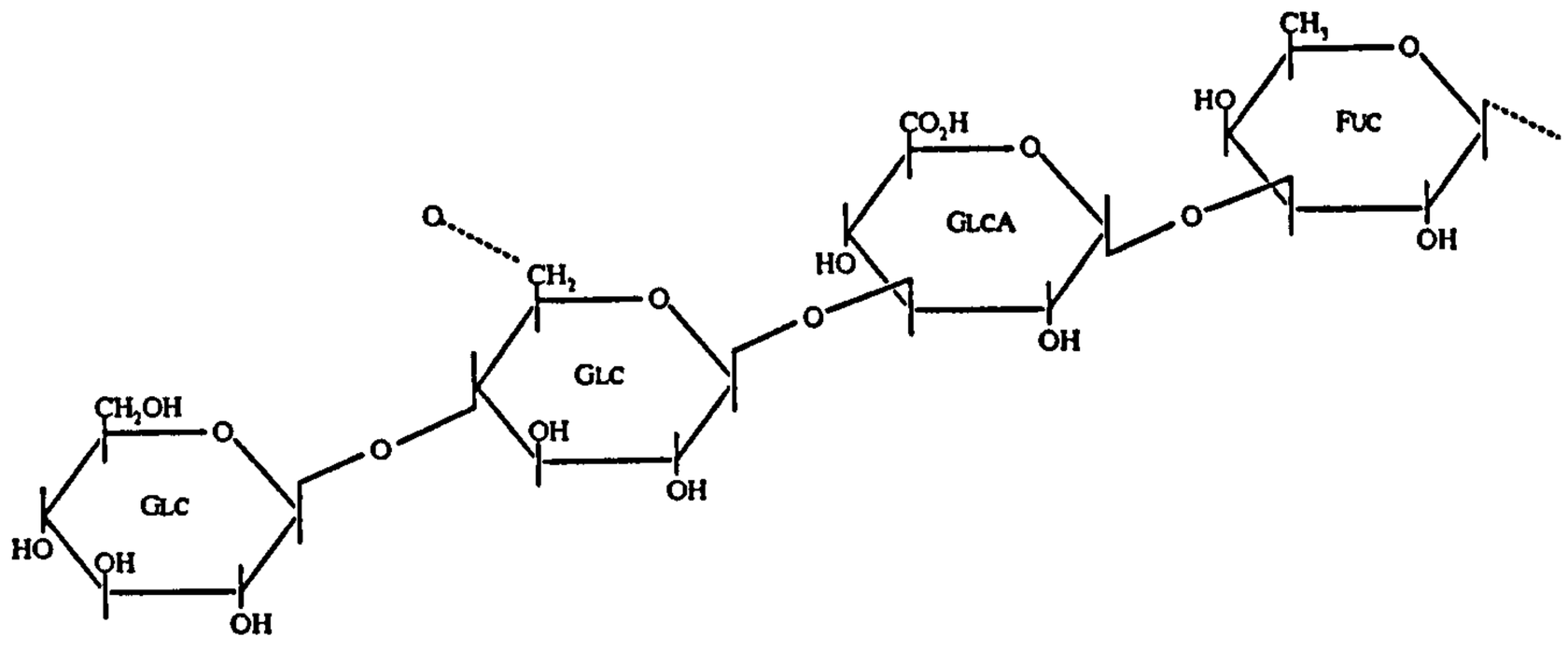

Figure A1.6 : Structure of *Klebsiella* Type 54 heteropolysaccharide.

Appendix 3 : Media Recipes

Klebsiella Medium (KM)

KH_2PO_4	3 g
K_2HPO_4	7 g
casamino acids	10 g
(or ammonium sulphate)	5 g
$MgSO_4$	0.1 g

Dissolve in 1 l distilled water and supplement with 1 % (unless stated otherwise) glucose (autoclaved separately).

Ruthenium Red Staining Solutions

Pre-staining fixative solution

3.6 % v/v glutaraldehyde in water	0.5 ml
0.2 M cacodylate buffer (pH 7.5)	0.5 ml
1.5 $mg.ml^{-1}$ ruthenium red solution (in water)	0.5 ml

Ruthenium red staining

2 % w/v osmium tetroxide	0.5 ml
0.2 M cacodylate buffer (pH 7.5)	0.5 ml
1.5 $mg.ml^{-1}$ ruthenium red solution (in water)	0.5 ml

Phosphate Buffered Saline (PBS)

NaCl	8 g
KH_2PO_4 (anhydrous)	0.2 g
Na_2HPO_4 (anhydrous)	1.15 g
KCl	0.2 g

Dissolved in 1 l distilled water. Autoclave at 121 °C/17 $lb.in^{-2}$ as necessary.

Phosphate Buffer (0.1 M)

Make solutions : 0.2 M Na_2HPO_4 and 0.2 M NaH_2PO_4 in distilled water.
Mix both components in the correct proportions to give the desired pH.
Dilute with an equal volume of distilled water. Autoclave at 121 °C/17 $lb.in^{-2}$ as necessary.

e.g. For pH 6.0	For pH 7.0
6 ml 0.2 M Na_2HPO_4	61 ml 0.2 M Na_2HPO_4
94 ml 0.2 M NaH_2PO_4	39 ml 0.2 M NaH_2PO_4
Dilute to 200 ml with distilled water.	Dilute to 200 ml with distilled water.

***Bacillus subtilis* Growth Medium (Hughes *et al.*, 1970)**

casein hydrolysate	0.5 %
yeast extract	0.5 %
$MgSO_4$	1 mM
β-glycerophosphate	60 mM
glucose	1 %

Glucose and $MgSO_4$ were autoclaved separately. This was supplemented with filter sterilised salts solution, to a final concentration of 0.02 $ml.l^{-1}$:

$MnCl_2$	0.2 %
$CuSO_4$	0.5 %
$ZnSO_4$	6.5 %
$FeSO_4$	0.5 %
HCl	10 %

Wall Medium

DL-alanine	4 ml, 10 $mg.ml^{-1}$
DL-glutamic acid	8 ml, 5 $mg.ml^{-1}$
DL-aspartic acid	20 ml, 2 $mg.ml^{-1}$
1 M $MgSO_4$	0.5 ml
glucose	5 ml, 40 % (autoclaved separately)

± L-tryptophan (2.5 ml 16 $mg.ml^{-1}$) or alternatively 2.5 ml sterile distilled water.

Medium for Nalidixic Acid Treatment (PBS/YE/CASA)

Casamino acids	3 g
Yeast Extract	0.3 g

Dissolve in 1 l PBS. Autoclave at 121 °C/17 $lb.in^{-2}$. Add filter sterilised nalidixic acid as required.

Appendix 4 : Gram Staining Procedure

Making a bacterial film

Degrease a microscope slide in methanol.
Place a drop of distilled water on the slide.
Homogenise a small loopful of pure bacterial colony growth from an agar plate in the water.
Allow to dry in air (or with gentle heating)
Fix by passing through a Bunsen flame.
The sample is now ready to stain.

Gram Staining Procedure

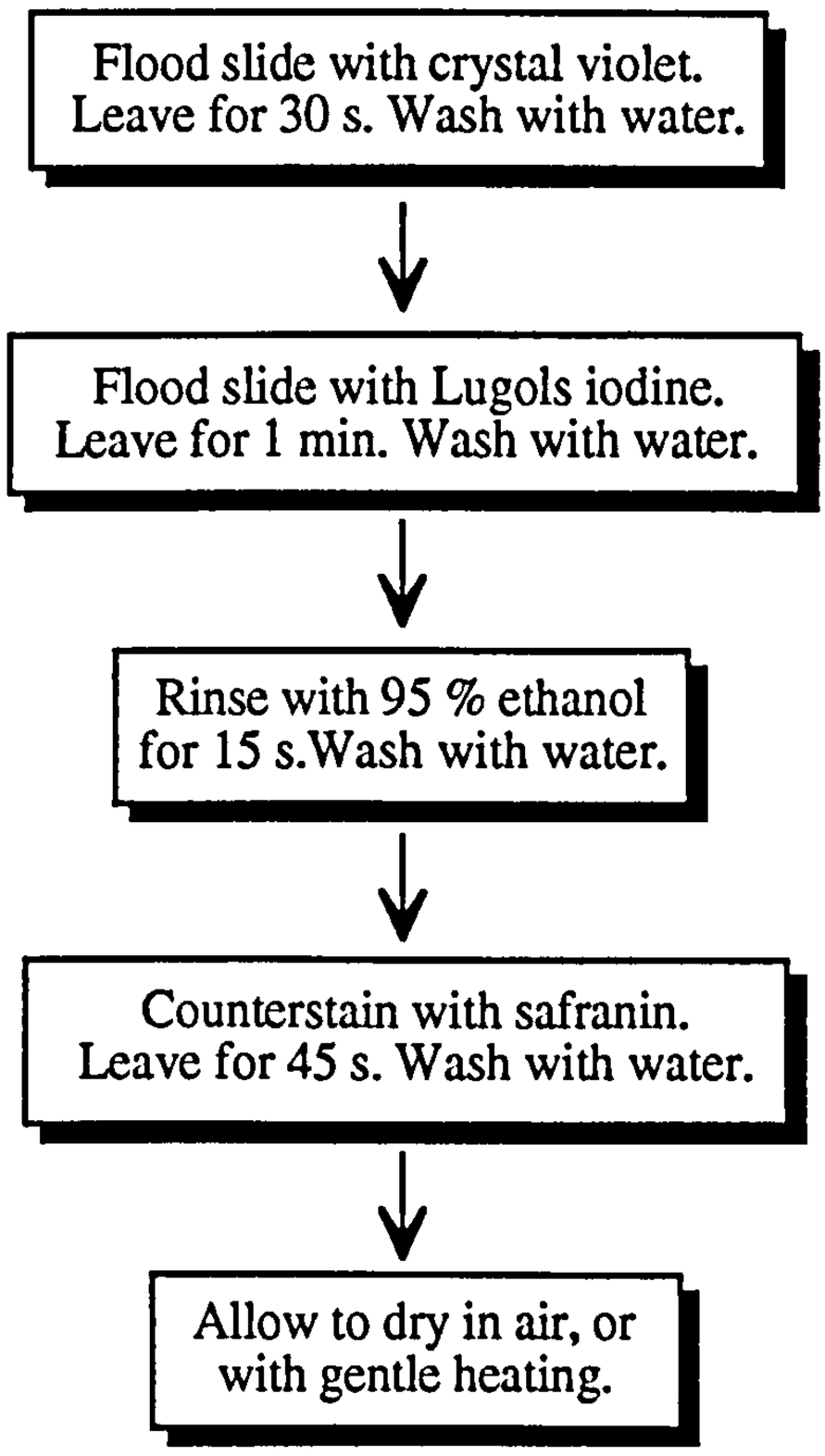

Microscopic examination

Examine slide under x100 oil immersion objective.

Gram positive cells stain purple.
Gram negative cells stain pink.

Appendix 5 : Electron Microscopy of Bacterial Species

Figures A5.1(a) to A5.1(d) show scanning electron micrographs of the bacterial species used in some of the dielectrophoretic experiments to enable visual comparison of cell shape and size.

Staph. aureus is a Gram positive cocci shaped cell often forming clusters upon growth and division. Measurements from figure A5.1(a) show that individual cells had an average size of 0.7 μm in diameter, though groups of similar cells in suspension can be several microns and may be visible by eye as particulates.

The Gram negative cells shown in the *Ent. cloacae* micrograph (figure A5.1(b)) appeared to have suffered during the preparation procedure, becoming somewhat distorted and clumped. Cells which were undamaged appeared as rod shaped cells of 1.6 to 1.7 μm length and 0.4 to 0.5 μm in width with rounded polar end caps.

B. subtilis as shown in figure A5.1(c) were again slightly damaged due to the preparation. These cells are Gram positive rod shaped bacteria and the single undividing cells were 1.8 to 2 μm in length by 0.65 μm wide. Some of the cells in the micrograph appeared longer than these dimensions and also slightly curved. These cells were in the process of division and thus had increased length.

The Gram negative *E. coli* 10418 is shown in figure A5.1(d). These cells are rod shaped and have a mean length of 1.5-2 μm. These cells represent the control sample for the nalidixic acid treatment of figure 4.4.1.

All of these species studied were taken from the stationary phase of culture growth to minimise the occurrence of dividing cells and thus to obtain more uniform cell sizes. During the exponential phase, the majority of cells are actively growing and dividing, often producing elongated cell structures.

(a)

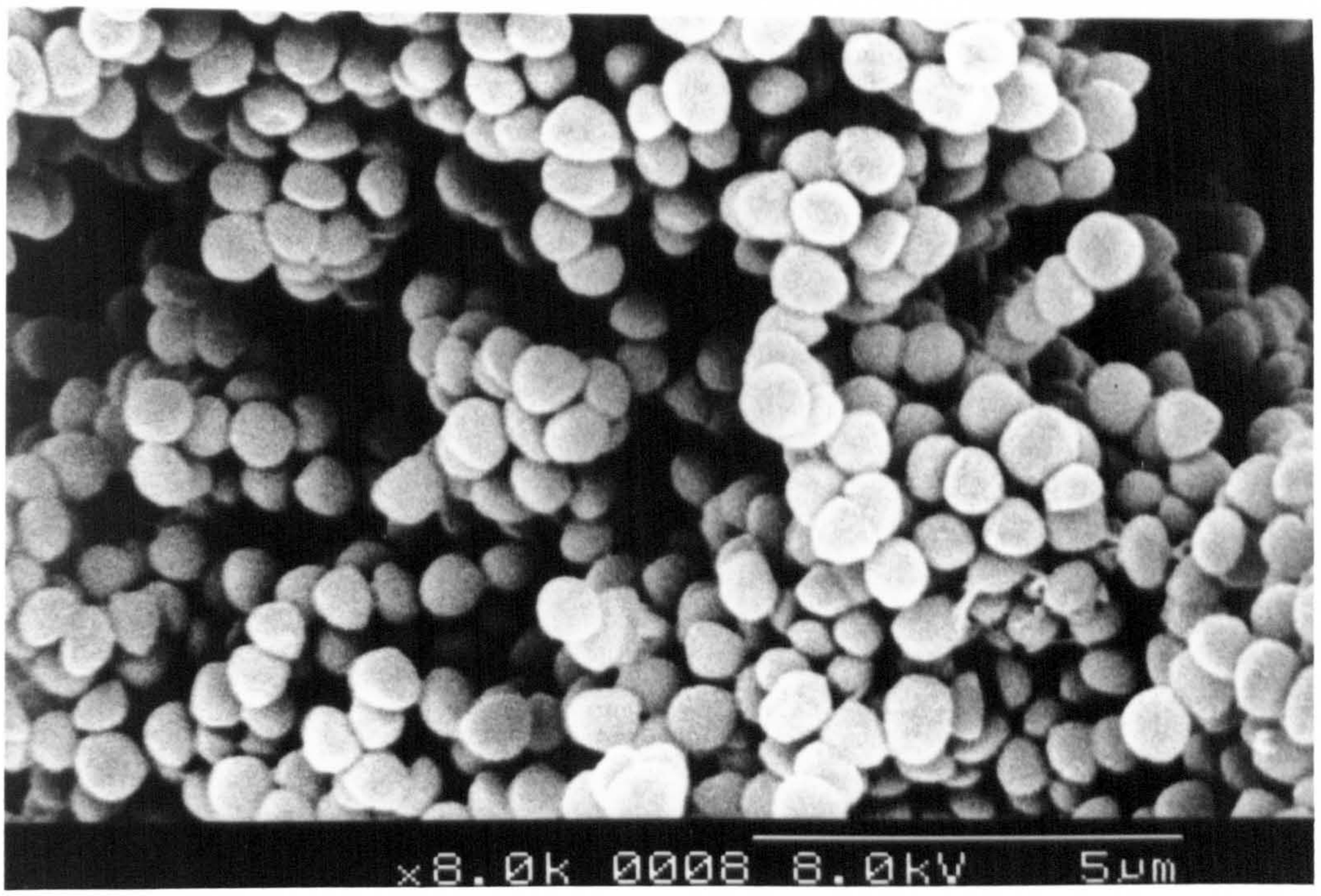

(b)

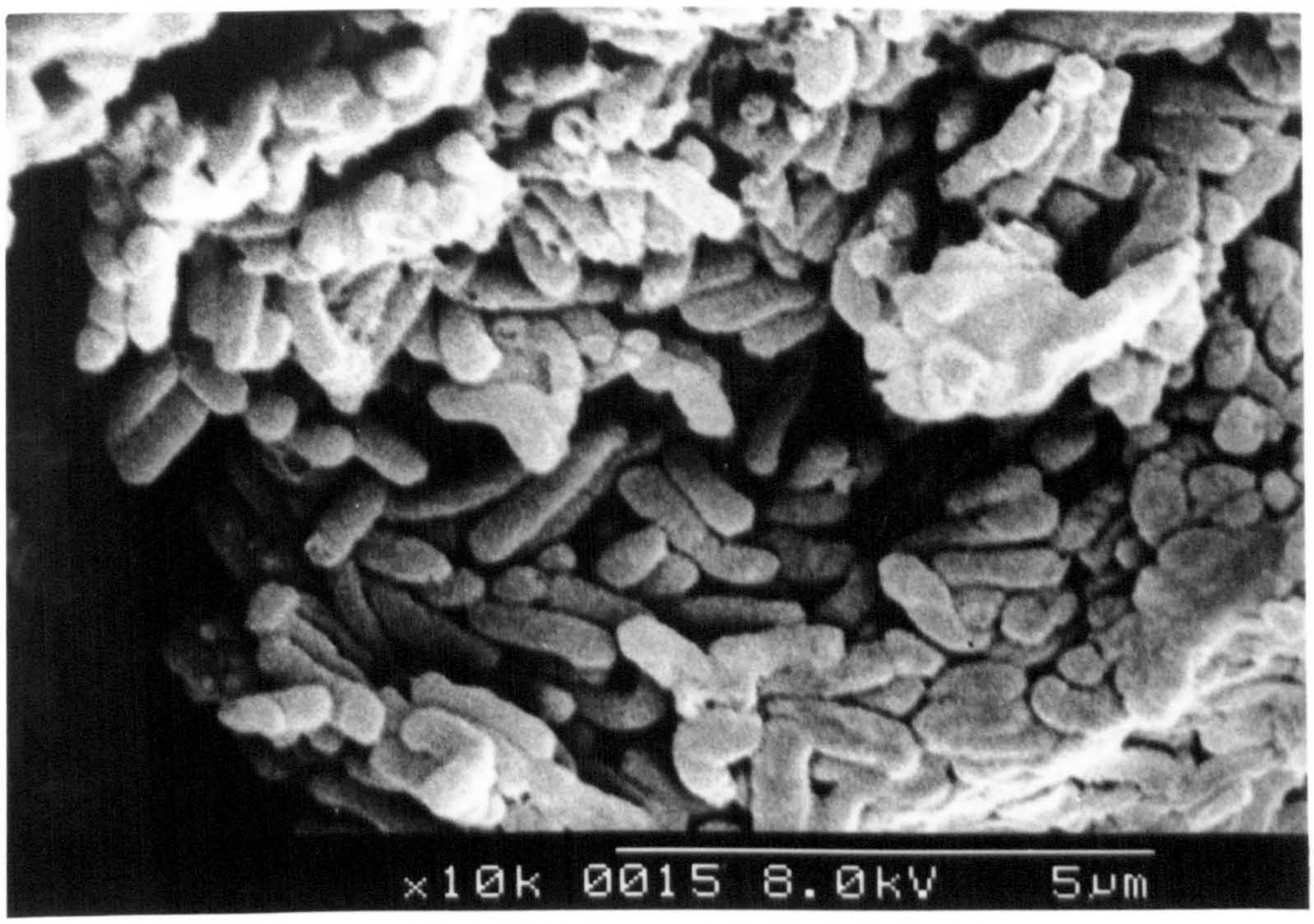

(c)

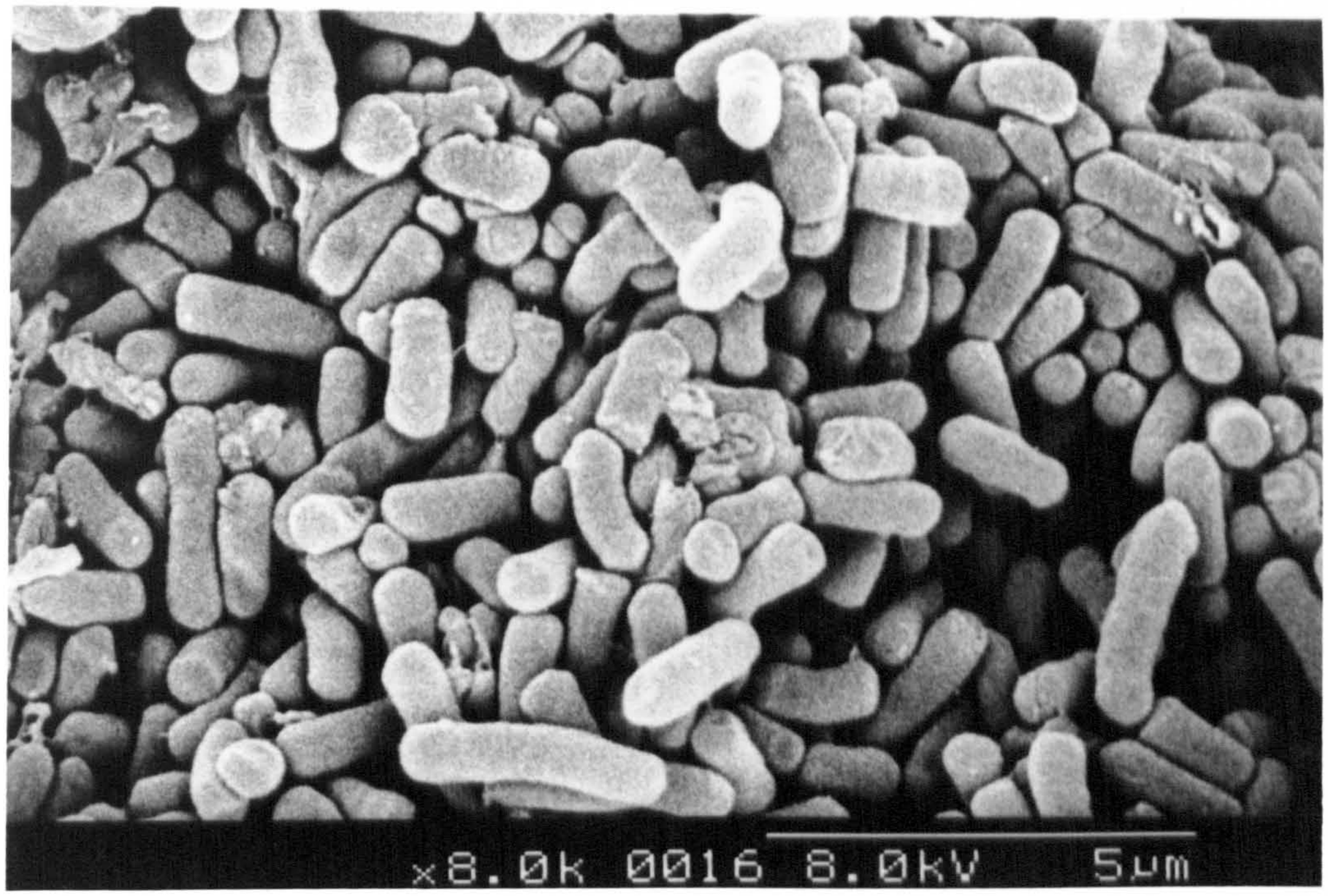

(d)

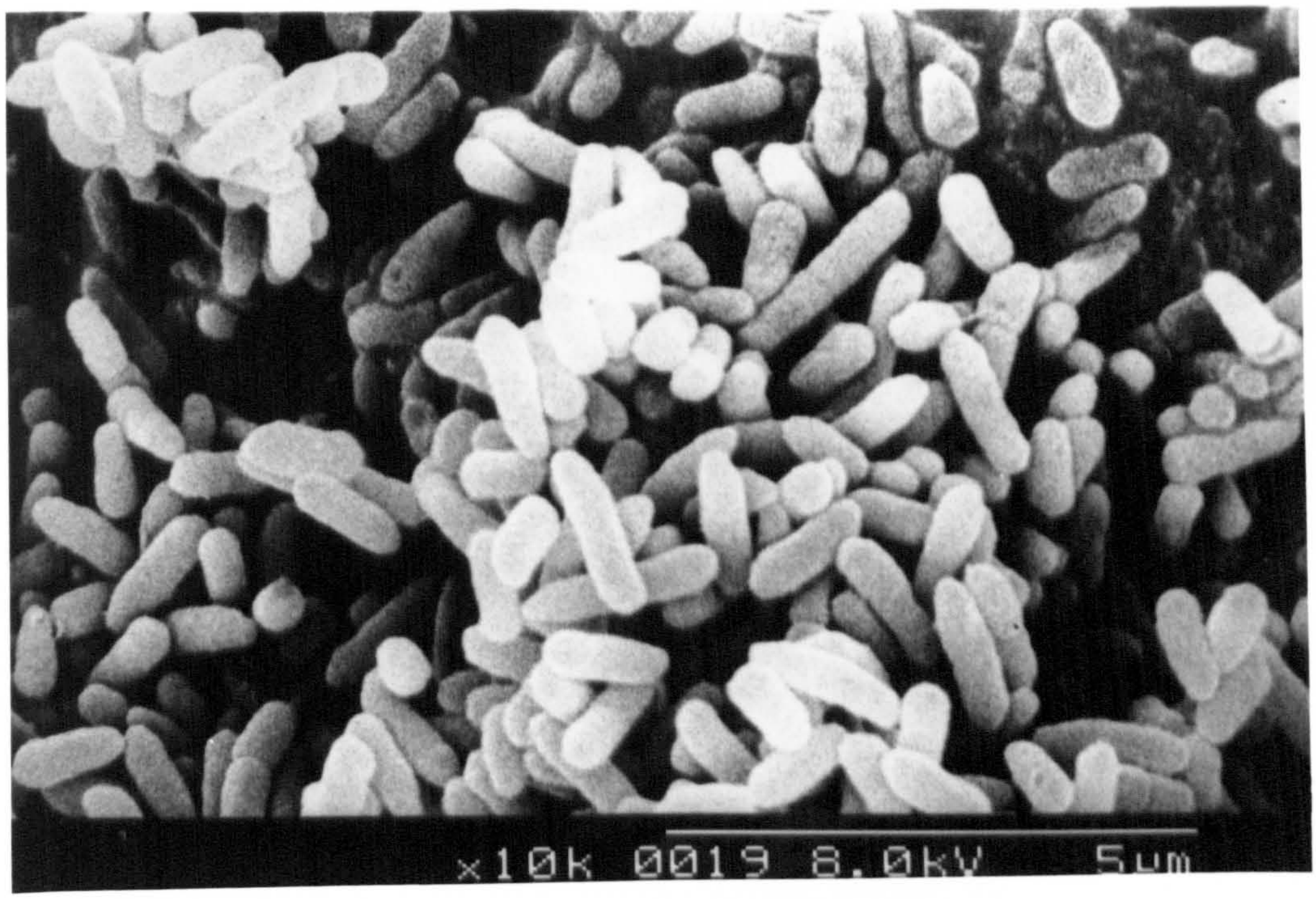

Figure A5.1 : Scanning electron micrographs of several bacterial species. (a) *Staph. aureus*, (b) *Ent. cloacae*, (c) *B. subtilis*, (d) *E. coli* 10418. Accelerating voltage 8 kV.

REFERENCES

Ackermann E. (1962) Biophysical Science. Prentice Hall, New York, pp. 208-211.

Adelberg E.A., Mandel M. & Chen G.C.C. (1965) Optimal conditions for mutagenesis by N'-methyl-N'-nitro-N-nitrosoguanidine in *Escherichia coli* K12. *Biochem. Biophys. Res. Comm.* **18**, 788-795.

Allison D.G. & Sutherland I.W. (1987) The role of exopolysaccharides in adhesion of freshwater bacteria. *J. Gen. Microbiol.* **133**, 1319-1327.

Amako K., Meno Y. & Takade A. (1988) Fine structures of the capsules of *Klebsiella pneumoniae* and *Escherichia coli* K1. *J. Bacteriol.* **170**, 4960-4962.

Anderson J.S., Matsuhasi M., Haskin M. & Strominger J.L. (1965) Lipid-phosphoacetylmuramylpentapeptide and lipid-phospho-disaccharide-pentapeptide : presumed membrane transport intermediates in cell wall synthesis. *Proc. Nat. Acad. Sci.* **53**, 881-889.

Anderson A.J., Green R.S., Sturman A.J. & Archibald A.R. (1978) Cell wall assembly in *Bacillus subtilis* : location of wall material incorporated during pulsed release of phosphate limitation, its accessibility to bacteriophages and concanavalin A, and its susceptibility to turnover. *J. Bacteriol.* **136**, 886-899.

Archer G.P., Betts W.B. & Haigh T. (1993a) Rapid differentiation of untreated and treated *Cryptosporidium parvum* oocysts using dielectrophoresis. *Microbios* **73**, 165-172.

Archer G.P., Render M.C., Betts W.B. & Sancho M. (1993b) Dielectrophoretic concentration of micro-organisms using grid electrodes. *Microbios* **76**, 237-244.

Archer G.P., Quinn C.M., Betts W.B., Allsopp D.W.E. & O'Neill J.G. (1995) Physical separation of untreated and ozone treated *Cryptosporidium parvum* oocysts using non-uniform electric fields. *In* Protozoan Parasites and Water. Betts W.B., Casemore D., Fricker C., Smith H. & Watkins J. (Eds.) The Royal Society of Chemistry, Cambridge, pp. 143-145.

Archibald A.R. (1985) Structure and assembly of the cell wall in *Bacillus subtilis*. *Biochem. Soc. Trans.* **13**, 990-992.

Archibald A.R. & Coapes H.E. (1976) Bacteriophage SP50 as a marker for cell wall growth in *Bacillus subtilis*. *J. Bacteriol.* **125**, 1195-1206.

Archibald A.R., Glassey K., Green R.S. & Lang W.K. (1989) Cell wall composition and surface properties in *Bacillus subtilis* : anomalous effect of incubation temperature on the phage-binding properties of bacteria containing varied amounts of teichoic acid. *J. Gen. Microbiol.* **135**, 667-673.

Arnold W.M. & Zimmermann U. (1988) Electrorotation: development of a technique for dielectric measurements on individual cells and particles. *J. Electrostat.* **21**, 151-191.

Arnold W.M., Gessner A.G. & Zimmermann U. (1993) Dielectric measurements on electro-manipulation media. *Biochim. Biophys. Acta* **1157**, 32-44.

Asami K., Hanai T. & Koizumi N. (1980) Dielectric analysis of *Escherichia coli* suspensions in the light of the theory of interfacial polarisation. *Biophys. J.* **31**, 215-228.

Atkins P.W. (1978) Physical Chemistry. Oxford University Press, Oxford.

Bar-Or Y. (1990) Hydrophobicity in the aquatic environment. *In* Microbial Cell Surface Hydrophobicity. Doyle R.J. & Rosenberg M. (Eds.) American Society for Microbiology, Washington, pp. 211-228.

Bayer M.E. (1968) Areas of adhesion between wall and membrane of *Escherichia coli*. *J. Gen. Microbiol.* **53**, 395-404.

Bayer M.E. (1990) Visualisation of the bacterial polysaccharide capsule. *In* Bacterial Capsules: Current Topics in Microbiology and Immunology, Volume 150. Jann K. & Jann B. (Eds.) Springer-Verlag, Berlin.

Bayer M.E. & Sloyer J.L. (1988) Measurement of the surface charge of *E. coli* in relation to antigenic variations. *Abstracts of the Annual Meeting of the American Society for Microbiology* **Abstr. D-58**, 80.

Bayer M.E. & Thurow H. (1977) Polysaccharide capsule of *E. coli* : microscope study of its size, structure and sites of synthesis. *J. Bacteriol.* **130**, 911-936.

Becker F.F., Wang X-B, Huang Y., Pethig R., Vykoukal J. & Gascoyne P.R.C. (1994) The removal of human leukaemia cells from blood using interdigitated microelectrodes. *J. Phys. D : Appl. Phys.* **27**, 2659-2662.

Bernhardt J. & Pauly H. (1973) On the generation of potential differences across the membranes of ellipsoidal cells in an alternating electrical field. *Biophysik* **10**, 89-98.

Betts W.B. (1994) Technical Report : Dielectrophoretic assessment of antibiotic sensitivity. Mycotech, Institute For Applied Biology, University of York.

Betts W.B. (1995a) The potential of dielectrophoresis for the real-time detection of micro-organisms in foods. *Trends In Food Sci. & Technol.* **6**, 51-58.

Betts W.B. (1995b) Technical Report : Effects of electric fields on porcine sperm physiology. Mycotech, Institute For Applied Biology, University of York.

Betts W.B. & Hawkes J.J. (1994) UK Patent 2238619B.

Betts W.B., Allsopp D.W.E. & Goodall D.M. (1995) Coupling of dielectrophoresis and capillary electrophoresis for microbiological applications. BBSRC Realising Our Potential Award (ROPA). Grant reference 87/SYS04701.

Beveridge T.J. & Graham L.L. (1991) Surface layers of bacteria. *Microbiol. Rev.* **55**, 684-705.

Beynon L.M., Dumanski A.J., McLean R.J.C., MacLean L.L., Richards J.C. & Perry M.B. (1992) Capsule structure of *Proteus mirabilis* (ATCC 49565). *J. Bacteriol.* **174**, 2172-2177.

Birdsell D.C. & Cota-Robles E.H. (1967) Production and ultrastructure of lysozyme and ethylenediaminetetraacetate-lysozyme spheroplasts. *J. Bacteriol.* **93**, 427-437.

Bone S. & Zaba B. (1992) Bioelectronics. John Wiley & Sons, Chichester.

Boulnois G.J. & Roberts I.S. (1990) Genetics of capsular polysaccharide production in bacteria. *In* Bacterial Capsules : Current Topics in Microbiology and Immunology, Volume 150. Jann K. & Jann B. (Eds.) Springer-Verlag, Berlin, pp. 1-18.

Bowman W.C. & Rand M.J. (1980) Textbook of Pharmacology. 2nd edition. Blackwell Scientific Publications, Oxford.

Braun V. (1975) Covalent lipoprotein from the outer membrane of *Escherichia coli*. *Biochim. Biophys. Acta* **415**, 335-377.

Braun V., Gnirke H., Henning U. & Rehn K. (1973) Model for the structure of the shape-maintaining layer of the *Escherichia coli* cell envelope. *J. Bacteriol.* **114**, 1264-1270.

Bridson E.Y. (1990) The Oxoid Manual. 6th Edition. Unipath Ltd., Basingstoke.

British Society for Antimicrobial Chemotherapy Working Party (1991) A guide to sensitivity testing. Report of the Working Party on Antibiotic Sensitivity Testing of the British Society for Antimicrobial Chemotherapy. Academic Press Ltd., London.

Burdett I.D.J. & Murray R.G.E. (1974) Septum formation in *Escherichia coli* : characterisation of septal structure and the effects of antibiotics on cell division. *J. Bacteriol.* **119**, 303-324.

Burt J.P.H., Pethig R., Gascoyne P.R.C. & Becker F.F. (1990) Dielectrophoretic characterisation of Friend murine erythroleukaemic cells as a measure of induced differentiation. *Biochim. Biophys. Acta* **1034**, 93-101.

Buysman J.R. & Koide F.T. (1971) Ion concentration profile normal to cell membrane. *J. Theor. Biol.* **32**, 1-23.

Carstensen E.L. (1967) Passive electrical properties of micro-organisms. II. Resistance of the bacterial membrane. *Biophys. J.* **7**, 493-503.

Carstensen E.L. & Marquis R.E. (1968) Passive electrical properties of micro-organisms. III. Conductivity of isolated cell walls. *Biophys. J.* **8**, 536-548.

Carstensen E.L., Cox H.A. Jnr., Mercer W.B. & Natale L.A. (1965) Passive electrical properties of micro-organisms. I. Conductivity of *Escherichia coli* and *Micrococcus lysodeikticus*. *Biophys. J.* **5**, 289-300.

Carstensen E.L., Maniloff J. & Einolf C.W. Jnr. (1971) Electrical properties and ultrastructure of *Mycoplasma* membranes. *Biophys. J.* **11**, 572-581.

Chapman D.L. (1913) A contribution to the theory of electrocapillarity. *Phil. Mag.* **25**, 475-481.

Chen C.S. (1972) On the Nature and Origins of Biological Dielectrophoresis. PhD Thesis, Oklahoma State University.

Chopra I. & Ball P. (1982) Transport of antibiotics into bacteria. *Adv. Microb. Physiol.* **23**, 183-240.

Chopra I. & Linton A. (1986) The antibacterial effects of low concentrations of antibiotics. *Adv. Microb. Physiol.* **28**, 211-259.

Chung K.L. (1971) Thickened cell walls of *Bacillus cereus* grown in the presence of chloramphenicol : their fate during cell growth. *Can. J. Microbiol.* **17**, 1561-1565.

Chung K.L. (1973) Influence of cell wall thickness on cell division : electron microscopy study with *Bacillus cereus*. *Can. J. Microbiol.* **19**, 217-221.

Coehn A. (1898) *Ann. Physik.* **64**, 217. (Cited by Pethig, 1979).

Costerton J.W. (1979) The role of electron microscopy in the elucidation of bacterial structure and function. *Ann. Rev. Microbiol.* **33**, 459-79.

Costerton J.W., Ingram J.M. & Cheng K.J. (1974) Structure and function of the cell envelope of Gram negative bacteria. *Bacteriol. Rev.* **38**, 87-110.

Costerton J.W., Irvin R.T. & Cheng K. J. (1981) The bacterial glycocalyx in nature and disease. *Ann. Rev. Microbiol.* **35**, 299-324.

Crane J.S. & Pohl H.A. (1968) A study of living and dead yeast cells using dielectrophoresis. *J. Electrochem. Soc.* **115**, 584-586.

Crane J.S. & Pohl H.A. (1972) Theoretical models of cellular dielectrophoresis. *J. Theor. Biol.* **37**, 15-41.

Crane J.S. & Pohl H.A. (1977) Use of the balanced cell technique to determine properties of single yeast cells. *J. Biol. Phys.* **5**, 49-74.

Cutnell J.D. & Johnson K.W. (1989) Physics. John Wiley & Sons Inc., USA., p. 508.

Davies J.T., Haydon D.A. & Rideal E. (1956) Surface behaviour of *Bacterium coli*. I. The nature of the surface. *Proc. Roy. Soc. London* **145**, 375-383.

Davis B.D., Dulbecco R., Eisen H.N. & Ginsberg H.S. (1980) Microbiology. 3rd edition. Harper & Row, Hagerstown, MD.

Dealler S.F. (1991) Antibiotics induce rapid bacterial zeta potential changes. *J. Antimicrob. Chemother.* **28**, 470-473.

Debye P. & Falkenhagen H. (1928) *Phys. Zeit.* **29**, 401. (Cited by Chen, 1972).

Debye P. & Hückel E. (1924) *Phys. Zeit.* **25**, 49. (Cited by Chen, 1972).

Deitz W.H., Cook T.M. & Goss W.A. (1966) Mechanism of action of nalidixic acid on *Escherichia coli*. III. Conditions required for lethality. *J. Bacteriol.* **91**, 768-773.

De Souza A.M. & Sutherland I.W. (1994) Exopolysaccharide and storage polymer production in *Enterobacter aerogenes* type 8 strains. *J. Appl. Bact.* **76**, 463-468.

Dickson J.S. & Siragusa G.R. (1994) Cell surface charge and initial attachment characteristics of rough strains of *Listeria monocytogenes*. *Lett. Appl. Microbiol.* **19**, 192-196.

Doyle R.J., McDannel M.L., Streips U.N., Birdsell D.C. & Young F.E. (1974) Polyelectrolyte nature of bacterial teichoic acids. *J. Bacteriol.* **118**, 606-615.

Doyle R.J., McDannel M.L., Helman J.R. & Streips U.N. (1975) Distribution of teichoic acid in the cell wall of *Bacillus subtilis*. *J. Bacteriol.* **122**, 152-158.

Duckworth M. (1977) Teichoic acids. Chapter 5. *In* Surface Carbohydrates of the Procaryotic Cell. Sutherland I.W. (Ed.) Academic Press, London, pp. 177-208.

Duguid J.P. (1951) The demonstration of bacterial capsules and slime. *J. Path. Bact.* **63**, 673-685.

Duguid J.P. & Wilkinson J.F. (1953) The influence of cultural conditions on polysaccharide production by *Aerobacter aerogenes*. *J. Gen. Microbiol.* **9**, 174-189.

Duguid J.P. & Wilkinson J.F. (1954) Note on the influence of potassium deficiency upon production of polysaccharide by *Aerobacter aerogenes*. *In* Wilkinson J.F., Duguid J.P. & Edmunds P.N. (1954) The distribution of polysaccharide production in *Aerobacter* and *Escherichia* strains and its relation to antigenic character. *J. Gen. Microbiol.* **11**, 59-72.

Dukhin S.S. & Shilov V.N. (1974) Dielectric Phenomenon and the Double Layer in Disperse Systems and Polyelectrolytes. Wiley, New York.

Dukhin S.S., Sorokina T.S. & Chelicdze T.L. (1969) *Colloid J.* **31**, 564. (Cited by Chen, 1972).

Dyar M.T. (1948) *J. Bacteriol.* **56**, 821. (Cited by Richmond and Fisher, 1973).

Edwards D.I. (1980) Antimicrobial Drug Action. Macmillan Press Ltd., London.

Einolf C.W. & Carstensen E.L. (1969) Passive electrical properties of micro-organisms. IV. Studies of the protoplasts of *Micrococcus lysodeikticus*. *Biophys. J.* **9**, 634-643.

Einolf C.W. & Carstensen E.L. (1973) Passive electrical properties of micro-organisms. V. Low frequency dielectric dispersion of bacteria. *Biophys. J.* **13**, 8-13.

Eisberg R.M. & Lerner L.S. (1981) Physics: Foundations and Applications. Volume II. McGraw-Hill Inc., USA. p. 1005.

Ellwood D.C. & Tempest D.W. (1969) Control of teichoic acid and teichuronic acid biosynthesis in chemostat cultures of *Bacillus subtilis* var. *niger*. *Biochem J.* **111**, 1-5.

Everitt C.T. & Haydon D.A. (1968) Electrical capacitance of a lipid membrane separating two aqueous phases. *J. Theor. Biol.* **18**, 371-379.

Fischer W., Schmidt M.A., Jann B. & Jann K. (1982) Structure of the *Escherichia coli* K2 capsular antigen. Stereochemical configuration of the glycerophosphate and distribution of galactopyranosyl and galactofuranosyl residues. *Biochemistry* **21**, 1279-1284.

Fomchenkov V.M., Brezgunov V.N., Gavrilyuk B.K., Smolyaninov V.V. & Bunina Z.F. (1979) A study of the effects of antibiotics on orientational and dielectrophoretic spectra of bacterial cells. *J. Biol. Phys.* **7**, 45-56.

Formanek H., Formanek S. & Wawra H. (1974) A three dimensional atomic model of the murein layer of bacteria. *Eur. J. Biochem.* **46**, 279-294.

Franklin T.J. & Snow G.A. (1975) Biochemistry of Antimicrobial Action. 2nd Edition. Chapman & Hall Ltd., London.

Fricke H. (1925) The electrical capacity of suspensions of red corpuscles of a dog. *Phys. Rev.* **28**, 682.

Fricke H. (1955) The complex conductivity of a suspension of stratified particles of spherical or cylindrical form. *J. Phys. Chem.* **59**, 168-170.

Gale E.F. (1962) The synthesis of proteins and nucleic acids. *In* The Bacteria, Volume 3. Gunsalus I.C. & Stanier R.Y. (Eds.) Academic Press, New York, pp. 471-576.

Ghuysen J.-M. & Shockman G.D. (1973) Biosynthesis of peptidoglycan. *In* Bacterial Membranes and Walls. Leive L. (Ed.) Dekker, New York, pp. 37-130.

Gilbert P., Evans D.J., Duguid I.G., Evans E. & Brown M.R.W. (1991a) Cell surface properties of *Escherichia coli* and *Staphylococcus epidermidis*. *In* Microbial Cell Surface Analysis : Structural and Physicochemical Methods. Mozes N., Handley P.S., Busscher H.J. & Rouxhet P.G. (Eds.) VCH Publishers Inc., New York, pp. 339-356.

Gilbert P., Evans D.J., Evans E., Duguid I.G. & Brown M.R.W. (1991b) Surface characteristics and adhesion of *Escherichia coli* and *Staphylococcus epidermidis*. *J. Appl. Bact.* **71**, 72-77.

Gilbert P., Caplan F. & Brown M.R.W. (1991c) Centrifugation injury of Gram negative bacteria. *J. Antimicrob. Chemother.* **27**, 550-551.

Giordano A., Magni A., Trancassini M. & Cipriani P. (1993) Outer membrane proteins and lipopolysaccharide changes after exposure of *Pseudomonas aeruginosa* to antibacterial drugs. *Microbiologica* **16**, 281-286.

Gittens G.J. (1962) PhD Thesis, University of London.

Gittens G.J. & James A.M. (1963) Some physical investigations of the behaviour of bacterial surfaces. VI. Chemical modification of surface components. *Biochim. Biophys. Acta* **66**, 237-249.

Glauert A.M. & Thornley M.J. (1969) The topography of the bacterial cell wall. *Ann. Rev. Microbiol.* **23**, 159-198.

Goss W.A., Cook T.M. & Deitz W.H. (1965) Mechanism of action of nalidixic acid. II. Inhibition of deoxyribonucleic acid synthesis. *J. Bacteriol.* **89**, 1068-1074.

Gotschlich E.C., Fraser B.A., Nishimura O., Robbins J.B. & Liu T-Y (1981) Lipid on capsular polysaccharides of Gram-negative bacteria. *J. Biol. Chem.* **256**, 8915-8921.

Gouy G. (1910) *J. Physique* **9**, 457. (Cited by Chen, 1972).

Grahame D.C. (1947) The electrical double layer and the theory of electrocapillarity. *Chem. Rev.* **41**, 441-501.

Grant I.S. & Phillipps W.R. (1990) Electromagnetism. 2nd edition. John Wiley & Sons, Chichester.

Grant E.H., Sheppard R.J. & South G.P. (1978) Dielectric Behaviour of Biological Molecules in Solution. Clarendon Press, Oxford.

Greig R.G. & Jones M.N. (1976) The possible role of steric forces in cellular cohesion. *J. Theor. Biol.* **63**, 405-419.

Hammond S.M., Lambert P.A. & Rycroft A.N. (1984) The Bacterial Cell Surface. Kapitan Szabo, Washington.

Hancock I.C. (1991) Microbial cell surface architecture. *In* Microbial Cell Surface Analysis : Structural and Physicochemical Methods. Mozes N., Handley P.S., Busscher H.J. & Rouxhet P.G. (Eds.) VCH Publishers Inc., New York, pp. 21-59.

Hancock I. & Poxton I. (1988) Bacterial Cell Surface Techniques. John Wiley & Sons, Chichester.

Hancock R.E.W. & Bell A. (1988) Antibiotic uptake into Gram negative bacteria. *In* Current Topics in Infectious Diseases and Clinical Microbiology, Volume 2 : Perspectives in Antiinfective Therapy. Jackson G.G., Schlumberger H.D. & Zeiler H.J. (Eds.) Friedr. Vieweg & Sohn, Braunschweig, Wiesbaden, pp. 21-28.

Handley P.S. (1991) Detection of cell surface carbohydrate components. *In* Microbial Cell Surface Analysis : Structural and Physicochemical Methods. Mozes N., Handley P.S., Busscher H.J. & Rouxhet P.G. (Eds.) VCH Publishers Inc., New York, pp. 87-107.

Harris C.M. & Kell D.B. (1985) On the dielectrically observable conseqences of the diffusional motions of lipids and proteins in membranes. II. Experiments with microbial cells, protoplasts and membrane vesicles. *Eur. Biophys. J.* **13**, 11-24.

Harrison A.B. (1994) Personal Communication.

Harrop P.J. (1972) Dielectrics. Butterworths, London.

Hawkes J.J., Archer G.P. & Betts W.B. (1993) A dielectrophoretic spectrometer for characterising micro-organisms and other particles. *Microbios* **73**, 81-86.

Henry D.C. (1931) *Proc. Roy. Soc. London Ser. A* **133**, 106. (Cited by James, 1991).

Hogg S.D. & Manning J.E. (1987) The hydrophobicity of 'viridans' streptococci isolated from the human mouth. *J. Appl. Bact.* **63**, 311-318.

Horowitz P. & Hill W. (1989) The Art of Electronics. 2nd Edition. Cambridge University Press, Cambridge, pp. 879-881.

Horská E., Pokorny J. & Labajová M. (1993) Changes of surface charge and hydrophobicity of the outer bacterial membrane depending on the cultivation medium. *Biológia, Bratislava* **48**, 343-347.

Hrebenda J., Hrebenda B. & Brzostek K. (1985) Influence of penicillin and nalidixic acid on growth and cell division of *Escherichia coli* K-12. *Acta Microbiologica Polonica* **34**, 19-24.

Hughes R.C., Tanner P.J. & Stokes E. (1970) Cell wall thickening in *Bacillus subtilis*. *Biochem. J.* **120**, 159-170.

Ingraham J.L., Maaløe O. & Neidhardt F.C. (1983) Growth of the Bacterial Cell. Sinauer Associates Inc., Sunderland, USA, pp. 227-265.

Inoue T., Pethig R., Al-Ameen T.A.K., Burt J.P.H. & Price J.A.R. (1988) Dielectrophoretic behaviour of *Micrococcus lysodeikticus* and its protoplast. *J. Electrostat.* **21**, 215-223.

Irimajiri A., Hanai T. & Inouye A. (1979) A dielectric theory of "multistratified shell" model with its application to a lymphoma cell. *J. Theor. Biol.* **78**, 251-269.

Irvin R.T. (1990) Hydrophobicity of proteins and bacterial fimbriae. *In* Microbial Cell Surface Hydrophobicity. Doyle R.J. & Rosenberg M. (Eds.) American Society for Microbiology, Washington, pp. 137-177.

Jacques M., Lebrun A., Foiry B., Dargis M. & Malouin F. (1991) Effects of antibiotics on the growth and morphology of *Pasteurella multocida*. **137**, 2663-2668.

James A.M. (1991) Charge properties of microbial cell surfaces. *In* Microbial Cell Surface Analysis : Structural and Physicochemical Methods. Mozes N., Handley P.S., Busscher H.J. & Rouxhet P.G. (Eds.) VCH Publishers Inc., New York., pp. 221-262.

Jann B. & Jann K. (1990) Structure and biosynthesis of the capsular antigens of *Escherichia coli*. *In* Bacterial Capsules : Current Topics in Microbiology and Immunology, Volume 150. Jann K. & Jann B. (Eds.) Springer-Verlag, Berlin, pp. 19-42.

Kauffmann F. & Vahlne G. (1945) Über die Bedeutung des serologischen Formenwechsels für die Bakteriophagenwirkung in der Coli-Gruppe. *Acta Pathol. Microbiol. Scand.* **22**, 119-137.

Kelemen M.V. & Rogers H.J. (1971) Three dimensional molecular models of bacterial cell wall mucopeptides (peptidoglycans). *Proc. Nat. Acad. Sci.* **68**, 992-996.

Kell D.B. & Harris C.M. (1985) On the dielectrically observable conseqences of the diffusional motions of lipids and proteins in membranes. I. Theory and overview. *Eur. Biophys. J.* **12**, 181-197.

Kirkwood J.G. & Shumaker J.B. (1952) The influence of dipole moment fluctuations on the dielectric increment of proteins in solution. *Proc. Nat. Acad. Sci.* **38**, 855-862.

Lang W.K., Glassey K. & Archibald A.R. (1982) Influence of phosphate supply on teichoic acid and teichuronic acid content of *Bacillus subtilis* cell walls. *J. Bacteriol.* **151**, 367-375.

Lin I.J. & Jones T.B. (1984) General conditions for dielectrophoretic and magnetohydrostatic levitation. *J. Electrostat.* **15**, 53-65.

Lohia A., Majumdar S., Chatterjee A.N. & Das J. (1985) Effects of changes in osmolarity of the growth medium on *Vibrio cholerae* cells. *J. Bacteriol.* **163**, 1158-1166.

Lorian V. (1980) Effects of subminimum inhibitory concentrations of antibiotics on bacteria. *In* Antibiotics in Laboratory Medicine. Lorian V. (Ed.) Williams & Wilkins, Baltimore, pp. 342-408.

Lorian V. (1985) Low concentrations of antibiotics. *J. Antimicrob. Chemother.* **15**, Suppl. A., 15-26.

Loubeyre C., Desnottes J.F. & Moreau N. (1993) Influence of sub-inhibitory concentrations of antibacterials on the surface properties and adhesion of *Escherichia coli*. *J. Antimicrob. Chemother.* **31**, 37-45.

Lugtenberg B., Peters R., Bernheimer H. & Berendsen W. (1976) Influence of cultural conditions and mutations on the composition of the outer membrane proteins of *Escherichia coli*. *Molec. Gen. Genet.* **147**, 251-262.

MacArthur A.E. & Archibald A.R. (1984) Effect of culture pH on the D-alanine ester content of lipoteichoic acid in *Staphylococcus aureus*. *J. Bacteriol.* **160**, 792-793.

Mackie E.B., Brown K.N., Lam J., Costerton J.W. (1979) Morphological stabilisation of capsules of group B streptococci, types Ia, Ib, II and III, with specific antibody. *J. Bacteriol* **138**, 609-617.

Markx G.H., Huang Y., Zhou X-F. & Pethig R. (1994) Dielectrophoretic characterisation and separation of micro-organisms. *Microbiology* **140**, 585-591.

Marquis R.E. & Carstensen E.L. (1973) Electric conductivity and internal osmolality of intact bacterial cells. *J. Bacteriol.* **113**, 1198-1206.

Marshall K.C. & Cruickshank R.H. (1973) Cell surface hydrophobicity and the orientation of certain bacteria at interfaces. *Arch. Mikrobiol.* **91**, 29-40.

Marshall A.J.H. & Piddock L.J.V. (1994) Interaction of divalent-cations, quinolones and bacteria. *J. Antimicrob. Chemother.* **34**, 465-483.

Marvin H.J.P. & Witholt B. (1987) A highly efficient procedure for the quantitative formation of intact and viable lysozyme spheroplasts from *Escherichia coli*. *Analytical Biochem.* **164**, 320-330.

Maxwell J.C. (1891) A Treatise on Electricity and Magnetism. 3rd edition. Volume 1. Clarendon Press, Oxford. Chapter IX.

McKenny D., Willcock L., Trueman P.A. & Allison D.G. (1994) Effect of sub-MIC antibiotics on the cell surface and extracellular virulence determinants of *Pseudomonas cepacia*. *J. Appl. Bact.* **76**, 190-195.

Mindich L. (1973) Synthesis and assembly of bacterial membranes. *In* Bacterial Membranes and Walls. Leive L. (Ed.) Dekker, New York, pp. 1-36.

Mognaschi E.R. & Savini A. (1985) Dielectrophoresis of lossy dielectrics. *IEEE Trans. Indust. Appl.* **IA-21**, 926-929.

Morris V.J. & Jennings B.R. (1975) The effect of neomycin and streptomycin on the electrical polarisability of aqueous suspensions of *Escherichia coli*. *Biochim. Biophys. Acta* **392**, 328-334.

Morris V.J. & Jennings B.R. (1977) The effect of antibiotics on the electrical polarisability of aqueous suspensions of bacteria. *Biochim. Biophys. Acta* **497**, 253-259.

Mozes N. & Rouxhet P.G. (1990) Microbial hydrophobicity and fermentation technology. *In* Microbial Cell Surface Hydrophobicity. Doyle R.J. & Rosenberg M. (Eds.) American Society for Microbiology, Washington, pp. 75-105.

Mozes N., Léonard A.J. & Rouxhet P.G. (1988) On the relations between the elemental surface composition of yeasts and bacteria and their charge and hydrophobicity. *Biochim. Biophys. Acta* **945**, 324-334.

Müller H. (1933) The theory of the diffuse double layer. *Cold Spring Harbor Symp. Quant. Biol.* **1**, 1-8.

Muller T., Fiedler S., Schnelle T., Ludwig K., Bordoni F., Jung H. & Fuhr G. (1996a) High frequency electric fields for trapping of viruses. *Biotechnol. Techniques* **10**, 221-226.

Muller T., Gerardino A., Schnelle T., Shirley S.G., Bordoni F., Degasperis G., Leoni R. & Fuhr G. (1996b) Trapping of micrometer and submicrometer particles by high-frequency electric fields and hydrodynamic forces. *J. Phys. D - Appl. Phys.* **29**, 340-349.

Nagle J.F. & Tristram-Nagle S. (1983) Hydrogen bonded chain mechanisms for proton conduction and proton pumping. *J. Membrane Biol.* **74**, 1-14.

NCTC (1995) Curator of National Collection of Type Cultures. Personal Communication.

Neidhardt F.C. (1987) *In Escherichia coli* and *Salmonella typhimurium*. Cellular and Molecular Biology, Volume 1. Neidhardt F.C. (Ed.) American Society For Microbiology, Washington D.C.

Neumann E., Sowers A.E. & Jordan C. (1989) Electroporation and Electrofusion in Cell Biology. Plenum Press, New York.

Nikaido H. (1973) Biosynthesis and assembly of lipopolysaccharides and the outer membrane layer of Gram negative cell wall. *In* Bacterial Membranes and Walls. Leive L. (Ed.) Dekker, New York, pp. 131-208.

Nikaido H. (1989) Outer membrane barrier as a mechanism of antimicrobial resistance. *Antimicrob. Agents Chemother.* **33**, 1831-1836.

O'Konski C.T. (1960) Electric properties of macromolecules. V. Theory of ionic polarisation in polyelectrolytes. *J. Phys. Chem.* **64**, 605-619.

Oncley J.L. (1943) The electric moments and the relaxation times of proteins as measured from their influence upon the dielectric constants of solutions. *In* Proteins, Amino Acids and Peptides. Cohn E.J. & Edsall J.T. (Eds.) Reinhold Publishing Corp., New York.

Ørskov I. (1984) *Klebsiella. In* Bergey's Manual of Systematic Bacteriology, Volume 1. Krieg N.R. & Holt J.G. (Eds.) Williams & Wilkins, Baltimore.

Ørskov I. & Ørskov F. (1984) Serotyping of *Klebsiella. Methods Microbiol.* **14**, 143-164.

Ørskov F. & Ørskov I. (1990) The serology of capsular antigens. *In* Bacterial Capsules : Current Topics in Microbiology and Immunology, Volume 150. Jann K. & Jann B. (Eds.) Springer-Verlag, Berlin, pp. 43-64.

Ørskov F., Sharma V. & Ørskov I. (1984) Influence of growth temperature on the development of *Escherichia coli* polysaccharide K antigens. *J. Gen. Microbiol.* **130**, 2681-2684.

Ou L-T & Marquis R.E. (1970) Electromechanical interactions in cell walls of Gram positive cocci. *J. Bacteriol.* **101**, 92-101.

Oyston P.C.F. & Handley P.S. (1990) Surface structures, haemagglutination and cell surface hydrophobicity of *Bacteroides fragilis* strains. *J. Gen. Microbiol.* **136**, 941-948.

Paakanen J., Gotschlich E.C., Mäkelä P.H. (1979) Protein K : a new major outer membrane protein found in encapsulated *E. coli*. *J. Bacteriol.* **139**, 835-841.

Pauly H. (1962) Electrical properties of the cytoplasmic membrane and the cytoplasm of bacteria and of protoplasts. *IRE Trans. Biomed. Electron.* **9**, 93-95.

Perkins R.L. & Miller M.A. (1973) Scanning electron microscopy of morphological alterations in *Proteus mirabilis* induced by cephalosporins and semi-synthetic penicillins. *Can. J. Microbiol.* **19**, 251-255.

Pethig R. (1979) Dielectric and Electronic Properties of Biological Materials. John Wiley & Sons, Chichester.

Pethig R. (1991a) Biological electrostatics : dielectrophoresis and electrorotation. *Inst. Phys. Conf. Ser.* **No. 118** (Section 1), 13-26.

Pethig R. (1991b) Application of AC electrical fields to the manipulation and characterisation of cells. *In* Automation in Biotechnology. Karube I. (Ed.) Elsevier, Amsterdam, pp. 159-185.

Pethig R., Huang Y., Wang X-B & Burt J.P.H. (1992) Positive and negative dielectrophoretic collection of colloidal particles using interdigitated castellated microelectrodes. *J. Phys. D. : Appl. Phys.* **24**, 881-888.

Plummer D.T. & James A.M. (1961) Some physical investigations of the behaviour of bacterial surfaces. III. The variation of the electrophoretic mobility and capsule size of *Aerobacter aerogenes* with age. *Biochim. Biophys. Acta* **53**, 453-460.

Pohl H.A. (1951) The motion and precipitation of suspensoids in divergent electric fields. *J. Appl. Phys.* **22**, 869-871.

Pohl H.A. (1958) Some effects of non-uniform fields on dielectrics. *J. Appl. Phys.* **29**, 1182-1188.

Pohl H.A. (1973) Biophysical aspects of dielectrophoresis. *J. Biol. Phys.* **1**, 1-16.

Pohl H.A. (1978) Dielectrophoresis : The Behaviour of Matter in Non-Uniform Electric Fields. Cambridge University Press, Cambridge.

Pohl H.A. (1983) Natural oscillating fields of cells. *In* Coherent Excitations in Biological Systems. Fröhlich H. & Kremer F. (Eds.) Springer-Verlag, Berlin, pp. 199-210.

Pohl H.A. & Hawk I. (1966) Separation of living and dead cells by dielectrophoresis. *Science* **152**, 647-649.

Pohl H.A. & Crane J.S. (1971) Dielectrophoresis of cells. *Biophys. J.* **11**, 711-727.

Pohl H.A. & Crane J.S. (1972) Dielectrophoretic force *J. Theor. Biol.* **37**, 1-13.

Pohl H.A., Braden T., Robinson S., Piclardi J., & Pohl D.G. (1981) Life cycle alterations of the micro-dielectrophoretic effects of cells. *J. Biol. Phys.* **9**, 133-154.

Polder D. & Van Santen J.H. (1946) *Physica* **12**, 257. (Cited by Chen, 1972).

Pover P.S. (1990) Colony counting and other petri dish applications of image analysis. *Binary* **2**, 77-79.

Poxton I.R. & Sutherland I.W. (1976) Isolation of rough mutants of *Klebsiella aerogenes* and their synthesis of polysaccharides. *J. Gen. Microbiol.* **96**, 195-202.

Price J.A.R. & Pethig R. (1986) Surface-charge measurements on *Micrococcus lysodeikticus* and the catalytic implications for lysozyme. *Biochim. Biophys. Acta* **889**, 128-135.

Price J.A.R., Burt J.P.H. & Pethig R. (1988) Applications of a new optical technique for measuring the dielectrophoretic behaviour of micro-organisms. *Biochim. Biophys. Acta* **964**, 221-230.

Quinn C.M. (1995) Dielectrophoresis of micro-organisms treated with antimicrobial agents. DPhil thesis, University of York.

Quinn C.M., Archer G.P., Betts W.B. & O'Neill J.G. (1995) An image analysis enhanced rapid dielectrophoretic assessment of *Cryptosporidium parvum* oocyst treatment. *In* Protozoan Parasites and Water. Betts W.B., Casemore D., Fricker C., Smith H. & Watkins J. (Eds.) The Royal Society of Chemistry, Cambridge, pp. 125-132.

Richmond D.V. & Fisher D.J. (1973) The electrophoretic mobility of micro-organisms. *Adv. in Microb. Physiol.* **9**, 1-29.

Rogers H.J. (1983) Bacterial Cell Structure. Van Nostrand, Wokingham.

Rogers H.J., Perkins H.R. & Ward J.B. (1980) Microbial Cell Walls and Membranes. Chapman and Hall, London.

Rohr T.E. & Troy F.A. (1980) Structure and biosynthesis of surface polymers containing polysialic acid in *Escherichia coli. J. Biol. Chem.* **255**, 2332-2342.

Rosenberg E. & Sar N. (1990) Changes in bacterial surface hydrophobicity during morphogenesis and differentiation. *In* Microbial Cell Surface Hydrophobicity. Doyle R.J. & Rosenberg M. (Eds.) American Society for Microbiology, Washington, pp. 229-247.

Rosenberg M. & Doyle R.J. (1990) Microbial cell surface hydrophobicity : history, measurement, and significance. *In* Microbial Cell Surface Hydrophobicity. Doyle R.J. & Rosenberg M. (Eds.) American Society for Microbiology, Washington, pp. 1-37.

Russell A.D. & Chopra I. (1990a) Mode of action of antibiotics and their uptake into bacteria. *In* Understanding Antibacterial Action and Resistance. Ellis Horwood, Chichester, pp. 39-94.

Russell A.D. & Chopra I. (1990b) Genetic and biochemical basis of resistance to chemotheraputic antibiotics. *In* Understanding Antibacterial Action and Resistance. Ellis Horwood, Chichester, pp. 146-181.

Salton M.R.J. (1960) Surface layers of the bacterial cell. Chapter 3. *In* The Bacteria. A Treatise on Structure and Function, Volume 1: Structure. Gunsalus I.C. & Stanier R.Y. (Eds.) Academic Press, London, pp. 97-151.

Savoia D., Malcangi A. & Martinetto P. (1990) The effect of sub-inhibitory concentrations of some antibiotics on the hydrophobicity of Gram negative bacteria. *J. Chemotherapy* **2**, 20-25.

Schaechter M., Maaløe O. & Kjeldgaard N.O. (1958) Dependency on medium and temperature of cell size and chemical composition during balanced growth of *Salmonella typhimurium*. *J. Gen. Microbiol.* **19**, 592-606.

Schlegel H.G. (1986) General Microbiology. 6th Edition. Cambridge University Press.

Schnaitman C.A. (1974) Outer membrane proteins of *Escherichia coli*. IV. Differences in outer membrane proteins due to strain and cultural differences. *J. Bacteriol.* **118**, 454-464.

Schnelle T., Müller T., Voigt A., Reimer K., Wagner B. & Fuhr G. (1996) Adhesion-inhibited surfaces. Coated and uncoated interdigitated electrode arrays in the micrometer and submicrometer range. *Langmuir* **12**, 801-809.

Schwan H.P. (1957) Electrical properties of tissue and cell suspensions. *In* Advances in Biological and Medical Physics, Volume 5. Lawrence J.H. & Tobias C.A. (Eds.) Academic Press, New York, pp. 147-209.

Schwan H.P. (1966) Alternating current electrode polarisation. *Biophysik* **3**, 181-201.

Schwan H.P. (1981) Dielectric properties of biological tissue and biophysical mechanisms of electromagnetic-field interaction. *In* Biological Effects of Nonionising Radiation. Illinger K.H. (Ed.) ACS Symposium Series **No. 157.**

Schwan H.P., Schwarz G., Maczuk J. & Pauly H. (1962) On the low-frequency dielectric dispersion of colloidal particles in electrolyte solution. *J. Phys. Chem.* **66**, 2626-2635.

Schwarz G. (1962) A theory of the low-frequency dielectric dispersion of colloidal particles in electrolyte solution. *J. Phys. Chem.* **66**, 2636-2642.

Sellwood J. & Wyn-Jones P. (1996) Viruses in water : present knowledge and future opportunities. *Microbiology Europe* **4**, 10-16.

Sher L.D. (1968) Dielectrophoresis in lossy dielectric media. *Nature* **220**, 695-696.

Shockman G.D. (1965) Symposium on the fine structure and replication of bacteria and their parts. IV. Unbalanced cell wall synthesis : autolysis and cell wall thickening. *Bacteriol. Rev.* **29**, 345-358.

Singh A., Pyle B.H. & McFeters G.A. (1989) Rapid enumeration of viable bacteria by image analysis. *J. Microbiol. Meth.* **10**, 91-101.

Sjogren R.E. & Gibson M.J. (1981) Bacterial survival in a dilute environment. *Appl. Env. Microbiol.* **41**, 1331-1336.

Sleytr U.B. & Messner, P. (1983) Crystalline surface layers on bacteria. *Ann. Rev. Microbiol.* **37**, 311-319.

Smoluchowski M. von (1921) Handbuch der Elektrizitat und des Magnetismus, Volume 2. Barth, Leipzig, pp. 366-385.

Sonnenfeld E.M., Beveridge T.J., Koch A.L. & Doyle R.J. (1985) Asymmetirc distribution of charge on the cell wall of *Bacillus subtilis*. *J. Bacteriol.* **163**, 1167-1171.

Springer L. & Roth I.L. (1973) The ultrastructure of the capsules of *Diplococcus pneumoniae* and *Klebsiella pneumoniae* stained with ruthenium red. *J. Gen. Microbiol.* **74**, 21-31.

Stern O. (1924) *Z. Electrochem.* **30**, 508-516.

Strange R.E. & Dark F.A. (1956) An unidentified amino-sugar present in cell walls and spores of various bacteria. *Nature* **177**, 186-188.

Stratford M. & Wilson P.D.G. (1990) Agitation effects on microbial cell-cell interactions. *Lett. Appl. Microbiol.* **11**, 1-6.

Stryer L. (1995) Biochemistry. 4th Edition. Freeman & Co., New York, p. 46.

Sutherland I.W. (1967) Phage induced fucosidases hydrolysing the exopolysaccharide of *Klebsiella aerogenes* Type 54 [A3(Sl)]. *Biochem. J.* **104**, 278-285.

Sutherland I.W. (1972) Bacterial exopolysaccharides. *Adv. Microb. Physiol.* **8**, 143-213.

Sutherland I.W. (1982) Biosynthesis of microbial exopolysaccharides. *Adv. Microb. Physiol.* **23**, 79-150.

Sutherland I.W. (1994) Personal Communication.

Sutherland I.W. & Norval M. (1970) The synthesis of exopolysaccharides by *Klebsiella aerogenes* membrane preparations and the involvement of lipid intermediates. *Biochem. J.* **120**, 567-576.

Teissié J., Prats M., Soucaille P. & Tocanne J.F. (1985) Evidence for conduction of protons along the interface between water and a polar lipid monolayer. *Proc. Nat. Acad. Sci.* **82**, 3217-3221.

Tempest D.W. (1969) Quantitative relationships between inorganic cations and anionic polymers in growing bacteria. *Symp. Gen. Microbiol.* **19**, 87-111.

Tipper D.J. (1970) *J. Systematic Bacteriol.* **20**, 361. (Cited by Ghuysen & Shockman, 1973).

Tortora G.J., Funke B.R. & Case C.L. (1995) Microbiology : An Introduction. 5th edition. Benjamin Cummings, California.

Troy F.A. (1979) The chemistry and biosynthesis of selected bacterial capsular polymers. *Ann. Rev. Microbiol.* **33**, 519-60.

Tsien H.C., Shockman G.D. & Higgins M.L. (1978) Structural arrangement of polymers within the wall of *Streptococcus faecalis*. *J. Bacteriol.* **133**, 372-386.

Tuomanen E., Cozens R., Tosch W., Zak O. & Tomasz A. (1986) The rate of killing of *Escherichia coli* by β-lactam antibiotics is strictly proportional to the rate of bacterial growth. *J. Gen. Microbiol.* **132**, 1297-1304.

Van der Mei H.C., Rosenberg M. & Busscher H.J. (1991) Assessment of microbial cell surface hydrophobicity. *In* Microbial Cell Surface Analysis : Structural and Physicochemical Methods. Mozes N., Handley P.S., Busscher H.J. & Rouxhet P.G. (Eds.) VCH Publishers Inc., New York. pp. 263-287.

Van der Mei H.C., de Vries J. & Busscher H.J. (1993) Hydrophobic and electrostatic cell surface properties of thermophilic dairy streptococci. *Appl. Env. Microbiol.* **59**, 4305-4312.

Vaz W.L.C., Goodsaid-Zalduondo F. & Jacobson K. (1984) Lateral diffusion of lipids and proteins in bilayer membranes. *FEBS Letters* **174**, 199-207.

Von Helmholtz H. (1879) (Cited by Pohl, 1978).

Wadström T. (1990) Hydrophobic characteristics of staphylococci : role of surface structures and role in adhesion and host colonisation. *In* Microbial Cell Surface Hydrophobicity. Doyle R.J. & Rosenberg M. (Eds.) American Society for Microbiology, Washington, pp. 315-333.

Wagner K.W. (1914) Erklärung der dielektrischen Nachwirkungs-vorgänge auf Grund Maxwellscher Vorstellungen. *Arch. Elektrotech.* **2**, 371-389.

Wagner K.W. (1924) Die Isolierstoffe der Electroteknik. Schering H. (Ed.) Springer, Berlin.

Ward J.B. (1973) The chain length of the glycans in bacterial cell walls. *Biochem. J.* **133**, 395-398.

Weiner I.M., Higuchi T., Rothfield L., Saltmarsh-Andrew M., Osborn M.J. & Horecker B.L. (1965) Biosynthesis of bacterial lipopolysaccharide. V. Lipid-linked intermediates in the biosynthesis of the O-antigen groups of *Salmonella typhimurium*. *Proc. Nat. Acad. Sci.* **54**, 228-235.

Weisberger C. & Troy F.A. (1990) Biosynthesis of the polysialic acid capsule in *Escherichia coli* K1. *J. Biol. Chem.* **265**, 1578-1587.

Whelan P.M. & Hodgson M.J. (1989) Essential Principles of Physics. 2nd Edition. Hazell Watson & Viney Ltd, Great Britain. p.366.

Wilkinson J.F. (1958) The extracellular polysaccharides of bacteria. *Bacteriol. Rev.* **22**, 46-73.

Wilkinson J.F., Duguid J.P. & Edmunds P.N. (1954) The distribution of polysaccharide production in *Aerobacter* and *Escherichia* strains and its relation to antigenic character. *J. Gen. Microbiol.* **11**, 59-72.

Wilkinson J.F., Dudman W.F. & Aspinall G.O. (1955) The extracellular polysaccharide of *Aerobacter aerogenes* A3(Sl) (*Klebsiella* Type 54). *Biochem. J.* **59**, 446-451.

Wolfe S.L. (1981) Biology of the Cell. 2nd Edition. Wadsworth Publishing Company, California. Chapter 17, pp. 480-497.

Wright A., Dankert M. & Robbins P.W. (1965) Evidence for an intermediate stage in the biosynthesis of the *Salmonella* O-antigen. *Proc. Nat. Acad. Sci.* **54**, 235-241.

Wright A., Dankert M., Fennessey P. & Robbins P.W. (1967) Characterisation of a polyisoprenoid compound functional in O-antigen biosynthesis. *Proc. Nat. Acad. Sci.* **57**, 1798-803.

York District Hospital (1994) Personal Communication.

"In complete darkness we are all the same. It is only our knowledge and wisdom that separates us. Don't let your eyes deceive you."

Janet Jackson